Cardiovascular Signal Compression Using a New Wavelet Energy Based Diagnostic Distortion Measure

M. Sabarimalai Manikandan

Cardiovascular Signal Compression Using a New Wavelet Energy Based Diagnostic Distortion Measure

A

Thesis Submitted

in Partial Fulfilment of the Requirements

for the Degree of

DOCTOR OF PHILOSOPHY

By

M. SABARIMALAI MANIKANDAN

Department of Electronics and Communication Engineering

Indian Institute of Technology Guwahati

Guwahati, Assam-781 039, INDIA

August, 2008

To my parents and family members
A. Mottaiyan, M. Annalakshimi and M. Senthil Murugan, M. Azhaghu Meena
for their blessings

To my teachers
Prof. K. I. Ramachandran and Prof. Elangovan
for their invaluable helps during my hardships of life

To my dear friends
N. Raghunath, P. Krishnamoorthy, Genemala Haobijam and Joormana Brahma
for their encouragements and moral supports

Certificate

This is to certify that the thesis entitled "**TITLE OF THE THESIS**", submitted by Author, a research student in the *Department of Electronics and Communication Engineering , Indian Institute of Technology, Guwahati*, for the award of the degree of **Doctor of Philosophy**, is a record of an original research work carried out by him under my supervision and guidance. The thesis has fulfilled all requirements as per the regulations of the Institute and in my opinion has reached the standard needed for submission. The results embodied in this thesis have not been submitted to any other University or Institute for the award of any degree or diploma.

Dated:
Guwahati.

Supervisor Name
Desigination
Dept. of Electronics and Communication Engg.
Indian Institute of Technology
Guwahati - 781 039
India.

Acknowledgements

I would like to express my sincere gratitude to Prof. Samarendra Dandapat for his guidance, suggestions and encouragement to successfully complete this research work. He has always been kind and motivating advisor, and introduced me to the field of medical signal and image processing. I sincerely thank him for the excellent research environment he has created for students to learn and pursue research work.

I would like to express my special thanks to the members of the thesis committee, Prof. P. K. Bora, Dr. S. R. M. Prasanna, and Dr. A. Mitra, for sparing their valuable time to evaluate the progress of my research work.

I would also like to express my thanks to the academicians at the Electronics and Communication Department of IIT Guwahati, Prof. A. Mahanta, Prof. A. K. Gogoi, Dr. S. Majhi, Dr. J. S. Sahambi, Dr. C. Mahanta, Dr. H. B. Nemade, Dr. R. Bhattacharjee, Dr. Roy P. Paily, Dr. K. Rakesh Singh, Dr. P. R. Sahu, Dr. R. Sinha, Dr. A. Rajesh, Dr. A. K. Mishra, and others for their moral support and valuable suggestions during the initial years of my Ph.D. studies.

It is a great pleasure to express my special thanks to Prof. P. K. Bora, Dr. S. R. M. Prasanna, Dr. Roy P. Paily and Dr. Harshal B. Nemade for their constant encouragements and moral supports throughout my research work. Sincere thanks are also extended to their family members.

I thank all the members of the research and staff of the department, namely L. N. Sharma, Sanjib Das, S. Josephine, Utpal Kumar Sharma, Pranab Jyoti Goswami, Sidananda Sonowal, Jharna Rani Rabha and Nabajyoti Dutta for their helps directly or indirectly during my research work.

It is a pleasure to express my sincere thanks to L. N. Sarma and S. R. Nirmala for their valuable suggestions, constant supports and the discussions we had at different stages of my work.

I thank Dr. Rajesh, Dr.(Mrs.) Mala Borthakur and electro medical and speech technology laboratory group members for their support in the subjective evaluation of the method. Special thanks to Dr.(Mrs.) Mala Borthakur for giving advice on my health conditions and suggestions.

I would like to express my thanks to all of my friends for their care, helps, and moral supports. I would also like to express my sincere thanks to H. S. Jeyanna and K. C. Narasimhamurthy for their suggestions and helps.

I would like to thank the whole IITG community for their help and cooperation during my stay at IITG.

Last but not the least; I would like to express my deep gratitude to my parents, sister and brother, who have always been there behind me with their love, support, encouragement and prayers during the hard times of my life.

(M. Sabarimalai Manikandan)

Abstract

This thesis presents an adaptive wavelet based compression method for cardiovascular signals. Generally, the performance of the lossy compression system depends on the methodologies used for compression and the quality measure used for evaluation of distortion. However, in order to introduce a closed loop rate or quality control, one needs an adequate distortion measure since it plays an important role in rate-distortion optimization technique used for finding optimal coding parameters.

Generally, compression method with two-stage design employs global wavelet thresholding followed by fixed linear quantization approach. But this may introduce a severe signal distortion since a subband consists of wavelet coefficients with great magnitude differences and exhibits varying dynamic range according to the signal characteristics. Therefore, first an adaptive wavelet compression approach based on the preprocessing step, multiresolution signal decomposition (MSD) technique, classification of wavelet coefficients, constraint threshold control zero-zone nearly uniform midtread quantization (TCZNUMQ), modified index coding (MIC) and Huffman coding schemes is proposed in this work. Generally, the amplitude distribution of wavelet coefficients of most ECG signals has sharp concentrations around zero in their distributions, and the relevant wavelet coefficients of the signal contents appear very close in a sequence order within a wavelet subband. The proposed approach exploits the above properties using TCZNUMQ and MIC schemes for achieving substantial improvements in compression performance. In this approach, the wavelet coefficients are classified into frames based on the statistics of subband coefficients for providing better quantization. The classified coefficients are then quantized using the constraint TCZNUMQ scheme in an adaptive manner. In this quantizer design, the zero-zone width is defined by the threshold parameter T for wavelet thresholding and the outer-zone width is chosen according to the distortion specification. A constraint on the TCZNUMQ scheme is studied to further reduce the computational cost of the conventional two-stage scheme. Since indexes or location of the nonzero wavelet coefficients are in sequence order, the modified index coding scheme is used to compress the integer significance map by exploiting the redundancy among the indexes.

The performance of compression method is tested using the well-known MIT-BIH arrhythmia (`mita`) database which contains varying characteristics of various ECG signals and different noises. The effect of noise filtering is one of the features in the wavelet transform based ECG signal compression. In such a case, smoothing of low-level background noise of the ECG signal causes a large percentage root mean square difference (PRD) value but no clinical feature distortion and, conversely, a small average distortion may severely deteriorate clinical performance if the error is concentrated in the regions of significant features. Moreover, noise present in the input decreases compression rate of the coder since the coder spends extra bits on approximating the noise for a user-specified PRD with a desired accuracy.

To overcome the limitations of the conventional PRD and wavelet based weighted (WWPRD) measures, a wavelet energy based diagnostic distortion (WEDD) measure for local and global assessment of compressed signals is presented. The WEDD measure is the weighted percentage root mean square difference between the subband coefficients of the original and compressed signals with weights equal to the relative wavelet subband energies of the corresponding subbands. In MSD technique, the higher subbands carry finely detailed information and the lower subbands carry shape based information, and it is noticed that the noise is well explained by a few levels that contain fine details and its effect disappears at the lower subbands. Therefore, the dynamic weights based on wavelet energy feature provides the actual contribution of the subbands that are used to discriminate different frequency subbands, particularly subbands corresponding to the background noise. Thus, the WEDD measure appears to be a correct representation of the amount of signal distortion at all subbands. This measure reliably computes the distortion not only within a distortion type at different distortion levels but also across different distortion types.

The rate-distortion (R-D) optimization is the key technique in an adaptive wavelet based compression method. This optimization technique requires an effective distortion measure to determine the optimal coding parameters. Therefore, the quality controlled wavelet based compression methods are presented for guaranteeing reconstruction quality measured using the WEDD criterion. The compression methods are based on: 1) the adaptive wavelet compression with joint thresholding and quantization scheme; 2) the adaptive wavelet subband compression with joint thresholding and quantization scheme; and 3) the set partitioning in hierarchical trees (SPIHT) algorithm based compression scheme. Experiments on several noisy records show that the quality controlled compression method with the new WEDD criterion provides an excellent coding performance, and outperforms the PRD and WWPRD criteria based compression methods.

Contents

List of Figures

List of Tables

List of Acronyms

1-D	One-dimensional
2-D	Two-dimensional
AAE	Average absolute error
ABSM	Arithmetic coding of binary significance map
ALQ-TRE	Adaptive linear quantization combined to a modified two-role encoder
AN	Amplitude normalization
ASEC	Analysis by synthesis ECG compressor
aVF	augmented voltage foot
aVL	augmented voltage left arm
aVR	augmented voltage right arm
AV	Atrioventricular
AVR	Average
AWGN	Additive white Gaussian noise
AZTEC	Amplitude zone time epoch coding
B2D	Binary to decimal conversion
BAWP	Best adapted wavelet packet bases
BSM	Binary significance map
BW	Biorthogonal wavelet
CAB	Cut and align beats
CAD	Cardiovascular disease
CAHM	Cardiac auscultation of heart murmurs
CC	Correlation coefficient
CDR	Compressed data rate
COTES	Coordinate reduction time encoding system
CR	Compression ratio
CSAPA	Combined scan along polygonal approximation
CUSAPA	Cubic-splines and scan along polygonal approximation
`cuvt`	Creighton university ventricular tachyarrhythmia database
CWT	Continuous wavelet transform
DCCR	Distortion constrained codevector replenishment
DCCR+SPIHT	DCCR and set partitioning in hierarchical trees
DCCR+SPIHT+BPC	DCCR with set partitioning in hierarchical trees and bit-plane coding
DCT	Discrete cosine transform
DLT	Discrete Legendre transform
DOWT	Discrete orthonormal wavelet transform

DR	Decoding rate
DWT	Discrete wavelet transform
DF	Decimation factor
DSI	Discrete sinc interpolation
ECG	Electrocardiogram
ED	Euclidean distance
EPE	Energy packing efficiency
EPE+WT	Energy packing efficiency and wavelet transform
EZW	Embedded zero-tree wavelet
FIR	Finite impulse response
FNC	Fixed number of coefficients
FOP	First-order predictor
FOI	First-order interpolator
FPWCZ	Fixed percentage of wavelet coefficients to be zeroed
FT	Fourier transform
GDQ	Guaranteeing desired quality
GSVQ	Gain-shape vector quantization
GW-AVQ	Gold washing-adaptive vector quantization
HC	Hybrid compression
HDISM	Huffman coding of difference of integer significance map
HPD	High-pass decomposition
HPDISM	Huffman coding of processed difference of integer significance map
HPR	High-pass reconstruction
HRBSM	Huffman coding of run-length encoded version of the binary significance map
HT	Haar transform
HT8BSM	Huffman coding of 8 bits/element table version of the binary significance map
IIR	Infinite impulse response
ISM	Integer significance map
JTQ	Joint thresholding and quantization
KLT	Karhunen-Loeve transform
KLT+MRS	Karhunen-Loeve transform and multirate sampling
LPD	Low-pass decomposition
LPR	Low-pass reconstruction
LP+WT	Linear prediction and wavelet transform
LSPIHT	Layered set partitioning in hierarchical trees
LQ	Linear quantization
LTP	Long-term prediction
LZW	Lempel-Ziv-Welch
M1	Root mean squared prediction error
M2	Mean absolute prediction error
M3	Standard error
M4	Correlation coefficient
MAE	Mean absolute prediction error
MAX	Maximum amplitude error
MC-AVQ	Multichannel adaptive vector quantization

MC-LTP	Multichannel long-term prediction
MCP	Mean correct prediction
MIC	Modified index coding
MIN	Minimum
MMSE	Minimum mean square error
MOS	Mean opinion score
MSAPA	Modified scan along polygonal approximation
MSD	Multiresolution signal decomposition
MSE	Mean square error
MSVQ	Mean-shape vector quantization
MR	Mean removal
MRA	Multiresolution analysis
`mitsva`	MIT-BIH Supraventricular arrhythmia database
`mita`	MIT-BIH arrhythmia database
NCC	Normalized cross correlation
NMAX	Normalized maximum amplitude error
NMSE	Normalized mean square error
NPE	Normalized prediction error
N-PR CMFB	Nearly perfect reconstruction cosine-modulated filter bank
NRDPWT	Nonrecursive discrete periodized wavelet transform
NUMQ	Nearly uniform midtread quantizer
NZWC	Nonzero wavelet coefficients vector
OM	Objective measure
OWT	Optimally warped transform
OZWC	Optimal zonal wavelet coding
PAN	Period and amplitude normalization
PCG	Phonocardiogram
PEC	Parameter extraction compression
PN	Period normalization
PRD	Percentage root mean square difference
PS	Period sorting
PSNR	Peak signal to noise ratio
PWCZ	Percentage of wavelet coefficients zeroed
QDASPIHT	Quality-on-demand algorithm and set partitioning in hierarchical trees
QMF	Quadrature mirror filters
QNZWC	Quantized nonzero wavelet coefficients vector
RE	Retained energy
RL	Regression line
RLE	Run-length encoding
rMSE	Relative mean square error
RMSE	Root mean square error
RQG	Retrieved quality guaranteed
RWSE	Relative wavelet subband energy
S1	First heart sound
S2	Second heart sound

SA	Sinoatrial
SAPA	Scan-along polygonal approximation
SBC	Subband coding
SDF	Spectral density function
SM	Similarity measure
SNR	Signal-to-noise ratio
SPIHT	Set partitioning in hierarchical tree
SQ	Scalar quantization
SROCC	Spearman rank-order correlation coefficient
SRR	Sample reduction ratio
StdErr	Standard error
STP	Short-term prediction
TCZNUMQ	Threshold control zero-zone uniform scalar quantization
TDC	Time domain compression
TDL	Target distortion level
TDR	Target data rate
TM	Template matching
TP	Turning point
TSVD	Truncated singular value decomposition
TWC	Thresholded wavelet coefficient
USQ	Uniform scalar quantizer
VAR	Variance
VCG	Vector cardiography
VF	Ventricular fibrillation
VM	Vanishing moments
VQ	Vector quantization
VT	Ventricular tachycardia
WC	Wavelet coefficients vector
WDD	Weighted diagnostic distortion
WEDD	Wavelet energy based weighted diagnostic distortion
WHOSC	Wavelet-transform higher order statistics-based coding
WLDECG	Wavelet-based, low-delay ECG compression
WPFDEC	Wavelet packets feasibility study for the design of an ECG compressor
WPFEC	Wavelet packets feasibility ECG compressor
WPT	Wavelet packet transform
WWPRD	Wavelet based weighted percentage root mean square difference
WPRD	Weighted percentage root mean square difference
ZOI	Zero-order interpolator
ZOP	Zero-order predictor

1

Cardiovascular Signal Compression: An Introduction

Contents

1.1 Introduction

Recent developments in digital technologies, sensors, efficient signal processing tools and wireless communication technologies enables to store and transmit biomedical signals for diagnosing patients diseases. Nowadays cardiovascular disease (CVD) is one of the most widespread health problems with unpredictable and life-threatening consequences in most regions throughout the world. For detection and identification of cardiac problems, the long-term measurement and real-time evaluation of cardiovascular signals is an essential task. For CVD diagnosis, electrocardiogram (ECG) and phonocardiogram (PCG) signals are commonly used for heart disease diagnosis. They provide essential information to the cardiologist and is used for both monitoring and diagnostic purposes. The ECG and PCG monitoring devices generate large amounts of digital data. The ECG signals, for example, received from recording systems such as 12-lead ECG, the vector cardiography (VCG) high-resolution ECG, exercise ECG, etc. are digitized at the sampling rate ranging from 100 to 1000 Hz with resolution in the range of 8 to 12 bits per sample. The PCG signals are stored in WAV format that are digitized with 8-16 bit sample resolution at a sampling frequency of 2000-22050 Hz. Thus, the ECG and PCG monitoring systems generate large amount of cardiac data every year. In recent years, miniaturized ECG recorder enables recording of the signals in urgent situations or remote location and the transmission of ECG data via well-established telecommunication channels to the specialist diagnostic center. The amount of cardiac data depends upon the sampling frequency, sample width, the number of leads and recording time, etc. There is clearly a need for compression without introducing clinical distortion for both storage and transmission of these signals.

Many compression methods for ECG signals have been proposed by exploiting the short-term correlation between adjacent samples, the considerable similarity between adjacent ECG beats (long-term correlation) and between the intra-lead ECG beats. They can be divided into three broad categories: time domain compression methods, frequency domain compression methods, and time-frequency domain compression methods. In recent years, the wavelet based methods have shown promise because of its interesting properties such as time-frequency localization, energy compaction, cross-subband similarity and straightforward implementation, etc. Among low computational complexity wavelet based ECG compression methods, many are based on thresholding of wavelet coefficients. A fundamental goal of any data compression is to reduce the bit rate for transmission or data storage without introducing the significant signal distortion. Since quality will be essential constraint for diagnosis, many automatic quality controlled compression methods have been attempted based on the well-designed lossy compression algorithm and percentage root mean square difference (PRD) measure for guaranteeing reconstruction quality. But, a number of researchers indicated the disadvantages of the use of PRD measure as a quality control criterion.

Most of the wavelet thresholding based methods are based on a two-stage design, where the wavelet coefficients are hard-thresholded first and then nonzero wavelet coefficients are quantized using the fixed uniform scalar quantization (USQ) schemes. The compression issues of the wavelet thresholding methods

are 1) a fixed number of coefficients from the sorted wavelet coefficients vector may not assure a good quality reconstruction because of the varying characteristics of various ECG signals. 2) In may two-stage schemes, fixed numbers of bits are assigned to wavelet coefficients that may produce severe signal distortion and hence decrease the coding efficiency of the compression algorithm. Since a vector consists of wavelet coefficients with different dynamic range, it is not efficient to allocate a fixed number of bits to represent wavelet coefficients because of the varying characteristics of various ECG signals. Even if we assign different but fixed numbers of bits to wavelet coefficients according to dynamic range of the vectors, the coding efficiency may still be poor because of wavelet coefficients with great magnitude differences within the coefficients vector of a ECG signal. In such a case, we need a classification technique and dynamic bit allocation which may enhance the compression performance of the adaptive wavelet coding method. In such a scheme, the signal distortion can be observed from two stages: discarded wavelet coefficients by thresholding with threshold T and quantization of nonzero wavelet coefficients with step size Δ. Thus, the distortion and the rate are the tradeoffs that must be considered simultaneously. We thus attempt issues related to the thresholding and uniform scalar quantization schemes to improve coding performance of the adaptive subband coding scheme in this work. 3) In two-stage schemes, a desired value of PRD maintained at the thresholding phase cannot be guaranteed after quantization phase since the fixed quantization step size is followed. We thus present a threshold control zero-zone nearly uniform midtread quantizer which has many advantages. 4) Common disadvantages of PRD measure are that a smoothing of low-level background noises of the ECG causes a large PRD value but no clinical feature distortion and, conversely, a small average distortion can severely deteriorate a signal clinical performance if all the error is concentrated in a significant feature region. In such a case, the PRD may not be subjectively meaningful since small and large numerical distortions do not correspond to "good" and "bad" subjective quality, respectively. Thus, quality assessment of a distorted ECG signal is an open problem today. We therefore explore the feasibility of the multiresolution signal decomposition and wavelet energy based features in developing a new quality measure that can be used for local and global assessments of distorted signals. 5) The performance tests are carried out using the well-known `mita` database which contains varying characteristics of various ECG signals and different noises and PRD measure. The effect of noise filtering is one of the features in the wavelet based compression, and is noticed in various compression works reported in the literature. In this case, noise degrades the compression performance of the coder since the coder spends extra bits on approximating the noise with the specified distortion accuracy. However, rate-distortion (R-D) optimization is the key technique in lossy compression methods to efficiently determine a set of optimal coding parameters. Thus, the R-D optimization requires an ability to measure distortion.

The above constructs show that in order to provide a better automatic quality control for wavelet based compression of cardiovascular signals, we need three most important components: a well-designed adaptive subband coding methodology, a subjectively meaningful objective quality measure for local and global assessment, and simple automatic quality control algorithm to perform the quality control quickly and accu-

rately. This research work attempts to present a better quality driven wavelet coding scheme by considering the design philosophy of those components.

1.2 Overview of Cardiovascular Signals

The cardiovascular system is composed of heart and blood vessels which facilitate the circulation of blood throughout the body. Mechanical events of the cardiac cycle are initiated and synchronized by electrical events [1–4]. Electrocardiography and phonocardiography are the fundamental parts of cardiovascular assessment. They are the essential tools for investigating cardiac arrhythmias and are also useful in diagnosing cardiac disorders [4,5]. Therefore, we present a brief outline of the electrocardiogram and phonocardiogram signals in this section.

1.2.1 The Electrocardiogram

The electrocardiogram (ECG) continues to be a critical component of the evaluation of patients who have signs and symptoms of emergency cardiac conditions [6, 7]. Cardiac impulses normally originate in the sinoatrial (SA) node and then are conducted through the atrial tissue to the atrioventricular (AV) node and into the bundle of His [8]. The ECG signal represents the changes in electrical potential in the cardiac muscles during the cardiac cycle as recorded on the surface of the body. Each ECG cycle contains number of time-varying local waves. These waves are examined by observing or extracting the feature parameters such as amplitudes, intervals and shapes of the waves. Information related to the characteristics of local wave patterns are important. The alteration of the local wave patterns during the ECG signal processing may mislead to wrong diagnosis. Hence, the preservation of the original clinical information is an essential requirement for a compression system. A two cycle ECG signal with various amplitudes and time intervals is shown in Fig. 1.1. P, Q, R, S, T and U are some of the local waves present in a typical ECG cycle. This section explains diagnostic criteria for the individual components of ECG waveforms. To recognize electrocardiographic abnormalities the range of normal wave patterns must be understood. The details of the diagnostic features can be found in many literatures, say [3–5, 8].

P wave: P wave represents the composite electrical activation of right and left atria. The duration of the P wave is usually in the range of 80 to 100 ms. The maximum normal amplitude of P wave on the surface of the body is 0.25 mV. Normal P wave is gently rounded and it is never pointed or peaked. A tall P wave ($>$0.25 mV) signifies right atrial enlargement (RLE) and a widened P wave indicates left atrial enlargement (LAE). P wave may be decreased in height due to hyperkalemia.

PR interval: The time interval between the atrial depolarization and the beginning of ventricular depolarization is called PR interval. The PR interval is a refractory period which represents the delay in transmission of impulses from atria to ventricles. The PR interval is measured from the beginning of the P wave to the beginning of the Q wave or the beginning of the R wave if the Q wave is absent. Normal duration of the

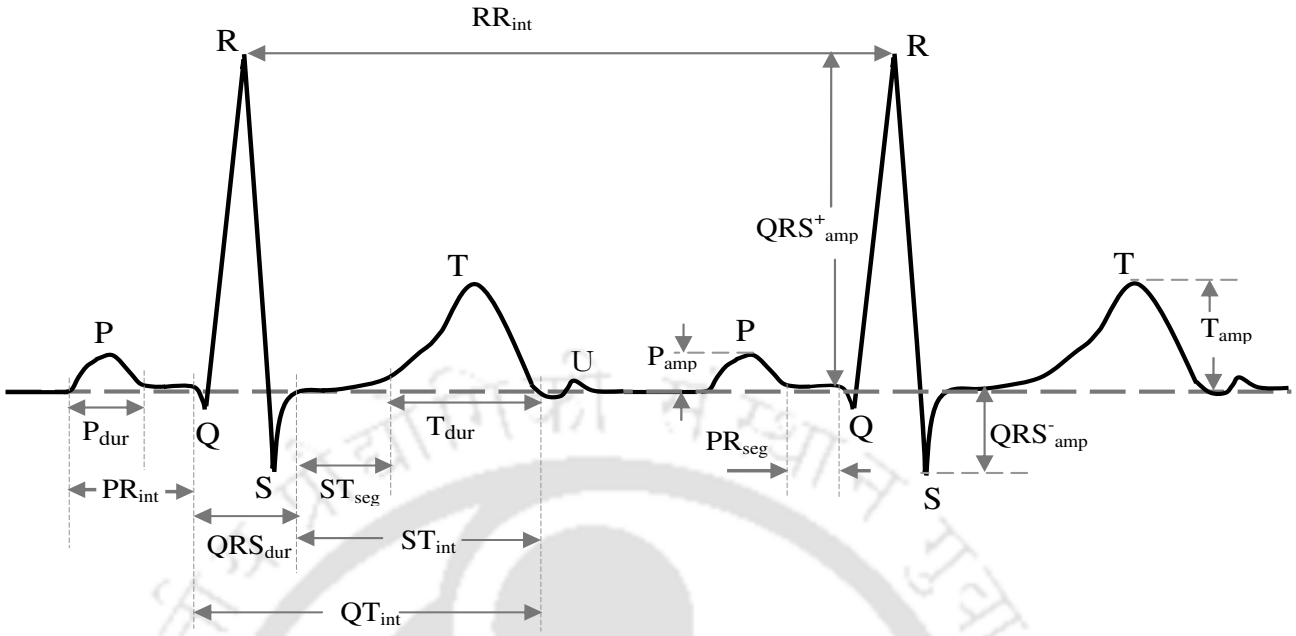

Figure 1.1: The electrocardiogram (ECG) signal and some diagnostic parameters.

PR interval is 120-200 ms. Very short PR intervals are observed in patients with pheochromocytoma and Wolfe-Parkinson-White Syndrome. ECG signals from patients with 1st degree AV block, 2nd degree AV block (Mobitz I) and rheumatic heart diseases exhibit prolonged PR intervals.

Q wave: Q wave is the first downward deflection of the QRS complex. Q wave represents the depolarization of the intraventricular septum. A normal Q wave is a narrow deflection of small amplitude (duration: $<$40 ms, amplitude: 25% of the amplitude of the R wave). A wide or deep Q wave may signify myocardial infarction.

R wave: R wave is the first upward deflection of the QRS complex. It represents a part of the ventricular depolarization cycle. If the R wave progression is reversed or greatly disturbed, it suggests the presence of a bundle branch block.

S wave: S wave is the first downward deflection after R wave. It represents the remaining part of time period for ventricular depolarization. S waves have irregular shapes in the presence of bundle branch blocks.

QRS complex: The QRS complex is the electrical wave that signals the depolarization of the myocardial cells of the ventricles. The duration of the QRS complex is normally 60 ms to 100 ms. If the duration of QRS complex is greater than 100 ms, then the electrical conduction is probably impaired within the ventricles (abnormal intraventricular conduction velocity).

ST segment: The ST segment corresponds to the plateau of the action potentials of all fibres after the depolarization of all the ventricular muscle cells. The QRS complex terminates at the J point. The ST segment lies between the J point and the beginning of the T wave. It represents the period from the end of

systole to the beginning of repolarization of the ventricles. It may appear as a flat line between the QRS complex and the T wave or it may be upsloping from the J point from 0.1 mV to 2 mV and may be of 80 ms to 120 ms duration. The appearance of the ST segment changes dramatically in the presence of ischemia or during a myocardial infarction. During ischemia, the ST segment will become depressed with a long duration and a large amplitude before it joins the T wave. The ST segment is elevated during an acute myocardial infarction. The ST segment is very important in the diagnosis of heart problem.

T wave: T-wave represents ventricular repolarization. The duration of T wave is typically 100 ms to 250 ms and its amplitude is less than 0.5 mV. The normal T wave is asymmetrical, the first half has a more gradual slope than the second half. Abnormally shaped T waves can signify acute episodes of cardiac ischemia or infarction.

QT interval: The QT interval is measured from the beginning of the QRS complex to the end of the T wave. It represents the total time required for depolarization and repolarization of the ventricles. The duration of the QT interval varies between 350 ms to 450 ms. At higher heart rates, the duration of the ventricular action potentials decreases which shortens the QT interval. Prolonged QT-interval may be associated with delayed ventricular repolarization which may cause ventricular tachyarrhythmias leading to sudden cardiac death.

U wave: U wave is a small deflection that follows the T wave. U waves result from repolarization of the mid-myocardial cells. The abnormal U wave is inverted or tall with an amplitude of 0.2 mV or more. Many electrocardiograms have no discernible U waves. It may cause hypokalemia, diabetes and cardiomyopathy.

PP and RR interval: The PP interval represents the duration of the atrial cycle which is an indicator of atrial rate. The RR interval is the ventricular rate which represents the duration of ventricular cardiac cycle.

The potentials generated in the heart are conducted to the body surface and this electrical activity of the heart is recorded from the body by surface electrodes. Standardized electrode positions are used for the recording of electrocardiograms. The recordings obtained through different pairs of electrodes result in different waveform shapes and amplitudes. In clinical practice, there are 12 conventional leads, which may be physiologically divided into two groups depending upon their orientation to the heart [3]. These are orientated in the frontal or coronal plane of the body. The frontal plane leads consist of bipolar limb leads viz standard leads I, II and III, and unipolar limb leads viz augmented limb leads aVR (augmented voltage right arm), aVL (augmented voltage left arm), and aVF (augmented voltage foot). These are orientated in the transverse or horizontal plane of the body. The horizontal plane leads consist of unipolar chest (precordial) leads V1 to V6. The 12-lead ECG is formed by the 3 bipolar surface leads: I, II, and III; the augmented Wilson terminal referenced limb leads: aVR, aVL and aVF; and the Wilson terminal referenced chest leads: V1, V2, V3, V4, V5 and V6. These 12-lead ECG signals are used for diagnosis of the heart diseases [8, 9]. A variety of cardiac disorders are associated with specific patterns of ECG. Diagnostic criteria for ECG abnormalities are summarized in [9] which are most important for cardiovascular signal processing applications.

1.2.2 The Phonocardiogram

Auscultation is the most common and cost effective non-invasive technique and heart sound analysis can provide important information relating to the heart condition for diagnosis of cardiovascular disorders [10]. Heart valve disorders are analyzed using phonocardiogram (PCG) which is a recording of the acoustic waves produced by the mechanical action of the heart [11, 12]. It is a very useful and effective method for the diagnosis of heart diseases (anatomical modifications of ducts, cavities and holes where blood passes, changing its dynamic and the vibrations). The cardiac cycle consists of two periods, systole and diastole. Four classes of sound components may be audible on heart auscultation: the primary components (S1, S2, S3, and S4) are short beats, the other classes of sounds are murmurs, clicks and snaps. The sound emitted by a human heart during a single cardiac cycle consists of two dominant events, the first heart sound (Sl) and the second heart sound (S2). S1 is a low, slightly prolonged "lub", caused by vibrations set up by the sudden closure of the mitral and tricuspid valves as the ventricles contract and pump blood into the aorta and the pulmonary artery at the start of the ventricular systole. The second sound S2 is a shorter, high-pitched "dup", caused when the ventricles stop ejecting, relax and allow the aortic and pulmonary valves to close just after the end of the ventricular systole. S2 consists of two major components, one due to the closure of the aortic valve (A2) and the other due to the closure of the pulmonary valve (P2) [12]. The A2 is the loudest component and is discernible at all the auscultation sites whereas the P2 component is the softer component. The S3 and S4 heart sounds are caused by the rapid ventricular filling during early diastole and the ventricular filling due to atrial contraction, respectively. In addition to these four heart sounds, other transient sounds namely opening clicks, snaps and prolapsed sounds are produced by valvular stenosis during systole and diastole. In this work, the PCG signals taken from the cardiac auscultation of heart murmurs (`CAHM`) and the `qdheart` databases [21, 22]. In these databases, PCG records are stored in WAV format with different sampling rates and resolutions. These databases include records of many different valvular pathologies (normal sounds, third heart sound, fourth heart sound, aortic insufficiency, aortic stenosis, mitral stenosis and murmurs, noises, etc.).

1.2.3 Cardiac Data Acquisition

Clinicians can evaluate the conditions of a patient's heart from the ECG and perform further diagnosis. The amplitude of the ECG signal as measured on the skin ranges from 0.1 mV to 5 mV [17]. The recording of the electrical field generated by the His and Purkinje activities produces a signal in the ECG with an amplitude range of about 1 to 10 μV which is useful in the identification of conduction abnormalities [4]. The frequency extends from 0.05 Hz to 130 Hz [5, 15–17]. It has been found that notches and slurs may be superimposed on the slowly varying QRS complexes. The recommendations of the committee on electrocardiography of the American heart association suggest a conversion rate of 500 HZ with a 9-bit precision [14]. In practice, sample rates from 100 Hz to 1000 Hz are used with 8-bit to 16-bit precision [17].

Table 1.1: Some cardiac data and its characteristics

Cardiac data		Frequency range	Digitization		data rate
	Signal range		sampling rate	resolution	(per channel)
ECG	10 μV - 5 mV	0.05 - 500 Hz	100-1000 Hz	8 - 16 b/sample	3.96 kbps[1]
PCG	80 dB	5- 2000 Hz	8 k - 22.05 kHz	8 - 16 b/sample	352.8 kbps[2]
Heart rate (HR)	45 - 200 beats/min	N/A	1 sample/min	9 b/sample	0.15 bps
Respiratory rate (RR)	2 - 50 breaths/min	0.1 - 10 Hz	1 sample/min	6 b/sample	0.1 bps
Blood pressure (BP)	40 - 300 mm Hg (arterial) 0 - 15 mm Hg (venous)	dc - 60 Hz	1 sample/min	8-10 b/sample	0.33 bps
Temperature (Temp.)	32 - 40 ^{o}C	0 - 0.1 Hz	1 sample/min	6 b/sample	0.1 bps
Blood flow (BF)	1 - 300 mL/s	0 - 20 Hz	1 sample/sec	9 b/sample	0.15 bps
Cardiac output (CO)	4 - 25 L/min	0 - 20 Hz	1 sample/min	6 b/sample	0.1 bps

Note:- 1. MIT-BIH arrhythmia `mita` database (F_s = 360 Hz, 11 b/sample) and 2. `qdheart` PCG database (F_s = 22050 Hz, 16 b/sample). Some of the clinical data specifications are taken from: http : //www.engr.wisc.edu/bme/faculty/webster_john.html

The information rate is thus approximately 11-22 Mbits/hour/lead. Therefore, data compression methods for ECG signals have gained popularity in recent years to meet the requirements of storage as databases for subsequent and serial comparisons and of transmission of these signals over wire/wireless communication networks. The main goal of any such technique is to derive maximum data compression without sacrificing the clinically significant information.

During the data acquisition stage heart sound signals are directly collected from patients and saved as waveforms. PCG is the complex and highly nonstationary signal [5]. Characteristics of heart sound signals have been assessed in terms of both intensity and frequency. According to Ref. [10], it is found that the first and second heart sounds fall in the frequency range of 80-120 Hz and 120-150 Hz, respectively. The third and fourth heart sounds are found to be of low frequencies in the range of 70-90 Hz and 50-70 Hz, respectively. Average murmurs are found to have usually higher frequencies in the range of 100-600 Hz. The frequencies of heart sounds mostly would occur below 1000 Hz [5, 13]. The PCG signals are digitized at a sampling frequency of 8000-22050 Hz with 8-16 bit resolution. The data rate for ECG (MIT-BIH arrhythmia database [18–20]) signal is 3960 bps whereas PCG (PCG database [21, 22]) data rate is 352.8 kbps. The ECG and PCG data rates are much higher than the other cardiac data namely heart rate, blood pressure and cardiac output as shown in Table 1.1. The ECG and PCG recorded for several minutes using heart patient's monitoring instruments can produce several hundred megabytes of cardiac data. As a result, the volume of the data increases significantly, which leads to a high cost in storing and transmitting such PCG data. Therefore, it is necessary to develop an effective compression method which has capability to reduce the volume of data for storing and to speed up the transmitted data for wireless telemedicine applications [23]- [34]. The main goal of any such method is to derive maximum data compression without introducing clinically significant distortions.

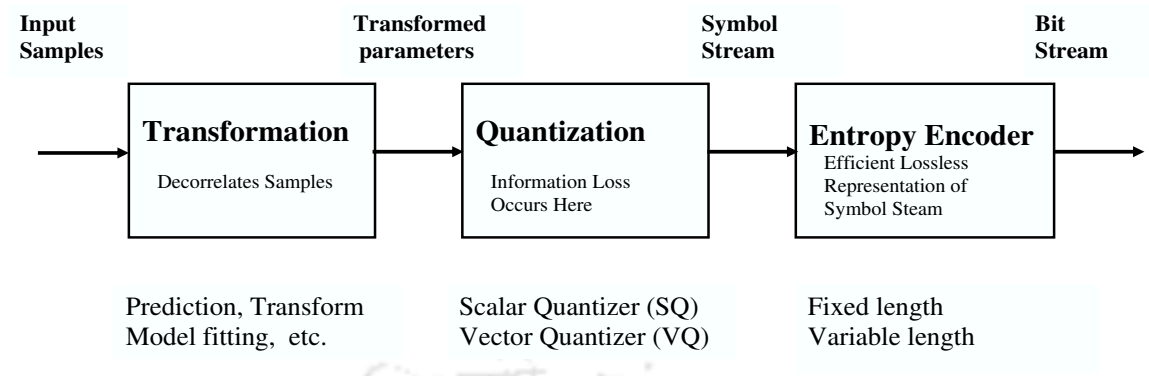

Figure 1.2: Basic components in a data compression system.

1.3 Classical Data Compression System

A digital data compression system consists of one or more of the following processes which may be combined with each other or with additional signal processing blocks such as signal transformation, quantization and entropy coding [35–37]. Fig. 1.2 shows the block diagram of a digital data compression system. The first stage consists of transformation block where the extraction of significant information, the prediction, the decomposition and the signal modeling are accomplished. The purpose of this stage is to produce a more efficient or compact representation of input signal. The second stage is the quantization block which aims at reducing the number of possible output symbols. The type of quantization has a significant effect on the quality of the compressed signal and its bit rate. This relationship is given as rate-distortion (R-D) curve. The third stage is the symbol encoding block. The criteria for testing the performance of compression method includes four components: compression measure, compression error, coding delay and coder complexity. The compression measure and the compression error are usually dependent on each other and are used to create the rate-distortion function of any method. Coder complexity is part of practical implementation consideration. Coder complexity includes both time and space complexity. Among the three (low, medium and high) levels of complexity, high complexity coder provides the best results in bit rate reduction by utilizing highly adaptive algorithms and/or extensive use of long-term signal memory [36].

Signal Transformation: In data compression, the objective of signal transformation is to concentrate the signal energy in fewer coefficients. The transformation can be achieved by prediction, transform and model fitting algorithms. Linear prediction (LP) algorithms such as short-term prediction (STP) and long-term prediction (LTP) are efficiently employed for removal of sample correlation [37]. The input signal can be decomposed into several subsignals (sets of coefficients) for separate processing by linear transformation (Fourier transform (FT), discrete cosine transform (DCT), Karhunen-Loeve transform (KLT), Walsh transform, etc.) or by filtering with a subband or wavelet filter bank [36, 37].

Quantization: The transformed coefficients or parameters are quantized to produce a stream of sym-

bols. Quantization is the process of replacing the continuous amplitude samples with approximate discrete values which are taken from a finite set of allowed values [36, 38]. The goal of quantization is to quantize the transformed coefficients or parameters so that the entropy of the resulting distribution of bin indexes is small enough and the symbols can be entropy coded at some target low bit rate. The quantization process results in a discrete amplitude signal which is different from the continuous amplitude signal by the quantization error or noise. Information loss occurs in the quantization stage. When each set of parameters (or a sequence of signal values) is quantized separately, the process is known as scalar quantization (SQ). When the set of parameters is quantized jointly as a single vector, the process is known as vector quantization (VQ) or block quantization [39, 40]. Some of the scalar quantizers [36] are: uniform quantizer (midtread quantizer and midriser quantizer), dead zone quantizer, nonuniform quantizer, logarithmic quantizer, adaptive quantizer and differential quantizer. The vector quantization (VQ) is an efficient data compression method for speech signals and images [39–41]. In VQ, the optimal encoder operates on a nearest neighbor or minimum distortion fashion and determines the closest codeword in its collection by an exhaustive search. A constrained search can speed up the encoding but may not guarantee to find the overall nearest neighbor in the codebook. The choice of distortion measure permits us to quantify the performance of a VQ in a manner that can be computed and used in analysis and design optimization. The performance of VQ depends crucially on the dimension, size of the codebook, the choice of code vectors in the codebook and the distortion criterion [40–42].

Entropy Coding: After quantization of data into a finite set of values, it can be encoded using an entropy coder to provide additional compression [37]. The entropy or statistical coder encodes a given set of symbols with the minimum number of bits required to represent them. If the original signal is transformed and quantized, then the application of lossless coding techniques [35] such as Huffman, Lempel-Ziv-Welch (LZW) or arithmetic can provide further compression without any additional loss of information. An efficient data compression system can be designed using methodologies which exploit irrelevancy and redundancy of the cardiovascular signals.

1.3.1 Signal Irrelevancy and Redundancy

For heart disease analysis, electrocardiography data is continuously recorded for 12-72 hours to monitor ischemia, ventricular and supra-ventricular dysrhythmias, conduction abnormalities, QT interval and heart rate variability [5]. The ECG signals are typically sampled at different sampling frequencies ranging from 100 Hz to 1000 Hz. For good signal quality, typically 8 to 16 bits of precision is used for samples. Hence, the amount of ECG data that has to be stored or transmitted depends upon the sampling frequency, the number of quantization levels, the number of leads and the recording time. Hence, ECG record management system and telecardiology application requires reliable and efficient compression techniques for storage and continuous transmission purposes [27]. The standard features of an ECG signal are the P wave, the QRS complex and the T wave. Additionally, small U wave (followed by the T wave) is present occasionally.

These local waves are separated by baseline or isoelectric regions. The local waves are characterized by the feature parameters such as amplitude, duration and shape. Alterations of these features are considered as diagnostic criteria for cardiac abnormalities. In medical practice, ECG signals are recorded for longer time for diagnosis of cardiovascular diseases. It can be observed that there is a concatenation of nearly similar cardiac events or periods which yields beat to beat correlation while looking at the long-term ECG signal. Digital sampling of ECG signals is generally performed by sampling at uniform intervals with rates high enough to record the fastest or short signal components [43]. Hence, many redundant samples are recorded in slow wave regions and baseline regions or isoelectric regions. Multi-channel ECG signals have three types of correlations [5, 6]: the intra-beat, the inter-beat and the inter-channel/lead. The intra-beat correlation represents the correlation between the successive samples in an ECG cycle. The inter-beat correlation represents the correlation between successive beats in a single-channel ECG signal. The correlation that exists between the signals from different channels is termed as inter-channel correlation. Similarly, phonocardiography has correlations across the intra- and inter-heart sounds and also has long silence regions. The above signal irrelevancy and redundancy are exploited using different compression methodologies in ECG and PCG data compression methods. Note that the quality of the compressed signals is most important for diagnosis of heart diseases at the diagnostic center.

1.3.2 Coding Efficiency

Redundancy reduction ability is evaluated in terms of the following compression measures: the sample reduction ratio (SRR), the compression ratio (CR), the compressed data rate (CDR) and the decoding rate (DR). The sample reduction ratio (SRR) is defined as the ratio of the number of samples within a block to the number of retained or stored samples for compression [43]. This compression measure is utilized where the retained samples are coded at the same sample resolution. The amount of compression is often measured by the compression ratio (CR) which is defined as the ratio between the bit rate of the original signal and the bit rate of the compressed signal. The CDR (bits per second) is defined as the ratio of the product between the sampling rate (samples per second) and the amount of the compressed data (bits) to the number of samples within a block. The entropy in bits per sample is also used in many reported ECG compression methods. The coding efficiency can be measured easily. But measurement of clinical quality of the distorted signal is a challenging problem in many biomedical signal processing applications.

1.3.3 Distortion or Quality Measures

In literature many lossy compression methods are proposed. Lossy compression methods may distort the clinical information in the signal. The quality measures in the literature can be classified into two groups: subjective and objective. Subjective evaluation is cumbersome as the physicians can be influenced by several critical factors including the knowledge, environmental conditions and motivation. Therefore a simple

mean square error (MSE) measure and its variants are commonly used for quality assessment [43]. The MSE is the L_2 norm of the arithmetic difference between the original and the compressed signals. A squared error distortion measure is an assignment of cost, $d(\mathbf{x},\widetilde{\mathbf{x}})$, of reproducing any original vector $\mathbf{x}$ as a reproduction vector $\widetilde{\mathbf{x}}$. Given such a distortion measure, the performance of a compression method is quantified by an average distortion $E[d(\mathbf{x},\widetilde{\mathbf{x}})]$. These types of distortion measures are called as objective distortion measures. A compression method will be good if it yields a small average distortion value. Ideally a distortion measure should be manipulable to permit analysis and computable so that it can be evaluated and used in minimum distortion methods. It should be subjectively meaningful so that large or small value can correlate with bad and good subjective quality. The objective distortion measures are grouped into three categories viz global measure, local measure and similarity measure. For a given original discrete sequence $x(n) = \{x(1),x(2),x(3).....,x(N)\}$ and a reconstructed or compressed sequence $\widetilde{x}(n) = \{\widetilde{x}(1),\widetilde{x}(2),\widetilde{x}(3).....,\widetilde{x}(N)\}$ the MSE is defined as

$$\text{MSE} = \frac{1}{N}\sum_{n=1}^{N}[x(n)-\widetilde{x}(n)]^2 \tag{1.1}$$

where N is the number of samples in the original vector. MSE distributes the error equally over all portions of the ECG signal. Every portion of the ECG cycle has a different diagnostic meaning and relevance. It is a common practice to measure the performance of a compression method by normalized MSE. This corresponds to normalizing the average distortion by the average energy. The global error measures include normalized MSE (NMSE), root MSE (RMSE), normalized RMSE (NRMSE), percentage root mean square difference (PRD) and signal to noise ratio (SNR). Some of the local error measures are maximum amplitude error (MAX) or peak error (PE), normalized MAX (NMAX) and standard error (StdErr). The similarity measures are normalized cross correlation (NCC) and the diagnostic distortion measures namely weighted PRD (PRD), weighted diagnostic distortion (WDD) and wavelet based weighted PRD (WWPRD). Among these, the PRD is widely used in many compression methods. In general, the PRD is a normalized value which indicates the error between original and compressed signals [43]. It can be expressed as $\text{PRD} = (\text{RMS}_e/\text{RMS}_v)\times 100$, where RMS_e and RMS_v are the RMS values of the error and the ECG signal respectively. This corresponds to normalizing the average error by the RMS value of the signal. The mathematical expressions for other objective measures will be described in the next chapter. Since a highly distorted signal can be useless from a clinical point of view, a meaningful distortion measure is essential for local and global assessment. However, assessment of compressed signal quality is an open problem today.

1.4 Classification of ECG Compression Methods

A digital information source is said to possess redundancy if either [35]: 1) the symbols are not equally likely, or 2) the symbols are not statistically independent. All data compression methods seek to minimize

data storage by reducing the redundancy [36]. Redundancy in a set of discrete samples exists when signal samples are statistically dependent [44]. Data compression methods, which are successfully used for speech, image and video signals, can be employed for ECG signals. ECG data compression should be accomplished without sacrificing the clinical information.

ECG Data compression (or data reduction) methods are divided into three categories [44–49]: lossless (reversible) compression and lossy (irreversible) compression. In lossless data compression, the signal samples are considered to be realizations of a random variable or a random process. Lossless compression method, also referred to as entropy coding, is performed by removing redundancy which exhibits in terms of statistical dependence between samples. Typical lossless methods (null suppression, run-length coding, differencing, Huffman coding, arithmetic coding, LZ family) are less suitable as the reconstruction is perfect while compression ratio is poor. On the other hand lossy methods may produce high compression ratio. In lossy methods, quantization of the input data leads to higher CR at the expense of reversibility. This may be acceptable as long as no clinically significant distortion is introduced to the signal. The CR levels of 2 to 1 are too low for most practical applications. Therefore, lossy compression methods which can achieve high compression ratio value at the cost of introduction of small reconstruction errors are preferred in practice.

Based on the input signal representation, the lossy compression methods are broadly classified into two major groups: one-dimensional (1-D) and two-dimensional (2-D) compression methods. These compression methods can be further subdivided into two major categories: 1) time domain methods, 2) frequency domain methods and 3) wavelet (time-frequency) domain methods. Two or more major categories can be combined to improve data compression efficiency which is referred here as hybrid compression method. In this work, more importance is given to 1-D ECG compression method because of its general acceptance and applicability in continuous cardiovascular signal transmission via mobile cellular networks [25–27, 32–34]. Therefore, compression system to be designed should be simple (low complexity), fast and efficient so as to make the system attractive for use in portable and mobile heart monitoring systems.

1.4.1 Time Domain Compression Methods

Time domain compression (TDC) methods detect redundancies by direct analysis of actual signal samples. Table 1.2 shows different TDC compression methods for ECG signals. TDC method exploits the intra-beat redundancy due to correlation between successive samples. Four categories of data handling approaches are used in this method [44–46]: the statistical coding techniques, the redundancy reduction techniques, the adaptive sampling techniques and the parameter extraction based (PEC) techniques. In adaptive sampling, the sampling rate of the original waveform is varied while in redundancy reduction the waveform is initially sampled at a constant rate and nonessential samples are eliminated later.

Table 1.2: Summary of some of the time domain ECG compression methods.

Methods	Based on the following concepts	Compression perfromances
polynomial predictors [44]	finite difference method, previous samples, tolerance (peak error) comparison,	efficient for step like data
polynomial interpolators [45]	both previous and future samples, preset error threshold	amplitude distortion
3^{rd} order interpolator [50]	important points (IP): amplitude, time and slope	seamless, smooth reconstruction
voltage triggered [52], [53]	stores sample if the absolute value of transient and permanent sample difference $>$ triggering threshold voltage	sloping baselines artefacts which misleads diagnosis
2-point projection [52], [54]	linear extrapolation, first order interpolator with two degree freedom (FOI-2DF)	effective on noise free ECG fails for highly noisy signal
AZTEC [55], [43]	ZOI, plateaus (amplitude) and slope (duration) parameters	discontinuities (step-like), poor P and T fidelity
TP [56], [43]	processes three points, reference point $x(0)$ is compared with other two points ($x(1)$ and $x(2)$) to find turning point	short term time distortion or local time shifts
CORTES [43]	AZTEC and TP, parabolic smoothing filter, TP to high frequency regions and AZTEC to isoelectric regions	amplitude distortion due to post processing
SAPA algorithms [57]	FOI with 2DF, three slope, center slope criterion for identifying permanent sample	SAPA-2 is effective, high CR, less sensitive to noise
fan [58–61]	FOI with 2DF, two slope, actual sample criterion for identifying permanent sample	high fidelity, slope distortion if CR is high
adaptive AZTEC [62]	AZTEC with adaptive error threshold determined from first three moments of the $x(n)$	post processing needed, CR depends on noise level
SLOPE algorithm [63]	repeatedly delimiting linear segments (LS) using some heuristics and Huffman coding for parameters of LS	clinically acceptable signal
CORNER detection [64]	smoothing, corner detection by curvature and displacement merging of consecutive LSs and Huffman coding for merged LSs	better than AZTEC in terms of SNR and RMSE
MSAPA [65]	SAPA-2 with integer division instead of real division	poor P wave and ST segment fidelity
CSAPA [65]	combines MSAPA and TP algorithms, MSAPA for fast and efficient compression, TP for retaining ST segment	high fidelity than SAPA and MSAPA
AZTDIS [66]	smoothing, simplified AZTEC, displacement to select samples, merging of consecutive LSs and Huffman coding of merged	improved SNR and RMSE compared to AZTEC
CUSAPA [67]	combines the CUbic splines and SAPA-1, SAPA-1 to high frequency regions, cubic splines to low frequency segments	good quality, superior noise reduction, more time
cubic splines [68]	cubic splines by calculating the spline coefficients, least squares norms to select number of coefficients	-
improved adaptive AZTEC [70]	adaptive AZTEC with $X_{\max}$ and $X_{\min}$ for finding the first three moments, all values are reset to zero before starting next cycle	better than adaptive AZTEC,

1.4.1.1 Statistical Coding Techniques

Data compression by entropy coding is obtained by means of assigning variable-length codewords to a given quantized data sequence according to their frequency of occurrence [44, 45]. This compression method

attempts to remove signal redundancy that arises when the quantized signal levels do not occur with equal probability. For achieving the desired coding, it is desirable to know the statistics of the source. If the statistics are stationary and are known a priori, a nonadaptive encoding procedure can be specified. In many cases, however, the statistics are not well-known and/or the statistics of the measurement source may be nonstationary. In these conditions, a nonadaptive encoding procedure can result in a bandwidth expansion instead of reduction. To avoid this problem, adaptive encoding techniques can be devised where the code assignments are based on the most recent statistics measured by the encoder itself. The encoding is generally a reversible process. Some of the encoding techniques used in literature are [36, 37]: Gamma coding, Huffman coding, arithmetic coding, Exp-Golomb coding, Ziv-Lempel coding, etc. These techniques are commonly utilized in many compression methods at the final stage to further increase the compression efficiency.

1.4.1.2 Redundancy Reduction Techniques

Redundancy reduction is a technique for eliminating data samples which can be implemented by examining the preceding or succeeding samples or by comparing with arbitrary reference patterns [44]. Many techniques for redundancy reduction are possible: the polynomial predictors and interpolators, the exponentials and the sine waves. However, the polynomial predictors [45] and polynomial interpolators [45] are most effective and these are widely used. Some of the redundancy reduction techniques are zero order predictor (ZOP), first order predictor (FOP), higher order predictor, predictive coding [46, 47], zero order interpolator (ZOI), first order interpolator (FOI), third order polynomial interpolator and second difference [48–50]. A polynomial predictor is an algorithm that estimates the value of each new data sample based on the past performance of the data [44]. If the new value falls within the tolerance range of the estimated new value, it is rejected as redundant since it is known that the data value can be reconstructed within the specified tolerance or preset error. The specified tolerance may be a peak error or a mean square error for the approximation. The most efficient ZOP technique uses a floating aperture or step method wherein the tolerance corridor $\pm\varepsilon$ is centered around the last saved data point [45]. In general, the ZOP has proven to be very efficient for step-like data. The first-order predictor (FOP) uses the first-order extrapolation polynomial. The extrapolation equation is a straight line drawn between the past two sample points. The optimum linear predictor (LP) predicts the next sample point by using linear combinations of past samples. The optimum linear predictor uses a set of coefficients which minimizes the mean square error between the predicted and the actual value. Two methods of applying the optimum linear predictor for compression have been investigated. In the first method, the predicted value of the present data point is found using P previous actual sample data points. The difference between the predicted value and the actual value is then binary coded and transmitted. In the second method, an aperture is placed about the predicted value. An excellent review of the predictors and interpolators is reported in [44]. In predictive coding method [46], the transmitter and receiver predict the next sample value by using the stored past sample values. The transmitter transmits not the original

sample value but the difference between it and its predicted value. At the receiver this error term is added to the receiver prediction to reproduce the sample value. Cox et al. [47] reported a compact digital coding of the ECG signal. The second difference is employed to reduce the redundancy. Then, Huffman coding technique is used to code the frequent residuals and the fixed length coding used for infrequent residuals. Finally, bounds on average code word length are calculated. Pahlm et al. [48] studied the integer based predictors and the minimum mean square error (MMSE) predictors at varying sampling rates and digital resolutions for both the long-term ECG signals and the ECG signals recorded at rest condition. The residuals are obtained using the following 1st, 2nd and 3rd differences. In many cases, the MMSE predictors perform better than 2nd differences at the cost of increased complexity entailed in using MMSE prediction. Finally, it is concluded from the studies that the 2nd differences approach is superior at any sampling rate and digital resolution for resting ECG signals.

An effective prediction requires that the characteristics of the data remain relatively constant from one time interval to the next [45]. If the data are varying continuously in a random manner or if they are perturbed by high-frequency noise, the redundancy reduction efficiency of the predictor will generally be low for reasonable system accuracies. Examining such data indicates that a greater number of redundant samples could have been eliminated if both future and past data samples were used. The process of polynomial curve fitting to eliminate redundant data samples is termed interpolation. Low-order polynomial interpolators have been found to be very efficient in ECG data compression. The zero-order interpolator (ZOI) is similar to the ZOP in the sense that a horizontal line is used to represent the largest set of consecutive data samples within a prescribed peak-error tolerance. The first-order interpolator (FOI) (linear method) assumes that data will continue in the same direction (slope) once it has started. Instead of drawing a horizontal line as is the case in the zero-order method, a line is drawn to establish a slope. The third order polynomial interpolator algorithm [50] was employed in ECG data compression with seamless joints. The third order algorithm is a peak error controlled one. Every interpolated segment is reconstructed in such a way that the error between the original and the reconstructed waveforms will always be within a preset limit. This important point (IP) contains three information values: amplitude, time and slope. It compresses the ECG by a fraction of about 6.5:1 for 1% peak error (or about 9.7:1 for 2% peak error), and produces a seamless, smooth reconstructed signal. Most of the tolerance comparison direct ECG data compression techniques employ polynomial predictors and interpolators. These techniques attempt to reduce redundancy in a data sequence by examining a successive number of neighboring samples.

1.4.1.3 Adaptive Sampling Techniques

Adaptive sampling is a technique for adjusting the sampling rate of a given source to its information rate [44, 51]. Adaptive sampling allows the sampling rate to change according to the activity of the source. Because of the problems with uniform sampling for cardiac signal, the alternative of sampling at irregular intervals is intrinsically attractive. Signals are sampled more frequently during the transient periods and

less frequently otherwise. ECG signals are well suited for adaptive sampling since they are periodic and contain some segments of rapid and slow changes. The basic difference between adaptive sampling and redundancy reduction is that in adaptive sampling, the sampling rate of the original data waveform is varied while in redundancy reduction the waveform is initially sampled at a constant rate and nonessential samples are eliminated later [44]. In adaptive sampling, an output is provided only when the data change exceeds the predetermined tolerance. Adaptive sampling is attempted using the following algorithms: the voltage-triggered [52, 53], the two-point projection [52, 54], the second differences [48, 54], the amplitude zone time epoch coding (AZTEC) [55], the turning point (TP) [56], the coordinate reduction time encoding system (CORTES) [43], the scan along polygonal approximation (SAPA) [57], the fan [58–61], the adaptive AZTEC [62], the slope detection algorithm [63], the corner detection [64], the modified SAPA (MSAPA) [65], the combined SAPA (CSAPA) [65], the cubic-splines and SAPA (CUSAPA) [67–69], the improved adaptive AZTEC [70], etc. Each adaptive sampling method processes the closely spaced samples to select a smaller set of samples and their associated time values called permanent samples. All methods are based on the idea of replacing the sequence of transient samples by line segments and use at least one parameter, called 'ERR', to specify the degree of approximation to be allowed in replacing the transient samples by line segments [71–73]. Permanent sample and time values produced by each method are used to reconstruct the waveform. The reconstruction uses linear interpolation between the permanent samples. These techniques are based on the specified error tolerance comparison or significant point extraction. In general, higher value of the specified error threshold will result in higher CR and lower compressed signal quality and vice-versa [74]. An excellent review and summary of few statistical, redundancy reduction and adaptive sampling techniques can be found in [74]. Clinical evaluations of the AZTEC, TP and fan algorithms is presented in [75]. Some of the experimental results and the limitations of the techniques are presented here.

Several researchers have compared the performance of different adaptive sampling algorithms on previously measured cardiac signals. The step (voltage-triggered), two-point projection and fan methods are applied on normal, abnormal and noisy ECG signals [52]. The AZTEC [55] decomposes raw ECG samples into plateaus and slopes. The AZTEC provides a significant compression ratio but the reconstruction of the ECG signal is unacceptable for accurate analysis by the cardiologist. Because the AZTEC results in significant discontinuities (step-like) and distortion in the reconstruction of the P and T waves due to their slow varying slopes [74]. The reconstructed signals need postprocessing to produce smoothed signals. This least-squares (parabolic filter) technique produces a smoothed signal by finding the best polynomial fit to each set of seven sample points in the reconstructed signal [43]. This smoothing produces a new waveform with reduced noise and no discontinuities. But it introduces the loss of amplitudes of QRS peaks and valleys. The amplitude information is very important in some diagnoses such as ventricular hypertrophy. The AZTEC technique ECG signals with a compression ratios of 4:1 and 5:1 fairly reproduces QRS configuration. Reproduction of ST/T complexes is less satisfactory making less accurate calculation of a depression [75]. The TP algorithm [56] is based upon the notion that ECG signals are normally oversampled

at four or five times faster rate than the highest frequency component present. Thus, the TP algorithm is used for the purpose of reducing the sampling frequency of an ECG signal from 200 Hz to 100 Hz without diminishing the elevation of large amplitude QRS complexes. The TP method is simple but introduces the short term time distortion or the local time shifts due to the unequally spaced time intervals. The CORTES algorithm [43] is a hybrid of TP and AZTEC algorithms. The CORTES algorithm employs the idea of the AZTEC to discard clinically insignificant samples in the isoelectric region with a high CR and then applies the TP method to reduce the amount of data for the clinically significant high frequency regions [74]. The CORTES provides nearly as great data reduction as AZTEC with approximately the same small compression or reconstruction error as TP. The parabolic smoothing is applied only to the AZTEC portion of the CORTES signal to eliminate this distortion. The adaptive AZTEC algorithm [62] represents a modification of the AZTEC technique extended with several statistical parameters used to calculate the variable threshold. This algorithm calculates the statistical parameters (mean value (μ), standard deviation (σ) and third moment (M)) of the ECG signal which are used in on-line. The experimental results show that the noisy signals compressed by the adaptive AZTEC algorithm [62] are as good as the noise free signals but the compression ratio is poor. The compression ratio highly depends on the level of the noise. The corner detection algorithm [64], is an efficient algorithm which locates significant samples and at the same time encodes the linear segments between them using linear interpolation. It is used for real time ECG compression and the results are compared with the AZTEC algorithm. The performance evaluation shows that under the same bit rate, a considerable improvement of the signal to noise ratio (SNR) and root mean square error (RMSE) can be achieved by employing the corner algorithm. The improved modified AZTEC [62] is presented to amend the effectiveness of the adaptive AZTEC technique. The comparative study is carried out on fidelity of the reconstructed signals using the smoothing filters. The compression results of the modified AZTEC are improved by incorporating the following two steps: i) For the evaluation of the statistical parameters namely the mean, the standard deviation and the third moment for the next compression cycle, X_{max} and X_{min} values are initialized to the first sample of the segment under consideration after each plateau or slope. ii) The statistical parameters of previous segments are not considered for the evaluation of parameters of the next compression cycle. The least-squares polynomial smoothing filters are employed to produce smooth reconstruction. However, the smoothing technique may introduce the amplitude distortion.

The Fan is a technique of adaptive sampling that selects samples with an irregular temporal spacing that specifies each waveform with the minimum number of samples required for a given maximum error or tolerance ε [58–61]. It draws the longest possible line between the starting point and the ending point so that all intermediate samples are within the specified error ε. Since the Fan technique guarantees that the error is less than or equal to the preset error tolerance, it produces better signal fidelity under the same compression ratio. Three SAPA algorithms (SAPA-1, SAPA-2 and SAPA-3) are developed for real time ECG compression and their performances are compared with the AZTEC algorithm [57]. Although SAPA-3 achieves highest compression, it tends to smooth out Q-wave details. The theoretical basis of the SAPA

algorithm is that a good approximation to a curve is obtainable from the piecewise linear segments inside the corridor formed by a preset error tolerance [65]. A major disadvantage of the SAPA-2 algorithm is that three division operations are required for calculating the slopes. This problem is later solved in modified SAPA (MSAPA) algorithm. In MSAPA, the integer division was utilized instead of real division which may be rapidly performed using a table searching technique and which also decreases the number of comparisons required. Although the MSAPA algorithm achieves fast and efficient data compression by approximating original ECG signals by lines, it occasionally produces a loss of the P wave and ST segment [65]. This is solved in the combined SAPA (CSAPA) algorithm that combines MSAPA and TP algorithms. At first, CSAPA algorithm applies MSAPA to ECG signals while simultaneously detecting the R wave and S point. Once the S point is detected, TP is substituted for ECG data reduction until the end of the ST segment. The reconstruction procedures of MSAPA and CSAPA are similar to the SAPA-2 algorithm. The decompression of CSAPA is the same as the MSAPA algorithm except that the ST segment is recovered by a method similar to the TP algorithm. The two algorithms named as modified SAPA and combined SAPA are tested using the 15 different ECG signals including ischaemic episodes, tachycardia, inverse QRS complexes and powerline noise. A curve smoothing technique can also be utilized to smooth peak and valley points of the curve but its disadvantage is the introduction of amplitude distortion of the ECG waveform.

The cubic-spline is a very popular method presently used for data approximation, interpolation, curve fitting and smoothing. The spline approximation in ECG data compression was reported in [68]. Data compression is achieved using cubic splines by calculating the spline coefficients which will be used later on to reconstruct the original data. The number of spline coefficients is much less than the number of original data points. These coefficients are computed in such a way that the approximation error between the original and the new signal is minimum. Least-squares norms are used as a measure of closeness in calculating the coefficients. The CUSAPA combines the SAPA-1 algorithm and the cubic-splines piecewise polynomial approximation [67]. The algorithm applies the SAPA algorithm to the high-frequency portions of the ECG signal (i.e., the QRS complex) and the cubic-splines approximation to the lower-frequency segments (i.e., the S-Q segment). To ensure a low reconstruction error for the spline processed segments and to achieve fast compression, an attribute grammar is developed to locate the best initial spline knot locations. These initial locations are then used to determine the optimal locations and the corresponding spline coefficients. The selective application of either the SAPA or the cubic-spline algorithms requires the detection and isolation of the QRS segments. The CUSAPA algorithm produces the best reconstructed signal among all other techniques with superior noise reduction [67]. The disadvantage is the extended time needed for processing.

From the survey of above direct data compression methods, the following conclusions can be drawn. Many adaptive sampling techniques have been reported for the reduction of large amount of ECG data. It is observed that in all the methods, the threshold tolerance ε is applied to select the significant or permanent samples. Some of these techniques are sensitive to the sampling rate, the quantization step size, and the

noises and artifacts in the signal. However, the selection of tolerance is difficult for noisy ECG signals. Some of the methods use more than one parameters to achieve the desired data reduction. But the simultaneous selection and tuning of these parameters is difficult in the case of real time applications. Furthermore, in most of the methods, the compressed signal is obtained by interpolating the stored samples. Therefore, design of interpolation scheme without varying shape and duration features of the ECG signal is the practical problem in these methods. Although the direct time domain methods are simple to implement, they will produce a serious distortion at high compression ratios.

1.4.1.4 Parameter Extraction Compression Techniques

Parameter extraction is a technique that reduces the bandwidth required to transmit a given data sample by means of an information-describing irreversible transformation. The parameter extraction compression (PEC) techniques employ preprocessors to extract a set of parameters or features that are used to model the original signal. These parameters or features are quantized using the scalar and/or the vector quantizer and then some entropy coder is applied to increase the compression efficiency. The PEC techniques include the modeling schemes (Linear prediction models, vector quantization (VQ) models, neural and network models, etc.) and the extraction of ECG features (template matching, cycle-to-cycle, waveform partitioning (complex block, plain block), etc.) [76–92]. The PEC technique is based upon the notion that the ECG signal is generally composed of a number of beats repeated at fairly regular intervals. A number of researchers have attempted to exploit the intra-beat and inter-beat redundancies of the ECG signal with the use of the template matching and beat subtraction schemes. Many PEC techniques have employed some combination of the above schemes. These PEC techniques can roughly be divided into three categories.

1) Linear prediction (LP) based methods [77, 79, 82, 83]: Linear prediction techniques are used for the compression of ECG signals by exploiting the correlation between adjacent samples and the correlation between adjacent beats if the ECG signal has a quasi-periodic nature. In LP based methods, the n^{th} sample of a signal is predicted by its P past samples. Then, the error between the predicted and original samples is sent or stored instead of the original sample itself. The residual (error) signal is quantized using scalar or vector quantization and further compressed using the Huffman coding scheme. A compression can be achieved if the dynamic range of the error is less than that of the original signal. Since the poor quantization rule applied to the residual signal may introduce clinical distortion, the residual quantization size is an important parameter of the compression method. Note that the residual signal has the same number of samples as the original signal and thus the transmission rate is directly proportional to the number of bits used for a residual sample. The performance of the compression system may degrade if signal block contain noise which is difficult to avoid.

2) Vector quantization (VQ) based methods [85–89]: In VQ based methods, the input ECG signal is segmented directly into vectors uniformly with fixed length and then vector quantized. These VQ based methods focus on the utilization of the correlation among small segments of ECG signals. The VQ schemes

are also used to exploit the intra-channel correlation in the multichannel case. This correlation consists of both intra-beat correlation and inter-beat correlation. An ECG signal compression system based on VQ schemes has two parts: the encoder and the decoder. First, the codebook is generated by a training procedure and it can be updated according to the input vector. This codebook is available for both the encoder and the decoder. For a test input vector, the encoder finds a representative vector in the codebook such that the distortion can be very small. Each codevector is associated with a unique index. The index, rather than the codevector itself, is transmitted during the encoding process. A binary codeword (Huffman codeword) is assigned to each permissible vector template which is then transmitted. To obtain a reconstructed signal at the decoder, the index is served as a pointer to find the corresponding vector from the codebook. The goal of VQ methods is to produce the best possible reproduction vector for a given rate R with minimal distortion. However, a distortion criterion which represents a distance or error between the input vector and codevector should be subjectively relevant. The choice of distortion criterion permits us to quantify the performance of a VQ in a manner that can be computed and used in analysis and design optimization. For simplicity, squared error distortion criterion is employed in most of the VQ based methods.

3) Template matching (or Beat subtraction) methods: These methods include ECG beat segmentation, beat normalization, beat matching and subtraction and coding of residual signal. The residual signal is obtained by subtracting the detected ECG beat from the average beat (or the beat from the template database). The run-length and Huffman coding schemes are employed for the residual data or the differenced residual data and for the period of the ECG complex [76, 80, 84]. Note that compression performance of these methods depends on the repetition of the ECG beats, the endpoints detection and the updation of the beat templates. The residual template pattern library will be synchronously updated in both the encoder and decoder via a simple updating rule [84]. Note that the ECG signal can be regular and irregular in real time case [83]. Changes in the QRS complex can be efficiently handled in these compression systems.

Short term prediction (STP) and long term prediction (LTP) algorithms [79] are employed for compression of ECG signals. STP and LTP algorithms exploit the intra-beat correlation and inter-beat correlation, respectively. The complexity of the algorithm is fully loaded by the detection of ECG features, the template matching [84] and the encoding of its residual by a VQ. Zigel et al. [83] introduced ASEC algorithm used with defined weighted diagnostic distortion (WDD) [81] measure in order to efficiently encode every heartbeat, with minimum bit rate while maintaining a predetermined distortion level. The `mita` database is used to evaluate the compression algorithm and the results were compared with other known compression methods such as AZTEC [55] algorithm, SAPA-2 [57], and LTP [80]. A mean compression rate of approximately 100 bps (CR value of about 30:1) had been achieved with a good reconstructed signal quality (WDD below 4% and PRD below 9%). Two types of tests such as the quantitative (the PRD and the WDD) test and the qualitative (by mean opinion score (MOS) of cardiologists) test which includes the blind and semi-blind tests were performed for the evaluation. An accurate QRS detector invariant to different noise sources and varying morphologies is an important issue in these methods. Predictive coding does it by coding an error

term formed as the difference between the current sample and its prediction. These techniques are not optimal since the processed samples are still somehow correlated or dependent and mainly depends on accurate beat segmentation and end points of the ECG beats.

VQ algorithms are widely employed for compression of image and speech signals [40, 41]. These are extended to the ECG signal compression which employs VQ either directly on the samples or on its transformed coefficients. A novel ECG signal compression based on VQ for coding feature vector is reported in [85, 86]. In the mean shape vector quantization (MSVQ) and the gain shape vector quantization (GSVQ) based methods [87, 89], each block is preprocessed by subtracting its mean value and normalized by its dynamic range of the input. Then, the shape and the mean value are coded using VQ and scalar quantization. In most of the algorithms, a simple squared error distortion measure is used to select the codebook which varies with time varying PQRST complex morphologies. The selection of distortion measure is important in VQ based coding scheme [86]. Large training sequence is needed so that all the statistical properties of the PQRST complexes are captured. The performance of VQ algorithm depends crucially on the dimension, the codebook size, the choice of code vectors in the codebook and the distortion measure. Best compression results are obtained with VQ on scales with long duration and low dynamic range, and scalar quantization on scales of short duration and high dynamic range. Note that the usual duration of computer evaluated ECG records is 10 seconds [17]. Many VQ algorithms do not consider the difficulties such as the controversial issues of selecting a distortion measure and the creation, and updation of codebook in the encoder and decoder for continuous ECG signal transmission system.

Chena et al. [84] introduced an efficient data compression scheme for biomedical ECG and arterial pulse waveforms. This compression consisted of the following processes: the beat segmentation and normalization, two-stage pattern matching and template replenishing mechanism and the residual beat coding. Three different residual beat coding methods such as Huffman/run-length coding (method-1) Huffman/run-length coding in discrete cosine transform domain (method-2) and vector quantization (method-3) are employed. The coding performance in terms of CR versus PRD distortion measure was compared over other methods including the TP algorithm, the Fan algorithm, the AZTEC algorithm, the m-AZTEC algorithm and the CORTES algorithm for ECG data compression using the 20 files of ECG data sequence sampled at 300 samples per second and quantized at 16 bits per sample. It was concluded that method-3 is superior to both method-1 and method-2.

In [76, 79, 80, 82–84], each ECG beat is treated as a separated vector. These methods utilize the correlation between adjacent samples and the correlation between adjacent beats to achieve low bit rate at the cost increased computational time. The methods require that the endpoints detection of each ECG beat be determined prior to the compression phase that is a difficult task under noisy conditions. The accurate beat segmentation, beat normalization and beat replenishing schemes maximize the correlation between the current and previous beats or the current and beat pattern available in the template database. The processing stage before compression phase provides a better choice of similar beat vector from the template database, or

results in residual signal with lesser dynamic range. Template matching is done using a simple normalized correlation coefficient (NCC) criterion. The template assigned to be subtracted from the current beat vector will be the one with the largest value of NCC. However, as will be demonstrated, the presence of some degree of noise diminishes the NCC as a measure of similarity in real time case. Two stage pattern matchings such as beat vector matching and residual vector matching are employed to reduce bit rate. Finally the authors concluded that it is not very suitable to irregular ECG signals, such as drastically varying pattern shape [84]. Therefore, the algorithm for irregular signal, such as ventricular fibrillation (VF) and ventricular tachycardia (VT) detection and compression is needed and is discussed in [83]. The compression system is more computationally complex than most of the reported ECG compression algorithms. It includes the following stages regularity detection, beat segmentation, period estimation and beat normalization, beat pattern matching and subtraction, residual pattern matching, residual coding, side information coding, updating algorithms according to the beat morphology variations, and the irregular signal compression algorithm.

1.4.2 Frequency Domain Compression Methods

Another class of lossy techniques employs the concept of transformation in which data are compressed in some other domain, such as frequency domain, instead of time domain [93, 94]. It is derived from the fact that transforms of the ECG signal possess the features of energy preservation, energy compaction, and decorrelation [95, 96]. In FDC method, the rationale is to efficiently represent a given data sequence by a set of transform coefficients. The FDC methods include the Karhunen-Loeve transform (KLT) [95–97], the Walsh transform [98–102], the Fourier transform (FT) [103–105], the discrete cosine transform (DCT) [106–110], the discrete Legendre transform (DLT) [112–114], the optimally warped transform (OWT) [113], and the subband coding (SBC) [115–121]. A brief outline of the transform compression systems is presented and then limitations of these systems are described. These compression methods generally consist of the following steps: the preprocessing, the transformation, the thresholding or/and quantization scheme(s), and the entropy coding of the quantized indexes and side information. The purpose of the transformation is to convert the signal block into a transform coefficients vector. Typically, the adjacent samples of the signal block are correlated and the transformation tries to decorrelate the signal samples and also to pack the signal energy in a few transform coefficients. Then, the nonzero transform coefficients of the thresholded vector can be optimally quantized by choosing the scalar and vector quantization schemes based on system complexity requirements. In general, the nonzero transform coefficients are referred as significant coefficients whilst zero coefficients are referred as insignificant coefficients which may be due to noise components. In some methods, the quantization is performed directly on transform coefficients without applying the thresholding process. Finally, the reconstructed signal can be obtained by applying the inverse transform to the quantized nonzero transform coefficients. The variance criterion [93] and quality control criterion [97] are used to retain transform coefficients for reconstruction of the ECG signal. The retained transform coefficients are transmitted or stored using fixed number of bits per coefficients. Finally

the Huffman and arithmetic codings can be used for further compression. Note that in transform based compression methods it is vital to select the transform so that it can represent the maximum amount of signal energy with the minimum number of transform coefficients [96]. The experimental results of some of the transform based ECG signal compression methods are presented here.

Ahmed et al. [93] tested the performances of the KLT, the DCT, the Haar transform (HT) and the identity transform (IT) using the variance criterion. The motivation for considering the suboptimal transforms is that the computational problems associated with the calculation of KLT basis functions cause it to be impractical for large values of N [94]. The HT and the DCT are considered and their performance are evaluated for ECG data compression. The basis vectors for the HT are sampled rectangular waves whilst those for the DCT are sampled sinusoids. The MSE estimate for the DCT comes closest to that of the KLT. For a given number of transform coefficients the MSE of the DCT approach is smaller and larger than the MSE of the HT and the KLT approaches, respectively. Feasibility of using a fast Walsh transform algorithm for real-time microprocessor based ECG data-compression system has been investigated [98]. The FFT based method requires $N\log_2 N$ complex multiplications whereas the fast Walsh transform of the ECG signal can be computed using $N\log_2 N$ additions and subtractions. Walsh spectrum of a typical ECG shows an exponentially decaying energy content with increasing spectral index. Therefore, Berti et al. [100] suggested the logarithmic quantization of the expansion-coefficient amplitudes in addition to an exponential decrement of the number of quantization levels. For a spectral reduction of 2:1, the method reached a CR of 3.05:1 with a very low MSE of 0.011 without the filter and 0.0025 with the filter. The superiority of the double logarithmic quantization scheme [100] compared to the existing logarithmic and linear techniques has been proved experimentally. Reddy et al. [103] presented Fourier descriptors (FD's) for ECG data compression. Two-lead ECG data are segmented into QRS complexes and S-Q intervals. The magnitudes of Fourier descriptors decrease rapidly for higher harmonics. While compression ratios of 10:1 are feasible for the S-Q interval, the clinical information requirements limited this ratio to 3:1 for the QRS complex. Nashash [104] proposed a method that relied on modeling quasi-periodic ECG signals by a set of time-varying Fourier coefficients. A higher CR with lower heart rates and a lower CR with higher heart rates can be obtained. Philips and Jonghe [112] have discussed a compression method based on the approximation of the ECG signal by higher-order polynomial expansions. The variable coding method is applied to reduce the correlation between the coefficients of the two intervals. For the same value of PE, the compression ratio of the DCT is only half of CR of the PT. The dip in the negative portion of the QRS complex disappears in the DCT reconstruction. However, the signals reconstructed by the DLT based method often suffer from ringing or Gibbs-effects. The DCT and DLT are sensitive to errors in QRS detection. Since the local bandwidth of an ECG signal is not definitely constant, the DCT cannot be optimal for ECG compression [113]. Philips [113] presented the adaptive compression for ECG signal using the OWT based method. The ECG records employed in [112] are used for the comparison of the DCT, DLT, and OWT performance. The error of the DLT based method is larger than the OWT based method error especially near the QRS

complexes. The results presented in this paper demonstrated the benefits of the OWT based method for ECG compression. But, the OWT based method requires more computation than the fixed transform schemes: approximately $7n_\alpha NL$ multiplications and $5n_\alpha NL$ additions are required in each iterations, where L is the number of data points, n_α is the number of step size and the N is the approximation order. Sine the OWT behaves like an adaptive filter, it guarantees both an accurate reconstruction of the QRS complexes and a maximal noise removal. Alberto and Antonio [114] presented an ECG compression scheme (variable bit rate rate fixed quality) based on the method proposed by Philips [112]. For medical analysis it is more interesting to reduce the compression ratio locally with an accurate representation of the original signal. The use of variable length discrete Legendre polynomials, a nonuniform quantizer and variable length Huffman technique improves the performance of the basic Philips coder [112].

Batista et al. [109] presented an ECG compressor based on optimized quantization of DCT coefficients. The ECG signal is partitioned in blocks of fixed size, and each DCT block is quantized using a quantization b vector and a threshold T vector that are specifically defined for each signal. These vectors are obtained so that the estimated entropy is minimized for a given distortion. The quantized coefficients are coded by an arithmetic coder. The PRD criterion is adopted as a measure of the distortion introduced by the compressor. Tests are carried out using the 2-minute sections of all 96 records of the `mita` database. For different PRD values, the corresponding CRs are computed, and an average CR of 9.3:1 is achieved for PRD equal to 2.5%. The authors concluded that the proposed method is compared favorably with the other compressors, producing considerably smaller PRD for a given CR. The significant gains in CR is achieved using different optimized b and T vectors for different signal blocks. It is observed that when block size increases CR increases for a given distortion, but it also increases the computation time. Thus, the decision about block size is fundamentally open. An average CR of 9.3:1 is achieved for a PRD value equal to 2.5% for an ECG compressor based on optimized quantization of DCT coefficients [109]. Borsali et al. [110] proposed an ECG compression method combining two approaches viz the ECG beat alignment and the polynomial modeling. The QRS complexes are first detected and then aligned in order to reduce high frequency changes from beat to beat. The complexity of the method is high since the method is a combination of two approaches. Alen and Belina [106] discussed the implementation of DCT based compression routines for ECG. The average value and the width of each band are calculated and the coefficients are approximated using uniform quantization. It is concluded that the overall suitability of the DCT in ECG signal compression method is enhanced by the basic algorithm which allows the dynamic allocation and subband thresholding. Madhukar and Murthy [108] presented a compression algorithm based on the parametric modeling of the discrete cosine transformed single lead ECG signal. A maximum compression ratio of 40:1 is achieved with normalized root mean squared error (NRMSE) in the range of 5% to 8%. Benzid et al. [111] presented a constrained ECG compression algorithm using the block-based DCT and considers the PRD as a controlled quality criterion. The adaptive linear quantization strategy is employed for the nonzero DCT coefficients and then the arithmetic coder is used for further compression of the quantized nonzero

coefficients. The authors have been motivated for the use of PRD as a controlled quality criterion in their works due to its widely employed quality measure and its low cost computational time [111]. One difficulty with squared error distortion criterion is that although the global error over a signal block contained more number of beats may be small, the error for an individual beat, or portion of a beat, may be large in general case [97]. Thus, the signal compression must be realized essentially without loss of the diagnostic features necessary for a physician to interpret the ECG. Note that the effect of signal compression with respect to ECG's has substantial implications [93]. In order to ensure that compressed signals can be properly used for clinical evaluation, the quality control criterion such as relative mean square errors ξ_s for each block $s = 1, 2$ and 3 (for blocks are $\widehat{\text{PQ}}$, $\widehat{\text{QRS}}$ and $\widehat{\text{ST}}$, respectively) is employed locally for each ECG beat.

Another way to eliminate the correlation of ECG signal is to decompose it in the frequency domain into several bands such that the data from each subband contain poorly correlated data. This is the basic concept of subband coding, an interesting approach is subband coding that is inspired by speech processing. As the lower band signals contain most of the spectrum energy, a larger number of bits are allocated to these subband signals. The subband signals from the higher bands contain noise-like signals which are not vital to our later reconstruction and therefore are encoded with less bits. The sub-band splitting is performed by an analysis filter bank. Reconstruction of the decoded signal is performed by a synthesis filter bank operating on the sub-band signals derived from their bit efficient representation. In general, the sub-band coding system consists of two basic components: i) the analysis/synthesis subsystem and ii) the coding subsystem. Naturally, both components must be carefully designed to achieve good performance. Tai [115] presented a six-band sub-band coder for encoding of the ECG signal. The frequency band decomposition is performed by means of quadrature mirror filters (QMF). The results show an average SNR of 29.97 dB and average bit rate of 0.81 bits per sample. In another work, the ECG signal is decomposed into four subsignals using a QMF bank in a tree structured fashion and the resulting stages of the tree are decimated by a factor of two [116]. In this method the subsignal with the lowest frequency content is encoded by using a DCT based compression scheme and the other subsignals are quantized using deadzone quantizers. The resulting data are coded using runlength coding of zero valued samples and pulse code modulation with variable length coding of the nonzero samples. Compression ratios as high as 5.7:1 is obtained with a PRD=7.0%. The performance is also tested with filtered ECG signal. A low-pass filter with a cutoff frequency of 125 Hz is used which results in a CR and PRD of 5.3:1 and 2.9%, respectively. It is observed that the PRD measure is sensitive to smoothing of background noise. Both finite impulse response (FIR) and infinite impulse response (IIR) filter banks are considered as main components in a sub-band coding system [118]. This system can provide compression ratios between 5:1 and 15:1 without loss of clinical information. Ramakrishnan and Saha [119] presented a compression technique for single channel ECG based on the automatic QRS detection, period and amplitude normalization (PAN), and vector quantization of the PAN beats. The period normalization is done by multirate processing. The codebook obtained is made available both at the encoder and at the decoder. This technique achieves high compression ratios of

100 to 200. The disadvantages of the technique are that it requires a codebook a priori and also high coding time compared to other techniques such as AZTEC, SAPA, etc [119]. Finally, the authors recommended it for off-line applications only. Blanco et al. [120] presented a low complexity algorithm using the nearly perfect reconstruction cosine-modulated filter bank technique (N-PR CMFB) with 16 channels and filter length 192 for ECG data compression. It applies subband decomposition to ECG signal block without QRS detection and ECG beat segmentation. Thus, the algorithm implemented in this work is extremely easy. Then, the thresholding technique with threshold T based on the target PRD value is applied in order to obtain a good degree of compression. The algorithm begins by fixing an initial T, which is the same for all subbands, to check the target PRD value. If it is not reached, a new T is chosen iterating the previous step until the predetermined accuracy limit is reached. In the entropy coder stage, the non-discarded samples are coded with the original precision (16 bits) and Then the number of consecutive zeros is coded with different precision by run-length coding procedure reported in this work. Since the segment cannot be too long due to the delay and the buffer size, the maximum segment length of 4096 samples, which is equivalent to 11.38 seconds is considered. This technique always provides the best degree of compression, particularly when a small predefined PRD value of 0.5% is requested. The computational complexity of the N-PR CMFB is less compared to other subband decomposition techniques. Although objective is the quality of compressed signal, the PRD as a performance measure is not sufficient to decide whether the retrieved signal is suitable or not [120]. In [121], ECG compression with retrieved quality guaranteed is presented which utilizes the 191-order 16-channel N-PR CMFB technique [120] to split the incoming signals into several subband signals, thresholding of the subband signals based on the target PRD value and finally, both the significant coefficients and significance map are encoded using the Huffman coder. Since the method does not require any a priori signal information, and can thus be applied to any ECG, it is computationally simple, enabling real time implementation [121].

Among the transforms, the KLT is the optimum transform in the sense that the least number of basis functions is required for random signal representation with respect to the mean square error criterion. Although KLT approach is shown to provide a high compression ratio, the computational time needed to calculate the KLT basis functions is very intensive [74, 97]. Therefore, the suboptimum transforms with fast algorithms are popular for ECG signal compression. In [97], to improve computational efficiency of the KLT based method, each ECG beat is first divided into three consecutive blocks $\widehat{\text{PQ}}$, $\widehat{\text{QRS}}$ and $\widehat{\text{ST}}$ which can be approximately associated with the atrial activation, ventricular activation and ventricular repolarization, respectively. Then, the multirate sampling stradegy is used for downsampling the resulting blocks with the sampling rates estimated from the spectral density function (SDF). The average CR over the `mita` database for the variance criterion with 0.98 is CR$\approx$53, while the same for the quality control criterion with 0.15 is C$\approx$32. This can be improved by using optimal quantizer. Typically, the quality control criterion provided a lower average CR compared to variance criterion over each 10-min ECG segment meanwhile the quality of the compressed signal based on the variance criterion is poor [97]. However, the compression efficiency

of this method depends on the performance of the preprocessing techniques used for blocks separation and downsampling, and the postprocessing techniques employed at the reconstruction. The block separation technique demands prior study of the spectral densities of the structural components and the duration interval of the components. The goal of transform based method is to reduce the bit rate significantly while keeping signal distortion at a clinically acceptable level. Data compression systems have a general tradeoff between distortion (or quality) and rate. An increase of the number of basis functions in the transform representation reduces distortion. Many efficient transform methods produce smooth compressed signals. Consequently, these methods may give compressed signals with insignificant errors (or irrelevant information loss). Squared error distortion criterion such as the MSE and the PRD criteria is widely used to quantify error between the original and reconstructed signals. Note that the `mita` database widely used, contains the records with some degree of powerline interference and with varying levels of noise and other artifacts. When the signal plus noise information are compressed, most of the noise in the original recordings gets filtered during compression. If the MSE/PRD is employed to measure error between the reconstruction and the noisy signal then high values of MSE/PRD can be obtained due to the presence of the noise [96]. Thus, high PRD values do not always represent the actual distortion between the original signal and smoothed reconstructed signals since a significant fraction of the error is directly attributable to noise filtering. This effect is also true for quality controlled compression method reported in [97] which employs relative MSE criterion locally to controlling quality of reconstruction of the blocks ($\widehat{\text{PQ}}$, $\widehat{\text{QRS}}$ and $\widehat{\text{ST}}$). Moreover, the quality control criterion with same tolerance is employed for different clinical content of the blocks. This may degrade the quality of the small structured components of the ECG signal. In recent years, wavelet and wavelet packet transforms can be efficiently implemented and thus wavelets have been applied extensively to the nonstationary characteristics of ECG signal processing applications such as denoising, feature extraction, particularly data compression [122–125]. More details of wavelet transform based ECG data compression can be found in [123].

1.4.3 Wavelet Transform Based ECG Compression Methods

Unlike the harmonic base functions of the Fourier analysis, which are precisely localized in frequency but infinitely extend in time, the wavelet transform (WT) has good localization in both frequency and time domains, having fine frequency resolution and coarse time resolutions at lower frequency, and coarse frequency resolution and fine time resolution at higher frequency. Since this matches the characteristic of most signals, it makes the wavelet transform with new classes of basis functions suitable for time-frequency analysis. The WT has several attractive properties that make it natural for processing of the ECG signal, which is characterized by local waves such as QRS complexes, P, T waves and etc. with different frequency contents, with noises and artifacts. The primary properties of the WT are *Locality*, *Multiresolution*, *Energy compaction (or Compression)* and *Easy implementation*. The locality and multiresolution properties jointly enable the WT to efficiently match a wide range of signal characteristics, from high frequency components

to slowly varying (low frequency) components. This can be effectively used for feature extraction of nonstationary ECG signals. The WT ability to match a wide variety of signals leads to the compression property. Moreover, the computational time is significantly less since the algorithm involves the use of discrete WT (DWT) in a multiresolution framework. As a result of these properties, ECG signal modeling and processing methods based in the wavelet domain are, in many cases, much more effective than classical time domain or frequency domain approaches. The WT technique is used as a first stage of a lossy compression method for efficient coding of the ECG signals by preserving feature coefficients integrity and removing redundancy to achieve higher compression with controlled distortion in compressed signal. The principle of WT involves the hierarchical decomposition of an original ECG signal into a series of successively lower resolution signals. At each resolution level, the wavelet coefficients corresponding to a particular local wave is larger than those that do not correspond to the waves. Therefore, wavelet coefficients related to the interested local contents are kept, while discarding others that are unrelated to the ECG signal characteristics. Then, resulting quantized wavelet coefficients are more effectively compressed by a lossless coder such as run-length, LZW, Huffman and arithmetic coding schemes. In this way, the amount of stored or transmitted data can be effectively reduced. From the compressed data, the original signal may be reconstructed with very little loss of information. The performance of the wavelet based method depends on the mother wavelet, length of the wavelet filters, number of decomposition levels, thresholding and quantization approaches to wavelet coefficients and coding of significance map.

The WT based methods outperform the traditional time domain and frequency domain methods [127]. In literature, WT based methods consist of following stages: preprocessing (QRS detection, PQRST complexes separation, mean removal (MR) and amplitude normalization (AN), period normalization (PN)), the DWT and encoding of wavelet coefficients. Based on the encoding of the coefficients, these methods are grouped into three categories: *i*) threshold methods [126–143], *ii*) embedded coding methods [144–149], *iii*) vector quantization (VQ) methods [150–154]. In literature, the hybrid compression (HC) methods for ECG signal are reported with some combination of the coding algorithms that result in good compression performance with the cost of increased time and space complexity. These methods are suitable for offline processing for the acceptable distortion level provided by the clinician. A detailed review of the wavelet based ECG compression methods is presented in the next chapter.

1.4.4 Two-Dimensional ECG Compression Methods

In two-dimensional ECG compression algorithms, 2-D transformation is applied on 2-D representation of 1-D ECG signals to improve the compression efficiency [154, 155]. The concepts employed in 2-D ECG compression methods are shown in Table 1.3. In literature, 2-D ECG compression methods CAB+2-D DCT [155], 2-D wavelet packet transform (WPT) [156], 2-D DCT [157], truncated singular value decomposition (TSVD) [158], JPEG2000 [159], CAB and modified SPIHT [160] and JPEG2000 coding for ECG with irregular periods [161] exploit both sample-to-sample and beat-to-beat correlation. These methods

Table 1.3: 2-D ECG compression methods

Method	QRS detection	PN	AN	MR	PS	Block/ Frame	Transform	Coefficient coding
Lee [155]	Yes, BPF	No	No	No	No	Block	CAB and 2-D DCT	Uniform quantization (UQ) and run-length coding
Moghaddan [156]	Yes, BPF	Yes	Yes	No	No	Frame	WPT, db4/sym4	Saving largest WPT coefficients and corresponding indexes
Uyar [157]	Yes, DWT	No	No	Yes	No	Frame	2-DCT	UQ with zonal coding and Huffman coding
Wei [158]	Yes	Yes	No	Yes	No	Frame	SVD	Uniform quantization
Bilgin [159]	Yes	Yes	No	No	No	Frame	DWT (9/7-tap, J=5)	JPEG2000 and Differential Coding
Tai [160]	Yes, DF	No	No	No	No	Block	DWT (db8, J=3)	CAB and Modified SPIHT
Chou-M1 [161]	Yes	No	No	No	Yes	Frame	DWT	JPEG2000
Chou-M2 [161]	Yes	Yes	No	No	Yes	Frame	(9/7-tap, J=5)	
Wang [154]	Yes, DWT	Yes	No	No	No	Block	DWT (9/7-tap, J=3)	VQ with DCCR and DPCM

BPF: bandpass filtering; DF: digital filtering; Frame indicates entire aligned beats

consist of the following steps: 1) preprocessing (QRS detection, period normalization (PN), amplitude normalization (AN), mean removal (MR), period sorting (PS)) for construction of 2-D array, 2) 2-D transformation (DCT, DWT, SVD, etc.), and 3) encoding. These algorithms result in high compression ratio with low reconstruction or compression error by exploiting inter sample and inter-beat correlation. The performance of the 2-D compression algorithm depends on the QRS detection which may be affected due to various noises and time varying ECG morphologies. It requires high time and space complexity for the algorithms employed in preprocessing stage. For example, if one frame includes 600 seconds of ECG samples, the latency will be at least 10 minutes [161]. Many algorithms do not mention the dimension of the array, $M \times N$ for real time implementation where M and N are the number of beats/cycle and the number of samples within the cycle, respectively. The 2-D compression method is suitable for offline processing. The performance of the 2-D compression method can be degraded if the quasi periodicity is not satisfied.

Since the length of each beat is different, an appropriate algorithm is needed to align the beats for maximizing the beat to beat correlation. The sampling rate [156], zero padding [155], [160], [154] and cubic spline interpolation [159] algorithms are employed for a given maximum/mean beat length. The 2-D array with $M \times N$ is constructed where M is the number of beats and N is the number of samples in the aligned beats. Then the constructed 2-D array is sliced into blocks for 2-D transformation. In some methods, the transformation is directly performed on 2-D array. The transformed coefficients are coded using the image coders. The additional information such as maximum amplitude and the beat length are coded using differencing. In 2-D WPT [156], maximum keeping algorithm saves the largest values in WPT

coefficients along with the corresponding indexes required for decoding. It can be predicted that better results are achievable by preserving all transform coefficients and applying vector quantization or dynamic bit allocation algorithms to different space frequency regions in 2-D wavelet domain [156]. Wang and Meng [154] presented a 2-D ECG compression algorithm based on wavelet transform and vector quantization. A theoretical introduction to the use of two-dimensional (2-D) coding techniques for the particular case of electrocardiogram (ECG) signals is presented [162]. It is clearly concluded that an error in the estimation of the period of the ECG signal has little influence on the behavior of the system. These compression methods result in high compression ratio with low reconstruction error by exploiting inter sample and inter-beat correlation. The compression performance degrades if the quasi periodicity is not well satisfied. Small local waves distortions may be introduced and these local distortions cannot be reflected by PRD measure. The distortion and compression ratio can be calculated either for each ECG beats or for the entire aligned beats. If calculated for the entire aligned beats, the resultant PRD value will be small due to the normalization by the large energy value. Furthermore, every segment in the PQRST complex has a different diagnostic meaning and significance. A given distortion in one segment does not necessarily have the same weight as the same distortion in another segment. The issues related to compression performance measures are not addressed estimating the local distortions and memory requirements. It requires high time and space complexity for the algorithms employed in preprocessing stage. For example, if one frame includes 600 seconds of ECG samples, the latency will be at least 10 minutes [161]. Many algorithms do not mention the dimensions of the array, $M \times N$ for real time implementation where M and N are the number beats/cylce and the number of samples within each cycle, respectively. Regarding the matrix size and block size, as expected, the bigger the matrix size, the higher the coding efficiency of the system, although the fact that the overall coding delay and its enhanced complexity must be also be taken into account [162]. In many 2-D compression methods, the effect of smoothing of background noise is shown [158, 160]. The effect of noise removal i.e., the amount of noise removed by compression filtering may not be same for all testing records conditions. Under this situation, the comparison of the method with other methods or the compression results provided with the use of PRD measure are not significant for real time applications.

1.4.5 Quality Controlled ECG Compression Methods

Main goal of any compression method is either to control the data rate or the quality of the compressed signal by automatically adjusting the coding parameters. If the quality of a compressed ECG signal is not guaranteed, the compression process itself will become less useful [129]. Since the quality is indispensable for diagnosis, some ECG compression methods attempt to control its compressed quality using some squared error distortion criterion. In this section, we discuss different approaches of the quality controlled ECG compression methods, and illustrate the advantages and disadvantages of those approaches.

Nagarajan et al. [127] selected the best wavelet packet basis that minimizes the number of bits needed to represent the ECG, subject to the constraint that the PRD is always within an apriori bound PRD_b . Such

constrained minimization problem is in rate-distortion theory. This bound is based on the initial performance of the compression method and could be defined by the clinician after correlating the information contained in the compressed signal and the resulting PRD. However, ensemble averages do not ensure capturing clinically relevant features in the PQ, QRS and ST portions, since each portion makes widely differing contributions to the variance [97]. Blanchett et al. presented a KLT-based quality controlled compression (KLT+QCC) of ECG in which beat-by-beat quality controlled criterion is shown to be necessary to ensure clinically adequate reconstruction of each beat [97]. The KLT+QCC method employed the relative mean square error (rMSE) as a quality measure and the number of retained transformed coefficients is chosen such that the rMSEs for each block (PQ, QRS and ST) is less than or equal to a prespecified tolerance. The noise filtering is demonstrated during sampling rate conversion of PQ, ST and QRS blocks. Thus, the quality control criterion may provide a lower CR over noisy PQ, ST and QRS blocks. Chen and Itoh [129] presented a compression method guaranteeing desired signal quality (GDQ) [129] based on discrete orthonormal wavelet transform (DOWT) and an adaptive quantization strategy, by which a user specified PRD of the reproduced ECG segments is guaranteed at high compression ratio (CR). The authors observed that if the same PRD value is specified for a noiseless block and the noisy one, the CR obtained for the noisy block will be lower than that of the noiseless block because a smaller quantization bin size is used for the noisy signal and this will spend extra bits on approximating the noise with the specified accuracy. Although noise elimination process is used prior to the compression process, the filtering algorithm may degrade the quality of the signal, and there exists a practical difficulty in measuring the quality of the denoised signal. Moreover, the PRD and other similar error measures have many disadvantages, which result in poor diagnostic relevance [83]. In [129] the weighted PRD is suggested to characterize the distortion of the selected local waves. However, an open problem on the this criterion is how to determine the weights for each local wave viz. P, Q, QRS, etc.

Zigel et al. [83] presented an analysis by synthesis ECG compressor (ASEC) algorithm based on analysis by synthesis coding, and consists of a beat codebook, long and short-term predictors, and an adaptive residual quantizer. The compression algorithm uses a defined weighted diagnostic distortion (WDD) measure in order to efficiently encode every heartbeat, with minimum bit rate, while maintaining a predetermined distortion level. However, the ASEC algorithm attempts to minimize a different metric called weighted diagnostic distortion, which is claimed to be better matched to diagnostic distortion than PRD, but requires complex parameter extraction to calculate, as is done within the ASEC procedure [145], [151].

Miaou and Yen proposed a quality driven gold washing adaptive vector quantization (QDQW+AVQ) for the wavelet based ECG compression [151] where multiple distortion thresholds (*dth*'s) are automatically adjusted according to a user-specified reconstruction quality (desired PRD). Later, Miaou and Lin proposed a wavelet-based quality-on-demand algorithm for the compression of ECG signal [146] using a set partitioning in hierarchical tree (SPIHT) in which the resulting PRD falls within the preset bound of the desired PRD. Note that PRD may not be a good measure of clinical acceptability of the compressed sig-

nal [151]. Moreover, Lu et al. ([145], 2000) notice, in their evaluation of the quality of compressed signal, that the chief effect of wavelet compression is the smoothing of the low-level background noise. Although the compression error of SPIHT (in PRD) is larger, the clinical features of the compressed signal appear to be faithfully preserved. Blanco et al. developed a filter bank based algorithm for ECG compression with retrieved quality guaranteed (RQG) where the threshold is chosen so that the quality of the retrieved signal is guaranteed. A target PRD (PRD_{target}) is established a priori to control the quality of the reconstruction. Tests are carried out using noisy ECG records from the `mita` database and the PRD criterion to evaluate the quality of the retrieved signal. In RQG [121], it is considered from Ref. [83] that for the `mita` database, the compressed signal with PRD1 (computed with zero mean original signal block) values under 9% represent good, or very good, results, whereas if the value is greater than 9% its quality group cannot be determined. One can argue that these are not valid assumptions with the use of global error criteria since the noise filtering capability and distortion of the local waves are dissimilar across the lossy compression methods. Thus, it should be noted that the use of optimum thresholding where threshold value is obtained from noise characteristics can provide a better rate-distortion performance [125].

Alesanco et al. [139] presented a new real-time ECG coding scheme compatible with packetized telecardiology applications. The compression scheme contains the preprocessing stage (baseline removal, QRS detection, Beat segmentation and noise measure), template matching, wavelet transform, coefficient selection based on rate or RMS error, adaptive pulse code modulation and Huffman coding schemes. The threshold is selected according to the noise power estimated in the preprocessing stage. Noise power in each beat is estimated as the power remaining after high-pass filtering (cutoff frequency equal to 20 Hz) in the repolarization interval. The threshold automatically updated according to the measured noise level avoids spending bit rate for noise coding. However, measurement of noise power of ECG beats with time varying characteristics may be difficult with the use of high-pass filter because there are many sources of noise such as power line interference, muscle contraction noise, poor electrode contact and baseline wandering due to respiration, having different frequency characteristics, in a clinical environment. Later, Alesanco and Garcí [149] presented a simple method for guaranteeing ECG quality in real-time wavelet lossy coding based on the SPIHT algorithm and WWPRD measure. The effect of ECG baseline artifacts in compression performance is discussed and the artifacts are removed before the compression phase. But noise measurement criterion may be difficult to incorporate in well designed SPIHT strategy which codes the wavelet coefficients by exploiting the redundancies among wavelet subbands. Thus, noise degrades compression performance of the SPIHT coder. In conclusion [149], in order to avoid the effect of noise coding, an adaptive approach that varies the threshold should be used. However, this may not be a remedy for quality controlled SPIHT coding strategy.

Blanco et al. [142] developed a simple wavelet packets feasibility study for the design of an ECG compressor (WPFDEC) scheme where the same thresholding and entropy coding schemes utilizing the PRD as the target to terminate compression is adopted. The compression performance of the WPFDEC is compared

with the SPIHT and filter-bank methods. Benzid et. al [143] proposed an ECG compression method based on the adaptive wavelet coefficients quantization combined to a modified two-role encoder (ALQ-TRE). The resulting wavelet coefficients are thresholded iteratively until a user-specified PRD is matched using the iterative algorithm given in [121]. Then, the compression performance of this method was compared with the filter-banks [121] and SPIHT [145] based methods. The authors concluded that the compression performance of the ALQ-TRE method is better than the filter-banks [121] and SPIHT [145] based methods. Benzid et. al ([111], 2008) proposed a constrained ECG compression algorithm using the block-based discrete cosine transform (DCT). It employed the block-based DCT, the adaptive quantization, the look-up table and the arithmetic coding. The iterative algorithm employed as similar to [121] considers the PRD as a controlled quality criterion. The experiments are carried out using the 2-min of data (each) from the `mita` records 100, 101, 102, 103, 107, 109, 111, 115, 117, 118 and 119. The authors reported that the method presents a high compression performance than the filter-banks [121] and SPIHT [145] based methods. Many ECG compression methods show and illustrate the effect of smoothing of background noise [126, 134, 145, 158, 160]. The well designed compression method may fast remove the wavelet coefficients due to high-frequency noises dominated in higher subbands for data compression. Thus, the effect of noise removal, the amount of noise removed by compression filtering, may not be similar for every method and testing record. Under this situation, the comparison of the compression methods or the compression results provided with the usage of PRD measure are not significant for real time applications. The employment of the PRD measure in evaluating ECG compression methods has no practical value [74]. The above facts have motivated a great deal of research on objective quality measure based on weighted distortion criterion approach. Recently, a wavelet based weighted PRD (WWPRD) [190] measure is reported that provides a local or subband error estimation, with weights equal to the normalized absolute sum of wavelet coefficients in the corresponding subbands. However, local PRD value of insignificant errors in higher subbands dominates a global PRD value while local PRD value of significant errors in other subbands may not reflect any contribution to the global PRD. This may lead to confusion in the judgement of the quality of the compressed signal. Thus, WWPRD criterion does not provide an optimal coding parameters set in a rate-distortion optimization procedure for a given quality specification. The effectiveness of the quality criteria are investigated thoroughly and their disadvantages are described in next Chapter.

1.5 Phonocardiogram Signal Compression Methods

A PCG recorded for several minutes using monitoring instruments can produce several hundred megabytes of data. As a result, the volume of the data increases significantly, which leads to high cost in storing and transmitting such PCG data. Therefore, it is necessary to develop an effective lossy compression method which has the capability to reduce the volume of data necessary for storing and to speed up the transmitted data for wireless telemedicine applications [23, 25, 27, 32, 34].

Table 1.4: Methodologies employed for wavelet threshold based PCG compression.

Method	Preprocessing			WT/WPT		Coefficient Coding				Distortion Measure	PCG Database
	MR	SRC	Block N	wavelet name	Level L	Thresholding		Coding of NZWC	Coding of SM		
						Global/local	target				
Alajarín [211]	-	-	4096	Db8	4	Global	RE	LQ, Huffman	RLE, Huffman	PRD	-
Kao [34]	-	DS	2048	BW 9/7	4	Local	CR/λ_s	-	-	PRD	qdheart
Moreo [212]	-	-	4096	Db10	4	Global	PRD_w	-	RLE, Huffman	PRD_w	-
Sabari [214]	Yes	-	1024	BW 9/7	5	SPIHT coding strategy				PRD	qdheart

∗ Note:-SRC: sampling rate conversion; BW: bi-orthogonal wavelet; Db: Daubechies; DS: down-sampling; WT: Wavelet transform; WPT: Wavelet packets transform; EPE: energy packing efficiency; RE: retained energy;λ_s: threshold values; PRD_w: wavelet PRD; SM: Significance map and LQ: linear qunatization.

A few wavelet based PCG compression algorithm are reported for PCG signals in literature [34,211,212, 214]. These algorithms are grouped into tree based method and the threshold based method. The tree based method exploits magnitude correlation across the wavelet subbands [214]. In threshold based methods, the wavelet coefficients of the original signal are compared to some thresholds based on the target criteria such as retained energy (RE), distortion level and compression ratio (CR). The wavelet coefficients with values below the thresholds are set to zero. The wavelet threshold based method generally consists of one or more of the following processing stages: preprocessing, wavelet transformation, coefficients thresholding or/and the coefficients quantization and the entropy coding [34, 211, 212]. In these methods, thresholding or/and quantization is done globally. The nonzero thresholded wavelet coefficients vector is encoded using the linear quantization (LQ) with 16 bits resolution and the Huffman coding algorithm [211]. On the other side, the binary significance map (BSM) vector which consists of ones and zeros is created to store the locations of the significant coefficients and then the runs of ones and zeros in the BSM vector is coded using the runlength coder and then Huffman coding algorithm. Finally, Huffman and arithmetic coding is employed to further increase the compression ratio [211]. The compression methodologies used for the wavelet based PCG compression methods reported in the literature are summarized in Table 1.4. Recently, Benzid et al. [215] proposed a quality-on-request PCG compression algorithm using the DCT. It is based on an automatic thresholding of the DCT coefficients obtained after transforming the original signal into the frequency domain. The threshold is found for the desired peak signal to noise ratio (PSNR) as the controlled quality criterion. The linear quantization and the iterative Lloyd quantization approaches are compared when applied on the nonzero DCT coefficients. The lossless two-role encoder [143] is used for improvement of compression efficiency.

We have comprehended all popular methods and described the major critical compression issues related to methodologies employed for cardiovascular signal compression. The issues are presented by considering the major requirements needed for an automatic quality controlled compression system which must be

designed to achieve high data compression without introducing clinically significant information distortions. The set of optimal coding parameters is chosen according to a target criterion for a specific application. The coding performance can be improved by optimizing the parameters of a coder in the rate-distortion (R-D) sense. The compression performances are evaluated using the set of ECG records and the squared error and absolute error criteria. For specified target values, the numerical results of the coding efficiency (compression ratio or compressed data rate (CDR) in bits per second or entropy rate in bits per sample) and the percentage error are calculated and compared with the other compression methods under different test conditions. A direct comparison of the ECG compression methods is improper without the formation of standards, because of the following factors: a) use of various test records (sampling rate and resolution), b) characteristics of test signal, c) characteristics of noises and artifacts, d) different lengths of data and block used for testing purpose, e) calculation of overall compression performance procedure, f) methodology validation metrics such as compression ratio, distortion criterion, coding delay and coder complexity, g) noise filtering capability of compression methodology, h) with or without an entropy coder, etc. Some of the above factors are well described in [74, 103, 125], and the benefits of the standardization efforts are well presented in [74]. In many methods, the exact compression ratio achieved and the corresponding percentage error are not given, and the quality of the compressed signals does not seem to be adequate for morphological studies [103]. Therefore, to facilitate a perfect comparison, a large set of records from a common database needs to be processed by all the methods and their compressed signal quality needs to be evaluated with a common objective criterion which is consistent with subjective evaluation. This survey reports the compression performances of the recent works and gives a rough idea of current significant progress in cardiovascular signal compression methods. The objectives and organization of the thesis are presented in the following section. The review of some of compression methods will be presented with different sets of experiments in the next Chapter. We present the main objectives and organization of the thesis in the following Section.

1.6 Objective of the Thesis

Most of the energy in an ECG signal is concentrated in the low-frequency region. At each subband of the wavelet transform the energy distribution is concentrated in a small number of wavelet coefficients. Therefore, the wavelet transform of most ECG signals are sparse, resulting in a larger number of small wavelet coefficients and a smaller number of large coefficients. Thus, amplitude distributions of wavelet coefficients typically have sharp concentrations around zero in their distributions. Furthermore, significant wavelet coefficients for each signal block appear very close in a sequence order within a wavelet subband. A significant improvement in coding performance could probably be achieved by using different optimized threshold T and resolution b values for different signal blocks.

1.6.1 Adaptive Subband Coding Based on Threshold Control Zero-zone Quantization and Modified Index Coding Schemes

Many wavelet thresholding schemes apply thresholding followed by fixed linear quantization approach but it may introduce a severe signal distortion. Since a vector consists of wavelet coefficients with different dynamic range, it is not efficient to allocate a fixed number of bits to represent wavelet coefficients because of the varying characteristics of various ECG signals. Even if we assign different but fixed numbers of bits to wavelet coefficients according to dynamic range of the vectors, the coding efficiency may still be poor because of wavelet coefficients with great magnitude differences within the coefficients vector of a ECG signal. In such cases, classification of wavelet coefficients into frames based on the statistic of subband coefficients and dynamic bit allocation can provide a considerable gains in compression performance. Most of the threshold based schemes are based on a two-stage design, where the wavelet coefficients are hard-thresholded first and then nonzero wavelet coefficients are quantized using the fixed USQ scheme. In such a case, as a result of two separate thresholding processes a greater number of wavelet coefficients are set to zero than is actually required. In two-stage schemes, the loss of information can be seen to have two different sources: discarded wavelet coefficients concentrated around zero in their distributions and the quantization of nonzero wavelet coefficients. Then, such a scheme does not guarantee a user-specified specification maintained in thresholding stage at the output of the quantizer, and does not reach desired specification accurately and smoothly. Thus, we need a threshold driven zero-zone quantizer, where the width of zero-zone is limited by the threshold parameter T found in the previous stage, in order to guarantee a user-specified specification in the two-stage design based compression scheme. In guaranteeing algorithms, it is possible to reduce the computational cost if the relationship between the thresholding and quantization can be exploited in rate-distortion sense. The relationship between the T and Δ has a strong impact in compression rate and distortion. Thus, considerable gains in compression performance can be achieved if the optimal choice of the zero-zone width T for thresholding and the outer-zone width Δ for quantization is used for compression of the wavelet coefficients.

We present an adaptive subband coding based on the preprocessing, 5-level 9/7-tap filters wavelet decomposition, energy based classification of wavelet coefficients, constraint threshold control zero-zone uniform scalar quantization (TCZNUMQ) and modified index coding (MIC) schemes, and use of Huffman coding. The TCZNUMQ scheme is the modified midtread quantizer which is completely characterized by the two parameters: zero zone width T and outer zone width Δ. Then, the parameters T and Δ provide a flexibility to control a number of wavelet coefficients to be zeroed and a resolution of relevant wavelet coefficients to be preserved, respectively. By exploiting rate-distortion property of a TCZNUMQ, the optimal choice of the zero zone width and the outer zone width will be studied, and furthermore, we will show that how an optimal parameters set can be efficiently computed for a specific minimization problem. A few number of wavelet coefficients may be used for the representation of the ECG signal which is characterized by a cyclic occurrence of patterns (QRS complexes, P and T waves) with different frequency contents. Since sig-

nificant wavelet coefficients exhibit localized patterns with considerable close in the order sequence within subbands, the wavelet index coding scheme is used to code positions or locations of significant coefficients. The wavelet index coding combines two ideas such as differential coding and variable length coding for exploiting redundancy of an integer significance map (ISM) vector. In this work, the ISM vector created by storing positions of the significant coefficients and then the modified index coding scheme is applied to code block of integers in the ISM vector efficiently. The performance of the proposed adaptive subband coding is discussed in Chapter 3 with several experimental results.

1.6.2 Wavelet Energy Based Diagnostic Distortion Measure

Traditionally, the percentage root mean square difference (PRD) and maximum amplitude error (MAX) measures are widely used to quantify the quality of a distorted signal due to its simplicity and mathematical convenience. These are adopted as a measure of the global distortion and local distortion introduced by the compressor, respectively. Several researchers have argued that the PRD does not correlate well with subjective quality rating of compressed signal. In spite of complicated algorithms, the diagnostic meaningful distortion measure, the WDD measure does not appear to be superior to the simple PRD and MAX measures. Common disadvantages of PRD criterion are that a smoothing of low-level background noise of the ECG signal causes a large PRD value but no clinical feature distortion and, conversely, a small average distortion can severely deteriorate a signal clinical performance if all the error is concentrated in a significant feature region. Another simple measure is the WWPRD that provides structured error estimation. But its local PRD value of insignificant errors dominates a global PRD value while local PRD value of significant errors may not reflect any contribution to the global PRD. Thus, the common error measures, the PRD and WWPRD, are very unreliable, resulting in wrong predictions of quality. An objective error measure will be subjectively meaningful if “small” and “large” values correspond to “very good” and “bad” subjective quality. However, measurement of distorted signal quality is of fundamental importance for many ECG processing algorithms.

In this thesis, a novel wavelet energy based weighted diagnostic distortion (WEDD) measure is proposed. The proposed measure is a weighted percentage root mean square difference between the wavelet subband coefficients of the original and compressed signals with weights equal to the relative wavelet subband energies of the corresponding subbands. Dynamic weights based on wavelet energy feature represent the actual contribution of the subbands that are used to discriminate different frequency subbands, particularly subbands corresponding to noise. The WEDD measure appears to be a correct representation of the amount of signal distortion at all subbands and correlates well with subjective rating compared to the PRD and WWPRD measures. Thus, WEDD measure is more suitable for local and global assessment of a distorted signal. The performance of WEDD measure and its advantages will be discussed in Chapter 4.

1.6.3 Quality Controlled Compression of Cardiovascular Signals

A number of researchers indicated the disadvantages of the use of PRD measure as a quality control criterion. Meanwhile, methods are commonly tested using the `mita` database in which the records contain various PQRST morphologies and noises. The effect of noise filtering is one of the features using the wavelet transform for ECG signal compression and is observed in various compression results reported in the literature. In such a case, large values of PRD are measured between the original signal and the reconstruction for good noise filtering capability methodology. Thus, noise decreases compression rate of any coder since it will spend extra bits on approximating the noise in order to maintain the desired quality in PRD. As a remedy, one can then suggest the use of denoising algorithm before compression phase but it may introduce other types of distortions and also demands an objective quality criterion for the assessment of a denoised signal in the automatic compression system case. Although the use of optimum thresholding where threshold is derived from noise level can increase compression efficiency, an effective noise power estimation algorithm is demanded for processing varying characteristics of various PQRST morphologies and noises. However, this may not be an effective solution for the well designed methods with different coding procedure for wavelet coefficients (e.g., quality-on-demand compression scheme in the SPIHT framework). However, rate-distortion (R-D) optimization is the key technique in lossy compression methods to efficiently determine a set of optimal coding parameters. Thus, the R-D optimization requires an ability to measure distortion. The above constructs show that in order to introduce an automatic rate or quality control one needs an adequate distortion measure for the distorted signal. Moreover, the choice of the distortion criterion that must be used in quality-control is of critical importance when noise suppression and signal compression is established simultaneously. In this cases, the WEDD can provide a better approximation to the ECG signal distortion than the currently used PRD (or MSE). Thus, a simple WEDD measure for local and global assessment presented in Chapter 4 is brought forward.

In this thesis, quality controlled wavelet ECG compression methods are presented for guaranteeing reconstruction ECG quality measured using the WEDD criterion, which appears to be a correct representation of the amount of signal distortion at all subbands. The compression methods are based on: 1) the adaptive wavelet coding with joint thresholding and quantization strategy (Approach 1); 2) the adaptive subband coding with joint thresholding and quantization strategy (Approach 2); and 3) the set partitioning in hierarchical trees (SPIHT) coding strategy (Approach 3). Combining the WEDD measurement criterion and the well-designed coding strategy, the quality control algorithm provides a considerable coding gain. The algorithm will search for an optimal parameters threshold T and coefficient resolution b continuously in order to meet the desired quality specified in WEDD with high compression rate. The proposed algorithm not only achieves a good compression performance, but also reaches the desired quality accurately within the preset error tolerance ε and quickly. The proposed concept of automatic quality control is applied to the compression of ECG signal in Chapter 5 and its coding performance is studied for PCG signals in Chapter 6. The PCG compression method is based on a combination of the multirate sampling and adaptive sub-

band coding strategies. Experiment results show that the method achieves higher compression ratio while maintaining the desired quality under noisy environments.

1.7 Organization of the Thesis

The evolution of ideas discussed in this thesis are organized as follows:

Chapter 2 reviews the electrocardiogram compression methods and objective quality measures. The performance of the present wavelet thresholding and quantization approaches and the distortion measures used for assessment of compressed signal is studied with different sets of experiments. Finally, the motivation for the present research work is presented.

In **Chapter 3** an adaptive subband coding approach using the preprocessing, multiresolution signal decomposition, classification of wavelet coefficients, threshold control zero-zone nearly uniform midtread quantization (TCZNUMQ) and modified index coding (MIC) schemes are presented. Finally the performance of the rate- and distortion-driven compression algorithms are described.

In **Chapter 4** a novel objective weighted distortion measure for local and global assessment of compressed signal is proposed. The qualitative and quantitative analysis of the proposed measure is performed on different types of distortion.

In **Chapter 5** a quality controlled wavelet ECG compression methods are presented for guaranteeing reconstruction quality measured using the wavelet energy based diagnostic distortion (WEDD) criterion is presented. The performance of the method is evaluated with different sets of experiments.

In **Chapter 6** we present a better PCG compression method based on the combination of multirate sampling strategy and adaptive wavelet compression scheme. The performance of the method is tested using the PCG signal blocks taken from the `qdheart` and `CAHM` databases which include normal sounds, murmurs, stenosis, noise and other pathologies.

Finally, **Chapter 7** summarizes the present research works and gives some directions for further work.

2

Wavelet Based ECG Compression Methods and ECG Distortion Measures: A Review

Contents

2.1 Introduction

This chapter reviews the electrocardiogram compression methods and distortion measures used for evaluation of the compressed signal quality. Data compression is a method to reduce the bandwidth required to transmit a given amount of information in a given time or to reduce the time required to transmit a given amount of information in a given bandwidth. ECG data compression must be accomplished without sacrificing the diagnostic information in a signal. The multi-lead long-term ECG signals have three correlations viz. inter-sample correlation, inter-beat correlation and inter-lead correlation. The ECG signals may contain long or short isoelectric regions between two local events or waves. Redundancy exists whenever adjacent signal samples are statistically dependent and/or the quantized signal amplitudes occur with unequal probability. These properties are exploited in the reported ECG compression methods using different methodologies.

Many ECG compression methods are reported which exploit one or more of the correlations present in the signal. These can be divided into three major groups: 1) direct methods (e.g., AZTEC, adaptive AZTEC, TP, CORTES, SAPA, FAN, DPCM), 2) transform methods (e.g., Fourier, Walsh, KLT, DCT, wavelet transform (WT)) and 3) parameter extraction methods (e.g., LP, STP and LTP, average beat subtraction method, vector quantization methods, neural nets methods). The transform methods usually achieve higher compression ratios and are insensitive to the noise contained in original ECG signals [129]. In the transform method, the original signal in time domain is converted into a transform domain where the actual compression is performed. Among the transforms, WT is the most effective transform and it has received significant attention because of its good localization properties in time and frequency domains, energy compaction ability and efficiency in recent years. In WT based methods, the compression is performed in time frequency plane. The WT based methods outperform the traditional time domain and frequency domain compression methods, and produces smooth compressed signals. We thus review WT based methods, and we present compression issues involved in the threshold based methods.

In the case of ECG signal compression, the goal is not only to achieve good compression but also to preserve the diagnostic or clinical features in the signal. It is well known that the most efficient criterion for judging the performance of any ECG compression method is the clinical quality and visual inspection of the compressed signals. For convenience, objective quality criteria are often used to evaluate the performance of ECG compression methods. Traditionally, two different error measures are used for the compressed signals: the sum of squared errors and the maximum absolute error. The most widely used squared error distortion criterion for the compressed signal is called the percentage root mean difference (PRD) between the original and the compressed signals. However, PRD may not be a good measure of quality of the compressed signal, and also low PRD value does not necessarily mean clinical acceptance in the case of wavelet based methods. This chapter reviews previous approaches to quantifying the quality of distorted ECG signals.

This chapter is organized as follows. In Section 2.2, we present a brief outline of wavelet transform and

multiresolution signal decomposition techniques for analyzing and characterizing frequency contents of the ECG signals. In Section 2.3, we discuss one-dimensional wavelet based ECG compression methods. In Section 2.4, we present different quality assessment approaches proposed in the literature for distorted ECG signals. In Section 2.5, we compare the test results of different quality assessment approaches for most widely used datasets from `mita` database compressed with global thresholding based method and SPIHT coding method. This Section also summarizes the quality measures for the local and global assessment approaches and discusses their difficulties and limitations. In Section 2.6, we evaluate compression performance of the wavelet threshold based methods in which the optimal parameters can be chosen according to the specific criteria. We present limitations of the uniform scalar quantization approaches, and describe how the family of zero-zone uniform scalar quantization approaches can be used within the framework of threshold based method. This section also validates the performance of the quality controlled ECG compression methods, and highlights the compression issues of the methods.

2.2 Wavelet Transform

In many signal processing applications, mathematical transformations are applied to a signal in order to extract information which may not be readily available from the original signal. A wavelet based signal processing technique is an effective tool for nonstationary ECG signal analysis and characterization of local waves (P, T and QRS complex morphologies). The detail of wavelets and wavelet transforms can be found in many books and literatures, say [180–187]. In this section, we describe the wavelet transform and multiresolution analysis, the multiresolution signal decomposition and reconstruction techniques from the point of cardiovascular signals.

A wavelet family $\psi_{a,b}(t)$ is the set of elementary basis functions generated by dilations and translations of a unique admissible mother wavelet $\psi(t)$: $\psi_{a,b}(t) = \frac{1}{\sqrt{|a|}}\,\psi\left(\frac{t-b}{a}\right)$ where a and b ($a, b \in \Re$, $a \neq 0$) are the scaling (dilation) and translation (shifting) parameters, respectively, t is the time and the factor $|a|^{-\frac{1}{2}}$ is used for energy normalization across the different scales to ensure that all wavelets have the same energy. The duration of the mother wavelet $\psi_{a,b}(t)$ is either compressed or expanded depending upon the choice of a (i.e., for $a < 1$ the wavelet is compressed and for $a > 1$, the wavelet is dilated in time). The mother wavelet is a bandpass function centered at $t = 0$ in time and $f = f_o$ in frequency. That is $f = f_o$ is the center frequency of the mother wavelet. Then, center frequency and bandwidth for the derived wavelet are given by $\omega_a = \frac{\omega_o}{a} = 2\pi\frac{f_o}{a} = 2\pi f_a, \Delta f_a = \frac{\Delta f_o}{a}$ where ω_o is the center frequency of the mother wavelet and Δf_o is its bandwidth. The ratio between the center frequency and its bandwidth is constant for any value of the scaling a. The wavelet transform is a two-dimensional transformation with the dimensions being a, the scale or inverse frequency parameter, and b, the shift parameter.

The continuous wavelet transform (CWT) [184, 185] of a signal is defined as the correlation between

the signal $x(t)$ with the family wavelet $\psi_{a,b}$ for each a and b

$$\mathrm{CWT}_x^{\psi}(a,b) = \frac{1}{\sqrt{|a|}} \int_{-\infty}^{\infty} x(t) \cdot \psi^* \left(\frac{t-b}{a} \right) dt \tag{2.1}$$

where $\psi_{a,b}(t)$ is the basis function or the mother wavelet and the asterisk denotes complex conjugate. The scaling parameter a will decide the oscillatory frequency and the length of the wavelet; the translation parameter b will decide its shifting position. The components of the wider (more dilated) basis functions (large scale a) give information about the lower frequency components of the signal as a function of time (b in the transformed space). Similarly, the components for small scale a provide high-frequency information about the signal as a function of time. In the CWT, the frequency bands grow and shrink with the scale a. This allows good frequency resolution at low frequencies and good time resolution at high frequencies. Hence, the CWT can extract both local and global variations of a signal $x(t)$. Low scales contain high-frequency information about the signal and high scales contain low-frequency information about the signal. The CWT can also be considered as the output of a bank of bandpass filters whose center frequencies and bandwidths vary depending on the scaling parameter a in addition to the spectral properties of the wavelet function. The variable bandwidth introduces different resolutions at different scales and thus, the CWT has a multiresolution capability. If the signal $x(t)$ or one of its derivatives has discontinuities, then the modulus of the CWT of $x(t)$, $|\mathrm{CWT}_x(a,b)|$ exhibits local maxima around the time of occurrence of the discontinuities and the lines of constant phase converge towards the point of discontinuities. Thus, the CWT exhibits the property of zooming in on the sharp temporal variations in a signal.

2.2.1 Discrete Wavelet Transform

The transformation is achieved by dilating and translating the mother wavelet continuously over $\Re$ and hence it generates substantial redundant information. Therefore, instead of continuous dilation and translation, the mother wavelet maybe dilated and translated discretely. To do so, set $a = a_o^j$ and $b = kb_o a_o^j$, with $j,k \in Z$, where a_o and b_o are fixed constants with $a_o > 1$, $b_o > 0$. Then, the discretized wavelet [185] becomes

$$\psi_{a,b}(t)|_{a=a_o^j, b=kb_o a_o^j} = \frac{1}{\sqrt{|a_o^j|}} \psi \left(\frac{t - kb_o a_o^j}{a_o^j} \right) \tag{2.2}$$

$$= a_o^{-j/2} \psi(a_o^{-j} t - kb_o) = \psi_{j,k}(t). \tag{2.3}$$

and the corresponding discrete wavelet transform (DWT) is given by

$$\mathrm{DWT}_x^{\psi}(j,k) = \mathrm{w}_{j,k} = \int_{-\infty}^{\infty} x(t) \psi_{j,k}^*(t)\, dt. \tag{2.4}$$

By careful selection of a_o and b_o, the family of dilated mother wavelets constitutes an orthonormal basis of $L^2(\Re)$. An orthonormal basis is a basis that consists of a set of vectors S such that $u \bullet v = 0$ for each distinct pair of $u, v \in S$. The usual choice is to follow a dyadic grid on the time-scale plane by selecting $a_o = 2$ and $b_o = 1$: $a = 2^j$ and $b = k2^j$. With this, the wavelet transform is called a dyadic-orthonormal wavelet transform. There are several implications of the orthonormal basis. The first is that there will be no information redundancy among the decomposed signals due to the orthonormal properties. The second is that with this choice of a_o and b_o there exists an elegant algorithm, which is known as the multiresolution signal decomposition technique, to decompose a signal into scales with different time and frequency resolutions. The discrete wavelet family $\psi_{j,k}(t) = \frac{1}{\sqrt{2^j}}\,\psi(2^{-j}t - k)$ constitutes an orthonormal basis of the Hilbert space $L^2(\Re)$ consisting of finite-energy signals. For a signal $x(t) \in L^2(\Re)$, we have

$$x(t) = \sum_{j=-\infty}^{\infty} \left(\sum_{k=-\infty}^{\infty} \mathrm{w}_{j,k}\, \psi_{j,k}(t) \right). \tag{2.5}$$

The $\mathrm{w}_{j,k}$ are called the wavelet transform coefficients of $x(t)$. The wavelet transform is a reversible transform, and the reconstruction is possible if admissibility and regularity conditions are satisfied. Daubechies proved that the necessary and sufficient condition for stable reconstruction is that the energy of the wavelet coefficients must lie between two positive bounds

$$A\|x\|^2 \leq \sum_{j,k} |\langle x, \psi_{j,k} \rangle|^2 \leq B\|x\|^2 \tag{2.6}$$

where $A > 0$ and $B < \infty$. Here, $\|x\|$ is the energy of the signal $x(t)$. When this condition is satisfied, the basis functions, $\psi_{j,k}$ are referred to as a frame with frame bounds A and B. When $A = B$ the frame is called a tight frame and the wavelets behave exactly like an orthonormal basis [184]. When $A \neq B$, perfect reconstruction is still possible, but at the expense of a dual frame, $\psi'_{j,k}$. In the dual frame scenario, the reconstruction wavelet is different than the analysis wavelet. The advantages of the dyadic DWT are (1) reduction in the complexity and redundancy of the CWT, and (2) maintenance of most of the nice properties of the CWT such as linearity, shift covariance, scale covariance and the zooming property [183, 184].

2.2.2 Multiresolution Analysis

In this subsection, some of the key ideas of multiresolution analysis (MRA) theory and its implementation in the context of ECG signal decomposition are presented. A complete treatment of MRA theory can be found in [184, 185]. Wavelet analysis requires a description of two basic functions, the scaling function $\phi(t)$ and the wavelet $\psi(t)$. An orthonormal, compactly supported wavelet basis of $L^2(\Re)$ is formed by the dilation and translation of a single function $\psi(t)$, called the wavelet function: $\psi_{j,k}(t) = 2^{-j/2}\,\psi(2^{-j}t - k)$. The function ψ has M_v vanishing moments up to order $M_v - 1$, and it satisfies the following two-scale

difference equation:$\psi(t) = \sqrt{2}\sum_k g_k \psi(2t-k)$. The wavelet function $\psi(t)$ has a companion, the scaling function $\phi(t)$, which also forms a set of orthonormal bases of $L^2(\Re)$, $\phi_{j,k}(t) = 2^{-j/2}\ \phi(2^{-j}t-k)$. The scaling function $\phi(t)$ satisfies $\int_{-\infty}^{\infty}\phi(t)dt = 1$ and the scaling equation is given by $\phi(t) = \sqrt{2}\sum_k h_k\phi(2t-k)$ where $\{g_k\}$ and $\{h_k\}$ are called the filter coefficients which have the same finite length for a certain basis. The filter length is related to the number of vanishing moments M_v in $\psi(t)$. In the wavelet representation of signals, $\{h_k\}$ behaves as a low-pass filter and $\{g_k\}$ behaves as a high-pass filter to signals.

An MRA is a sequence of closed subspaces $\{V_j; j \in Z\}$ in $L^2(\Re)$ such that they lie in a contained hierarchy $\cdots \subset V_{-2} \subset V_{-1} \subset V_0 \subset V_1 \subset V_2 \subset V_3 \subset \cdots$ where the basis for the subspace V_j is a set of orthonormal, translated functions, and each of these function sets is a fixed dilation of the scaling function, $\{\phi_{j,k}; k \in Z\}$. As j goes to infinity V_j enlarges to become all energy signals $L^2(\Re)$. As j goes to negative infinity V_j shrinks down to only the zero signal. The multiresolution analysis is a sequence of closed linear subspaces that satisfies the following conditions:1) $V_j \subset V_{j-1}$ with $\overline{\bigcup_j V_j} = L^2(\Re)$ and $\bigcap_j V_j = \{0\}$; 2) $f(t) \in V_0 \Leftrightarrow f(2^{-j}t) \in V_j$; 3)$f(t) \in V0 \Rightarrow f(.-k) \in V_0$ for all $k \in Z$; 4) $\{\phi_{0,k}; k \in Z\}$ is an orthnormal basis in V_0 where $\phi_{0,k} = \phi(t-k)$ denotes the translation of the ϕ. Then, $\phi_{j,k}(t)$ is called a scaling function for V_j. Multiresolution approximation is a nested sequence of linear spaces. The orthogonal complement W_j of V_j in V_{j-1} can be thus defined $V_{j-1} = V_j \bigoplus W_j$. It is clear from the definitions that every signal in V_{j-1} is a sum of a signal in V_j and W_j. This shows that the spaces W_j are the differences (in the subspace sense) between adjacent spaces V_{j-1} and V_j. The wavelet basis $\{\psi_{j,k}; k \in Z\}$ forms the orthonormal basis of the subspace W_j. Based on this, for any $j < J$ we have the following equation:$V_j = V_J \bigoplus_{k=0}^{J-j-1} W_{J-k}$ where all subspaces W_j are orthogonal. To get a better idea of multiresolution analysis, let's decompose a signal, $x(t)$, in V_0 a few times. One can use the breakdown:

$$\begin{aligned} V_0 &= V_1 + W_1 \\ &= V_2 + W_2 + W_1 \\ &= V_3 + W_3 + W_2 + W_1 \\ &= V_4 + W_4 + W_3 + W_2 + W_1 \\ &= V_5 + W_5 + W_4 + W_3 + W_2 + W_1. \end{aligned}$$

This shows that V_0 contains the original data which has the finest resolution; the projection of the data on $\{V_j; j = 1,2,3,4,5\}$ has increasingly coarser resolution.

The data projected onto the subspace V_j is referred as the decomposition of data at resolution level j. We define the projection of a function $x \in V_0$ on V_j to be $x^j(t)$. Then, the j^{th} resolution level of the function has the form $x_a^j(t) = \sum_k \mathrm{A}_{j,k}\phi_{j,k}(t)$, where $\mathrm{A}_{j,k}$ is the projection of the function $x(t)$ on the basis $\phi_{j,k}$;$\mathrm{A}_j(k) = \int x(t)\phi_{j,k}(t)dt$. Next, the projection of $x(t)$ is defined on the subspace W_j to the difference $x_d^j(t) = \sum_k \mathrm{D}_{j,k}\psi_{j,k}(t)$, where $\mathrm{D}_{j,k}$ is the projection of the function $x(t)$ on the basis $\psi_{j,k}$;$\mathrm{D}_j(k) =$

$\int x(t)\psi_{j,k}(t)dt$. Any finite energy signal $x(t)$ can be decomposed over this wavelet orthogonal basis

$$\begin{aligned} x(t) &= \sum_{j,k\in Z} \langle x(t), \psi_{j,k}(t)\rangle \psi_{j,k}(t) \\ &= \sum_{k\in Z} \langle x(t), \phi_{j,k}(t)\rangle \phi_{j,k}(t) + \sum_{l\le j,k\in Z} \langle x(t), \psi_{l,k}(t)\rangle \psi_{l,k}(t) \\ &= \sum_{k=-\infty}^{\infty} A_J(k)\phi_{J,k}(t) + \sum_{j=-\infty}^{J}\sum_{k=-\infty}^{\infty} D_j(k)\psi_{j,k}(t) \\ &= \sum_{j=-\infty}^{\infty}\sum_{k=-\infty}^{\infty} w_j(k)\psi_{j,k}(t). \end{aligned} \tag{2.7}$$

Then, the original function $x(t) \in V_0$ can be represented by

$$\begin{aligned} &= x(t) = x_a^J(t) + \sum_{j=J}^{1} x_d^j(t \\ &= \sum_{k=-\infty}^{\infty} \mathrm{A}_J(k)\phi_{J,k}(t) + \sum_{j=J}^{1}\sum_{k=-\infty}^{\infty} \mathrm{D}_j(k)\psi_{j,k}(t). \end{aligned} \tag{2.8}$$

These scaling and wavelet functions together resolve the signal into its coarse and detail components. The first summation gives a function that is a low resolution or a coarse approximation of $x(t)$; the second one represents the higher or finer resolution to give detailed information of the signal. It can be seen that the decomposed traces contain progressively lower frequencies with the increase of decomposition levels. This leads to various decompositions:

$$\begin{aligned} x(t) &= \mathrm{A}_1(t) + \mathrm{D}_1(t) \\ &= \mathrm{A}_2(t) + \mathrm{D}_2(t) + \mathrm{D}_1(t) \\ &= \mathrm{A}_3(t) + \mathrm{D}_3(t) + \mathrm{D}_2(t) + \mathrm{D}_1(t) \\ &= \mathrm{A}_4(t) + \mathrm{D}_4(t) + \mathrm{D}_3(t) + \mathrm{D}_2(t) + \mathrm{D}_1(t) \\ &= \mathrm{A}_5(t) + \mathrm{D}_5(t) + \mathrm{D}_4(t) + \mathrm{D}_3(t) + \mathrm{D}_2(t) + \mathrm{D}_1(t) \\ &= \cdots\cdots\cdots\cdots \end{aligned} \tag{2.9}$$

where $\mathrm{D}_j(t)$, in W_j, is called the detail at level j and $\mathrm{A}_j(t)$, in V_j, is called the approximation at level j. Based on the multiresolution analysis, any signal $x(t)$ can be completely decomposed in terms of the approximations provided by scaling functions $\phi_{j,k}(t)$ and the details provided by the wavelets $\psi_{j,k}(t)$.

2.2.3 Wavelet Filter Banks for ECG Signal Decomposition

In this subsection, we briefly describe signal decomposition and reconstruction techniques. A more detailed description of these can be found in wavelet references [184–187]. The dyadic wavelet transform is im-

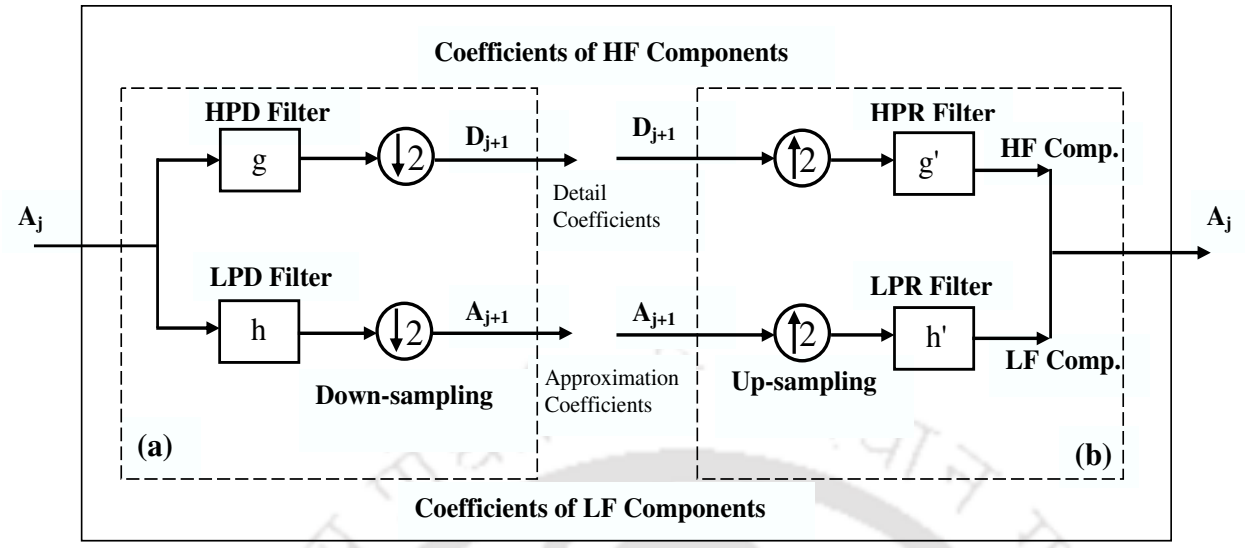

Figure 2.1: Subband filtering scheme for single level decomposition. (a) Analysis (Decomposition) structure: low-pass decomposition (LPD) and high-pass decomposition (HPD) filters. (b) Synthesis (Reconstruction) structure: low-pass reconstruction (LPR) and high-pass reconstruction (HPR) filters.

plemented using a multiresolution pyramidal decomposition technique. An attractive feature of the wavelet series expansion is that the underlying multiresolution structure leads to an efficient discrete-time algorithm based on a filter bank implementation. In particular, using the scaling function $\phi(t)$ and the wavelet function $\psi(t)$, one can define the $A_j(k)$ and $D_j(k)$ coefficients as $A_j(k) = \langle x(t), \phi_{j,k}(t) \rangle, D_j(k) = \langle x(t), \psi_{j,k}(t) \rangle$ and $A_j(k) = A_{j+1}(k) + D_{j+1}(k)$. The j^{th}scale coefficients (A_j) are filtered by two finite impulse responses of low-pass and high-pass digital filters with coefficients h and g, respectively. After this operation, down-sampling gives the next coarser, $j+1$ scaling coefficients (A_{j+1}) and wavelet coefficients (D_{j+1}). This process is illustrated in Fig. 2.1(a), where $\downarrow 2$ denotes a down-sampling operation by a factor of 2. In Fig. 2.1(b), the synthesis or reconstruction process is shown. The filters used in the synthesis or reconstruction structure are low-pass (h') and high-pass (g') synthesis filters. From the MRA technique, the decomposed signals at scale 1 are $A_1(k)$ and $D_1(k)$, where $A_1(k)$ is the smoothed or approximated version of the original signal $A_0(k)$ and $D_1(k)$ is the detailed representation of the original signal $A_0(k)$ in the form of wavelet transform coefficients. They are defined as $A_1(k) = \sum_{n=-\infty}^{\infty} h(n-2k)A_0(n)$ and $D_1(k) = \sum_{n=-\infty}^{\infty} g(n-2k)A_0(n)$ where h and g are the associated filter coefficients that decompose $A_0(k)$ into $A_1(k)$ and $D_1(k)$, respectively. The next higher scale decomposition is based on the signal $A_1(k)$. The decomposed signal at scale 2 is given by $A_2(k) = \sum_{n=-\infty}^{\infty} h(n-2k)A_1(n)$ and $D_2(k) = \sum_{n=-\infty}^{\infty} g(n-2k)A_1(n)$. Higher scale decompositions are performed in the same way as described above. The implementation of the multiresolution signal decomposition technique is shown in Fig 2.2. After the signal $A_0(k)$ is filtered by h and g, it is decimated by a factor of two. The resulting signal from h is $A_1(k)$, a smoothed version of the original signal $A_0(k)$ because

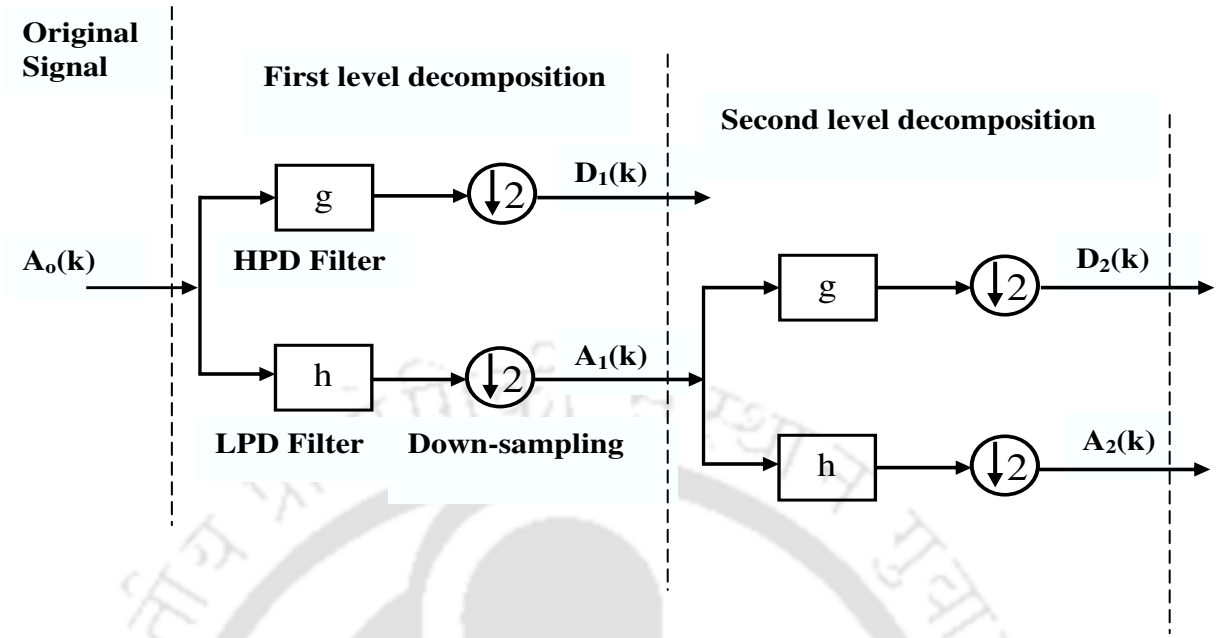

Figure 2.2: Signal decomposition structure. Decomposition of $A_0(k)$ into 2 scales. h=low-pass decomposition filter; g = high-pass decomposition filter; $A_1(k)$ and $A_2(k)$ are the approximate coefficients of the signal $A_0(k)$ at level 1 and 2, respectively. $D_1(k)$ and $D_2(k)$ are the detail coefficients at level 1 and 2, respectively.

the filter h has a low pass frequency response. The filtered signal $D_1(k)$ is a detailed version of $A_0(k)$ and contains higher frequency components, i.e., sharp edges, transitions, and noises. In other words, signal $D_1(k)$ contains the details that have been removed from signal $A_1(k)$. Signal $D_1(k)$ is called the wavelet transform coefficient at scale one. The time resolutions of $A_1(k)$ and $D_1(k)$ are now half that of $A_0(k)$ due to the decimation by a factor of two. As a result, if $x(n)$ has N sample points for the entire observation time, then signals $A_1(k)$ and $D_1(k)$ will have $N/2$ sample points for the same observation period. At each decomposition level, the length of the decomposed signals is half of the length of the signal in the previous stage.

The efficiency of wavelet analysis stems from its fast pyramid algorithm. The algorithm has two structures. The forward algorithm (decomposition structure) is used to compute the discrete wavelet transform (DWT). The backward algorithm (reconstruction structure) is used to compute the inverse DWT (IDWT). The decomposition and reconstruction structures are illustrated schematically in Fig. 2.2 and 2.3, respectively. The forward algorithm uses linear filters, low- and high-pass to decompose the signal into low- and high-frequency components, and also combines these filters with down-sampling operations (which accounts for the algorithms speed). The backward algorithm simply inverts the process, by combining an upsampling process with linear filtering operations. The original ECG signal passes through two complementary filters and emerges as two signals (low-pass and high-pass components). The decomposition

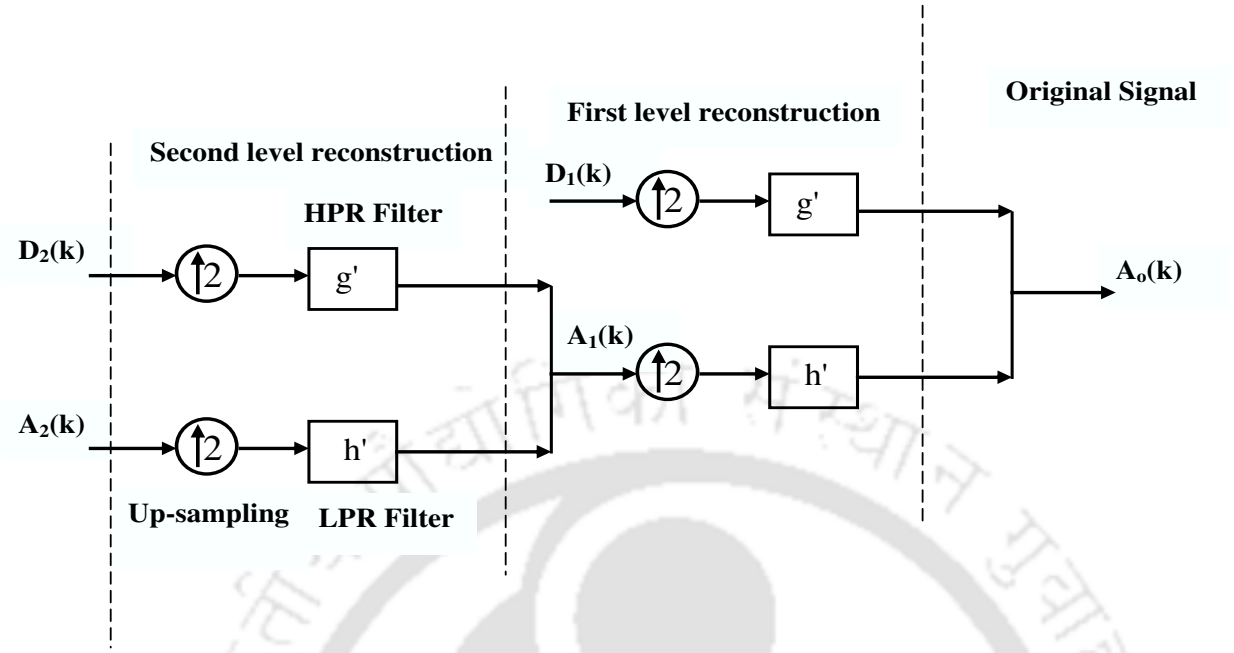

Figure 2.3: Signal reconstruction structure. h'=low-pass reconstruction (LPR) filter; g' = high-pass reconstruction (HPR) filter; $A_1(k)$ and $A_2(k)$ are the approximate coefficients at level 1 and 2, respectively. $D_1(k)$ and $D_2(k)$ are the detail coefficients at level 1 and 2, respectively. $A_0(k)$ is the original or approximated signal.

process can be iterated with successive low frequency components being decomposed in turn, so that one signal is broken down into many lower-resolution components as shown in Fig. 2.4. In reference to Figs. 2.2 and 2.3, the decomposition and reconstruction processes are described as follows. For each decomposition level, the LF and HF signal coefficients are obtained using the decomposistion filters $\{h\}$ and $\{g\}$. This process is repeated depending upon the number of decomposition levels desired. Fig. 2.4 illustrates the analysis part of a five-level decomposition scheme using subband coding.

Reconstructing the HF (or LF) component at level 5 from the detail (or approximation) coefficient vector is performed by upsampling the coefficient vector at level 5 and convolving the result with the high-pass (or low-pass) reconstruction HPR (or LPR) filter. The synthesis structure for a five-level decomposition is shown in Fig. 2.5. The reconstruction structure can be represented by the synthesis filter bank as a cascade of filters that can be used to extract signal synthesized at different levels of resolution. Successive details $\{D_j(n); j = 1,2,3,4,5\}$ and approximations $\{A_j(n); j = 1,2,3,4,5\}$ of the original signal are shown in Fig. 2.5. The multiresolution signal decomposition (MSD) technique decomposes a given signal into its detailed and smoothed versions. The BW 9/7-tap wavelet filters are used to calculate the detail signals. The high-frequency information of the signal is contained in $D_1(n)$ and lower components are observed in $D_5(n)$. The effects of high-frequency noise are produced at small scales as shown in Fig. 2.5. The effects of baseline

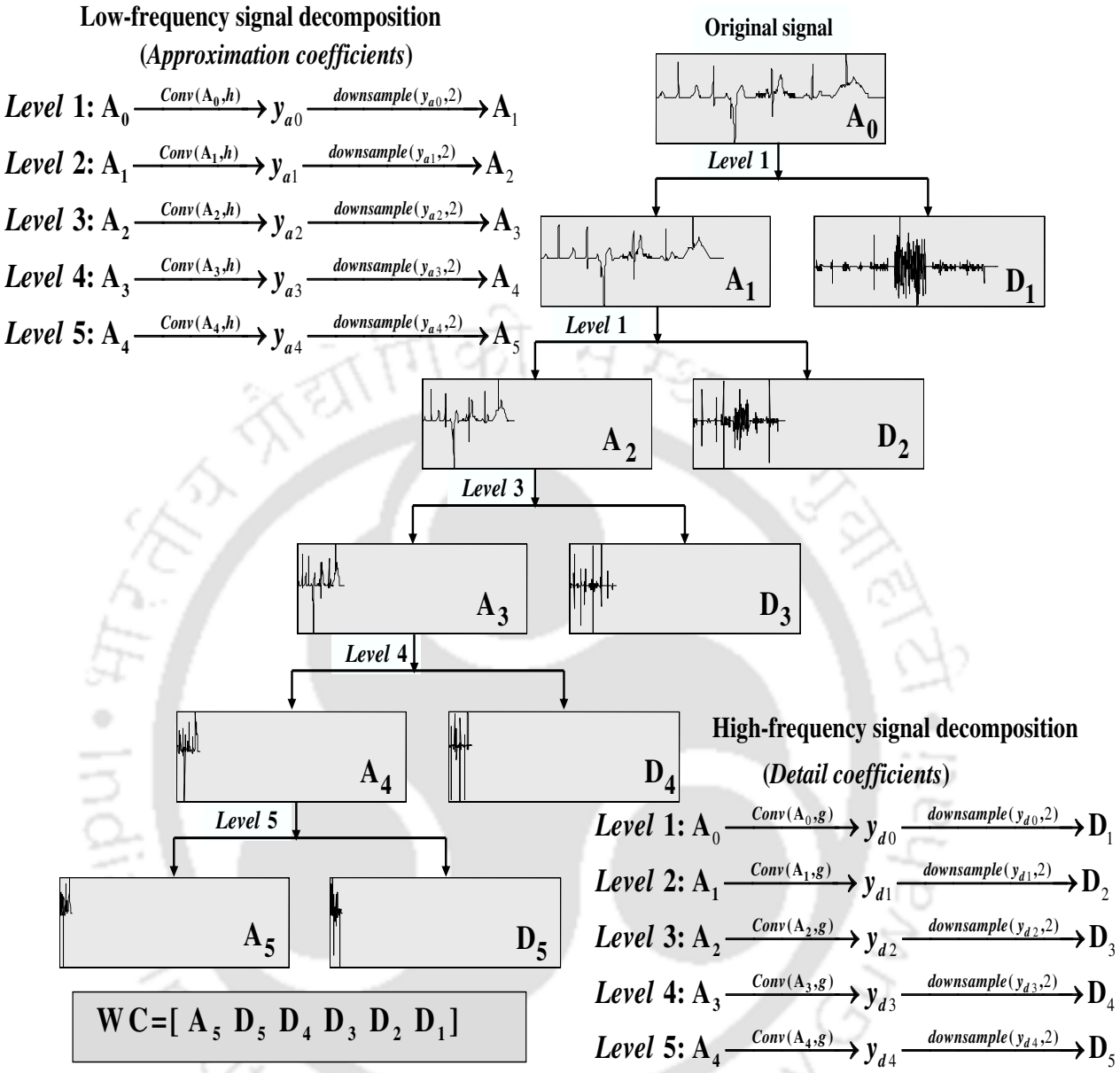

Figure 2.4: Five-level wavelet decomposition of simulated ECG signal. WC is the wavelet coefficients vector. Approximation coefficients: A_5, A_4, A_3, A_2 and A_1. Detail coefficients: D_5, D_4, D_3, D_2 and D_1.

drift are mainly at large scales as shown in $A_5(n)$ of Fig. 2.5. $A_5(n)$ contained low-frequency information such as baseline drift, P/T waves of the original signal. As the level of detail information $D_j(n)$ is added to the reconstruction, the approximation resembles the original signal. Therefore, the WT is a suitable tool to analyze the ECG signal which is characterized by the patterns (QRS complexes, ST segment, P, T and U waves) with different frequency content. The progressive quality/resolution of the reconstruction is observed from the approximation signals shown in 2.5. The reconstruction of these approximation and detail

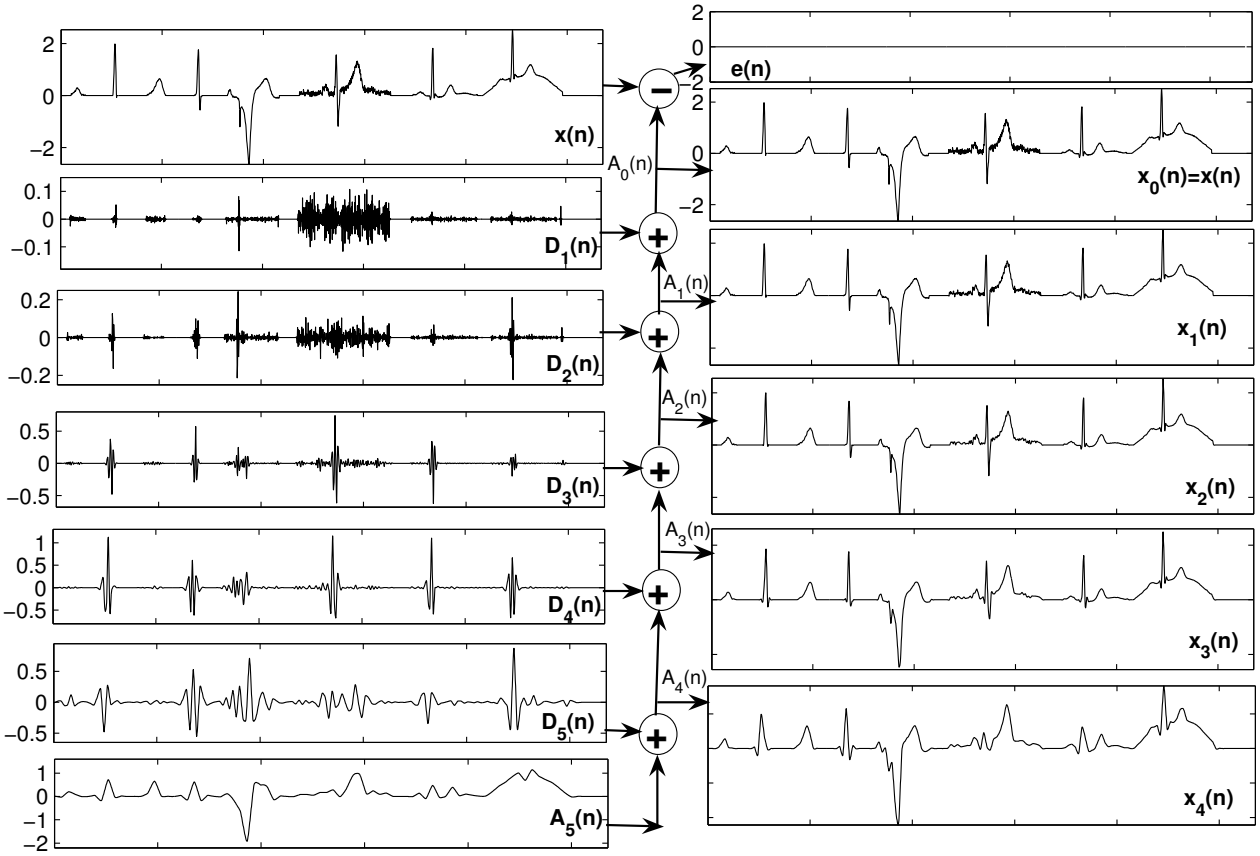

Figure 2.5: The synthesis (reconstruction) structure for a five-level decomposition of the test ECG signal.

signals are obtained using the wavelet coefficients $\{A_5,\ D_5,\ D_4,\ D_3,\ D_2\}$. Half of the wavelet coefficients are discarded. Therefore, by using the wavelet transform it is possible to achieve a good compression of a signal. This is done by performing the wavelet analysis on the ECG signal and disregarding non-significant coefficients. Experiment shows that the low-frequency shapes in the signal is the most important for perfect reconstruction. Some of the major observations on the ECG signal and the MSD of the ECG signal are given below for the point of signal compression:

(i) In general, ECG is a nonstationary signal whose waves and segments have time varying characteristics. These waves and segments may be localized in time domain. The PQRST morphology may change subject to physiological variations due to the patient and to corruption due to noise sources. Two types of the ECG signals can be seen that are regular PQRST morphology ECG signal and irregular ECG signal such as ventricular fibrillation (VF) and ventricular tachycardia (VT). We can know the degree of importance of the local waves, segments and noises affecting the ECG signal using the efficient MSD technique.

(ii) The high-frequency components of the local waves and different QRS complex morphologies are

reflected in the higher subbands which have larger dimensions and these components are localized in the higher subbands. The coefficients due to spikes of the PQRST morphology are essential for perfect reconstruction and hence these coefficients are referred as significant coefficients and the errors due to these coefficients are referred as significant errors.

(iii) The low-frequency components of the waves such as P, T and U, and ST segments are observed in lower subbands. Since the durations of these local waves are larger as compared to the durations of the spikes/notches appeared in the PQRST complexes, wavelet coefficients look to be distributed within the smaller subband dimensions.

(iv) The power line and muscular noises, baseline wandering and motion artifacts affecting the ECG signal also appear at different frequency bands, thus having different contribution at the various subbands. The high frequency noises can be seen in the higher subbands that do not exist in lower subbands. This phenomenon is shown in Fig. 2.5. The low-frequency baseline artifact is reflected in the lower subbands that can be seen in $A_5(n)$ of the figure. The coefficients due to noise are referred as insignificant coefficients and their errors are referred as insignificant errors.

(v) Amplitude distribution of the significant and insignificant coefficients over the scales depends on the type of the wavelet filters used for the MSD technique and the signal contents. The selection of the mother wavelet determines the amplitude distribution and the signal representation. Set of statistical features can be used to detect and characterize the signal contents in time and frequency planes.

(vi) The visual quality of the reconstruction $x_2(n)$ shown in Fig. 2.5 without contribution of the details $D_2(n)$ and $D_1(n)$, provides a better data reduction, is upgraded as compared to original signal. However, diagnostic accuracy may be degraded if the coefficients of the higher subbands are set to zero.

(vii) The low-frequency shape components are decorrelated at the lower subbands. The decomposition process results in small coefficients in the lower subbands which are essential for the preservation of the shapes of the small local waves.

(viii) Larger subband dimension contains a few significant coefficients and smaller subband dimension contain a few insignificant coefficients. These properties can be exploited so as to achieve a high compression gain with the preservation of all clinical information.

The DWT provides a representation of the signal on wavelet coefficients partly localized in time and frequency and is not redundant. Processing of the wavelet coefficients may allow their representation on a smaller number of bits than needed for representing the original signal. Therefore, a major role of any compression approach is to retain significant coefficients available across the subbands and to code the retained coefficients with less error so that all the clinical features are faithfully preserved. Many approaches

reported in the literature retain the significant coefficients according to a criterion specific for the application. In the following section, we discuss the coding schemes reported for wavelet coefficients of the ECG signal.

2.3 One-Dimensional Wavelet Based ECG Compression Methods

In ECG data compression, the wavelet and the wavelet packet transform are used to exploit the redundancy in the signal. After the signal is transformed into the wavelet domain, many coefficients are so small that no significant information is lost in the signal by setting these coefficients to zero [145]. Many 1-D and 2-D wavelet based compression methods are reported in literature. The 2-D ECG compression method achieved high compression ratio with low reconstruction error at the cost of increased time and space complexity for preprocessing techniques like accurate QRS detection, ECG segmentation, period normalization (PN), amplitude normalization (AN), mean removal (MR) and period sorting (PS). The 2-D compression methods are suitable for off-line processing because of the computational complexity involved and the use of long duration ECG signal. Therefore, 1-D wavelet based compression method is widely attempted that includes the following stages: the preprocessing, the DWT and the encoding of wavelet coefficients. The approaches such as blocking, baseline and noise artifacts removal, wavelet filters, number of decomposition levels employed in the first two stages are generally similar in most of the reported compression methods in literature. The selection of the mother wavelet determines the signal representation and the different mother wavelets provide different performance depending on the ECG signal characteristics. The selection of the mother wavelet and the decomposition level is commonly based on the minimal distortion of the compressed signal for a given compression ratio. In most cases, the mother wavelet is chosen by comparing the compression results of a few wavelets on a set of test signals. However, the BW 9/7-tap wavelet filters and the decomposition level chosen between 4 to 6 are commonly used in reported wavelet based methods. Therefore, researchers have proposed different coding approaches which are used to code the wavelet coefficients of the ECG signal with less number of bits so as to achieve good compression ratio. Based on the approaches used for coding of wavelet coefficients, the approaches are grouped into four categories: tree methods, vector quantization methods, linear prediction methods and threshold methods. Note that signal distortion occurs at the coefficient coding stage of the methods. Wavelet based ECG compression methods and their salient features are shown in Table 2.1.

2.3.1 Tree Based Methods

The embedded zero tree wavelet (EZW) and set partitioning in hierarchical trees (SPIHT) schemes are spatial tree based methods [144], [145]. This EZW algorithm is based on two main concepts [144]: the prediction of the absence of significant information across scale by exploiting self-similarity inherent in the signal and an entropy-coded successive-approximation quantization. This quantization scheme outputs an embedded bit stream by extracting at each step another significant bit for each coefficient which has been

Table 2.1: One dimensional wavelet and wavelet packets based ECG compression methods

Compression	Preprocessing					Transform		Coefficient Coding			target	computation/
method	QRS	PN	AN	MR	Block, N	Wavelet	Level, L	Thresholding,TH	Quantizer	Entropy Coding	criterion	implementation
WP+KLT [126]	Yes	Yes	No	No	512/1024	Coiflet-12	-	KLT, TH by variance, logarithmic quantizer and difference of beat lengths			RMS	one-third of KLT
BAWP [127]	No	No	No	No	4096	coiflet 8 VM	4	median absolute deviation	2-banks,each with 3 quantizers	Runlength coding	PRD	increased $O(n)$ to $nlog_2 n$, real-time
WT+LP [128]	Yes	Yes	Yes	Yes	PAN:256	Db4	8	N_c highest coefficients	Reordering of coefficients, LP and USQ		-	off-line
EZW [144]	No	No	No	No	1024	BW-9/7	-	embedded zero tree (EZW) coder		Adaptive Arithmetic	CR	fast, real-time
KLT+QCC [97]	No	PQ, QRS and ST block				MR Sampling and KLT		by relative MSE (rMSE)	logarithmic quantizer as in [126]		rMSE	better than [126]
GDQ [129]	No	No	No	No	1024	Db10	5	Block quantizer, Adaptive quantizer		Lempel-Ziv-Welch	PRD	less than [144] [128]
GW-AVQ [151]	No	No	No	No	1024	Db8	5	goal PRD based	Adaptive Vector Quantizer: 5 numbers		PRD	-
SPIHT [145]	No	No	No	No	1024	BW-9/7	6 layer	set partitioning in hierarchial trees (SPIHT) coder			CR	fast and easy
OZWC [131]	No	No	No	No	2048	Coif.4	4	optimal zone, size=32	USQ	Huffman based adaptive	-	fast, real-time
QDSPIHT [146]	No	No	No	No	1024	BW-9/7	-	SPIHT encoder with goal PRD: time=$\eta_\varepsilon(T_{SPIHT^{-1}}+T_{IDWT})$			PRD	less
WT-DCCR [152]	No	No	No	No	1024	BW-9/7	5	goal PRD based	Tree Vectors and DCCR mechanism in VQ		PRD	on-line
WT+EPE [134]	No	No	Yes	Yes	-	bior4.4	5	Energy based	Fixed No. of bits	Run-length for BSM	-	fast,real-time
LSPIHT [147]	No	No	No	No	1024	BW-9/7	10, 2 layer	layered SPIHT algorithm			-	real-time
FPWCZ [137]	No	No	No	Yes	NA	bior4.4	6	PWCZ	USQ	B2D, D2B and Huffman	-	fast,real-time
RQG [121]	No	No	No	No	2048	191-O,16-CH,N-PR CMFB		based on PRD_{target}	USQ	B2D, D2B and Huffman	PRD	simple,real-time
WLDECG [138]	block separation				adaptive	bior4.4	5	TH by allocated bits	flexible bit allocation	run-length for BSM	-	low delay, real-time
EREP [139]	Yes	template matching			512	Coiflet-12	-	TH by RMS/ bit rate	Amplitude coding (adaptive PCM), Huffman and data packetization		RMS/ Bit rate	real-time
NRDPWT [140]	No	No	No	Yes	1024	Db,6-tap	10	lossless SPIHT coder with modified quantization process			-	real-time
WPFDEC [142]	No	No	No	No	1024/2048	CDF 9/7	4 layer	target PRD	8-bit USQ	B2D, D2B and Huffman	PRD	simple,real-time

∗ Note:- BW: biorthogonal wavelet, VM: vanishing moments, PAN: period and amplitude normalization, DCCR: distortion constrained codevector replenishment, B2D: binary to decimal conversion, D2B: decimal to binary, PWCZ: percentage of the wavelet coefficients that must be zeroed, BSM: binary significance map, USQ: uniform scalar quantizer, O: order, CH: channel, N-PR CMFB: nearly-perfect reconstruction cosine modulated filter bank. LP: linear prediction, MR: multirate. The details given here are quoted from the reference cited.

found to be significant. The EZW allows to stop the compression whenever the desired CR or quality is met. Following this significant work, Said and Pearlman developed an alternative exposition of the underlying principles of the EZW algorithm and presented an extension that achieved even better results. These coding methods are extensively employed for coding of wavelet or wavelet packets coefficients of the the image, the ECG and the audio [145]. Recently, the performance of the SPIHT coder was evaluated for the PCG signal [214]. The ECG compression results obtained with SPIHT are shown to be superior in efficiency and considerably lower in complexity than any previous method. Since a highly distorted ECG signal can be useless from the point of diagnostic accuracy, the introduction of a precise quality (or distortion) control mechanism is essential for a well-designed compression method. Thus, Miaou and Lin [146] proposed a wavelet-based quality-on-demand algorithm for the compression of ECG signal using the SPIHT algorithm and the PRD as a quality measure for compressed ECG signal. However, the quality measure being guaranteed was PRD, which does not reflect the actual clinical distortion and the actual behavior of the method. Recently, Alesanco and Garcya [149] presented a simple and efficient method for guaranteeing reconstruction quality measured using the SPIHT algorithm and the distortion index wavelet weighted PRD (WWPRD). The compression performance of this method is evaluated using the signal block from the noisy `mita` records. The authors concluded that noise in ECG signals increases the bit rate due to effects of noise coding [149]. To prevent this problem, an adaptive approach that updates threshold according to noise level

in the block should be used [149]. Thus, noise power in each ECG beat was estimated as the power remaining after high-pass filtering (cutoff frequency equal to 20 Hz) in the repolarization interval [139]. Then, the number of wavelet coefficients to be transmitted is selected according to the measured noise level in the ECG beat. However, the noise estimation procedure may not be adaptively used in efficient and simple SPIHT coding scheme which exploits the self similarity across different subbands [145].

2.3.2 Vector Quantization Based Methods

The VQ algorithm alone provides a compression technique for sampled ECG signals, but it can also be used as the quantization step in a general compression system by combining it with signal decomposition techniques such as transforms or subband or wavelet filter banks and with lossless coding. Such cascades can provide better performance at the cost of added complexity. In these methods, the compression is performed by quantizing the wavelet coefficients into a reduced set of reference vectors. Many VQ based compression algorithms are reported in the literature for the single lead and the multi-lead ECG signals. Miauo and Yen [151] proposed a quality driven gold washing adaptive vector quantization (GW-AVQ) and its application to ECG data compression. Although the adaptive nature of the GW-AVQ algorithm provides the robustness for wide variety of the ECG signals, the performance of the GW-AVQ algorithm is highly dependent on the distortion threshold dth which is found according to a specified quality criterion, such as the PRD for ECG signals. The performance of the algorithm for the direct AVQ and WT+AVQ technique is evaluated using the four sets of test data, each is 15-min long which are all taken from the `mita` database, including records 101, 111, 208, and 228. Note that these records contain different noise sources and the PRD criterion has many disadvantages which will be demonstrated in the next Section. Miauo et al. [151] proposed wavelet-based ECG compression using dynamic vector quantization with tree codevectors in single codebook (WT+DCCR). The distortion constrained codevector replenishment (DCCR) mechanism is incorporated with VQ for the quality guarantee of reconstructed signal vectors. For ECG records in full length (slightly exceeds 30 min) from `mita` database, the compression performance of the WT+DCCR is better than the SPIHT coder for the given same compressed data rate (CDR). Although the WT+DCCR method obtains a very low CDR with acceptable compressed quality, it suffers from high computational complexity due to the high vector dimension and codebook size. Sun and Tai [89] proposed a beat based ECG compression using gain shape vector quantization that exploits the redundancy among the adjacent heart beats (interbeat correlation). The Okada algorithm and the QRS detection algorithm using DWT are used for the detection of QRS complex. Finally, the authors observed that the beat based method yields slightly better performance while using the wavelet based QRS detector. It is well known that quantizing a set of wavelet coefficients (vector) is more efficient than quantizing a wavelet coefficient (scalar) individually according to the rate-distortion optimization theory. However, from a practical point of view, VQ still suffers from several common drawbacks, including distortion measure and requires an effective algorithmic solution.

2.3.3 Linear Prediction and Template Matching Based Methods

Linear prediction (LP) method is based on the compression of the linearly predicted wavelet coefficients of the signal [128]. The error corresponding to the difference between the wavelet coefficients and the predicted coefficients is minimized in order to get the best predictor. In these methods, the input signal is divided into blocks and each block goes through a discrete wavelet transform; then the resulting wavelet coefficients are linearly predicted. These signals are compressed using various entropy coding schemes, including run-length and Huffman coding schemes. Ramakrishnan and Saha [128] proposed a novel ECG coding technique based on the LP of chosen wavelet coefficients of period and amplitude normalized (PAN) PAN beats. The variance of the resultant residuals is less than that of the original wavelet coefficients. Thus, lower number of bits is used for each residual coefficient than the number of bits required for each wavelet coefficient. This technique exploits both inter-beat and intra-beat correlations. With the this technique, a mean transmission rate of 180 bits per second (bps) is achieved with good fidelity of reconstruction. Ahmeda and Abo-zahhad [133] described a hybrid technique based on the combination of wavelet transform and linear prediction to achieve very effective ECG data compression. With PRD less than 4%, an average CR of 20:1 has been achieved when the technique is applied to different normal and abnormal signals from the `mita` database. However, the complexity of compression processes composed of beat detection, amplitude and period normalization, and an interpolation filter can downgrade their computational efficiency. Furthermore, the aliasing effect may occur due to improper designs of interpolation filter and down-sampling factors [158].

Kim et al. [138] presented a wavelet based low-delay ECG compression (WLDECG) algorithm for continuous ECG transmission for telecardiology applications over a wireless network. To attain both low delay and high quality, it employs waveform partitioning, adaptive frame size adjustment, wavelet compression, flexible bit allocation and header compression. The ECG signal with one period can be divided into two contiguous blocks of N samples based on the standard deviation σ of each block: a complex block with high σ and a plain block with low σ. For each block, centering and normalization are performed first and then wavelet transformation with the BW wavelet filters and five layer decomposition level is applied. The wavelet coefficients are then arranged in descending order to compose significant coefficients whose magnitudes are greater than the threshold determined by allocated bits. The coded bit stream consists of a set of coded significant coefficients and a run length encoded version of the BSM which indicates the positions of significant coefficients. The mean PRD values of the WLDECG algorithm is lower than WT+EPE [134] and EZW [144] for fast heart rate cases (cu01 and cu04 from `cuvt` database) and for high level of noise cases (118e00 and 119e00 from MIT-BIH noise stress test `mitnst` database). With respect to the `mita` database, the mean PRD of 1.067% (WLDECG) is lower than those of the 1.137% (WT+EPE) and 1.184% (EZW). But PRD values of the WLDECG are higher than the WT+EPE and EZW for the `mita` records 103, 107, 207, and 208. Thus, it shows that comparison of average compression performances of the methods may not be effective since noise filtering characteristics may not be similar across the compression methods

which contain thresholding or/and quantization stages. Alesanco et al. [139] presented a new real-time ECG coding scheme compatible with packetized telecardiology applications. The compression scheme contains the preprocessing stage (baseline removal, QRS detection, Beat segmentation and noise measure), template matching, wavelet transform, coefficient selection based on rate or RMS error, adaptive pulse code modulation and Huffman coding schemes. The compression performance of this method depends on the accurate segmentation of the beats of real time ECG signals and the measurement of total noise power of the beats which have different frequency contents.

2.3.4 Threshold Based Methods

Among the four categories, the wavelet thresholding based methods are low complexity algorithms [134, 137, 142]. The methods described in the literature utilize the preprocessing, wavelet transform, thresholding or/and quantization of the wavelet coefficients, binary significance map (BSM) and lossless entropy coding of the quantizer indexes and the BSM vector. In most of the methods, the first step of the wavelet coefficients coding is the thresholding process with threshold found based on the specific criteria such as the retained energy (RE), energy packing efficiency (EPE), percentage of wavelet coefficients zeroed (PWCZ), quality or distortion specification, compression ratio, etc. In this step, hard or soft thresholding rule is employed that discards the coefficients below the threshold and keeps the other coefficients with their resolution. The approaches such as global or local (or subband) thresholding are used in the literature. Since most of the signal energy is found in the lower subbands with smaller number of coefficients and the larger number of small coefficients contribute lesser energy, the perfect reconstruction is possible by choosing the optimal threshold and by keeping the resolution of retained coefficients. The nonzero wavelet coefficient (NZWC) vector and the BSM vector are created. The nonzero wavelet coefficients of the NZWC vector are quantized using the linear quantization (LQ) [137] and the resulting quantized indexes are encoded using the lossless coder. On the other side, the BSM vector which consists of '1s' and '0s' is created to store the locations of the significant coefficients and then the runs of ones and zeros in the BSM vector are coded using the run-length coder. Finally, Huffman and arithmetic coding can be employed to further increase compression ratio.

Chen and Itoh [129] presented a new ECG compression method based on orthonormal wavelet transform and an adaptive quantization strategy by which a predetermined PRD can be guaranteed with high compression ratio and low implementation complexity. The presented method is implemented with 10-taps designed by Daubechiess, layer of five, the buffer size of $N = 1024$ samples, and the Lempel-Ziv-Welch (LZW) encoder is chosen as the entropy encoder for simplicity. To make the results independent of the features of a specified ECG signal, four types of ECG signals with different features including a 10-min record (216000 samples) taken from the `mita` record 200 sampled at 360 Hz with 11-bit resolution, an atrial fibrillation record, an angina pectoris record and a normal ECG record are considered for testing. The later three are all 1-min long (15000 samples) and sampled at 250 Hz with 16-bit resolution. The `mita` record

200 is compressed at the specified PRDs of 7%, 9%, and 13%. The results of the evaluation show that no diagnostic information is lost for the ECG signals reproduced at specified PRDs of 7% and 9%, respectively while the compressed signal at PRD of 13% has degenerated in some Q-waves and ST-segments. Thus, the authors finally recommended a weighted PRD criterion for characterization of local waves of the compressed signals. The noise coding phenomenon is also described very well in the use of noisy ECG signals.

Nagarajan et al. [127] presented a constraint ECG compression by introducing a constraint on PRD and using adaptive wavelet packet decomposition. The constraint is based on the initial performance of the algorithm after taking into consideration the visual quality and the clinical information contained in the compressed signal. A Coiflet with eight vanishing moments was used to decompose the signal. The length of ECG vector (N) and the depth of decomposition (J) were fixed as 4096 and 4, respectively. Further, two banks of quantizers were used depending on the entropy at each node of the wavelet packet tree. Each bank had three quantizers that could be classified as coarse, medium, or fine. The coefficients were thresholded and runlength coded if the entropy of a node was less than unity. A scaled value of the median absolute deviation was used for thresholding. The bit resolution of the coefficients was reduced to 6, 7, or 8-bit depending on the quality of the quantizer if the entropy of a node was greater than unity. By generalizing wavelet decomposition it efficiently deals with the nonstationarity of the ECG, producing a better compression within the given constraint. The cost paid to achieve these benefits is in the form of increased number of computations. The order of computation increases from $O(N)$ to $O(N\log_2 N)$. The MIT-BIH ECG Compression test (`mitct`) database (168 annotated records from 38 subjects) is used to evaluate the performance of the algorithm. These test signals were sampled at 250 Hz with a 12-b resolution and exhibit a wide variety of arrhythmias, conduction disturbances, and noise. They are selected because their characteristics could pose a problem for the ECG compression method.

Rajoub [134] proposed an efficient ECG compression using the wavelet transform based on preprocessing, discrete wavelet transform (DWT), grouping of coefficients based on EPE, coefficients thresholding, the fixed quantization and the coding of significance map. The ECG signal is first preprocessed, the DWT is then applied to the preprocessed signal. Normalization and mean removal guarantees that all significant coefficients be less than one. Thus, reducing the number of bits needed to represent each coefficient [134]. The preprocessed ECG signal is decomposed by using the DWT up to the fifth level using the bior4.4 wavelet filters. Secondly, the wavelet coefficients are divided into three groups and each group is thresholded using a threshold T based on a desired EPE values. The BSM is then generated by scanning the wavelet coefficients and outputting a '1' if the scanned coefficient is significant, and a '0' if it is insignificant coefficient. Finally, the compression is achieved by 1) using a variable length code based on run length encoding to compress the significance map and 2) using direct binary representation for representing the significant coefficients. The dataset-I and II records from the `mita` database are used for performance evaluation. The PRD3 measure is used as distortion measure which was calculated with both mean value and

baseline value of 1024. Regardless of the performance of PRD3 measure the coding performance is compared with SPIHT algorithm reported in [145]. The author observed that the compressed ECG signals are smoothed versions of the original signals. In [137, 142], an 8 bits/element table (T8), formed from a binary table (01000001....010) where, every 1 indicates the chronological position of the corresponding nonzero coefficient in the initial wavelet coefficients. The Huffman coding was used to code both the quantized indexes and T8 to increase the compression ratio. Blanco et al. [142] presented a wavelet packets (WP) thresholding based ECG compression method. The number of WP layers is set as 4 and the bior9.7 wavelet filters is used for the decomposition. By using WP, the energy is suitably packed in fewer wavelet coefficients, so the first objective is addressed by simply thresholding quantized coefficients. To achieve quality reconstruction, both the thresholding and entropy coding schemes are carried out as in [137], utilizing the PRD as the target to terminate compression. For comparisons with the SPITH algorithm, the PRD values of SPIHT are considered for the specified compression ratios. Finally, the authors show that the proposed scheme outperforms the compression ratio reported in the literature by other thresholding based approaches. Both the threshold and scalar quantizer are signal specific. Experimental results show that it is possible to achieve a considerable gain in the compression ratio for a fixed distortion by using thresholding and then quantization. Since the design of quantization is a tradeoff between rate and distortion, different approaches used in the threshold based methods are discussed in the following section.

2.3.5 Quantization Approaches for Wavelet Coefficients

The second step of the wavelet compression is quantization. The purpose of quantization is to reduce data entropy by compromising the precision of the data and to reduce the irrelevance in a signal [188, 189]. Reducing entropy allows more compression. The quantizer typically performs an operation such as truncation or rounding to the nearest integer, thus creating an integer valued output. This process may introduce quantization errors, distortion or noise, to the signal. Thus, the original signal may not be recovered exactly after quantization. It is therefore very important to design a quantization strategy which selectively quantizes the wavelet coefficients and preserves the ECG quality. There is a tradeoff between signal quality and degree of quantization. It also has significant impact on the bit rate of the encoder. Thus, the performance is governed by the rate-distortion theory. A large quantization step size can produce high compression ratios with unacceptably large clinical feature distortion. Unfortunately, finer quantization leads to lower compression ratios. Then, the question is how to quantize the wavelet coefficients most efficiently. The design of the quantizer has a significant impact on the amount of compression obtained and loss incurred in a lossy compression scheme. Therefore, we present different quantization approaches applied to the wavelet coefficients of the ECG signals. In this section, we also present some of other simple quantization schemes which are reported for subband coding of images and then we describe the issues involved in the reported quantization schemes in order to present the motivation for the present research work.

The scalar quantizer is the simplest of all lossy compression schemes that is widely employed to code

the retained wavelet coefficients. In [126], each group of coefficients is quantized using the number of bits per coefficient, b, which is given by

$$b = 1 + \left\lfloor \log_2 \left(1 + \frac{c_l - c_s}{2 \times \text{TOL}} \right) \right\rfloor \tag{2.10}$$

where c_l and c_s denotes the largest and the smallest coefficient within the group, TOL specifies the maximum allowable quantization error per coefficient, and $\lfloor . \rfloor$ denotes the integer part. A value of TOL=0.008 is used, and the number of bits is restricted within $5 \leq b \leq 16$. In [129], uniform quantization with bin or step size of Δ is used for each wavelet subband coefficients. The Δ is found according in adaptive manner for a desired quantization MSE. In [131], a uniform scalar quantizer with 16-bit resolution is used because of its simplicity and ease of implementation. Results presented in [131] indicate that the number of quantization levels to be used has an impact on the quality of the compressed signal and the compression ratio. But the rate-distortion performance may be improved if the number of quantization levels of the quantizer is chosen based on the dynamic range of the significant coefficients vector. In [134], the retained coefficients are grouped and then encoded by assigning a fixed number of bits for each coefficient. A sign bit ('1' for negative coefficient and '0' for a positive coefficient) is added to encode the sign of the retained coefficient. The retained coefficients are stored using 7 bits signed representation and then the compression performances are compared with the results of the SPIHT and the ASEC algorithms. Note that there is no bits assigned to the integer part of the coefficient because it is always zero due to the preprocessing steps that were applied to the ECG signal before applying the DWT. Disadvantages of this approach will be discussed in later with a set of experiments. In [137], the nonzero wavelet coefficients (NZWC) were transformed into in the range 0-255 using the 8 bits linear quantizer defined by

$$\text{QNZWC} = 255 \times \frac{\text{NZWC} - \text{NZWC}_{\text{min}}}{\text{NZWC}_{\text{max}} - \text{NZWC}_{\text{min}}} \tag{2.11}$$

where QNZWC denotes the quantized NZWC vector, NZWC_{max} and NZWC_{min} denotes the maximum and minimum value of the NZWC vector. Note that fixed quantization scheme is used for the coding of the coefficients of the time varying PQRST morphology. In general, for a given quantizer resolution, the quantization step Δ is determined for each signal based on its dynamic range. The quantizer replaces each coefficient with $\Delta[\text{NZWC}/\Delta]$, referred as quantized NZWC (QNZWC). This is the simplest quantization rule which is often used in the wavelet based methods.

An excellent overview of scalar quantization scheme and its variants are discussed for coding of wavelet coefficients of the image [195]. In [195], the issues of different quantization schemes are discussed. We provide here the limitations of the schemes reported in [195], since there is no analytical framework of quantization for coding of wavelet coefficients of the ECG signals. The JPEG 2000 uses a dead-zone uniform scalar quantizer to wavelet coefficients resulting from the DWT of image samples [195]. The

midtread quantizer [195, 196] with step size Δ yields quantization indexes q

$$q = Q(c) = \text{sign}(c)\left\lfloor \frac{|c|}{\Delta} + \tau \right\rfloor \tag{2.12}$$

where c denotes a wavelet coefficient of the ECG signal block and τ is a parameter controlling the width of the central zero-zone. When $\tau = 0.5$, the quantizer is uniform, while $\tau = 0$ corresponds to the case in which the zero-zone width is 2Δ. The wavelet coefficients inside the interval $(-\Delta, \Delta)$ are quantized to zero. Thus, this interval is referred as dead-zone (or zero-zone) [195]. The width of zero-zone interval is 2Δ while all other intervals are of width Δ. The inverse quantizer is given by

$$\tilde{c} = \overline{Q^{-1}}(q) = \begin{cases} 0, & q = 0 \\ \text{sign}(q)(|q| + \xi)\Delta & q \neq 0 \end{cases} \tag{2.13}$$

where parameter ξ is in the range [0,1] (typically $\xi = 0.5$). An increase of Δ implies that greater compression can be achieved, but with low quality compressed signal. It is known that compressed quality and rates are controlled by the amount of quantization applied to each coefficient. The quantization step sizes are specified relative to the nominal dynamic range of the coefficients. Part II of the standard generalizes the zero-zone midtread quantizer to allow more flexible zero-zone selection while maintaining the fixed width Δ for all other intervals [195]. In [200], the performance of the three quantizers such as uniform scalar quantizer, zero zone midtread quantizer and trellis coded quantization is tested for coding wavelet coefficients of the image. Among these three quantizers, the performance of the USQ with control zero-zone is significant and its computational complexity is lower than the universal trellis coded quantizer [200]. For each threshold T, the best choice of parameter Δ in the rate-distortion sense can be determined by some searching algorithm. However, for natural image, the value of Δ should be among $1.2T - 1.8T$, specifically $\Delta = 1.55T$, for good compression performance [200, 201]. In this way, only one parameter (the threshold T) should be adjusted to determine the specific quality or rate. Then, this quantizer is applied to the the wavelet coefficients of the ECG signal. In [200, 202, 203], the wavelet coefficients vector is quantized with a quantizer defined in (2.14), where T is $0.5\Delta < T < \Delta$.

$$d_p = \begin{cases} ((2p-1)\delta, (2p+1)\delta) & p = -2, -3, -4, ... \\ (-3\delta, -T) & p = -1 \\ (-T, T), & p = 0 \\ (T, 3\delta), & p = 1 \\ ((2p-1)\delta, (2p+1)\delta), & p = 2, 3, 4, ... \end{cases} \tag{2.14}$$

$$O_p = \begin{cases} 0, & p = 0 \\ p\Delta, & p = \pm 1, \pm 2, \pm 3, ... \end{cases} \tag{2.15}$$

where, Δ is the quantization step size, δ is the half of the step size, d_p is the p^{th} decision level, O_p is the p^{th} output level and T is the threshold of the zero-zone. If the threshold, $T = \delta$, then the characteristics of

this quantizer is same as that of midtread quantizer. The width of the zero-zone is $2T$. In [142], the nonzero wavelet coefficients of the threshold vector are quantized using fixed quantizer as mentioned before in (2.11) with 8 bits resolution. In [143], the nonzero wavelet coefficients (NZWC) of the thresholded vector are quantized as in (2.16)

$$\mathrm{QNZWC} = (2^b - 1) \times \frac{\mathrm{NZWC} - \mathrm{NZWC}_{\min}}{\mathrm{NZWC}_{\max} - \mathrm{NZWC}_{\min}} + 2^b \tag{2.16}$$

where b is the quantizer resolution. The parameter b stands for the quantization resolution determined in such a way that the PRD of the compressed signal resulting from the quantized wavelet coefficients, denoted QPRD, meets the specified accuracy of QPRD. The minimal resolution $(b+1)$ is chosen and attributed to the quantizer from the set of bits $\{7,8,9,10,11\}$. If a suitable distortion measure is defined, an effective optimal quantizer can be designed by a simple iterative algorithm. The advantages and disadvantages of the above quantizers are presented in section 2.6 with different sets of the experiments.

2.4 Quality Assessment Approaches for the Distorted ECG Signal

A major problem in evaluating lossy compression methods is describing the type and the amount of distortion in compressed ECG signals. A compression system typically consists of one or more of the following stages, which may be combined with each other or with additional signal processing: sampling, signal decomposition, thresholding or/and quantization, entropy coding. Most of the reported compression methods employ thresholding of samples (or coefficients) and quantization. This process may distort the small and sharp diagnostic features present in the signal. In wavelet compression, signal distortion can be seen to have two different origins: discarded wavelet coefficients and quantization of retained coefficients. Thus, an assessment of clinical features of the compressed signal is most essential in the medical signal compression. Different distortion measures are employed for quality assessment of compressed ECG signals.

Usually two types of quality measures are employed: subjective measure and objective measure. The mean opinion score (MOS) is one of the most popular and widely accepted subjective measure. In this measure, the signal quality is evaluated by visual inspection of diagnostic features such as amplitudes, durations and shapes of the ECG waves. Cardiologists are the ultimate judges of ECG signal quality. They express their judgements of diagnostic feature qualities according to a given MOS scale. The MOS is a mapping of the level of diagnostic features such as amplitude, duration and the shape of the PQRST complexes' distortions into either the descriptive terms such as bad, not bad, good, very good and excellent or into equivalent numerical ratings in the range of 1-5 [190]. Finally, the scores are averaged across the subjects to obtain the final value of MOS. This measure is correlated with the diagnostic information in the signal but it is time-consuming and expensive. In this work, the mean opinion score (MOS) is used as a basis for validating our proposed objective measure.

There are two classes of objective quality assessment measures. The first class includes non-diagnostic

distortion measures. The non-diagnostic objective distortion or error measures are grouped into three categories namely global error measures, local error measures and similarity measure. The second class of objective error measures consider diagnostic features in an attempt to incorporate visual inspection quality by physicians. It includes diagnostic distortion measures viz WPRD, WDD and WWPRD. This section reviews previous approaches to quantifying the clinical quality of distorted ECG signal.

2.4.1 Non-Diagnostic Distortion Measures

In this section, we discuss two groups of distortion measures such as global and local commonly used to measure the compressed ECG signal quality in the literature.

2.4.1.1 Global Error Criteria

In this subsection, some of the non-diagnostic distortion measures are discussed. The mean square error (MSE) between the original and the compressed ECG signals is used as a measure of quality of the compressed signals and the limit to which an ECG signal could be compressed with an acceptable reconstruction quality is determined. For a given discrete sequence $x(n) = \{x(1), x(2), ..., x(N)\}$, consisting of N samples, and an estimated or reconstructed version of the same sequence $\widetilde{x}(n) = \{\widetilde{x}(1), \widetilde{x}(2), ..., \widetilde{x}(N)\}$, the mean square error (MSE) is expressed as

$$\text{MSE} = \frac{1}{N} \sum_{n=1}^{N} [x(n) - \widetilde{x}(n)]^2 \tag{2.17}$$

Geometrically, this distortion measure is the mean of the square of Euclidean distance between the input and the output vectors. MSE distributes the error equally over all portions of the ECG signal. Every portion of the ECG cycle has a different diagnostic meaning and relevance. This is the simplest distortion measure while it is not subjectively meaningful in many cases. It is difficult to define the clinically acceptable MSE value for a given compression method due to different dynamic ranges of ECG signals. To eliminate this shortcoming, the normalised mean square error (NMSE) between the original and the reconstructed ECG signals is computed [98, 102]. The NMSE is expressed as

$$\text{NMSE} = \frac{\sum_{n=1}^{N} [x(n) - \tilde{x}(n)]^2}{\sum_{n=1}^{N} [x(n)]^2} \tag{2.18}$$

Generally, normalization is required to make the error measure independent of the amplitude scale of the original signals. ECG signal amplitudes vary for different subjects and leads. Therefore, the measured error value should be normalized to conform within a standard range. Root mean square error (RMSE) is another measure employed to evaluate the distortion introduced by compression and quantization [64, 115, 126]. It

is defined as

$$\text{RMSE} = \sqrt{\frac{1}{N}\sum_{n=1}^{N}[x(n)-\tilde{x}(n)]^2} \tag{2.19}$$

It is questionable whether root mean square distortion is always a good measure of ECG signal fidelity [76]. The modified version of RMSE, i.e., normalized root mean square error (NRMSE), is used as an error measure [108, 119, 128]. NRMSE is defined as

$$\text{NRMSE} = \sqrt{\frac{\sum_{n=1}^{N}[x(n)-\tilde{x}(n)]^2}{\sum_{n=1}^{N}[x(n)]^2}} \tag{2.20}$$

In addition to NRMSE, the histogram of the error samples is used for evaluation of compression methods. Percentage rms difference (PRD) is a normalized error value which indicates the error between original and compressed signals. It is given by

$$\text{PRD} = (\text{RMS}_e/\text{RMS}_v) \times 100 \tag{2.21}$$

where RMS_e, RMS_v are the rms error and the rms value of the ECG signal, respectively. In most ECG compression algorithms, PRD is computed with different normalized value [43, 65, 79, 109, 114, 120]. Based on the normalization process, PRD measures are used as PRD1 [109, 166], PRD2 [109, 155, 161, 166] and PRD3 [120, 134]. Most of the compression methods tested using `mita` database adopts the addition of 1024-baseline for storage purposes. The records in `mita` database have different mean values. PRD1 is calculated after subtracting the mean value and the baseline of 1024 from the original signal [83, 120]. PRD1 is defined as

$$\text{PRD1} = \sqrt{\frac{\sum_{n=1}^{N}[x(n)-\tilde{x}(n)]^2}{\sum_{n=1}^{N}[x(n)-\mu_0-1024]^2}} \times 100 \tag{2.22}$$

where μ_0 is the mean of the original signal. PRD2 is defined as [155]- [161]

$$\text{PRD2} = \sqrt{\frac{\sum_{n=1}^{N}[x(n)-\tilde{x}(n)]^2}{\sum_{n=1}^{N}[x(n)-1024]^2}} \times 100 \tag{2.23}$$

PRD2 is determined with the inclusion of mean value of the ECG signal. PRD3 is defined as [134, 138],

$$\text{PRD3} = \sqrt{\frac{\sum_{n=1}^{N}[x(n)-\tilde{x}(n)]^2}{\sum_{n=1}^{N}[x(n)]^2}} \times 100 \tag{2.24}$$

PRD3 measure calculation includes both the mean value, μ_0 and the baseline of 1024. PRD3 value is very low for the given set of original and reconstructed signal as compared to the values of PRD1 and PRD2. But the reconstruction with low PRD value does not necessarily imply diagnostic acceptance. However, it is meaningless to compare the values of three PRDs with different offsets. If the signal $x(n)$ has a fluctuating baseline, the variance of the signal will be higher, and the PRD will be artificially lower. The PRD and other

similar error measures have many disadvantages which result in poor diagnostic relevance. Signal to noise ratio (SNR) is also employed as a measure of quality [64]. It is defined as

$$\text{SNR} = 10\log_{10}\left(\frac{\sum_{n=1}^{N}[x(n)-\mu_0]^2}{\sum_{n=1}^{N}[x(n)-\tilde{x}(n)]^2}\right) \tag{2.25}$$

The SNR value is larger at the high activity regions compared to other regions [64]. The normalized cross correlation measure is employed to evaluate the similarity between the original signal and the compressed signal [129]. The NCC is defined as

$$\text{NCC} = \frac{\frac{1}{N}\sum_{n=1}^{N}[x(n)-\mu_0]\ \sum_{n=1}^{N}[\tilde{x}(n)-\mu_r]}{\sqrt{\frac{1}{N}\sum_{n=1}^{N}[x(n)-\mu_0]^2}\sqrt{\frac{1}{N}\sum_{n=1}^{N}[\tilde{x}(n)-\mu_r]^2}} \tag{2.26}$$

where μ_0 and μ_r are the mean values of the original signal and the compressed or reconstructed signal, respectively. The correlation measure is used for finding similarity of the shape between the original and the reconstructed local waves [192].

A simple distortion measure, percentage area difference (PAD), was proposed as an alternative to existing ways of evaluating the performance of ECG compression methods [193]. This distortion measure corresponds to the area enclosed between the original and the reconstructed signal. The PAD is defined, in continuous time within a signal segment, as

$$PAD = \frac{\left|\int_{t_i}^{t_f} x(t) - \int_{t_i}^{t_f} \tilde{x}(t)\right|}{(t_i - t_f)(x_{max} - x_{min})} \times 100 \tag{2.27}$$

where t_i and t_f are the initial and final time instants of the segment and x_{max} and x_{min} are the maximum and minimum values in the original signal. The numerator term represents the absolute error in terms of area difference between the original and the reconstructed signal. The denominator is a normalization factor represented by the area chosen as reference. In this measure, the integration of the original signal was performed using the trapezoidal rule. The measure uses two different trapezoidal rules for integration of the original and the reconstructed signals for a given initial and final time instants.

2.4.1.2 Local Error Criteria

For local error criterion, the maximum amplitude error (MAX) or peak error (PE) is used in ECG compression methods to find out the maximum error and determine its position within a cycle [67], [120], [133], [112], [191], [166], [141]. MAX is defined as

$$\text{MAX}_i = \max_{n=1}^{N_{ci}}\{|x(n)-\tilde{x}(n)|\} \tag{2.28}$$

where, N_{ci} is the number of samples within an i^{th} cycle. Another version of MAX is the normalized maximum amplitude error (NMAX), which shows the largest absolute value of error normalized by the dynamic range of the signal within a cycle [119], [128]. The NMAX for the i^{th} cycle is defined as

$$\text{NMAX}_i = \frac{\max_{n=1}^{N_{ci}}\{|x(n)-\tilde{x}(n)|\}}{\max_{n=1}^{N_{ci}}\{x(n)\}-\min_{n=1}^{N_{ci}}\{x(n)\}} \tag{2.29}$$

The mean NMAX for the entire signal is determined by averaging over all the cycles.

In general, the existing global measures such as PRD, SNR and PSNR are not capable of showing the local distortions in the signal. Standard error (StdErr) [161] is proposed as a local distortion measure for ECG signals. The authors have shown results with non-zero mean values. According to the equations given in [[161], (4) and (5)] for MaxErr and StdErr, the MaxErr provides the largest absolute value of errors and the StdErr is the standard deviation of errors. The MaxErr cannot be same for error signal with and without mean value whereas StdErr is same for both cases. The MaxErr cannot reflect true compression error due to different non-zero mean values of different ECG cycles. Hence, choosing a predefined error level is difficult under this condition. If the MaxErr is calculated with zero mean error signal, then the StdErr is given by

$$\text{StdErr} = \sqrt{\frac{1}{N_c-1}\sum_{n=1}^{N_c}[\text{error}(n)]^2} = \sqrt{\frac{1}{N_c-1}\sum_{n=1}^{N_c}[x(n)-\tilde{x}(n)]^2} \tag{2.30}$$

StdErr is approximately equivalent to RMSE where the denominator is N_c instead of N_c-1. Hence, this expression does not reflect local effects. This definition shows that the StdErr is also global performance indicators like MSE and PRD measures. The PRD and MAX are the attractive measures due to their simplicity and mathematical convenience. However, the correlation between PRD/MAX and subjective judgement of quality is not close enough for most applications. The above facts have motivated a great deal of research on diagnostic distortion measures.

2.4.2 Diagnostic Distortion Measures

The second class of objective error measures considers diagnostic features to incorporate visual inspection quality by physicians. Diagnostic distortion measures include weighted PRD (WPRD), weighted diagnostic distortion (WDD) and wavelet based weighted PRD (WWPRD). In this section, we discuss different diagnostic distortion measures which are used for evaluation of ECG signal quality.

2.4.2.1 Weighted PRD Criterion

A compression method may achieve a low PRD value by ignoring the local wave between QRS complexes, totally losing the P-wave, and faithfully reproducing the QRST complex. It is difficult to avoid the degeneration of local information in the reproduced ECG signal. PRD measure fails to characterize the local

distortion of an ECG signal [129]. To improve this situation, the weighted PRD (WPRD) is used which is defined as

$$\text{WPRD} = \sqrt{\frac{\sum_{k=1}^{M} w_k \gamma_k}{\sigma}} \tag{2.31}$$

where w_k are the weights, γ_k are the reconstruction MSE of the diagnostic features such as P-wave, Q-wave, QRS-wave and ST-wave and σ is the power of the original signal. The weights can be chosen according to the desired diagnostic effect of the feature. For example, a larger weight could be applied to the ST-segment if the ST-waves need to be carefully treated. However, there is no procedure reported to select the optimal weights for each local waves. The WPRD measure depends on the accurate extraction of local waves within each beat and the weights for the significant waves. It may be impossible to get a good collection of the weights without the guidance of experienced cardiologists [129].

2.4.2.2 Weighted Diagnostic Distortion Criterion

The weighted diagnostic distortion (WDD) [191] measures the relative error in the diagnostic information. The WDD is based on comparing the PQRST complex features of the two ECG signals, the original ECG signal and the reconstructed or compressed one. The WDD measure uses diagnostic feature vector which consists of 18 features (durations, amplitudes and shapes). The WDD (in percentage) is defined as

$$\text{WDD}(\beta, \tilde{\beta}) = \Delta\beta^T \cdot \frac{w}{tr[w]} \cdot \Delta\beta \times 100 \tag{2.32}$$

where β and $\tilde{\beta}$ denotes the diagnostic feature vectors of the original and the compressed or reconstructed signal, respectively. $\Delta\beta$ is the normalized difference vector and w is a diagonal weighting matrix. This matrix is used to emphasize certain regions in the ECG cycle. Although the WDD measure correlates well with visual inspection, it suffers from high computational complexity due to the requirement of accurate evaluation of all diagnostic features and the calculation of optimal weights for the significant features. The nonstationary nature of ECG signal and the artifacts may lead to a false classification of diagnostic features. The source error due to the classification and the comparison of irregularity of the wave shapes may degrade the accuracy of the WDD measure. The complexity of the WDD calculation can be decreased by the extraction of fewer features or by developing more efficient extraction algorithms. However, there is no standard protocol to implement WDD measure for compression of real time ECG signals.

2.4.2.3 Average Absolute Error Criterion

In biomedical data reduction, the diagnostic distortion measure and visual inspection measure are performed to test the clinical acceptability of the compressed signal. The diagnostic distortion measure is implemented by comparing the PQRST complex features of the original signal with the compressed one. Nine diagnostic

parameters such as amplitudes and durations are extracted from each ECG cycle and then, the average absolute error (AAE) is calculated without giving any weight to the local waves [192]. Some of the diagnostic features are $P_{amp}, QRS_{+amp}, QRS_{-amp}, T_{amp}, P_{dur}, QRS_{dur}, T_{dur}, PR_{int}, ST_{int}$ and ST_{slope}. Two vectors of diagnostic parameters, one for the original signal (f_o^i) and the other for the compressed signal (f_r^i), are defined as $f_o^i = \{f_o^1, f_o^2, f_o^3, ...f_o^K\}$ and $f_r^i = \{f_r^1, f_r^2, f_r^3, ...f_r^K\}$ where K is the number of ECG features. The absolute error, (λ_i) for i^{th}, in a diagnostic feature is defined as $\lambda_i = \frac{f_o^i - f_r^i}{f_o^i}$ and the average absolute error (AAE) is calculated as

$$\text{AAE} = \frac{1}{K}\sum_{i=1}^{K}\lambda_i \tag{2.33}$$

where λ_i is the normalized absolute error for i^{th} diagnostic parameter. This measurement leads to a measure of diagnostic accuracy of the distorted ECG signals but it requires more effective feature extraction algorithms for real time implementation case.

2.4.2.4 Wavelet based Weighted PRD Criterion

Recently a wavelet based quality measure, Wavelet based Weighted PRD (WWPRD), is proposed [190]. This measure is based on decomposition of the ECG segment of interest into subbands and weighted score is given to the band depending on the dynamic range and its diagnostic significance. The PRD measure is used as error measure for each band, which is called as WPRD. The Wavelet based weighted PRD (WWPRD) is given as

$$\text{WWPRD} = \sum_{j=1}^{L+1} w_j \, \text{WPRD}_j \tag{2.34}$$

where, L is the number of decomposition levels, w_j is the weight of the j^{th} subband and WPRD_j is the PRD value of the j^{th} subband. In WWPRD measure, the weight of each subband is calculated as the ratio of sum of the absolute value of coefficients within that band and the sum of absolute value of wavelet coefficients in all the bands. The WWPRD measure provides structured error estimation criterion that will focus on diagnostic quality for reconstructed signals rather than random behavior of error which will be distributed equally between all the samples of the compressed signal. Qualitative and statistical analysis have proved that the WWPRD is well correlated with the clinically evaluated results. The contribution of insignificant error of some subbands are more in WWPRD measure. Consequently, the WWPRD measure will increase the overlapping of the quality groups and leads to confusion in the judgement of the reconstructed signal quality.

2.5 Evaluation of Distortion Measures

In this section, effectiveness of the distortion or quality measures are analyzed with different sets of experiments. Their advantages and limitations reported in the literature are discussed to have an effective comparison and to demonstrate the importance of the distortion measures in ECG compression.

2.5.1 Performance of PRD Criteria

In most ECG compression algorithms, PRD is computed with different energy normalized value [43, 65, 79, 109, 114, 120]. Based on the normalization process, PRD measures are defined as PRD1 [109, 166], PRD2 [109, 155, 161, 166] and PRD3 [120, 134]. Compression methods using `mita` database adopts the addition of 1024-baseline for storage purposes. Figure 2.6(a) shows the mean values of 48 ECG records in `mita` database. It is observed that the records in `mita` database have different mean values. PRD1 calculation includes subtraction of the mean value and the baseline of 1024 from the original signal [83, 120] for evaluation of signal energy. Estimation of PRD2 value includes subtraction of 1024 baseline for evaluation of signal energy. In PRD3 measure, the calculation of signal energy includes the mean value and the base line of 1024. Figure 2.6(b) shows the three PRD values evaluated for all 48 ECG records. The PRD values are evaluated for DCT and DWT based compression methods with a RE value of 99.7%. Two types of compression schemes, DCT and DWT, are used to evaluate the PRD values because the distortions are qualitatively different in these two types of schemes. Evaluation of PRD values with two different compressed signals can help establish the general nature of PRD characteristics. It is observed that PRD3 value is lower compared to the values of PRD1 and PRD2 for the records. Lower value of PRD3 does not necessarily imply diagnostic acceptance. Experiments show that there is a wide variation of PRD2 values for different ECG records. ECG records with higher mean values have lower PRD2 values for both the compression schemes. For the evaluation of PRD2 values, signal energy used for error normalization does not subtract or consider the mean in the signal. This is the reason for dependence of PRD2 values on the mean values of the signal. As the mean value does not have any correlation with the diagnostic information in the signal, PRD2 is not suitable for evaluation of compressed signals. There is little variation of PRD1 values across different records for the same RE value. This is due to the fact that signal energy used for error normalization subtracts the mean and the baseline of 1024. Among the three PRDs, PRD1 is most suitable for evaluation of distortions in an ECG signal. It is meaningless to compare the values of PRDs with different offsets.

For comparison between PRD1, PRD2 and PRD3 measures, their values are shown in Table 2.2. In this experiment, some of the frequently used `mita` ECG records 100, 103, 107, 111, 117, 119, 121, 123, 202 and 232 are used for evaluation. The first 1024 samples are taken from each of the record. Each block of samples are transformed using DCT and DWT. The decompressed signals are obtained from the retained coefficients based on RE criterion. PRD2 values depend on the mean μ_o value of the original

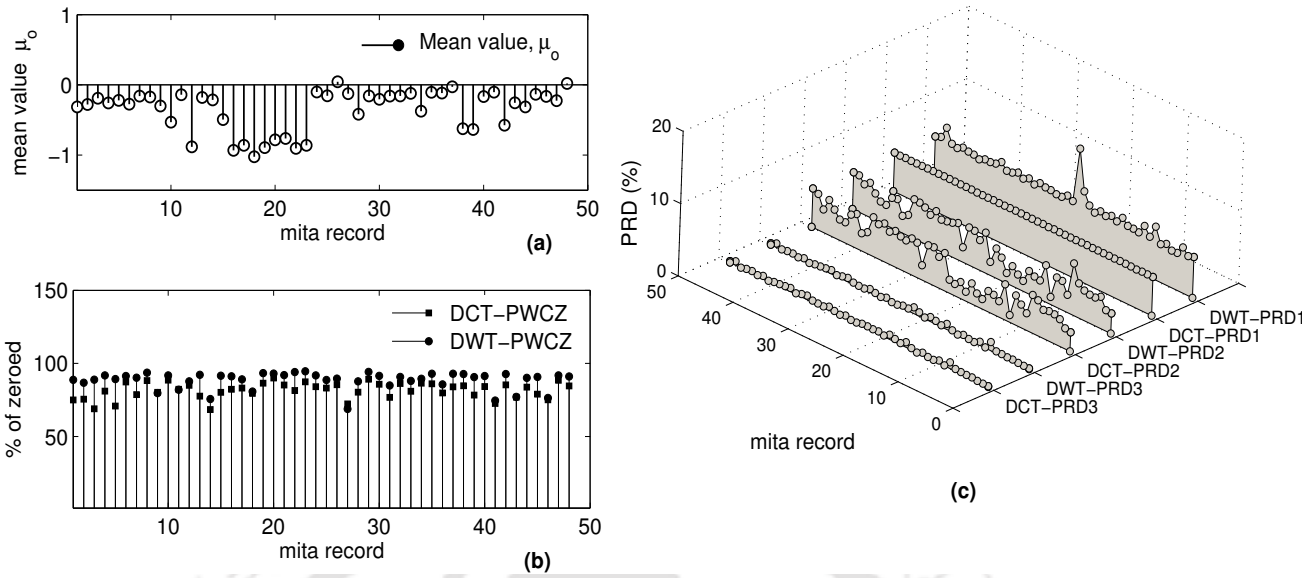

Figure 2.6: Performance of PRD and its variants under different mean values. (a) Mean value of `mita` records. (b) percentage of zeroed at RE value of 99.7%. (c) PRDs of compression error.

signal. The PRD1 values are approximately same for both the compression schemes. But there is large variation in PRD2 values due to different mean values of the signals. Choosing the clinically acceptable level is difficult if the PRD2 and PRD3 values are used. An user predefined PRD has been attempted in many compression methods [137, 139, 142, 143, 146, 149]. For a given PRD2 value of 5.0%, the methods can reach a target value for each segment. But the quality of the reconstructed signals are questionable for processed signals with nonzero mean value. In DWT case, if the reconstructed signal (record 231) with PRD2 value of 4.825% is considered within the clinically acceptable range then the reconstructed signal (record 123) is also acceptable for clinical evaluation. But the diagnostic features in the compressed signal of record 123 are severely distorted. The compressed signals are shown in Fig. 2.7(c1). The PRD1 value of the compressed signal is 13.04% which is larger than PRD1 values obtained for other segments. In the reported works, very good or good quality is defined for the PRD1 value ranging between 0 to 9%. The compressed signal for the record 107 with PRD1 value of 7.39% is shown in Fig. 2.7(b1). It can be observed that the duration of the P wave is prolonged in the compressed signal. The alteration of the features may affect the diagnostic accuracy. It proves that the PRD1 measure does not reflect local wave distortion.

Most of the compressed signal qualities of the DWT based method is good but the PRD1 values are large due to removal of the noise. It shows that the PRD1 measure is sensitive to insignificant errors or noise in the signal. So, a compression method might achieve a low PRD at a high CR but the high amplitude regions (e.g. QRS complex) may be reproduced with significant error. This distortion can be seen in Fig. 2.7(d4) for the case of `mita` record 117. The PRD1 values obtained for DCT and DWT based reconstruction are 5.427% and 5.569%, respectively. Due to noise filtering (low-pass filter) effect of transform, the DWT

Table 2.2: Performance of PRD measures for the reconstructed signals of transform based methods.

mita record	Mean value	DCT				DWT			
		PCZ (%)	PRD1	PRD2	PRD3	PCZ (%)	PRD1	PRD2	PRD3
100	-0.314	75.000	5.455	2.732	0.211	88.732	5.749	2.879	0.222
103	-0.258	81.055	5.404	4.124	0.347	91.737	5.231	3.992	0.336
107	-0.174	88.184	5.442	5.333	0.950	93.615	7.390	7.242	1.290
111	-0.141	82.324	5.466	4.171	0.187	81.972	5.515	4.208	0.188
117	-0.861	83.106	5.427	1.476	0.318	89.014	5.569	1.515	0.327
119	-0.893	86.426	5.457	2.919	0.744	93.333	5.287	2.828	0.721
121	-0.783	90.039	5.396	1.380	0.265	93.052	5.929	1.516	0.291
123	-0.905	81.445	5.441	1.738	0.404	94.085	13.040	4.165	0.968
202	0.044	85.449	5.477	5.354	0.222	89.578	5.274	5.156	0.214
231	-0.133	78.906	5.393	4.919	0.327	90.704	5.290	4.825	0.321

method results in large PRD1 value which is slightly higher than PRD1 of DCT method. Meanwhile, for a fixed retained energy, the DWT method produced smooth reconstructed signal than the DCT based method. Despite their widely accepted use as distortion measures, PRD1, PRD2 and PRD3 do not indicate precisely the quality of the signal. In other words, a low value of these measures does not guarantee total preservation of the essential features of the original record. The decompressed signal has to be evaluated by visual inspection. Therefore, the compression results of a quality controlled method based on PRD criterion are questionable.

The MSE and PSNR are directly related and PSNR is normally used for measuring the ECG coders objective performance. However, this measure is not generally a good measure for ECG. Better subjective quality may be obtained by using more complicated distortion measures such as the general quadratic distortion measures with input dependent weights like the arithmetic segmented distortions [64]. The compression results of corner detection based ECG compression method is compared with the results of the AZTEC under the same bit rate. The author stated that the SNR values shown in [[64], Table 1] are not constant for all regions of an ECG signal. The SNR value is larger at the high activity regions and smaller otherwise. Thus, the content of clinical information is in fact more finely preserved than that indicated by the SNR value. This result shows that the measured SNR value does not quantify the local wave distortion. It is expected that the distortion maeasure should capture the errors in the clinical information.

2.5.2 Performance of MAX Criteria

The maximum amplitude error (MAX) or peak error (PE) is used in ECG compression methods to find out the maximum error and determine its position within a cycle. This error is used to evaluate the localized clinical error in the signal. The effectiveness of local error measures are analyzed by compressing two

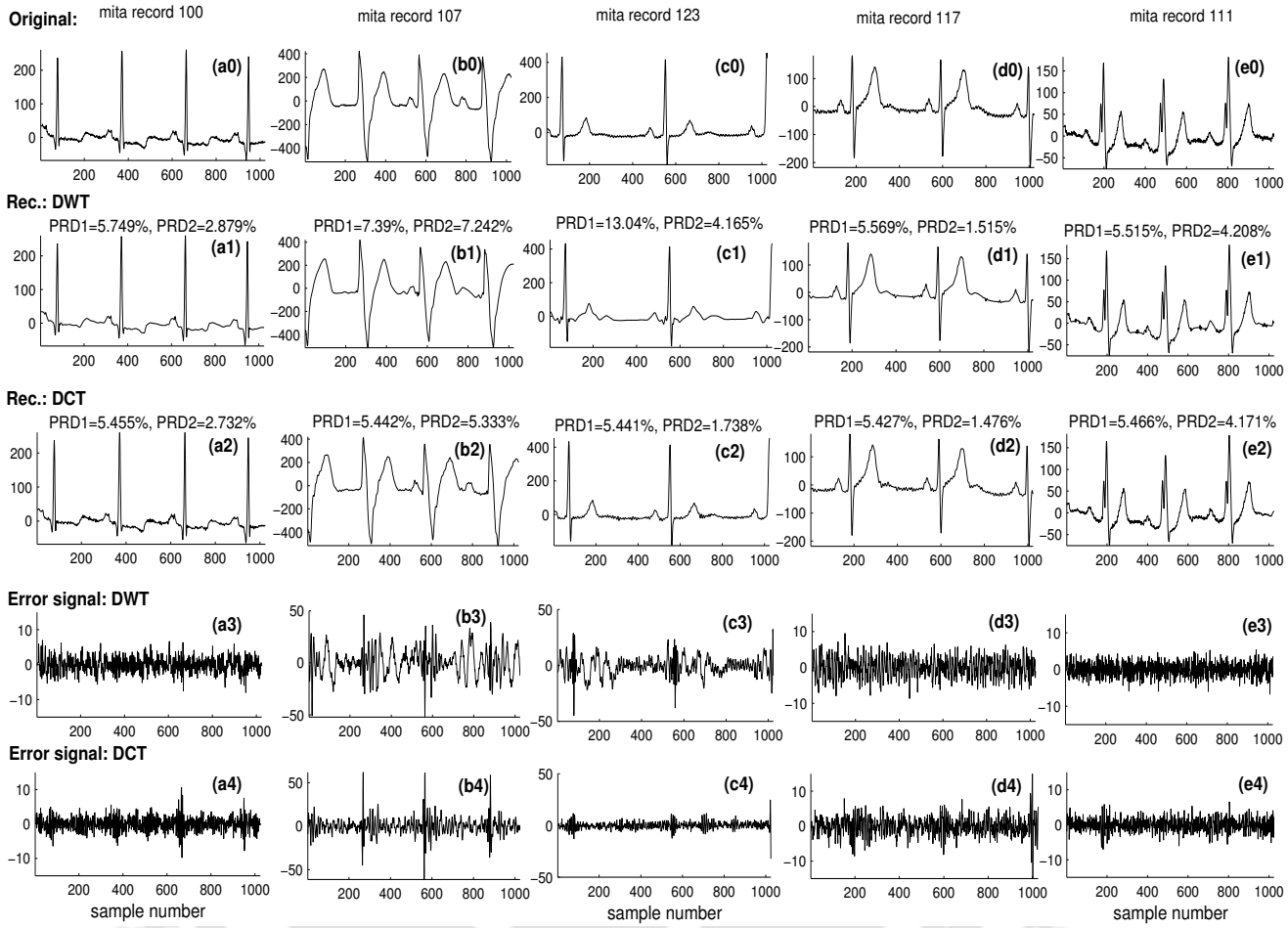

Figure 2.7: Performance of PRD and its variants. (a0-e0) Original signals. (a1-e1) Reconstructed signals DWT. (a2-e2) Reconstructed signals DCT. (a3-e3) Error signals of DWT based reconstruction. (a4-e4) Error signals of DCT based reconstruction.

different ECG segments taken from `mita` record 123 and 111. The original segments are transformed into sets of coefficients and then the reconstruction is performed from the retained coefficients based on the RE criterion. The reconstructed signals are shown in Fig. 2.8 along with the original signals and the error signals for visual comparison. The local effects due to thresholding process is studied by the MAX value. For RE value of 99.9% and 99.0%, the reconstructed and the error signals of the processed segments taken from the `mita` 123 and 111 are shown in Fig. 2.8. The MAX value of 0.0295 is measured at sample number of 71 of Fig. 2.8(c1) which is from the diagnostic feature (P wave) region of the segment shown in Fig. 2.8(b1) whereas the MAX value of 0.0146 at sample number of 250 is measured from the isoelectric region of the segment shown in 2.8(c2). This can be improved by weighting each error sample by the absolute value of its original sample, which is shown in Fig. 2.8(d2). Now the maximum error occurs in the QRS complex location. But the average MAX for an ECG segment is obtained by averaging over all the blocks.

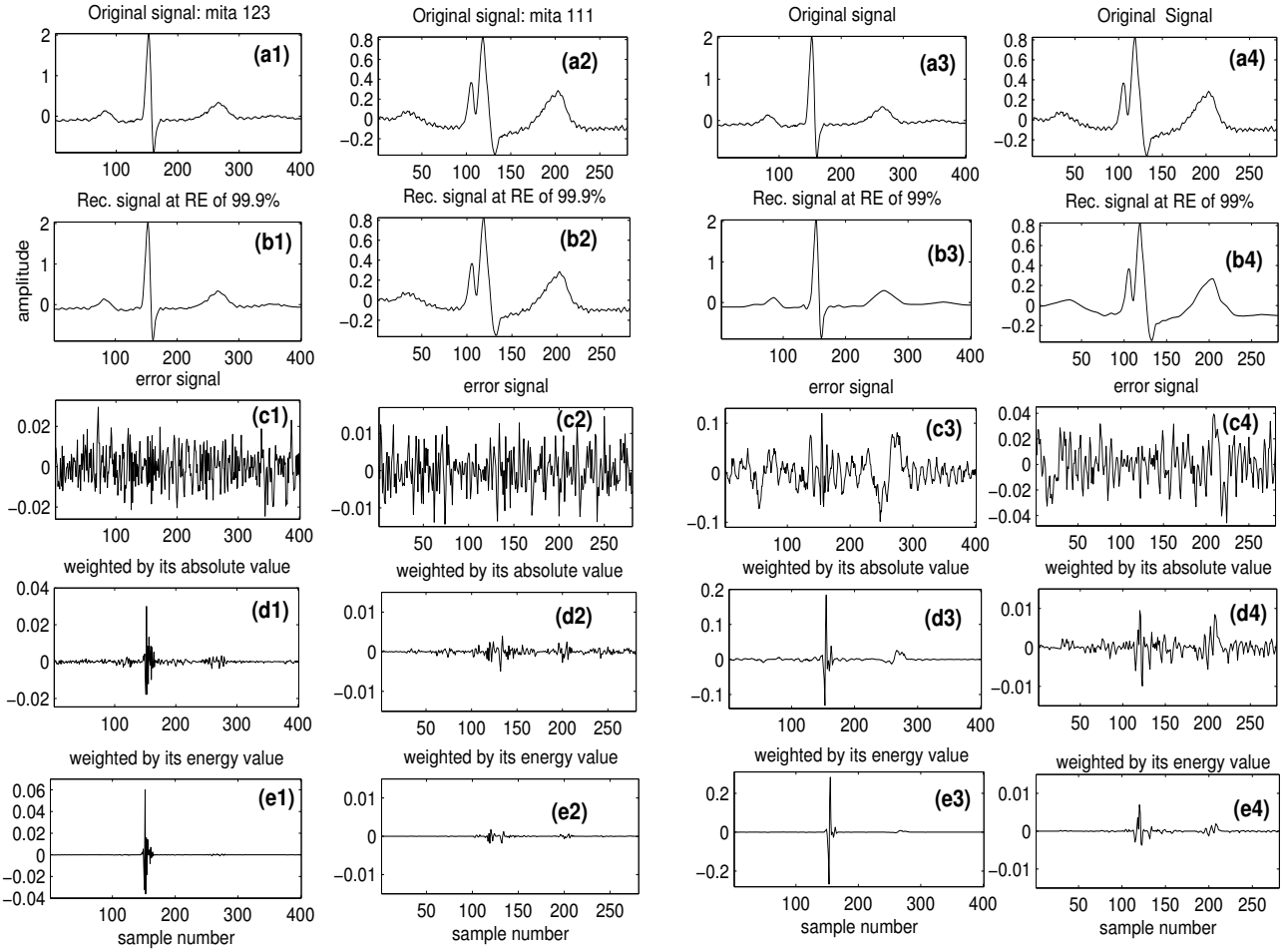

Figure 2.8: Performance of the quality measure in time-domain. (a) the original signals (`mita` record 123 and 111) . (b) the reconstructed signals. (c) Error sample. (d) Error sample weighted by absolute value of its original sample. (e) Error sample weighted by energy value of its original sample.

From Fig. 2.8(c(1-4)), it can be observed that the MAX error in the isoelectric regions also contributed some amount to the average MAX. The error measure can be improved further by weighting the error sample by the energy value of its original sample. The improvement in the error distribution is shown in Fig. 2.8(d(1-4)). But it will not show which local waves are distorted within an ECG cycle. For characterizing the local effects, the MAX and NMAX are used in ECG compression methods to find out the maximum error and determine its position within a cycle. The mean NMAX for the entire signal is determined by averaging over all the cycles. Moreover, the ECG segment contains isoelectric regions that do not contribute any diagnostic information. For these regions, all local error measures result in a nonzero value. Meanwhile a given distortion in one region does not necessarily have the same influence as the same distortion in another regions.

Table 2.3: Comparisons of diagnostic distortion measure for `mita` record 117 with CR=8:1

Compression Method	Diagnostic features									AAE
	P_{amp}	QRS_{+amp}	QRS_{-amp}	T_{amp}	P_{dur}	QRS_{dur}	T_{dur}	PR_{int}	ST_{int}	(%)
AZTEC (%)	1.64	216	5.61	8.8	2.62	27.5	2.8	1.7	3.6	30.03
FAN (%)	5.26	400	5.61	11.76	56.8	11.7	6.65	1.64	1.73	55.68
DSI (%)	0.65	31.6	3.3	5.88	2.72	4.0	2.75	1.70	0.88	5.94

2.5.3 Performance of Average Absolute Error Criterion

The diagnostic distortion measure is evaluated by comparing the PQRST complex features of the original signal with the compressed one. For evaluation of diagnostic distortion measure, nine diagnostic parameters such as amplitudes and durations are extracted from each ECG cycle and then, the average absolute error is calculated without giving any weight to the local waves. Some of the diagnostic features are $P_{amp}, QRS_{+amp}, QRS_{-amp}, T_{amp}, P_{dur}, QRS_{dur}, T_{dur}, PR_{int}$ and ST_{int}. Diagnostic features are extracted from the original ECG signal using digital filters, non-linear transformation and decision rule processor [167, 168]. The QRS detection is performed in a two step process: The ECG signal is first preprocessed to enhance QRS complex while suppressing motion artifact and muscle noise, P and T waves. The output of the preprocessor is subjected to a decision rule that gives the position of the QRS if the output of the processor exceeds a threshold. Based on QRS detection, the locations of P wave and T wave is detected using a search window. The preprocessor consists of band pass filter and differentiator which enhances the QRS complexes. Some of the detected significant diagnostic features (location of waves) are marked in Fig. 2.9. A vector of diagnostic parameters one each, for the original signal (f_o^i) and the compressed signal (f_r^i), is defined as $f_o^i = \{f_o^1, f_o^2, f_o^3, ...f_o^9\}$ and $f_r^i = \{f_r^1, f_r^2, f_r^3, ...f_r^9\}$ respectively, where K is the number of ECG features. The absolute error (λ_i) for i^{th} diagnostic feature is defined as $\lambda_i = \frac{f_o^i - f_r^i}{f_o^i}$ and the average absolute error is calculated as $AAE = \frac{1}{K}\sum_{i=1}^{9}\lambda_i$ where λ_i is the normalized absolute error for i^{th} diagnostic parameter.

Diagnostic distortion measure which is measured in terms of average absolute error (AAE) is independent of mean value and baseline drift. The relative absolute error is measured for each diagnostic parameters and the experimental results are shown in Table 2.3. The discrete sinc interpolator (DSI) based compression method results in an AAE value of 5.94% which is much lower than AAE of 30.03% and 55.68% of AZTEC and Fan algorithms respectively [192]. Also for QRS_{+amp} feature, the DSI algorithm results in an absolute error of 31.6% which is because of significantly reduced amplitude in QRS complex. The Fan method with compression ratio 8:1 reproduces QRS complexes but reproduction of ST/T complexes is very poor which gives less accurate calculation of ST depression/elevation. The DSI method results in AAE of 4.27, 2.22 and 5.88, for P position, R position and T position, respectively. From this experiment problems of the measurement of diagnostic accuracy is studied. This feature extraction is employed in the WDD measure.

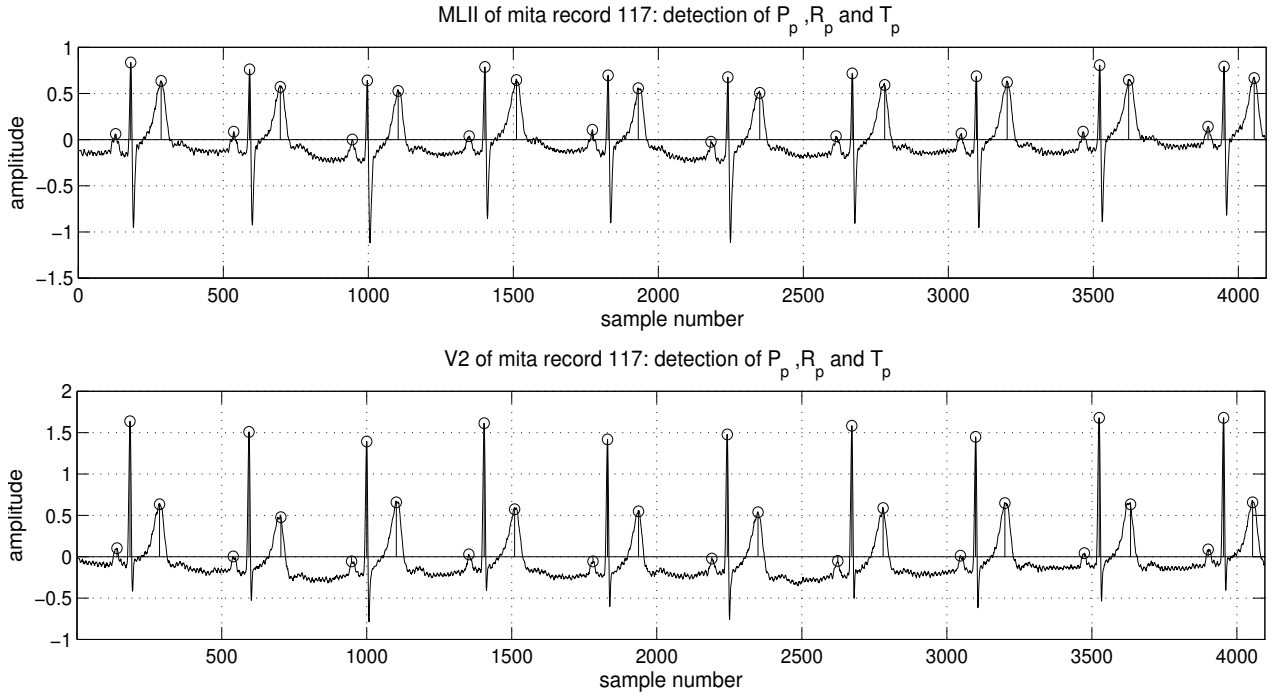

Figure 2.9: Detection of P waves, QRS complexes and T waves.

Although the WDD measure correlates well with visual inspection, it suffers from high computational complexity mainly due to the requirement of accurate classification of all diagnostic features, knowledge of the test conditions and the calculation of optimal weights for the significant features of interest [145]. Furthermore, non-stationarity of ECG cycles, time-varying morphologies, missing beats and noise may lead to false detection of diagnostic features and introduce errors. The WDD measure is performed in time and feature classification domain space and hence it will increase the complexity of the transform based compression algorithms.

2.5.4 Performance of Wavelet based Weighted PRD Criterion

The WPRD is a diagnostic error criterion that depends on estimation of ECG local waves and weighting their significance. The weights are computed based on the absolute value and the energy value of the wavelet coefficients. ECG signals taken (each) from selected `mita` records are compressed by using the DCT and DWT based coding schemes. The compressed signals are shown in Fig. 2.7. Then, the WWPRD [190] measure is used for assessment of the compressed signal quality. Local errors calculated using the WWPRD measure are shown in Table 2.4. It is well know that the transform methods provide a smooth reconstruction. Hence, a large wavelet PRD value can be obtained due to zeroing of coefficients in high order subband. The contribution of the insignificant error of some subbands are more in WWPRD measure. Consequently, this makes the signal to fall into wrong signal quality group. Although WWPRD is a diagnostic error measure

Table 2.4: Performance of WWPRD measures for the compressed signals of DWT and DCT based methods.

Record	WWPRD [190]: WT based compression methods							WWPRD [190]: DCT based methods						
	A_5 (%)	D_5 (%)	D_4 (%)	D_3 (%)	D_2 (%)	D_1 (%)	Total (%)	A_5 (%)	D_5 (%)	D_4 (%)	D_3 (%)	D_2 (%)	D_1 (%)	Total (%)
100	0.606	0.422	0.752	0.958	3.394	5.692	11.823	0.901	0.254	0.214	1.282	3.904	4.887	11.442
103	0.743	1.013	0.968	0.715	2.573	3.284	9.294	1.264	0.466	0.475	1.321	3.429	3.091	10.046
107	1.697	1.778	1.433	1.799	2.446	1.186	10.339	0.446	0.498	0.959	2.293	2.569	1.160	7.926
111	0.272	0.167	0.573	1.363	5.812	5.944	14.130	0.917	0.251	0.662	2.065	4.683	5.531	14.108
117	0.571	0.424	0.829	2.644	2.485	4.031	10.985	0.715	0.460	0.513	2.423	3.271	4.739	12.120
119	0.957	1.054	1.376	2.279	2.938	2.732	11.337	0.855	0.458	1.389	3.385	2.304	2.701	11.092
121	0.948	0.708	1.069	4.590	3.729	4.361	15.405	0.550	0.443	1.008	4.322	3.357	4.345	14.026
123	2.304	1.887	1.280	1.925	3.487	2.564	13.447	0.332	0.264	0.386	1.599	2.430	2.457	7.468
202	0.376	0.349	0.447	1.152	7.398	5.959	15.680	0.740	0.407	0.688	1.928	5.313	5.351	14.426
231	1.262	0.628	1.263	1.199	1.747	3.560	9.659	1.007	0.164	0.517	1.940	2.414	3.273	9.314

and simple to calculate, it is sensitive to insignificant errors due to smoothing of low level background noise. Furthermore, insignificant errors in some subbands may dominate the global error while significant errors in other bands may not reflect any contribution to the global error. This may lead to confusion in the judgement of the reconstructed signal quality. In most of the methods, the performance of the compressor is evaluated using the noisy records. Under this test condition, the local and global error measures may lead to false conclusions. The argument lies in the fact that if the same WWPRD value is specified for a noiseless ECG segment and the noisy one, the CR obtained for the noisy segment will be lower than that of the noiseless segment because a smaller quantization step is used for the noisy signal.

2.5.5 Comparison of the Distortion Measures

To test the performance of the distortion measures under filtered signal (background noise removed) condition, the `mita` record 123 is chosen and the noise present in the signal is filtered. The original and the filtered signals are shown in Fig 2.10. P and R wave of the filtered signal is distorted at different distortion levels for testing purposes. The reconstructed signals with P and R wave distortions are shown shown in Fig. 2.10. These distortions are measured using different error measures employed in literature and these results are shown in Table 2.5. From the table and the figure, it can be observed that the non-diagnostic distortion measures such as RMSE, PRD1, MAX, NMAX, SNR and CC provides the quantity of error. It does not provide which diagnostic features are distorted. This can be observed in WWPRD if the local errors of the WWPRD measure are provided for verifications. The results shown in the table and figure demonstrate that the distortion measure in wavelet domain provides information on distortion of the diagnostic features whereas other time domain distortion measures such as RMSE, PRD1, SNR, MAX, NMAX and NCC only quantifies the error. The WWPRD measure provides the errors between the distorted P wave/R wave and

Table 2.5: Performance of non-diagnostic and diagnostic error measures

Distortion	Non-diagnostic Measure						WWPRD Measure						
	RMSE	PRD1	SNR	MAX	NMAX	NCC	A_5	D_5	D_4	D_3	D_2	D_1	Total
Experiment 1 : Figs. 2.10 (a), (b), (c) and (d)													
P-wave	16.1	6.32	23.98	106.5	36.6	0.9981	3.5786	1.5442	0.3938	0.2848	0.1232	0.1444	6.069
R-wave	15.7	6.14	24.22	231.8	79.7	0.9981	0.7668	0.2166	1.0535	0.9826	1.6733	0.5577	5.251
with noise	15.9	6.22	24.11	57.5	19.8	0.9981	1.1291	0.5051	0.7228	0.9218	1.1415	1.693	6.113
Experiment 2 : Figs. 2.10 (a), (e), (f) and (g)													
P-wave	27.3	10.70	19.40	116.8	40.1	0.9943	7.5221	1.5844	0.33	0.2416	0.103	0.1226	9.904
R-wave	27.4	10.72	19.39	432	148.5	0.9943	0.1208	0.228	0.5424	1.9927	3.1595	1.5806	7.624
with noise	28	10.97	19.18	96.7	33.2	0.9943	2.6213	0.7263	1.2061	1.5552	1.85	3.171	11.13
Experiment 2 : Figs. 2.10 (a), (h), (i) and (j)													
P wave	38.8	15.19	16.36	0.126	43.5	0.9891	10.6235	1.4974	0.2525	0.1832	0.0766	0.0878	12.7209
R wave	37.4	14.66	16.67	0.692	238	0.9891	0.3464	0.3653	0.5423	1.9759	4.5813	2.2818	10.0929
with noise	38.1	14.95	16.51	0.114	39.3	0.9891	4.6187	1.133	1.4266	2.2192	2.78	4.2031	16.3806

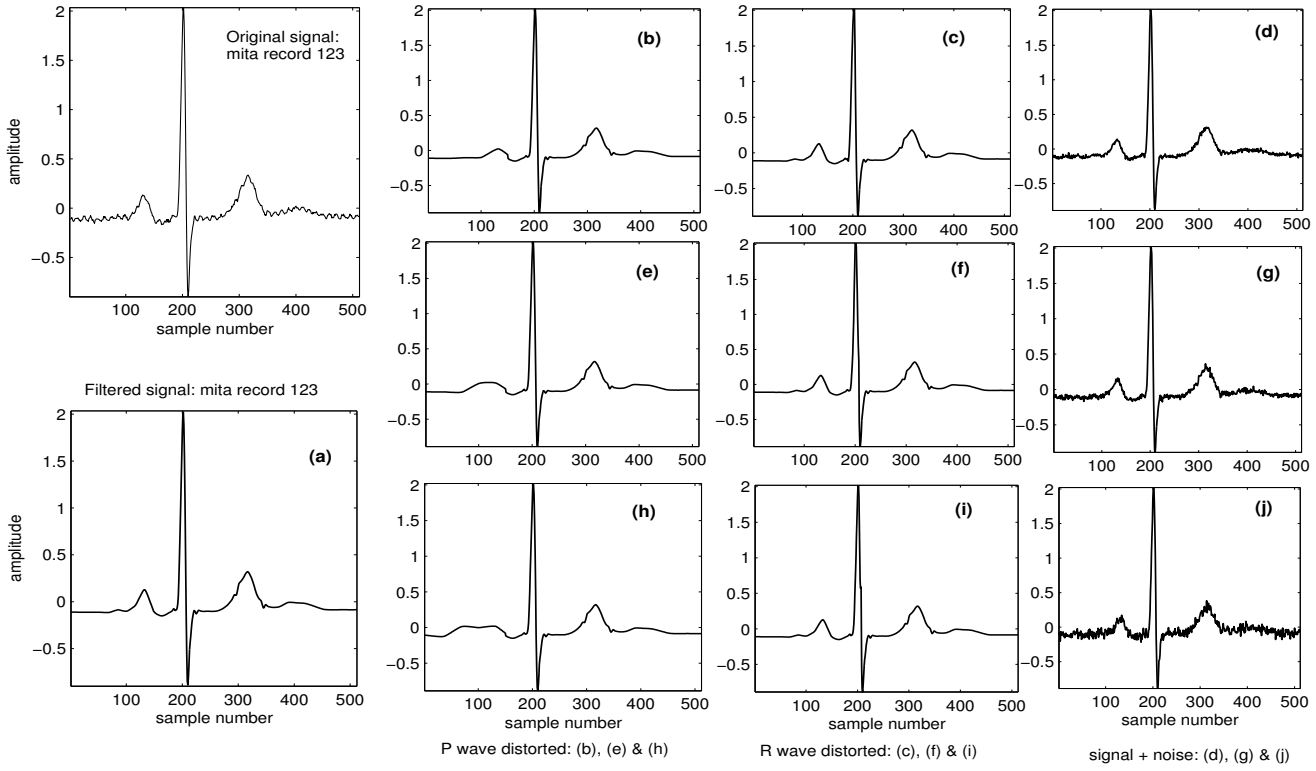

Figure 2.10: Performance of the distortion measures. (a) Filtered signal of the original signal taken from `mita` record 123. (b,e,h) P-wave distorted signals. (c,f,i) R-Wave distorted signals. (d,g,j) noisy signals

the original P wave/R wave at the frequency bands of P wave and R wave, respectively.

However, the inclusion of insignificant error is more in the case of WWPRD measure. In most cases,

Table 2.6: Performance of the ECG distortion measures

Characteristics of distortion/ quality measures	Objective quality or distortion measures								
	RMSE	PRD1	PRD2	PRD3	SNR	NCC	MAX	NMAX	WWPRD
global error measure (GEM)	√	√	√	√	√	√			
sensitive to mean (S2M)			√	√					
sensitive to baseline (S2B)				√					
local EM (LEM)							√	√	
diagnostic distortion measure (DDM)									√
sensitive to noise (S2N)	√	√	√	√	√	√	√	√	√

the resulting WWPRD by the band D_1 and D_2 are high due to the presence of noise. In [190], the total error is calculated by adding all the weighted errors which are contributed by the band A_5 and from D_5 to D_1. This may mislead the judgement of the signal quality when the signal contains more noise if the noise elimination algorithm is not employed in the compression method. It can be observed that the reported WWPRD measure is more sensitive to smoothing of low level background noise. The performance of all objective distortion measures are summarized in Table 2.6.

Many wavelet based ECG compression methods are reported and the tests are carried out using the noisy records from the `mita` database and the percentage root mean square difference (PRD) criterion in the literature. A major design goal of any compression method is to obtain the best clinical quality with the highest compression ratio (CR) using the optimal coding parameters such as threshold or/and quantization bit obtained for a quality or distortion specification. But the measurement of distortion in the compressed signal is difficult because the distortion introduced by different types of compressors are very diverse. The effect of noise filtering is one of the features using the wavelet transform for compression and it is demonstrated in various compression results reported in the literature. In this case, the magnitude of insignificant errors may not be of much relevance from the point of view of clinical quality of the compressed signal. The effects of noise on the rate-distortion performance of the proposed methods and the SPIHT based methods are demonstrated in the previous chapter. Although PRD does not exactly correspond to the result of a clinical subjective test, it is easy to calculate and compare, so it is widely used in the ECG compression literature. Common disadvantages of PRD and WWPRD criteria are that a smoothing of low-level background noises of the ECG causes a large PRD value but no clinical feature distortion and, conversely, a small average distortion can severely deteriorate a signal clinical performance if all the error is concentrated in a significant feature region. The weighted diagnostic distortion (WDD) measure correlates well with subjective test but it suffers from high computational complexity, and there is no standard protocol for its implementation.

Thus, in order to introduce closed loop CR or quality control, one needs an adequate diagnostic distortion measure for the compressed signal. Moreover, the choice of which distortion measure must be used for compressed signal is of critical importance when noise suppression and signal compression is established

simultaneously. In the area of ECG signal compression, little attention has been paid towards the evaluation of distortion of clinical information. A suitable objective distortion measure can help proper evaluation of the well-designed ECG compression methods under noisy environments. Otherwise, the quality of the compressed signal has to be evaluated by subjective test, visual inspection of the clinical features. However, performing subjective test is difficult task in closed loop rate or quality control method in which the optimal coding parameters are adaptively chosen to compress time-varying signal characteristics effectively. Thus, the compression system typically involves tradeoff between the rate and quality of the output. Undoubtedly, there is a need for an objective quality measure for local and global assessment. Thus assessment of distorted signal quality is an open problem today.

2.6 Evaluation of ECG Compression Methods

In this section, the compression issues in the reported methods are described and investigated with different sets of experiments. Tests are carried out using the `mita` database and the PRD measurement criteria to evaluate the quality of the compressed signal and to select optimal coding parameters. Some of the preliminary experimental results are presented in this section.

2.6.1 Effects of Preprocessing (Mean Removal and Amplitude Normalization)

Mean value of an ECG data plays an important role in the evaluation of the compression method. The compression performance is tested using different ECG databases which consist of ECG signals recorded under different conditions. The nonzero mean value of the signal effects the performance of the compression method. It is found in the literature that some of the compression methods are evaluated with nonzero mean ECG signals. With nonzero mean ECG signals, the performance of compression methods is shown to improve. In a wavelet based compression method [134], the thresholds are selected based on the energy packing efficiency. This reduces the number of significant wavelet coefficients. The preprocessing consists of mean removal and amplitude normalization. This preprocessing technique is given as

$$x_p = \left[\text{zeros}(1,M) \quad \left(\frac{x_i}{x_{max}}\right) - \text{mean}\left(\frac{x_i}{x_{max}}\right) \quad \text{zeros}(1,M)\right] \tag{2.35}$$

where x_p is the processed signal, x_i is the original signal, x_{max} is the maximum amplitude of the original signal and M is the number of zeros. Many authors aimed for this type of preprocessing technique in which amplitude normalization and mean removal guarantee that the magnitudes of all significant wavelet coefficients are always less than one. It is claimed that due to processing, there is no need to assign any bit to the integer part of the coefficient [134]. To evaluate the effect of a nonzero mean value in an ECG signal and the limitations of this type of preprocessing, the following experiment is carried out.

Table 2.7 shows the energy contribution efficiency (ECE) values for six subbands of the first 5.69 second

Table 2.7: ECE values of the approximation and details for 2048 samples of mita record 117

ECE values (%)	without preprocessing			with preprocessing given in [134]		
	with mean	without mean	with mean and P=1024	with mean	without mean	with mean and P=1024
ECE_{A_5}	97.8037	64.0699	99.9026	63.6064	63.6064	63.6064
ECE_{D_5}	0.8999	14.7214	0.0399	13.6024	13.6024	13.6024
ECE_{D_4}	1.1157	18.2517	0.0495	19.4544	19.4544	19.4544
ECE_{D_3}	0.1669	2.7297	0.0074	3.066	3.066	3.066
ECE_{D_2}	0.0105	0.1725	0.0005	0.21	0.21	0.21
ECE_{D_1}	0.0034	0.0549	0.0001	0.0608	0.0608	0.0608

ECG data of mita record 117. In this experiment 9/7 biorthogonal wavelet is used for decomposition of the signal to the six subbands. The input signal has a nonzero mean. The energy values in the third and the sixth columns are obtained with addition of a baseline shift of 1024. It is required to make the samples positive for storage purpose. It is observed that energy distribution as shown in the third column across the bands is most suitable for compression because the signal energy is most compactly packed into the lowest frequency band. But this result is misleading as the energy packing efficiency of the lowest frequency band will increase with a higher mean value. There is no diagnostic information in the mean value. With different mean values, it is practically not feasible to maintain the same signal quality with a fixed ECE value. For proper evaluation and comparison of performances, the mean normalization should be carried out before further processing.

The preprocessing technique cannot always guarantee the absolute value of the largest wavelet coefficients less than one. For example, for the mita record 107, 119, 200, the preprocessed signals have wavelet coefficients with their absolute values greater than one. For record 107, some of the coefficients have values -1.5051, -1.4535, -1.4414, -1.4282, -1.5006, -1.2511, -1.2681, -1.1680, 1.0520, -1.0458 and -1.5684. For coding of the coefficients, the signal is reconstructed after zeroing the integer part of the coefficient as given in the literature [134]. The results are shown in Fig. 2.11. It is observed that this coding procedure does not reproduce the signal faithfully. Due to zeroing of the integer part of the coefficients, visible distortion has occurred. This proves the limitation of the proposed preprocessing technique with the suggestion for zeroing of the integer part of the coefficient.

2.6.2 Effects of Quantization on the Desired RE or EPE Criterion

In threshold based methods, the coefficients are retained based on criteria viz. fixed number of coefficients (FNC) [128], retained energy (RE), energy packing efficiency (EPE) [134], percentage wavelet coefficients zeroed (PWCZ) [137] and desired PRD value [121] [143]. Fixed number of coefficients from the sorted coefficient vector may not assure a very good reconstructed signal quality. High frequency components contained in time varying local waves may be lost since some of these important coefficient may have

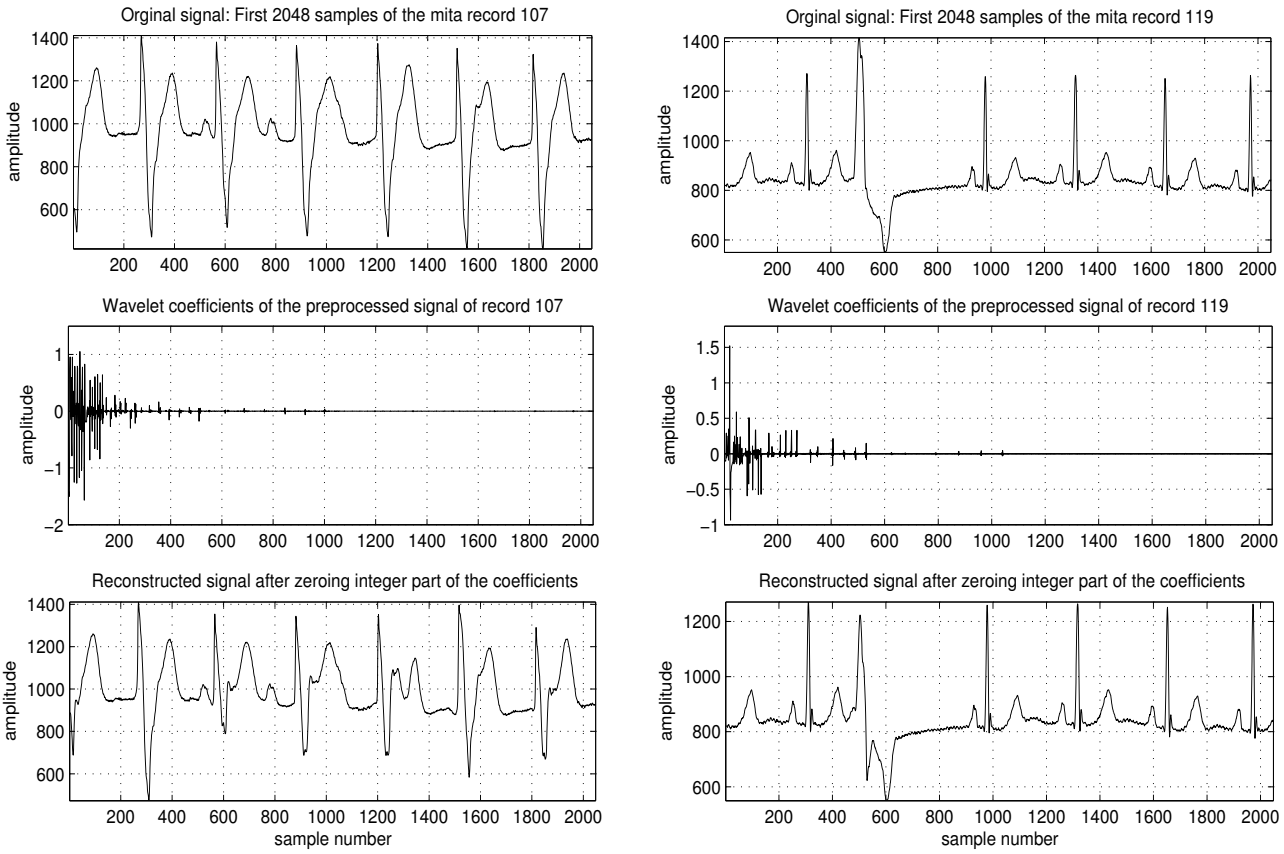

Figure 2.11: First 2048 samples of the `mita` record 107 and 119 and their wavelet coefficients of the preprocessed signals. Reconstructed signals are obtained after zeroing the integer part of the coefficients.

smaller amplitude values. Distortion of the original signal can be observed in two different origins: discarded high order coefficients by thresholding and quantization of retained coefficients. In the reported works, fixed uniform quantization of retained wavelet coefficients has been considered. In many methods, the percentage of RE/EPE was used for guaranteeing the quality of the reconstructed signal. For each block, many coefficients with varying amplitudes are retained in order to achieve a desired percentage of the RE/EPE. If the quantization step used in the next step is chosen to be too large, then some of the retained coefficients may also be rounded to zero because of the large dynamic range of the coefficients. Most of the reported works achieved a target value by adapting the threshold(s) with fixed quantization step.

In this experiment, limitations of a predefined retained energy (RE) or energy packing efficiency (EPE) is evaluated. The quantization is commonly performed using the rounding operation in many compression methods [112, 113]. Some of the methods have shown that the preservation of energy may result in better reconstruction. This criterion may be true if the resolution of the coefficients are preserved. In case of large quantization step sizes, the retained energy may decrease or increase. To demonstrate quantization effects,

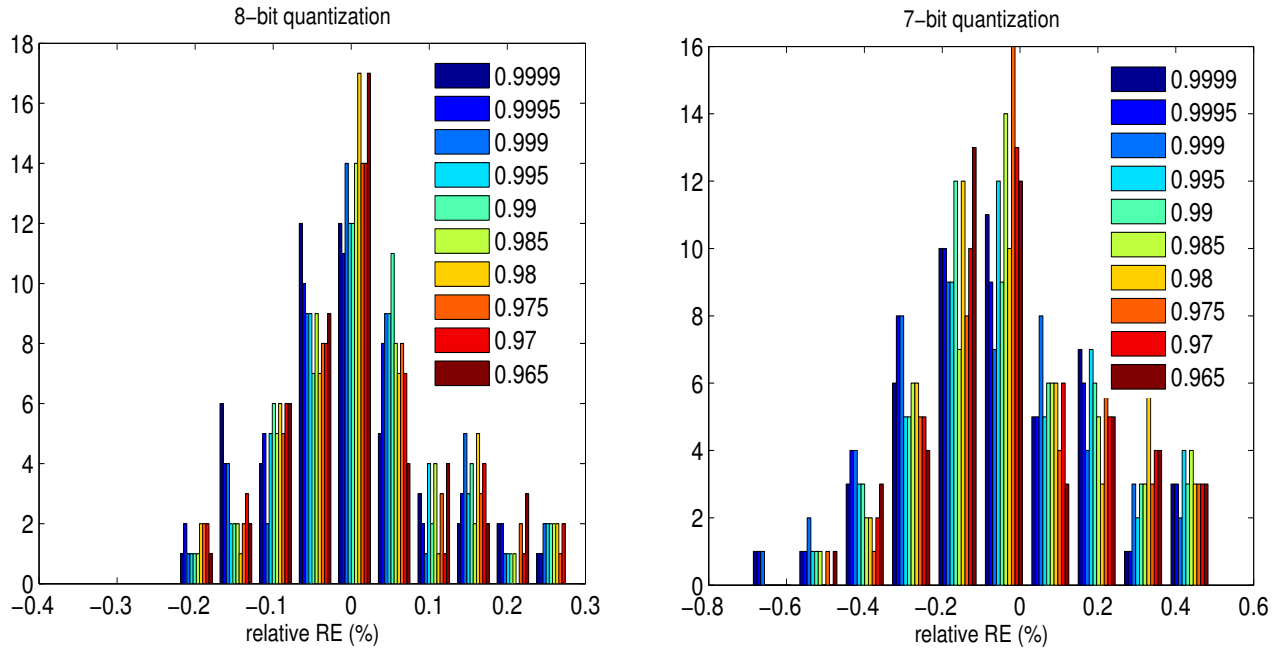

Figure 2.12: Quantization effects on a desired RE. (a) relative RE variations due to 8 and 7-bit quantization.

initial 1024 samples taken from (each) 48 `mita` records are transformed using DWT. These transformed coefficients are thresholded based on retained energy (RE) criteria and then the nonzero thresholded coefficients are quantized using a uniform scalar quantizer with 6, 7, 8 and 9 bits. The experimental results are shown in Fig. 2.12 as histogram plots. The horizontal axis shows the relative error values of between the reconstructed signal energy and the retained energy value. The positive or negative values indicate whether the coefficient is smaller or greater than a predefined value. The vertical axis shows the number of records out of 48 results in the corresponding relative RE value. It is observed that the distribution of this error value has a lower spread for higher number of bits. Higher number of bits will result in better preservation of the targeted energy in the compressed signal. However, the compression performance in terms of CR value will degrade for higher number of bits. On the other hand, lower number of bits will result in better compression performance at the cost of more variation in the retained energy. So, a time varying bit allocation may prove a better solution for the above problem.

The dynamic range is dependent on the nonstationarities of the ECG signal whose morphologies and segments have a time varying characteristics. Hence, fixed quantization step may not be appropriate for compressing the nonstationary ECG signals. Thus, the use of a varying quantization step along with varying number of coefficients by varying threshold T values per block/lead/subject may be suitable for perfect reconstruction of ECG signals with different morphologies. A better compression performance can be obtained by finding the optimum threshold(s) with varying quantization bits.

2.6.3 Effects of Quantization on the Desired PWCZ Criterion

In many ECG compression methods [137], a fixed number of coefficients are retained in order to achieve a certain percentage of the energy. The coefficients are retained based on percentage wavelet coefficients zeroed (PWCZ) criterion. The PWCZ is expressed by

$$\mathrm{PWCZ(T)} = \frac{\mathrm{card(WC_T)}}{dim(\mathrm{WC})} \tag{2.36}$$

where WC denotes the wavelet coefficient vector. It is obtained by ordering the approximation coefficients and the details coefficients. The denominator of the equation (2.36) indicates the dimension of the wavelet coefficient (WC) vector. For a user specified PWCZ, the threshold T is obtained using the dichotomy algorithm. All the coefficients with absolute value less or equal to T are zeroed. The nonzero wavelet coefficient (NZWC) vector is obtained by discarding the zeroed coefficients. These nonzero coefficients are then quantized using fixed quantization in (2.11). This quantization process has a major problem. Noise is introduced in the reconstructed signals if full precision of the minimum value $\mathrm{NZWC_{min}}$ is used for dequantization or a user specified PWCZ cannot be maintained during dequantization. The retained coefficients are further rounded during dequantization or quantization based on the quantizer rule. These effects are shown in Fig. 2.13 and Table 2.8. Figure 2.13 shows the number of additional zeros due to quantization. The results are shown for 48 `mita` records and for different PWCZ (%) values. Two subfigures are shown for results of two block sizes. It is observed that more number of additional coefficients are zeroed for lower values of PWCZ. These additional zeros will introduce unexpected error in the signal and may result in an inefficient compression performance. Table 2.8 shows the percentage increase in the number of additional zeros for two data records with four block sizes. It is observed that more number of coefficients are zeroed with lower values of PWCZ. An ideal solution may be obtained for a PWCZ value of 90%. But this will result in a poor performance of the compression method in terms of compression ratio. For a PWCZ of 80% [[137], Table I], the thresholds are determined for the `mita` records 100, 103, 107, 109, 115, and 119 and quantized. During dequantization, the following number of zeros can be observed: 67, 78, 104, 58, 79 and 118, respectively. Care must be taken as this target cannot always be guaranteed. This experiment shows that study of relationship between these two parameters viz threshold and quantization step is important in target criteria algorithm. In general, the value of PWCZ ranges from 0 to 100. Sometimes the method for example PWCZ of 50% and 70% introduces noise in the reconstructed signal. The reconstructed signals of the record 107 and 119 for the above two PWCZ values are shown in Fig. 2.14. Large noise may be introduced in the reconstructed signal for PWCZ value below 50%. Hence, it requires efficient noise elimination algorithm during post processing. It may affect the shape of the local waves if the noise level is high. This defect makes the algorithm invalid for lower range of distortion level. Hence, the lower bound for PWCZ should be specified for faithful reproduction in ECG signal compression.

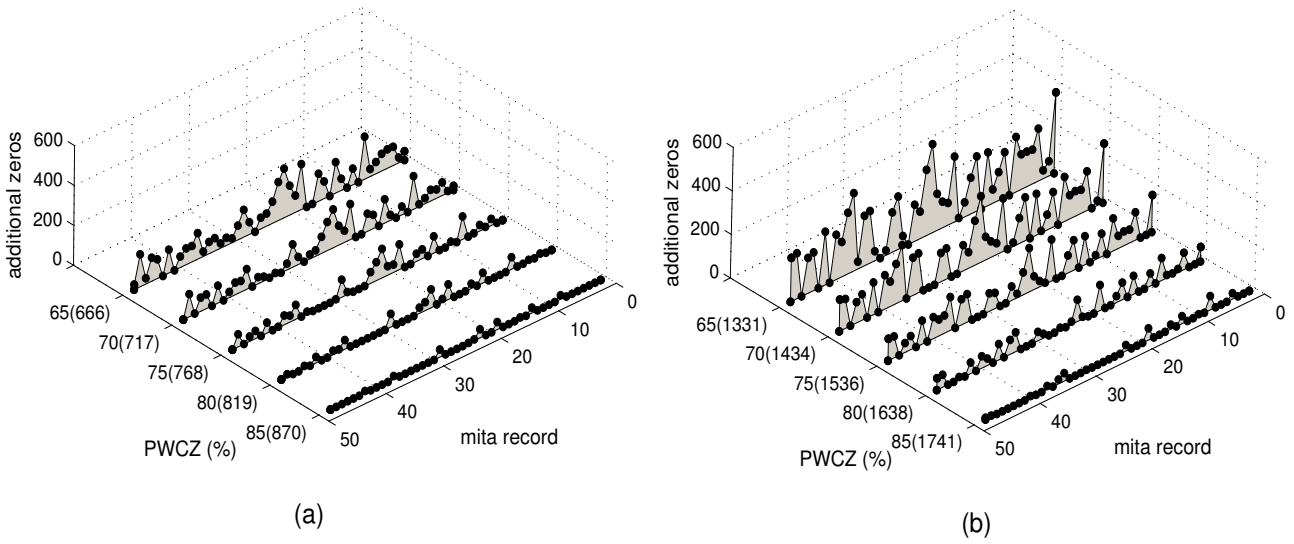

Figure 2.13: Quantization effects on a desired PWCZ (%). The number of zeros for each PWCZ (%) is given within the parenthesis. Additional number of zeros after 8-bit linear quantization as in [137]. (a) for block size of 1024 samples. (b) for block size of 2048 samples.

Table 2.8: Analysis of PWCZ criterion based threshold method: ↑ PWCZ (%) after 8-bit quantization.

Target	N=1024		N=2048		N=4096		N=21600		N=43200	
PWCZ (%)	107(↑ %)	119(↑ %)	107(↑ %)	119(↑ %)	107(↑ %)	119 (↑ %)	107(↑ %)	119(↑ %)	107(↑ %)	119(↑ %)
40	115.09	118.49	76.59	75.85	108.17	113.67	112.77	118.98	**104.76**	**111.14**
50	72.66	74.37	41.60	44.69	66.70	70.66	70.17	75.15	**63.79**	**68.94**
60	43.51	45.31	25.67	8.97	38.89	42.42	41.84	45.94	**36.51**	**40.76**
70	23.29	24.90	14.36	17.14	19.04	22.11	21.56	25.13	**17.00**	**20.67**
80	7.41	9.38	6.34	7.19	5.43	6.83	6.36	9.47	**5.75**	**6.27**
90	0.00	0.65	0.27	0.65	0.00	0.00	0.00	0.00	0.00	0.00

2.6.4 Effects of Quantization on the Desired PRD Criterion

Quality controlled/guaranteed compression methods have used either MSE or PRD for evaluating the compressed signals [137]. In these methods, a desired PRD value is assigned for the compressed signal. In lossy compression method, the loss of information is due to thresholding and quantization of nonzero coefficients. Most compressed methods based on PRD target criterion do not consider the quantization error. Though a desired PRD value is targeted, the final distortion value may vary due to the quantization. This is demonstrated with the results shown in Table 2.9 for selected `mita` records. The results are shown for three target PRD2 values. In this experiment, the desired PRD target value of PRD2_T and PRD2_Q shows the PRD values of the compressed signal. It is observed that the targeted PRD value is not maintained in the compressed signal. Maximum deviation has occurred for target PRD value of 1%. For this target PRD value, the

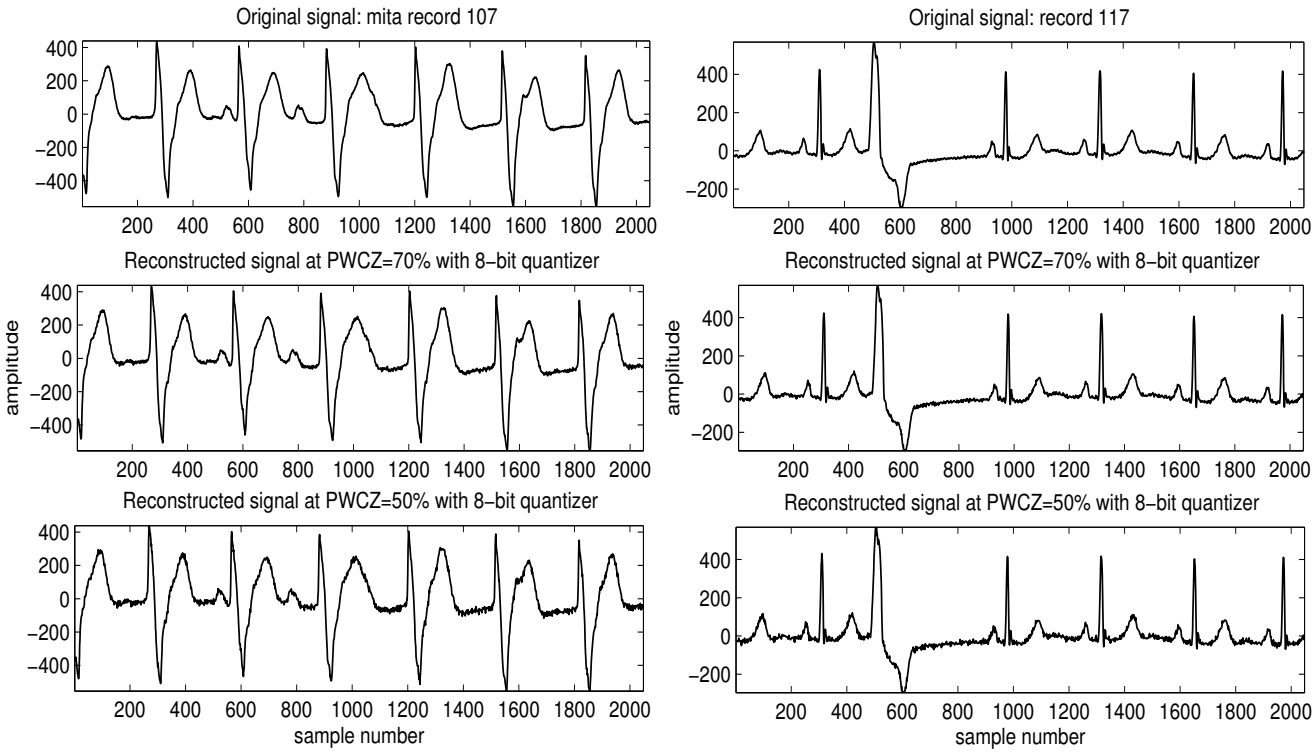

Figure 2.14: Quantization effects on a desired PWCZ (%). The number of zeros for each PWCZ (%) is given within the parenthesis. Additional number of zeros after 8-bit linear quantization as in [137]. (a) for block size of 1024 samples. (b) for block size of 2048 samples.

`mita` 111 record shows two hundred percent increase in its PRD value. Quantization effect is responsible for this deviation from the target PRD value. Though the deviation from the target PRD values reduces due to selection of higher target PRD values, higher target PRD values are not expected from an efficient compression method point of view. Experiments with PRD1 values demonstrate similar results. These results prove that quantization effects cannot be neglected during implementation of quality controlled/guaranteed compressed methods based on target PRD values. In literature, the compression methods have used a fixed quantization step with either a constant or a variable threshold T. It may be useful to estimate the PRD value with quantization error during the iterative process so that its value can be maintained close to the target value. For a fixed distortion level, it is possible to achieve a considerable gain in the CR value by varying both the threshold and the quantization parameters.

2.6.5 Scalar Quantization Approaches for Wavelet Coefficients

In multiresolution ECG signal decomposition, we can observe that there are large numbers of small magnitude coefficients in higher subbands and are only small numbers of large coefficients. Most of the energy in an ECG signal is concentrated in the small size low frequency subbands. Large wavelet coefficients are

Table 2.9: Variation of PRDs with variable T found based on target PRD2 and fixed quantization step.

Test record	PRD2=1%		PRD2=2%		PRD2=3%	
	$PRD2_T$	$PRD2_Q$	$PRD2_T$	$PRD2_Q$	$PRD2_T$	$PRD2_Q$
100	0.96	**1.91**	2.03	**2.33**	2.99	3.12
101	1.04	1.37	2.05	2.14	3.00	3.04
102	0.98	1.51	2.02	2.16	3.00	3.06
103	1.00	1.37	1.95	2.12	3.03	3.10
107	0.98	1.36	1.97	2.11	3.03	3.11
109	1.03	1.34	1.99	2.09	3.00	3.04
111	0.97	**2.15**	2.01	**2.47**	3.03	3.23
115	1.04	1.26	2.00	2.06	3.01	3.03
117	0.98	1.03	2.00	2.01	3.01	3.02
118	0.99	1.10	1.96	2.00	3.02	3.04
119	1.02	1.30	2.01	2.09	2.95	3.00

more important than small wavelet coefficients. Therefore, large wavelet coefficients get quantized accurately while small coefficients are discarded in the compression methods. In this section, we investigate the performance of different approaches for quantization of the wavelet coefficients of the ECG since there is a tradeoff between signal quality and bit rate (or degree of quantization).

Scalar quantization is an example of a lossy compression method where it is easy to control the CR or quality. The quantization error is perceived as noise or distortion that depends on the type quantizer. The uniform quantizer is the most commonly used scalar quantizer due to its simplicity. It is also referred as a linear quantizer in some of the compression methods. In USQ, the decision levels are uniform and the reconstruction levels are also equally spaced and located in the middle of the decision levels [195, 196, 200]. There are many ways to choose the decision levels or boundaries and the output or reconstruction levels. We concentrate on the uniform scalar quantizers such as midtread quantizer, midrise quantizer and dead zone quantizer in this section. To design a uniform quantizer, we have to determine the dynamic range of the coefficients vector, the desired coefficients resolution (number of quantization levels) and select the proper type of quantizers (e.g., midtread or midrise or dead zone). The quantizer is generally described as a function Q that maps a transformed coefficient to a quantization index q. For a given wavelet coefficient c, the quantizer output is a signed integer q given by $q = Q(c)$. Given q, the decoder produces an estimate of c as $c = \overline{Q^{-1}}(q)$ [195]. These quantizers are completely characterized by the quantization step size Δ. Since the midrise quantizer does not have the zero output level, large number of small magnitude wavelet coefficients are quantized into first output level. This may introduce quantization noise and its magnitude depends on the quantization step size. The quantization noise may result in some noticeable distortion of amplitude, duration and shape features of the ECG segment at lower quantizer resolution. Although the midrise quantizer has more number of output levels, it will introduce the quantization noise and the signal

distortion caused by rounding and clipping of the coefficients simultaneously. The quantization noise can be avoided in compression system by accommodating the zero output value. The zero output level is useful in waveform coding scheme where we need to represent zero value of the signal or in transform coding where we set large number of small coefficients to zero. Due to this reason, the midtread quantizer is popular in the transform coding scheme.

We study the performance of these quantizers using the ECG signal block from the commonly used `mita` records 107, 117 and 119 [137, 142, 143, 203]. In this study the block size of 1024 samples is chosen and then the wavelet coefficients obtained for the 5-level 9/7-tap filters DWT of the signal block are directly quantized using the above three quantizer with different resolution $b = \{6, 7, 8, 9, 10\}$. The quantization and the dequantization are performed according to the expression for the quantizers presented in section 2.3.5. For each quantizer resolution, the entropy H_Q in bits per coefficient is determined without entropy coding. The PRD1 and PRD2 criteria are used to measure the distortion between the original and the compressed signals. To reveal the visual quality of the compressed signals, the original signal and the compressed signals obtained with 6-, and 8-bit quantization for records 107, 117 and 119 are shown in Fig. 2.15. The compressed and original signals are examined to obtain the subjective quality ratings. Fig. 2.15(a) shows that the clinical features are distorted due to quantization noise introduced by the midrise quantizer. As can be seen in Fig. 2.15(b), the clinical features are preserved in the compressed signals when the midtread quantization is employed. Furthermore, the main effect of the smoothing of background noise can be seen for higher quantizer resolution since the coefficients due to noise that lie inside the zero zone interval are quantized to zero. Therefore, we give more importance to midtread quantizer and its variants. Table 2.10 shows the entropy of the midrise and midtread quantizers with various numbers of quantization levels, the subjective ratings and the PRD values. Note that PRD2 is commonly used for comparing the compression performance with other algorithms, and the number of bits required for quantization is selected according to the measured PRD2 value. But we have considered PRD1 measure for comparison purposes. Experiment shows that midtread quantizer achieves good rate-distortion performance and the output of this dequantizer is free from quantization noise. There are two main sources for signal distortion:1) the zeroing of the wavelet coefficients in the zero zone interval and 2) the quantization of the coefficients in the outer zone interval. An increase of step size can lead to higher compression, but ”very bad” quality of compressed signal. It is well known that signal distortion and rates are controlled by the widths of the zero zone and the outer zones applied for quantization. Since the zero zone and the outer zone widths are equal to the step size Δ, the midtread quantizer may not be quite flexible to control the tradeoff between the rate and signal distortion.

Since large zero zone quantization rule is often used in many transform based image and video coding schemes [195, 198, 199, 201], we also apply this approach to quantize the wavelet coefficients of the ECG signal [202]. The zero zone quantizer is characterized by two parameters such as zero zone width and outer zone width. In many applications, the width of the zero zone is equal to twice the outer zone width.

Table 2.10: Performance of the midrise, midtread and zero zone quantizers.

mita Record	b	Midrise quantizer, $Q1$				Midtread quantizer, $Q2$				Zero zone quantizer, $Q3$				COMP($Q3, Q2$)	
		H_Q	PRD1 (%)	PRD2 (%)	MOS	H_Q	PRD1 (%)	PRD2 (%)	MOS	$H(b)$	PRD1 (%)	PRD2 (%)	MOS	H_Q % ↓	PRD1 % ↑
107	6	0.7366	16.2916	15.9658	2	0.919	4.015	3.935	3.5	0.725	5.393	5.285	1.5	21.110	25.552
	7	0.9943	8.3299	8.1633	2.75	1.205	2.372	2.324	4.25	0.990	3.132	3.069	3.5	17.842	24.266
	8	1.3011	4.4261	4.3376	3.5	1.633	1.550	1.519	5	1.299	1.939	1.901	4.75	20.453	20.062
	9	1.7664	2.4088	2.3606	4	2.243	0.940	0.921	5	1.764	1.258	1.233	5	21.355	25.278
	10	2.4608	1.3122	1.2860	4.75	3.015	0.545	0.534	5	2.460	0.747	0.732	5	18.408	27.042
117	6	0.7896	17.4699	4.7516	1.25	1.090	5.936	1.615	4	0.791	7.488	2.037	1.75	27.431	20.727
	7	1.1966	9.2168	2.5069	2.75	1.579	3.731	1.015	4.5	1.190	4.839	1.316	4	24.636	22.897
	8	1.7582	5.2628	1.4314	3.5	2.379	2.244	0.610	4.75	1.747	3.151	0.857	4.5	26.566	28.785
	9	2.6648	2.9114	0.7919	4.25	3.312	1.164	0.317	5	2.661	1.796	0.489	5	19.656	35.189
	10	3.8305	1.4945	0.4065	4.75	4.174	0.571	0.155	5	3.830	0.804	0.219	5	8.242	28.980

This quantization rule is followed here to study its rate-distortion performance. The entropy rates of the zero zone quantizer with different resolutions are summarized and their compressed signals are shown in Fig. 2.15(c). As shown in Table 2.10, the midtread quantizers obtain better compression performance than midrise quantizer. In Fig. 6, we compare the zero zone quantizer $Q3$ with the midtread quantizer $Q2$ approach. Since the objective measure will be employed in an automatic quality control system, we have considered the measured PRD1 values instead of MOS values for performance comparison. At the range of $6 \leq b \leq 10$, the average H_Q of $Q3$ and $Q2$ are 1.4476 and 1.8030, respectively and the average PRD1s of $Q3$ and $Q2$ are 2.493 and 1.844, respectively. The H_{Q3} is improved by 19.71% at the cost of increased PRD1 of 24.44 % for the specific ECG signal from the mita 107. The behavior of the quantizer is same for other signals from the mita 117 and 119. Experiments show that the performance of the quantizers depend on the distribution of the wavelet coefficients of the ECG signal. Thus, for a given distribution, the optimal quantizer can be completely described by the parameters such as zero zone width and outer zone width.

In [203], a larger zero-zone (defined by threshold T) is expected to set more high-frequency coefficients to zero in order to achieve high compression performance [203]. The authors observed that for good compression performance Δ should be among $1.2T - 1.8T$. Finally, they fixed the relationship between the quantization step size Δ and the threshold T as $\Delta = 1.55T$ which is a satisfactory choice for ECG signals tested. However, this fixed relationship may not always result in good compression performance for the ECG signals with varying PQRST morphologies [202]. The reason lies on the fact that although a large threshold T preferred for the zero zone is ensured by selecting a large quantization step size Δ, the outer zone with this Δ value can produce unacceptably large clinical distortion due to rounding or clipping of the significant coefficients. Unfortunately, smaller outer-zone width leads to lower compression ratios with good compressed signal quality. Furthermore, global quantization approach may introduce severe clinical

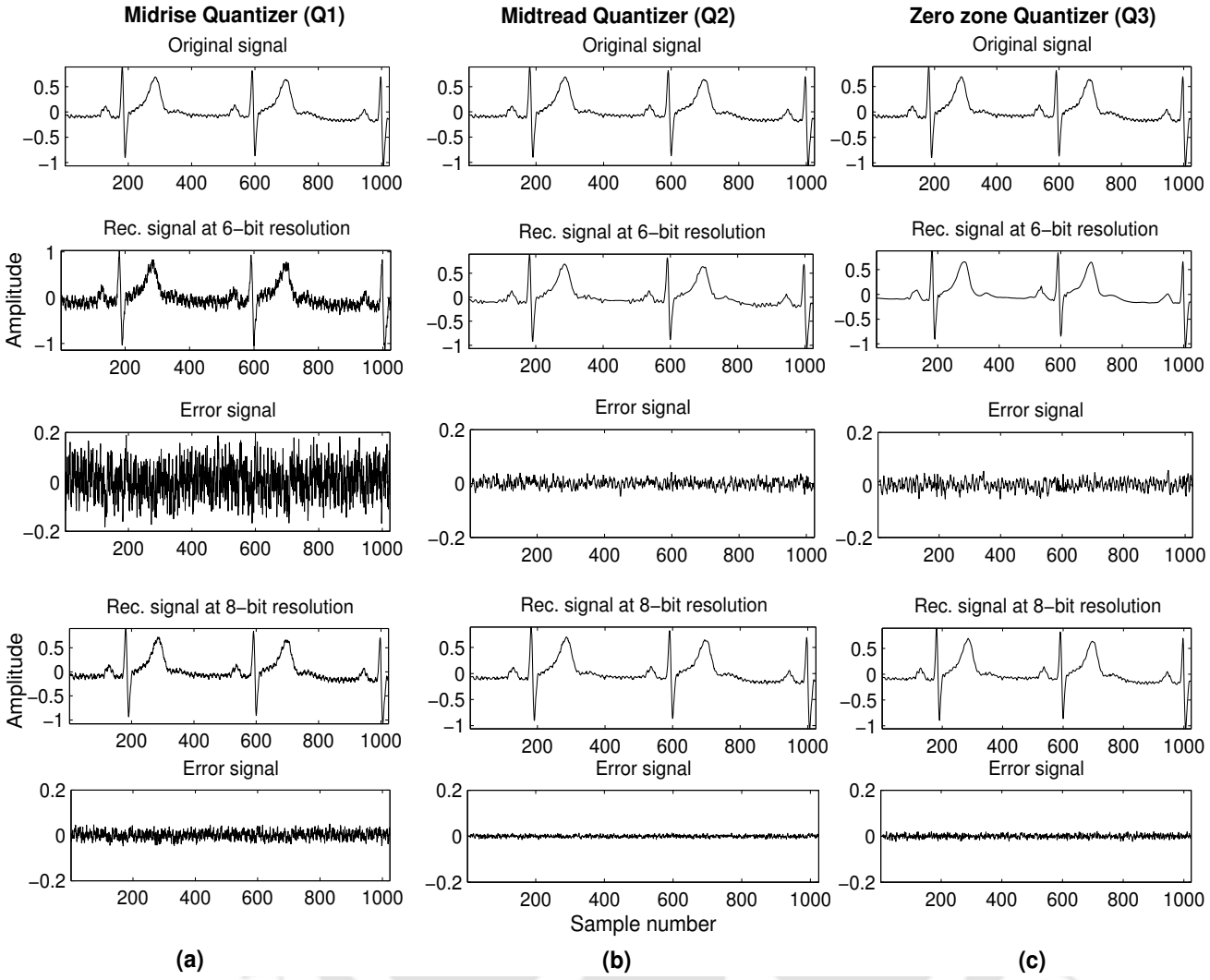

Figure 2.15: Performance of the uniform scalar quantizers for 6- and 8-bit resolution: (a) Midrise quantizer, (b) Midtread quantizer, (c) Zero zone quantizer ((with the zero zone width to be twice the outer zone width).

distortion since more small magnitude coefficients are set to zero due to large step size Δ obtained for large dynamic range of the wavelet coefficients vector. The question is how to quantize the wavelet coefficients most efficiently. In [202], to improve the compression performance, the zero zone quantizer is applied to the three frames of the coefficients created based on the energy contribution efficiency of the subbands. However, there are the questions of how many quantization levels and what type of reconstruction values (e.g. centroid, uniform) used to give reasonable good compression performance.

In [143], the wavelet coefficients are thresholded with a threshold T found iteratively for a user specified PRD2 value. In the next step, the nonzero wavelet coefficients (NZWC) are quantized adaptively by the linear quantizer as in (2.16) of the lowest possible resolution. This adaptive quantization strategy provides an optimal dynamic bit allocation according to the nature of each ECG signal if the threshold T is greater

than half of the step size of midtread quantizers [202]. If the rate-distortion property of a zero zone quantizer in terms of zero zone and outer zone widths can be exploited, it is possible to reduce the computational cost. Moreover, an optimal quantizer design requires a distortion criterion since the uniform scalar quantizers are optimized in an operational rate-distortion sense. In fact, the quantization and dequantization introduces distortion to the compressed signal. The PRD2 is used as a distortion criterion since it is easy to calculate and compare. Although it does not mean that a lower PRD2 value provides a better clinical quality, this criterion is often used in the literature to choose a quantizer resolution. Because the subjective quality criterion is so difficult to adopt in minimization problem of the optimal quantizer design, a meaningful objective distortion criterion which measures the quantization errors is required to achieve optimal compression. In general, an optimal choice of the quantization parameters viz. zero zone width and the outer zone width with an effective distortion criterion can provide a good rate-distortion performance. The above issues will be considered in a design of optimal quantizer in this work to retain the coding performance and to provide a simultaneous signal denoising and compression.

2.6.6 Quality Controlled Coding Methods Based on PRD and WWPRD Criteria

In general, the optimal coding parameters are chosen according to a criterion specific for the application [145]. Since quality is essential for diagnosis, some quality-controlled ECG coding strategies are reported based on the PRD criterion. But PRD does not always correspond to a better clinical quality [140, 145]. Meanwhile, wavelet based schemes are commonly tested using the `mita` database which contains many noisy records [145]. Lu et al. [145] notice, in their evaluation of the quality of compressed signal, that the chief effect of wavelet compression is the smoothing of the low-level background noise. Otherwise, the clinical features appear to be faithfully preserved. Ku et al. [140] quoted that at the range of $4 \leq$ compression ratio $(\mathrm{CR}) \leq 12$, SPIHT [145] is slightly better than NRDPWT-6 [140]. This result is because of noisy ECG signals in the datasets. The wavelet coefficients due to noises are observed in low octave bands and these coefficients are fast removed by the quantization scheme [140]. This property may cause to lower the whole coding performance of the method in the usage of highly noisy signals. When the noise elimination process is not used prior to the compression process, there exists a practical difficulty in treating the noisy signals. This emphasizes the need for noise elimination or measure algorithm in the preprocessing stage. But there will be a difficulty in evaluating the quality of the denoised signals in the case of noise filtering algorithm at this stage. In threshold based methods, the threshold is beat-to-beat automatically updated according to the measured noise power using the high-pass filtering (cutoff frequency equal to 20 Hz) in the repolarization interval. In this method, the optimum threshold for which the RMS is minimum is reached when the power of the discarded coefficients equals the noise power estimated in the preprocessing stage. But measurement of noise power of ECG beats whose local waves and segments have a time varying characteristics is difficult in the general case. The threshold may not be optimal when the discarded coefficients vector contains small wavelet coefficients of the high-frequency

Table 2.11: Illustration of the adaptive quantization strategy using the mita record 117.

Quantizer resolution (b)	PRD_{tar}=2%, PRD_T=1.99%					PRD_{tar}=0.5%, PRD_T=0.496%				
	QPRD2 (%)	QPRD1 (%)	Threshold (T)	Step size (Δ)	Entropy (H_Q)	QPRD2 (%)	QPRD1 (%)	Threshold (T)	Step size (Δ)	Entropy (H_Q)
6	2.15	7.95	15.78	18.44	0.68	1.87	6.93	2.06	18.44	1.67
7	2.03	7.51	15.78	9.15	0.75	1.13	4.18	2.06	9.15	2.02
8	2.00	7.39	15.78	4.56	0.81	0.69	2.54	2.06	4.56	2.34
9	1.99	7.36	15.78	2.27	0.87	0.54	2.01	2.06	2.27	2.61
10	1.99	7.36	15.78	1.14	0.93	0.51	1.89	2.06	1.14	2.90

PRD_T denotes the obtained PRD after the thresholding process (before quantization).

components of the local waves. Moreover, this noise measurement criterion is difficult to incorporate in well designed SPIHT algorithm which codes the wavelet coefficients by exploiting the redundancies among wavelet scales. Noise decreases the CR of the SPIHT coder for a specified PRD value since the coder will spend extra bits on approximating the noise with the specified accuracy. Furthermore, the choice of the distortion criterion that must be used in quality control is of critical importance when noise suppression and signal compression is established simultaneously. In this experiment, the performance of the recently reported wavelet thresholding based method [143] which outperforms other methods is tested using the widely used mita database records and the PRD2 measurement criterion. We study the performance of this method for a user specified PRD2 value based on the following parameters and dataset used in the implementation [143]: $N = 43,200$ samples, 5-level, bior4.4 wavelet, $b = \{6,7,8,9,10\}$ and test dataset: mita records 100, 101, 102, 103, 107, 109, 111, 115, 117, 118, and 119. Two criteria such as the PRD2 and the entropy H_Q of the quantizer are considered. Table 2.11 illustrates the adaptive quantization strategy when applied to the mita record 117 for the user specified PRD2 values of 2% and 0.5%. The QPRD2 (PRD2 after quantization) is found for each quantizer resolution. The tolerance for the adaptive thresholding and the adaptive quantization strategies are chosen equal to $\varepsilon = 1\%$and $\varepsilon_Q = 10\%$, respectively. Note that the mean of the signal block is -0.8172. As we have demonstrated in the previous section that the PRD1 is better than the PRD2 and the PRD3 measures, the QPRD1 is thus calculated and preferred here to select an optimal quantization bit for a specified tolerance ε_Q. Table 2.11 shows that QPRD2 increases when the quantizer resolution b decreases while the dynamic range of the nonzero wavelet coefficients (NZWC) vector is fixed. Since the threshold T is greater than $\frac{\Delta}{2}$, the increment of the QPRD2 values is mainly due to the round off error and the overload error. From Table 2.11, it is clearly noticed that for $b = 6$ the linear quantizer fulfills the requirement that is $\varepsilon_Q = 10\%$. Note that the QPRD1 value is 7.95% for this quantizer resolution. For a specified PRD_{tar}=0.5%, it is clear that T is smaller than $\frac{\Delta}{2}$ for a set of $b = \{8,7,6\}$ and then the resulting errors are due to quantized nonzero wavelet coefficients (QNZWC) and zeroed nonzero coefficients. It is also observed that the quantizer may not fulfills the tolerance requirement

Table 2.12: Local and global objective error measures.

mita Record	Bit rate controlled SPIHT								Quality controlled SPIHT		
	target CR	Error Measures	Local/Subband Error, PRD_s (%)						global / **total** (%)	target value	obtained CR	decreased CR
			A_5	D_5	D_4	D_3	$\mathbf{D_2}$	$\mathbf{D_1}$				
100	8:1	PRD1	2.83	1.72	2.54	4.49	33.83	84.11	4.93	4.93%	5.5:1	31.2%
		WWPRD [190]	0.86	0.31	0.52	0.71	**3.26**	**4.77**	**10.43**	10.43%	3.92:1	51%
107	16:1	PRD1	3.01	4.67	18.93	34.72	78.34	99.89	4.851			
		WWPRD [190]	**2.09**	0.74	1.35	1.38	**1.90**	**1.19**	**8.65**			

for $b = \{8,7,6\}$. This experiment shows that computation time of the adaptive quantization strategy can be reduced by providing some constraint. Finally, average compression performances are studied using the same dataset for the target PRD2 value of 2.75%, 3.30% and 4.65%. This test is performed to determine the QPRD1 value and to evaluate the compressed signal quality. The QPRD2 values of 2.89%, 3.51% and 4.84%, and the QPRD1 values of 5.15%, 6.31% and 8.63% are obtained for average b values of 7.73, 7.18 and 6.82, respectively. The local waves of some of compressed signals are distorted for the target PRD2 value of 3.30%. From this experiment, the deficiency of the PRD2 as a quality measure is demonstrated and also the problems of this adaptive quantization strategy are illustrated to provide a faster and better adaptive quantization mechanism with meaningful distortion criterion.

In this experiment, the performance of the SPIHT coding strategy [145] is evaluated using signal block of 1024 samples. The high efficiency, high speed, and low complexity make the SPIHT algorithm an attractive candidate for compression of biomedical signals [145]. Note that the performance of the threshold based methods depends on many optimal parameters. Since the 9/7-tap biorthogonal wavelet (BW) filters for WT and SPIHT coding are proven to offer an excellent coding gain [145], they are also adopted here. We hereby show the effectiveness of the PRD1, and WWPRD criteria based quality controlled SPIHT coding strategy. The ECG signals from the `mita` record 100 and 107 are compressed at CR=8:1 and CR=16:1, respectively. The original and the compressed signals are shown in Figs. 2.16(a) and (c), respectively and the behavior of local and global error measures are shown in Table 2.12. In WWPRD criterion, insignificant errors in bands D_2 and D_1 dominate the global error while significant errors in other bands are low. Thus, the selection of upper bound distortion (D) level is very difficult since the WWPRD measure is not subjectively meaningful in the sense that the small and large values correspond to "good" and "bad" quality, respectively [see Fig. 2.16 and Table 2.12]. Moreover, experiments show that the rate-distortion performance of the SPIHT coder is poorly seen in the PRD1 and WWPRD measurement criteria. The signal block from the `mita` record 100 with SNR=45 dB is compressed for PRD1=4.93% and WWPRD=10.43% which are obtained for a target CR value of 8:1 [see Fig. 2.16(a) and (b)]. The compression ratios achieved are 5.5 and 3.92, respectively. Thus, the compression ratio is decreased by 31.2% and 51%, respectively [for example, 100*((8-5.5)/8)=31.2%].

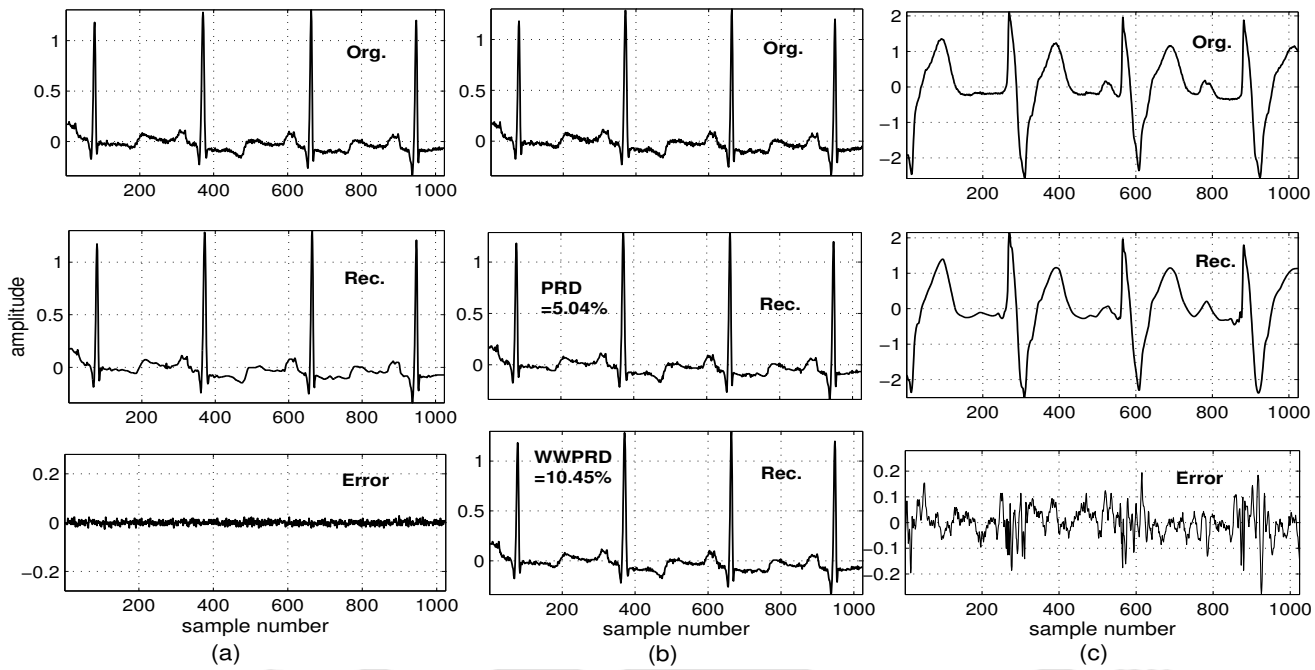

Figure 2.16: Compression results of the SPIHT coder. (a) `mita` rec. 100 (CR=8:1, PRD=4.93% and WWPRD=10.43%). (b) Compression of noisy signal for a target error percentage: At the case of PRD=5.04% and WWPRD=10.45%, the compression ratios of SPIHT are 5.5 and 3.92, respectively. (c) `mita` rec. 107 (CR=16:1, PRD=4.851% and WWPRD=8.65%).

This phenomenon is shown in Fig. 2.16(b) which reveal the clinical quality of the compressed signals for each specified error percentage. We observe that not only the significant feature is retrieved, but also the signal quality is upgraded because the insignificant coefficients dominated in subbands D_2 and D_1 are removed for data compression. For a given quality specification, rate-distortion performance of the well designed SPIHT based quality controlled compression methods based on the PRD and WWPRD criteria is poor due to noise coding. Therefore, in order to introduce automatic quality control one needs an adequate objective distortion measure for measurement of error of the compressed signal.

2.7 Motivation for the Present Research Work

The wavelet transform has proven to be an effective tool in noise reduction, clinical features extraction and particularly ECG data compression because of its interesting properties such as time-frequency localization, energy compaction, cross-subband similarity and straightforward implementation, etc. Therefore, in recent years many wavelet transform based ECG compression schemes have been attempted by biomedical research community. By examining the ECG signals, the facts can be concluded that the ECG beat signals generally show the short-term correlation between adjacent samples, the considerable similarity between adjacent ECG beats (long-term correlation) and between the intra-lead ECG beats. Most existing

wavelet based ECG compression schemes exploit such correlation between adjacent samples and correlation between adjacent ECG beats. These schemes are classified into two major groups: the one-dimensional (1-D) ECG compression and the two-dimensional (2-D) ECG compression. In the first group, the wavelet transform directly to the one-dimensional ECG data and in the second group, the compression scheme deals with two-dimensional (2-D) transformation of the ECG data. Although the 2-D wavelet based ECG data compression scheme achieves higher compression efficiency but it is acceptable for most clinical compression for storage purposes except for real-time transmission of such data. For example, if one frame includes 600 seconds of ECG data, the latency is at least 10 minutes. Therefore, it is an off-line algorithm.

The 1-D ECG compression schemes are simpler but their compression efficiency is lower. Generally, the 1-D ECG compression schemes consist of following steps: 1) preprocessing (blocking, mean removal, elimination ECG artifacts), 2) wavelet transformation, and 3) coding of wavelet coefficients. As far as block size is concerned, increasing block size increases compression rate for a given distortion but also increases computation time and memory requirements of the adaptive wavelet coding schemes. Thus, the decision about block size in the ECG compression is fundamentally open. However, various experiments show that increasing the block size above a certain point results in a very low compression rate gain while the computation time significantly increases and also the quality assessment of local distortions will be more complex. The usual duration of computer evaluated ECG records is 10 seconds.

The signal block extracted from the raw ECG records may contain mean, noises and varying characteristics of various PQRST morphologies. But the mean and noises do not contribute any medical importance during clinical evaluation of the ECG signal. The effects of processing signal block with mean value in the wavelet thresholding based method with different desired criteria are demonstrated in our works. The experiments show that the mean value affects the amplitude distribution of the wavelet coefficients, increases significantly the variance of the wavelet coefficients vector of the signal block. Thus, the coding parameters such as threshold T and quantization b are not optimal in the case of mean preservation. Therefore, each signal block is preprocessed for subtracting its mean value prior to wavelet decomposition stage. Mean removal does not alter the clinical features present in the signal block whereas filtering of varying frequency characteristics of various noises may introduce clinical features distortion. The compression method presented in this Chapter apply directly over the zero-mean ECG signal block without any pre-filtering. The ECG signal can, in any case, be preprocessed as usual in order to reduce the noise level. Nevertheless, wavelet filtering that is implicitly performed when implementing the thresholding or/and quantization, making the system robust and allowing the direct application over the raw ECG signal.

According to the techniques used for coding of wavelet coefficients, these techniques can roughly be divided into three categories: vector quantization schemes (direct VQ, adaptive VQ, tree vector VQ, mean shape VQ, and gain shape VQ, etc.), tree based schemes (EZW, SPIHT, modified EZW, modified SPIHT, and layered SPIHT, etc.), and threshold schemes (rate or quality driven threshold adaptation with fixed USQ, RE or FPWCZ driven threshold adaptation with fixed USQ, and subband coefficient coding using USQ,

etc.). Among low computational complexity schemes, many are based on wavelet coefficient thresholding. Many wavelet thresholding schemes apply thresholding followed by fixed linear quantization approach but it may introduce a severe signal distortion. Since a vector consists of wavelet coefficients with different dynamic range, it is not efficient to allocate a fixed number of bits to represent wavelet coefficients because of the varying characteristics of various ECG signals. Even if we assign different but fixed numbers of bits to wavelet coefficients according to dynamic range of the vectors, the coding efficiency may still be poor because of wavelet coefficients with great magnitude differences within the coefficients vector of a ECG signal. It is observed that each of the subbands has a different energy level and variance, with less energy being in the higher detail subbands. Thus, each signal (each frame in case of classification) is quantized using a separate quantizer so as to quantize different wavelet coefficients in different subbands or frames according to their variance or energy. Thus, we need frame classification and dynamic bit allocation schemes.

Most of the threshold based schemes are based on a two-stage design, where the wavelet coefficients are hard-thresholded first and then nonzero wavelet coefficients are quantized using the fixed USQ schemes. The uniform midtread quantizer has the zero-zone and outer-zone regions and is completely specified by the quantization step size Δ. In such a case, as a result of two separate thresholding processes a greater number of wavelet coefficients are set to zero than is actually required. For a given zone width Δ, the number of small wavelet coefficients around the zeroth zone to be zeroed meanwhile the resolution of the significant coefficients required to be preserved are modified simultaneously. In this scheme, the loss of information can be seen to have two different sources: discarded wavelet coefficients concentrated around zero in their distributions and the quantization of nonzero wavelet coefficients. Then these schemes do not guarantee a user-specified specification at the output of the quantizer. Moreover, these schemes do not reaches desired specification accurately and smoothly. The relationship between the T and Δ has a strong impact in compression rate and distortion. Thus, we need a threshold driven zero-zone quantizer, where the zero-zone of a quantizer is limited by the threshold found in the previous stage, in order to guarantee a user-specified specification in the two-stage design based adaptive wavelet compression scheme. In two-stage schemes, thresholding and quantization are performed independently. In guaranteeing algorithms, it is possible to reduce the computational cost if the similarity between the threshold and the zero-zone width of a quantizer is exploited in rate-distortion sense. Furthermore, considerable gains in compression performance can be achieved if the optimal choice of the zero-zone width T for thresholding and the outer-zone width Δ for quantization is used for compression of the wavelet coefficients.

A major design goal of any wavelet based scheme is to achieve low reconstruction error with the high compression ratio using the optimal coding parameters (e.g., the threshold T and the outer-zone width Δ) chosen according to a criterion specific for the application. In literature, the optimal parameters are usually chosen based on the criteria such as compressed data rate (CDR), retained energy (RE), energy packing efficiency (EPE), percentage of wavelet coefficients to be zeroed (PWCZ) and quality specification mea-

sured using the PRD index. The CR, RE, EPE and PWCZ criteria can be easily measurable in closed loop control. However, the overall coding performance is commonly evaluated in an operational rate-distortion (R-D) or rate-quality (R-Q) curve. This curve provides a maximum compression rate achievable for a desired distortion (D_L) level. In such a case, the distortion measurement criterion is also important to perform the compressed signal quality evaluation. However, the quality and the bit rate are the tradeoffs that must be considered simultaneously. But measurement of distorted signal quality is a challenging problem in the ECG signal denoising and compression methods. The quality measures used to quantify the dissatisfaction of the distorted ECG signal in the literature can be classified into two groups: subjective and objective. The subjective test is the obvious way of measuring clinical quality. However, such a subjective test is tedious, time consuming and results depend on various other factors such as the physicians background, motivation, etc. Moreover, it cannot be incorporated into automatic quality controlled compression systems. On the other hand, objective measure is repeatable and simple but it does not always match with the subjective one. Thus, assessment of distorted signal quality is an open problem today.

Since signal quality is essential for diagnosis, in recent years, the well-designed compression schemes are devised for guaranteeing reconstruction quality measured using the PRD index between the reconstruction and the original signal. Although PRD does not well correlates with the subjective evaluation, it is widely used in the ECG compression methods because of its simplicity. It is shown that although some distortion measures correlate well with subjective quality measure for a given compression scheme, they are not reliable for an evaluation across different schemes. Therefore, the objective measure should be coder-independent, so that it can compare the subjective qualities of various compression methods possibly entailing quite different types of distortion introduced in the coding process. The above facts have motivated a great deal of research on weighted distortion measures. The weighted PRD is suggested to quantify the distortion of the selected local waves. However, an open problem on the this criterion is how to determine the weights for each local waves viz. P, Q, QRS, etc.. The weighted diagnostic distortion (WDD) measure correlates well with subjective test but it suffers from high computational complexity, and there is no standard protocol for its implementation. Another simple measure is the wavelet based weighted PRD (WWPRD) that provides a local or subband error estimation, with weights equal to the normalized absolute sum of wavelet coefficients in the corresponding subbands. But insignificant errors in higher subbands dominate the global error while significant errors in other bands may not reflect any contribution to the global error. This may lead to confusion in the judgement of the quality of the compressed signal. Thus, the conventional PRD and WWPRD measures are not subjectively meaningful in the sense that the small and large values does not correspond to “good” and “bad” quality of the compressed signal, respectively.

Moreover, in literature, the tests are carried out using the well-known `mita` database which contains varying characteristics of various ECG signals and different noises. The effect of noise filtering is one of the features in the wavelet transform based ECG signal compression, and is also noticed in the various compression works reported in the literature. This property may cause to lower the whole coding performance

of the method in the usage of highly noisy signals. This lies on the fact that noise degrades the compression performance of the coder since the coder will spend extra bits on approximating the noise with the specified distortion accuracy. In this case, the direct comparison of compression performance of the different methods are meaningless since the PRD and the WWPRD criteria do not reflect the actual behavior (noise filtering and signal distortion) of the compression methods. The well-designed compression method fast removes the wavelet coefficients due to high-frequency noises dominated in higher subbands for data compression, and thus the wavelet based method may cause a large PRD value but no clinical feature distortion for a user-specified PRD value. This is demonstrated and discussed well in Chapter 2 by implementing the quality driven DCT based ECG compression and quality driven wavelet based ECG compression methods. Experiment shows that one cannot adopt the PRD ranges defined for the quality groups, which are expressed for the particular compression method, to guarantee the preservation of the clinical features of the compressed signal obtained using the different compression methodologies. As a remedy, one can then suggest ideal filtering of the noise. Although noise elimination process is used prior to the compression process, the filtering algorithm may degrade the quality of the signal, and there exists a practical difficulty in measuring the quality of denoised signal in closed loop rate or quality control algorithms. On the other hand, the choice of which distortion measure must be used for compressed signal is of critical importance when noise suppression and signal compression are established simultaneously and the input noise level is difficult to estimate or avoid. The above issues should be considered even the quality control mechanism reaches a desired specification within the predefined accuracy. The conventional PRD measure is performed in time-domain and the diagnostic meaningful WDD measure is performed in feature-space domain. But wavelet based schemes provide the good signal reconstruction quality and the high compression ratio simultaneously. The most widely used objective quality criterion for the distorted ECG signal is the PRD and therefore they apply the inverse wavelet transform to the de-quantized coefficients in order to perform the PRD measurement in time domain in the adaptive algorithm. This may increase the computational complexity of the quality driven wavelet based compression scheme.

The above constructs show that in order to provide a better automatic quality control for wavelet based compression of cardiovascular signals, we need three most important components: a well-designed adaptive subband coding methodology, a meaningful objective quality measure for local and global assessment, and simple automatic quality control algorithm to perform the quality control quickly and accurately. This research work attempts to present a better quality driven wavelet coding scheme by considering the design philosophy of those components.

3

Adaptive Subband Coding Based on Threshold Control Zero-zone Quantizer and Index Coder

Contents

3.1 Introduction

A fundamental goal of data compression is to reduce the bit rate for transmission or data storage while maintaining an acceptable compressed signal quality or a diagnostic accuracy. Numerous lossy compression methods for ECG signal have been developed, such as direct time domain methods, parameter extraction methods, frequency domain methods, wavelet domain methods and hybrid coding methods using different compression techniques. Among low computational complexity wavelet based ECG compression methods, many are based on thresholding of wavelet coefficients [134, 137, 142, 143, 211]. In these methods, the two stage design is employed for coding of the wavelet coefficients, where the wavelet coefficients are hard thresholded iteratively until a predefined EPE/PWCZ/PRD/RE value is reached first and then nonzero wavelet coefficients are quantized. The coding performance of the wavelet thresholding based method depends on the mother wavelet, the length of wavelet filters, the number of decomposition levels, the thresholding and quantization approaches and the compression of significance map vector for a given signal block of N samples. Signal distortion can be observed from two stages: discarded wavelet coefficients by thresholding with threshold T and quantization of nonzero wavelet coefficients with step size Δ. We thus attempted compression issues related to the thresholding and uniform scalar quantization schemes to improve rate-distortion performance of threshold based method in this research work.

The fixed number of coefficients from the sorted wavelet coefficients (WC) vector may not provide a good quality reconstruction because of varying characteristics of various ECG signals. In this case, a better signal quality may be obtained by using varying number of wavelet coefficients per block/lead/subject. Since a WC vector consists of wavelet coefficients with great magnitude differences, it is not an efficient way to assign a fixed number of bits to represent every wavelet coefficient. In many wavelet thresholding methods, linear quantizer with fixed resolution is used for the nonzero wavelet coefficients (NZWC) vector. For a fixed resolution b, quantization step size Δ will be large for a larger dynamic range of the NZWC vector while it will be smaller for a small dynamic range. In midtread quantizer case, as a result of thresholding process implicitly performed during quantization a greater number of nonzero wavelet coefficients are set to zero. Thus, a desired value of RE/EPE/PWCZ/PRD assured at the thresholding phase cannot be guaranteed at the output of the coder. Furthermore, experimental results in Chapter 2 demonstrate that the above design procedure cannot reach predefined compression ratio or quality specification quickly and accurately. This can be solved by choosing a smaller step size so that the desired value will be maintained but this may degrade coding performance. It proves that the definition of threshold T and quantizer resolution b has a strong impact on compression ratio and distortion. Therefore, an adaptive thresholding and quantization scheme may be suitable for wavelet thresholding based method. A significant improvement in coding performance could probably be achieved by using different optimized b and T values for different signal blocks. We thus attempt a design of adaptive joint thresholding and quantization strategy by examining the similarity between the hard thresholding and midtread quantization in this work.

Most of the energy in an ECG signal is concentrated in the low-frequency region, at each subband of the wavelet transform the energy distribution is concentrated in a small number of wavelet coefficients. Therefore, the wavelet transform of most ECG signals are sparse, resulting in a larger number of small wavelet coefficients and a smaller number of large coefficients. Thus, amplitude distributions of wavelet coefficients typically have sharp concentrations around zero in their distributions. Furthermore, significant wavelet coefficients for each signal block appear very close in a sequence order within a wavelet subband. In this chapter, the above properties will be exploited, using the threshold control zero-zone nearly uniform midtread quantizer (TCZNUMQ) and wavelet index coding (WIC) schemes, to achieve a good rate-distortion performance.

This chapter is organized as follows. In Section 3.2, threshold control zero-zone nearly uniform midtread quantization (TCZNUMQ) and modified index coding (MIC) schemes are presented. This section discusses the preprocessing stage function, choice of wavelet filters and number of decomposition levels for the decomposition, statistical analysis of the wavelet coefficients, the classification of the wavelet coefficients into frames based on relative wavelet subband energy measure. The performance of different criteria for the selection of threshold and the thresholding rules are discussed with different sets of experiments. In Section 3.3, target distortion level (TDL) and target data rate (TDR) driven wavelet threshold based ECG compression algorithms are presented based on the TCZNUMQ and MIC schemes. In Section 3.4, the performance comparison of the proposed method and other ECG compression methods is presented. Analysis of computational complexity and evaluation of clinical quality of the compressed signal are discussed in this section. Finally, some important discussions are presented in Section 3.5.

3.2 Construction of Adaptive Subband Coding Scheme

In this section, we study the performance of different methodologies used for the signal compression in several experiments. This study demonstrates different compression issues involved in the wavelet thresholding based methods and then we present a remedy for each of issues to provide a better compression method. In this work, we have put more efforts on the experimental analysis of different compression methodologies. However, theoretical analysis of the methodologies presented here will be attempted in our future research works. With reference to some interesting results obtained, we present a better wavelet thresholding based compression method to overcome the limitations of the existing methods. The proposed compression method consists of the following steps: 1) Preprocessing (Blocking and mean removal). 2) Decomposition of the signal using the wavelet transform and energy based classification of wavelet coefficients. 3) Thresholding of the wavelet coefficients of the frames based on the energy packing efficiency criterion. 4) Compression of the nonzero wavelet coefficients vector using the proposed adaptive TCZNUMQ scheme. 5) Compression of the significance map using the proposed modified index coding (MIC) scheme. and 6) Huffman coding of the quantized indexes and the output of the MIC scheme.

3.2.1 Preprocessing: Blocking and Mean Removal

The raw ECG signal $\{x(n), \mathrm{M}\}$ is segmented into nonoverlapping blocks of N samples and then the mean removal is performed for each block. For a desired data rate, each block is encoded and decoded separately. The block length is selected to represent the best tradeoff between the compression performance and the storage space for the computational requirements. However, a block length should be selected such that it enables real time computer aided diagnosis for remote patient health care monitoring system. In literature, block of 512, 1024, 2048, 4096, 21600 and 43200 samples are chosen for testing purpose. Some signal distortion and degradation of the reconstructed ECG samples are obtained if the number of ECG samples is chosen to be significantly large. Various results show that increasing the block size above a certain point results in a very modest CR gain while the computational time and memory space requirement significantly increases. Thus, the decision about block length is fundamentally open. The usual duration of computer evaluated ECG records is 10 seconds [17, 139]. However, the optimum block length with a good compromise between complexity and compression performance will be selected by performing different sets of experiments in this work.

Each block extracted from the raw ECG records may contain mean, noises and varying characteristics of various PQRST morphologies. But the mean and noises do not contribute any medical importance during clinical evaluation of the ECG signal. The effects of processing signal block with mean value in wavelet thresholding based method with different desired criteria are demonstrated in the previous Chapter. The experiments show that the mean value affects the amplitude distribution of the wavelet coefficients, increases significantly the variance of the wavelet coefficients vector of the signal block. Thus, the coding parameters such as threshold T and quantization b are not optimal in the case of mean preservation. Therefore, each signal block is preprocessed for subtracting its mean value prior to wavelet decomposition stage. Mean removal does not alter the clinical features present in the signal block whereas filtering of varying frequency characteristics of various noises may introduce distortions in the clinical features. The compression method presented in this Chapter apply directly over the zero-mean ECG signal block without any pre-filtering. The ECG signal can, in any case, be preprocessed as usual in order to reduce the noise level. Nevertheless, wavelet filtering is implicitly performed when implementing the thresholding or/and quantization. Thus, the resulting method achieves simultaneous denoising and compression if such property is desired. The effect of the use of noisy ECG signal will be discussed using various noisy records taken from the `mita` database.

3.2.2 Wavelet-Multiresolution Signal Decomposition

Wavelet transforms have been proven to be very efficient in nonstationary signal analysis. Wavelet transform (WT) decomposes a given signal into several scales at different levels of resolution. Wavelet based signal processing over conventional techniques offers definite advantages such as coefficient compaction property of wavelet, weakening of noise in wavelet domain, and the removal of redundancy. From the decomposed

signals, it is possible to recover the original time domain signal without losing any information. This reverse process is called the inverse WT or signal reconstruction. These two processes form a WT pair. With the orthonormal basis, there will be no information redundancy among the decomposed signals due to the orthonormal property of the basis function and the basis lends itself to a simple implementation using a pyramidal signal decomposition technique. Once the filters have been defined, one applies the recursive decomposition algorithm which offers the hierarchical, multiresolution representation of signal. The usefulness of wavelets for data compression and denoising rests mainly in the fact that the WT can be turned into sparse expansions. It means that any signal can be quite accurately represented by a small part of the initial number of coefficients only, the ones that are small enough being set to zero.

In wavelet thresholding based compression methods, there are several parameters that need to be determined or well-known: i) the type of mother wavelets that is, a particular pair of low-pass and high-pass filters; ii) the length of wavelet filters; the number of decomposition levels; iv) significance of wavelet subbands; v) the criterion for threshold selection and the thresholding rule; vi) the type of quantizer and its quantization strategy; and vii) type of encoding scheme used for the compression of significance map and quantized values. The selection of these parameters will be discussed with several experiments in this research work. Our goal is to reduce the bit rate significantly while keeping signal distortion at a clinically acceptable level. For the ECG signal, this means minimizing the distortion in the P-wave, QRS complex, and the T-wave, etc. the features of most interest in terms of clinical diagnosis. Since a highly distorted signal with high CR can be useless from a clinical point of view, answer to the Boolean question about the diagnosis of the compressed signal (1-YES, 0-NO) is opted in this work.

3.2.2.1 Wavelet Filters and Decomposition Level

The choice of mother wavelet is very important for obtaining effective data compression, because the wavelet affects distribution of the wavelet coefficients and the design of the compression system [144, 145]. The best mother wavelet depends on the specific features of the signal to be compressed and thus a signal based selection of the mother wavelet is necessary for optimal compression with respect to high compression ratio with less reconstruction error. In literature, the mother wavelet can be selected from a wavelet filter bank library or selected by comparing the actual compression performance of several different mother wavelets on a set of experimental signals. However, the choice of the mother wavelet is fixed a priori in this work. For the selection of wavelet filter pairs, we referred many wavelet based compression methods. During literature review and our ground study we have observed that the biorthogonal wavelet (BW) filters exhibit superior performance. We selected the BW 9/7-tap filters. They were chosen because i) they are symmetrical filters [145] and ii) they have been adopted because they performed slightly better overall than the other filters employed for wavelet coding of ECG signals [144–146, 152]. The detail of wavelet filters for coding can be found in [144, 145]. The number of decomposition levels (J) determine the coarsest frequency resolution of the wavelet transform and should be at least four for adequate compression [145]. In

literature, the number of decomposition levels employed for ECG signal varies from 4 to 6 [137, 152]. In this research work, the number of decomposition levels is set as 5 since this number of levels provided good compression ratios at a low computational cost in the previous works. However, it exploits sufficient energy compaction capability of DWT for ECG signals according to our experience.

3.2.2.2 Wavelet Subbands: Approximation and Detail

In our work, a raw ECG signal is first segmented into blocks and then mean removal is performed. Each signal block consists of N samples. Then the zero-mean signal block $\{x(n), \mathrm{N}\}$ is successively decomposed into a set of subsignals A_J and $(\mathrm{D}_j)_{(1\leq j\leq J)}$ using the BW 9/7-tap filters bank DWT structure. We will have $J+1$ coefficient subbands if a J-level wavelet decomposition is taken for each signal block. The decomposition subbands are the approximation subband A_J and the detail bands D_J, D_{J-1}, D_{J-2},..... D_1, where A_J is the smoothed version of $x(n)$ and $(\mathrm{D}_j)_{(1\leq j\leq J)}$ are the difference subsignals between the original signal and its smoothed version at j^{th} resolution, respectively. In this work, a five level decomposition structure is used for decomposition of the ECG signal. The wavelet coefficients (WC) vector is given by $\mathrm{WC} = [\ \mathrm{A}_5 \quad \mathrm{D}_5 \quad \mathrm{D}_4 \quad \mathrm{D}_3 \quad \mathrm{D}_2 \quad \mathrm{D}_1\ ]$. Multiresolution signal decomposition is used to achieve two important properties. The first is the localization property and the second property is the partitioning of the signal energy at different frequency bands.

3.2.2.3 Statistical Distribution of the Wavelet Coefficients

Amplitude distributions of the wavelet coefficients of subbands are different due to varying characteristics of ECG morphologies. Therefore, an analysis of amplitude distribution of the wavelet coefficients is essential for an effective data compression and will be discussed in this section. Seventy-eight 1024 sample segments of ECG signals are selected from three different ECG databases, 15 each from the MIT-BIH Supraventricular arrhythmia (`mitsva`) database (128 Hz, 10 b/sample), the Creighton university ventricular tachyarrhythmia `cuvt` database (250 Hz, 12 b/sample) and 48 from the MIT-BIH arrhythmia (`mita`) database (360 Hz, 11 b/sample). The 78 signal blocks are decomposed up to five-level using a BW 9/7-tap wavelet filter set and their amplitude distributions of wavelet coefficients are shown in Fig. 3.1. Black (low active regions) and gray (high active regions) in the figure represent the smaller amplitude wavelet coefficients and larger amplitude coefficients, respectively. For all the signal blocks, high activity regions toward low frequency subbands and these regions are most important for perfect reconstruction. The distribution serves to motivate that the threshold can provide potential benefits in an efficient wavelet coding. For the ECG signals, high activity regions are clustered and separated from surrounding low activity regions.

The analysis of the distribution of wavelet coefficients of ECG signal block is very important in order to understand their behavior at each subband. The experimental results are demonstrated using the wavelet coefficients of widely used `mita` records 107, 111, and 117. Histogram of the wavelet coefficients at each subband is shown in Fig. 3.2. It can be observed in the plots that 90% of the wavelet coefficients are very

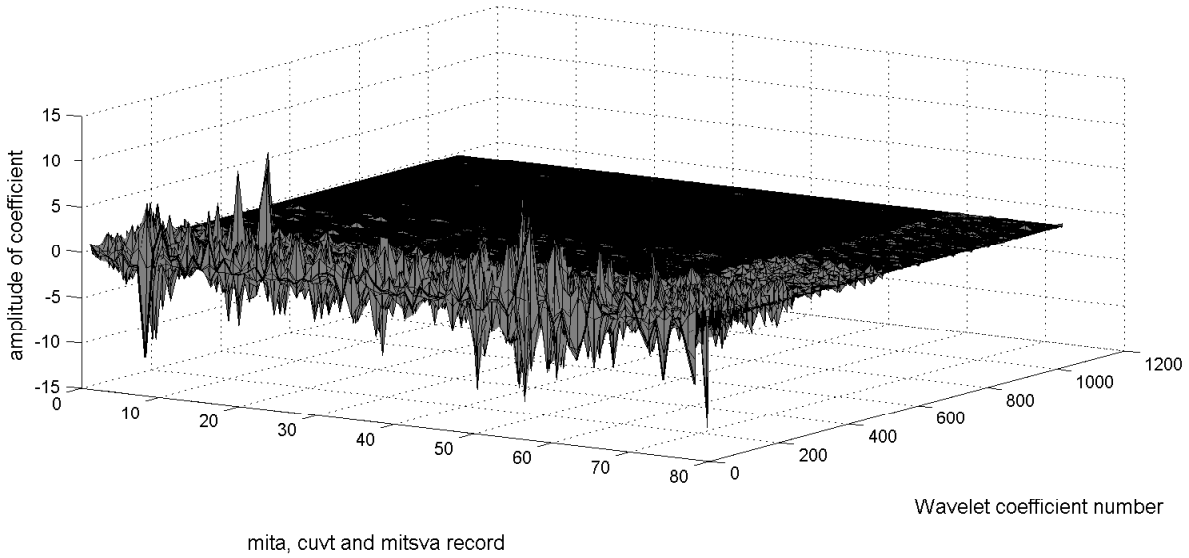

Figure 3.1: Subband coefficients obtained by five-level decomposition of the ECG signal blocks taken from from `mita`, `cuvt` and `mitsva` databases using a BW 9/7-tap wavelet filter set. Black indicates the least active regions and gray depicts the most active regions. Large coefficients toward low frequency subbands and, more importantly, spatial clustering of the wavelet coefficients within each subband.

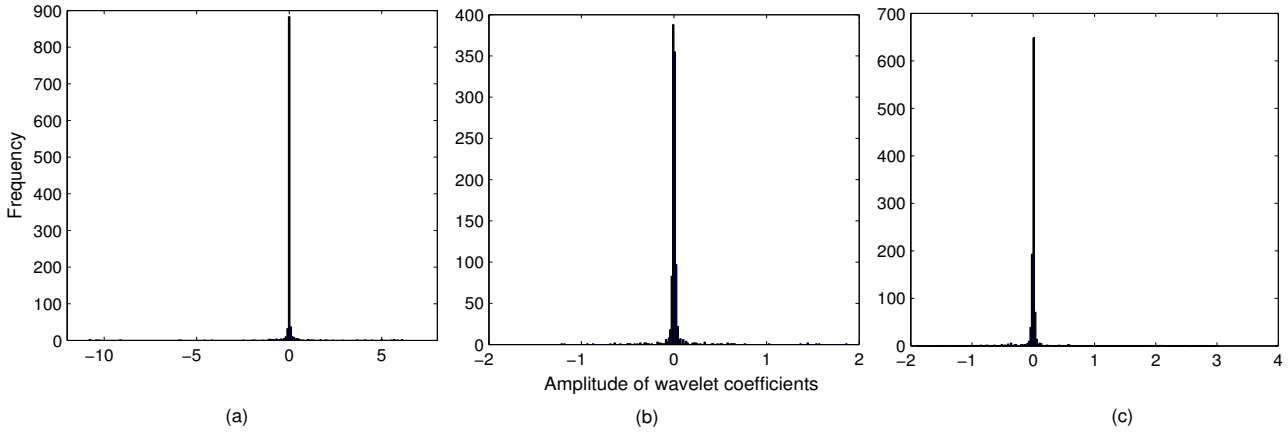

Figure 3.2: Histograms of the wavelet coefficients of the ECG signals: (a) `mita` record 107, (b) `mita` record 111, and (c) `mita` record 117. For all test records, histogram shows a very sharp peak around zero-bin.

small and lie in a very narrow dynamic range around the origin. The behavior of the wavelet coefficients is illustrated in Table 3.1.

The histograms of the wavelet coefficients in the subbands of the test signals are shown in Fig. 3.3 and the statistics of the wavelet coefficients at each subband for each signal are shown in Table 3.1. It describes the minimum and maximum (MIN and MAX) wavelet coefficient at each subband, the mean and variance (MEAN and VAR) of the wavelet coefficients in each subband, and the range of each shape after

Table 3.1: Statistics of the wavelet coefficients in the subbands of the mita records 107, 111 and 117.

Subband	Record	MIN	MAX	MEAN	VAR	$\frac{(MIN-MEAN)}{VAR}$	$\frac{(MAX-MEAN)}{VAR}$	Kurtosis	Skewness
D_1	107	-0.0698	0.0447	-0.0003	0.0001	-985.1056	638.7301	23.7366	-1.1975
	111	-0.0192	0.0207	-0.0002	0	-418.8797	458.0309	3.0836	0.1282
	117	-0.0257	0.0949	-0.0003	0.0001	-389.2535	1456.23	39.1735	3.1112
D_2	107	-0.2637	0.3357	0.0014	0.0017	-158.1285	199.4455	30.0072	1.9289
	111	-0.068	0.0901	-0.0007	0.0004	-151.9918	205.2720	3.9731	0.3778
	117	-0.2052	0.1233	0.0004	0.0005	-449.4682	268.652	40.9713	-2.9418
D_3	107	-1.0664	1.1350	0.0098	0.0287	-37.452	39.1571	29.3646	0.9046
	111	-0.4017	0.4228	0.0007	0.0064	-62.5934	65.6792	16.2483	-0.5408
	117	-0.7447	0.5635	0.0006	0.0106	-70.4471	53.203	29.3471	-1.5583
D_4	107	-1.8602	1.9308	0.0336	0.2233	-8.4815	8.4962	10.5954	0.7168
	111	-0.6916	0.7639	0.0228	0.0321	-22.2212	23.0518	11.2744	0.9467
	117	-1.8468	2.0833	0.0446	0.1876	-10.0824	10.868	16.8848	1.4213
D_5	107	-5.9295	4.1871	-0.0763	2.7962	-2.0933	1.5247	7.5217	-0.7816
	111	-0.4973	1.5627	0.096	0.1307	-4.5391	11.2217	11.5105	2.799
	117	-1.9039	1.7422	-0.0115	0.2531	-7.4754	6.928	9.5788	-0.3768
A_5	107	-10.8152	6.1451	-0.6365	27.9633	-0.364	0.2425	2.4839	-0.6864
	111	-1.221	1.8693	0.0696	0.5122	-2.5201	3.5139	3.1743	0.5786
	117	-1.364	3.0256	-0.1161	0.8925	-1.3982	3.520	6.2842	1.9237

normalizing by the MEAN and VAR. At each subband, the values of the validation metrics are shown for each record to study the behavior of the low activity and high activity regions of the different signals. The importance of each subband is determined by Table 3.1: 1) The amplitude range of the wavelet coefficients (i.e., [MIN, MAX]) and their variances (i.e., VAR) of the lower subbands (A_5, D_5, D_4 and D_3) are larger than those of higher subbands (D_2 and D_1) which proves that the wavelet coefficients at the lower subbands have higher importance. It shows that the subbands D_2 and D_1 contain large number of small wavelet coefficients. 2) After subtracting the MEAN and scaling by the VAR, the range of the coefficients becomes smaller and similar for the blocks in the lower subbands. 3) The approximation subband A_5 and detail subband D_5 consist of a wider range and larger coefficients and variances than the other subbands. These subbands contain the most important coefficients. Thus, the subband D_5 will be thresholded and quantized separately and the subband A_5 that contains the most smoothed version of the original signal will be kept with full resolution for reconstruction purposes. This procedure might result in lower compression but also in good reconstructed signal quality.

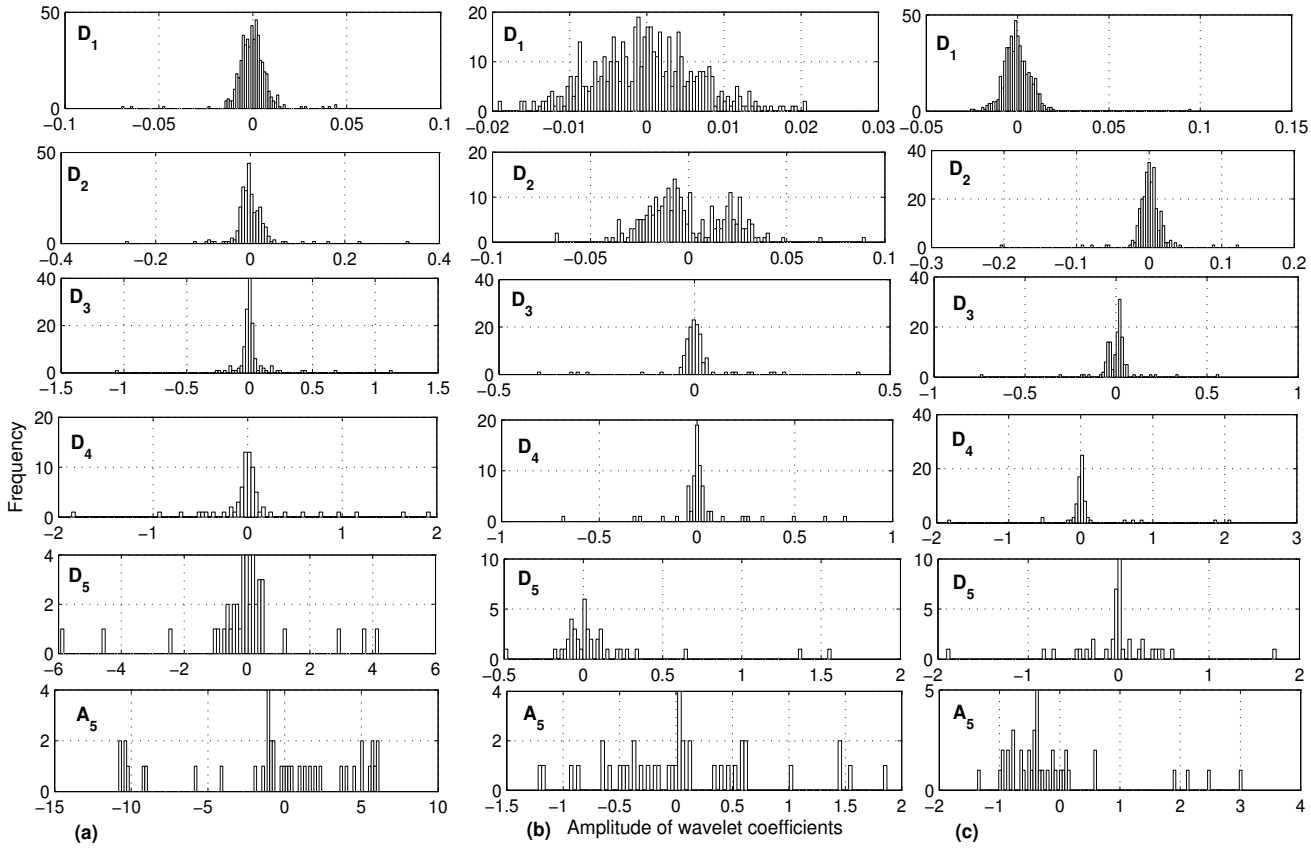

Figure 3.3: Histograms of the wavelet coefficients in the subbands of the test ECG signals: (a) `mita` record 107, (b) `mita` record 111, and (c) `mita` record 117.

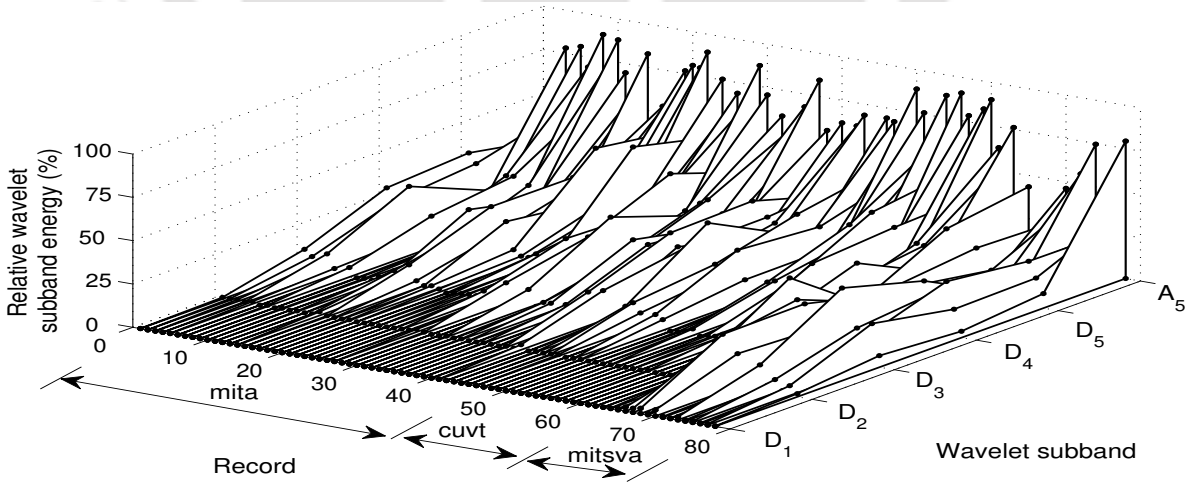

Figure 3.4: Relative wavelet subband energy (RWSE) distribution of each record taken from `mita`, `cuvt` and `mitsva` databases. We can note that the RWSE of the bands D_2 and D_1 is lesser as compared to the other bands.

3.2.2.4 Energy Based Classification of Wavelet Coefficients

From the behavior of the wavelet coefficients and their distribution, it can be observed that most of the wavelet coefficients lie in a narrow range around the origin, and the higher subbands contain smaller wavelet coefficients and variances. The importance of the subbands is discussed in the previous sections. Looking at Table 3.1 and Fig. 3.4, we see that in each record, subbands A_5, D_5 contain more energy and larger coefficients and variances than the other subbands. To analyze the energy distribution of the wavelet coefficients, for each subband the relative wavelet subband energy (RWSE) is computed as the ratio of the energy of the wavelet coefficients in that subband and the total energy of the coefficients. The RWSE of the j^{th} subband is given as

$$\text{RWSE}_j = \frac{\sum_{k=1}^{K_j} c_j^2(k)}{\sum_{j=1}^{J+1}\sum_{k=1}^{K_j} c_j^2(k)}, \quad j = 1,2,....(J+1) \tag{3.1}$$

where K_j denotes the number of wavelet coefficients in the j^{th} subband and $c_j(k)$ is the k^{th} wavelet coefficient of the j^{th} subband. The RWSE of the approximation subband (A_5) and detail subbands (D_5-D_1) are calculated for the ECG records taken from different ECG databases. The RWSE values of all subbands of `mita` ECG records are shown in Fig. 3.4. The RWSE values are calculated from zero mean ECG signal to observe the energy distribution in subbands of PQRST complex features. The energy plots of records follow waterfall characteristics. It shows that the RWSE values of higher detail bands (D_2 and D_1) are small. It is observed that more energy is packed in few large magnitude wavelet coefficients and less energy is concentrated in more number of small magnitude wavelet coefficients. The compression is carried out in the wavelet domain by retaining wavelet coefficients associated with signal contents and discarding all other wavelet coefficients. The relevant coefficients in each subband are used to represent the original ECG signal with less reconstruction error. We can note that the coefficients of high frequency components of the ECG signal are small in the WC vector. These coefficients may be discarded when the global thresholding is applied. Therefore, we attempt local thresholding rule in this work. Based on the observation of the amplitude distribution of the wavelet coefficients within subbands and their subband energies, the wavelet coefficients are divided into three frames based on the RWSE values of the subbands. The first frame F_1 contains only approximation band coefficients A_5, the second frame F_2 has detail band coefficients D_5, and the third frame F_3 consists of detail bands from four to one. These frames or classes are given by $F_1 = [\ A_5\ ]$, $F_2 = [\ D_5\ ]$, and $F_3 = [\ D_4\ D_3\ D_2\ D_1\ ]$.

Generally, once the signal block is decomposed using the multiresolution signal decomposition technique, statistics of the wavelet coefficients at each subband is computed to perform classification of coefficients before compression process for achieving substantial gains in coding performance. The study shows that each of the subbands has a different energy level, dynamic range and variance, with less energy being in the high detail subbands. The relative wavelet subband energy introduced provides information about the

relative energy associated with different frequency bands present in the signals. The resulting energy distribution provides a suitable tool for detecting and characterizing signal contents and then the classification into frames is performed that serves to distinguish between the subband coefficients according to their relative energy levels for better adaptive thresholding and quantization. Once classification of wavelet coefficients is performed, the next task is thresholding, which is neglecting certain wavelet coefficients. In two-stage scheme, for each frame, the optimal number of the retained wavelet coefficients is determined based on the signal distortion or compression rate. For doing wavelet thresholding one has to decide the value of a threshold and how to apply the same. Moreover, the choice of thresholding functions and threshold values are critical in compression methods.

3.2.3 Wavelet Thresholding and Threshold Selection

The original signal can be approximately reproduced with reduced data by selecting the large amplitude coefficients in the frames and discarding the small amplitude coefficients with suitable thresholds. Wavelet thresholding idea is especially effective for signals with sparse representations where most of the signal energy is contained in a few large components. While the idea of thresholding is simple, finding a reasonable threshold for each signal block is not an easy task. Since the threshold plays a key role in the reconstruction, variant techniques for threshold determination are investigated to choose a better algorithm for threshold selection. The iterative algorithm with some criteria is reported for threshold finding in wavelet thresholding based ECG compression works [134,137,142,143,211]. Then, the global thresholding procedure is followed in most of the compression methods reported for the ECG and PCG signals in the literature.

3.2.3.1 Criterion for Threshold Selection

Before the thresholding phase, one needs to formulate the criterion for the selection of wavelet coefficients and the corresponding cost functions. The threshold T can be set manually by the user, although the lack of a direct relation between its value and the losses of the compression due to thresholding makes manual setting not suitable. There are many criteria for threshold estimation: The frequently used criteria are: only wavelet coefficients whose magnitude is higher than the predefined threshold are retained and its corresponding cost function is defined as the number of the retained coefficients (Criterion-1).; The optimal number of the retained wavelet coefficients is determined as the compromise between the number of the retained coefficients and the reconstruction error (Criterion-2). In wavelet based ECG compression methods [134, 137, 211], threshold T is determined based on the following criteria: i) fixed number of coefficients (FNC) extracted from sorted wavelet coefficients in descending order; ii) the energy packing efficiency (EPE) [134]; iii) the percentage wavelet coefficients to be zeroed (PWCZ) [137]; and iv) the distortion level measured using the RMSE and PRD metrics [142, 143]. The EPE is defined as the percentage of the total energy preserved in a certain subband after thresholding [134]. For a given value of PWCZ/FNC, the number of retained

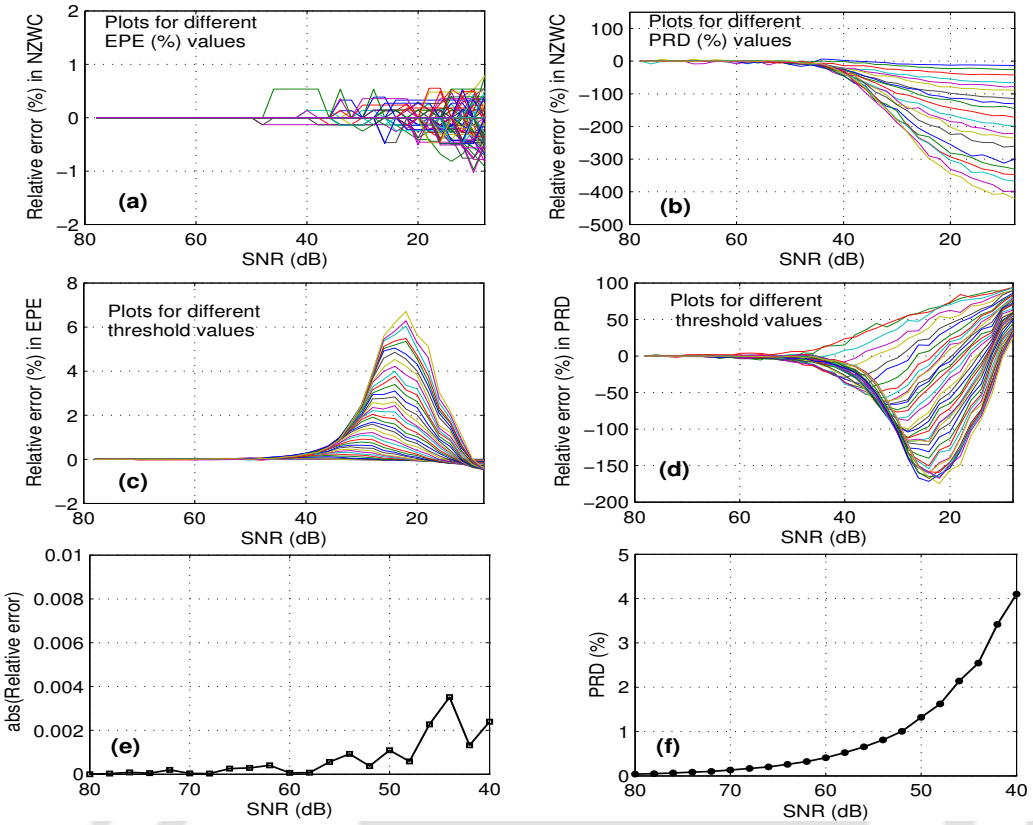

Figure 3.5: Evaluation of EPE and PRD criteria for threshold selection under noisy conditions. (a) Relative variation in number of NZWC at each EPE value for different SNR values. (b) Relative variation in number of NZWC at each PRD value for different SNR values. (c) Relative variation in EPE at each threshold value for different SNR values. (d) Relative variation in PRD at each threshold value for different SNR values.(e) Average EPE value versus SNR value.(f) Average PRD value versus SNR value.

wavelet coefficients is same for all test signal blocks. The threshold T iteratively determined, based on the algorithm for a desired PWCZ may not be efficient for the test signal blocks with varying PQRST morphologies since the decay rate of the sorted absolute wavelet coefficients of those signal blocks may be fast or slow. The slow decay rate implies that the wavelet coefficients of the ECG signal will be more spread out. Moreover, the decay rate remains unknown for nonstationary ECG signals. Thus, the method based on the above threshold findings may distort clinical features of the signal. It can be improved by using a varying number of wavelet coefficients for reconstruction. Therefore, for the class of signals that have fast or slow decaying wavelet coefficients, the EPE/PRD criterion for threshold finding will be effective in compressing those signals. However, energy and error measurement criteria are sensitive to noise level in the signal. It is well known that the suitable threshold is output if the resulting EPE/PRD value falls within the preset bound of the desired EPE/PRD.

It is well known that the wavelet thresholding procedure removes noise by thresholding only the coeffi-

cients of the detail subbands while keeping the low resolution coefficients unaltered. The WT based method may produce smooth reconstructed signals with less significant errors. If we use the PRD measure between the smoothed reconstruction and the noisy signal we can obtain a large value of PRD due to the presence of unwanted noise. The iterative algorithm performs a threshold adjustment procedure until a desired PRD is reached and reaches a desired PRD value with a small threshold for the noisy signal than the noiseless signal case. Thus, the resulting threshold value may not be an optimal one for the given signal characteristics. Therefore, we analyze the effects of noise on threshold parameter estimation for a given EPE/PRD value. This is performed with the use of the simulated white noise and the experimental results are shown in Fig. 3.5. Percent relative error metric is used for validation of the algorithms. For a given value of EPE, the threshold values and the numbers of nonzero wavelet coefficients (NZWC) are found by varying signal to noise ratio (SNR). Fig. 3.5(b) shows that the threshold T estimation is more sensitive to noise energy in the case of PRD criterion based iterative algorithm. The change in PRD values with respect to SNR values are shown in Fig. 3.5(f). It shows that if the noise energy is larger the value of PRD will also be higher. This behavior is not reasonable because the effect of the noise energy on morphologies is less. Note that the SNR values are limited so that the morphology signal change is minimum. Similarly, for each SNR value the cumulative sum of the energy of wavelet coefficients found and its characteristics are observed. For the range of SNR, the energy values are approximately equal for an interested EPE value. Since the wavelet transform provides the energy compaction and sparse representation properties, the EPE criterion is relative insensitivity to low noise level compared to PRD which takes into account the differences of the samples of the original and smoothed signals. These experiments show that the performance of the energy criterion based threshold finding is better within the reasonable SNR range. In this case, one would like to prepare less sensitive measurement criterion for threshold finding. Therefore, we attempt energy packing efficiency criterion in this Chapter. This threshold finding is not only easier to analyze but also provides more facility to find the desired compression signal quality measured using the energy criterion than the several other methods. In general, a smaller threshold T will result in higher signal quality due to the preserving of more signal energy. A higher T will get an opposite result. Therefore, the significant coefficients in the frames are retained by selecting a suitable threshold value based on the desired EPE for each frame. Finally, it is also possible to set one of the parameters used to measure the performance of the compression, CR or PRD1, as the target value.

3.2.3.2 Wavelet Thresholding Rule

Given a threshold T, two popular wavelet thresholding rules such as hard thresholding, and soft thresholding are used in the literature [204–206]. Both hard thresholding and soft thresholding methods which correspond, respectively, to the strategies "kill or keep" and "kill or shrink", compare the wavelet coefficient to a given threshold and set coefficient to zero if its magnitude is smaller than the threshold whose value may differ from frame to frame [205, 206]. A wavelet coefficient $F_i(k)$ is defined as significant with respect

to a threshold T_i if $|F_i(k)| \geq T_i$, otherwise $F_i(k)$ is said to be insignificant. The intuition is that because the wavelet transform is good at energy compaction capability, large number of small wavelet coefficients are more likely due to noise, and small number of large coefficients due to signal contents [205]. The threshold thus acts as an oracle which distinguishes between the insignificant coefficients and the significant coefficients. The hard thresholding operator is defined as:

$$H_T(F_i(k), T_i) = \begin{cases} F_i, & |F_i(k)| \geq T_i \\ 0, & \text{otherwise} \end{cases} \tag{3.2}$$

The soft thresholding operator on the other hand is defined as:

$$S_T(F_i(k), T_i) = \begin{cases} sgn(F_i(k)) \bullet (|F_i(k)| - T_i), & |F_i(k)| \geq T_i \\ 0, & \text{otherwise} \end{cases} \tag{3.3}$$

Wavelet thresholding essentially creates a region around zero where the coefficients are considered negligible. Outside of this region, the wavelet coefficients are kept to full precision. As for which to choose between the two thresholding rules, many research works reported several reasons for denoising. If the wavelet coefficients distribute densely close to the threshold, hard thresholding will preserve their magnitudes whereas the soft thresholding will reduce their magnitudes for a given threshold T_i. By considering the quantization rule and its performance in rate-distortion sense, the hard thresholding rule is adopted in this work.

3.2.3.3 Threshold Finding Algorithm and Results of Wavelet Thresholding Phase

In this section a simple threshold finding algorithm with EPE criterion is presented and tested using the signal blocks taken from the most widely used `mita` database. Many threshold based methods use a unique threshold value T for all wavelet coefficients. But varying T controls the CR and the distortion. The presented algorithm finds a threshold for each frame continuously to meet the desired EPE value assigned for that frame. Experimental results show that most of the energy is concentrated in frame F_1. As a result, thresholding of approximation coefficients in the first frame will distort the base of the PQRST morphologies. Thus, the first frame F_1 is not thresholded in this work. This procedure helps to preserve the low frequency components (low pass shape) of the ECG signal that are most important for reconstruction. As a result, the morphologies of P-wave and T-wave, the small q-wave and the ST segment may not be distorted. This preserves the diagnostic information in the signal to a large extent. Meanwhile, the thresholds for the higher frames are set higher in order to attain a good performance in the rate-distortion sense. Using the RWSE values, the EPEs are chosen to decide the thresholds T_2 and T_3 for the second and third frames, respectively. For a specified EPE, the threshold value is determined using the simple sorting algorithm (SA) shown in Table 3.2. For the specified EPE_{F_2} and EPE_{F_3}, the respective thresholds T_2 and T_3 are calculated using a simple algorithm [134]. Thresholded wavelet coefficient (TWC) vector is given as,

Table 3.2: Sorting algorithm (SA) for determining the threshold T value and thresholding process.

Step 0: Initialization
(a) Give a required EPE_i (in percentage) value for the i^{th} frame.
(b) Get the wavelet coefficients of the i^{th} frame. $\mathrm{F}_i(\mathrm{p})$, $p = 1, 2, 3, \ldots\ldots \mathrm{P}_i$.
Step 1: Calculate the total energy of the i^{th} frame by $\mathrm{TE}_i = \sum_{p=1}^{\mathrm{P}_i} [\mathrm{F}_i(p)]^2$.
Step 2: Calculate the retained energy of the i^{th} frame by $\mathrm{RE}_i = (\frac{\mathrm{EPE}_i}{100}) \times \mathrm{TE}_i$.
Step 3: Sorting of the absolute value of the wavelet coefficients in the F_i in descending order.
Step 4: Find the threshold (T_i) value. $\mathrm{E}_c = 0$; $p = 0$;

```
{
    while E_c < RE_i
        E_c = E_c + [F_i(p)]^2; // calculation of energy
        p = p + 1;
}
  T_i = F_i(p); // threshold value
{
    for (p = 1; p ≤ P_i; p = p + 1)
      if F_i(p) < T_i
          F̄_i(p) = 0 ;
      else
          F̄_i(p) = F_i(p);
}
```

TWC = [F_1 $\overline{F}_2$ $\overline{F}_3$], where $\overline{F}_2$ and $\overline{F}_3$ are the second and the third frame thresholded coefficient vectors. The nonzero wavelet coefficient (NZWC) vector is constructed by removing the zero valued coefficients from TWC. The integer significance map (ISM) is a positive integer vector which contains the positions of the significant or nonzero coefficients. The NZWC and positive integer vectors are coded in the next section.

The EPE values for the second and the third frame is assigned based on the RWSE values of approximation and detail coefficients of each ECG record. The smaller EPE value results in larger compression ratio but most of the diagnostic information is lost in the compressed signal. The shapes of P and T waves may be altered. Sometimes PR segment and small Q wave are lost in the reconstructed signal. The small Q wave is important for diagnosis of myocardial infarction. Hence, proper selection of EPE value is important for each ECG record. For all `mita` records, the reconstruction error (PRD1 value) versus energy packing efficiency ($\mathrm{EPE}_{\mathrm{F3}}$) are shown in Fig. 3.6. It can be observed that the PRD1 value varies for each record for a specified $\mathrm{EPE}_{\mathrm{F3}}$ value and hence a proper selection of EPE value is important for each record. The PRD1 value cannot reflect the exact amount of distortion of the PQRST complex features. For a given ECG signal, the value of PRD1 is same for dissimilar distortions introduced by the compression method. A compression method might achieve a low PRD1 error ignoring the local wave between QRST complexes, totally losing the small P-wave, and faithfully reproducing the QRST complex. Therefore, to ascertain that the clinical

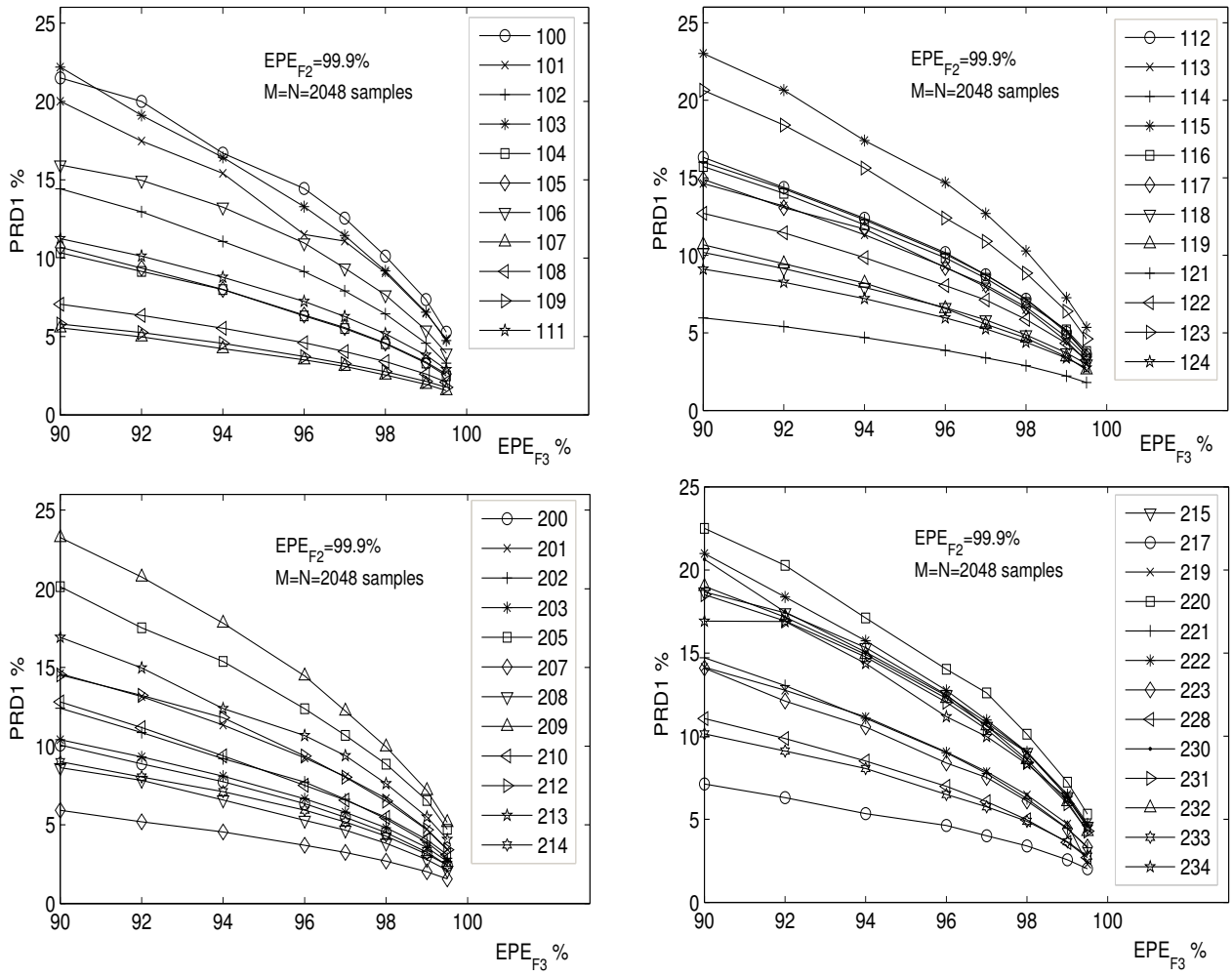

Figure 3.6: PRD1 versus EPE_{F3} of all records of the MIT-BIH arrythmia database.

information is preserved, the compressed signal quality is evaluated by comparing it visually with the original signal. In this work, more importance is given to the quality of judgement via visual inspection rather than the objective measures.

3.2.4 Threshold Control Zero-zone Nearly Uniform Midtread Quantization Scheme

The possibility of compression by thresholding or/and quantizing wavelet coefficients relies on the assumption that details at higher subbands are less relevant to the reconstruction. A common way to reduce the number of bits required for the compression phase is to quantize the coefficients and apply some lossless compression such as Huffman or arithmetic coding on the quantized coefficients or their representative indexes. The quantizers used in standard compression methods are designed to approximately minimize the MSE between the original and reconstructed signals for a given bit rate. In ECG compression method, the

nonzero wavelet coefficients or the wavelet coefficients can be quantized using the scalar quantization (SQ) schemes or the vector quantization (VQ) schemes. Comparing SQ versus VQ should take into consideration three aspects: compression ratio achieved and its signal quality, computational complexity and coding delay. The compression issues involved in quantization strategy are discussed in Chapter 2 with different sets of experiments. We present here issues of the simple quantization strategy with frequently used quantization rules and then propose a better adaptive quantization strategy for wavelet coding.

3.2.4.1 Limitation of the Quantization Approaches

The thresholding phase attempts to discard the irrelevant coefficients and to preserve relevant coefficients of the signal contents. Then, one can store or transmit the nonzero (or significant or relevant) wavelet coefficients using a fixed codeword length. The codeword length usually equals the number of bits per sample and this criterion may result in less coding error. In [134], each decimal part of the significant coefficients are stored by assigning a fixed number of bits (7- or 9-bit signed representation) by assuming that no integer exists according to the preprocessing algorithm aimed. This encoding procedure may produce considerable coding errors if the number of bits used to code each significant coefficient is not sufficient. Since the dynamic range is not considered, this encoding procedure results in a large reconstruction error. Thus, it degrades overall rate-distortion performance of the method. In [137, 142, 211], a linear quantization scheme with fixed resolution (8-bit for ECG, 10-bit for PCG) is used to quantize the nonzero wavelet coefficients (NZWC) vector. These methods use a unique quantization step size Δ to quantize coefficients in NZWC vector obtained for each record. This Δ value is defined to minimize the squared mean error between the original and reconstructed signals for a desired criterion specification. For lower values, the error of compression dramatically increases having a negative effect on compression performance. Since the dynamic ranges of NZWC vectors obtained for signal blocks are different, a low degree of quantization strategy can lead to low compression ratios associated with high distortions.

Many compression methods control target criteria such as EPE [134], PWCZ [137], RE [211] and PRD [142] at the thresholding phase which maintains a desired target value with specified tolerance ε by performing a threshold adjustment procedure and uses the linear quantization strategy with fixed resolution for all records. However, a desired target value may not be guaranteed at output of the quantization phase since the quantization step of compression is analogous to the threshold value in the thresholding function. The quantization is the lossy operation which usually reduces the resolution of the significant coefficients of interest. The values can vary significantly according to the density of the significant coefficients within the quantization zone range [-δ, δ]. The relevant coefficients of each signal with different amplitudes are retained using the threshold T obtained for a desired target value. Then the quantization step Δ is found for each signal based on the dynamic range of the NZWC vector for a specified quantizer resolution b. Because of the varying dynamic range due to different frequency contents of the signal, if the step size obtained is larger than the threshold T then some of the significant coefficients may be rounded to zero or to the first

Table 3.3: Performance of the modified midtread quantizer for different quantization levels.

b	Without correction of threshold T			With correction of threshold T			Test ECG data
	CR ($\mu \pm \sigma$)	PRD1 (%) ($\mu \pm \sigma$)	PRD2 (%) ($\mu \pm \sigma$)	CR ($\mu \pm \sigma$)	PRD1 (%) ($\mu \pm \sigma$)	PRD2 (%) ($\mu \pm \sigma$)	
8	16.91±2.473	8.088±3.562	11.745±4.192	16.91±2.473	8.088±3.562	11.745±4.192	MIT-BIH
7	19.48±2.763	8.235±3.531	11.983±4.056	19.48±2.763	8.235±3.531	11.983±4.056	arrhythmia
6	22.42±3.452	8.575±3.428	12.408±3.799	22.54±3.31	8.577±3.427	12.410±3.797	database (48 records)

output level. The rounding to zero or to the first output level is based on the conventional uniform midtread and midrise quantizers, respectively. Thus, there are two main sources for introducing signal distortion: 1) discarding of wavelet coefficients by thresholding; and 2) quantization of the retained wavelet coefficients. But many quality controlled compression methods do not consider the signal distortion due to quantization scheme. Moreover, some of the wavelet coefficients that lie in the zero-zone region of the quantizer may be rounded to zero. This indirectly confirms that a method with a fixed linear quantization may result in unacceptable compressed quality. This can be solved by choosing a smaller step size such that it matches the threshold T. But it degrades overall compression efficiency of the method.

Recently, the modified midtread quantizers have been reported in [202, 203] for global and local (or frame) coding procedures. In [202], two approaches are studied for compression of wavelet coefficients: 1) threshold T_i is optimized for a desired target value at the thresholding phase and then the appropriate step size Δ is chosen so that the target is maintained at the output of the quantizer; 2) the optimal ratio between the threshold T_i for the zero-zone and the step size Δ is attempted to study the gains in compression performance. The performance of the adaptive quantization schemes are evaluated using the 48 records from the `mita` database. The first one minute of data are taken from each record and the BW 9/7-tap filters DWT is applied on the block of samples up to five-level of decomposition. The wavelet coefficients in the second and third frames are thresholded using thresholds T_2 and T_3 which are selected at $EPE_{F2} = 99.9\%$ and $EPE_{F3} = 93\%$, respectively. The thresholded coefficients are quantized using the quantizer with $b = \{6, 7, 8\}$. For each bit, the compression ratio, the PRD1 and the PRD2 are calculated for the same EPE of the frames. The performance of the quantizer is summarized in Table 3.3. For the $b = \{7, 8\}$, no signal block meets the condition that the threshold value is less than half of the step size. So, threshold correction is not required for the quantization $b = \{7, 8\}$. Thus, the average compression ratio, average PRD1 and average PRD2 are same with and without correction, which is shown in Table 3.3. For the 6-bit quantization case, two records, 108 and 207, have the threshold value less than the half of the quantization step size. But the average compression ratio is better than the results obtained for the 7- and 8-bit quantization at the cost of small increment in the average values of PRD1 and PRD2.

To study the performance of the quantization effect on `mita` record 108 and 207, a variable threshold T is used while keeping the step size of the quantizer constant. Here, the threshold value is slightly greater than

Table 3.4: Performance of the modified midtread quantizer for specific records.

Record	b	EPE_{F2} (%)	EPE_{F3} (%)	Without correction of threshold T			With correction of threshold T			
				CR	PRD1(%)	PRD2(%)	$EPE_{F3}(\%)$	CR	PRD1 (%)	PRD2 (%)
108	6	99.9	93	11.25:1	5.632	9.743	90.5	13.2:1	5.642	9.761
	7	99	86	13.86:1	5.605	9.695	-	-	-	-
	8	99.9	83	13.49:1	6.045	10.458	-	-	-	-
207	6	99.9	93	20.12:1	6.001	6.314	89.69	24.05:1	6.071	6.387
	7	99	86	24.18:1	5.854	6.159	-	-	-	-
	8	98	80	23.78:1	6.981	7.346	-	-	-	-
117	7	99	86	24.94:1	4.850	17.601	-	-	-	-
	6	99.9	93	25.76:1	3.357	12.182	-	-	-	-

Figure 3.7: Performance of the joint thresholding and quantization strategy. (a) Original ECG signal is taken from lead II of `mita` record 117. (b) Reconstructed signal at threshold T_2 and T_3 selected at EPE_{F2} =99% and EPE_{F3} =86% for 7-bit quantizer. (c) Reconstructed signal at threshold T_2 and T_3 selected at EPE_{F2} =99.9% and EPE_{F3} =93% for 6-bit quantizer.

half of the step size. The compression results for the new threshold values are shown in Table 3.4. After the correction of threshold for the 6-bit quantization, the records 108 and 207 are compressed with compression ratios of 13.2:1 and 24.05:1, respectively. The PRD and PRD1 values are almost equal to the values obtained without correction of threshold value. But the energy packing efficiency, EPE_{F3} , is less than the desired value which is summarized in Table 3.4. The modified threshold value increases the compression efficiency of the system with the desired reconstruction error. Same compression ratio can be achieved with 7-bit

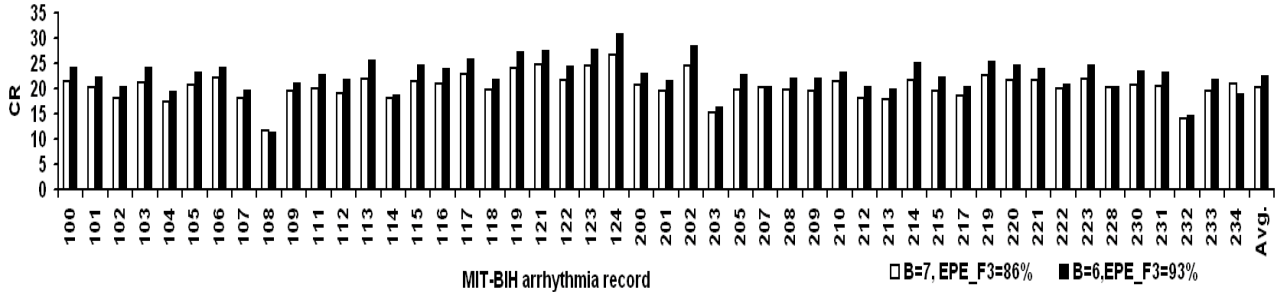

Figure 3.8: Compression results of the proposed technique at b=7, EPE_{F3} = 86% and b=6, EPE_{F3} =93%.

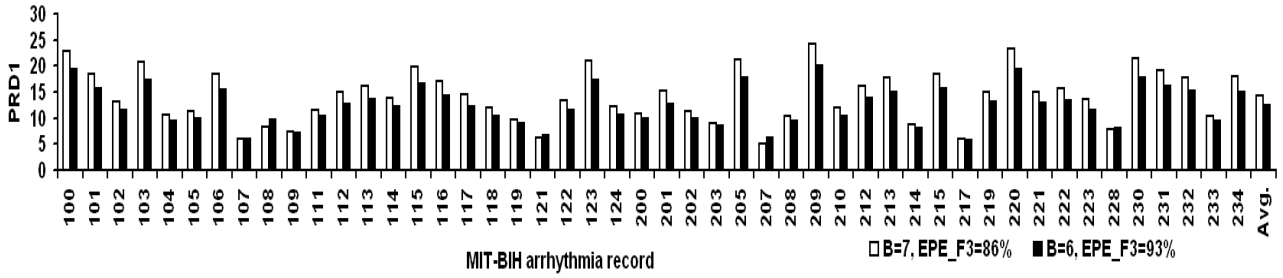

Figure 3.9: PRD results of the proposed technique at b=7, EPE_{F3} = 86% and b=6, EPE_{F3} =93%.

quantization without the correction of threshold value for the threshold T_2 and T_3 selected at EPE_{F2} = 99% and EPE_{F3} =86%. The PRD1 and PRD2 values of the records 108 and 207 are less than the reconstruction error of the 6-bit quantizer with correction. For the record 117, the technique achieves a CR value of 24.94:1 with a PRD1 value of 17.601%. In this case, the 6-bit quantization results in a CR value of 25.76:1 with PRD1 value of 12.182 for the threshold T_2 and T_3 selected at EPE_{F2} = 99.9% and EPE_{F3} =93%. To reveal the visual quality of the compressed signal obtained for the 7- and 6-bit quantization, the original and the reconstructed signals are shown in Fig. 3.7(b) and (c). It can be observed that the quality of the compressed signal obtained for the 6-bit quantization is better than the one obtained for the 7-bit quantization. The QRS complex amplitude of second ECG beat, which is shown in Fig. 3.7(b), is reduced because of the low EPE_{F3} for 7-bit quantizer. To evaluate the effects of 6-bit and 7-bit quantization with their respective EPE values, 48 `mita` records are tested using the proposed technique. The CR and PRD2 values are shown in Fig. 3.8 and 3.9. It is observed that, except for the records 108, 121 and 207, the 6-bit quantizer with the threshold T_2 and T_3 selected at EPE_{F2}= 99.9% and EPE_{F3} =93% achieves higher compression ratio with lower PRD1 values compared to the 7-bit quantization with the threshold T_2 and T_3 selected at EPE_{F2} = 99% and EPE_{F3} =86%. The overall performance is better with the 6-bit quantization because of the selection of higher EPE values for the thresholding process.

Based on our results in [202], the value of δ should lie between $0.85T_i - 0.95T_i$ for the i frame for a set of test ECG signals. In [203], the relationship between the step size Δ and the threshold T is fixed as

$\Delta = 1.55T$ for ECG signal compression. This choice has been empirically tested to give reasonably better performance. However, when the above condition is not met the result may not be optimal. It is well known that the parameters threshold T and Δ have a strong impact on compression and reconstruction error. Thus, considerable gains in compression ratio could probably be achieved by using different optimized parameters set for different blocks. The limitations of the above quantizers in the point of ECG compression are illustrated with sets of experiments in Chapter 2.

3.2.4.2 Background and Problem Statement

Several wavelet transform techniques have been proposed over the years which utilize lossy compression for denoising of images corrupted with noise [205,206]. The signal denoising has been widely achieved using the nonlinear techniques, particularly wavelet thresholding where insignificant coefficients likely due to noise are removed while significant coefficients consisting of important signal features are retained with full precision (i.e., without quantization). The compression has been achieved in the sense that a fewer number of nonzero wavelet coefficients are retained and a few number of bits are used to quantize nonzero wavelet coefficients without introducing significant distortion. Many reported techniques exploit the similarity between soft thresholding and quantization to achieve simultaneous denoising and compression. The midtread quantizer is completely defined by its fixed quantization step-size Δ where the reconstruction values are optimized by the centroid of the distribution on the bins [206]. In practice, the center of a bin is often used as the reconstruction value for convenience purposes [198].

In wavelet based ECG coding methods, the compression of the wavelet coefficients are achieved by the hard thresholding followed by scalar uniform quantization. In wavelet based methods, higher subband coefficients of the ECG signal have sharp concentrations around zero bin in their distributions. Therefore, a zero-zone of the midtread quantizer is modified in a suitable way to reduce those small wavelet coefficients since it is similar to hard thresholding rule. Meanwhile, one likes to keep the wavelet coefficients located outside the zero-zone with good resolution. An excellent overview of scalar quantization scheme and its variants is discussed for coding of wavelet coefficients of the image [195]. In uniform midtread quantizer, the zero-zone width is limited by quantization step size Δ. The modified midtread quantizer is usually characterized by two parameters: the zero-zone width T and the outer-zone width Δ. Since zero-zone width does not equal outer-zone width of the quantizer, the quantizer is nearly uniform but not uniform. Therefore it is named as nearly uniform midtread quantizer (NUMQ). It is well known that the wavelet coefficients that lie inside the zero-zone region are set or quantized to zero. In many applications, the width of the zero-zone is 2Δ while the outer-zones of equal width Δ. It implies that the compression can be achieved in two ways: 1) by adjusting zero-zone width while all other widths are half of the zero-zone width; and 2) by choosing the outer-zone width for a required number of quantization levels while zero-zone width is twice the outer-zone width. Since many high frequency subband wavelet coefficients of most natural signals are very small, there will be no noticeable loss in the compressed signal if they are quantized to zero [203].

Therefore, it is desired to have a larger zero-zone to set more high frequency coefficients to zero to achieve the necessary compression [203, 206]. In this case, the outer-zone width increases in magnitude as the zero-zone width increases. Thus, it may quantize the nonzero wavelet coefficients in the outer-zone coarsely and this may introduce significant features distortion if those nonzero coefficients are really from the relevant features of the ECG signal. When the second quantization procedure is opted it may not remove the small wavelet coefficients likely due to noise significantly to achieve good compression results.

The nearly uniform midtread quantizer (NUMQ) is reproduced here in brief. The NUMQ has $2L+1$ zones, consists of one zero-zone plus L symmetric levels of zones on each side, with zero-zone width $2T$ and outer-zone width Δ [198]. The decision levels of the quantizer are defined for a quantizer with $2L+1$ zones that L levels of zones of equal quantization step size Δ on each side. The quantization rule of the quantizer [198] is defined as

$$\mathbf{y} = \begin{cases} y_{-\infty}, & x < -T-(L-1)\Delta \\ y_{-m}, & -T-m\Delta \le x < -T-(m-1)\Delta \\ y_0, & |x| \le T \\ y_m, & T+(m-1)\Delta < x \le T+m\Delta \\ y_{\infty}, & x > T+(L-1)\Delta \end{cases} \tag{3.4}$$

where $1 \le m < L$, x is the input value and $\{y_i\}$ denote the reconstructed or output values. The optimal reconstruction values are the centroids of the input values lying between two levels. In wavelet based image coding techniques, the modified midtread quantizer is widely used to achieve simultaneous denoising and compression [205, 206]. These techniques exploit the close similarity between the extended zero-zone midtread quantization and the soft thresholding structures, and approximate the denoising process using the lossy quantization [205]. In [205], *BayesShrink* threshold T_B defines the zero-zone width and the quantized nonzero wavelet coefficients are found in minimum description length (MDL) rule over the number of quantization levels L and step size Δ. The compression performance of the technique in [205] depends upon the magnitude of the additive noise. With respect to the ECG signals, the above quantizer solution is most suitable if the threshold parameter T_B is successfully defined for varying characteristics of the signal with different noises and artifacts. This design can be used to quantize higher detail subbands of the corrupted ECG signal with an apriori knowledge of the distribution to appropriately model these subband coefficient histograms and a noise threshold parameter T_B estimated appropriately. Thus, it requires an apriori study of characteristics of the noises and artifacts to be present in the recorded ECG signals and modeling of the histograms of the subband coefficient. However, if high compression rate is demanded at the output of a variable rate coder with the quantizer design in [205], it provides a poor compression results when the power of the input corrupting noise is low (i.e., high SNR). This happens because of the smaller zero-zone width, defined by the noise power dependent threshold T_B, and the rest of the nonzero coefficients to be then quantized coarsely with large distortion [206]. Therefore, it does not balance the tradeoff between the compression rate and distortion.

To overcome the above problem, the threshold parameter T_B and the number of quantization levels required in the quantizer are adapted [206]. To provide a better explanation with the ECG signal compression aspects, we provide a brief summary of the quantizer design philosophy [206] and then describe the limitation of this quantizer design. The zones on the positive side are indexed as $m = 0, 1, ...L$. Let $z_{-L}, ..., z_{-1}, z_0, z_1, ..., z_L, ...$ denote the boundaries of the outer-zones with reconstruction or output values $y_{-L}, ..., z_{-1}, z_0, y_1, ..., y_L$. In standard midtread quantizer, the zero-zone width is fixed by $\Delta_z = \frac{\text{MAX}(|WC|)}{2L+1}$. Based on the modeling of the histograms, the adaptive subband coder (adaptation of the zero-zone and reconstruction levels of the quantizer) is reported in order to perform simultaneous denoising and compression of the image. As per the quantizer design philosophy, the decision on the zero-zone width is made by comparing Δ_z with noise threshold parameter T_B. For design of the quantizer in [206], the zero-zone width is defined as

$$z_0 = \begin{cases} T_B, & \text{if } \Delta_z \leq T_B \\ \Delta_z, & \text{if } \Delta_z > T_B. \end{cases} \tag{3.5}$$

where T_B is the *BayesShrink* threshold parameter. The expression in (3.5) is slightly modified to perform zero-zone decision operation in closed form. The value of z_0 used to design the outer-zone width Δ. For the positive side of the quantizer, the decision levels of the quantizer are defined as $z_m = z_0 + m\Delta$ where $\Delta = \frac{\text{MAX}(|WC|) - z_0}{L}$. The decision levels for the negative side are calculated as $z_{-m} = -z_0 - m\Delta$ using the symmetry of the quantizer. This quantizer adapts its zero-zone and reconstruction levels according to the input noise level, the statistics of the noise-free signal and the compression rate required [206]. The results show that this scheme works better than the two stage schemes employed for simultaneous denoising and compression. As we stated in the previous section, the compression rate depends upon the two parameters zero-zone width T_B (thresholding) and the outer-zone width Δ (quantization). When the input noise level is low or no noise is present in the input (i.e., at high compression rates, $\Delta_z > T_B$), the coder in [206] functions like an adaptive subband coder that performs quantization of the wavelet coefficients by adjusting the outer-zone width Δ_z for a desired compression rate. In such a case, this adaptive subband coder may introduce a significant amount of quantization noise since the relatively larger width of the outer-zone Δ will be chosen in order to achieve a desired high compression rate when the input noise level is low. In this case, a significant improvement in compression rate and distortion could be achieved if the coder jointly selects the optimal values of the threshold (i.e., zero-zone width) T_B in the allowable outside region and the outer-zone width Δ for quantizing nonzero wavelet coefficients. Thus, the approach with constraint NUMQ scheme provides an optimal bit allocation and simultaneous signal denoising and compression with optimal parameters set. In ECG compression methods, the wavelet coefficients are thresholded iteratively until a user specified target value is reached with a preset error tolerance ε. As we demonstrated in the previous section, most of the signal energy is concentrated on a small number of wavelet coefficients while these coefficients are relatively large compared to the irrelevant coefficients, and less energy being in coefficients around zero in their distributions. The EPE/PWZC/RE criterion is chosen to select the threshold parameter T in most of

the reported works [134, 137, 211]. On the other hand, the methods set the insignificant coefficients to zero based on the threshold T achieved with rate- or quality-driven adaptive threshold algorithm [142, 143]. In all the methods, significant coefficients should be quantized at a finer resolution so that the criterion can be satisfied at the output of the coder. In such a case, the quantizer design, in (3.5), may not be efficiently embedded in those well-defined compression methods.

The above survey and investigation by several experiments show that an optimal quantization procedure can significantly improve the coding performance and reduce the computational cost, and can satisfy the specific application requirements. Therefore, a complete study of the thresholding and quantization procedures are presented to provide a fast algorithm for optimal nearly uniform midtread quantizer design, and to achieve simultaneous denoising and compression with good rate-distortion performance. In this work, the adaptive subband coder is attempted to perform: signal denoising with the noise threshold parameter and finer resolution of nonzero wavelet coefficients; signal compression by finding the optimal choice of the zero-zone width T and outer-zone width Δ in rate-distortion sense; and jointly signal denoising and compression with the optimal constraint noise threshold parameter T and outer-zone width Δ. The choice of NUMQ design parameters is discussed next.

3.2.4.3 Adaptive TCZNUMQ Scheme for Wavelet Coefficients

Although the concept of the modified midtread quantizer is extensively used for the image compression techniques and for achieving simultaneous denoising and compression, the optimal choice of the zero-zone width for thresholding and the outer-zone width for quantizing the nonzero wavelet coefficients is not studied elsewhere in reported ECG signal compression methods. In general, the compression framework involves the selection of optimal parameters T and Δ relating to the thresholding zero-zone width and the quantizing outer-zone width, respectively.

In this research work, we study the threshold control zero-zone nearly uniform midtread quantizer (TCZNUMQ) design. The zero-zone width is controlled by threshold parameter while the outer-zone width equals Δ. The zero-zone width of the quantizer equals T for the case of target driven threshold adaptation or is the optimal choice within the allowable region. For a given dynamic range of the NZWC vector, the outer-zone Δ width is calculated for varying quantizer resolution b within a reasonable range. The threshold control zero-zone nearly uniform midtread quantization for the frame i is illustrated in Fig. 3.10. The TCZNUMQ is equivalent to the thresholding with zero-zone width T_i followed by quantization with outer-zone width Δ. Parameter T_i is the width of the zero-zone of the i^{th} frame and the parameter Δ is the width of the outer-zones. Here, wavelet coefficients in the second and the third frames are adaptively thresholded and then quantized using the TCZNUMQ scheme. The wavelet coefficients in the first frame directly quantized without loss of any information. The nonzero wavelet coefficients in the three frames are kept with full precision that are denoted by c. They are quantized using the modified quantizer and the quantized nonzero wavelet coefficients are denoted by $\widetilde{c}$. The TCZNUMQ scheme maps a wavelet coefficient c to a quantiza-

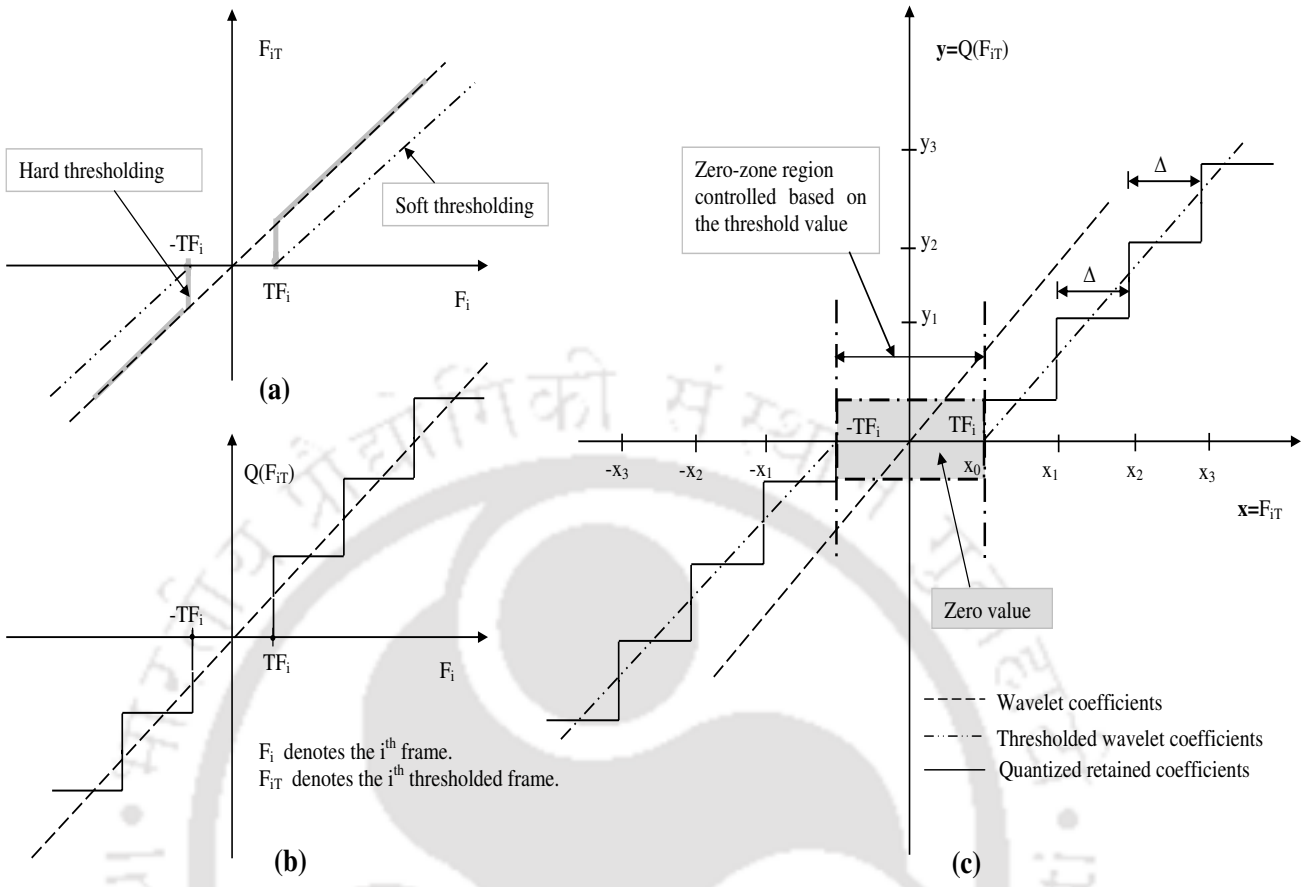

Figure 3.10: Similarity between the coefficients thresholding and coefficients quantization. Quantization is an approximation to the thresholding function. (a) Hard and soft thresholding functions. (b) Midtread quantization (c) Threshold control zero-zone nearly uniform midtread quantization: the zero-zone width is controlled by the threshold parameter T_i and the outer-zone width is Δ.

tion index q which is an integer. The quantization index q is a marker to the quantization zone where c lies. While reconstruction levels should be set at the centroids of the quantization bins to minimize mean squared reconstruction error, wavelet coefficients are here reconstructed at the midpoints of the quantization bins to reduce computation. The dequantizer receives a quantization index q and maps it to a value $\widetilde{c}$ that is close but it is not identical to c. Thus, the quantizer introduces signal distortion.

A uniform midtread quantizer can be defined by two parameters: the number of quantization levels and the quantizer step size Δ. The number of levels is generally chosen to be of the form 2^b to make the most efficient use of b bit binary codewords. The Δ depends on the dynamic range of the coefficient amplitude

and the quantizer resolution b. In standard midtread quantizer, the quantization step size is calculated as

$$\Delta_j = \left(\frac{\max(|c_j(k)|) - \min(|c_j(k)|)}{(2^{b_l} - 1)} \right), \quad j = 1,2,....J, \quad \text{and} \quad l = 1,2,....N_b. \tag{3.6}$$

The width of the zero-zone and outer-zone equals Δ_z. In our quantizer design, the zero-zone width equals the noise threshold parameter T_i of the i^{th} frame to perform the signal denoising or the target driven threshold adaptation for some applications. Note that the zero wavelet coefficients resulting from thresholding are kept as zeros and that the subsequent quantization does not set any additional wavelet coefficients to zero. Otherwise, for achieving simultaneous denoising and compression, the optimal choice of desing parameters are efficiently computed in the rate-distortion sense. In such a case, the threshold T_i is efficiently located in the allowable region to remove the wavelet coefficients which are expected only because of the noise.

For the zero-zone width T_j and the outer-zone width Δ_j, the quantization index for the k^{th} wavelet coefficient in the j^{th} subband is given by

$$q_j(k) = \begin{cases} \left\lfloor \frac{c_j(k)+T_j \cdot \Delta_j}{\Delta_j} \right\rfloor, & c_j(k) > T_j \\ 0, & -T_j \le c_j(k) \le T_j \\ \left\lceil \frac{c_j(k)-T_j \cdot \Delta_j}{\Delta_j} \right\rceil, & c_j(k) < -T_j \end{cases} \tag{3.7}$$

The above equation shows how design parameters T_j and Δ_j are used by the adaptive wavelet coder to quantize a wavelet coefficient $c_j(k)$ (i.e., k^{th} wavelet coefficient j^{th} subband) to quantization index $q_j(k)$. In this work, T_j is transmitted as side information to the decoder. If $T_j = 0.5$, then the proposed TCZNUMQ operates like a typical midtread quantizer with the quantization step size of Δ_j, and if $T_j = 0$, then the TCZNUMQ corresponds to the modified midtread quantizer where the zero-zone width is $2\Delta_j$. For a target driven threshold adaptive algorithm, the value of the T_j limits the width of the zero-zone while it is the optimal choice in the case of signal compression.

The quantized index q_j is stored and transmitted. Generally, the de-quantization is performed during the decoding process to find an approximation to the input wavelet coefficient c_j that is done in the multiplication of each quantized index q_j of the nonzero wavelet coefficient by the quantization step size Δ_j. For given $q_j(k)$ and T_j, the decoder produces de-quantized coefficients $\widetilde{c_j}(k)$,

$$\widetilde{c_j}(k) = \begin{cases} \Delta_j \cdot (q_j(k) + \xi - T_j), & q_j(k) > 0 \\ 0, & q_j(k) = 0 \\ \Delta_j \cdot (q_j(k) - \xi + T_j), & q_j(k) < 0 \end{cases} \tag{3.8}$$

The above equation shows how the decoder computes the quantized nonzero wavelet coefficients vector QNZWC. ξ is the parameter that varies in the range [0, 1]. It determines the reconstructed value $\widetilde{c_j}$ and

the ξ can be chosen so that the quality of reconstruction is good. For $\xi = 0.5$, the reconstructed values for each quantization zones are the midpoints of the zones. In practice, this procedure is often followed rather than the centroid of the distribution on the bin for convenience purposes [198]. At the de-quantization, the quantized wavelet coefficient $\widetilde{c_j}$ may not be equal to the amplitude of the input coefficient $c_j(k)$. In general, the quantization error is defined by $d(c,\widetilde{c_j}) = (c_j - \widetilde{c_j})$. The quantization error of the wavelet coefficients lies in the outer-zone width which is bounded by

$$\frac{-\Delta_j}{2} \leq e_j^q(k) \leq \frac{\Delta_j}{2} \tag{3.9}$$

An increase of Δ implies that greater compression can be achieved, with lower quality in the compressed signal. It is known that compressed quality and rates are controlled by the amount of quantization applied to each coefficient. The quantization step sizes are specified relative to the nominal dynamic range of the coefficients.

The distortion of the original signal can be seen to have two different origins: the discarded wavelet coefficients lie within the zero-zone region; the quantization of wavelet coefficients lie in the outer-zones. Without loss of generality, let N^T and N^q be the number of zeroed wavelet coefficients and the number of nonzero wavelet coefficients, respectively. The classical squared error distortion is defined by $d(c_j(k),\tilde{c}_j(k)) = (c_j(k) - \tilde{c}_j(k))^2$. For the optimization procedure, we use the mean square error as the distortion measure $D(T_j,\Delta_j)$. The mean squared error introduced by the coefficients c_j^z lies in the zero-zone of the quantizer, the thresholding zone for the j^{th} subband is given as:

$$D_j^T(T_j) = \frac{1}{N_j^T}\sum_{k=1}^{N_j^T}(c_j^z(k))^2. \tag{3.10}$$

The equation (3.10) equals the noise energy if the c_j^z are the wavelet coefficients of the noise. The mean squared error introduced by the quantization of the nonzero wavelet coefficient $c_j^q(k)$ can be calculated as:

$$D_j^q(\Delta_j) = \frac{1}{N_j^q}\sum_{k=1}^{N_j^q}(c_j^q(k) - \widetilde{c}_j^q(k))^2. \tag{3.11}$$

Then, the mean squared error due to the thresholding and quantization of wavelet coefficients c_j is given by

$$D_j(T_j,\Delta_j) = \frac{1}{N_j^T}\sum_{k=1}^{N_j^T}(c_j^z(k))^2 + \frac{1}{N_j^q}\sum_{k=1}^{N_j^q}(c_j^q(k) - \widetilde{c}_j^q(k))^2. \tag{3.12}$$

In global thresholding case, the $D(T,\Delta)$ is given by

$$D(T,\Delta) = \frac{1}{N^T}\sum_{k=1}^{N^T}(c^z(k))^2 + \frac{1}{N^q}\sum_{k=1}^{N^q}(c^q(k) - \widetilde{c}^q(k))^2. \tag{3.13}$$

where c denotes wavelet coefficients vector of the signal. With respect to the modified quantizer shown in (3.4) for the symmetric levels L, the entropy measure $H(T,\Delta)$ is defined as [198]:

$$H(T,\Delta) = -P_0 \log_2 P_0 - 2\sum_{l=1}^{L} P_l \log_2 P_l, \tag{3.14}$$

where $P_0 = \int_{-T}^{T} p(c)dc$, $P_l = \int_{T+(l-1)\Delta}^{T+l\Delta} p(c)dc$, and $P_L = \int_{T+(L-1)\Delta}^{\infty} p(c)dc$. The equation (3.14) provides the estimation of the entropy of all quantized wavelet coefficients for a given T and Δ. There are many possible ways to encode the quantized wavelet coefficients that are discussed in Chapter 2. In this work, the N^T wavelet coefficients within the range $[-T,T]$ are set to zero and then two vectors are derived from the thresholded wavelet coefficients (TWC) vector: the nonzero wavelet coefficients (NZWC) vector; and the significance map (SM) which consists of the locations or indexes of the nonzero wavelet coefficients. Finally, the N^q quantized nonzero wavelet coefficients and the SM are encoded either in fixed or variable codeword length manner. The quantized coefficients are denoted by $\{\widetilde{c}^q\}$. On average, the smallest number of bits needed to code $\widetilde{\mathbf{c}}^q$ is computed using Shannon entropy [205]. Thus, the codeword length for coding the bin indexes is computed as $H(\widetilde{\mathbf{c}}^q|T,\Delta) = -\sum_l P_l \log_2 P_l$ where P_l is the probability of a symbol in bin l. The number of bits needed to indicate the indexes of nonzero wavelet coefficients is $N^q \log_2 N$ (assuming fixed codeword length). The number of bits needed for SM can be further reduced using the proposed encoding scheme in the next section. Using the above distortion and entropy measures, the optimal values of the T and Δ can be obtained by solving the minimization problem.

The TCZNUMQ quantizer provides distinct advantages over other quantizers used for ECG compression: 1) it allows the adaptive threshold T control for the zero-zone width and thus provides adaptive thresholding to different subband characteristics based on specific criterion; 2) it allows to quantize the significant wavelet coefficients with minimal quantization error by adjusting the outer-zone width Δ. Thus, the adaptive quantization in outer-zone region does not introduce significant distortion and thus it performs denoising where the allowed loss is equal to the noise strength; 3) it reduces the computational cost without affecting the optimal performance by searching over a limited set of step sizes; 4) it allows to find the optimal values of the zero-zone width and the outer-zone width of the quantizer in rate-distortion sense. This procedure helps to achieve simultaneous denoising and compression regardless of the input noise level, where the zero-zone width equals either the noise threshold T_B or an optimal threshold T outside in the range $[-T_B,T_B]$. When a high compression rate is desired at the output of a coder and the noise power is low, for example, the proposed TCZNUMQ scheme based coder provides better compression performance than the wavelet coder with the quantizer designs in [205, 206]; and 5) it provides a desired rate/distortion quickly and accurately.

3.2.4.4 Results of Adaptive TCZNUMQ Scheme

In this section, we demonstrate the advantages of the proposed adaptive TCZNUMQ scheme over other widely used quantizers for the ECG signal compression. Tests are carried out using the `mita` records 107, 111, 117 and 119, the distortion measures namely PRD1 and PRD2, and the tolerance $\varepsilon = 1\%$. Note that these records have different morphologies, noises and mean values and widely used in the previous works. The signal block of 43200 samples is chosen from each record to compare the performance of the proposed scheme with the recently reported two-stage scheme [143]. Each signal block is compressed independently from the others. Once the zero-mean signal is decomposed up to five-level, the wavelet coefficients are thresholded iteratively, using the bisection algorithm, until a desired PRD1/PRD2 is reached with a specified tolerance ε. The resulting nonzero wavelet coefficients are quantized using the proposed adaptive TCZNUMQ scheme and the quantization scheme in [143]. In this test, the adaptive quantization schemes adopt the quantizer resolution for each iteration from the set $\{11,10,9,8,7,6\}$. The two two-stage schemes are: first is the distortion driven adaptive threshold and adaptive quantization algorithms reported in [143], where the algorithms function independently to perform compression; and second is the proposed two-stage algorithm with threshold control zero-zone quantization scheme. Table 3.5 illustrates the performance of the two two-stage schemes when applied to the records 107 and 117 for a desired PRD2 values of 2% and 1%. The compression results of the two two-stage adaptive algorithms are compared and some interesting properties are observed in this experiment. In [143], the results of the adaptive quantization scheme for the `mita` record 117 and the desired PRD1 value of 2% are illustrated with the tolerance $\varepsilon = 10\%$. The authors concluded that for $b = 6$ the quantizer fulfills the desired requirement, PRD2=2% with $\varepsilon = 10\%$ [143]. In [143], the quantization errors are due to the quantized NZWC or/and the resulting zero coefficients after quantization. In our scheme, the errors are only due to the quantized coefficients since the quantization of the nonzero coefficients do not set any additional coefficients to zero. In such an adaptive quantization scheme with $\varepsilon = 10\%$, for a large value of desired PRD2, the deviation will be larger. Moreover, target PRD2 values may not be reached smoothly and accurately. For the same record and specifications, the compression results are shown in Table 3.5. Note that the mean values of the records 107 and 117 are -0.8172 and -0.2275, respectively. When the threshold T is larger than the decision interval of the zero-zone of the quantizer, the increment of PRD2 is small. Otherwise, the increment is large which is illustrated in Table 3.5 for the desired PRD2=1% and both the `mita` records. This phenomenon is observed, in the case of record 107, for the quantizer resolution of $\{7,6\}$ and $\{8,7,6\}$ with the PRD2 values of 2% and =1%, respectively. Thus, it is possible to reduce the computational cost. In such cases, the constraint on the threshold control zero-zone reduces the computation by three times as compared to that required for the conventional adaptive quantization procedure. Note that the reduction in computation is dependent on a desired PRD2 value for finding the threshold. However, a considerable amount of computation can be reduced in the allowable range of PRD2 values which can result in better quality of the compressed signal.

The quantization errors may be significant compared to the errors due to zeroing of the irrelevant wavelet

Table 3.5: Performance comparison of the two two-stage adaptive algorithms: without threshold control zero-zone (TCZ) strategy [143]; with TCZ quantization strategy.

target	b	mita record 107						mita record 117					
		W/O TCZ [143]		T	Δ	W/ TCZ		W/O TCZ [143]		T	Δ	W/ TCZ	
PRD2 (%)		PRD1 (%)	PRD2 (%)			PRD2 (%)	PRD1 (%)	PRD1 (%)	PRD2 (%)			PRD2 (%)	PRD1 (%)
	6	4.972	4.800	16.388	70.799	4.669	4.836	7.953	**2.150**	15.782	18.441	**2.152**	7.998
	7	2.948	2.846	16.388	35.121	2.950	3.055	7.505	2.028	15.782	9.148	2.030	7.511
2	8	2.312	2.232	16.388	17.492	2.226	2.305	7.390	***1.997****	15.782	4.556	***1.998****	7.391
	9	2.131	**2.057**	16.388	8.729	**2.055**	2.129	7.364	1.990	15.782	2.274	1.990	7.364
$\varepsilon = 1\%$	10	2.082	***2.010****	16.388	4.360	***2.009****	2.081	7.357	1.988	15.782	1.136	1.988	7.357
	6	5.158	4.979	5.311	70.799	4.309	4.464	6.687	1.807	5.404	18.441	1.759	6.508
	7	3.112	3.005	5.311	35.121	2.466	2.554	4.384	1.185	5.404	9.148	1.197	4.427
1	8	1.853	1.789	5.311	17.492	1.701	1.762	3.887	**1.051**	5.404	4.556	**1.051**	3.889
	9	1.250	1.207	5.311	8.729	1.238	1.283	3.746	***1.012****	5.404	2.274	***1.013****	3.746
	10	1.095	**1.057**	5.311	4.360	**1.056**	1.094	3.709	1.002	5.404	1.136	1.002	3.709
$\varepsilon = 1\%$	11	1.051	***1.014****	5.311	2.179	***1.014****	1.052	3.699	0.999	5.404	0.567	0.9998	3.699

Table 3.6: Compression performance of the two-stage scheme [143] and the proposed TCZNUMQ scheme.

target	mita record 107						mita record 117					
	Benzid et al. [143]			Proposed Method			Benzid et al. [143]			Proposed Method		
PRD1 (%)	PRD1 (%)	(T,Δ)	H	PRD1 (%)	optimal (T,Δ)	H	PRD1 (%)	(T,Δ)	H	PRD1 (%)	optimal (T,Δ)	H
1	1.00	(11,5.82)	2.18	1.00	(10,5.14)	1.87	1.05	(10,1.31)	3.99	1.06	(10,1.25)	3.49
2	2.05	(9,17.17)	1.27	2.04	(8,15.29)	1.05	2.03	(9,2.43)	2.65	2.04	(9,2.31)	2.32
3	3.03	(8,30.10)	1.10	3.02	(8,29.93)	0.826	3.07	(9,4.13)	1.84	3.07	(9,4.14)	1.66
4	4.07	(10,45.94)	0.916	4.07	(7,45.40)	0.659	4.02	(9,6.50)	1.50	4.04	(8,6.37)	1.23
5	5.03	(8,54.92)	0.788	5.02	(7,53.41)	0.580	5.08	(8,8.56)	1.24	5.08	(7,8.53)	0.952

coefficients concentrated around zero in their distributions. Thus, for the $\varepsilon = 1\%$, the quantizer with $b = 8$ fulfills the requirement for the record 117 and the PRD2=2%. Note that ***1.997%**** denotes the attained PRD2 at the output of the two-stage scheme. In the two two-stage schemes, the entropy rates obtained are approximately equal. But the improvement in the compression can be achieved for the optimal choice of design parameters T and Δ. Since PRD2 is dependent on mean value, the PRD1 is used in the optimization problem. The compression results of the two-stage scheme [143] and the proposed TCZNUMQ scheme are shown in Table 3.6. It shows that the proposed TCZNUMQ scheme obtains better compression performance than the two-stage scheme. At the range of $1 \leq \text{PRD1}(\%) \leq 5$, the average rates of the TCZNUMQ and two-stage are 1.00 and 1.25, respectively for the test record 107. Thus, the compression performance is

improved by 24.21%. For the test record 117, the compression performance is improved by 13.97%. These experiments show that the proposed adaptive TCZNUMQ scheme works better than other quantization schemes in wavelet based ECG compression methods.

3.2.5 Modified Index Coding Scheme for Significance Map

In wavelet thresholding based methods, the compression is done in two stages: 1) compression of the nonzero wavelet coefficients (NZWC) vector and 2) compression of the significance map. Transmission or storage of indices of the significant coefficients or significance map is important for perfect reconstruction at the decoder. The significance map is defined as the indication of whether a particular wavelet coefficient is zero or nonzero in a given wavelet coefficients vector. For wavelet based image coding, many approaches to efficiently code the significance map by exploiting the properties of the wavelet transformed image [217]. In most of the wavelet thresholding based ECG compression methods [134, 135, 137, 138, 142, 211], the significance map which is the binary vector that stores the information generated by scanning the wavelet coefficients in TWC vector and representing a '1' if a nonzero (or significant) wavelet coefficient is scanned and representing a '0' if a zero (or an insignificant) coefficient is scanned [134]. This is referred as binary significance map (BSM) [134, 135] and is compressed using the 8 bits/element table (T8) [137] or the RLE [138,211] and Huffman coding algorithms [137,142]. In [134,135], the BSM is compressed efficiently using a variable-length code based on run length encoding algorithm. The compression efficiency of the threshold based method depends on the number of bits used to code the NZWC vector and the number of bits used to code the significance map. Considerable gains in compression ratio could probably be achieved if a significance map is compressed in an efficient way. Therefore, we attempt an efficient coding scheme for significance map by exploiting the characteristics of the ECG signal and the distribution of the significant coefficients at each subband of the wavelet transform.

Most of the energy in an ECG signal is concentrated in the low-frequency region. The wavelet transformation causes the significant part of the signal energy to be concentrated at the low-frequency components, with majority of the coefficients having little energy. It can be observed that at each subband of the wavelet transform the energy distribution is concentrated in a small number of wavelet coefficients. Therefore, the wavelet transform of most ECG signals are sparse, resulting in a larger number of small wavelet coefficients and a smaller number of large coefficients. A few number of wavelet coefficients may be sufficient to represent the ECG signal which is characterized by a cyclic occurrence of patterns (QRS complexes, P and T waves) with different frequency contents. Moreover, significant wavelet coefficients for each signal block appear considerably close in the order sequence within a wavelet subband. Since nonzero coefficients in the TWC vector exhibit localized patterns at each subband, thus significance map is created by storing the indexes or locations of nonzero wavelet coefficients. The resultant is referred as integer significance map (ISM). The use of first order forward difference for the indexes leads to increases the closeness of the indexes of the significant coefficients within subbands. This is described as follows. The first order forward

difference of a set of positive integers I is a new set $\hat{I}$ where $\hat{I} = I(n+1) - I(n)$. Set $\hat{I}$ has one element less than the initial set I that is stored and transmitted. This is referred as differencing further in this work. Resulting set $\hat{I}$ can be much more efficiently coded since differencing increases the probability of occurrence of symbols within a set or subset. Thus, the first difference of the indexes of the significant coefficients can be coded with a Huffman encoding in a highly efficient way.

The proposed modified index coding (MIC) combines two ideas such as differencing and Huffman encoding to compress the ISM. The first step of this concept is similar to the one introduced in a lossy image codec based on index coding [217]. Let us explain first the index coding with an example and then we focuss on our proposed MIC scheme. A finite wavelet coefficient index set is given by $I = \{k : k \in \mathbb{Z}^+, k \leq K\}$, where K is a positive number that is the length of the WC vector and k is the index of the wavelet coefficient in the WC vector. If we assume A is a subset of I then how to code the set or the subset A in an efficient way. Assume W to be the amplitudes of a hypothetical set of wavelet coefficients for one signal block, $\mathrm{W} = \{-141.87, 47.44, -56.72, 83.62, -13.79, -1.21, 0.46, 0.59, -14.50, 1.38, 0.10, 0.65, 13.60, -8.47, 5.01, 6.59, -14.52, 5.30, 6.10, -2.33, 7.35, 1.02, -24.49 - 2.33, 11.35\}$. With a threshold $T = 10.15$, the significant or nonzero wavelet coefficients are

$$I = \{-141.87, 47.44, -56.72, 83.62, -13.79, -14.50, 13.60, -14.52, -24.49, 11.35\} \tag{3.15}$$

and their wavelet indexes in set W are

$$I = \{1, 2, 3, 4, 5, 9, 13, 17, 23, 25\} \tag{3.16}$$

In this example, the number of significant coefficients is 10. The elements in a wavelet index set I are all positive integers. We want to code this index set I. Since the elements of I are ordered in a monotonically increasing order, we can take the forward difference of two adjacent elements to produce a difference set $\hat{I}$ of initial set I,

$$\hat{I} = \{1, 1, 1, 1, 1, 4, 4, 4, 5, 2\}. \tag{3.17}$$

The elements in set $\hat{I}$ are referred as skips. And it is straightforward to get set I from the difference set $\hat{I}$ by taking the partial sums of $\hat{I}$. Thus I and $\hat{I}$ contain the same information and it means that there is no information loss. The difference set $\hat{I}$ can be compressed by means of a Huffman coding or a variable length coding procedure which assigns codewords of variable lengths to the possible outcomes $\hat{I}$ such that highly probable outcomes are assigned shorter codewords, and vice versa. Huffman coding is based on the frequency of occurrence of the skips values in difference set $\hat{I}$. In this example, the frequency histogram of of skips values of the set $\hat{I}$ is given by

$$\hat{I}_h = \{5, 3, 1, 1\}. \tag{3.18}$$

and then the probability set P which provides probabilities of the skips values of the set $\hat{I}$, is given by

$$P = \{0.5, 0.3, 0.1, 0.1\}. \tag{3.19}$$

As a variable-length encoding scheme, Huffman encoding has been shown to be one of the most leading techniques being used in various applications dealing with data compression. In fact, as it is widely practised, the combination of run length encoding and Huffman encoding provides a near optimal encoding technique which is easy to implement. In this work, we use the combination of differencing encoding and Huffman encoding schemes since the length of the wavelet index set I is small and it does not have any repeated symbols like runs of ones and runs of zeros in the binary significance map. The run length coding is more suitable to code the binary significance map. In this work, Huffman coding is employed which minimizes the average code length required for difference set $\hat{I}$. The Huffman coding is performed in an efficient way by examining the probabilities (or count) of the symbols in the difference set $\hat{I}$.

Generally, more number of large wavelet coefficients are localized in wavelet subbands such as approximation subband and lower detail subbands having the smaller sizes. Thus this property results in a more number of ones in difference set $\hat{I}$, and its probability is naturally high compared to that of other symbols which are available in the set. Thus its count is coded by assigning a fixed number of bits. A few larger values are observed in difference set $\hat{I}$ due to long skip between the localized patterns. This may reduce the coding efficiency of the Huffman coder. Therefore, we have employed a skips detector with threshold I_T assigned based on prior study of distribution of localized wavelet coefficients in WC vector or adaptively found by exploiting local skip statistics of the set I. The detector finds and assigns a zero to values of skips in the set $\hat{I}$ above I_T while that large skip is stored. The large skips removed set is referred as S. The large skips are coded using fixed-length coding. The number of large skips maybe small and thus its code length is small. The codebook is generated which consists of four parts. The first part contains the code assigned to ones count. The second part carries the code used to represent the symbols in set S. The third part carries the code used to represent counts of those symbols. Finally, the fourth part contains the code of the large skips. As a measure of the compression efficiency of an encoding scheme, we use the average codeword length. Let $\mathbf{S} = (S, p)$ be an information source and (C, f) be an encoding scheme for symbol set $S = \{s_1, s_2, s_3, \ldots\ldots\ldots s_q, \}$ where S denotes source symbols s_q, $1 \leq i \leq q$, p_i denotes the probability of the source producing symbol s_q, C denotes a code for the source S and $C(i)$ is the codeword assigned to source symbol s_q. The entropy of the source S is given by

$$H = -\sum_{i=1}^{q} p_i \log_2 p_i \tag{3.20}$$

and the average codeword length of (C, f) is given by

$$L_c = \sum_{i=1}^{q} \text{length}[f(s_i)]\ p(s_i) \tag{3.21}$$

As we will see, the proposed modified index coding produces the most efficient scheme in the sense of having the smallest average codeword length among the encoding schemes used for the ISM. Finally, the proposed modified index coding schemes consists of the following steps:

Step 1: Obtaining the thresholded wavelet coefficients (TWC) vector of the frame or the WC vector depending on the thresholding procedure.

Step 2: Creation of integer significance map (ISM) by storing the locations of nonzero wavelet coefficients in the TWC vector.

Step 3: Applying difference encoding to the ISM and results in DISM set(s).

Step 4: Detecting larger skips in the difference set and replacing those skips with the zero value. Thus it results in two sets: processed DISM set and large skips subset.

Step 5: Compression of the processed DISM using the Huffman coding algorithm and representation of the large skips using the adaptive fixed-length coding procedure.

Step 6:Finally, generation of codebook for each significance map.

The compression performance of the reported various encoding schemes and the proposed MIC schemes such as Huffman coding of difference of ISM (HDISM) and Huffman coding of processed difference of ISM (HPDISM) is tested using more than 150 significance maps. The widely used encoding shemes for the compression of significance map are the arithmetic coding of binary significance map (ABSM), the Huffman coding of 8 bits/element table (T8) version of the BSM (HT8BSM) and the Huffman coding of run length encoded version of the BSM (HRBSM). The significance map resulting from the wavelet coefficients vector of the ECG signal by thresholding is expressed by the binary strings and the wavelet indexes of the entire wavelet subbands for testing purposes. In the first experiment, we have considered the signal block of 1024 and 2048 samples and the widely used `mita` records 107 and 117. For different values of percent retained energy (RE), the BSM and ISM are created, and then these maps are compressed using the reported encoding schemes and the proposed encoding schemes, respectively. The compression ratio calculated for each encoding scheme is shown in Fig. 3.11. It can be observed that for both the signal block lengths the compression performances of the proposed encoding schemes such as HDISM and HPDISM are better compared to the other encoding schemes. Meanwhile, the compression ratios achieved using the HPDISM encoding are higher as compared to that of the HDISM encoding scheme. In the second experiment, fifty significance maps created using the following specifications such as the percent RE value of 99.5% and the signal block of 1024 samples taken from fifty records, and then significance map of each signal block is encoded separately. Note that difference sets obtained for these significance maps may have diverse skip values and also may have various localized patterns. The compression performance of the encoding

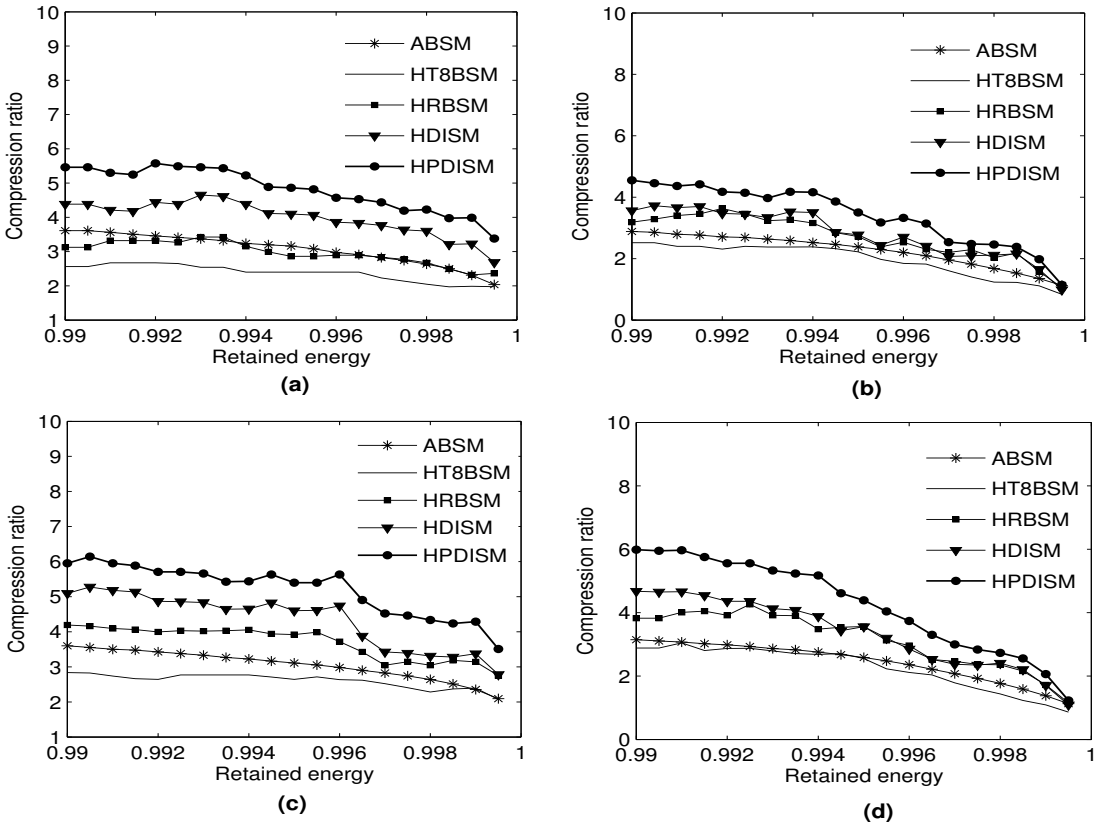

Figure 3.11: Compression performance of the various encoding schemes for the significance maps which are generated from the processed ECG signal with (a) 1024-samples taken from the `mita` record 107; (b) 1024-samples taken from the `mita` record 117; (c) 2048-samples taken from the `mita` record 107; and (d) 2048-samples taken from the `mita` record 117.

Table 3.7: Average compression performance of different encoding schemes for 150 significance maps.

Encoding scheme for SM	N=1024 samples		N=4096 samples	
	Compression ratio (CR)	Coding time, t_{esm} (ms)	Compression ratio (CR)	Coding time, t_{esm} (ms)
	ACR $\pm \sigma$	$At_{esm} \pm \sigma$	ACR $\pm \sigma$	$At_{esm} \pm \sigma$
HT8BSM	1.89 $\pm$ 0.48	158.2$\pm$ 33.83	2.11 $\pm$ 0.52	585 $\pm$ 97.7
HRBSM	2.40 $\pm$ 0.61	57.6 $\pm$ 22.03	3.19$\pm$0.85	167.2 $\pm$78.1
HDISM	2.94 $\pm$ 0.95	60.8$\pm$23.9	3.51 $\pm$ 1.03	202.9 $\pm$ 94.3
HPDISM	3.55 $\pm$ 1.11	47.73$\pm$ 22.7	4.15 $\pm$ 1.20	153.2$\pm$ 83.06

schemes for the case of different significance maps is shown in Fig. 3.12. These experiments show that compression performance of the proposed HPDISM encoding scheme is better for varying distribution of various significance maps.

The compression ratio and encoding time (t_{esm}) are measured for different significance map encoding schemes, averaged across the 150 significance maps and the results are shown in Table 3.7. The standard

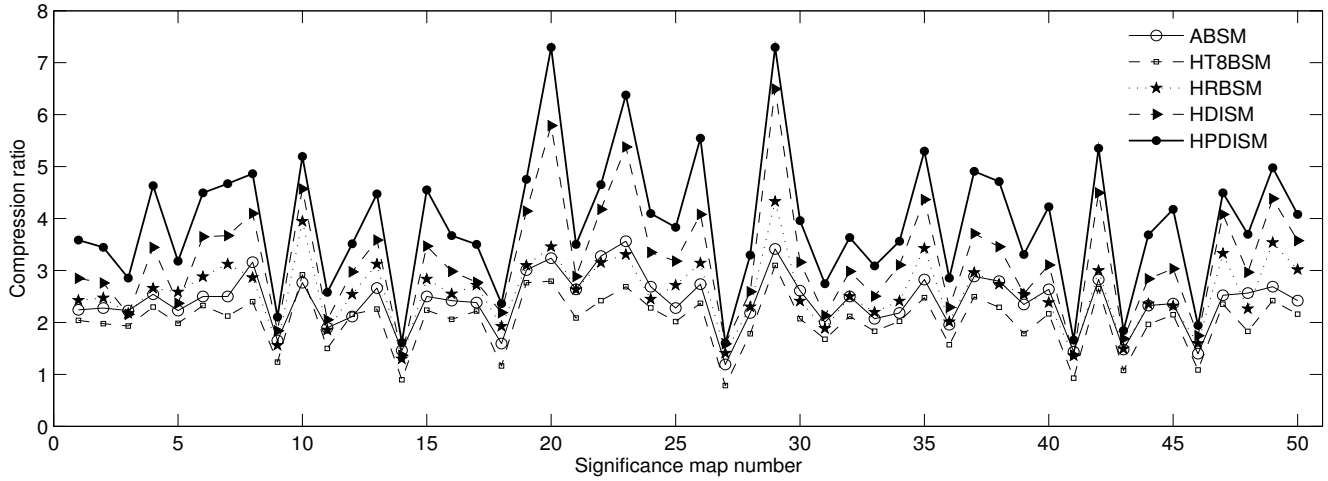

Figure 3.12: Compression performance of the proposed encoding schemes for varying distribution of various significance maps.

deviation of the measured values are also summarized. Table 3.7 shows that HPDISM performs better than the other schemes with the highest compression ratio and lowest coding time. Especially remarkable is the increase in compression performance of the proposed HPDISM compared to the widely employed HT8BSM algorithm in ECG compression method or to the HRBSM algorithm used in the transform based methods. It is shown that by employing the proposed steps for encoding significance map becomes significantly faster and the compression ratio is also higher compared to other coding schemes employed for significance map. By exploiting the local distribution of the wavelet indexes, we have shown that an intuitive way of coding of difference set symbols results in a much more efficient compression of the significance map without increasing the coding time. We thus follow the encoding procedure of the HPDISM scheme described in this section to code the significance maps. The HPDISM is referred as modified index coder (MIC) in this thesis. Overall compression performance with the combined quantized nonzero wavelet coefficients vector and the processed DISM of the significance map will be discussed in the next Section.

3.2.5.1 Performance of the Modified Index Coding Scheme

In this section, tests are carried out using the most widely employed `mita` datasets and the frequently used signal duration. We compare the performance of the proposed encoder for significance map derived from the frames. The performance of the proposed scheme is compared with the HT8BSM [137] and the arithmetic encoding of significance map for 5.62 seconds and 60 seconds duration signals, respectively in Fig.3.13 and 3.14. Dataset-I is used for the testing purpose. From Fig.3.13(a), it can be observed that the proposed scheme requires less number of bits compared to the HT8BSM and arithmetic encodings. The arithmetic coding scheme requires less number of bits for 60 seconds duration signals compared to 5.62 second signal

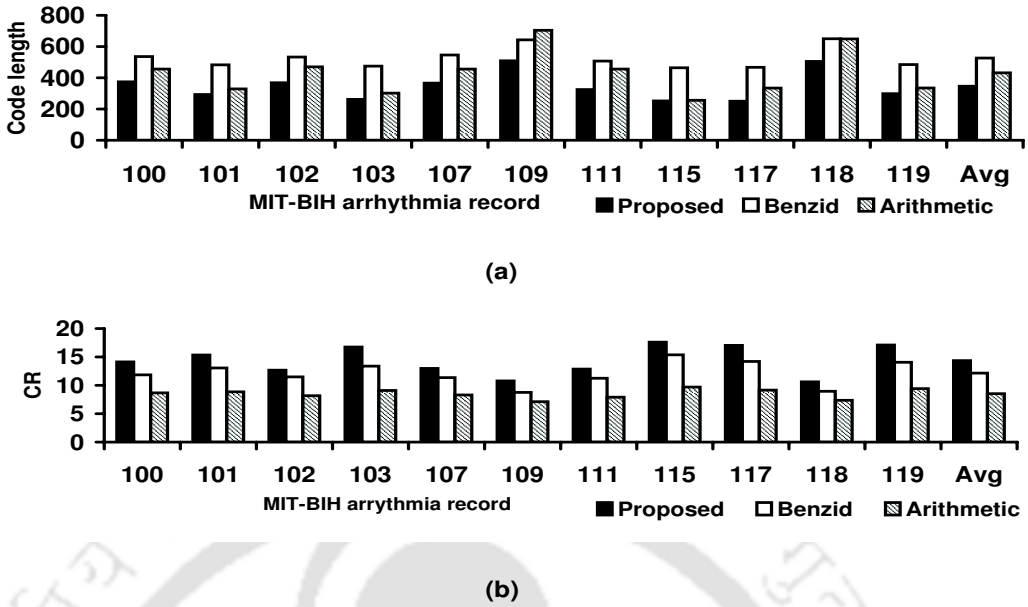

Figure 3.13: Performance of the modified index coding scheme for 5.62-sec duration samples. (a) Comparison of codeword lengths of the proposed, Benzid and Arithmetic coding. (b) Compression results of the different encoding methods applied to code the significance map.

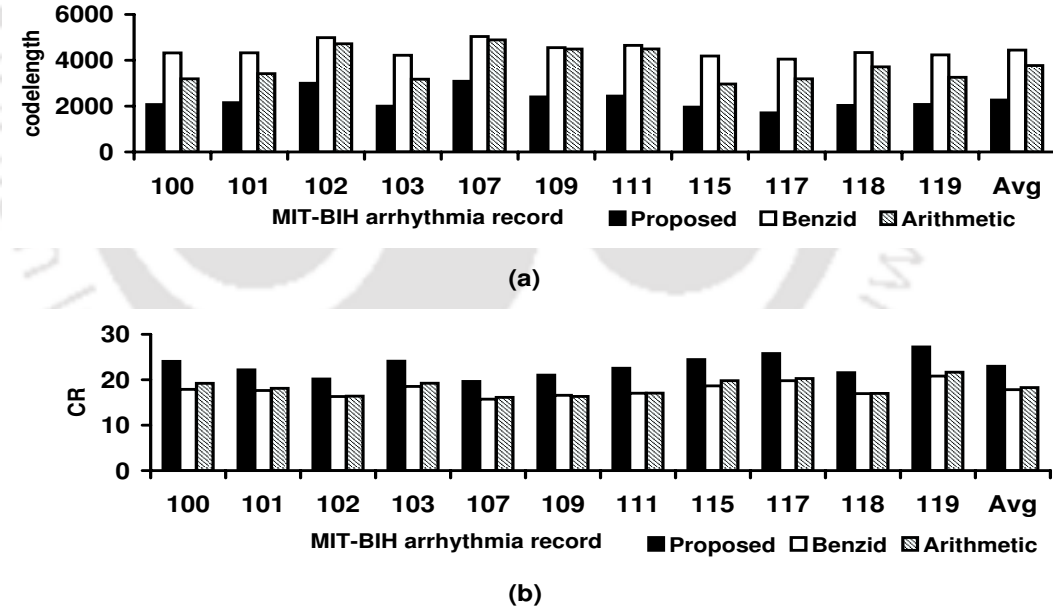

Figure 3.14: Performance of the modified index coding scheme for 60-sec duration samples. (a) Comparison of codeword lengths of the proposed, Benzid and Arithmetic coding. (b) Compression results of the different coding methods.

since the length of the sequence is large. The results show that the performance of the proposed scheme is better than others even for the small duration test signal blocks. The proposed entropy coder achieves high

compression efficiency because the number of indexes in the details band is less and the indexes are in an incremental pattern.

To show the coding gain, the proposed entropy coder is evaluated with the dataset-II records: 104, 107, 111, 112, 115, 116,117, 118, 119, 201, 207, 208, 209, 212, 213, 214, 228, 231 and 232 with different block lengths and the EPE values. The overall performance of the proposed MIC is compared with the HT8BSM encoding for binary significance map (BSM). The effectiveness of the coder is tested for different block lengths and the experimental results are shown in Fig. 3.15. It can be observed that the code length of the proposed MIC scheme is less compared to the HT8BSM encoding scheme for all the tested data records. Due to the localization of the wavelet coefficients, the indices of the nonzero wavelet coefficients in each subband results in an incremental pattern. Consequently, integer significance map is encoded efficiently with less number of bits by exploiting the redundancy among the indexes of the nonzero wavelet coefficients using the difference encoding, large skips finding and Huffman encoding. Thus, the proposed modified index coder achieves high compression efficiency. This compression methodology will be used in the automatic data rate control algorithm and quality control algorithm in the following Section.

3.3 Rate- and Distortion-Driven Subband Coding Algorithms

In this section, distortion level and data rate control algorithms are presented for the compression of the ECG signal. These are based on the concepts of energy based thresholding, adaptive quantization scheme based on the threshold control zero-zone nearly uniform midtread qunatizer (TCZNUMQ) and modified index coding (MIC) scheme. Compression performance of these two algorithms is evaluated in terms of number of iterations required to reach a target PRD/CDR, reconstructed signal quality and coding delay. The ECG signal is compressed using both target algorithms and features of the ECG signal are evaluated by visual inspection. The issues, on the use of PRD/RMSE as a quality measure and the data rate variability are investigated with different sets of experiments. Issues related to real time implementation using fixed block length and fixed data length are also addressed. Computational complexity of the proposed algorithms is studied by considering different block lengths with and without entropy coder (EC). The proposed algorithms are evaluated using different sets of ECG records. SPIHT based ECG compression algorithm is also implemented and considered as a reference for comparison with the proposed target CDR algorithm since it has the best compression performance. The signal quality is evaluated by verifying the diagnostic features of the original and decompressed signal which is referred to as correct diagnosis test in this work. For each set of ECG data, the compressed data rate bound is determined after correlating the percentage of correct diagnosis and the compressed data rate.

In data compression, there is always a tradeoff between the data rate and the amount of distortion. Most ECG compression algorithms reduce the data rate with a predefined PRD value. This results in data rates which vary with time varying morphologies, mean value and noise level. It is desirable to store or transmit

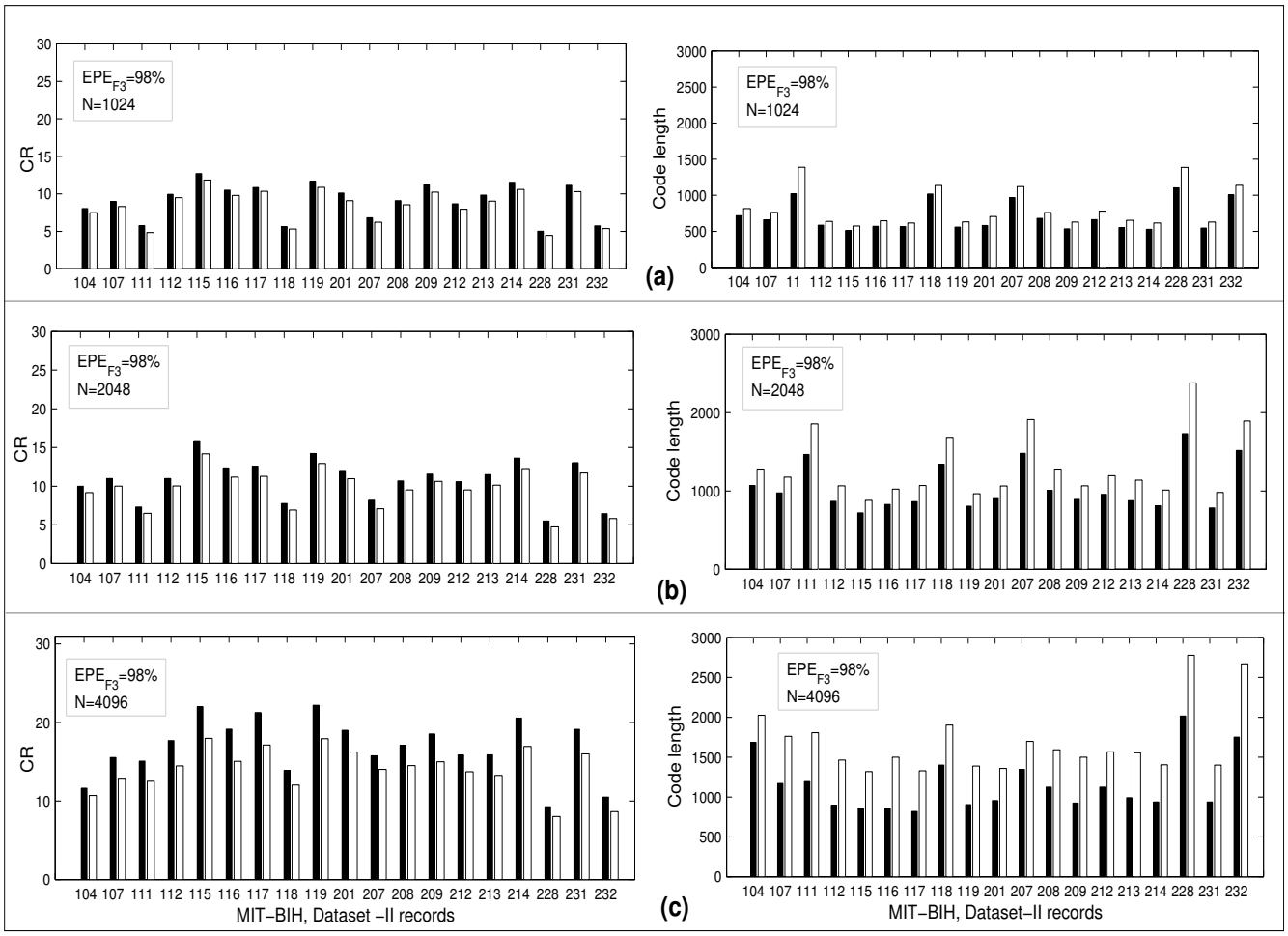

Figure 3.15: Comparison of codeword lengths and compression ratios of the proposed MIC (■) and the HT8BSM encoding (□). (a) N=1024. (b) N = 2048. (c) N = 4096. Here, $EPE_{F2} = 99.9\%$ and $EPE_{F3} = 98\%$.

data at the specified rate. Therefore, the proposed coder is implemented with a target value of compressed data rate or compression ratio. The compressed data rate depends on the ratio between the sampling rate and the signal bandwidth, the number of bits used for the amplitude resolution, the time varying morphologies of local waves within each block, the number of ECG cycles, the number of leads and the noise level. Consequently, it is imperative that any performance comparison between different algorithms should be based on identical values of the system parameters. The data length and the block length also affect the speed of the compression algorithms. Achieving lower CDR (or high CR) from large discrete sequence will not be helpful in real time mobile telecardiology applications. It will be worth if the compression algorithm gives the achievable upper bound of compressed data rate with negligible clinical information loss by considering small length of data.

3.3.1 Determination of Coding Parameters

The major task of any compression system is to find the optimal coding parameters. For a given signal block, let $H(T,\Delta)$ be the entropy of wavelet coefficients quantized by using T and Δ, and $D(T,\Delta)$ a measure of the distortion introduced in the signal by thresholding and quantization. In this work, optimization problem can then be stated in two ways: 1) For a given rate $H(T,\Delta)$, determine design parameters T and Δ in such a way that it minimizes distortion $D(T,\Delta)$; 2) For a given distortion $D(T,\Delta)$, determine parameters T and Δ in such a way that it minimizes rate $H(T,\Delta)$. At each iteration of the algorithm, the optimal parameters set is found for a given optimization problem. A simple bisection algorithm can be used to iteratively find optimal design parameters. The effects of the energy packing efficiency, quantization bit, input data length and block length are investigated in the following section.

3.3.1.1 Effects of Energy Packing Efficiency

In this subsection, the effects of the EPE on different ECG signals are evaluated. Different block lengths such as lengths of 1024, 2048 and 4096 samples are chosen to observe the thresholding effect on the compressed signal quality. The amount of reconstruction error is measured in terms of PRD1 values. It is well known that improper thresholding introduces distortion in the diagnostic features. Therefore, comparison of the original clinical information with those in the reconstructed signal is important. For all `mita` records, the compression error (PRD1 value) versus energy packing efficiency (EPE_{F3}) is shown in Fig. 3.16. It can be observed that the PRD1 value varies for each record for a specified EPE_{F3} value. Hence, a proper selection of EPE value is important for each test ECG record. The measured PRD1 value cannot reflect the exact amount of distortion of the PQRST complex features. For a given ECG signal, the value of PRD1 is same for dissimilar distortions introduced by the compression algorithms. A compression algorithm might achieve a low PRD1/RMS error ignoring the local wave between QRST complexes, totally losing the small P-wave, and faithfully reproducing the QRST complex. Therefore, to ascertain that the clinical information is preserved, the reconstructed signal quality is evaluated by comparing it visually with the original signal. For this, correct diagnosis (CD) test is performed with the help of physicians. In this work, more importance is given to the visual inspection for quality judgement. CD is determined from the total number of binary answers to the questions about the diagnosis ($1-$YES, $0-$NO) by the physicians. For each block, the number of correct reconstruction at different EPEs are summarized in Table 3.8. It is concluded that the signal quality is a function of EPE_{F3} value and block length, N. For $EPE_{F3} = 97\%$ and N = 1024, the number of correct diagnosis is 39 out of 49 tested records. When the diagnosis test results given by the physicians are correlated with PRD1 values, it is observed that the compressed signal with high PRD1 value contains original PQRST complex features.

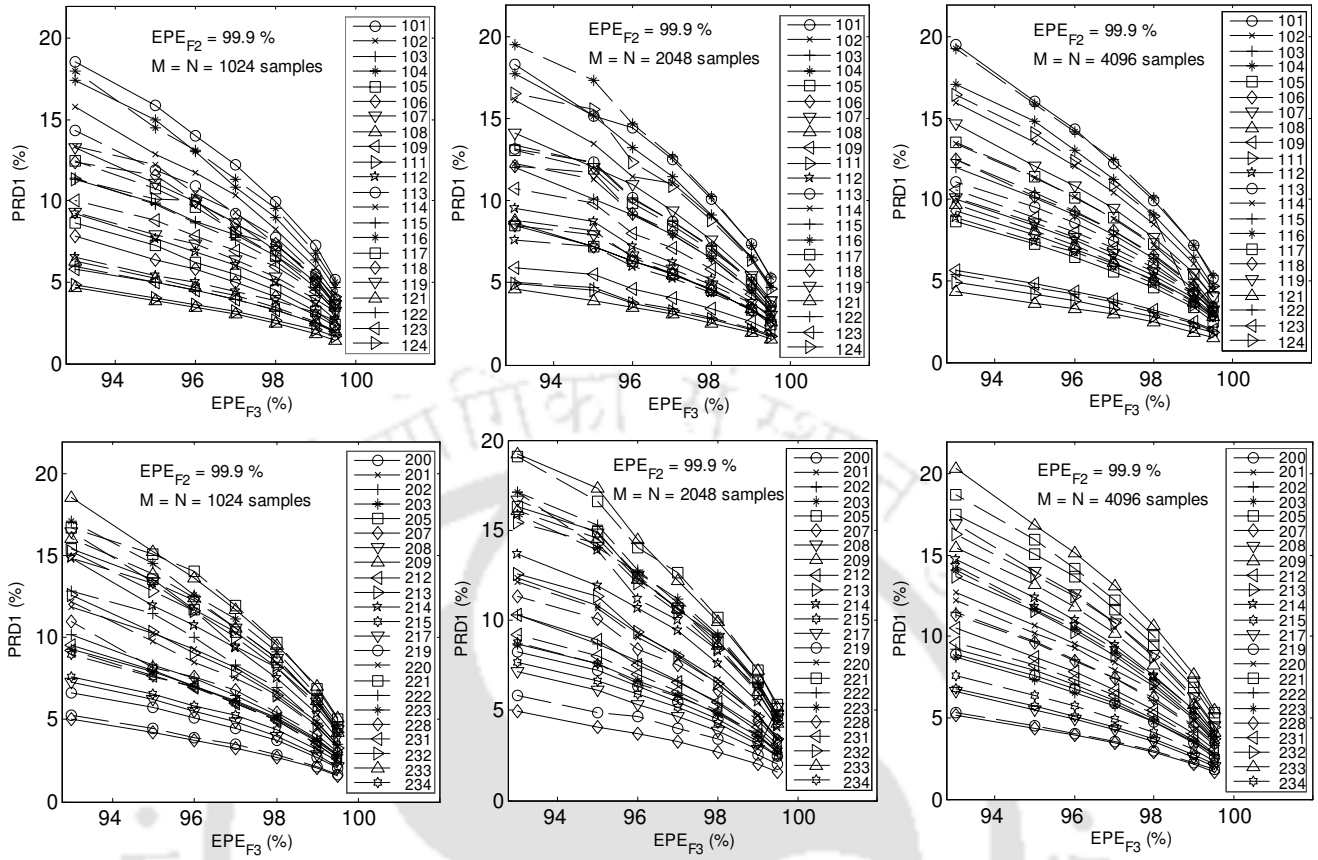

Figure 3.16: Reconstruction error, PRD1 as a function of energy packing efficiency (EPE) value.

Table 3.8: Average performance of Energy based thresholding for different block size (N) of records from MIT-BIH arrhythmia database. Correct diagnosis (CD) test is performed for all records. Here, data length, M=N.

EPE	Block length: N=1024 samples		Block length: N=2048 samples		Block length: N=4096 samples	
(%)	APRD1±σ	CD	APRD1±σ	CD	APRD1±σ	CD
99.5	3.32± 1.06	48/48 (100%)	3.48± 1.07	48/48 (100%)	3.39± 1.05	48/48 (100%)
99	4.51±1.54	48/48 (100%)	4.62±1.55	48/48 (100%)	4.52± 1.15	48/48 (100%)
98	6.23±2.19	45/48 (93.75%)	6.39± 2.23	45/48 (93.75%)	6.34±2.20	47/48 (97.92%)
97	7.55±2.69	39/48 (81.25%)	7.78±2.77	41/48 (85.42%)	7.74±2.74	43/48 (89.58%)
96	8.72±3.17	33/48 (68.75%)	8.93± 3.18	35/48 (72.92%)	8.93±3.19	39/48 (81.25%)
95	9.71±3.52	29/48 (60.42%)	10.95± 3.91	32/48 (66.67%)	9.98±3.57	37/48 (77.08%)
93	11.48±4.14	21/48 (43.75%)	11.86±4.26	29/48 (60.42%)	11.86±4.27	34/48 (70.83%)

Note:- APRD1: average PRD1 calculated without mean, σ: standard deviation.

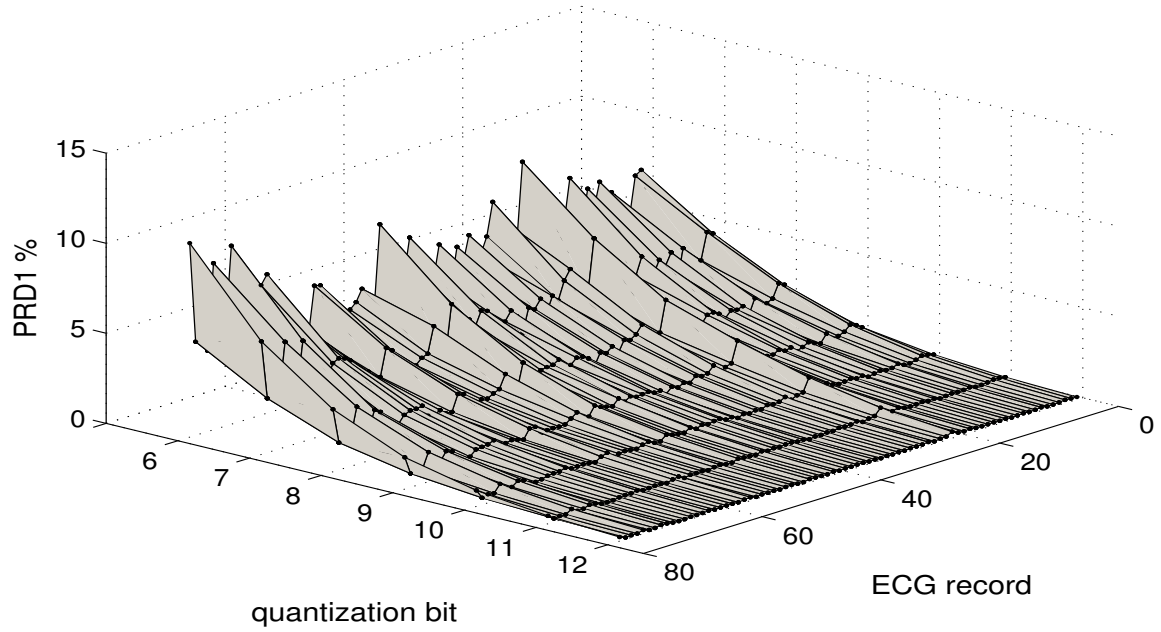

Figure 3.17: Rate-distortion curves: reconstruction error, PRD1 (%) as a function of quantization bit, b.

3.3.1.2 Selection of Quantization Bit

The wavelet coefficients vector of each ECG signal is quantized using the proposed quantization scheme with different resolution bits ranging from 5 to 11 per coefficient. The compression error introduced by the quantization process is calculated in terms of PRD1. The PRD1 values versus quantization bits, b, are shown in Fig. 3.17. The average, standard deviation and maximum PRD1 values for each quantizer resolution are shown in Table 3.9. It can be observed that the error is minimum with quantization bits greater than 9. The quantization error value is exponentially decreasing with increasing value of b. From these experimental results, the resolution bits, $b = \{6, 7, 8, 9\}$ are chosen for quantization in this work. In some cases, it is observed that the 6-bit quantizer results in higher CR values with lower PRD values but the preservation of clinical information may not be guaranteed. In this work at a desired distortion level and target data rate the NZTC vector is quantized with minimal distortion. It can be achieved using the simple adaptive quantization algorithm. For a desired PRD or CR value, there is a unique combination of number of bits per coefficient and number of coefficients retained that produces maximum data compression or minimum distortion level.

3.3.1.3 Selection of Data Length and Block Length

In ECG compression, different data lengths and block lengths are used for testing and comparison of their performances. To examine the effects of the data lengths and block lengths, a set of analysis is carried out

Table 3.9: Performance of quantization process for records from `mita`, `cuvt` and `mitsva` databases.

PRD1	Quantizer resolution, b (bits)						
(%)	6	7	8	9	10	11	12
average	5.7645	3.5570	2.0429	1.1194	0.5796	0.2912	0.1463
std	1.4599	0.8874	0.4918	0.2855	0.1530	0.0763	0.0381
max	10.7675	6.2769	3.8149	2.5145	1.4385	0.7291	0.3593

Table 3.10: Performance of the proposed algorithm for different data lengths and block lengths.

Test	PRD1	Compression ratio (CR)											
data		M=4096 samples				M=8192 samples					M=16384	M=32768	M=65536
	(%)	N=512	1024	2048	4096	512	1024	2048	4096	8192	16384	32768	65536
100	7.1	7.72±0.80	9.34±0.48	10.81±1.21	12.68	7.65±0.83	9.45±0.41	11.16±0.66	12.62± 0.07	13.76	14.69	15.36	15.79
115	5.0	8.20±1.29	10.07±1.01	12.57±0.08	14.05	8.24±0.92	10.06±0.79	12.14±0.84	13.77±1.09	14.96	16.0	17.67	18.01
119	3.51	6.07±0.45	7.95±0.22	10.28±0.10	11.73	5.84±0.5	7.63±0.46	9.73±0.321	10.97±0.05	12.02	14.51	15.07	14.83
cu01	5.0	6.53±1.01	7.89±1.02	10.14±1.43	12.04	6.20±1.11	7.43±0.90	8.67±1.09	9.38±0.66	10.11	9.92	10.35	11.47
800	7.1	4.77±0.62	5.56±0.60	6.23±0.54	6.68	4.23±0.72	4.86±0.84	5.51±0.86	5.88±1.06	6.11	6.20	6.97	6.11

and the results are shown in Fig. 3.18 and Table 3.10. The performance of the proposed algorithms with different block lengths for the data length, M = 65536 samples is shown in Fig. 3.18(a) and (b). The upper plot shows that the compression performance improves with increasing block length. The lower plot shows PRD1 values versus block lengths for the same records. It can be observed that PRD1 increment is very small as block length increases. Above a certain block length, the incremental change in the compression ratio is also small. The block length of 2048 or 4096 samples results in good compression performance. But the consideration of duration of the ECG signal for real time processing, internal memory and the computation time is also important. The experimental results shown in Figs. 3.18 (c) and (d) also establish that the percentage of correct diagnosis is high for these two block lengths. Table 3.10 shows the compression ratios for various block lengths at a given PRD1 value for the selected records. The results show that the performance of the proposed algorithm is better with a large block length. These observations are consistent with different test ECG signals. According to the results shown in Table 3.10 and Fig. 3.18, a block length of 2048 or 4096 and a data length of 4096 are recommended since the performance of the proposed algorithm will not improve significantly with a data length larger than 4096. If the block length and data length are large, small and sharp local waves may be distorted. The other two system parameters, EPE_i and b, are determined based on compression criteria, either distortion level or CDR in few iterations using the proposed algorithm which is discussed in the next section.

In the next section, using the above coding parameters, the TDL and TDR driven wavelet threshold based compression algorithms are implemented and their performances are evaluated. Effects of data rate variation on different signal parameters such as mean value variation, noise in the signal and the time

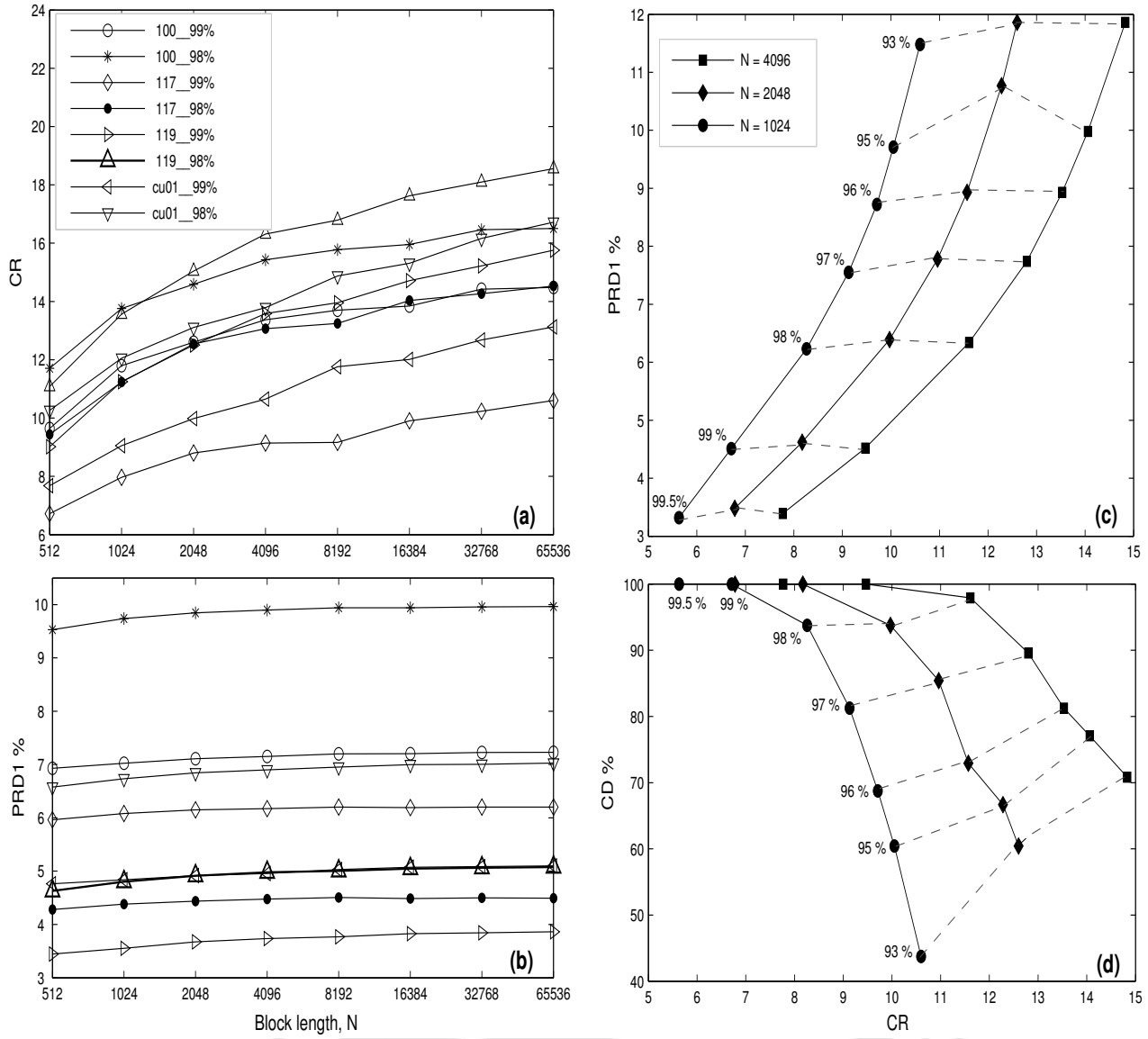

Figure 3.18: Compression performance for different data and block lengths. (a) Compression ratio (CR) and (b) average PRD1 of the of the proposed algorithm with data length, M = 65536 as a function of block length, N for the tested `mita` records 100, 117, 119 and `cuvt` record cu01. (c) Average PRD1 and (d) percentage of correct diagnosis (CD) as a function of CR at different EPE values, showing the average performance of all 48 `mita` records for different block lengths.

varying characteristics of PQRST complexes within a cycle are investigated for TDL algorithm. This data rate variability condition may not be acceptable for limited and well established channel. To solve this, TDR driven ECG compression algorithm is proposed and its performance is analyzed in terms of number of iterations required to meet the target value, compression efficiency, amount of clinical information lost and coding delay. Note that the energy packing efficiency is followed in the iterative algorithms. One might be argued that they are applied at increased computational cost. The reason for the use of EPE is illustrated

Table 3.11: Target distortion level (TDL) driven wavelet threshold based ECG compression algorithm.

Let us consider the ECG signal with length of M samples for a real time processing.
Step 1: Blocking and buffering N input samples.
The PRD1 can be written as follows:
PRD1 $= f(X_n, \widetilde{X}_n = \mathtt{f}(\mathrm{N}, \mathrm{EPE}_i, b)\ )$
// where, $X_n = \{x[0], x[1], x[2], ...x[\mathrm{N}-1]\}$, N is the block length,
// EPE_i is the energy packing efficiency of the i^{th} frame,and the quantization bits, b = {6, 7, 8, 9}.
Encoder:
Step 2: Decompose the signal, X_n, using 9/7 wavelet filters.
Step 3: Initialization
(a) Specify the target $\mathrm{PRD1_{tar}}$ or $\mathrm{RMSE_{tar}}$ value.
(b) Define the value of $\mathrm{EPE_{F2}}$ and the range of search for $\mathrm{EPE_{F3}}$ is [0 100]%.
(c) Get all three frames $\mathrm{F_1}$, $\mathrm{F_2}$ and $\mathrm{F_3}$.
(d) Get the relative bound error, e, for $\mathrm{PRD1_{tar}}$ calculation.
Step 4: Calculate $\mathrm{T_2}$ at desired $\mathrm{EPE_{F2}}$ by SA in Table 3.2.
(a) Get copy of $\mathrm{F_2}$ and threshold it at $\mathrm{T_2}$.
for ($k = 1;\ k <= \mathrm{K};\ k = k+1$)
// where K is the number of quantization bits. Here, K = 4.
{ **While** $|(\mathrm{PRD1}(\mathrm{EPE_3}) - \mathrm{PRD1_{tar}})/\mathrm{PRD1_{tar}}| \times 100 > e$
{ Step 5: Calculate $\mathrm{T_3}$ at $\mathrm{EPE_3}$ = ($\mathrm{EPE_{3min}}$+$\mathrm{EPE_{3max}}$)/2 ;
(a) Get the copy of $\mathrm{F_3}$ and threshold it at $\mathrm{T_3}$.
Step 6: Compute PRD1 by
(a) Get the thresholded wavelet coefficient (TWC) vector, TWC = [$\mathrm{F_1}$ $\mathrm{F_{2T}}$ $\mathrm{F_{3T}}$]
(b) Create the nonzero thresholded coefficient (NZTC) vector.
(c) Quantize the NZTC by using the proposed adaptive quantizer at desired resolution b bits.
(d) Reconstruct the signal by taking inverse DWT of the reordered QNZTC.
(e) Finally, calculate the PRD1.
Step 7: **If** PRD1 ($\mathrm{EPE_3}$) < $\mathrm{PRD1_{tar}}$
{ $\mathrm{EPE_{3min}}$ = $\mathrm{EPE_3}$; }
else
{ $\mathrm{EPE_{3max}}$ = $\mathrm{EPE_3}$; }
}
$\mathrm{EPE}_q(k)$ = $\mathrm{EPE_3}$;
Step 8: Compute the CR or CDR.
(a) Get the TWC vector, TWC = [$\mathrm{F_1}$ $\mathrm{F_{2T}}$ $\mathrm{F_{3T}}$] and the NZTC vector.
(b) Create the integer significance map (ISM) vector.
(c) Encode the ISM vector using the proposed index coding scheme.
(d) Finally, encode the QNZTC and the output of the index coder and calculate the CR.
$\mathrm{CR}_q(k)$=CR ;
}
Step 9: Get $\{\mathrm{EPE}_q(k)\}$ and $\{\mathrm{CR}_q(k)\}$ $\quad \forall\, k = 1, 2, ...\mathrm{K}$.
Step 10: Get combination of $\{\mathrm{EPE_3},\ b\}$ by $\{\mathrm{EPE_3},\ b\} = \max\{\mathrm{CR}_q\}$;
Step 11: Using $\mathrm{EPE_3}$ and b, compress the original signal X_n at $\mathrm{PRD1_{tar}}$ with high CR.

Reconstruction: 1) Decoding, 2) De-quantization and 3) Inverse DWT.

in the previous section. However this extension to simple threshold adaptation case is straightforward for a given maximum absolute value of wavelet coefficients in each class or frame. In this algorithms, the two-stage design philosophy is followed, where the subband coefficients are thresholded first and then quantized.

3.3.2 The TDL Driven ECG Compression Algorithm

The proposed TDL driven ECG compression algorithm is shown in Table 3.11. In the encoder part, the threshold T and the quantization bits, b, are iteratively determined for a given target error value. In this algorithm, the number of compressed bits varies with user specified error between the original and the reconstructed signals. For a given CR, the error depends on the methodology used for the compression and the time-varying PQRST complex morphologies. Distortion measure, PRD and its variants employed in literature, depends on the RMS value of the original signal and the amount of noise removed by the compression algorithm. The RMS value of the signal includes both mean and baseline value. Hence, the compression of the ECG signal with mean, noise and the dissimilar PQRST complex morphologies results in different data rates. Data rate variability condition may interrupt the real time ECG transmission via well established wireless networks. To demonstrate the variation in the data rate of block under a specified target PRD1 value, three types of experiments , variation of mean, variation of noise level are conducted as follows.

3.3.2.1 Variation of Mean

In most of the ECG compression algorithms, PRD and its variants are widely used to determine the signal distortion. Different versions of PRD measure such PRD1, PRD2 and PRD3 are discussed in the previous chapter. Among these, PRD2 is the most commonly used. PRD3 value is very low compared to the values of PRD1 and PRD2. But the compression with low PRD value does not necessarily imply diagnostic acceptance. The mean value of each ECG signal with block length of 1024 samples taken from `mita` database is measured and displayed in Fig. 3.19(a). The mean value of ECG signal from `mita` record 100 is -0.3135 and the baseline value is 959.82. The `mita` record 100 is compressed at a compression ratio of 8:1 using wavelet based ECG compression with large threshold control zero-zone quantizer. The signal error is measured using PRD1, PRD2 and PRD3 measures for different values of mean and baseline. The experimental results are shown in Figs. 3.19(c) and (d). The values of PRD1, PRD2 and PRD3 are 5.55%, 2.78% and 0.2146%, respectively. Large mean value for the signal results in small PRD2 value. The mean value in the signal does not have any medical relevance. This experiment also shows that the comparison of PRDs with different offsets is meaningless. It will be more pertinent if the mean value and the baseline of 1024 is removed from the original signal.

The data rate variation due to different mean value of the signal is studied by using `mita` records 100, 117 and 119. The experimental results of this test are shown in Fig. 3.19(b). Each point in Fig. 3.19(b) is the result of processing 1024 samples of ECG data with some mean value. Fig. 3.19(b) shows that for the same assigned PRD2 value with a relative error value of e = 1%, the algorithm results in variable data rate with variation of mean. For all test records, the largest CDR value is found with the zero-mean ECG signal while preserving all clinical information. Meanwhile smallest CDR value is obtained for the maximum

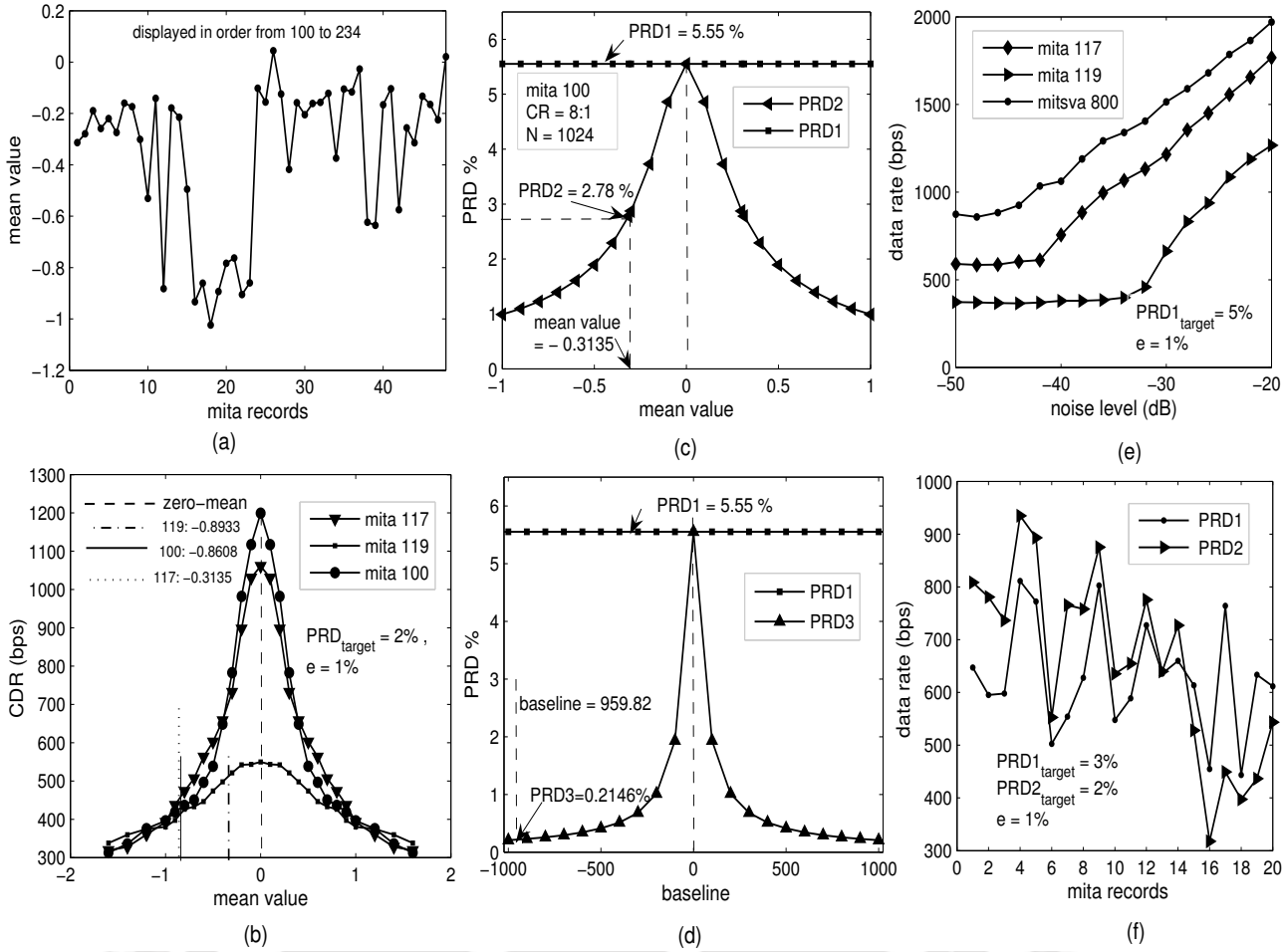

Figure 3.19: Experimental results of TDL algorithm.(a) mean value of the ECG signal with a block of 1024 samples. (b) The effect of mean values on compressed data rate (CDR). (c) The effect of mean values on PRD1 value. (d) The effect of baseline values on PRD1 value. (e) The effect of noise level on CDR value. (f) data rate variability due to time varying PQRST complex morphologies.

mean value with poor signal quality. The experimental results show that the target PRD2 value should be calculated from the zero-mean signals.

3.3.2.2 Variation of Noise Level

In many situations, the ECG signal contains noise which is not important for clinical diagnosis but it affects the error measures. The target error criterion employed in literature strongly depends on the smoothing or noise removal capability of the compression algorithms. Many compression algorithms are evaluated using `mita` database which contain noisy ECG records and the coding performance is compared with different compression methodologies. In this experiment, the effect of presence of noise is analyzed by varying the noise level. The target PRD1 is calculated from the zero-mean signals. For testing purpose, an additive

Table 3.12: Performance comparison of target distortion level based compression algorithms.

Algorithm	target PRD1	mita record 101		mita record 111		mita record 208		mita record 228	
		APRD1±σ	ACDR±σ	APRD1±σ	ACDR±σ	APRD1±σ	ACDR±σ	APRD1±σ	ACDR±σ
Direct AVQ [151]	3%	3.13±1.22	1678± 735	3.72± 1.65	2518±732	3.12± 0.70	1477± 496	3.29±2.35	2521± 868
WT+AVQ [151]		3.37±1.04	893±211	3.39±0.87	1143±270	3.25± 0.86	638± 114	3.09±1.57	950± 278
Proposed TDL		3.0001±0.023	517±138	2.999 ±0.008	771±134	3.0012±0.0179	561±112	2.998±0.01	743±221
Direct AVQ [151]	6%	5.81±1.21	528±413	6.07± 1.12	1277± 385	5.98±0.88	627± 300	5.67± 3.15	1276± 708
WT+AVQ [151]		6.27±1.43	410±73	6.26±1.19	450± 47	6.08±1.63	369± 90	5.33±2.88	466± 113
Proposed TDL		6.002±0.127	350±77	6.0015±0.073	431± 86	6.007±0.106	399±64	6.001±0.073	467±168
Direct AVQ [151]	9%	8.59±1.82	324±197	9.05±1.44	660±195	8.62±1.56	329± 227	7.79± 4.14	684± 473
WT+AVQ [151]		8.73±1.94	335±56	8.93±1.82	303±37	7.57±2.16	325± 98	7.64± 4.12	317± 56
Proposed TDL		9.03±0.207	297±54	9.009 ±0.147	340 ±50	8.998±0.182	337 ±46	9.009±0.177	352±121

Note:- APRD1: average PRD1, ACDR: average CDR, σ: standard deviation.

white Gaussian noise is added to each ECG signal from the mita record 117 and 119, and mitsva record 800. The compression results are shown in Fig. 3.19(e). It is observed that the data rate increases as the noise level increases at a given PRD1 value. This phenomenon is also observable with the usage of RMSE measure. Therefore, noise elimination is required prior to the implementation of compression algorithm. Many TDC algorithms smooth low-level background noise and results in more error while preserving all clinical information. Hence, there is a need for a distortion measure which is insensitive to noise elimination and more sensitive to the changes of the features of the ECG signal.

3.3.2.3 Time Varying PQRST Complex Morphologies

In this experiment, the effect of time varying morphologies on the compressed data rate (CDR) is investigated using selected mita records 200, 214, 231, 210, 106, 107, 113, 208, 104, 233, 103, 105, 230, 213, 115, 124, 117, 119, 123 and 116 which are referred as dataset-III. These records are chosen because they have different PQRST complex morphologies and low noise level. A block of 1024 samples is used from each record for the testing purpose. The compression results for these records are shown in Fig. 3.19(f). It shows that the resultant CDRs of the blocks are unequal for different local wave morphologies.

To investigate the CDR of each block from the same test record for a specified target PRD1 value, 15-min duration each of records 101, 111, 208 and 228, which are referred to as dataset-IV, is chosen for testing purpose [151]. A block of 1024 samples is chosen and a total number of 316 blocks are considered from each record. Each block is encoded and decoded separately at a given target PRD1 value. Three different target PRD1 values of 3%, 6% and 9% are considered for this experiment. The average CDR values of 316 blocks along with standard deviations at each target PRD1 value for a test ECG signal are shown in Table 3.12. The average PRD1 value and its standard deviation are also tabulated to observe its closeness with respect to the target value. Standard deviation of the PRD1 values of the proposed algorithm are small for all long duration test records. These experimental results show that the compression error value is close

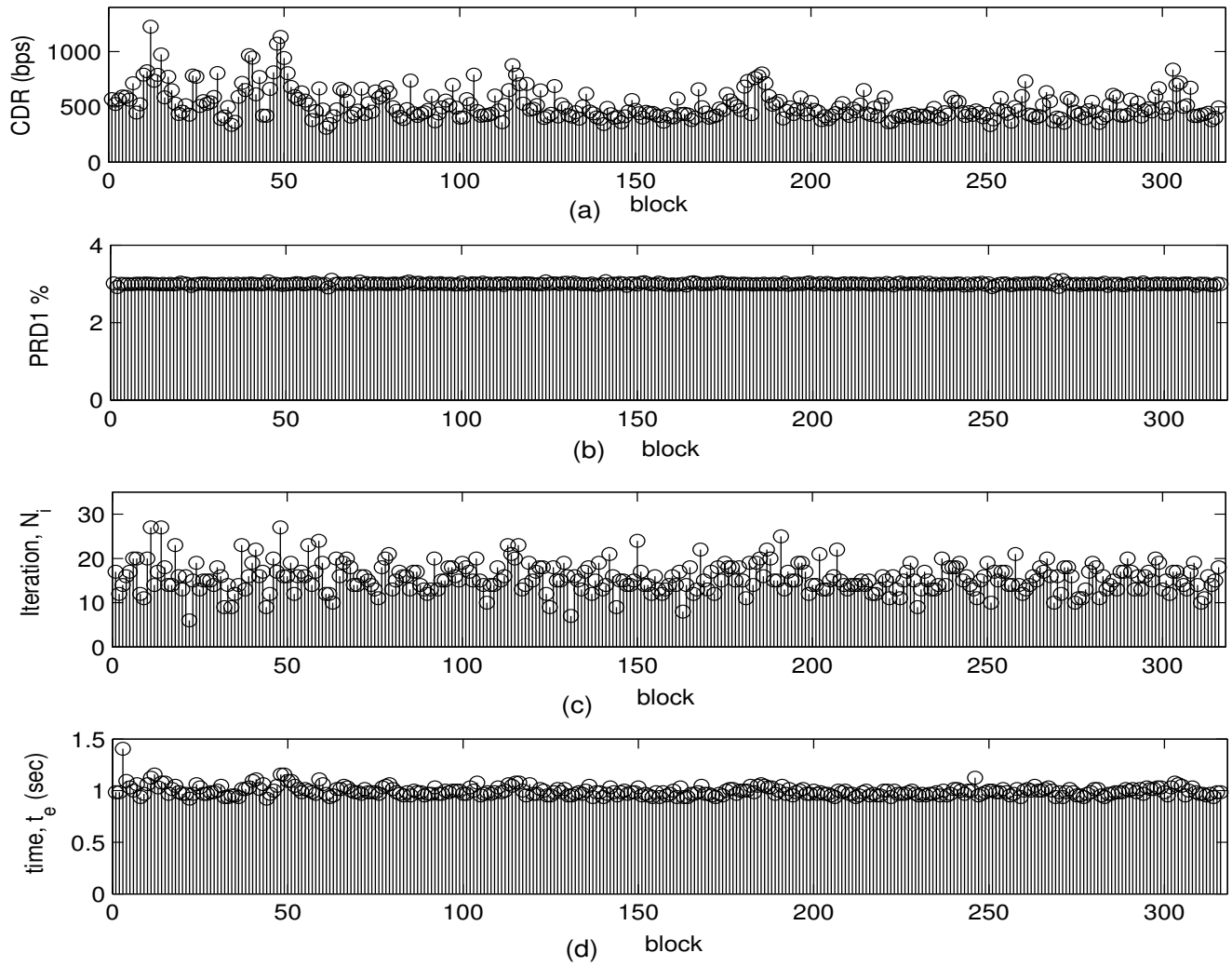

Figure 3.20: Type-III experiment results for test `mita` record 101. (a) Compressed data rate (CDR). (b) PRD1 values. (c) number of iterations, N_i. (d) the execution time, t_e (sec).

to the specified target value. To reveal this, the PRD1 value of each block is shown in Figs. 3.20 (b) and 3.21 (b) at a target PRD1 value of 3% for the tested `mita` record 101 and 111, respectively. Along with this, the CDR of each block, the number of iterations, N_i, required to achieve convergence and accuracy, and the execution time, t_e are shown in the figures. It is observed that the CDR values of the blocks are unequal and there is a large variation in CDR value of two blocks within a record. The experimental results in Table 3.12 show that there is a large variation in the CDR of the tested block for a record. In this situation, the minimum and maximum CDR of block is considered for real time case. The minimum and the maximum CDR values are 310 bps and 1224 bps, respectively for the test `mita` record 101. Similarly the minimum and the maximum CDR values are 356 bps and 1273 bps, respectively for the test `mita` record 111. These variations in the CDR values cannot establish an efficient ECG data transmission through limited

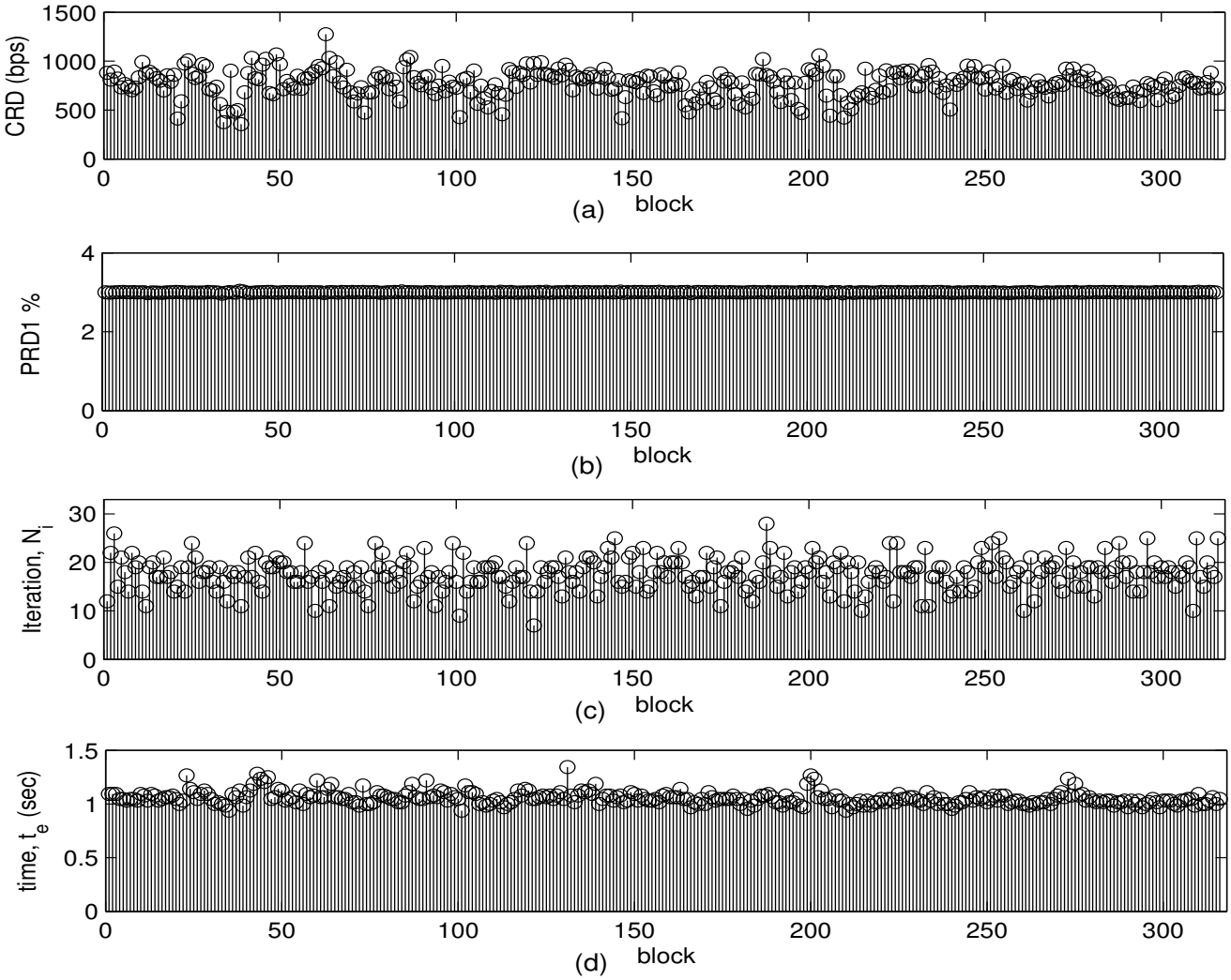

Figure 3.21: Type-III experiment results for test `mita` record 111. (a) Compressed data rate (CDR). (b) PRD1 values. (c) number of iterations, N_i. (d) the execution time, t_e (sec).

and assigned channel capacity.

The compression performance of the proposed algorithm is better than the direct AVQ and WT+AVQ algorithms. The standard deviations of CDR values of the proposed algorithm are less compared to AVQ and WT+AVQ algorithms for all test records with a target PRD1 value of 3%. But the performance of the proposed algorithm is worse than the WT+AVQ algorithm with a target PRD1 value of 6% for the `mita` records 101, 111 and 208. Similarly performance of WT+AVQ algorithm is better for the `mita` records 111 and 228 with a target PRD1 value of 9%. By comparing these experimental results, it cannot be concluded that the performance of the proposed algorithm is better than the other ECG coders. ECG signal compression algorithms with target PRD1/RMSE criteria will not assure that the local waves are faithfully reproduced. In most of the algorithms the coding efficiency at a given PRD1/PRD2/PRD3/RMSE

Table 3.13: Performance of the TDL algorithm. Block of 1024 samples taken from mita dataset-I.

$PRD1_{tar}$	3%	5%	7%	8%	9%
APRD1$\pm\sigma$	3.13$\pm$0.05	5.06$\pm$0.08	7.16$\pm$0.07	8.1$\pm$0.09	9.07$\pm$0.12
CD	100%	90.91%	63.63%	45.45%	18.18%
ACDR$\pm\sigma$	733$\pm$219	536$\pm$145	433$\pm$95	396$\pm$76	373$\pm$68
min. CDR	407	333	303	281	290
max. CDR	1067	764	633	582	548
N_i	18.8	15.2	15.8	13.4	13.6

Note:- APRD1: average PRD1, ACDR: average CDR, σ: standard deviation, CD: correct diagnosis.

value is compared with the specified target CR directly. Although the present algorithm maintains a user-specified PRD for each block of an ECG signal, some local distortions have occurred. For example, the small amplitude Q wave may be lost in the compressed signal. To detect such distortions, a distortion measure capable of quantifying the diagnostic distortion is needed. The quality is evaluated via correct diagnosis test by visual inspection in this work. This test result is shown in Table 3.8 in subsection 3.3.1.1.

It is reported [121], [142] that the quality of the reconstructed signal is either 'very good' or 'good' if the PRD1(%) value is between 0 and 9. But the defined PRD1 range is applicable only for the specific compression method. Because the compression artifacts in the decompressed signal depends on the type of methodology, viz. transform types (DCT, KLT, DWT), quantization, prediction, etc. used for the implementation of compression algorithm. Maintaining the PRD1 value below 9% will never assure that the original diagnostic features are faithfully reproduced in the reconstructed signal. Therefore, visual or clinical inspection of the reconstructed signal is always important for all type of compression algorithm even if the PRD1 value is small.

To demonstrate the need of visual or clinical inspection, a block of 1024 samples is used from each mita record of dataset-I. The coding parameters and the test PRD1 range (3% - 9%) are used as WPFEC [142]. Each block is compressed and decompressed at a target PRD1 value as mentioned above. The experimental results are shown in Table 3.13. The desired target distortion level is achieved with a lower CDR value using the TDL algorithm in few iterations. Clinical information in the reconstructed signals are evaluated by visually comparing them with the original signals. The percentage correct diagnosis (CD) is calculated from the number of CD at a target PRD1 value. It can be observed that 100% of CD is achieved only for a target PRD1 value of 3%. The percentage CD value is less for the target PRD1 value of 7% and above. Consequently, this PRD1 range cannot be used if the proposed compression algorithm is used with the same coding parameters. To reveal the visual or clinical quality of the signal for selected test records, the original signal, the compressed signal at a PRD1 value of 7% and the error signal are shown in Fig. 3.22. The distortions of the diagnostic features are marked in the compressed signals. The error signals are plotted to observe their distributions. The structured errors are also marked in the error signals. It is

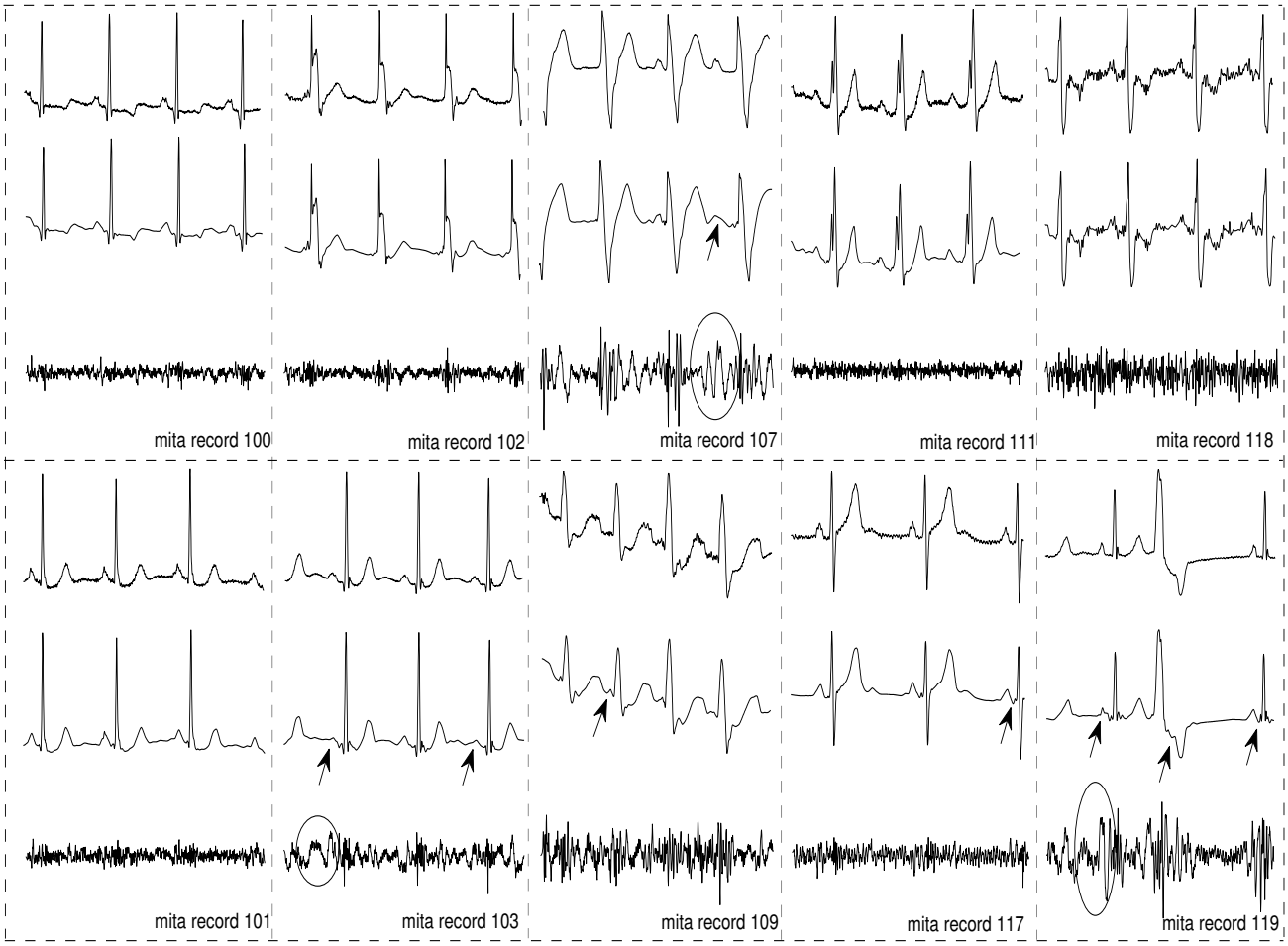

Figure 3.22: Compression results for arrhythmia ECG signal extracted from dataset-I at a target PRD1 = 7%. Some of the distortion of the diagnostic features are marked in the reconstructed signals. From top to bottom, the plots display the original ECG, the reconstructed ECG, and the difference between original and reconstruction.

observed that important diagnostic features are distorted and the small and short local waves are missing in Figs. 3.22. Hence, the compressed signal is not quality guaranteed by using a predefined PRD1 value. In WPFEC [142], PRD2 value is used as target which is meaningless because it depends on the mean value of the original signal. This effect is already discussed in the previous section. We prefer 100% CD for a PRD1 value of 3% for further analysis and comparison. Table 3.13 shows that the target TDL algorithm meets the required error value but it does not satisfy the requirements of data rate even if the PRD1 value is clearly defined at the clinically acceptable level. For example, for a PRD1 value of 3% the minimum and maximum CDR values are 407 bps and 1067 bps, respectively. This variation in CDR value leads to inefficient utilization of the required data rate or channel capacity ($\geq$ maximum CDR). Data rate variability may not fulfill the demand of compressed data rate. To rectify the above problem, the TDR driven wavelet compression is presented and its performance is analyzed with respect to the clinically acceptable quality.

Table 3.14: Target data rate (TDR) driven wavelet threshold based ECG compression algorithm.

The CR and the PRD1 can be written as: CR = $f(X_n$, M, N, EPE_i, b);
Step 1: Blocking and buffering N input samples.
// where, $X_n = \{x[0], x[1], x[2], ...x[M-1]\}$,M is the data length, N is the block length,
// EPE_i is the energy packing efficiency of the i^{th} frame, and the quantization bits, b = {6, 7, 8, 9}.
PRD1 = $f(X_n, M, N, EPE_i, b)$; $\forall n = 0, 1, 2, ...M-1$.
Encoder:
Step 2: Decompose the signal, X_n, using 9/7 wavelet filters.
Step 3: Initialization
(a) Specify the target CR_{tar} or CDR_{tar} value.
(b) Define the value of EPE_{F2} and the range of search for EPE_{F3} is [0 100]%.
(c) Get all three frames F_1, F_2 and F_3.
(d) Get the relative bound error, e, for CR_{tar} calculation.
Step 4: Calculate T_2 at desired EPE_{F2} by SA in Table 3.2.
(a) Get copy of F_2 and threshold it at T_2.
for ($k = 1$; $k <= K$; $k = k+1$)
// where K is the number of quantization bits. Here, K = 4.
{ **While** $|(CR(EPE_i) - CR_{tar})/CR_{tar}| \times 100 > e$
{ Step 5: Calculate TF_3 at EPE_3 = (EPE_{3min}+EPE_{3max})/2 ;
(a) Get copy of F_3 and threshold it at TF_3.
Step 6: Compute the compression ratio (CR).
(a) Get the thresholded Wavelet coefficient (TWC) vector, TWC = [F_1 F_{2T} F_{3T}]
(b) Create two vectors:
the nonzero thresholded coefficient (NZTC) vector and the integer significance map (ISM) vector.
(c) Quantize the NZTC by using the proposed quantizer at desired resolution, b bits.
(d) On the other side, encode the ISM vector using the proposed index coding scheme.
(e) Finally, encode the QNZTC and the output of the index coder and calculate the CR.
Step 7: **If** CR (EPE_3) < CR_{tar}
{ EPE_{3max} = EPE_3 ; }
else
{ EPE_{3min} = EPE_3 ; }
}
$EPE_q(k)$ = EPE_3 ;
Step 8: Reconstruct the signal and calculate the PRD1.
$PRD1_q(k)$=PRD1 ;
}
Step 9: Get $\{EPE_q(k)\}$ and $\{PRD1_q(k)\}$ $\forall k = 1, 2, ...K$.
Step 10: Get combination of $\{EPE_3, b\}$ by $\{EPE_3, b\} = \min\{PRD1_q\}$;
Step 11: Using the above EPE_3 and b, compress the original signal X_n at CR_{tar} with minimal distortion.

Reconstruction: 1) Decoding, 2) De-quantization and 3) Inverse DWT.
Note:- SA: sorting algorithm in Table 3.2.

3.3.3 The TDR Driven ECG Compression Algorithm

To meet the demands of well established channel/memory capacity, a new and simple TDR driven wavelet threshold based ECG signal compression algorithm is proposed and shown in Table 3.14. This algorithm attains the target CR/CDR by automatically adjusting the coding parameters in a few iterations.

The proposed TDR driven algorithm can be used to compress ECG signals for the given block length (N), the data length (M), and the desired CDR. In the following experiments, 15-min duration dataset-IV records with different ECG morphologies are selected to establish the robustness of the TDR driven algorithm. For a given target data rate, a block length of 1024 samples is coded and decoded separately.

Table 3.15: Compression results of the TDR algorithm.

Test ECG	CDR_{tar} (bps)	ACDR$\pm\sigma$ (bps)	APRD1$\pm\sigma$ (%)	$AN_i\pm\sigma$	$At_e\pm\sigma$ (sec)
101	495	494.85±3.36	5.24±3.01	11.05±2.0	1.43±0.24
	330	328.68±11.84	7.67±3.94	8.99±2.15	1.14±0.25
111	495	495.08±3.44	6.14±1.15	9.10±1.16	1.22±0.19
	330	329.72±1.98	9.91±2.57	6.73±1.91	0.876±0.21
208	495	494.96±3.33	4.02±1.70	9.90±1.98	1.33±0.24
	330	328.83±10.67	7.68±3.24	7.14±1.92	0.94±0.22
228	495	495.04±3.45	6.65±3.16	8.02±1.77	1.02±0.19
	330	329.11±9.35	10.01±5.62	7.32±2.78	0.97±0.26

Note:- APRD1: average PRD1, ACDR: average CDR, σ: standard deviation, AN_i: average number of iterations, At_e: average coding delay.

The experimental results are shown in Table 3.15. For a desired CDR = 495 bps (CR = 8:1) with relative error e = 1.25%, the compression performances such as the CDR, PRD1, the number of iterations, N_i, and the execution time, t_e are shown in Figs. 3.23 and 3.24 for the first two test `mita` records 101 and 111, respectively. From the experimental results, it can be observed that the CDR values are closer to the desired target CDR values. The resulting PRD1 error value remains same for many blocks except for a few noisy blocks in the test records. For noisy blocks, the PRD1 error values are higher than the less noisy blocks. The proposed algorithm results in optimal PRD1/RMS value at a desired CDR value for some combinations of b and EPE_i value which are automatically obtained in a few iterations. But the quality of the reconstructed signal cannot be judged from the measured PRD value because it does not reflect the distortion of the diagnostic features within the block of samples. Therefore, the assessment of signal quality is important via visual or clinical inspection which is focussed in the next section. From the experimental results, it can be observed that the number of iterations depends on the variables e, N, b and CDR. The experimental results show that the number of iterations required to achieve the desired CDR value decreases as e increases. The number of iterations N_i and execution time t_e are shown in Fig. 3.23(c) and (d), respectively for each test record. N_i depends on the target value and the relative bound error (e). The number of iterations to achieve convergence and accuracy, for the target CDR can be reduced by using an optimization technique.

3.4 Comparison with Other ECG Compression Algorithms

The performance of the proposed method is evaluated using two data sets: 2-min data (each) from records of dataset - I and 1-min data (each) from records of dataset - II. These two datasets are used because they consist of records of different rhythms, different morphologies, ectopic beats and noisy ECG signals. To compare with the compression performance of RQG [121], FPWCZ [137], NRDPWT-6 [140] and

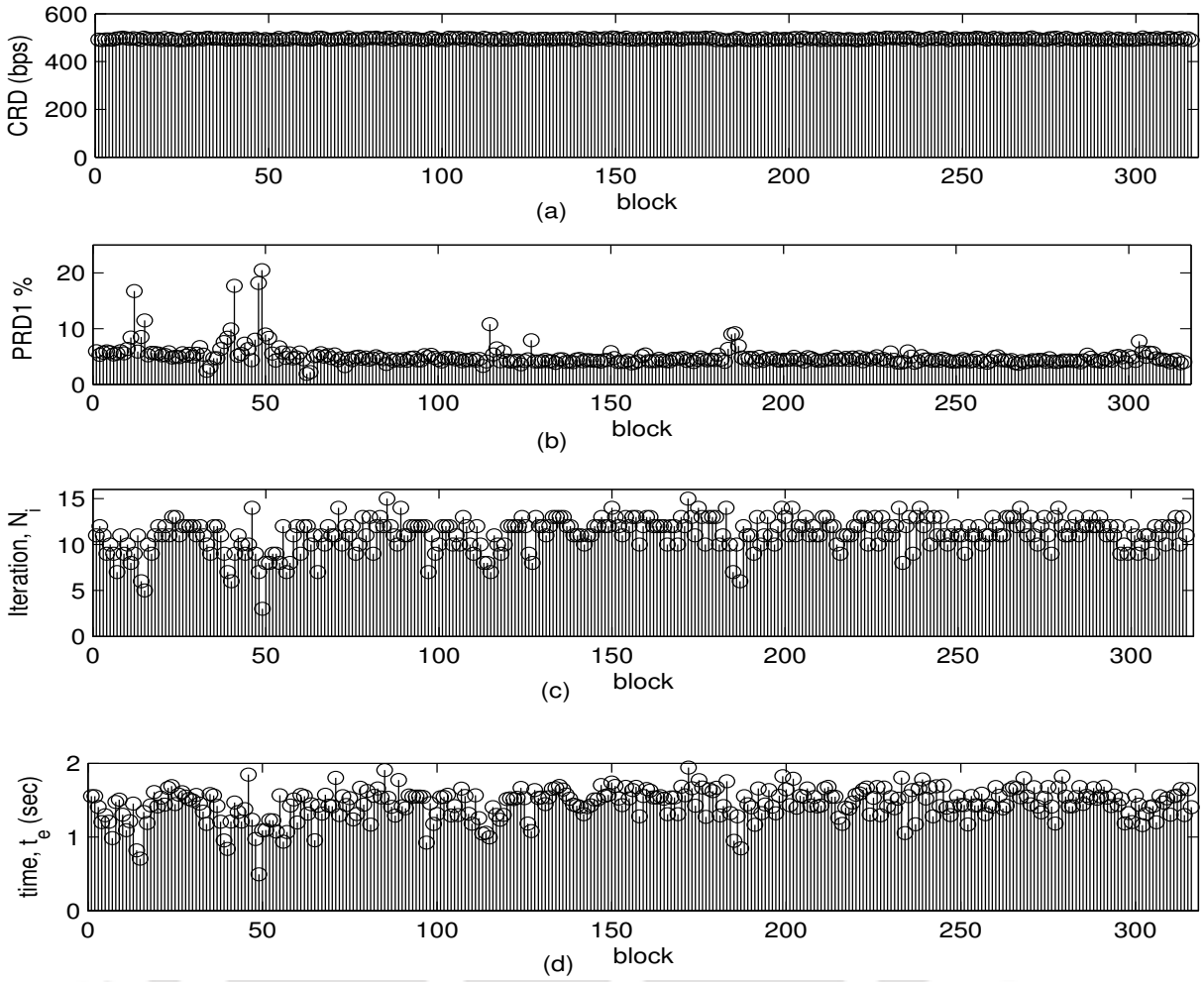

Figure 3.23: TDR experiment results for test `mita` record 101. (a) Compressed data rate (CDR). (b) PRD1 values of each block. (c) number of iterations, N_i. (d) the execution time, t_e (sec).

SPIHT [145] algorithms, block lengths (N) of 1024 and 2048 samples are chosen. The test ECG record is split into nonoverlapping blocks of N samples and each block is transformed and encoded separately. The experimental results of the proposed method for N=1024 are tabulated in Table 3.16. For a target CR, the average PRD and PRD1 values are measured. The standard deviation of the PRD values are also shown in the table. To compare the compression performance of SPIHT algorithm, same system parameters as proposed by Perlman [145] are used for the implementation . The average PRD1 (APRD1) values of the SPIHT method ranges from 1.72% to 9.64% for the average CR values ranging from 8:1 to 20:1, respectively . The APRD and APRD1 values obtained for the proposed method are less than those obtained in SPIHT and NRDPWT-6. The variance of PRD and PRD1 values are less for all target CR values compared to SPIHT [145] and NRDPWT-6 [140] algorithms. For the range of $4 \leq CR \leq 12$ and $16 \leq CR \leq 20$, the improvement in compression performance is calculated in terms of average PRD values. For the first CR

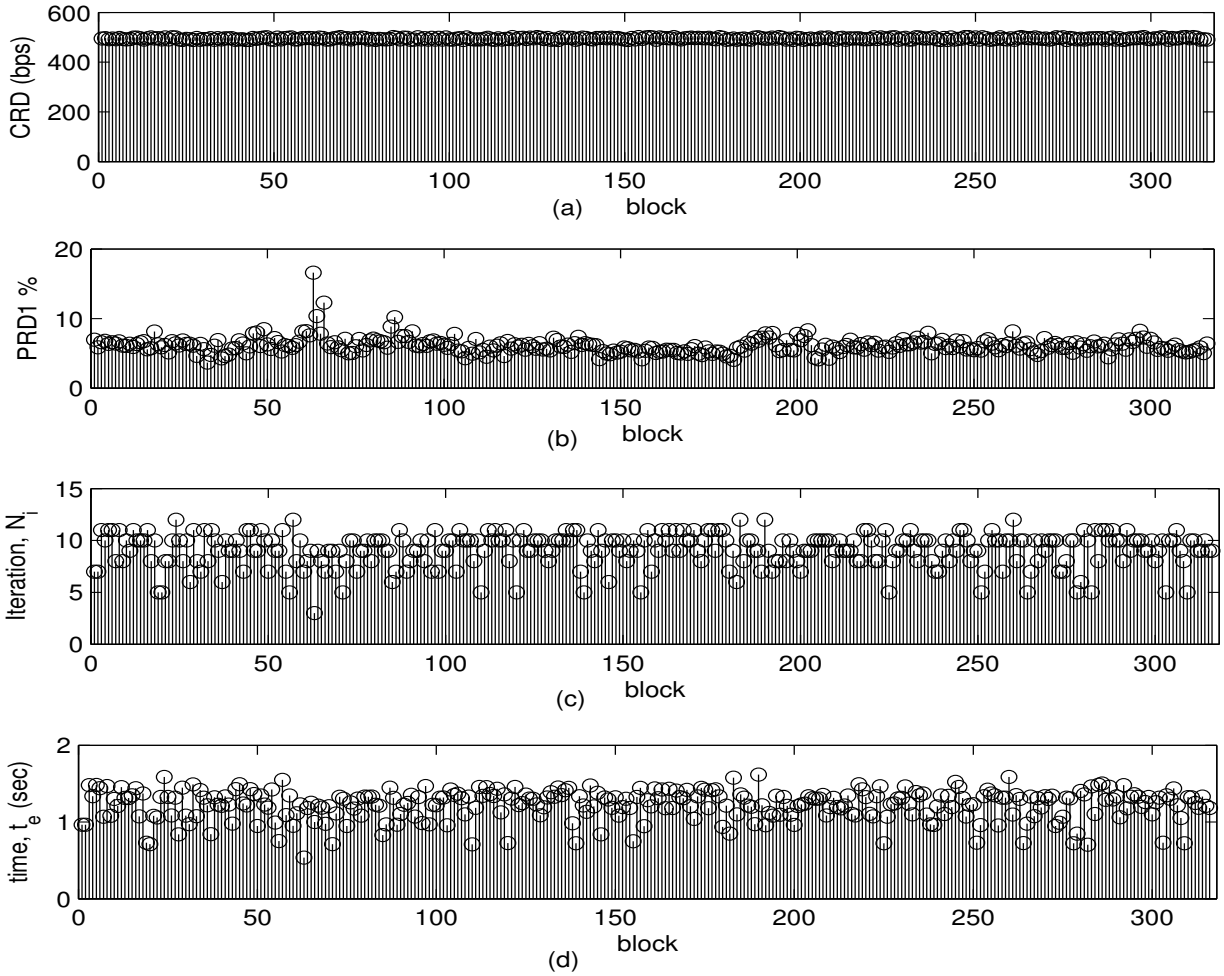

Figure 3.24: TDR experiment results for test `mita` record 111. (a) Compressed data rate (CDR). (b) PRD1 values of each block. (c) number of iterations, N_i. (d) the execution time, t_e (sec).

range, the PRD of the proposed method is less by 4.137% and 5.701% compared to SPIHT and NRDPWT-6, respectively. Similarly, the PRD is less by 22.94% and 18.29%, respectively for the second CR range. Experimental results show that the compression performance is better especially with high CR values.

With the records in dataset-I, the performance of the proposed and RQG [121], FPWCZ [137], NRDPWT-6 [140] and SPIHT [145] are compared and the results are shown in Fig. 3.25. The performance of the proposed method is evaluated using both the user defined PRD and CR algorithms. For a given CR value, the proposed method results in lower PRD values compared to SPIHT and NRDPWT-6 except at CR=4:1 where the PRD value of the proposed method is slightly higher than SPIHT and NRDPWT-6 due to smoothing of background noise. For the range of $4 \leq \text{CR} \leq 20$, the PRD is reduced by 27.31% and 13.44% compared to SPIHT and NRDPWT-6, respectively. The performance of the proposed method with user defined PRD algorithm is also compared with FPWCZ and RQG. From Fig. 3.25, it can be observed that higher CR

Table 3.16: Average PRD and PRD1 comparisons for the given CR_{tar}.

Test data	Method	CR_{tar}	4:1	8:1	12:1	16:1	20:1
dataset-I	Propsed	ACR$\pm\sigma$	4.03$\pm$0.08	7.99$\pm$0.05	12.01$\pm$0.07	16.05$\pm$0.08	20.02$\pm$0.04
		APRD$\pm\sigma$	1.07$\pm$ 0.46	1.97$\pm$ 0.70	2.75$\pm$ 1.05	3.43$\pm$ 0.95	4.43$\pm$ 1.37
		APRD1$\pm\sigma$	1.63$\pm$ 0.52	3.26$\pm$0.81	4.40$\pm$1.13	5.63$\pm$1.24	7.11$\pm$1.21
	SPIHT implemented	APRD$\pm\sigma$	1.05$\pm$ 0.44	2.05$\pm$ 0.84	2.94$\pm$ 0.97	4.21$\pm$1.26	5.99$\pm$ 1.78
		APRD1$\pm\sigma$	1.72$\pm$ 0.64	3.34$\pm$ 1.15	4.84$\pm$1.36	6.85$\pm$1.56	9.64$\pm$1.81
	NRDPWT-6 [140]	APRD$\pm\sigma$	1.01$\pm$ 0.39	2.12$\pm$ 0.81	3.01$\pm$ 0.90	4.13$\pm$1.16	5.50$\pm$ 1.63
dataset-II	Proposed	ACR $\pm\sigma$	4.01$\pm$0.03	8.04$\pm$0.03	12.05$\pm$0.09	16.07$\pm$0.02	20$\pm$0.08
		APRD $\pm\sigma$	1.13$\pm$ 0.43	2.42$\pm$1.06	3.57$\pm$1.41	4.67$\pm$1.96	6.38$\pm$2.92
		PRD1 $\pm\sigma$	1.97$\pm$ 0.82	3.49$\pm$1.31	5.19$\pm$1.86	6.80$\pm$2.59	9.1$\pm$3.56
	SPIHT [145]	APRD $\pm\sigma$	1.11	2.50	3.82	5.46	7.52
	NRDPWT-6 [140]	APRD $\pm\sigma$	1.21$\pm$0.55	2.66$\pm$1.24	3.83$\pm$1.66	5.19$\pm$2.20	6.87$\pm$ 2.90

Note:- ACR: average CR, APRD: average PRD, PRD: calculated with mean, APRD1: average PRD1, PRD1: without mean

values are achieved with the proposed method compared to RQG at fixed PRD values. For the range of $2.72 \leq$ APRD (%) ≤ 5.75, the average CR values of the proposed and RQG are 15.81 and 12.38, respectively. Thus, the proposed method improves the compression efficiency by 21.65%. In case of both the target criteria algorithms, the proposed method incurs good compression performance, especially at higher CR values. Note that the comparison is made on the numerical values of the CR and PRD. A complete comparison of the compression methods is very difficult to make since signal recoding conditions, noise levels, block size and noise filtering effect vary from method to method.

The average compression ratios and the average PRD values for the records of dataset-II at different EPE_{F3} values are calculated to compare with the performances of WT+EPE algorithm [134]. In WT+EPE algorithm [[134], Table II], the average CR values ranges from 8.6:1 to 20.55:1 for EPE_{D4-D1} values ranging from 99% to 85%, respectively. Proposed method approximately achieves the above CR values for $99.3\% \leq EPE_{F3} \leq 95\%$. For the above CR range, the compression performance is improved by 50.98%. Higher energy packing efficiency will guarantee better compressed signal quality. At a desired EPE_{F3} = 95%, the CR value of 26.35:1 and 12.68:1 is achieved for the records 119 and 232, respectively. The lower CR value for the record 232 is due to the presence of noise . Using target CR algorithm shown in Table 3.14, the CR value of 26.35:1 is achieved for the record 232 with automatically determined values of EPE_{F3} = 72.66% and b = 7. The resultant PRD2 and PRD1 value is 0.7494% and 14.914%, respectively. The PRD1 value is high due to the smoothing of background noise. It is reported that the maximum and minimum CR values achieved at EPE_{D4-D1} = 99% are 17:1 and 3:1, respectively [134]. Similarly, the reported CR value at EPE_{D4-D1} = 85% is around 24:1 and 16:1, respectively. Therefore, the standard deviation of the CR value is always important in addition to the average CR value. Although a high CR is achieved with wavelet based compression methods, they can be accepted only if the clinical information are

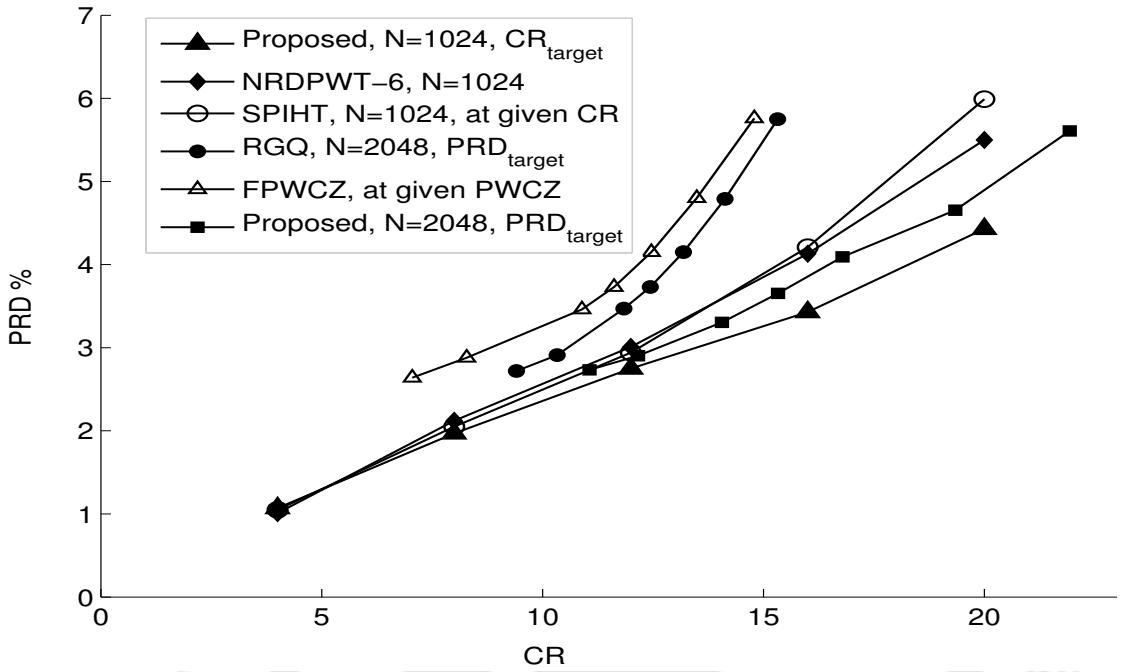

Figure 3.25: Comparison of average compression results of the proposed and SPIHT [145], FPWCZ [137], RQG [121], NRDPWT-6 [140] for the dataset-I.

perserved. The error measures such as PRD/PRD1/PRD2, MSE and RMS values do not show the amount of clinical information loss.

3.4.1 Quality Assessment of Compressed Signal by Visual Inspection

The clinical quality of the compressed signal cannot be predicted using the existing objective quality measures. Therefore, the visual or clinical inspection is required to evaluate the coder performance. To evaluate the clinical information in the compressed signal, correct diagnosis (CD) test is performed. In this test, 4096 samples are taken from 19 records of dataset-II, 15 records each from `cuvt` database and the `mitsva` database. A block length of 1024 samples is chosen for an effective comparison with the SPIHT scheme [145]. Each block is transformed and coded separately. It is shown that the CRs of the proposed TDR algorithm are very close to the CR targets. Average PRD1 value of 49 records is calculated at each target CR value. The fidelity of the compressed signal is evaluated through visual or clinical inspection. The average PRD1 values, the number of iterations, and the number of correct diagnosis are shown in Table 3.17.

The PRD values versus compression ratios for each record of the test dataset with a block length of 1024 samples are shown in Fig. 3.26. For `mita` database records, the proposed TDR algorithm achieves correct diagnosis of 100% for CR $\leq$ 12. The correct diagnosis of 100% is achieved for CR $\leq$ 8 and CR $\leq$ 4 for the tested ECG records from `cuvt` and `mitsva` database, respectively. The correct diagnosis of the SPIHT and the proposed algorithm is 100% when the target CR is below 4. For CR $\geq$ 8, the overall performance of the

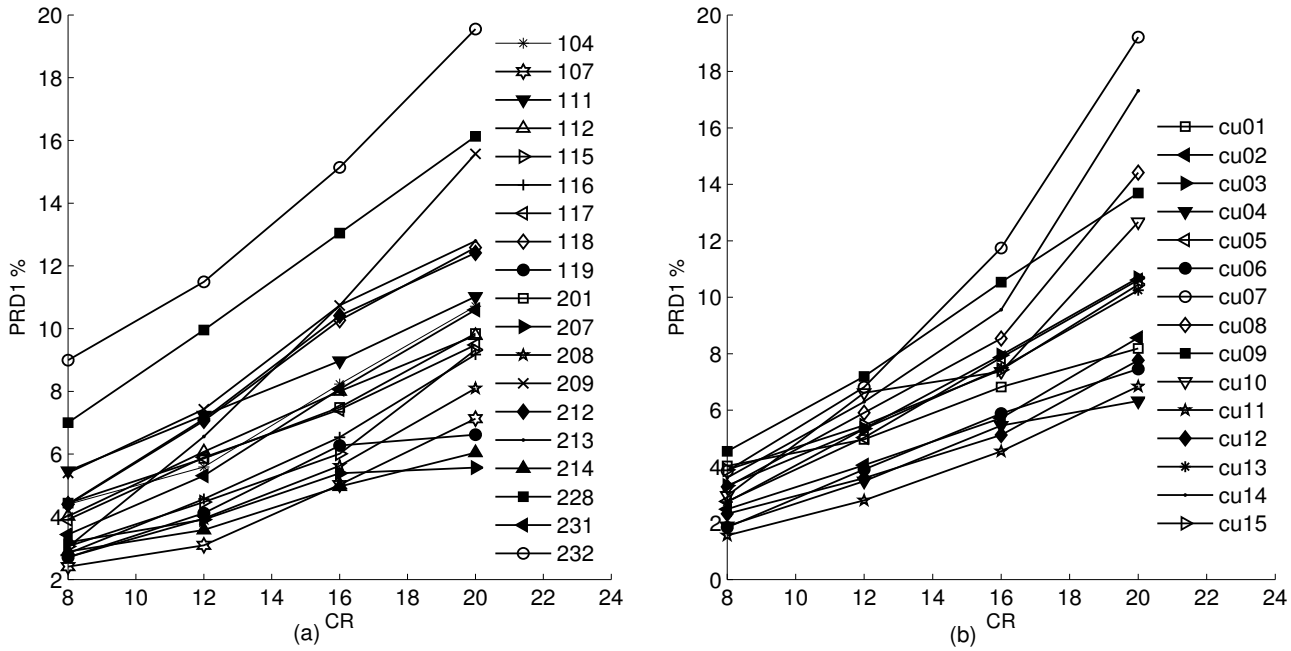

Figure 3.26: PRD1 versus CR of selected records from (a) the `mita` database (sampling rate = 360 samples/s, sample width = 11 b/sample) (b) the `cuvt` database (sampling rate = 250 samples/s, sample width = 12 b/sample).

proposed algorithm is better than SPIHT algorithm. Both the coding algorithms result in poor compressed signal quality for ECG signals from `mitsva` database. The performance of EZW based ECG coder [144] is degraded for the same ECG recording conditions. The proposed TDR algorithm achieves $4 \leq \text{CR} \leq 12$ while preserving all clinical information for signals from `mita` database. The use of compression for fast ECG retrieval is a debatable subject since high compression ratios usually introduce critical information loss that might impede accurate diagnosis. However, requirements for ECG signal quality differ depending on applications. The performance of the proposed TDR algorithm can be improved if a block length of 2048 or 4096 samples is used for compression at the cost of increased complexity. These experimental results show that the compression algorithm should define the type of clinical information to be transmitted or stored efficiently while preserving the original information.

3.4.2 Computational Complexity

Generally, the complexity of the algorithm is measured in terms of number of operations, clock cycles, memory access, etc. In ECG compression method, the time and space complexity will depend on the type of iterative algorithm whether it is based on target compression rate or PRD1. In case of target compression rate algorithm, the time complexity includes the entropy coder and it depends on the type of entropy encoder employed. For the target PRD1 algorithms, the complexity depends on the time required to pre-

Table 3.17: Performance comparison of TDR algorithm with implemented SPIHT based ECG coder in terms of PRD1 and CD. Here, M=4096, N=1024 and d = 0.2.

target CR	Algorithm	CR±σ	No. of iterations N_i±σ	mita database (360 Hz, 11 b/sample)		cuvt database (250 Hz, 12 b/sample)		mitsva database (128 Hz, 10 b/sample)		Over all CD (%)
				APRD1±σ	CD (%)	APRD1±σ	CD (%)	APRD1±σ	CD (%)	
4:1	Proposed TDR	4.07 ±0.083	9.94±1.614	2.02±0.86	100	0.94±0.36	100	4.53±1.12	100	100
	SPIHT	4:1	-	1.91±0.87	100	0.97±0.41	100	4.88±1.26	100	100
8:1	Proposed TDR	7.98 ±0.124	7.47±1.611	3.72±1.72	100	2.16±0.68	100	10.45±2.18	73.33	91.84
	SPIHT	8:1	-	3.88±1.92	100	2.49±0.83	100	11.09±2.65	60	87.76
12:1	Proposed	12.03 ±0.015	5.94±1.614	5.73±2.81	100	4.12±1.02	93.33	18.02±3.83	33	77.55
	SPIHT	12:1	-	5.81±2.87	100	4.54±1.24	93.33	18.85±4.85	20	73.47
16:1	Proposed TDR	16.01 ±0.113	4.52±1.982	7.82±2.56	89.47	6.46±1.23	80	–	–	85.29
	SPIHT	16:1	-	8.14±3.62	84.21	7.07±1.85	80	–	–	82.35
20:1	Proposed	19.98 ±0.107	3.42±1.980	10.86±3.21	78.95	9.96±2.63	46.66	–	–	64.71
	SPIHT	20:1	-	11.17±3.97	57.89	10.38±2.74	46.66	–	–	52.94

process a block to achieve the target PRD1 before the encoding process. In ECG compression methods, the wavelets and/or wavelet packets are used to convert statistically correlated ECG samples into uncorrelated coefficients. The computational complexity of the algorithms are of the order $O(\mathrm{N})$ and $O(\mathrm{N}\log\mathrm{N})$, respectively [144]. The thresholding process requires $\mathrm{K}\times\mathrm{N}_i$ operation per wavelet coefficient, where K and N_i is the number of quantization bits and number of iterations, respectively. The number of iterations N_i is inversely proportional to the relative error, e. The quantization process requires $\mathrm{K}\times\mathrm{N}_i\times 2^b$ operations per thresholded coefficient. The complexity of the Huffman algorithm is of the order $O(\mathrm{M}\log\mathrm{M})$, where M is the number of symbols. This complexity can be reduced by using an efficient algorithm. The computation time required for the proposed algorithm, t_e, can be expressed approximately as

$$t_e = t_{\mathrm{dwt}} + \mathrm{K}\times(t_{\mathrm{ti}} + t_{\mathrm{idwt}} + t_{\mathrm{prd1}}) + t_{\mathrm{fe}} \tag{3.22}$$

where, t_{dwt}, t_{idwt}, t_{prd1} and t_{fe} denote the time required for the DWT implementation, IDWT implementation, the PRD1 calculation and the final encoding process, respectively. t_{ti} is the total execution time required for the iterations per quantization bit which is calculated as, $t_{\mathrm{ti}} = \mathrm{N}_i\times(t_{\mathrm{thresh}} + t_{\mathrm{quantizer}} + t_{\mathrm{entropy}})$. The value of t_{fe} = 0 when K = 1. On HCL PC with Microsoft Windows XP, Intel Pentium-4 3.4 GHz CPU, 512 MB RAM and MATLAB 7.0, the execution time with and without entropy coder is shown in Table 3.18. Here, the same CR value is attained without the use of entropy coder at the cost of reduced percentage of CD. For all block lengths, the maximum coding delay is always less than the test signal duration. For the decoding process, time and space complexity are decreased compared to that of the encoding process. The execution time also depends on the type of programming language used for the ECG coders. The coding delay is large due to the usage of Huffman coding in the iterative process. Time required for the Huffman coding algorithm can be reduced by the use of an efficient algorithm.

Table 3.18: Execution time (seconds) with and without entropy coder. Reduced CD (%) by without entropy coder.

Test record	CR_{tar} d = 0.2	Execution time (seconds)						Reduced percentage of CD $= \frac{CD_{w/EC} - CD_{w/o\ EC}}{CD_{w/EC}} \times 100\%$		
		Proposed TDR algorithm with entropy coder (w/EC)			Proposed TDR algorithm without entropy coder (w/oEC)					
		N = 1024	N = 2048	N = 4096	N = 1024	N = 2048	N = 4096	N = 1024	N = 2048	N = 4096
dataset-II	8:1	1.13	1.32	1.54	0.103	0.210	0.830	0%	0%	0%
	12:1	0.687	0.836	1.07	0.098	0.146	0.622	10.52%	5.26%	0%
	16:1	0.353	0.542	0.853	0.083	0.128	0.431	26.31%	15.78%	10.52%

For the ECG records 117 and 232 from `mita` database, the compression performances of proposed and WPFDEC [121] algorithms are shown in Table 3.19 for comparison. An important criterion for judging any ECG compression algorithm is the clinical quality of the compressed signals. Therefore, the weighted mean opinion score error ($WMOS_e$) is calculated through the visual inspection and is summarized in Table 3.19. It can be observed that the performance of the proposed target data rate driven wavelet threshold based ECG signal compression algorithm is better than the other ECG coders. A 10-sec long ECG signal is used for computer aided analysis [138]. The performance of the proposed algorithm is evaluated using selected arrhythmia 10-sec long ECG signal (each) from the selected `mita` records 102/V5, 107/II, 111/II, 118/VI, and 119/II, referred to as dataset-V. Dataset-V consists of normal beat, atrial premature beat, ventricular beat and paced rhythm. At CR = 12:1, the ECG signals are coded and decoded for the evaluation of compressed signals. To reveal the clinical quality of the signals, the original, the reconstructed and the error signals are plotted in Figs. 3.27-3.31. The compressed or reconstructed signals show that the diagnostic information such as paced rhythm, paced rhythm with dissociated P wave, left bundle branch block, right bundle branch block with atrial premature beats and ventricular bigeminy present in the arrhythmia ECG signals are reproduced. All the structural diagnostic features are easily recognized and are faithfully reproduced, and the various beat morphologies can be clearly distinguished. The error signal is plotted to observe the distribution of errors. The experimental results show that the highly irregular rhythm can be retained with the proposed TDR based compression algorithm.

3.4.3 Evaluation of the Proposed Algorithm for Real Time Application

Different sets of ECG recordings are used to evaluate the suitability of the proposed compression method for real time applications. The normal duration of computer evaluated ECG records is 10-sec and this criterion is followed here. The record numbers of dataset-V are 100, 102, 103, 104, 107, 109, 111, 115, 117, 118, 119, 210, 215, 222, and 232 from the `mita` database, cu01 and cu04 from the `cuvt` database, 800 and 801 from the `mitsva` database and 1-sec data of 12 - lead ECG (created using 1-sec data of each leads from `mita` database). Dataset - V consists of a variety of rhythms, QRS complex morphologies, ectopic

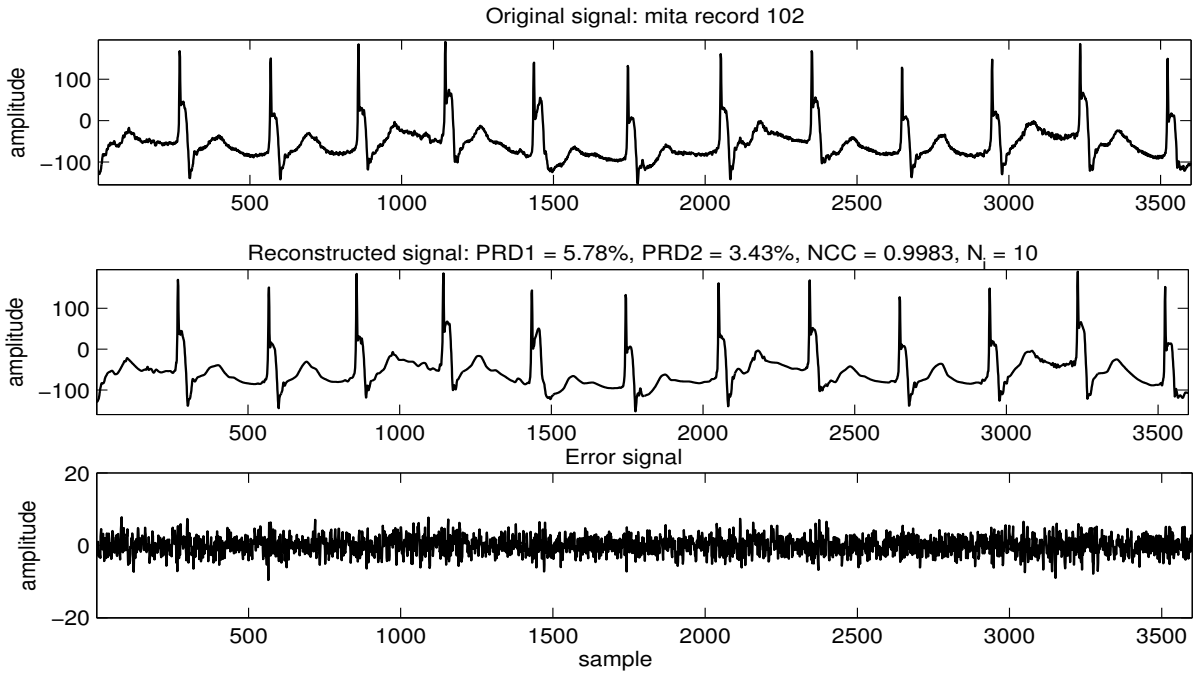

Figure 3.27: Compression results for arrhythmia ECG signal extracted from lead V5 of `mita` record 102 exhibiting a paced rhythm at a CR of 12:1.

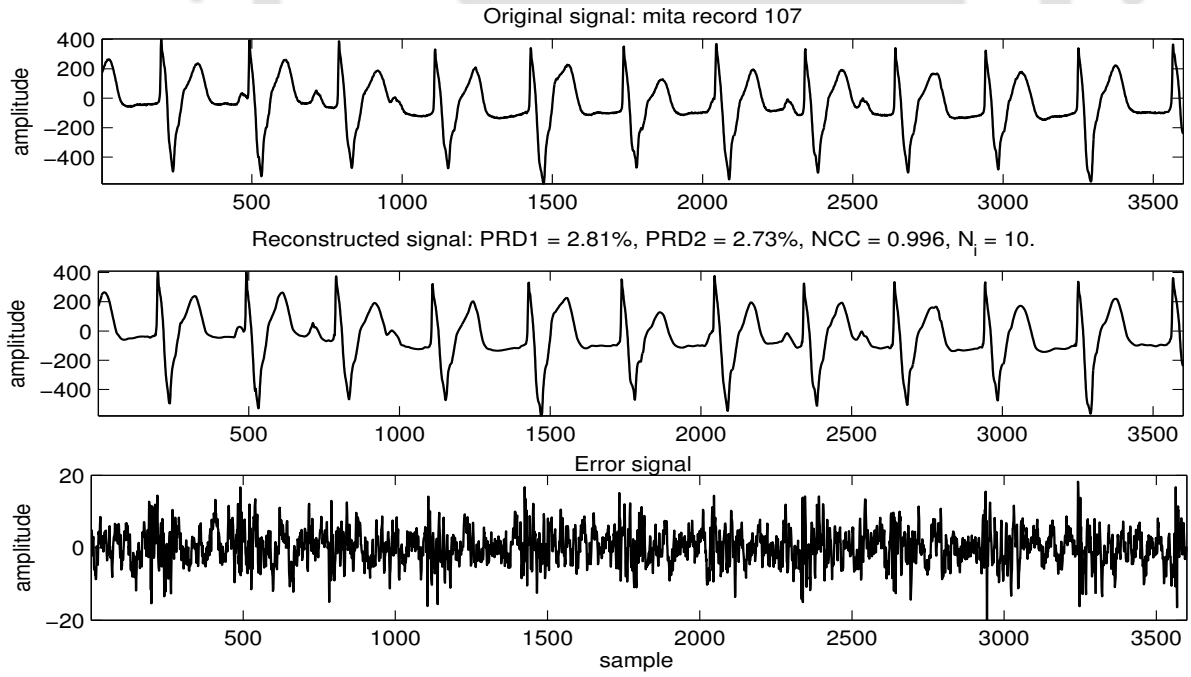

Figure 3.28: Compression results for arrhythmia ECG signal extracted from lead II of `mita` record 107 exhibiting a paced rhythm with dissociated P wave at a CR of 12:1.

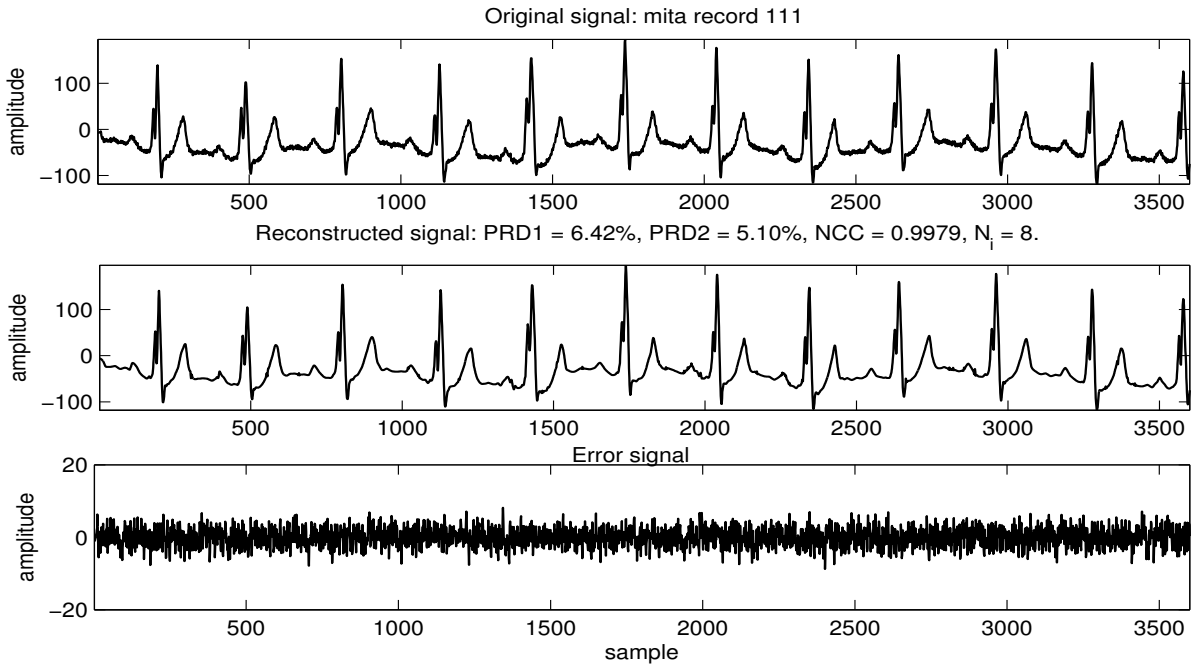

Figure 3.29: Compression results for arrhythmia ECG signal extracted from lead II of `mita` record 111 exhibiting a left bundle branch block at a CR of 12:1.

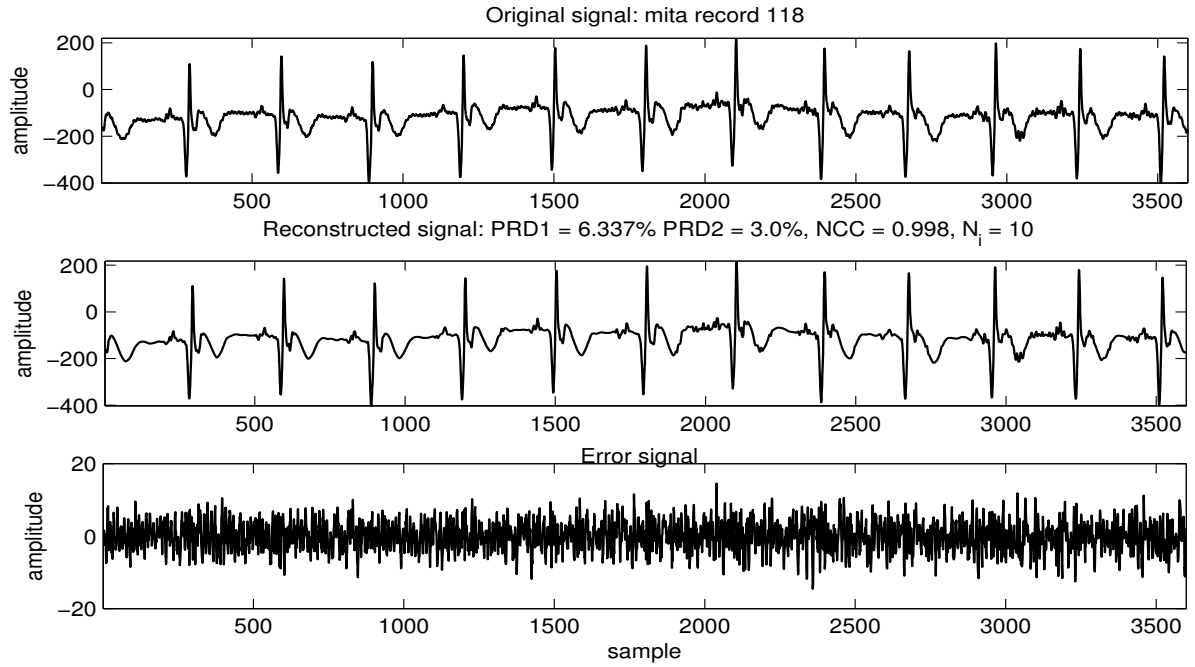

Figure 3.30: Compression results for arrhythmia ECG signal extracted from lead VI of `mita` record 118, exhibiting right bundle branch block with atrial premature beats at a CR of 12:1.

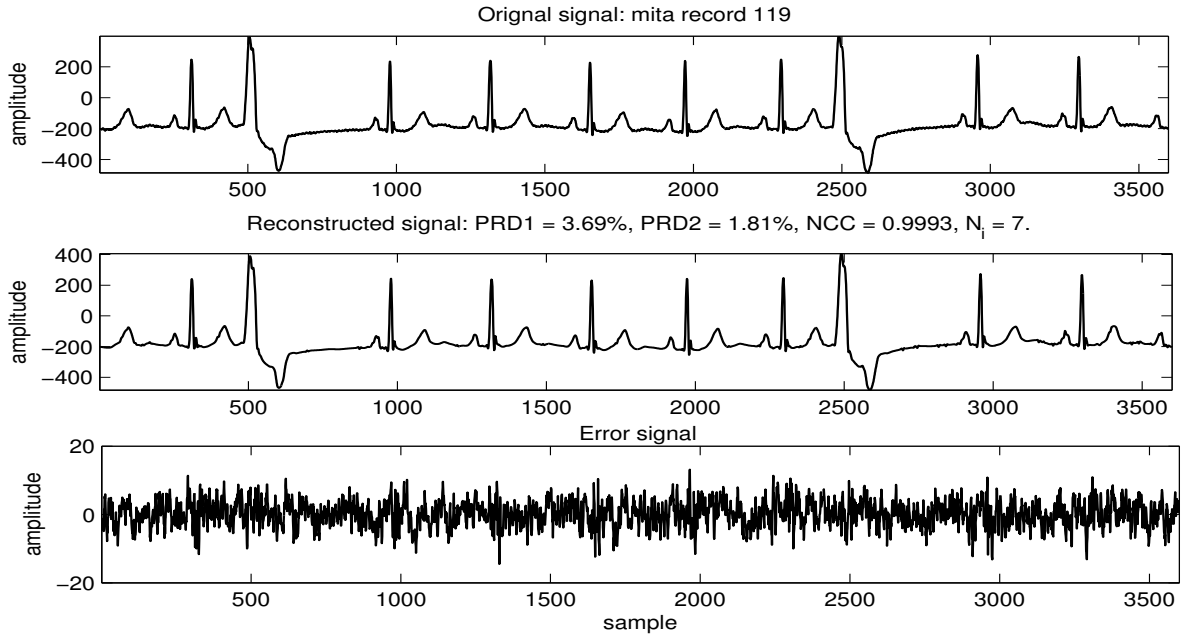

Figure 3.31: Compression results for arrhythmia ECG signal extracted from lead II of `mita` record 119 exhibiting ventricular bigeminy at a CR of 12:1.

beats, and noisy data and these ECG records are employed for evaluation of real time applications [144], [145], [131], [134], [121]. In this work, the performance of the proposed method is evaluated in terms of compressed signal quality and the coding delay at a desired data rate. The best criterion for the evaluation of compressed signal quality is the subjective test which is based on the physicians' visual perception. A weighted mean opinion score error ($WMOS_{error}$) [191] is calculated from the results of blind and semiblind tests conducted by four physicians for every tested signal. These tests are discussed in detail in Section 4.5 of the Chapter 4. Table 3.20 shows $WMOS_{error}$ of the proposed method with and without entropy coder for various types of ECG signals. At a CDR value of 495 bps, the maximum execution time with and without entropy coder is 1.42 s and 0.498 s, respectively. For both the cases, $WMOS_{error}$ is zero for the tested `mita` and `cuvt` records but it is large for the `mitsva` records 800 and 801. Similarly, at a CDR value of 792 bps, the execution time for encoding and decoding of 1 s long 12-lead ECG is 1.762 s and 0.682 s, respectively. Here, the coding delay is larger than the test signal duration due to the usage of Huffman coding in the iterative process while it is less without entropy coder. $WMOS_{error}$ for the two cases are 2.75% and 4.6%, respectively. The quality group is same for both the cases. It can also be observed that the proposed method doest not introduce any additional distortion at the end of each segment (1 s long) of 12-lead ECG. Time required for the Huffman coding algorithm can also be reduced by the use of efficient algorithm. For the specific ECG records 117 and 232 from `mita` database, the compression performances of proposed and WPFDEC [142] methods are summarized in Table 3.19 for comparison. The above experimental results show that the proposed method is suitable for real time telecardiology applications.

Table 3.19: Performance comparison of specific mita records. Here, M = 4096 and N = 2048.

mita record	WPFDEC [121]			Proposed TDR					
	CR	PRD (%)	PRD1 (%)	CR	PRD (%)	PRD1 (%)	RMS (μV)	NCC	$WMOS_e$ (%)
117	8.36	1.34	4.95	8.39	1.130	4.102	9.8	0.9992	0.0
232	7.35	5.0	8.68	7.37	4.059	8.03	9.3	0.9902	0.0

Table 3.20: Evaluation of clinical information by $WMOS_{error}$ at target CDR with and without entropy coder(EC) and the maximum execution time, t_e for encoding and decoding process.

10 s of each record of dataset-V (CDR = 495 bps and ε = 2.5%)							1 s of 12-lead ECG (CDR = 792 bps)	
Target algorithm	$WMOS_{err}$ (%)					maximum t_e (s)	$WMOS_{err}$ (%)	Execution time t_e (s)
	15 mita records	cu01	cu04	800	801			
w/ EC	0.0	0.0	0.0	28.5	34.38	1.42	2.75	1.762
w/o EC	0.0	0.0	0.0	36.2	37.6	0.498	4.6	0.682
Quality groups defined by MOS_{err} [191]: $0 \leq$ **very good** < 15, $15 \leq$ **good** < 35, $35 \leq$ **not good** < 50, **bad** ≥ 50								

3.5 Discussion

In this Chapter, the target distortion level (TDL) and target data rate (TDR) driven wavelet threshold based ECG compression algorithms are presented based on the classification of the wavelet coefficients, adaptive threshold control zero-zone nearly uniform midtread quantization (TCZNUMQ) and modified index coding (MIC) schemes. The advantages of the proposed adaptive quantization scheme is illustrated over the other quantization schemes used for the ECG compression. Experiments show that the constraints on the TCZNUMQ scheme reduces the computation of the two-stage techniques, wherein the distortion driven threshold adaptation is performed first and then the nonzero wavelet coefficients are quantized using linear quantizer. Moreover, the wavelet coding with the proposed TCZNUMQ scheme can provide for achieving simultaneous signal denoising and compression. A simple index coding scheme is presented for the significance map and then the performance is tested using the large number of integer significance maps. The results show that the index coding scheme compresses the significance map efficiently as compared to the other coding schemes used for the significance map.

The TDL (TDR) based ECG compression scheme achieved a desired distortion level (data rate) with low CDR (PRD1) by automatically adjusting the value of energy based threshold value and the resolution bits per coefficient in a few iterations. The proposed TDR algorithm is tested using three different sets of ECG data from mita, mitsva and cuvt databases. The compressed signal quality is assessed by both objective error measure and the correct diagnosis test through visual inspection. The CR/CDR bound of the TDR algorithm is determined for each set of ECG record after correlating the percentage of CD and the CR. For mita database records, the TDR algorithm achieved correct diagnosis of 100% for CR $\leq$ 12. The CD of

100% was achieved for CR $\leq$ 8 and CR $\leq$ 4 for ECG records from `cuvt` and `mitsva` database, respectively. All of the diagnostic features of the ECG are easily recognized and are faithfully reproduced, and the various beat morphologies are clearly distinguished within the above determined CR/CDR ranges. There is no standard objective measure for defining the clinically acceptable distortion level of the reconstructed signal. Even if the range of error value is defined, the experimental results of the TDL algorithm show that the variation in the CDR may not always fulfill the requirements of the dedicated transmission link. However, the performance of the presented TDL and TDR driven wavelet threshold based algorithm for the compression of the ECG signals is better than other wavelet based ECG coders.

The data rate variability of TDL algorithm is analyzed under different signal conditions such as mean value variation, noise level and time varying PQRST morphologies. The compression performance of the TDL and TDR based compression algorithms are compared. The issues on the use of PRD/RMSE as a quality measure are analyzed. The PRD distributes the error equally over all portions of the ECG signal and the measure fails to characterize the local distortion of an ECG signal. It is observed that the PRD criterion is not a subjectively meaningful measure since small and large numerical distortions do not correspond to "good" and "bad" subjective quality, respectively. Thus, the range of PRD value defined in reported algorithms did not necessarily result in clinically acceptable signal.

In literature, the tests are carried out using the well-known `mita` database which contains many time-varying and noise-contaminated ECG signals. Experiments show that the WT based method may produce smooth reconstructed signal. The noise in the input decreases the compression rate of the coder since the coder will spend extra bits on approximating the noise with the specified accuracy. Thus, the distortion measurement criterion plays an important role for choosing a set of optimal coding parameters. Therefore, we focussed on the evaluation of the TDR algorithm rather than the TDL algorithm in this Chapter. In this case, the subjective evaluation is used to quantify the dissatisfaction of the compressed ECG signal. Although the subjective test is the obvious way of measuring clinical quality, such a test is tedious, time consuming and results depend on various other factors such as the physicians background, motivation, etc. Moreover, it cannot be incorporated into automatic quality controlled compression systems. On the other hand, objective measure is repeatable and simple but it does not always match with the subjective one. However, measurement of quality is crucial because the distortion introduced by different types of compressors are very diverse. The above constructs show that in order to introduce closed loop CR or quality control one needs an adequate distortion measure for the compressed signal. Moreover, the choice of which distortion measure must be used for compressed signal is of critical importance when noise suppression and signal compression are established simultaneously. Therefore, we attempt the diagnostic distortion measure in the next Chapter.

4

Wavelet Energy Based Quality Measure for Local and Global Assessment of Distorted ECG

Contents

4.1 Introduction

Many wavelet based ECG compression methods are reported and the tests are carried out using the noisy records from the `mita` database and the percentage root mean square difference (PRD) criterion in the literature. A major design goal of any compression method is to obtain the best clinical quality with the highest compression ratio (CR) using the optimal coding parameters such as threshold or/and quantization bit obtained for a quality or distortion specification. But the measurement of distortion in the compressed signal is difficult because the distortion introduced by different types of compressors are very diverse. The effect of noise filtering is one of the features using the wavelet transform for compression and it is demonstrated in various compression results reported in the literature. In this case, the magnitude of insignificant errors may not be of much relevance from the point of view of clinical quality of the compressed signal. The effects of noise on the rate-distortion performance of the proposed methods and the SPIHT based methods are demonstrated in the previous chapter. Although PRD does not exactly correspond to the result of a clinical subjective test, it is easy to calculate and compare, so it is widely used in the ECG compression literature. Thus, in order to introduce closed loop CR or quality control, one needs an adequate diagnostic distortion measure for the compressed signal. Moreover, the choice of which distortion measure must be used for compressed signal is of critical importance when noise suppression and signal compression are established simultaneously. In the area of ECG signal compression, little attention has been paid towards the evaluation of distortion of clinical information. A suitable objective distortion measure can help proper evaluation of the well-designed ECG compression methods under noisy environments. Otherwise, the quality of the compressed signal has to be evaluated by subjective test, visual inspection of the clinical features. However, performing subjective test is a difficult task in closed loop rate or quality control method in which the optimal coding parameters are adaptively chosen to compress time-varying PQRST morphology effectively. A number of researchers have proposed variety of speech and image quality measures for local and global assessment. But very little effort has been made to provide an objective quality measure for the assessment of distorted ECG signal. The compression system typically involves tradeoff between the rate and quality of the output. Undoubtedly, there is a need for an objective measure for local and global assessment, and thus assessment of distorted signal quality is an open problem today.

In this chapter, a novel wavelet energy based diagnostic distortion measure is proposed for compressed ECG signal quality assessment. The proposed measure is a weighted percentage root mean square difference between subband coefficients of the original and compressed signals with weights equal to the relative wavelet subband energy of the corresponding subbands. These weights may represent the actual contribution of each subband that are used to discriminate different frequency subbands particularly bands corresponding to noise. The proposed measure appears to be a correct representation of the amount of signal distortion at all scales. Experiments show that the proposed measure works substantially better than the conventional PRD and the wavelet based weighted PRD (WWPRD) measures. The proposed measure

correlates well with subjective assessments and leads to provide a better evaluation of rate-distortion performance of the compression method. This Chapter is organized as follows. Section 4.2 discusses ECG distortion measures and their limitations. In Section 4.3, a novel wavelet energy based diagnostic distortion measure is proposed. In Section 4.4 preliminary evaluation of the WEDD measure is presented. In Section 4.5, subjective quality assessment of the clinical features of the compressed signal is presented. In Section 4.6, quantitative and qualitative analysis of the WEDD measure is performed.

4.2 Background and Problem Statement

In Chapter 2, various distortion measures used for evaluation of ECG signal quality are discussed. To be useful the distortion measure must possess the following two properties: 1) it must be subjectively meaningful in the sense that small and large distortions correspond to good and bad subjective quality, respectively; 2) it must be easily incorporated in rate-distortion optimization algorithm. Based on these properties and the behavior of the compression methods, the limitations of the distortion measures are summarized in this section.

The subjective and objective distortion measures are used to quantify the distortion of the compressed ECG signal. The subjective test is the obvious way of measuring clinical quality. However, subjective test is tedious, time consuming and results depend on various other factors such as the physician's experience, motivation, etc. Moreover, it cannot be incorporated into automatic quality controlled compression systems. On the other hand, objective measure is repeatable and simple but it does not always match with the subjective one. The non-diagnostic objective distortion measures are in terms of the squared error criteria viz. mean square error (MSE), normalized MSE (NMSE), root mean square error (RMSE), percentage root mean square difference (PRD), signal-to-noise ratio (SNR), normalized cross correlation (NCC), standard error (StdErr) and the absolute error criteria viz. maximum absolute error (MAX), normalized maximum absolute error (NMAX), etc. The most widely used global and local distortion criteria for compressed signal are the PRD and maximum absolute error (MAX), respectively. Smoothing of low-level background noises of the ECG causes a large PRD value but no clinical feature distortion and, conversely, a small average distortion can severely deteriorate clinical performance if the error is concentrated in the regions of significant features. For characterizing the local effects, the MAX is used in ECG compression methods. Isoelectric regions in an ECG signal do not contain any diagnostic information. But the MAX measure results in a nonzero value for smoothed isoelectric region at low CR situations. The global and local error measures may lead to false conclusions especially when the data are composed of signal and noise. The PRD and MAX are attractive measures due to their simplicity and mathematical convenience. However, their correlation subjective judgement of quality is not close enough for most applications. The above facts have motivated a great deal of research on diagnostic distortion measures.

To solve the above mentioned problems, researchers have proposed objective error measures which take into account the diagnostic distortion of the local waves such as P-wave, Q-wave, QRS complex, ST segment and T-wave. Chen [129] suggested a new distortion measure, the weighted PRD to improve the local distortion measure for evaluating the fidelity of the compressed ECG signal. However, there is no procedure reported to select the optimal weights for the local waves [129]. The weighted PRD measure depends on the accurate extraction of local waves within each beat and the weights for the significant waves. Although the WDD measure correlates well with visual inspection, it suffers from high computational complexity mainly due to the accurate evaluation of all diagnostic features and the calculation of optimal weights for the significant features. The nonstationarity of ECG signal and the artifacts may lead to a false detection of diagnostic features. This error may degrade the accuracy of the WDD measure. However, there are no standard protocols for finding the optimal weights and for implementing the weighted PRD and the WDD measures in closed loop quality control. A wavelet based quality measure, WWPRD, is based on the decomposition of the segment of interest into subbands and the weighted score is given to the band depending on the dynamic range and its diagnostic significance. The PRD measure is used as error measure for each subband is called wavelet PRD (WPRD). In WWPRD measure, the weight of each subbands is calculated as the ratio of sum of the absolute values of coefficients within that band and the sum of absolute values of wavelet coefficients in all the bands. The WWPRD measure provides a local or subband error estimation. However, it is observed in Chapter 2 that the insignificant errors in higher subbands dominate the global error.

In literature, the compression methods are commonly tested using the `mita` database which contains many time-varying and noise-contaminated ECG signals. In general, noise filtering capabilities of the transform based methods may not be similar for a specified compression rate. It is observed in Chapter 2 that not only the significant feature is reproduced, but also the compressed signal quality is upgraded because the insignificant coefficients dominating in higher subbands are removed for data compression. In this case, the conventional PRD or WWPRD does not always correspond to a better clinical quality. Moreover, noise decreases the compression ratio of any coder for a desired PRD value since the coder will spend extra bits on approximating the noise with the specified accuracy. Thus, noise will degrade the overall rate-distortion (coding) performance of any coder. Although some distortion measures correlate well with subjective quality measure for a given compression algorithm, they are not reliable for an evaluation across different algorithms. Therefore, the objective distortion measure should be coder-independent, so that it can compare the subjective qualities of various compression methods possibly entailing quite different types of distortion. Based on the results obtained in previous studies on weighted distortion measures, it appears that weighting works, however, there is no clear explanation for the reason why and how it works and how to choose an optimal set of weights. The above facts have motivated a great deal of research on objective distortion measures with clinical relevance. The multiresolution signal decomposition technique has already proven its ability in splitting signal and noise in time-frequency domain. The scope of this Chapter is to

explore the feasibility of wavelet energy feature in developing a new measure that can express the quality of distorted ECG signals either locally or globally.

4.3 Wavelet Energy Based Diagnostic Distortion Measure

The wavelet transform (WT) provides a description of the signal in the time-scale domain, allowing the representation of the temporal features of a signal at different resolutions. Therefore, it is a suitable tool to analyze the ECG signal which is characterized by local wave patterns (QRS complexes, P and T waves) with different frequency content. Moreover, the noise and artifacts appear at different frequency bands, thus having different contribution at various scales [147, 170]. The WT is established on basis functions formed by dilation and translation of a prototype wavelet function. They are much better suited for representing short bursts of high frequency signals or long duration, slowly varying signals. The ECG data to be compressed may contain signal and various noises. The noises are often stochastic signals with broadband, whose frequency bands will overlap with the interested signals. In the traditional signal processing, the out-of-band noise can be removed by applying a linear time-invariant filtering method. However, it cannot be removed from the portions where it overlaps the signal spectrum. Therefore, it is difficult to eliminate the noise from the signals effectively with general filtering methods. In addition, traditional methods require some information and assumptions about the signals that one wants to extract from the noise. The wavelet transform has already proven its ability in splitting signal and noise in wavelet domain. Recently, researchers from biomedical signal processing community have applied wavelet transform in signal compression, feature extraction and denoising. The reason for selection of wavelet domain processing of the ECG signal is due to varying characteristics of signal and presence of noise which restrict the application of conventional linear filtering scheme. The key idea in this technique is to utilize the wavelet localization property. As presented in Chapter 2, wavelet transforms are able to detect and localize frequency contents effectively. Therefore, we attempt to use the multiresolution signal decomposition technique for the quality assessment of distorted ECG signals in this Chapter.

The information can be organized in a hierarchical scheme of nested subspaces called multiresolution analysis in $L^2(\Re)$. In multiresolution signal decomposition (MSD), the signal $x(t) \in L^2(\Re)$ is decomposed to detailed and approximated versions using the scaled and translated versions of the wavelet ($\psi_{j,k}(t)$) and scaling functions ($\phi_{j,k}(t)$). The approximations are the low-frequency components of the signal and the details are the high-frequency components. The MSD is used to exploit two important issues. The first is the localization property in time and will appear by the presence of large coefficients at the time. The second property is the partitioning of the signal energy at different frequency bands. The MSD for a given signal $x(t)$ is given by

$$x(t) = \sum_{k=-\infty}^{\infty} \mathrm{A}_J(k)\phi_{J,k}(t) + \sum_{j=1}^{J}\sum_{k=-\infty}^{\infty} \mathrm{D}_j(k)\psi_{j,k}(t) \tag{4.1}$$

with $A_J(k) = \int_{-\infty}^{\infty} x(t)\phi_{J,k}(t)dt$ and $D_j(k) = \int_{-\infty}^{\infty} x(t)\psi_{j,k}(t)dt$ where J is the number of decomposition levels, $A_J = \{a_J(k)\}_{k\in Z}$ are the approximation coefficient vectors at resolution level J and $\{D_j = \{d_j(k)\}_{k\in Z}\}_{j=1,2,\ldots J}$ are the detail coefficient vectors. The wavelet coefficients vector is given by $C = [D_1\ D_2\ D_3 \cdots D_J\ A_J]$. The frequency range of subbands A_j and D_j are given by

$$\begin{aligned} &[0, 2^{-j-1}F_s], && \text{for approximation subbands} \\ &[2^{-j-1}F_s, 2^{-j}F_s], && \text{for detail subbands} \end{aligned} \tag{4.2}$$

where F_s is the sampling frequency. The signal $x(n)$ can be expressed as the summation of approximation $A_J(n)$ signals and detail $\{D_j(n)\}_{1\le j\le J}$ signals, that is:

$$x(n) = \sum_{j=1}^{J} D_j(n) + A_J(n), n = 1,\ 2,\ 3.....N. \tag{4.3}$$

The above MSD technique provides a mathematical tool with powerful structure and enormous freedom that decompose a given signal into several subsignals with different frequency bands. Eq. (4.3) provides a hierarchical and fast scheme for the computation of the wavelet coefficients of a given signal. The DWT is implemented using a multiresolution signal decomposition algorithm with the wavelet filters $h(n)$ and $g(n)$. The first step in signal decomposition consists of computing these approximation and detail coefficients using the filters $h(n)$ and $g(n)$, respectively. The approximation signal captures the low-frequency information and the detail signal captures the high-frequency information contained in the ECG signal. Then, the wavelet coefficients of any scale (or resolution) could be computed from the wavelet coefficients of the next higher resolutions. The low frequency part is divided again into high and low frequencies. Depending upon the number of decomposition levels, the end product of a multiresolution decomposition results in a set of these signals at different frequencies, as shown in Eq. (4.4)

$$x(n) = x_H(n) + x_{M_1}(n) + x_{M_2}(n)..... + x_{M_{J-1}}(n) + x_L(n) \tag{4.4}$$

where x_L is the low-frequency signal, x_H is the high-frequency signal and $x_{M_i}, j = 1, 2, ...J-1$ are the medium-scale signals. For example, if a five-level decomposition of the signal is done, it results in one approximation signal (low-frequency) and five detail signals (high- and intermediate-frequency).

The process of decomposition uses a subband filtering (filter bank) that is illustrated in Figs. 4.1 (a) and (b). The DWT can be computed using the low-pass filter $h(n)$, high-pass filter $g(n)$ and down-sampling process. Fig. 4.1 (b) illustrates the analysis part of a five-level decomposition scheme. The original sampled signal is filtered with the scaling function and the wavelet function and down-sampled by two, resulting in the approximation and detail coefficients at level one. The approximated signal is then used as the original signal and filtered with the scaling function and the wavelet to yield the coefficients at level two. This process is repeated depending upon the number of decomposition levels desired.

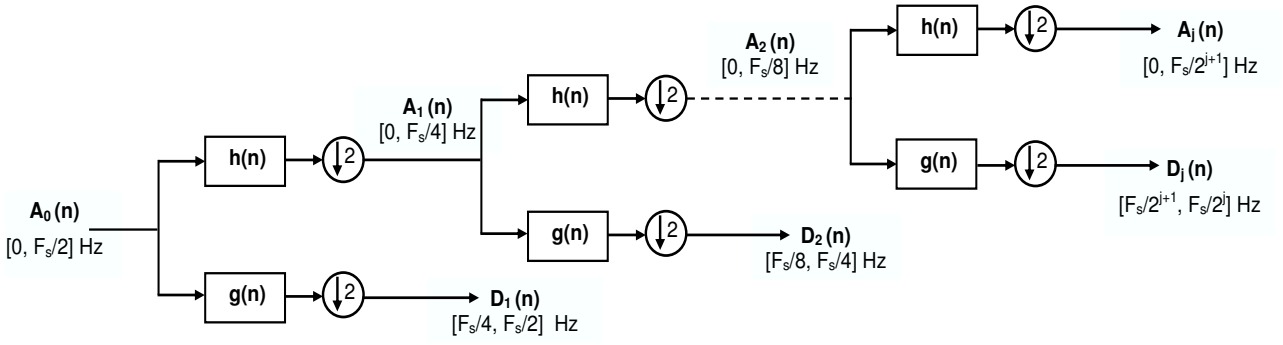

(a) Multiresolution signal decomposition: $A_0(n)$ is a sampled signal of $x(t)$ and F_s is the sampling rate. h(n) and g(n) are the low-pass and high-pass filters, respectively. $A_1(n)$ and $D_1(n)$ are the smoothed or approximated and detailed versions, respectively.

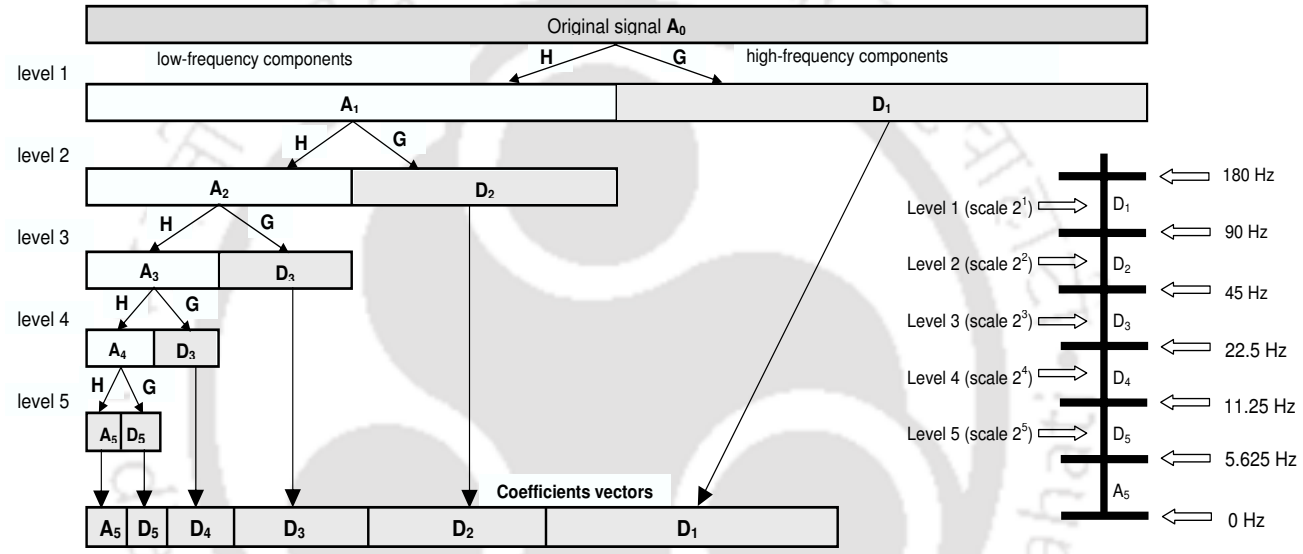

(b) Five level multiresolution signal decomposition of signal A_0. Frequency bands of the signal sampled at 360 Hz (MIT-BIH arrhythmia database).

Figure 4.1: The analysis part of the discrete wavelet transform implementation using the subband filtering and decimation process. Five-level multiresolution signal decomposition of original signal $A_0(n)$ or $x(n)$.

4.3.1 Local-wave Energies of the ECG Signal

The mean value of the original ECG signal and the compressed signal is measured and then it is subtracted from them as the first step. Both signals are decomposed using biorthogonal 9/7-tap wavelet filters [186] up to J decomposition level. In this work, the five-level analysis structure is used for the decomposition of the ECG signals. This level is sufficient for the ECG signal sampled between 250 Hz and 360 Hz [190]. For the sampling frequency of 360 Hz, the frequency bands A_5, D_5, D_4 and D_3 occupy the region of frequencies ranging from 0 Hz to 45 Hz. According to the power spectra of the ECG signal, noise and artifact [15], this frequency range has most of the coefficients of the local waves of the ECG. Fig. 4.2 shows the P-wave,

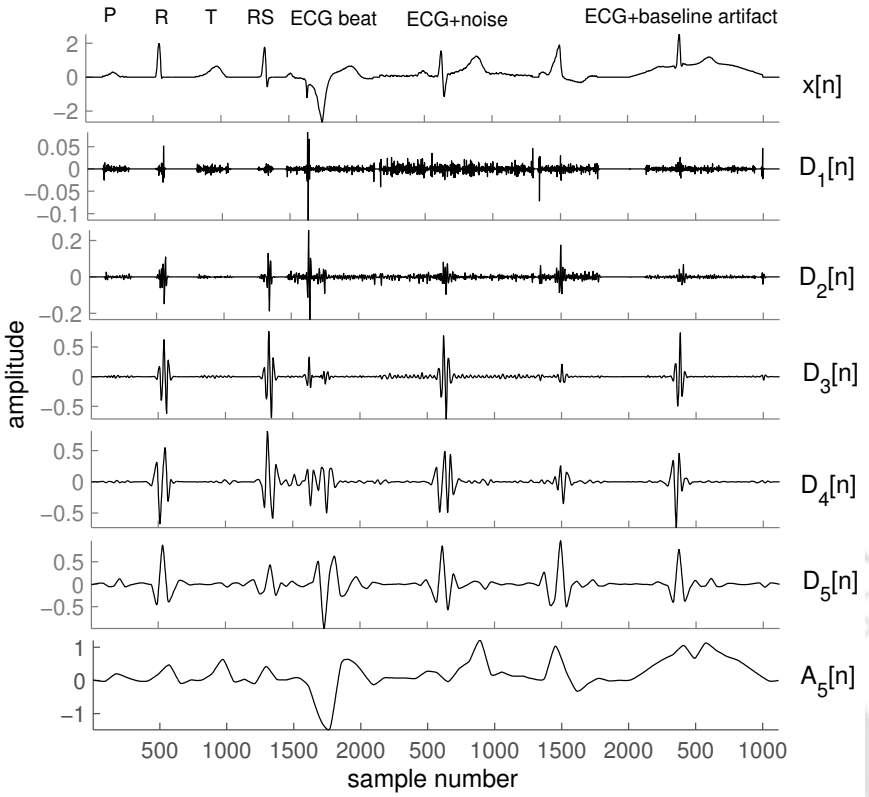

Figure 4.2: Test ECG signal $x[n]$ contains different PQRST complexes, noise and baseline artifacts. Multiresolution ECG signal decomposition using a 5-level 9/7 wavelet filters WT structure. Approximation $A_5[n]$ signal and detail $D_j[n]$ signals at resolution $j = 1,2,....5$. Noise components and fine details of ECG at D_1 and D_2. Components are localized in bands $D_j, j = 1,2,3,4$.

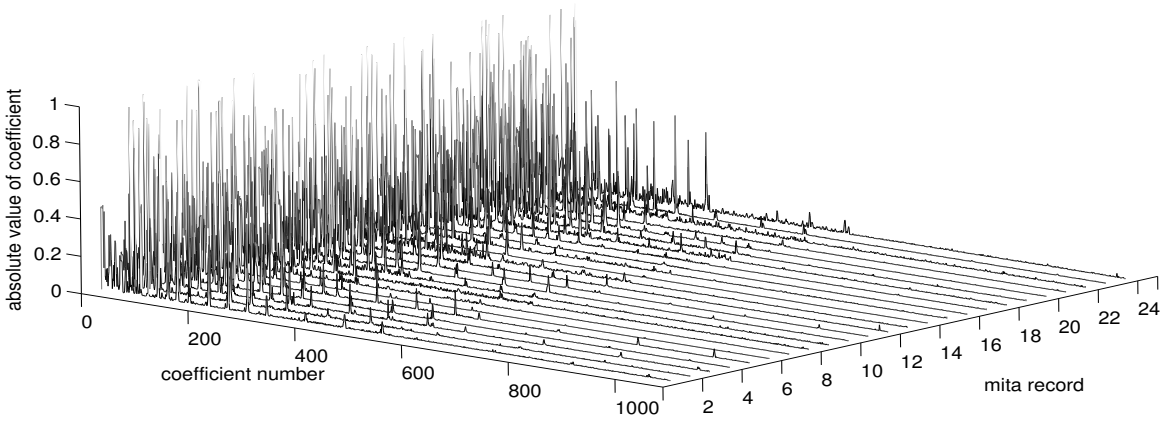

Figure 4.3: Absolute amplitude distribution of wavelet coefficients for first 2.84 s of signal from 48 records of the MIT-BIH arrythmia (`mita`) database. Large number of small coefficients in higher bands.

R-wave, T-wave, RS-wave, Q-wave, different QRS complex morphologies and noises, together with details band ($D_1 - D_5$) and approximation band A_5. It can be observed that small scales reflect the high frequency components of the signal and large scales reflect the low frequency components of the signal. The amplitude distribution of the wavelet coefficients of the decomposed ECG signals are shown in Fig. 4.3. It shows that the WT of most ECG signals are sparse, resulting in a large number of small coefficients and a small number of large coefficients. We notice that the noise is well explained by a few levels that contain fine details and its effect disappears at the coarser scales which is shown in Fig. 4.2. A measure of amplitude distribution of coefficients within the subbands is important to know the degree of importance. The wavelet subband energy (WSE) gives a good measurement of information of the signal contents and can be exploited to characterize the signal and noise contents. The relative wavelet subband energies of the subbands of the decomposed ECG signals are shown in Fig. 4.4. Most of the energy in an ECG signal is concentrated in the low-frequency band. If a signal has its energy concentrated in a small number of wavelet coefficients and their values will be relatively large. We notice that the subbands D_1 and D_2 contain most of the energy attributed to the noise and that the noise energy is practically nonexistent at the lower subbands. The relative wavelet subband energy estimate provides local information associated to the different frequency subbands present in the ECG segment and their corresponding degree of importance.

The observations on the distribution of the signal contents and the clinical distortions are summarized based on the Figs. 4.2 and 4.4, reported works in [190], 5-level decomposition tree and local thresholding. Band D_1 contains larger number of small coefficients due to the noise and a few small fine details of the ECG. Thresholding of the subband D_1 usually leads to noise suppression. Band D_2 contains the noise structure and high frequency of the QRS complex. Thresholding of the subband D_2 leads to amplitude reductions of the QRS components and local waves smoothing. These bands are weighted with a small value because their contribution to the spectrum is low. In most cases, the weight of the band D_1 is less than the weight given to the band D_2. The band D_3 consists of high frequency portion (spikes) of the QRS complex and its weight is higher than the other high frequency subbands. Thresholding of this subband leads to clinical distortion around the QRS complex region. The band D_4 consists of most of the QRS complex contribution and a small part of the P-wave. The weight of the band D_4 depends on the amplitude of the QRS complex. Thresholding of the subband D_4 leads to distortions in the QRS regions and in the PR and ST segment regions. The shape distortions of the QRS complex are severe. The band D_5 has large contribution of the P-wave and part of the T-wave and QRS complex. The weight of the band D_5 is mostly maintained by the P-wave and low percentage of the T wave and QRS complex. Distortions are on the PQRST features and flattening, missing of the P-wave are mostly seen with the thresholding of this band. Finally, the approximation band A_5 contains large contribution of the T-wave and some contribution of the P-wave and its weight includes the significance of the T and P waves and also the shape of the waves. Thresholding of the subband A_5 leads to severe distortions of the P- and T-waves.

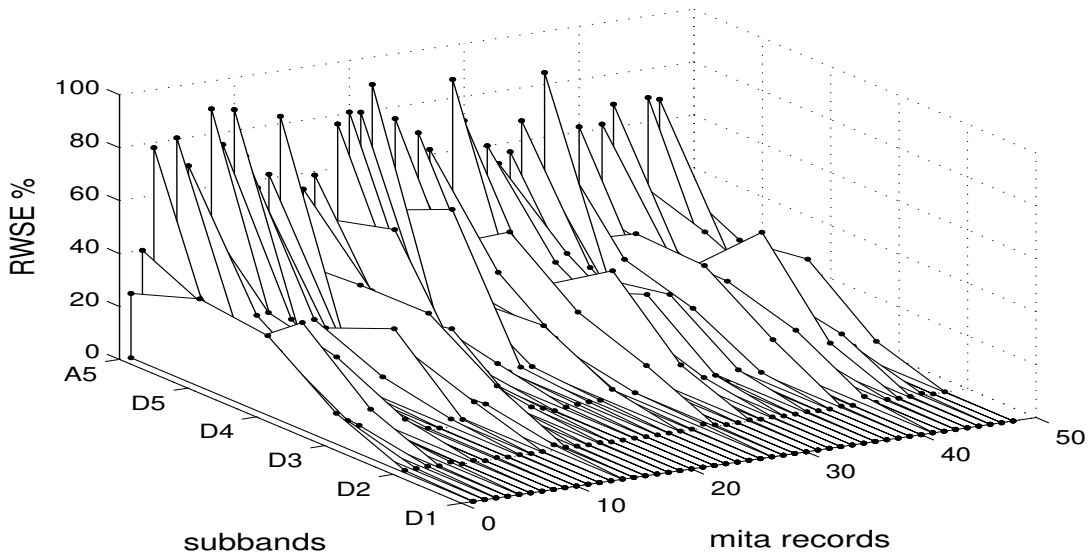

Figure 4.4: Relative wavelet subband energy (probability) distributions corresponding to five wavelet resolution levels.

4.3.2 Formulation of WEDD Measure

The MSD technique analyzes the ECG signal which is characterized by local wave patterns with different frequency content and the noise and artifacts affecting the ECG signal. If the signal is contaminated with high-frequency noise, the most affected subbands are D_1 and D_2. The relative or normalized wavelet subband energy gives a good measurement of information of the signal contents at all scales. The time-scale probability (energy) distribution is more suitable to discriminate different subbands, particularly bands corresponding to noise [147]. Thus, the wavelet energy estimates are used as weights to characterize the local clinical distortions of the compressed signal.

Let A_J be the approximation and $D_J, D_{J-1}, ..., D_1$ be the details in a J-level WT. The amplitude distribution of the wavelet coefficients of the decomposed ECG signals are shown in Fig. 4.3. The total energy of the wavelet coefficients E_t is expressed as

$$E_t = E_{\mathbf{A}_J} + \sum_{j=1}^{J} E_{\mathbf{D}_j} = \sum_{k=1}^{N_{A_J}} |A_J(k)|^2 + \sum_{j=1}^{J} \sum_{k=1}^{N_{D_j}} |D_j(k)|^2 \tag{4.5}$$

where N_{A_J} and N_{D_j} are the lengths of the approximation and the j^{th} level detail subband, respectively. Then, the dynamic weights that capture the actual contribution of the subbands are estimated as

$$\mathbf{w} = \left[\frac{E_{\mathbf{A}_J}}{E_t}, \frac{E_{\mathbf{D}_J}}{E_t}, \frac{E_{\mathbf{D}_{J-1}}}{E_t}, , ..., \frac{E_{\mathbf{D}_1}}{E_t} \right]^T \tag{4.6}$$

These weights are dynamic in nature because they are dependent on the dynamic range of the ECG signal.

A natural measure of the quality or distortion is the average distortion, where the average might be with respect to a probability model for the signal or, more commonly, a sample or time-average. It is common to normalize the distortion in some fashion to produce a dimensionless quantity. The most common distortion measure is the traditional squared error or error energy. This squared error distortion measure also plays an important role in rate-distortion function. Then, the squared error between the approximation subband $\mathbf{A}_J$ and the j^{th} detail subband $\mathbf{D}_j$ coefficient vectors of the original and compressed signals are calculated and are given by

$$E^{\text{err}}_{\mathbf{A}_J} = \sum_{k=1}^{N_{A_J}} (A_J[k] - \tilde{A}_J[k])^2 \tag{4.7}$$

$$E^{\text{err}}_{\mathbf{D}_j} = \sum_{k=1}^{N_{D_j}} (D_j[k] - \tilde{D}_j[k])^2 \tag{4.8}$$

where $E^{\text{err}}_{\mathbf{A}_J}$ and $E^{\text{err}}_{\mathbf{D}_j}$ are the error energy of the J^{th} approximation band and the j^{th} level detail band, respectively. The subband or local error is referred to as PRD_s which measures normalized root mean square difference between subband coefficients of the original and compressed signals. The PRD_s is defined as

$$\mathbf{PRD_s} = \left[\sqrt{\frac{E^{\text{err}}_{\mathbf{A}_J}}{E_{\mathbf{A}_J}}} \times 100, \quad \sqrt{\frac{E^{\text{err}}_{\mathbf{D}_J}}{E_{\mathbf{D}_J}}} \times 100, \ldots\ldots\ldots\ldots, \sqrt{\frac{E^{\text{err}}_{\mathbf{D}_1}}{E_{\mathbf{D}_1}}} \times 100 \right]^T. \tag{4.9}$$

The subband error normalization property is highly desirable for quality control algorithm and thus is performed in Eq. (4.9). The global error, total subband error is defined as

$$\text{WEDD} = \mathbf{w}^T \mathbf{PRD_s}. \tag{4.10}$$

The WEDD measure provides subband or local error estimation criterion that will focus on diagnostic quality for compressed signals. As will be demonstrated, the measure is insensitive to noise suppression and more sensitive to PQRST complex features distortion. We will show that a well-chosen set of weights can lead to better measure of clinical distortions. The WEDD measure will be a correct representation of signal distortion and will provide more meaningful results than the PRD measure, since errors due to ECG waves and complexes are weighted according to their contribution. Thus, the measure is more suitable for compression of noisy signal when the noise level is difficult to estimate, and for simultaneous noise suppression and signal compression approach. A block diagram of the procedure of obtaining six dynamic weights, calculation of the weighted subband error and total subband error is shown in Fig. 4.5. Any objective measure must ultimately be validated by comparing with subjective assessments. An objective measure is considered to be effective if it can reliably predict the score of a subjective quality rating scheme. The proposed distortion measure is validated with different sets of the experiments.

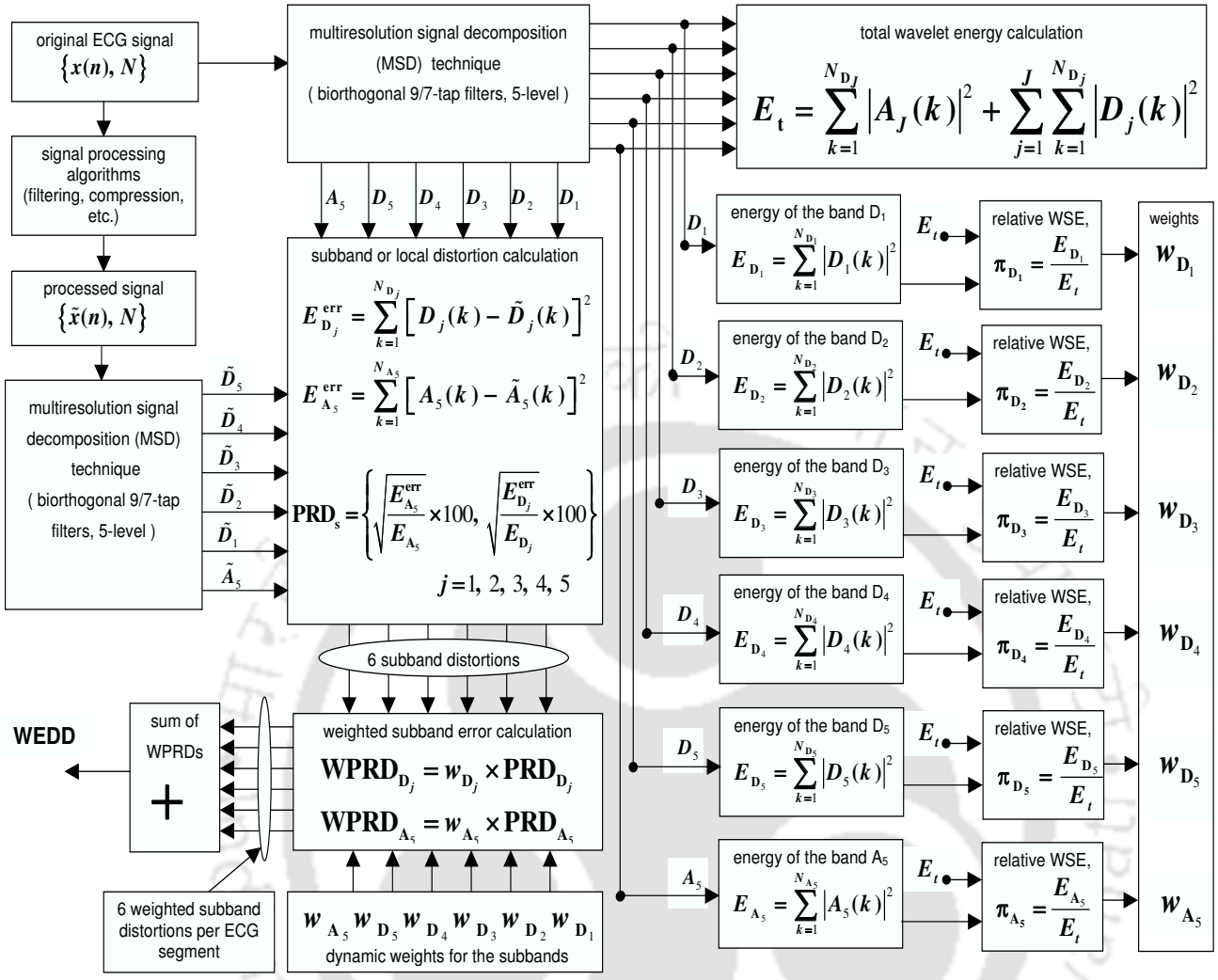

Figure 4.5: Block diagram of wavelet energy based diagnostic distortion (WEDD) measure.

4.4 Preliminary Evaluation of the WEDD Measure

For a preliminary evaluation of the proposed WEDD measure, tests are performed by applying the measure to three different types of distorted ECG signals with predictable results: i) ECG signal reconstruction after zeroing specified wavelet band coefficients; ii) ECG with noise; and iii) ECG with isoelectric region distortions. These types of distortions are considered because these occur during the zeroing of samples/coefficients based on threshold value in ECG compression algorithms, the improper quantization of samples/coefficients with small amplitudes and during the ECG signal transmission.

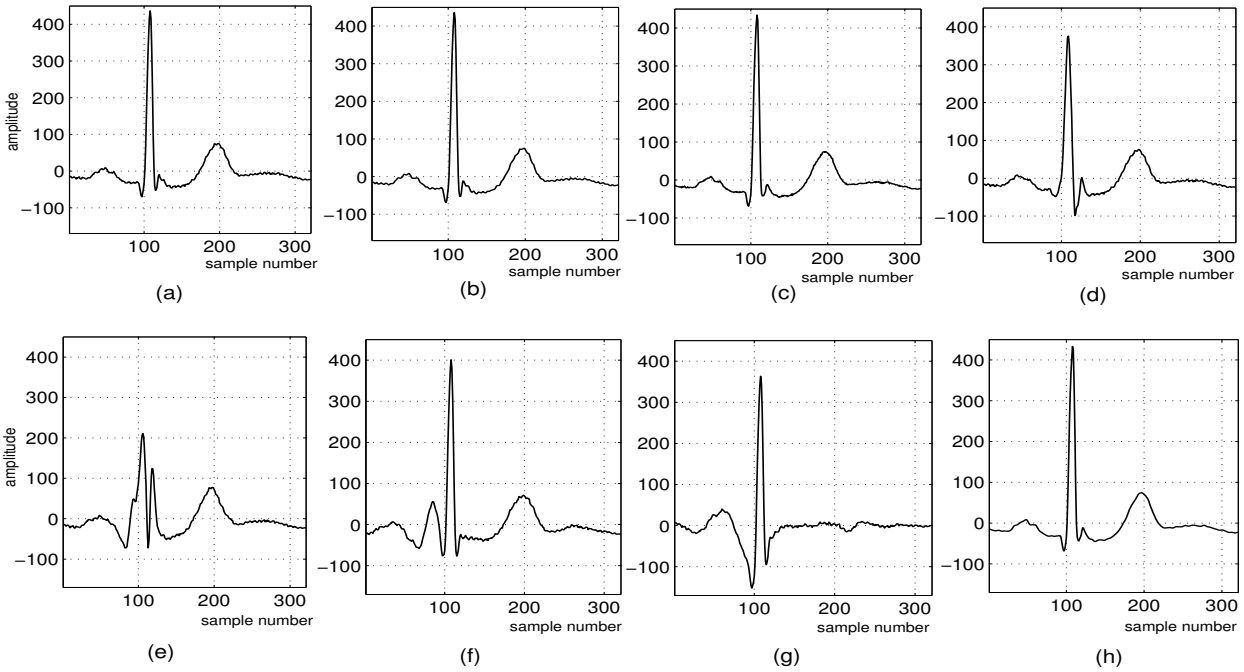

Figure 4.6: Evaluation of the subband errors. (a) Original signal from the `mita` record 103. Reconstructed signal after zeroing wavelet coefficients in (b) Detail band (D_1) (c) Detail band (D_2) (d) Detail band (D_3) (e) Detail band (D_4) (f) Detail band (D_5) (g) Approximation band (A_5) (h) Detail bands (D_1 and D_2).

4.4.1 Evaluation of the Local Errors by Zeroing of Wavelet Coefficients

Recently reported efficient wavelet based compression algorithms [126, 128, 129, 134, 142, 145] use thresholding process to retain a specified number of wavelet coefficients while zeroing other wavelet coefficients. The zeroing of wavelet coefficients may lead to distortion of diagnostic features. The reflection of local errors due to the zeroing of wavelet coefficients of particular subband is performed using the `mita` record 103. The original signal of the tested ECG segment is shown in Fig. 4.6 (a). The reconstructed signals after zeroing the detail bands D_1, D_2, D_3, D_4, D_5, the approximation band A_5 and the combined detail bands D_1 and D_2 are shown in Figs. 4.6(b)-(h). The WWPRD [190] and the proposed WEDD for each band are measured. The PRD1, MAX and NCC are also measured. The value of WEDD for each band, WWPRD, PRD1, MAX and NCC values are summarized in Table 4.1. From the results presented in Table 4.1, it can be observed that all measures detect differences between the original and zeroed band signals. The WEDD value is low for the zeroed detail band D_1 and D_2 case whereas WWPRD values are large. The reconstructed signal is shown in Fig. 4.6(b) and (c), respectively. It can be seen that the reconstructed signal qualities are good. The error in these bands may be referred to as insignificant error since it does not distort the diagnostic features except small amplitude reduction in the QRS complex. Zeroing the band D_3 slightly distorts the QRS complex which is shown in Fig. 4.6(d). The QRS complex is severely distorted when the band D_4 is zeroed and results in high WEDD value of 44.7802, as shown in Fig. 4.6(d). The T-wave

becomes nearly flat line when the A_5 coefficients are zeroed and its effect is shown in Table 4.1 and in Fig. 4.6(g). WEDD values in the eighth column of Table 4.1 shows that the WEDD measure emphasizes the significant error with respect to the amplitude of the features in time domain ECG signal while it diminishes the insignificant error. The above experimental results of the proposed WEDD measure proves that the error in the diagnostic features is reflected in their subbands. In case of WWPRD measure, the error value is high for the insignificant features. Hence it may not reflect the diagnostic distortion and may lead to confusion in the quality judgement. Similarly the PRD1, MAX and NCC measures give the value of global error, local error and similarity, respectively. Since global error measure is only an average measure, it alone cannot adequately quantify the performance of an ECG compression algorithm. These measures may not show which diagnostic feature is severely distorted even when the measure is applied block-wise, since the local waves of ECG are spatially variant. The proposed WEDD measure provides more substantive results than MSE based measures, since it provides errors of the local waves. These local errors are weighted dynamically based on the amplitude and shape of the ECG waves in the original signal. Thus, the proposed WEDD measure is more effective for assessing the quality of the diagnostic features in the reconstructed signal.

Table 4.1: Performance of the proposed measure when a particular subband is zeroed.

Zeroed	WEDD: Weighted PRD (%) of each band							WWPRD [190]: Weighted PRD (%) of each band							PRD1	MAX	NCC
band	A_5	D_5	D_4	D_3	D_2	D_1	Total	A_5	D_5	D_4	D_3	D_2	D_1	Total	(%)		
D_1	0.0258	0.0039	0.0283	0.0411	0.0035	0.0312	0.134	0.032	0.005	0.013	0.0622	0.1331	3.745	3.991	1.727	0.032	0.9999
D_2	0.3355	0.0343	0.0363	0.0138	0.1202	0.0019	0.542	0.417	0.044	0.0167	0.0209	4.5196	0.224	5.242	3.553	0.084	0.9994
D_3	0.6075	0.0401	0.0805	8.5993	0.0048	0.0003	9.333	0.7551	0.0515	0.0371	12.999	0.1794	0.0323	14.055	32.037	0.781	0.9473
D_4	0.3662	0.0335	44.780	0.0176	0.0007	0.0001	45.198	0.4551	0.0429	20.617	0.0266	0.0277	0.0071	21.176	68.360	1.38	0.7304
D_5	3.762	8.748	0.1498	0.0418	0.0015	0.0001	12.703	4.6759	11.215	0.069	0.0632	0.0572	0.0145	16.095	31.533	0.430	0.9491
A_5	38.845	0.1377	0.1314	0.0414	0.0015	0.0001	39.157	48.282	0.1765	0.0605	0.0626	0.0555	0.013	48.650	53.977	0.451	0.8418
D_1, D_2	0.3112	0.0349	0.061	0.0458	0.120	0.0313	0.6044	0.3869	0.0447	0.0281	0.0692	4.524	3.7549	8.808	3.936	0.078	0.9992

4.4.2 Performance of the WEDD Measure under Noisy Conditions

In many situations, the ECG signal contains noise which may not be important for clinical diagnosis but it contributes nonzero value in all the above mentioned error measures including WWPRD [190]. In WEDD measure, the error introduced by the noise is weakened by the proposed wavelet energy based weights, which are very small. These problems are considered and illustrated with the following experiment. The ECG segments from the noisy `mita` records 100, 108, 117 and 123 are compressed/decompressed and the reconstructed signal distortion is computed using non-diagnostic and diagnostic distortion measures. For the testing purpose, the additive white Gaussian noise of -30 dB is introduced in isoelectric region of the ECG segment from the `mita` record 123. Other `mita` records 100, 108 and 117 are processed with their noise levels in the records. The wavelet decomposition of these records have high frequency noise components in subbands D_2 and D_1. These subband wavelet coefficients are zeroed when the thresholding process is

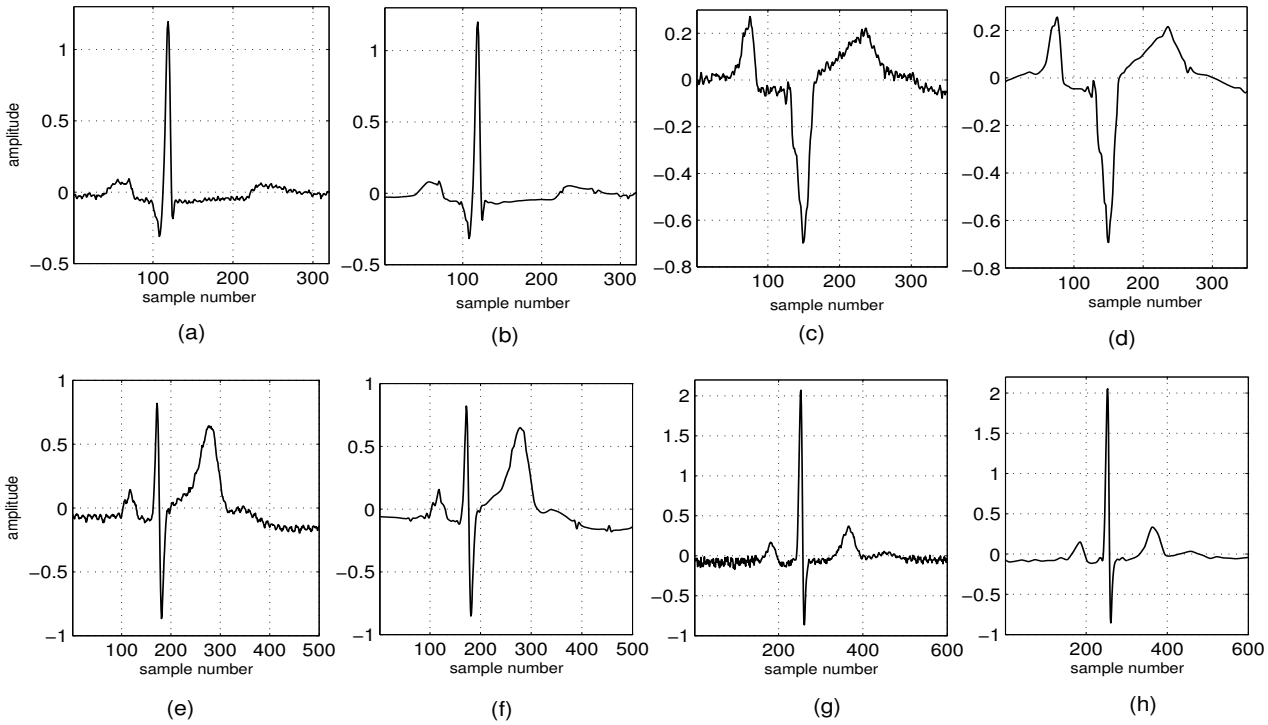

Figure 4.7: Performance of the proposed WEDD and other error measures for the noisy test signals. Original signals: (a), (c), (e) and (g) are from the `mita` record 100, 108, 117 and 123, respectively. Reconstructed signals: (b), (d), (f) and (h) of the compressed versions of the signals taken from the `mita` record 100, 108, 117 and 123, respectively. Here, the raw ECG signal taken from the `mita` record 100, 108 and 117 are processed. And the additive white gaussian noise of -30 dB is introduced in isoelectric region of ECG signal from record 123 for testing purpose.

employed in the compression algorithms. Now, a distortion measure is needed to measure the amount of diagnostic feature distortion without the inclusion of insignificant error.

The measured objective error values using non-diagnostic and diagnostic distortion measures are summarized in Table 4.2. For the visual inspection, the reconstructed signals are shown in Figs. 4.7(b), (d), (f) and (h). Table 4.2 illustrates the actual behavior of local and global error measures. The local errors introduced by the approximation band A_5 and the detail bands D_5 - D_1 are computed using the WWPRD [190] and the proposed WEDD measure for the effective comparison. In WWPRD, the error contributed to the total error value by the bands D_1 and D_2 is high compared to other wavelet bands shown in the table. These two bands provide high error value due to the smoothing of background noise. Hence, the WWPRD measure may not reflect the local wave distortion. For all the tested ECG segments, the resulting WWPRD value is very high. These values indicate that some diagnostic features are severely distorted within the ECG segment of the tested records. But the diagnostic features are preserved well which is shown in Fig. 4.7. The proposed measure provides low error value for these two bands. Consequently, the WEDD reflects the amount of diagnostic distortion. For example, the WWPRD value for the tested `mita` record 108 is

Table 4.2: Performance of the WEDD measure when the signal with noise and distortion in the isoelectric region.

Measure	Record	Weighted PRD (%) of each band							Non-diagnostic Measures: for mita records 100, 108, 117 and 123, respectively		
		A_5	D_5	D_4	D_3	D_2	D_1	Total			
WWPRD [190]	100	1.1121	0.247	0.8651	1.4829	3.5722	5.2015	12.4808			
	108	1.6623	0.4749	1.6152	3.0294	8.0238	6.5371	21.3427	PRD1	MAX	NCC
	117	1.5995	0.5718	0.8029	5.1285	2.9298	4.5792	15.6117	4.983	0.0279	0.9988
	123	0.9925	0.7628	1.0169	6.0858	6.1846	12.7361	27.7787	7.201	0.0387	0.9974
Proposed WEDD	100	0.3845	0.5753	1.331	0.7529	0.6117	0.0756	3.7311	5.731	0.0557	0.9984
	108	2.2423	0.7283	0.3058	0.253	0.3773	0.096	4.0026	8.3533	0.1011	0.9965
	117	1.9963	0.4777	1.125	0.2772	0.0623	0.0419	3.9804	-	-	-
	123	0.6399	1.1024	2.8355	0.7264	0.3853	0.3794	6.069	-	-	-

Note:- Additive white Gaussian noise (AWGN) of -30 dB is introduced in isoelectric region of mita 123. Other mita records 100, 108, and 117 are processed with their noise level in their respective records.

21.3427 while the WEDD value is 4.0026. The diagnostic features are preserved in the reconstructed signal of mita record 108, which are shown in Fig. 4.7(d). The WEDD for the test record 123 is 6.069%, which indicates that some of the diagnostic features are distorted. From Fig. 4.7 and Table 4.2, it can be observed that the tabulated WEDD values indicate the amount of error in diagnostic features. The judgement of the compressed signal quality is better using the estimated WEDD value than the WWPRD value under noisy condition. It can be also observed that the proposed WEDD measure is more sensitive to diagnostic features' distortion while it is less sensitive to distortion in the isoelectric regions and the presence of noise as compared to other error measures such as PRD1, MAX, NCC and WWPRD. The above experiments show that the proposed measure performs quite well for a wide range of distortion types.

4.5 Subjective Quality Measure

In order to analyze the proposed WEDD measure with reference to subjective or clinical quality test, the mean opinion score (MOS) test is performed in this section. Subjective test based distortion measure is used as reference because it represents the true quality of the reconstructed signal (gold standard) [191]. These tests are visually performed by the cardiologist and the biomedical signal processing group by reviewing the diagnostic features of the original and compressed signals. MOS test consists of a blind test and a semi-blind test [191]. The blind test analyzes both the original and the compressed signals individually and the different ECG signal features are interpreted by the observers. The semi-blind test compares the original and the compressed signals together. In this test, the observer provides an evaluation of the similarity between the original and the compressed signal features. In this work, semi-blind test is conducted for the evaluation of MOS rating. The MOS rating is decided according to the quality of the diagnostic features such as P-wave, PR-interval, QRS complex, T-Wave, ST-segment and QT-interval for every tested signal.

Table 4.3: Semi-blind MOS test applied to `mita` record 123 [Fig. 4.7(h)].

ECG features	Score 1	Score 2	Score 3	Avg.
P-wave	4	5	4	4.33
PR-segment	4	5	5	4.67
PR-interval	5	5	4	4.67
QRS complex	5	5	4	4.67
ST-segment	5	4	5	4.67
T-wave	4	4	5	4.33
QT-interval	5	5	4	4.67
MOS	4.57	4.71	4.43	4.57

The quality rating ranges from 1 (bad) to 5 (excellent) for each tested signal. The observer examines a set of ECG features and assigns a numerical rank for the signal under test. All such scores are recorded. The average rank of each ECG signal is determined. The MOS^{s} of one ECG segment from the i^{th} cardiologist is defined as

$$\mathrm{MOS}^{(s)}(i) = \frac{1}{\mathrm{N}_f} \sum_{n=1}^{\mathrm{N}_f} \mathrm{R}(n) \tag{4.11}$$

where $\mathrm{R}(n)$ is the rating of the n^{th} diagnostic feature and N_f is the number of diagnostic features which is seven in this work. The overall MOS for the tested signals is the average MOS of all the segments of the signal. The MOS of one segment from all N_c cardiologists is given by

$$\mathrm{MOS} = \frac{1}{\mathrm{N}_c} \sum_{i=1}^{\mathrm{N}_c} \mathrm{MOS}^{s}(i) \tag{4.12}$$

Using Eq. (6.2), $\mathrm{MOS}_{\mathrm{error}}$ for the semi-blind test of one segment from all N_c cardiologists is calculated as

$$\mathrm{MOS}_{\mathrm{error}} = \frac{5 - \mathrm{MOS}}{5} \times 100 \tag{4.13}$$

In this work, the $\mathrm{MOS}_{\mathrm{error}}$ measure is used as a gold standard [191]. It is necessary to determine a gold standard that can represent the diagnostic quality of each compressed signal. A signal that is judged to be of deficient quality would have a high $\mathrm{MOS}_{\mathrm{error}}$, whereas one that is thought to be of good quality would receive a low $\mathrm{MOS}_{\mathrm{error}}$. One can estimate the effectiveness of a metric by comparing the numerical values reported by an ECG quality system to those assigned by the subjective test group. The values of a good metric should be similar to the mean opinion scores. MOS for the tested ECG segment (in Fig. 4.7(h)) from record 123 is given in Table 4.3.

4.6 Quantitative and Qualitative Analysis of WEDD Measure

In this section, the performance of the proposed measure is compared with other diagnostic and non-diagnostic distortion measures. In order to assess the ability of the proposed WEDD measure in predicting the MOS_{error} and to compare with WWPRD, PRD and other non-diagnostic distortion measures, the compressed signals with different qualities are obtained using five different compression algorithms AZTEC, FAN, DCT, SPIHT [145] and DSI [192]. For evaluation purpose, the ECG signals are extracted from the 48 records included in the `mita` database, $08730\_01, 08730\_02, 08730\_05$ and 08730_07. These signals are chosen because they consist of a large variety of pathological cases and noisy ECG signals. The mean is removed from every ECG signal. Using the above mentioned records, 210 reconstructed signals are produced for the evaluation purpose.

4.6.1 Correlation between MOS_{error} and Distortion Measures

For every compressed signal, the non-diagnostic distortion measures and the diagnostic distortion measures are computed. RMSE, PRD1, PRD2, SNR, MAX, NMAE, CC, WWPRD and the proposed WEDD values are estimated. To evaluate the objective measures, the gold standard MOS_{error} is calculated from the results of the semi-blind test of two cardiologists for every tested signal.

To observe the relationship between gold standard and the distortion measures, the scatter plots of MOS_{error} versus objective distortion measures are shown in Figs. 4.8-4.10. The mean opinion score errors are linearly scaled to a range of [0, 100], where 0 and 100 represent the best and the worst ratings, respectively. The horizontal axis and the vertical axis represent the objective distortion measure and MOS_{error}, respectively. Each sample point in the scatter plot indicates the error value of one compressed signal. Scatter plot shows at a glance whether a relationship exists between two sets of sample points or not. The scatter plots of the global error measures are shown in Fig. 4.8. The scatter plot of MOS_{error} versus PRD2 is shown in Fig. 4.8(a). From the figure, it is observed that the sample points are dispersed over a wide space. This shows weak correlation between subjective and objective scores (PRD2 values). Fig. 4.8(b) shows the scatter plot of MOS_{error} versus PRD1. At higher values of PRD1, the points are widely spread. Hence, it results in poor correlation. But at low values of PRD1, the points are closer. Therefore, the PRD1 has better correlation compared to PRD2. The performance of PRD1 is better than PRD2 because it is measured without mean of the original signal. This relationship between two variables is analyzed by linear and nonlinear regression. Fig. 4.8(c) shows the scatter plot of MOS_{error} versus RMSE. It is observed that the data points are widely spread. In the above plots, if the data points make a straight line going from the origin out to high x- and y-values then the variables MOS_{error} and PRD1/PRD2/RMSE are said to have a positive correlation. Fig. 4.8(d) shows the scatter plot of MOS_{error} versus SNR. The sample points are not widely distributed. Here, the line goes from a high-value on the y-axis down to a high-value on the x-axis and hence, the variables MOS_{error} and SNR have a negative correlation.

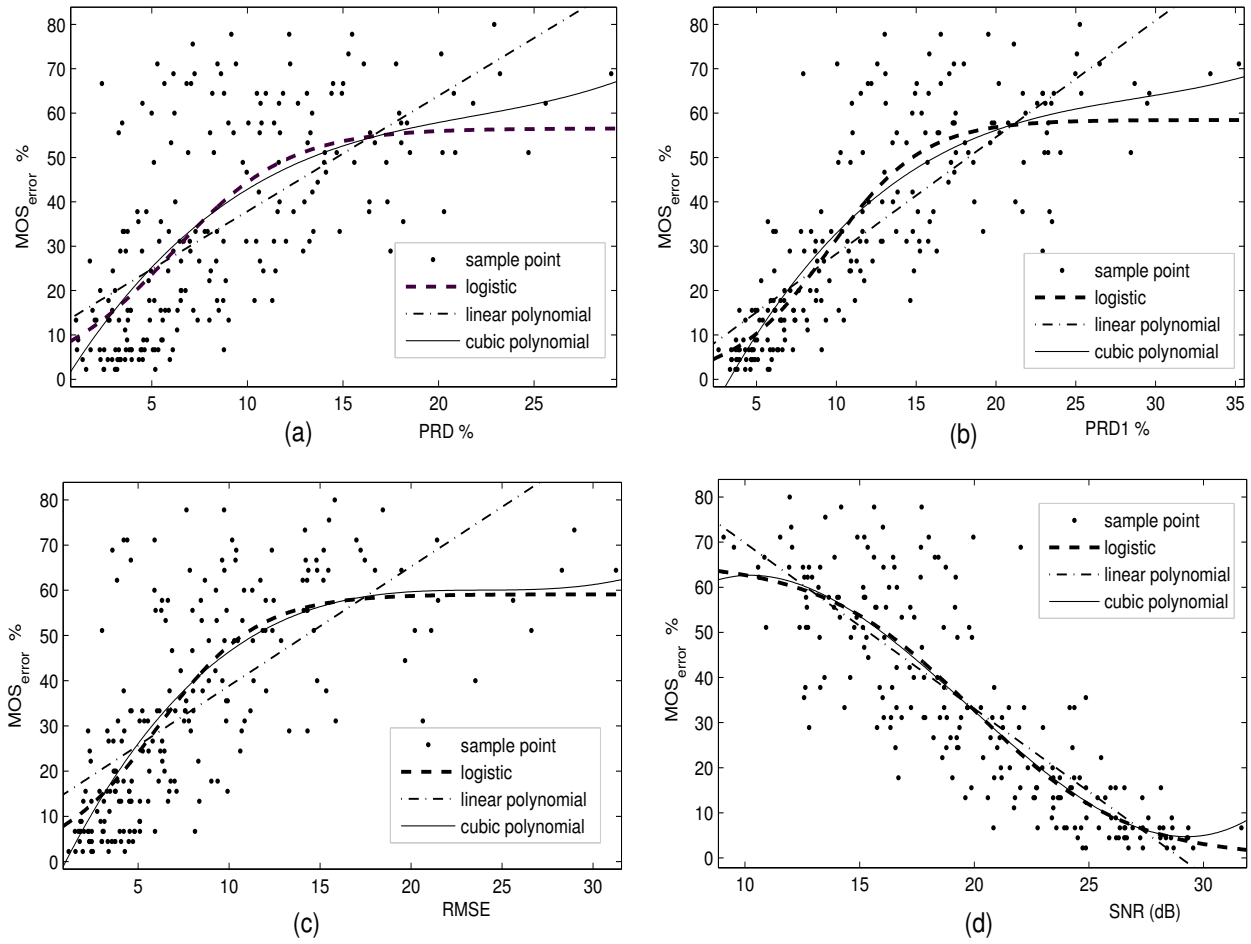

Figure 4.8: Relationship between measured gold standard (MOS_{error}) values versus values estimated via objective non-diagnostic distortion measures. Each point represents one test signal. (a) MOS_{error} versus PRD2, CC = 0.6342. (b) MOS_{error} versus PRD1, CC = 0.799. (c) MOS_{error} versus RMSE, CC = 0.6639. (d) MOS_{error} versus SNR, CC = -0.8354.

The scatter plots of local error measures (MAX, NMAX), MAE and similarity measure (NCC) are shown in Fig. 4.9. Fig. 4.9(a) shows the scatter plot of MOS_{error} versus MAX. Fig. 4.9(b) shows the scatter plot of MOS_{error} versus NMAX. Fig. 4.9(c) shows the scatter plot of MOS_{error} versus MAE. From these figures, it is observed that the sample points are dispersed widely. The correlation between the variables is very poor in MAX/NMAX/MAE case. The correlation values are 0.6173, 0.7215 and 0.647, respectively. But these measures have positive correlation since their lines extend from a high-value on the y-axis down to a high-value on the x-axis. Fig. 4.9(d) shows the scatter plot of MOS_{error} versus NCC. The correlation is good at high NCC values while NCC performs poor at low values. In this scatter plot, the line goes from a high-value on the y-axis down to a high-value on the x-axis and hence, the variables MOS_{error} and NCC have negative correlation. The correlation value of this measure is -0.7016.

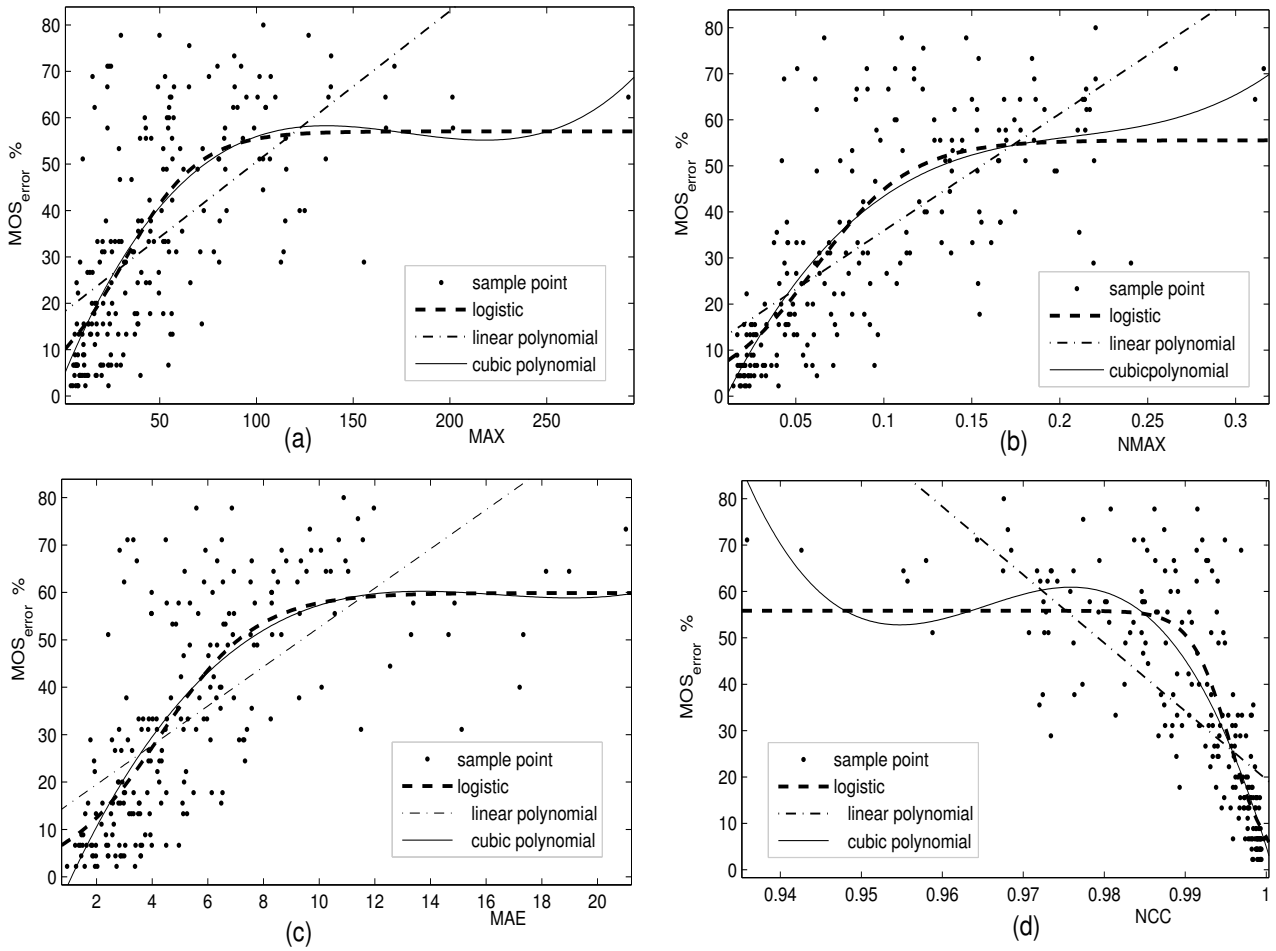

Figure 4.9: Relationship between measured gold standard (MOS_{error}) values versus values estimated via objective non-diagnostic distortion measures. Each point represents one test signal. (a) MOS_{error} versus MAX, CC = 0.6173. (b) MOS_{error} versus NMAX, CC = 0.7215. (c) MOS_{error} versus MAE, CC = 0.647. (d) MOS_{error} versus NCC, CC = -0.7016.

Table 4.4: Linear and Nonlinear regression function.

Type of fit	Regression function
Linear polynomial	$f_1(x) = b_1x + b_0$
Cubic polynomial	$f_2(x) = b_3x^3 + b_2x^2 + b_1x + b_0$
Logistic	$f_3(x) = \frac{b_0}{1+b_1 exp(\frac{-x}{b_2})}$

Note:- where x is the objective score and b_0, b_1, b_2 and b_3 are the model parameters.

Fig. 4.10 shows the scatter plot of MOS_{error} versus diagnostic distortion measures. Fig. 4.10(a) shows the scatter plot of MOS_{error} versus WWPRD. It is observed that the sample points are not tightly clustered

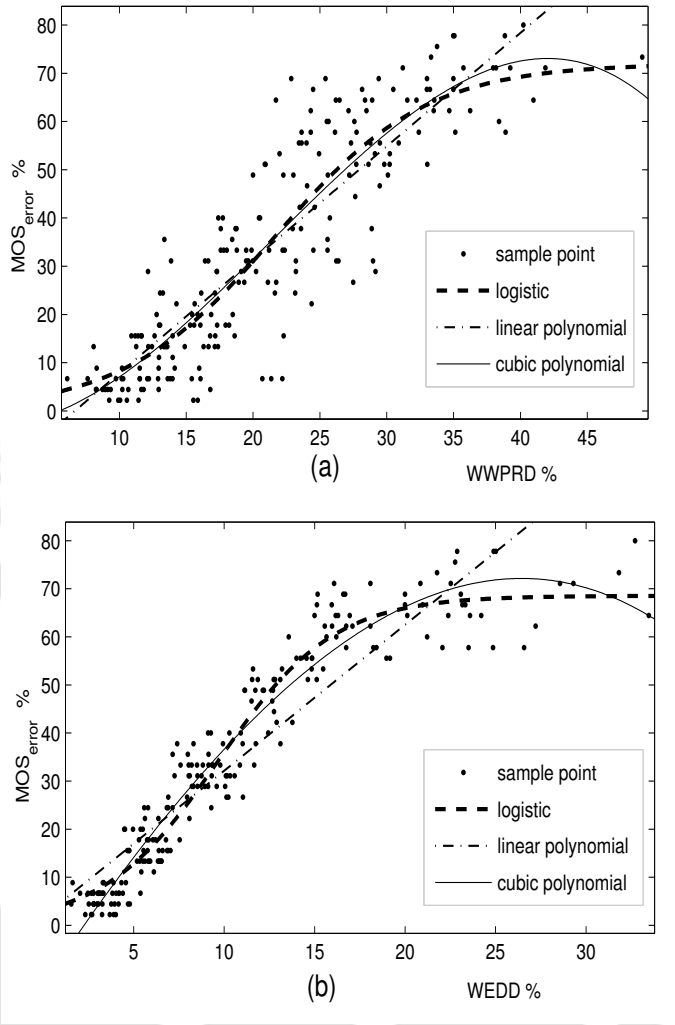

Figure 4.10: Relationship between measured gold standard (MOS_{error}) values versus values estimated via objective diagnostic distortion measures. (a) MOS_{error} versus WWPRD, CC = 0.8811. (b) MOS_{error} versus WEDD, CC = 0.9197.

together and are spread more widely along the horizontal direction. Hence it results in poor correlation. Fig. 4.10(b) shows the scatter plot of MOS_{error} versus proposed WEDD. Here the sample points are tightly packed and the plot resembles a line rising from left to right. The closer the sample points are, the higher is the correlation between the two variables. Since the slope of the line is positive, there is a positive correlation between the two sets of points. The performance of the proposed WEDD measure is better than WWPRD for the noisy signals.

Table 4.5: Variance (VAR) of the error calculated between distortion measures and their regression lines.

Regression Line (RL)	non-weighted distortion measure								weighted distortion measure	
	Global-OM					Local-OM		SM	Absolute w_l	Energy w_l
	RMSE	PRD2	PRD1	SNR	MAE	MAX	NMAX	NCC	WWPRD [190]	WEDD
Linear RL	290.26	310.29	187.68	156.85	301.75	321.24	248.89	263.59	116.08	80.00
Cubic RL	238.31	288.71	151.68	150.15	240.67	265.02	208.67	159.26	107.18	35.42
Nonlinear RL	239.20	288.44	150.75	149.21	240.11	213.46	267.78	155.71	106.49	31.70

Note:- OM: Obejective measure; SM: Similarity measure.

4.6.2 Statistical Predictability of Distortion Measure

In order to assess the ability of the proposed WEDD and other distortion measures to predict the MOS ratings, linear and nonlinear predictors are fitted to the various scatter plots. Table 4.4 shows the linear and nonlinear function which is used to provide a linear and nonlinear mapping between the objective and subjective scores. The linear and cubic polynomials are used as linear predictor which exactly fit the sample points as line. Logistic function is used for the nonlinear mapping. In this work, the model parameters are found numerically using a nonlinear regression process with MATLAB optimization toolbox. After the linear and nonlinear mapping, the following analysis is performed to evaluate the performance of the objective distortion measures.

Firstly, a measure of deviation from the regression line between subjective and objective measures is used for the evaluation of predicted quality compared to gold standard [191]. The regression line expresses the best prediction of the dependent variable ($\text{MOS}_{\text{error}}$) for the given independent variables (objective error measures). The deviation of a particular point from the regression line (its predicted value) is called the prediction error. The smaller the variability of the error values around the regression line, the better is the prediction. The VAR [191] measure is given as

$$\text{VAR} = \frac{1}{N_s}\sum_{n=1}^{N_s}[d(n)-\mu_d]^2 \tag{4.14}$$

where $d(n)$ is the vertical deviation of the n^{th} sample point from the regression line, N_s is the total number of sample points and μ_d is the mean value of $d(n)$, $n = 1,2,3,....N_s$. For each regression line (RL), the variance of the error between the actual and the predicted $\text{MOS}_{\text{error}}$ are summarized in Table 4.5. The VAR is zero for a good predictor. The VAR is low for the nonlinear predictor (logistic function) compared to polynomial predictor. Thus, the logistic predictor gives the best fit. The variance between the WWPRD and the $\text{MOS}_{\text{error}}$ is 106.49 and the variance between the WEDD and the $\text{MOS}_{\text{error}}$ is 31.70, which is three times better than the WWPRD case.

Secondly, to investigate the performance of the proposed measure, various statistical measures like root mean square prediction error (RMSE), mean absolute prediction error (MAE), standard error (SE) and

Table 4.6: Validation of the objective distortion measures.

Type of Regression Line (RL)	Metrics	non-weighted DM								weighted DM	
		Global-OM					Local-OM		SM	WWPRD [190]	WEDD
		RMSE	PRD2	PRD1	SNR	MAE	MAX	NMAX	NCC		
Linear polynomial	M1	16.9979	17.5748	13.6683	12.4953	17.3311	17.8821	15.7403	16.1984	10.7497	8.9238
	M2	13.8897	14.367	10.3427	9.5397	14.3147	14.6177	12.0759	12.9466	8.3673	7.0685
	M3	17.0764	17.6559	13.7315	12.553	17.4111	17.9647	15.813	16.2732	10.7994	8.9651
	M4	0.6639	0.6342	0.799	0.8354	0.647	0.6173	0.7215	0.7016	0.8811	0.9197
Cubic polynomial	M1	15.4021	16.9526	12.2876	12.2256	15.478	16.2421	14.4123	12.5912	10.3293	5.9385
	M2	11.756	13.7934	9.2926	9.1102	12.0152	12.5307	10.7778	9.4747	7.9886	4.8341
	M3	15.4375	16.9916	12.3159	12.2537	15.5136	16.2795	14.4454	12.6201	10.3531	5.9521
	M4	0.7354	0.6662	0.8413	0.843	0.7324	0.6996	0.7733	0.8326	0.8908	0.9653
Logistic	M1	15.4309	16.9448	12.2503	12.1874	15.4603	16.3268	14.5779	12.4512	10.2963	5.6198
	M2	11.7827	13.7173	9.2793	9.1423	11.8726	12.661	11.0407	9.552	8.0041	4.5321
	M3	15.5022	17.023	12.3069	12.2437	15.5317	16.4023	14.6452	12.5087	10.3439	5.6458
	M4	0.7343	0.6666	0.8424	0.8441	0.7331	0.6959	0.7674	0.8368	0.8916	0.969
SROCC		0.7433	0.68	0.8504	-0.8486	0.7439	0.7129	0.7799	-0.8479	0.8865	0.9624

Note:- M1: Root mean squared prediction error; M2: Mean absolute prediction error; M3: Standard error; M4: Correlation coefficient; SROCC: Spearman rank-order correlation coefficient.

correlation coefficient (CC) between $\mathrm{MOS}_{\mathrm{error}}$ and each distortion measure are computed. The prediction error is the difference between the true $\mathrm{MOS}_{\mathrm{error}}$ and the predicted $\overline{\mathrm{MOS}}_{\mathrm{error}}$ for an objective error. The regression line seeks to minimize the sum of the squared errors of the prediction. The square root of the average squared error of prediction, standard error (SE), is used to measure the accuracy of predictions made with regression line. The standard error is given by

$$\mathrm{SE} = \sqrt{\frac{\sum_{n=1}^{N_s}[\mathrm{MOS}_{\mathrm{error}}(n) - \overline{\mathrm{MOS}}_{\mathrm{error}}(n)]^2}{N_s - 2}} \tag{4.15}$$

where N_s is the number of sample points.

Performance of the objective measures is also evaluated with respect to two aspects of their ability to estimate subjective assessment of signal quality. The first measure is the prediction accuracy which gives the ability to predict the subjective quality ratings with low error. The second measure is the prediction monotonicity. The objective measure value should increase and decrease monotonically as the MOS increases and decreases. After the nonlinear mapping, the correlation coefficient between the predicted and true subjective scores is calculated to evaluate the prediction accuracy. The prediction monotonicity is evaluated by Spearman rank order correlation coefficient (SROCC) [194]. The monotonic relation is expressed using rank-order numbers instead of values. As a statistical test to check whether a relation between two

variables exists, SROCC test is better than the standard correlation coefficient (CC) because the latter will only work when there is a linear relation between the variables. In practical situations, assumption of a linear relation is often unrealistic.

The statistical evaluation results for all the distortion measures are summarized in Table 4.6. Using regression lines, the statical measures namely RMSE, MAE, SE and CC are calculated for each objective distortion measure. Comparison of the values given in column four (PRD2), five (PRD1) and six (SNR) of Table 4.6 shows that the performance of the PRD1 measure is better than the PRD2. But the SNR performance is better than PRD1 and PRD2 case. The numbers in M4 row of Table 4.6 have the following meanings. M4 is the correlation coefficient(CC) between the actual and predicted MOS values. Perfect prediction would yield the value CC = 1. The correlation coefficient of WWPRD is 0.8916, which is slightly better than PRD1 with CC of 0.8424. But it results in poor prediction for the noisy input signal. For the same test signal, the CC of WEDD is 0.969, which shows better prediction accuracy. Row M3 represents the standard error (SE). The standard error should be zero for a good prediction. The SE between the actual MOS_{error} and predicted MOS_{error} from WEDD is 5.6458 and from WWPRD it is 10.3439. The performance of WEDD is approximately two times better than WWPRD.

In order to justify the effectiveness of the proposed WEDD measure, the rank-order correlation between the WEDD and MOS_{error} is examined and it is compared with the rank-order correlation between the WWPRD and the MOS_{error}. The SROCC is 0.9624 for the proposed measure which is better than the WWPRD with SROCC value of 0.8865. These results prove that the subjective quality scores obtained from the proposed WEDD measure gives good prediction accuracy (higher correlation coefficient) and better prediction monotonicity (higher Spearman rank-order correlation coefficient) than PRD1 which is most widely used in the ECG compression methods.

One way of classifying signal quality can be defined by dividing the MOS_{error} into five quality groups. The quality groups are: Excellent, Very Good, Good, Not Bad and Bad. These quality groups and classified MOS_{error} ranges are shown in Table 4.7. This classification may suggest a reasonable means of evaluating the measures and comparing their findings with those of an independent observer. In this work, the technique used in [191], [190] for the determination of thresholds of each prediction range is followed. For the proposed measure, five prediction ranges are determined. Fig. 4.11 shows the PRD1, WWPRD and WEDD values of each quality group of signals and the prediction ranges. The horizontal axis and the vertical axis represent the quality groups and objective distortion measure, respectively. Each sample point in the scatter plot indicates the quality of the reconstructed signal. It is observed that the overlapping of quality groups in Fig. 4.11(a) and (b) is more compared to quality groups in Fig. 4.11(c). Overlapping of quality groups leads to confusion. For PRD1 and WWPRD measure, the prediction ranges given in [190] are used in this paper. The thresholds of each prediction range are determined manually making sure that all the signals in the prediction range fall within a minimum number of quality groups. The prediction ranges of PRD1, WWPRD, and WEDD measures and their quality groups are depicted in Table 4.8. This is referred to as

Table 4.7: Quality groups defined by MOS_{error}.

MOS_{error} (%)	0-10	10-25	25-40	40-55	> 55
ECG signal quality	Excellent	Very good	Good	Not Bad	Bad

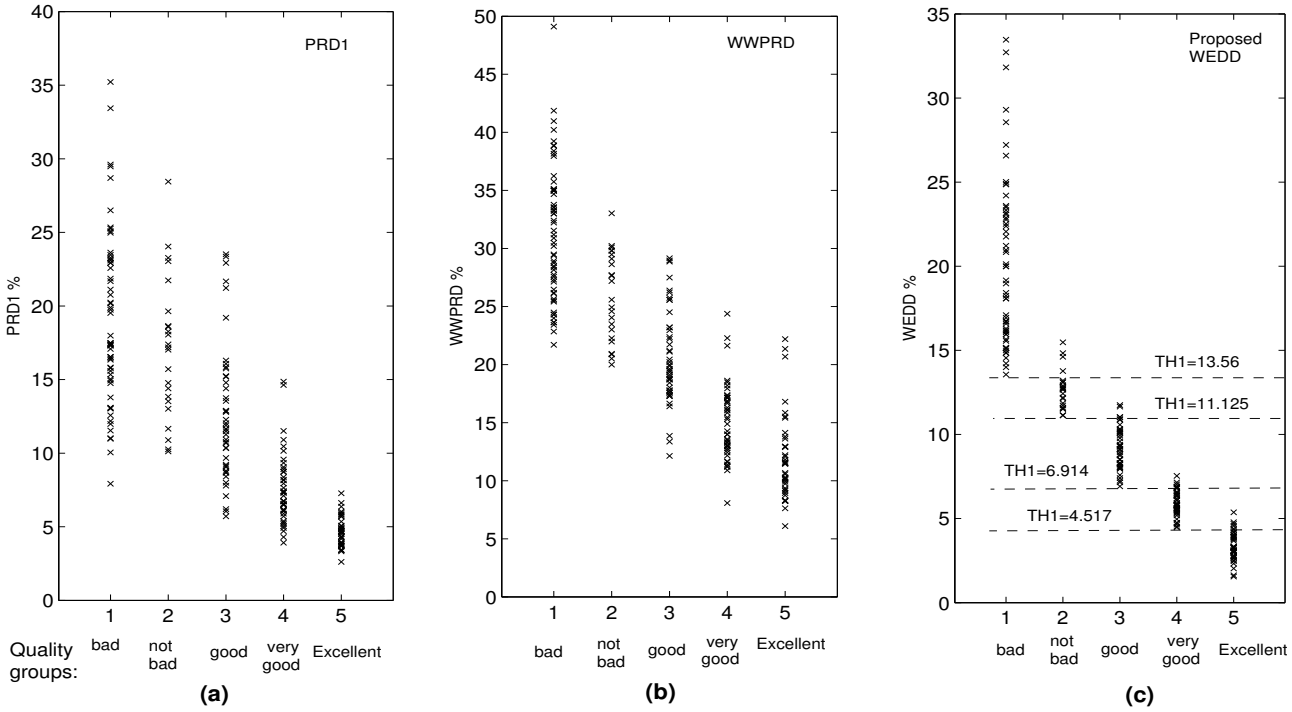

Figure 4.11: The scattering and threshold values of the prediction range for each quality group of reconstructed signals. (a) for the PRD1 measure, (b) for the WWPRD measure, (c) for the proposed WEDD measure.

confusion matrix [191]. The number (r_{mn}) inside the 5×5 confusion matrix indicates the percentage of signals from the m^{th} prediction range and the n^{th} quality group. Table 4.8 also demonstrates the prediction ability of the three distortion measures. The diagonal elements of the confusion matrix indicate the correct prediction by the distortion measure. From Table 4.8, it is observed that the determination of quality group is difficult when the tested signal has PRD1 value between 7.8% - 11.59% or a WWPRD value between 15.45% - 25.18%. But a WEDD value between 6.914% - 11.125% predicts a quality group of 'very good' or 'good'. The mean correct prediction (MCP) and the normalized prediction error (NPE) are computed as defined in [191]. The mean correct prediction of the proposed WEDD measure is 95%, which is higher than the other measured PRD1 and WWPRD with an MCP of 54.4% and 50.2%, respectively. The normalized prediction error of the proposed measure is 0.6876%, which is ten times less than the PRD1 and WWPRD case.

Table 4.8: Quality groups and their prediction range of PRD1, WWPRD and WEDD measure.

Distortion Measure	Prediction range	Quality groups					MCP (%)	NPE (%)
		Excellent	Very Good	Good	Not Bad	Bad		
PRD1 (%)	0-4.33	**89**	11	0	0	0	54.4	7.22
	4.33-7.8	43	**48**	9	0	0		
	7.8-11.59	0	38	**41**	8	13		
	11.59-22.57	0	3	28	**22**	47		
	>22.57	0	0	12	16	**72**		
WWPRD [190] (%)	0-7.4	**100**	0	0	0	0	50.2	7.5
	7.4-15.45	55	**39**	6	0	0		
	15.45-25.18	6	27	**42**	14	11		
	25.18-37.40	0	0	15	**20**	65		
	>37.40	0	0	0	50	**50**		
Proposed WEDD (%)	0-4.517	**100**	0	0	0	0	95	0.6876
	4.517-6.914	2	**98**	0	0	0		
	6.914-11.125	0	7	**93**	0	0		
	11.125-13.56	0	0	9	**91**	0		
	>13.56	0	0	0	7	**93**		

Note : MCP: Mean correct prediction; NPE: Normalized prediction error.

4.7 Discussion

In this chapter, a novel objective weighted distortion measure for compressed and denoised ECG signals is proposed. The proposed WEDD measure is the weighted percentage root mean square difference between the wavelet subband coefficients of the original and compressed signals with weights equal to the relative wavelet subband energies of the corresponding subbands. The dynamic weights based on wavelet energy feature provides the actual contribution of the subbands that are used to discriminate different frequency subbands, particularly subbands corresponding to noise. The WEDD measure appears to be a correct representation of the amount of signal distortion at all the subbands, and robust to insignificant errors in some bands. The performance of the proposed measure is gauged by its prediction accuracy and monotonicity. Experiments showed that the WEDD measure is subjectively meaningful since the small and large values correspond to "good" and "bad" quality, respectively. Thus, this criterion can lead to a better evaluation of the rate-distortion (R-D) performance of any coder. Experiments on several noisy records from the widely used MIT-BIH arrhythmia (`mita`) database showed the measure is more suitable for compression of noisy signal when the noise level is difficult to estimate or avoid and for simultaneous noise suppression and signal compression approach. Based on the observations, we are hopeful that this new approach will give new insights into comparison of various compression methods possibly entailing quite different types of distortion. We are now experimenting with different compression methods and working on generalizations

to other classes of signals. The WEDD measure is also useful in some interesting applications viz. optimal threshold selection for signal denoising, optimal wavelet selection for wavelet coding, dynamic bit allocation in rate-distortion optimization, ECG beat recognition system, noise floor estimation of a desired channel, etc.

भारतीय प्रौद्योगिकी संस्थान गुवाहाटी
Indian Institute of Technology Guwahati

5

Quality Controlled Compression of Electrocardiograms

Contents

5.1 Introduction

Many wavelet based lossy compression methods are well-designed and widely studied for the ECG signals by the biomedical research community. In general, a major design goal of any lossy compression is to obtain the best clinical quality with the lowest bit rate. However, the quality and the rate are the tradeoffs that must be considered simultaneously. When the amount of ECG data is very large, an automatic quality control mechanism for the compression method can be a useful approach in the real-time case. Moreover, one can interactively adjust some parameters associated with a compression algorithm according to the desired quality-rate consideration. Generally, the adaptive coding strategy that operates with a rate or distortion constraint requires two major components: the efficient and well-designed compression methodology and the objective measure for assessment of compressed signal quality. Many well-designed compression methods have been reported by the speech and image processing communities. In literature, thresholding methods, vector quantization (VQ) methods [150, 151], embedded zero tree wavelet (EZW) and SPIHT methods are widely used for coding of wavelet coefficients of the ECG signal. Among these, the threshold based and SPIHT based methods have been shown as the low complexity coding scheme and the methods achieve the reconstruction with good quality and high compression ratio simultaneously. However, despite the evident problem posed by the conventional distortion measure, very little attention has been given in the assessment of quality of distorted ECG signal that can be adopted into rate- or distortion-driven subband coding scheme.

Several quality controlled wavelet based ECG compression schemes have been proposed over the years which utilize PRD measure for assessment of distorted ECG signals. Common disadvantages of PRD criterion are that a smoothing of low-level background noise of the ECG causes a large PRD value but no clinical feature distortion and, conversely, a small average distortion can severely deteriorate a signal clinical performance if all the error is concentrated in a significant feature region. For characterizing the local effects, the MAX is used in ECG compression methods to find out the maximum error within the ECG segment. The ECG segment contains isoelectric regions that do not contribute any diagnostic importance. But the MAX measure results in a nonzero value for smoothed isoelectric region at low CR situations. Thus, the conventional distortion measures may lead to false conclusions especially when the data are composed of signal and noise. The PRD and MAX are the attractive measures due to their simplicity and mathematical convenience. However, the correlation between PRD/MAX and subjective judgement of quality is not close enough for most applications. Another simple measure is the wavelet based weighted PRD (WWPRD) that provides a local or subband error estimation. However, insignificant errors in higher subbands dominate the global error while significant errors in other bands may not reflect any contribution to the global error. This may lead to confusion in the judgement of the quality of the compressed signal. The works in Chapter 4 show that the WEDD measure outperforms PRD, MAX and WWPRD, consistently measuring the distortion both across different distortion types and within a given distortion type at different

distortion levels. Experiments show that the WEDD measure is a correct representation of the amount of signal distortion at all subbands.

In this chapter, we present the efficient methods for guaranteeing reconstruction quality measured using the WEDD measure which reflects the signal distortion in a more accurate way under noisy environments. The goal of this Chapter is to compare and contrast the three types of distortion measures such as the conventional PRD, the WWPRD and the WEDD in the lossy compression of ECG signals. In this work, the following three approaches using different way of thresholding and quantization procedures, and SPIHT coding procedure are chosen to demonstrate substantial gains in the performance of the proposed adaptive subband coding strategy with TCZNUMQ and MIC schemes. The first two approaches are based on the Huffman encoding applied on the quantized nonzero wavelet coefficients resulting from the threshold control zero-zone nearly uniform midtread quantizer and the output of the modified index coder, and the third approach is the SPIHT coding algorithm for the wavelet coefficients that are capable of determining the bit rate automatically according to a desired quality specification.

Approach 1-By Adaptive Wavelet Coding with Joint Thresholding and Quantization Strategy: In this approach, the processed signal block is first decomposed up to five-level using the WT which yields detail subband and an approximation subband. Then, the resulting wavelet coefficients vector is directly compressed using the distortion-driven joint thresholding and quantization (JTQ) strategy implemented in Chapter 3. Note that the classification of wavelet coefficients is not performed in this approach.

Approach 2-By Adaptive Subband Coding with Joint Thresholding and Quantization Strategy: This approach is generally based on the concept of the adaptive subband coding which includes the following steps: the decomposition of the processed ECG signal using the WT, the classification of the subband coefficients into number of frames or classes as described in Chapter 3, the compression of the classified coefficients using the distortion driven JTQ strategy where a different quantizer is used for quantizing each frame or subband, and use of the Huffman coding for the compression of output of the JTQ strategy. These approaches are designed to demonstrate considerable gains in an adaptive subband coding strategy. In this approach, the JTQ strategy forms the core of the adaptive subband coding scheme with subband classification serving to enhance the coding performance.

Approach 3-By SPIHT Coding Strategy: One interesting property of the SPIHT algorithm is its progressive coding capability which means the signal quality can be improved gradually as the compressed bit rate increases. Therefore, we would like to compare the coding performance of our proposed approaches with the SPIHT coding performance for different ECG signal conditions in this work. Finally, we present the results of three quality controlled ECG compression algorithms for a user-specified error percentage.

This chapter is organized as follows. In Section 5.2, a brief summary of existing quality controlled compression methods and major compression issues are described. Effectiveness of the distortion measures for guaranteeing reconstruction quality is investigated by several experiments in Section 5.3. In Section 5.4, approach 1-by adaptive wavelet coding with joint thresholding and quantization strategy with WEDD

measurement criterion is presented and tested using the well-known `mita` records. In Section 5.5, approach 2-by adaptive subband coding scheme where the wavelet coefficients are classified into frames first and then quantized using the TCZNUMQ scheme. In section 5.6, the quality controlled SPIHT coding strategy is presented and then rate-distortion performance of this coder is studied with the use of PRD and WWPRD measures. Finally the discussion is presented in Section 5.7.

5.2 Background and Motivation

In recent years, many efficient lossless and lossy ECG signal compression methods have been reported for efficient storage and transmission. Performance of these methods is evaluated in terms of compression rate, reconstructed signal quality and coding delay. The evaluation of lossless methods is a simple and straightforward task where the compression rate, the coding delay, etc. are employed. A major problem in evaluating lossy methods is the extreme difficulty in assessing the local wave distortions in the compressed signal. This is because the signal distortions introduced mainly depend on the type of methodology (AZTEC, TP, Fan, prediction, interpolation, FT, KLT, DCT, DWT, VQ, and etc.) used for compression. Quality assessment is important in lossy methods since most of the reported methods employ thresholding of samples/coefficients directly or indirectly (via quantization scheme). This process may distort the small and sharp local waves present in the original signal. In next section, the effectiveness of the distortion measures is tested using the different qualities of the compressed signals. The experiments attempt to evaluate the closeness of the objective quality measures with the subjective measure.
In this section, a brief discussion of the issues related to quality controlled ECG compression methods are discussed. All the reported compression methods have different approaches but with only one common design goal, that is, taking the quality of compressed signals as a necessary design constraint in their methods. Quality criteria for ECG compression are often based on the squared distortion error criterion. However, this is not always a relevant measure of clinical quality in the general case. In [145], it is noticed that the chief effect of wavelet compression is the smoothing of the low-level background noise. Thus, the compression error of SPIHT (in PRD) is larger while the clinical features appear to be faithfully preserved. If the noise level increases within the signal block or portions, the number of coefficients or bits should be increased in order to approximate the noise with the specified accuracy. Thus, the noise decreases the compression rate and leads to worst measure of rate-distortion (R-D) or rate-quality (R-Q) performance of well-designed ECG compression method like SPIHT coding scheme. This issue is well explained in [125], Provaznik and Kozumplik talk about wavelet transform in ECG data compression and observe that PRD can significantly arise as the powerline noise is suppressed by thresholding. They presented the following solutions: 1) the use of optimum thresholding where the threshold value derived from noise characteristics can increase compression efficiency. More sophisticated techniques employ a QRS complex detector and modify the wavelet coefficients between QRS complexes.; and 2) the removal of powerline noise before compression.

In RQG [121] and WPFDEC [142], it is described from the results in [83,191] that for the `mita` database, the compressed signal with PRD1 values under 9% represents good, or very good, results, whereas if the value is greater than 9% its quality group cannot be determined. A well-designed compression method removes the irrelevant wavelet coefficients, due to noise components, in some higher detail subbands quickly for achieving a better data compression, and thus result in a large PRD value but there is no clinical feature distortion for a given set of coding parameters. Therefore, one cannot adopt the PRD1 ranges of the quality groups, which are defined for the particular compression method, to guarantee the preservation of the clinical features since the denoising or/and distortions introduced by different types of compressors are very diverse.

To avoid the noise coding, in [139] an automatic compression approach that adjusts its threshold according to the measured noise level in the preprocessing stage is introduced. Noise power in each beat is estimated as the power remaining after high-pass filtering (cutoff frequency equal to 20 Hz) in the repolarization interval. But the measure of noise level may be difficult with the designed filter because there are many sources of noise such as power line interference, muscle contraction noise, poor electrode contact and baseline wandering due to respiration, having different frequency characteristics, in a clinical environment. Moreover, the noise coding phenomena is not considered, in recent paper [149], in the quality control algorithm based on the efficient SPIHT algorithm and the WWPRD criterion. Since SPIHT codes the wavelet coefficients exploiting the redundancies among wavelet scales instead of applying global threshold, we need either effective denoising algorithm before compression or meaningful objective distortion measure. Although noise elimination process is used prior to the compression process, the filtering algorithm may add some amount of denoising artifacts to the input signal, and there exists a practical difficulty in measuring the quality of the denoised signal.

Chen and Itoh in [129] used an adaptive scalar quantizer in order to match a predefined MSE. Recent works show that it is possible to achieve a considerable gain in the CR if the zero-zone and the resolution of significant coefficients are controlled individually. In filter-banks [121] and WPFDEC [142], a linear quantizer with fixed resolution is used to quantize the non-zero coefficients vector obtained for threshold T guaranteeing a desired PRD value. The coding efficiency with fixed number of bits assigned to a linear quantizer may be poor because of the time-varying characteristics of various ECG signals. Therefore, Benzid et al. in 2007 paper [143] proposed an ECG compression method based on the adaptive wavelet coefficients quantization combined to a modified two-role encoder (ALQ-TRE). The resulting wavelet coefficients are thresholded iteratively until a user-specified PRD is matched using the iterative algorithm given in [121]. In [143], after the thresholding with the threshold value found for a user-specified PRD, the DCT or DWT non-zero coefficients of the threshold vector are quantized using the adaptive linear quantization scheme. In such a case, as a result of two separate thresholding processes a greater number of wavelet coefficients are set to zero than is actually required. The relationship between the threshold T and the zero-zone of the quantizer has a strong impact on compression and distortion. The disadvantages in the global threshold-

ing, computational cost, rate-distortion performance, etc. of this two-stage scheme is well demonstrated in Chapter 3 with several experiments. Moreover, the PRD2 and MAX measures employed in [143] have many disadvantages.

In [129] the weighted PRD is suggested to characterize the distortion of the selected local waves. However, an open problem on this criterion is how to determine the weights for each local waves. In [83] the ASEC algorithm considers a WDD measure in order to efficiently encode every heartbeat, with minimum bit rate, while maintaining a predetermined distortion level. However, WDD measure suffers from high computational complexity [145], [151]. Moreover, there is no standard protocol for the WDD measure and the optimum weights for the features of interest [190]. To choose significant coefficients one needs an acceptable quantitative measure of compressed signal quality and protocols for careful studies of the tradeoffs of quality and bit rate in specific applications.

5.3 Guaranteeing Quality Using WEDD criterion

Guaranteeing the quality of a biomedical signal in lossy compression methods is most important since a highly distorted signal can be useless from a clinical point of view. In lossy compression, care must be taken with the signal distortion introduced by the lossy processes. The higher compression rate at the output of variable rate coder will be better for storage and transmission purposes but it may introduce severe signal distortion. However, the performance of most of the well-designed adaptive wavelet based compression method depends on the optimal estimates of the coding parameters for a given distortion specification. Therefore, the rate-distortion optimization is the key technique in coding method to efficiently find a set of optimal coding parameters. In adaptive ECG coding, the distortion (D)is measured using the PRD, the resulting wavelet coefficients are compressed iteratively until a predefined PRD is achieved with a desired tolerance ε. It is well-known that the `mita` database contains different morphologies and noises. Meanwhile the noise filtering property can be seen in the wavelet based compression methods and thus large PRD can be obtained for a better quality of compressed signal. In such a case, it becomes extremely difficult to compress such an ECG while keeping distortion within reasonable limits. The reason lies on the fact that noise decreases compression rate of the coder for a desired PRD value since the coder will spend extra bits on approximating the noise with the specified accuracy. Thus, the distortion measurement criterion plays an important role in rate-distortion optimization technique. Many methods with automatic quality control using the PRD criterion have been reported but the experiment shows that the criterion is not a subjectively meaningful measure since small and large numerical distortions does not correspond to “good” and “bad” subjective quality, respectively. Although the compression method is well-designed, measurement of quality of the compressed signal is so difficult using the conventional measures and is crucial because the distortion introduced by different types of compressors are very diverse [190, 191]. A number of researchers point to the disadvantages of the PRD measure that is incorporated in an automatic

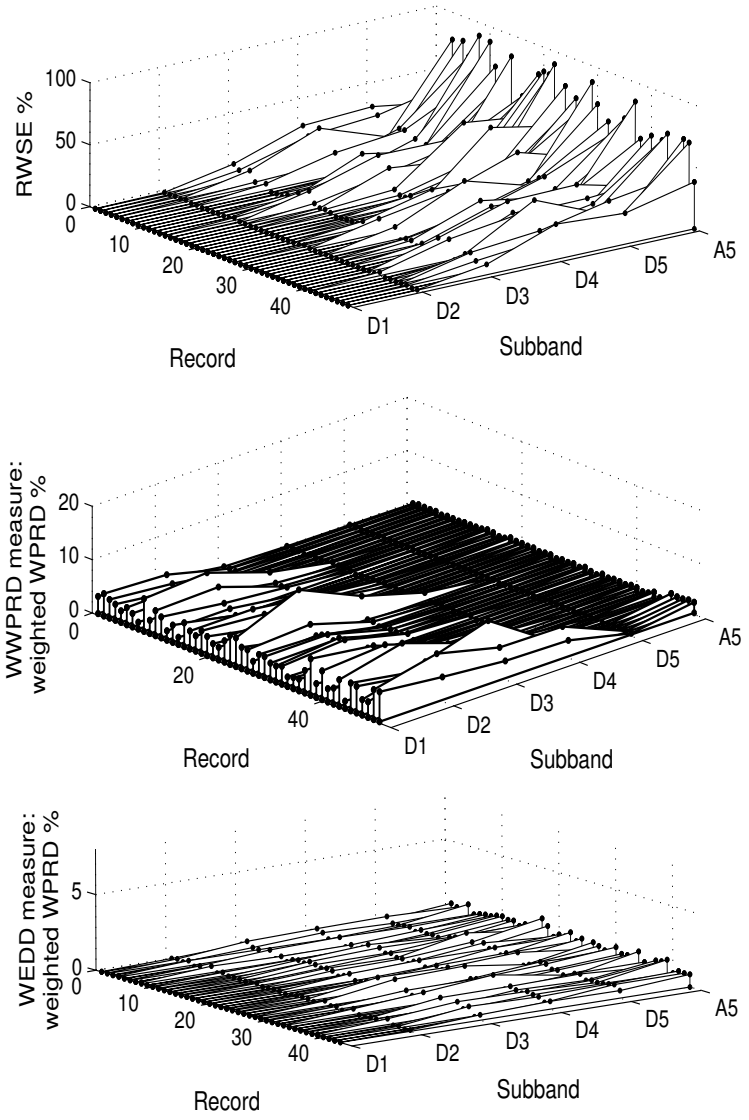

Figure 5.1: Assessment of local errors using the WEDD and WWPRD measures. (a) Relative wavelet subband energy of subbands of each record taken from `mita` database. (b) WWPRD measure: Weighted PRD of subbands of each tested `mita` record. (c) WEDD measure: Weighted PRD of subbands of each tested `mita` record.

quality control [83, 97, 125–127, 129, 131, 139, 140, 145, 146, 190, 191]. In this section different experiments are performed to evaluate the effectiveness of the distortion measures.

In the first experiment, 48 ECG signals taken from 48 `mita` records are processed at a compression rate of 8 using the algorithm reported in Chapter 3. The resulting compressed signals are evaluated via visual inspection. The WWPRD and the WEDD values are shown in Figs. 5.1 (b) and (c), respectively. Each point in the error plot of Figs. 5.1 (b) and (c) indicates the weighted WPRD of each subband of one test signal. It is observed that WWPRD measure provides large error value for the bands D_2 and D_1. These bands have

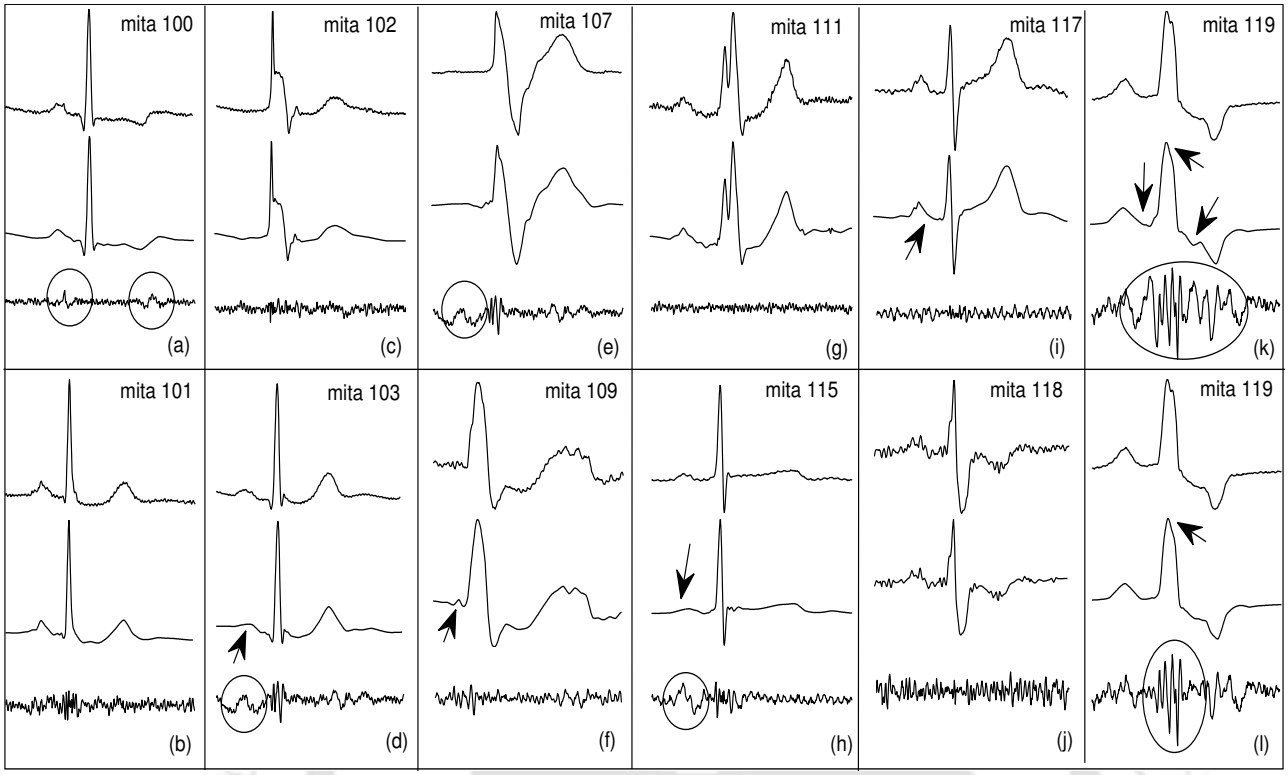

Figure 5.2: Compression results (PRD1=6%) of arrhythmia ECG signals extracted from dataset-I. Some of the distortion of the diagnostic features are marked in the compressed signals. From top to bottom, the plots display the original signal, the compressed signal and the difference between original and compressed signals.

the wavelet coefficients of high frequency noise for many test signals and also have less energy as shown in Figs. 5.1 (a). So, its errors are called insignificant errors [190]. It is known that in most of the compression methods, many coefficients in these bands are zeroed by thresholding or/and quantization scheme(s). It is observed that the visual quality of the compressed signals are good even if their WWPRD values are large. But the inclusion of insignificant errors is more in the case of WWPRD while it is negligible in WEDD. This experiment shows that WWPRD does not correspond to better clinical quality of the compressed signal in the general case.

In the second experiment, the commonly used dataset-I records (`mita` 100, 101, 102, 103, 107, 111, 115, 117, 118 and 119) are processed at a PRD1 value of 6%. The weighted local errors of the WEDD and WWPRD are shown in Table 5.1 and the reconstructed or compressed signals are shown in Fig. 5.2. It is observed that important diagnostic features are distorted and the small and short local waves are missing in Figs. 5.2 (a), (d), (h), (i), (k) and (l). In Figs. 5.2(h), (i) and (k), the duration of the small P wave is prolonged. Regardless of an apparent large error as reflected in the PRD's and in the WWPRD's, close examination of the signals of Fig. 5.2 reveals that all the local waves of the ECG and their diagnostic features

Table 5.1: Performance evaluation of objective quality measures. Here, PRD1=6%

Rec.	Fig.	WEDD:Weighted PRD (%) of bands							WWPRD:Weighted PRD (%) of bands						
	no.	A_5	D_5	D_4	D_3	D_2	D_1	Total	A_5	D_5	D_4	D_3	D_2	D_1	Total
100	5.2(a)	1.02	1.50	1.47	1.28	0.31	0.06	5.65	0.94	0.98	1.22	1.49	4.36	5.03	14.01
101	5.2(b)	1.56	1.11	1.51	1.06	0.67	0.08	5.99	1.52	1.01	0.74	1.42	5.49	5.33	15.52
102	5.2(c)	1.70	1.20	0.94	1.01	0.60	0.15	5.61	1.47	0.78	0.67	1.86	3.75	4.28	12.81
103	5.2(d)	2.25	2.77	1.40	0.33	0.18	0.02	6.97	4.54	1.31	1.14	2.93	3.00	3.63	16.56
107	5.2(e)	1.59	1.80	0.31	0.49	0.17	0.01	4.38	1.17	2.41	1.10	3.57	4.05	1.94	14.22
109	5.2(f)	3.89	0.50	0.58	0.29	0.22	0.05	5.52	3.07	0.31	1.61	3.79	6.51	4.43	19.73
111	5.2(g)	1.91	1.27	0.68	0.40	0.44	0.10	4.81	1.52	0.78	0.77	3.04	9.11	6.17	21.40
115	5.2(h)	1.22	1.49	1.91	0.94	0.27	0.03	5.86	2.19	1.18	0.82	2.22	2.15	3.53	12.09
117	5.2(i)	2.05	0.26	0.94	0.65	0.10	0.03	4.03	1.68	0.45	0.56	2.85	2.63	3.46	11.63
118	5.2(j)	2.18	1.16	0.55	1.10	0.48	0.03	5.50	1.98	0.44	1.43	3.02	8.46	3.65	18.96
119	5.2(k)	3.35	0.95	0.40	0.14	0.03	0.00	4.87	2.54	2.23	2.59	4.68	2.28	2.06	16.39
119	5.2(l)	3.35	0.51	0.27	0.14	0.03	0.00	4.30	2.55	1.21	1.72	4.68	2.28	2.06	14.50

are retained. The PRD1 and WWPRD have poor correlations with the visual quality of the compressed signals obtained for the widely used `mita` noisy records. In WWPRD criterion, insignificant errors in subbands D_2 and D_1 dominate the global error while significant errors in other bands may not reflect any contribution to the global error. This may lead to overlapping of the quality groups and to confusion in the judgement of the quality. The WWPRD criterion is not a subjectively meaningful measure since small and large numerical distortions do not correspond to "good" and "bad" subjective quality, respectively. Thus, the selection of upper bound distortion level is very difficult which is useful for clinical applications. Moreover, WWPRD criterion based compression algorithm may not reflect the best compression ratio of the coder when data are composed of signal and noise. Therefore, this criterion does not guarantee the optimality in the rate-distortion sense, which is the measure of the true performance of data compression. The proposed measure is superior over other measures in the sense that it is subjectively meaningful since the small and large values correspond to good and bad subjective quality, respectively. Thus, the WEDD measure is much more suitable for evaluating compressed signals than the other measures, and naturally leads to a new method for quality control in ECG signal compression.

In the third experiment, the effectiveness of the distortion measures for the noisy signals case is studied since the quality-driven wavelet coding scheme is widely tested with noisy records taken from the `mita` database and the threshold parameter plays an important role in the adaptive coding scheme. It is well-known that in the adaptive subband coding scheme, the optimal parameters are determined for a user-specified distortion or quality specification. As the name "distortion-driven subband coding scheme" implies, the quality or distortion is "constrained" that is achieved by adapting the threshold parameter in a two-stage scheme. Generally, the distortion-constrained keeps the reconstructed distortion of the scheme under con-

trol that guarantees the preserving of signal information if the distortion threshold is set properly. In the threshold adaptation, the quality-control method performs a threshold adjustment procedure until the desired PRD/WWPRD/WEDD is reached, obtaining the final compressed signal. In such a case, the distortion measurement criterion should consider the signal errors rather than noise errors due to the smoothing of low-level background noise. Otherwise, the resulting threshold parameter may not be an optimal one with respect to the compression rate for a given quality specification. In this experiment, variation of the threshold parameter under different noisy conditions is studied, and then drawbacks of the conventional measures used for rate-distortion optimization technique to find a set of coding parameters are addressed.

Four different kinds of noise have been considered in this experiment: simulated Gaussian white noise, powerline noise, muscular noise and motion artifact noise. White noise is artificially generated but more realistic sources of noise present in the ECG signals are also considered as powerline noise, muscular noise and motion artifact noise provided in the Physionet database. The powerline noise arises from the measurement equipment specially due to the power supply. This noise can be seen as a sinusoidal signal with random peak value and 50 Hz frequency added to the ECG source signal. The muscular noise present in the ECG signal has a spectrum that overlaps that of the ECG, but extends to higher frequencies. The electrode motion artifact is usually the result of intermittent mechanical forces acting on the electrodes, with significant amounts of baseline wander and muscle noise as well.

The test signal blocks taken from the `mita` database are corrupted by the noises and thus it cannot be directly used for this test. In order to perform this experiment, the soft-thresholding approach developed by David Donoho is used first to get the clean ECG signal from the mita records 107, 117 and 111. For evaluation purposes, the clean ECG signals are corrupted using the above noises and then they are considered as the original signals in this experiment. For each value of SNR, the error between the clean and the noisy signals are measured using the WEDD, WWPRD and PRD1 criteria. These measurement provide the information about the distortion where in the cases the clean signal is contaminated by noises, for example communications channel. When the magnitude of the additive noise is low in the signals (i.e., high SNR), the visual quality of the signal is good in the general cases. In such a case, the objective measure should results in a meaningful numerical value so that the quality can be predicted correctly in the quality assessment problem. Moreover, the measure should not depend on the noise errors for the rate-distortion optimization problem. If we use the PRD1 measure between the clean and noisy signals, we can get high values of PRD1 due to the presence of the noise. But the high values do not represent the actual signal distortion between the clean and the noisy signals, are due to noise errors. If the noise level is high (i.e., low SNR), the distortion consists of both the signal and noise errors. In this case, the objective measure should compute the signal errors rather than the noise errors. However, this is so difficult but crucial task for the distortion-driven subband coding scheme. Under this situations the performance of the distortion criteria is shown in Fig. 5.3. For testing purposes, two different clean ECG signals are obtained and corrupted by the simulated white noise and the realistic powerline noise. This experiment shows that the performance of the WEDD is better

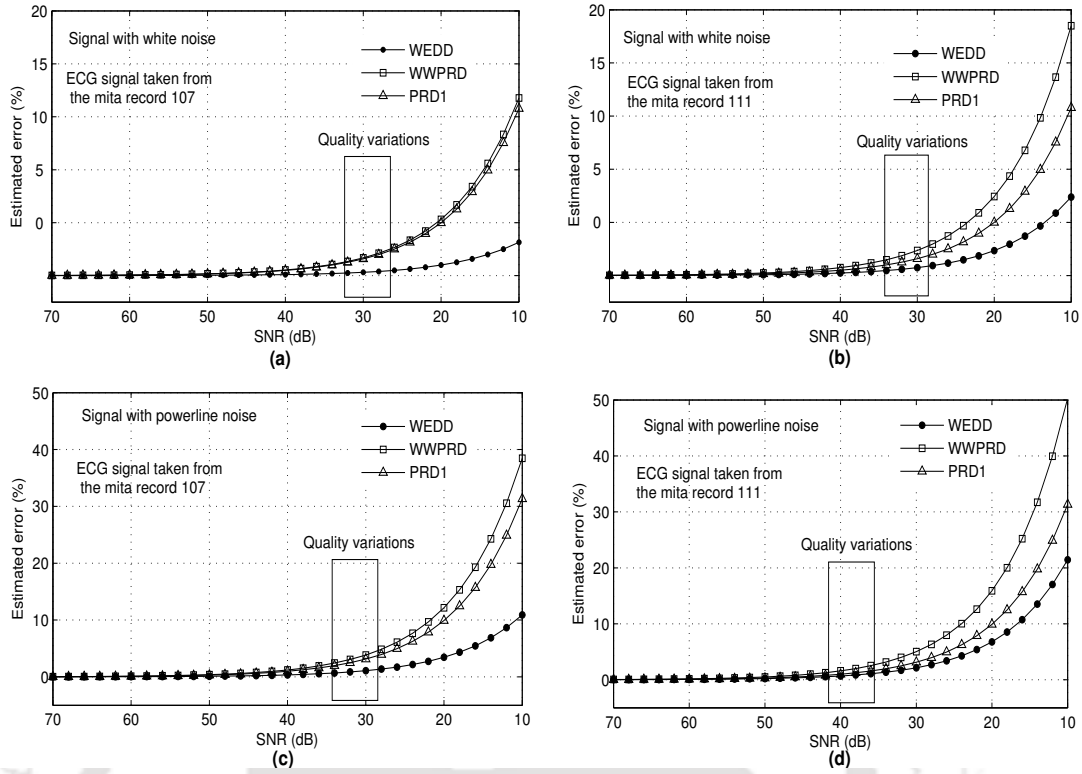

Figure 5.3: Performance of the WEDD, PRD1 and WWPRD measures for the clean signal and the signal with different noise and noise levels.

than the PRD1 and WWPRD measures. It can be seen that the signal quality is changed for the SNR ranges from 35 dB to 25 dB. However the amount of distortion estimated using the PRD1 and WWPRD measures are larger in the case of "excellent" and "very good" reconstructions. For different noise cases, the number of nonzero wavelet coefficients (NZWC) obtained with a user-specified estimated error of 2% in different distortion criteria are shown in Fig. 5.4. It is observed that in the WEDD case the number of NZWC obtained is lesser than the number of NWZC obtained in the PRD1 and WWPRD cases for a user-specified estimated error of 2%. Furthermore, the number of NZWC is dependent on the level of the input noise as in the cases of PRD1 and WWPRD driven threshold adaptation. Since the insignificant errors in some higher detail subbands dominates the global, threshold obtained is more sensitive to the background noise present in the input (even for the high SNR) in the WWPRD driven threshold adaptation. This experiment shows that the WWPRD and PRD1 may not provide better rate-distortion optimization. The performance of the WEDD measure is good for the the powerline and white noise cases with the considerable SNR. Note that the WEDD measure is sensitive to the modification of the signal contents. Since other artifacts, with a spectrum that overlaps that of the ECG, affect the signal contents and thus the WEDD measure results in large values. Thus, at this stage there is no final conclusion on the compression of the noisy ECG signals contaminated by such artifacts. However, the WEDD measure provides a better subjective results for

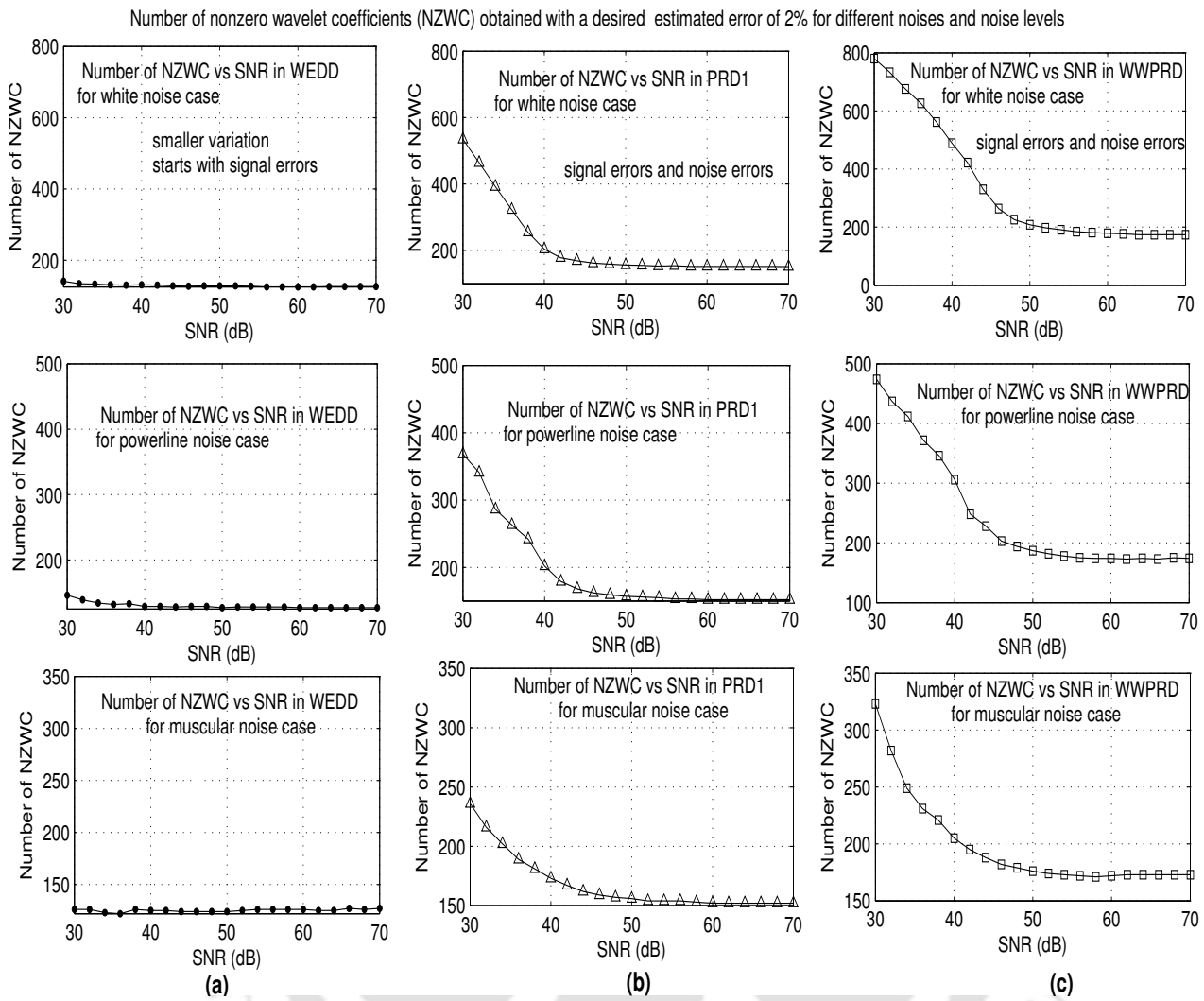

Figure 5.4: Performance of the distortion-driven threshold adaptive algorithm based on the WEDD, PRD1 and WWPRD criteria under different input signal conditions. (a) The number of NWZC obtained in the WEDD-driven driven threshold adaptive algorithm for the white, powerline and muscular noise cases (from top to bottom), (b) The number of NWZC obtained in the PRD1-driven driven threshold adaptive algorithm for different noises and noise levels and (c) The number of NWZC obtained in the WWPRD-driven driven threshold adaptive algorithm.

smoothed reconstruction where the low-level background noise is removed during the wavelet thresholding process. This is illustrated in the second experiment for set `mita` records which include different morphologies and noises, and the weighted local errors of the WEDD and WWPRD are shown in Table 5.1 and the reconstructed signals are shown in Fig. 5.2. Experiment shows that PRD1 and WWPRD measure fail to yield good judgement on the reconstructed signal quality.

As a remedy, one can then suggest ideal filtering of the noise. However, filtering may introduce signal distortion that is observed in this experiment, and anyhow the denoising in the preprocessing step requires

a objective quality measure for evaluation of the denoised signal in a closed loop CR or distortion control. Nevertheless, wavelet filtering is implicitly performed when implementing the thresholding or/and quantization, making the system robust and allowing the direct application over the raw ECG signal. The above experiments show that the WEDD measure outperforms PRD and WWPRD, consistently measuring the distortion both across different distortion types and within a given distortion type at different distortion levels. Furthermore, the WEDD measure is simple and it can be easily incorporated into any quality controlled wavelet coding algorithm. The main goal of this chapter is to demonstrate the possibility of attaining good compression ratios by using the well-designed quality-driven subband coding scheme and WEDD criterion for guaranteeing reconstruction quality under noisy environments.

5.4 Approach 1-By Adaptive Wavelet Coding with JTQ Strategy

Among the low complexity ECG compression methods, many are based on the global thresholding and quantization strategy [137, 142, 143]. In this approach the raw ECG signal $\{x(n), n = 0, 1, 2, ...M-1\}$ is blocked into nonoverlapping blocks of N samples and then the mean removal is performed for each block to examine the exact energy contribution of the local waves. Each block is encoded and decoded separately for a desired distortion level. The maximum block size is 4096 samples which is equivalent to 11.38 s duration for a sampling rate of 360 samples per second. The block size of 1024 or 2048 or 4096 samples are chosen for testing and comparison purposes [127, 134, 140, 142, 145]. The ECG signal blocks usually contain very low frequency components due to respiration and relative movements of electrodes and skin. A simple ECG baseline estimation method is used in this work. In monitor mode, a third-order Butterworth low-pass filter with cut-off frequency equal to 0.5 Hz or 1 Hz is used in forward/backward directions to avoid phase distortion. In diagnostic mode, the cut-off frequency is set at 0.05 Hz. After this estimation, baseline is subtracted from the ECG signal block. For each block, the BW 9/7-tap wavelet filters, with five decomposition level, is used for wavelet transformation. The subbands are the approximation band A_5 and the detail bands D_5, D_4, D_3, D_2, D_1. The wavelet coefficient (WC) vector is given by $WC = [\,A_5 \quad D_5 \quad D_4 \quad D_3 \quad D_2 \quad D_1\,]$. More energy is packed in few large magnitude coefficients and less energy is concentrated in more number of small magnitude coefficients. A good compression performance can be achieved by selecting the significant coefficients in each subband to represent the original ECG signal with minimum distortion. A considerable gain in the compression rate can be achieved for a desired distortion using the two-stage scheme which performs thresholding followed by quantization and Huffman coding of the quantized index and MIC output. Thus, they are employed in this work and their optimum values are determined according to a desired quality specification.

In this work, after applying global threshold to all coefficients, two vectors are created from TWC vector: nonzero wavelet coefficients vector which is constructed from TWC by discarding the zero valued coefficients and integer significance map (ISM). The compression is done by thresholding and quantization

of the WC vector and coding of the integer significance map using the proposed schemes in Chapter. Note that the TCZNUMQ scheme avoids further zeroing of retained wavelet coefficients at the thresholding phase meanwhile allowing to vary the outer-zone width Δ for quantization of the retained coefficients to meet a desired quality specification with highest compression rate. The bi-section algorithm finds the optimum threshold T and outer-zone width Δ so that a minimum entropy of the quantized coefficients is achieved for a given distortion level. For a given signal, let $H(T,\Delta)$ be the code length which includes the code of quantized nonzero wavelet coefficients obtained for the parameters (T,Δ) and the code of ISM and $D(T,\Delta)$ be a measure of the distortion introduced in the reconstructed signal by thresholding and quantization. The proposed optimization problem can then be stated as: for a given $D(T,\Delta)$, determine T and Δ in such a way that it minimizes $H(T,\Delta)$. By using the above compression methodology and the new WEDD measure, a simple quality control mechanism is presented in Table 5.2. In this algorithm the two-stage design philosophy is followed for testing purposes. The search ranges for the coding parameters are computed in the following section in order to reduce the computational cost. Note that the ranges defined below do not affect the rate-distortion optimization. The predefined bound of a WEDD can be reached by adaptively defining the T and Δ within the range defined. The coding parameters such as threshold T and quantization bit (b) are automatically determined for a user specified WEDD value. It is well known that thresholding and quantization contributes to the lossy effect of the compression method. Therefore, study of these two processes are essential for providing an effective coding algorithm. Some of the preliminary results of thresholding and quantization processes are discussed in the next two subsections.

5.4.1 Search Range for Threshold Adaptation

Seventy-eight 1024 sample segments of ECG signals are selected from three different ECG databases, 15 each from the MIT-BIH Supraventricular arrhythmia (`mitsva`) database (128 Hz, 10 b/sample), the Creighton university ventricular tachyarrhythmia `cuvt` database (250 Hz, 12 b/sample) and 48 from the MIT-BIH arrhythmia (`mita`) database (360 Hz, 11 b/sample). Experiment shows that the selection of threshold T plays an important role in transformed domain compression methods under different ECG recording conditions. Note that in iterative algorithm the threshold will be adapted according to the WEDD value. However this experiment may help to locate threshold T in the allowable region quickly if the WEDD values obtained for test signals are approximately similar at a particular T. By keeping this property, the following experiment is conducted here.

In this experiment, wavelet coefficients are thresholded based on the threshold value which is determined from a specified percentage retained energy (RE). This RE value is varied from 99.99% to 97% and then the TH value is determined for each RE value using a sorting algorithm. Then, thresholding is done by simple hard thresholding rule and the signal is reconstructed from the retained or the significant coefficients. The quality of the reconstructed signal is evaluated using PRD1, WWPRD and WEDD measures. The quality of the signal is also assessed via visual inspection of clinical information within a block. Numerical values of

Table 5.2: Approach 1-By adaptive global thresholding and quantization strategy in two-stage scheme.

Let us consider a signal with M samples for a real time processing.
Step 1: Blocking and buffering of N input samples.
The WEDD can be written as follows: WEDD $= f(x(n),\ \widetilde{x}(n) = \mathtt{f}(N,T,\Delta))$,
// where $x(n)$ is the original signal, $x(n) = \{x[0], x[1], ...x[\mathrm{N}-1]\}$
// $\widetilde{x}(n)$ is the reconstructed signal, N is the block size and Δ is the outer-zone width of the TCZNUMQ.
// The threshold T and outer-zone width Δ is automatically adapted according to $\mathrm{WEDD}_{\mathrm{tar}}$ criterion.
Encoding Process:
Step 2: Store the signal with N samples and perform removal baseline artifact.
Step 3: Apply DWT on input samples and store wavelet coefficients (WC) vector.
$\mathrm{WC} = [\ \mathrm{A}_5 \quad \mathrm{D}_5 \quad \mathrm{D}_4 \quad \mathrm{D}_3 \quad \mathrm{D}_2 \quad \mathrm{D}_1\ ]$.
Step 4: Calculate the energy based weights, $w = \{(w_l)_{(1\le l\le J+1)}\}$.
Step 5: Initialization
(a) Specify the target $\mathrm{WEDD}_{\mathrm{tar}}$ value and relative bound error (ε).
(b) Define the search range for threshold T, [$\mathrm{WC}_{\mathrm{min}}$, $\mathrm{WC}_{\mathrm{max}}$],
where $\mathrm{WC}_{\mathrm{min}}$ is zero and $\mathrm{WC}_{\mathrm{max}}$ is the maximum absolute value of coefficients in WC vector.
(c) Define the quantization bits, $b = \{6, 7, 8, 9, 10\}$.
(d) Set the value of WEDD to zero.
Iterative process:
for ($K = 1;\ k <= \mathrm{K};\ k = k+1$);
// where K is the number of quantization bits. Here, K = 5.
{ **While** $|(\mathrm{WEDD}(T) - \mathrm{WEDD}_{\mathrm{tar}})/\mathrm{WEDD}_{\mathrm{tar}}| \times 100 > \varepsilon$
{ *Step 6*: Calculate T = ($\mathrm{WC}_{\mathrm{min}}$+$\mathrm{WC}_{\mathrm{max}}$)/2 ;
(a) Get a copy of WC and apply thresholding rule for a determined threshold T by

```
{
  for (p = 1; p ≤ P_i; p = p + 1)
  if WC(p) < T
      TWC(p) = 0 ;
  else
      TWC(p) = WC(p);
}
```

Step 7: Compute WEDD by
(a) Get the TWC vector.
(b) Create the nonzero wavelet coefficients (NZWC) vector.
(c) Quantize the NZWC using the TCZNUMQ scheme and results in quantized NZWC (QNZWC).
(d) Convert reordered QNZWC into their subbands $\{\mathrm{A}_{\Delta J}, (\mathrm{D}_{\Delta j})_{(1\le j\le J)}\}$.
(e) Finally, calculate the amount of distortion by the WEDD measure.
Step 8: **If** WEDD (T) < $\mathrm{WEDD}_{\mathrm{tar}}$

```
{ WC_min = T ; }
else
{ WC_max = T ; }
```

}
$T_\Delta(k) = T$;
Step 9: Compute the compression rate (CR) for a user specified WEDD value as:
(a) Get the TWC and QNZWC vectors.
(b) Create the ISM from TWC and code the ISM using the modified index coding scheme coder.
(c) Finally, calculate the CR and store it, $\mathrm{CR}_\Delta(k)$ = CR ;
}
Step 10: Get $\{T_\Delta(k)\}$ and $\{\mathrm{CR}_\Delta(k)\}$ $\quad \forall\ k = 1, 2, ...\mathrm{K}$.
Step 11: Find the combination of {T, Δ} by $\{T,\ \Delta\} = \max\{\mathrm{CR}_\Delta\}$;
Step 12: Using the above T and Δ, compress the input signal $x(n)$ for a desired $\mathrm{WEDD}_{\mathrm{tar}}$ with high CR.

objective quality measures such as WEDD and WWPRD are shown in Fig. 5.5(a) and Fig. 5.5(b), respectively. Higher RE value means lower threshold value. Consequently, small magnitude wavelet coefficients

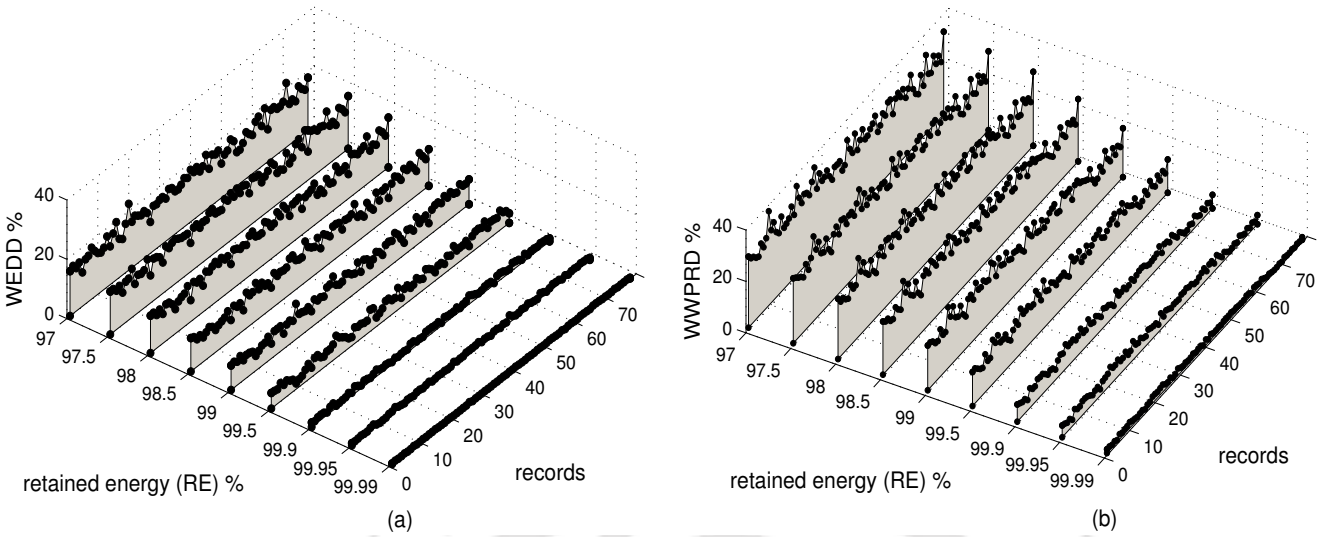

Figure 5.5: Thresholding of wavelet coefficients for a specified retained energy (RE). (a) WEDD versus RE (in percentage). (b) WWPRD versus RE (in percentage).

of low level background noise are set to zero. Other significant coefficients are retained. Thus, it results in low WEDD for RE values varying from 99.99% - 99.90% which is noticed in Fig. 5.5(a). It is observed that the reconstructed signal quality is good and the numerical value of WEDD measure is comparable with its signal quality defined via visual perception. But for the same reconstructed signal quality WWPRD values are larger with the same RE value range and the local error is shown in Fig. 5.6. The inclusion of insignificant error is more in WWPRD whereas it is negligible in WEDD case. This leads to confusion in the judgement of the signal quality for these test records. To see the variation of WEDD, WWPRD and PRD1 values, the average and standard deviation are calculated and are shown in Table 5.5. It demonstrates that the weighted PRD values obtained for the subbands D_2 and D_1 are approximately similar in the case of the 48 test records taken from the `mita` database. Furthermore, the weighted PRD values are small for all `mita` records. For a given RE value, a smaller standard deviation of WEDD values will be better for reducing computational cost of the threshold adaptation of a user-specified distortion level. From the results shown in Fig. 5.5, the minimum RE at which the original clinical information is reproduced faithfully can be determined. This minimum RE varies according to the block size N, sampling rate and characteristics of the ECG signal. For an RE value of 97%, the WEDD, WWPRD and PRD1 values are high. It is observed that the local waves are distorted severely during the cross validation of the measures for the given signal and the RE value. The analysis of local error distribution is more useful for automatic quality control.

Table 5.3: Performance of thresholding process for records from `mita`, `cuvt` and `mitsva` databases.

Retained energy (RE)		99.99%	99.95%	99.9%	99.5%	99%	98.5%	98%	97.5%	97 %
WEDD (%)	average	0.33	1.03	1.66	4.93	7.78	10.13	12.04	13.8	15.4
	std	0.11	0.36	0.49	1.19	1.4	1.67	1.79	1.92	2.15
	max	0.6779	2.5083	2.989	7.5658	12.0556	13.835	16.9064	18.35	22.4565
WWPRD (%)	average	2.3704	5.0965	6.9022	13.2893	17.3877	20.4293	22.8412	24.9672	26.9038
	std	0.6547	1.3062	1.6799	2.5126	2.8524	2.8697	3.0854	3.1197	3.384
	max	3.8227	8.1525	10.5432	19.5646	24.6514	28.6976	31.5015	33.907	37.6037
PRD1 (%)	average	1.0802	2.4172	3.4251	7.7475	10.9866	13.4576	15.6313	17.5684	19.2687
	std	0.226	0.5171	0.7055	1.6429	2.0294	2.5442	2.8832	3.4464	3.8786
	max	2.4704	5.6666	7.7523	17.9311	22.2648	27.6817	30.759	37.1043	41.9795

Table 5.4: Performance of quantization process for records from `mita`, `cuvt` and `mitsva` databases.

Quantizer resolution, b		6	7	8	9	10	11	12
WEDD (%)	average	3.9689	2.1649	1.1134	0.5461	0.2883	0.1377	0.0707
	std	0.8996	0.4664	0.2431	0.1306	0.0738	0.0336	0.0175
	max	6.4262	3.2164	1.7594	1.0994	0.4661	0.2879	0.1123
WWPRD (%)	average	10.8436	7.3524	4.5526	2.5868	1.3668	0.6854	0.3452
	std	3.1391	2.3417	1.5757	0.9798	0.5353	0.2692	0.1344
	max	18.9458	15.1936	9.3929	5.3434	2.9976	1.5943	0.7676
PRD1 (%)	average	5.7645	3.557	2.0429	1.1194	0.5796	0.2912	0.1463
	std	1.4599	0.8874	0.4918	0.2855	0.153	0.0763	0.0381
	max	10.7675	6.2769	3.8149	2.5145	1.4385	0.7291	0.3593

5.4.2 Search Range for Width of Outer-zone

The quantization is the lossy portion of compression system. In two-stage scheme, the outer-zone width Δ is searched for a given threshold T. In such a scheme, the nonzero wavelet coefficients required lying in the outer-zone regions are quantized with the number of quantization levels determined for a given specific criterion. As we have demonstrated, the quantization of relevant wavelet coefficients of the signal contents may introduce severe signal distortion than zeroing of large of number of small wavelet coefficients lying in the zero-zone width. However, the computational cost of the TCZNUMQ scheme can be reduced when the zero-zone width is defined by threshold T and if the amount of quantization distortion is known apriori for an adaptive coding strategy. Therefore, the study of the quantization of wavelet coefficients for different quantizer resolution is essential for a user specified distortion level.

The signal blocks with 1024 samples from dataset-III are chosen for evaluating the quantizer performance. The wavelet coefficients (WC) of each test ECG signal are quantized with different resolution bits ranging from 6 to 12 per coefficient. During the quantization process, wavelet coefficients around the zeroth zone decision level are rounded to zero and other coefficients are rounded to their nearest output level within

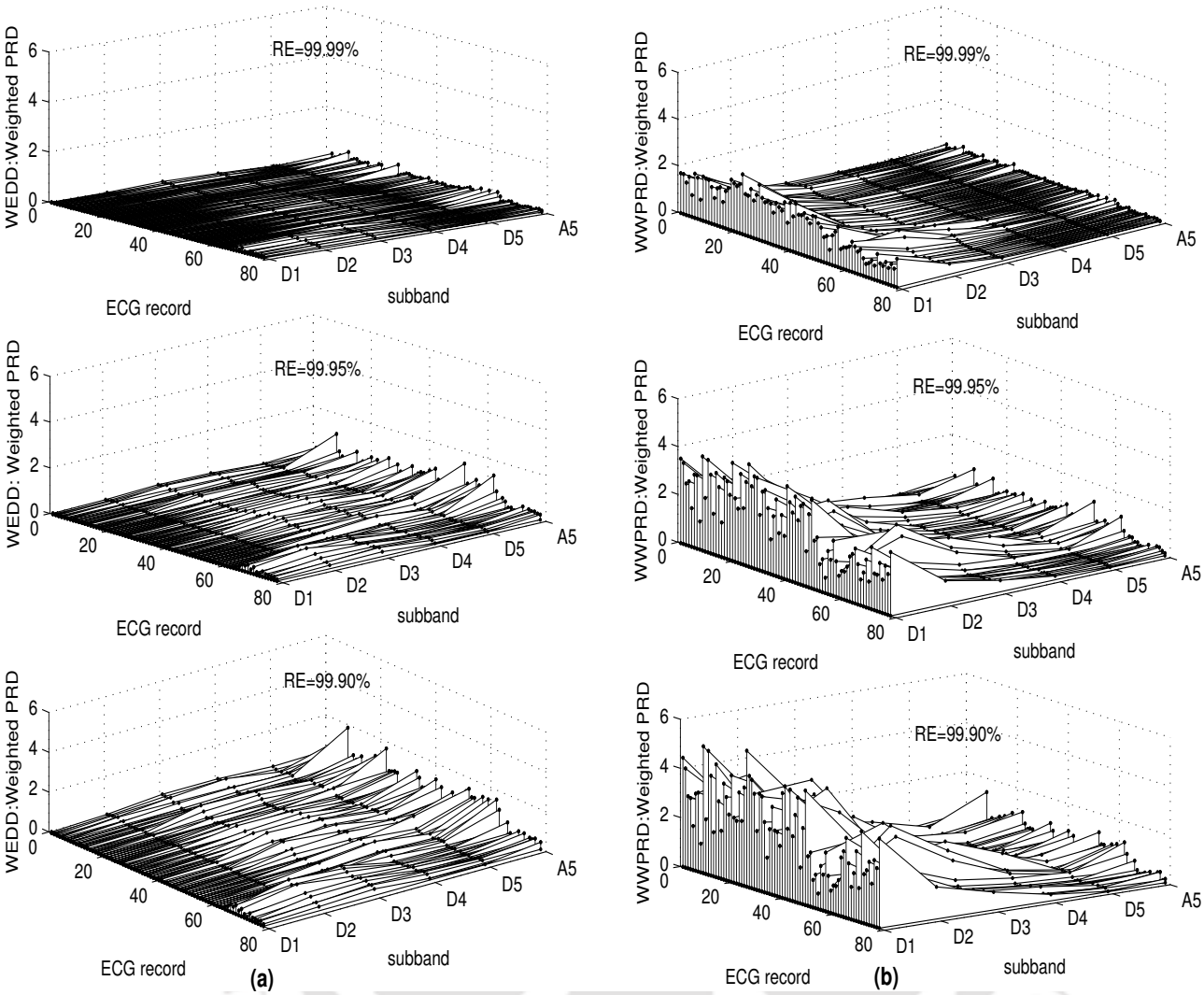

Figure 5.6: Effects of thresholding process for a desired RE (%) value. Visual inspection of weighted PRD of each subbands of record taken from `mita`, `cuvt` and `mitsva` databases. (a) WEDD measure. (b) WWPRD measure.

their decision level. The compression error introduced by the quantization process is calculated using the objective quality measures such as WEDD, WWPRD and PRD1. The WEDD and WWPRD versus quantization bits, b are shown in Fig. 5.7(a) and (b), respectively. These figures show the rate-distortion curves of seventy eight ECG signals. From these R-D curves, the optimum value of *b* which results in a minimum distortion can be determined for the quantization of nonzero wavelet coefficients. The quantization errors shown in Fig. 5.7(a) are small and nearly same for all tested records within the quantization bits ranging from 10 to 12. In 10-bit quantization of wavelet coefficients, average values of WEDD, WWPRD and PRD1 of 0.2883%, 1.366% and 0.579%, respectively are obtained for the compression of the ECG signals taken from dataset-III. Three different numerical values are obtained for a fixed resolution of wavelet coefficients.

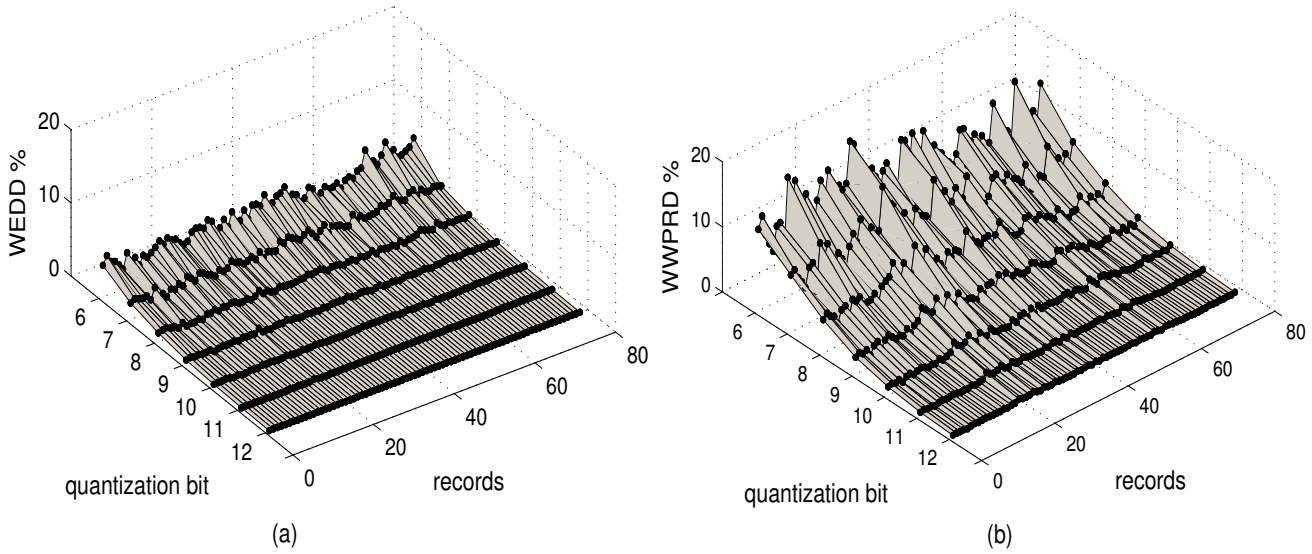

Figure 5.7: Quantization of wavelet coefficients of records taken from `mita`, `cuvt` and `mitsva` databases. (a) Rate distortion curves: WEDD (%) versus quantization bit, *b*. (b) Rate distortion curves: WWPRD (%) versus quantization bit, *b*.

Hence, the observation of weighted PRD values of subbands in the usage of quality measures (WEDD and WWPRD) and the reconstruction of clinical information are important. The cross validation of subband error is done for WEDD and WWPRD measure. In WWPRD, higher weighted PRD values are obtained for subbands D_1 and D_2 compared to the WEDD case for example in the thresholding process with small threshold value. But these subbands include more number of insignificant coefficients. It is observed that the inclusion of insignificant error is more in case of WWPRD whereas it is negligible in WEDD case. The average, the standard deviation and the maximum values of WEDD, WWPRD and PRD1 are shown in Table 5.4. The maximum WEDD, WWPRD and PRD1 values are less than 0.466%, 2.997% and 1.438%, respectively for coefficient resolution ranging from 10 to 12 bits. The WEDD measure adds up the errors due to rounding of significant coefficients to nearest level. But other measures namely WWPRD and PRD1 includes the errors of low level background noise due to zeroing of small magnitude coefficients around the zero zone. It is noted that the classified signal quality group is same for all compressed signals within that resolution range. Different qualities are obtained for coefficient resolution decreasing from 9 to 6 bits.

It is also observed that the average WEDD value is approximately doubled for decrementing quantization bit by one. This is not true in the case of WWPRD and PRD1. The variation of average WWPRD values are high for a quantizer with a resolution below 9-bit. Rate-distortion curves shown in Fig. 5.7 demonstrate that the error value is less for a resolution greater than 9-bit per coefficient and this resolution bound is considerable for coding with negligible clinical information loss. The quantization error value is exponentially decreasing with increasing value of *b*. From those experimental results, the resolution bits,

Table 5.5: Average compression performances of Approach 1-By adaptive global thresholding and quantization strategy in two-stage scheme.

WEDDtar, ε=6%		1%	2%	3%	4%	5%	6%	7%
WEDD (%)	1024	1.01±0.03	2.0±0.07	2.98±0.11	3.99±0.16	5.04±0.15	5.98±0.19	7.01±0.22
	2048	1.01±0.03	1.99±0.07	3.02±0.10	4.01±0.13	5.00±0.16	6.06±0.19	7.08±0.25
WWPRD	1024	6.03±1.87	8.93±2.66	11.06±2.90	12.69±3.16	14.44±3.33	15.77±3.50	16.98±3.44
(%)	2048	6.76±2.13	9.16±2.46	11.13±2.80	12.77±2.85	14.28±3.17	15.75±2.98	17.26±3.02
PRD1 (%)	1024	2.54±0.63	4.11±0.93	5.52±1.24	6.53±1.49	7.84±1.83	8.85±2.08	9.81±2.03
	2048	2.82±0.63	4.16±0.85	5.41±1.06	6.46±1.25	7.55±1.49	8.64±1.47	9.84±1.56
% of correct	1024	100	100	91.67	79.16	70.83	58.33	29.16
diagnosis	2048	100	100	100	91.67	79.16	66.66	41.66
compression	1024	3.81±1.76	7.13±3.52	10.17±4.43	12.11±4.57	14.36±5.05	15.81±5.07	17.22±5.22
ratio	2048	4.57±2.35	7.70±3.39	10.5±4.06	12.84±4.50	14.74±5.10	16.52±5.66	17.92±5.91
min(**max**)	1024	1.89(**8.09**)	2.89(**15.60**)	4.17(**19.69**)	4.97(**21.79**)	6.10(**26.38**)	7.69(**27.54**)	7.8(**28.16**)
CR	2048	2.01(**11.73**)	3.08(**17.16**)	3.59(**22.09**)	4.30(**25.57**)	4.94(**29.60**)	5.18(**33.37**)	6.05(**35.76**)
number of	1024	51.46±7.88	44.13±8.35	39.83 ±7.65	40.21±10.26	34.04 ±6.05	32.50±7.64	33.04±9.53
iterations, N_i	2048	47.71±2.91	45.08±6.24	37.21±4.12	37.88±7.33	36.13±10.85	34.21±9.70	30.88±10.62
coding delay	1024	1.44 ±0.21	1.238±0.157	1.19±0.23	1.14±0.11	0.96±0.187	0.95±0.19	0.95±0.205
t_d,(sec)	2048	1.61±0.06	1.47±0.166	1.32±0.125	1.28±0.205	1.20±0.28	1.16±0.319	1.14±0.27

$b = \{6,7,8,9,10\}$ are chosen in this work. The proposed algorithm automatically selects the threshold value and the quantization bit in few iterations for a user specified WEDD value. The above resolution bits are included in the iterative process for achieving the target WEDD value. From the experimental results shown in Section 5.4.1 and 5.4.2, the optimum threshold value (TH) and quantizer resolution (b) which results in minimum distortion level with high compression ratio are determined for the compression. The quality control criterion, WEDD, allows clinically acceptable reconstructions while maintaining high compression ratios. The overall performance of the proposed quality controlled ECG compression algorithm shown in Table 5.2 with the usage of above coding parameters is evaluated in the next section.

5.4.3 Results of the Quality-Driven Wavelet Coding with JTQ Strategy

The performance of the Approach-I is evaluated in terms of compression ratio, number of iterations required to reach convergence accuracy (N_i), compressed signal quality and coding delay (t_d). The ECG records taken from `mita` database are compressed and decompressed using the algorithm shown in Table 5.2. Then the percentage of correct diagnosis is specified for the above sets of records.

In the first experiment, twenty four records are created from widely used ECG datasets (dataset-I and dataset-II) by excluding repeated records, which is referred as dataset-IV. The records included in the

dataset-IV are mita 100, 101, 102, 103, 104, 107, 109, 111, 112, 115, 116, 117, 118, 119, 201, 207, 208, 209, 212, 213, 214, 228, 231, and 232. The first 1024 and 2048 samples (each) are taken from the records of dataset-IV for testing purpose. For these blocks of samples, assessment of the average WWPRD, the average PRD1, the percentage of CD, the average CR, the average b, the number of iterations (N_i) and the average coding delay of the proposed method based on $WEDD_{tar}$ ranging from 1% to 7% are shown in Table 5.5. The WEDD values are close to the target WEDD values. The closeness of resulting WEDD values to the target one depends on the relative bound error (ε) and its effect is discussed later. The percentage of correct diagnosis for the compressed block (1024 and 2048) of samples at a user specified WEDD value is determined and shown in Table 5.5. For both block sizes, correct diagnosability rate decreases for a target WEDD value of 3% and above. It is observed that the percentage of correct diagnosis is better in case of $N = 2048$ than $N = 1024$ for all target WEDD values. But the time spent for the local waves is more in the case of $N = 2048$. The average compression ratios and the standard deviations are shown in the table. Just comparing the average compression rate, the performance of the compression system for a user specified target error value cannot be concluded. It is well known that the compression ratio depends on the characteristics of local waves within a block which are taken from different subjects with same digitization parameters (sampling rate and sample resolution). The minimum and the maximum compression ratios achieved are also shown in the table. For a WEDD value of 3%, the minimum CR and the maximum CR values of 4.17 and 19.69 are obtained for the test records mita 232 and mita 207, respectively. For the compressed signal at CR=19.69:1, it is observed that the original clinical information are reproduced faithfully. Similarly, the original signal information are reproduced in the compressed signals of the test signals except for test signal from the mita record 109. For a WEDD value of 3%, the percentage of correct diagnosis is 95.83% and 100% for a block size of 1024 and 2048, respectively. From this experiment, the WEDD value of 2% is chosen as upper bound for 100% correct diagnosability. The increment in the average compression ratio for doubling the block size is small. But the maximum compression ratio achieved is better in the case of $N = 2048$. This test shows that the local waves within the block affects the compression ratio. Experiments show that the compression ratio is maximum for repeated ECG cycle within the block. The block size of 1024 samples is considered for further performance analysis in this work.

The complexity of this algorithm is evaluated in terms of the number of iterations (N_i) and the coding delay (t_d). These values are shown in Table 5.5 for each target WEDD value. The number of iterations depends on the relative bound error (ε), the block size (N), the target WEDD value and the ECG signal characteristics. For a specified ε=6%, N=1024 and $WEDD_{tar}$=3%, the target value is reached by N_i of 30 and N_i of 48 for the tested mita record 101 and 107, respectively. The average number of iterations decreases as target WEDD value increases. The resulting WEDD value is closer to the target WEDD value for the small relative bound error. The required (N_i) will be increased for a given ε, N and ECG signal $\{x(n), N\}$. The number of iterations versus relative bound error is shown in Fig. 5.8 for the test mita record 117 and 231. The required (N_i) will be increased for a given ε, N and ECG signal $\{x(n), N\}$. The number

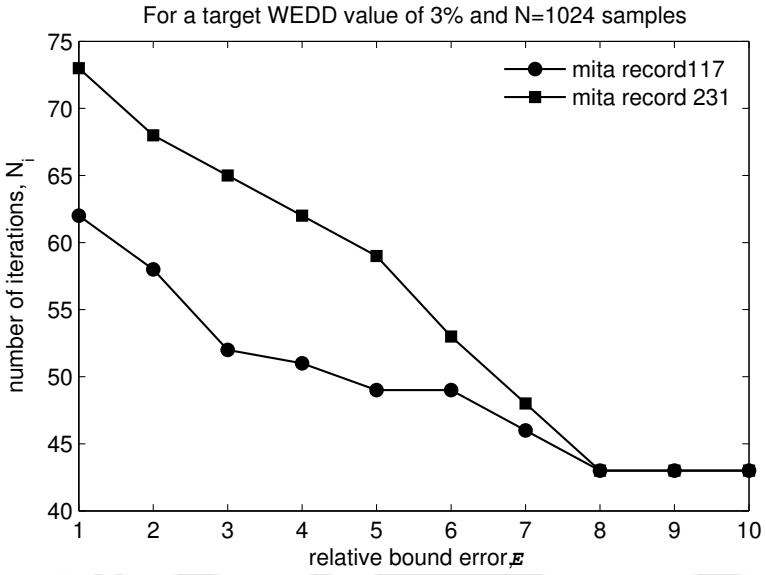

Figure 5.8: Number of iterations, N_i versus relative bound error, ε.

of iterations can be reduced by using the optimum quantizer resolution rather than adaptive quantization scheme within the iterative process. The N_i can also be reduced with minimization of the rate (R) and distortion (D) in terms of T and b using the optimization algorithm. In [143], [158], the coding delay is calculated in MATLAB environment and this method is followed here. For an Intel Pentium-4 PC with 3.4 GHZ CPU, 512 MB RAM and MATLAB 7.0, the coding delay of the proposed method is measured and the average values are shown in Table 5.5 for each target WEDD value. For both block sizes, the maximum coding delays are less than the duration of the original signals, 2.844 s for $N = 1024$ samples and 5.688 s for $N = 2048$ samples respectively. The coding delay includes the reading of the signal from the database directory, the searching of the optimum values of T and Δ for the user specified WEDD value and the signal compression. The experimental results demonstrate that the desired signal quality can be reached quickly and smoothly.

5.5 Approach 2-By Adaptive Subband Coding with JTQ Strategy

Many wavelet thresholding schemes apply thresholding followed by fixed linear quantization approach but it may introduce a severe signal distortion. Since a vector consists of wavelet coefficients with different dynamic range, it is not efficient to allocate a fixed number of bits to represent wavelet coefficients because of the varying characteristics of various ECG signals. Even if we assign different but fixed numbers of bits to wavelet coefficients according to dynamic range of the vectors, the coding efficiency may still be poor because of wavelet coefficients with great magnitude differences within the coefficients vector of a ECG signal. It is observed that each of the subbands has a different energy level and variance, with less

energy being in the higher detail subbands. Thus, each signal (each frame in case of classification) is quantized using a separate quantizer so as to quantize different wavelet coefficients in different subbands or frames according to their variance or energy. Thus, we need frame classification and dynamic bit allocation schemes.

In this approach, once the signal block is decomposed using the multiresolution signal decomposition technique, statistics of the wavelet coefficients at each subband is computed to perform classification of coefficients before compression process for achieving substantial gains in coding performance. The study shows that each of the subbands has a different energy level, dynamic range and variance, with less energy being in the high detail subbands. The relative wavelet subband energy (RWSE) is introduced to provide information about the relative energy associated with different frequency bands present in the ECG signals. The resulting energy distribution provides a suitable tool for detecting and characterizing signal contents and then the classification into frames is performed that serves to distinguish between the subband coefficients according to their relative energy levels. These classified wavelet coefficients are quantized using the threshold control zero-zone nearly uniform midtread quantization (TCZNUMQ) scheme presented in Chapter 3 in an adaptive manner where a different quantizer is used for quantizing each frame. This TCZNUMQ scheme is completely specified by the two design parameters: the zero-zone width and the outer-zone width and the reconstruction value is the center of a zone. In our quantizer design, the zero-zone width is limited by threshold T which allows to perform signal denoising where the zero-zone width equals noise threshold parameter T_B and the outer-zone width is chosen according to the distortion specification. The adaptive subband coding with JTQ strategy is explained in Chapter 3 and the quality control mechanism is explained in the previous section. The coding procedure is similar to the previous algorithm except the stage which performs the energy based classification of wavelet coefficients into frames. Brief summary of the Approach 2 is given below:

Step 0: Perform the blocking and baseline removal.

Step 1: Perform the multiresolution signal decomposition using the five-level 9/7-tap wavelet filters DWT which results in detail subbands and an approximation subband.

Step 2: Perform the classification of wavelet coefficients into frames based on the relative wavelet subband energy (RWSE) and energy packing efficiency criteria as described in Chapter 3.

Step 3: Quantize each frame or subband using the adaptive joint thresholding and quantization strategy which is implemented in two-stage design philosophy. Create the integer significance map and compress using the modified index coding (MIC) scheme as described in Chapter 3.

Step 5: Use Huffman coding for further compression of quantized indexes and the output of MIC scheme.

The performance of the Approach 2 is evaluated using the well-known dataset-IV which includes the `mita` records 100, 101, 102, 103, 104, 107, 109, 111, 112, 115, 116, 117, 118, 119, 201, 207, 208, 209, 212, 213, 214, 228, 231, and 232. The first 1024 samples (each) taken from the dataset-IV are used for

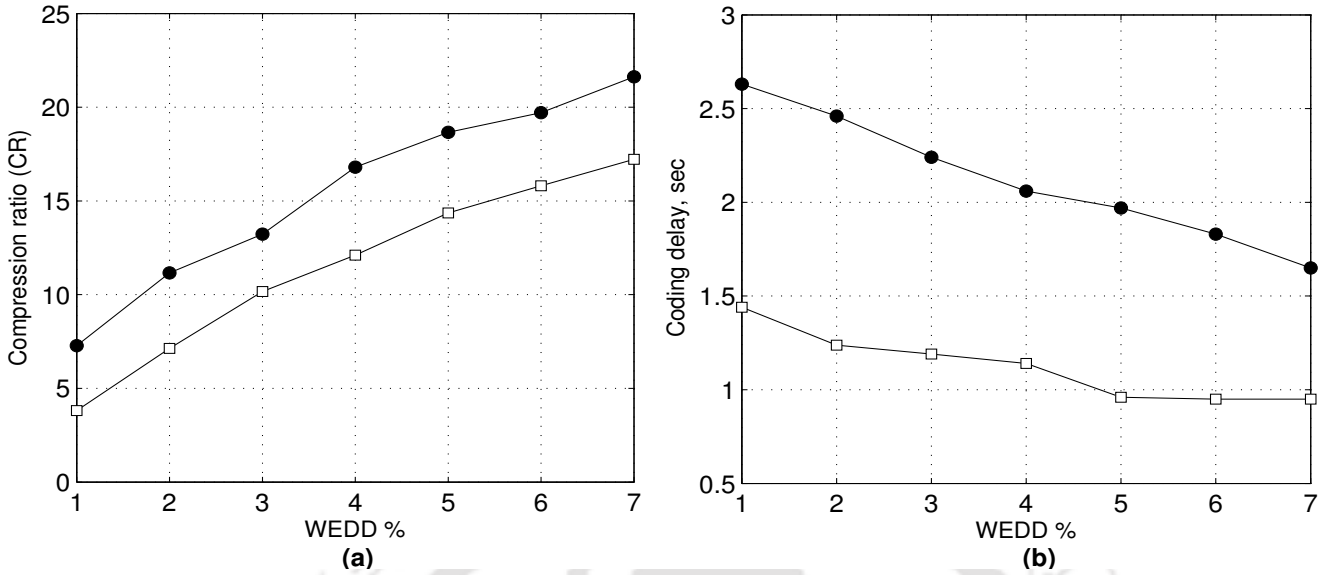

Figure 5.9: Performance of the proposed quality controlled compression approaches. (a) Average compression performance of the proposed Approach 1 and Approach 2. (b) Maximum coding delay of the proposed Approach 1 and Approach 2 for different values of WEDD.

testing purposes. In this experiment, each signal block is processed separately. The Approach 2 reaches user-specified WEDD accurately for all the test signals. The excellent coding performance of the Approach 2 as compared to the Approach 1 is shown in Fig. 5.9. The energy based frame classification technique enhances the compression performance of the Approach 2 but the computational time is more as compared to the Approach 1. However, the maximum computational time required is less compared to the duration of the signal block which equals 2.844 sec. Experiment shows that the classification technique employed is suitable for characterizing the subband coefficients of the signal and noise that is demonstrated in Chapter 4. Thus, the Approach 2 with the threshold control zero nearly uniform midtread quantization and noise threshold parameter estimation techniques can perform simultaneous denoising and compression of the signal in a single step.

5.6 Approach 3-By SPIHT Coding Strategy

The SPIHT coding was first presented in [145] as an efficient method for coding wavelet coefficients in image compression. In [146], the algorithm was introduced for ECG compression, obtaining very good results when being compared with other ECG compression methods. The SPIHT algorithm [145] is one of the most efficient coding scheme for the wavelet coefficients of ECG signals that has excellent coding performance for ECG, PCG, audio, image, medical image, video, etc [145, 214]. In [145], the ECG signal is first transformed into the wavelet domain and then encoded by the SPIHT algorithm. This is basically an efficient

quantization strategy for the resulting coefficients of wavelet transform. The SPIHT codes the wavelet coefficients exploiting the redundancies among wavelet subbands. The principles of the SPIHT algorithm are partial ordering of the transform coefficients by magnitude with a set partitioning sorting algorithm, ordered bit plane transmission and exploitation of self-similarity across different wavelet subbands. By following these principles, the encoder always transmits the most significant bit to the decoder. The operations in the algorithm are simple comparisons and bit manipulations, so that encoding and decoding are extremely fast. The SPIHT algorithm has demonstrated its efficiency for ECG compression both in obtaining high compression gain with low distortion. The SPIHT coding algorithm has the following features [145]: 1) the encoding and the decoding processes can be stopped at any desired bit rate or quality requirement; 2) different quality of compressed signals can be obtained by decoding subsets of the bit stream. The progressive coding capability of the SPIHT enables its inherent quality-controlling function in terms of some objective distortion criterion [146]. It is well known that the distortion criterion plays a crucial role in discovering the best compression (or rate-distortion) performance of the coder. Therefore, in this section the coding performance of the SPIHT algorithm with better rate-distortion optimization technique is studied and the results show that the SPIHT algorithm can improved compression rate while maintaining the visual quality.

5.6.1 Automatic Quality Controlled SPIHT Coding Procedure

The quality of a reconstructed signal can be refined gradually in the SPIHT scheme as the compressed bit rate increases. This is called progressive coding. Bisection method will be used in the proposed rate estimation method when an estimate is out of some bounds, say a lower bound R_L and an upper bound R_U. The initial bounds should be assigned such that the range covered in bracket $[R_L, R_U]=[R_{min}, R_{max}]$ is large enough to contain the desired solution. The minimum and the maximum bit rate are obtained from the coding performance of the SPIHT coder in the Chapter 3. A convenient assignment could be 1 bps and the rate of original data without compression. A block diagram of the proposed encoding procedure is given in Fig. 5.10. The performance of the SPIHT coder was studied in the Chapter 3. Since the the BW 9/7-tap wavelet filters to implement the DWT and the resulting coefficients of the ECG signal block are then encoded using the SPIHT strategy that are proven to offer an excellent coding gain, they are also adopted here. The partially encoded bits up to a predefined value are decoded using the decoding process of SPIHT. Then, the WEDD for a predefined bit rate is calculated. If the resulting WEDD falls within the preset bound of the desired WEDD, the encoded bits are sent or stored. Otherwise, the decoding process of SPIHT is continued until the next bit rate is reached, and the WEDD is calculated and re-examined gain. The process given above is repeated until a desired WEDD is achieved. Then, the resulting encoded bits are sent or stored and the process is repeated for the next ECG signal block.

The reported quality-control strategies are based on the PRD1 criterion and are tested using the noisy records from `mita` database. The encoded bits are sent or stored if the resulting PRD1 has reached a desired error percentage and falls within the convergence precision. In this case, the performance of the coder can

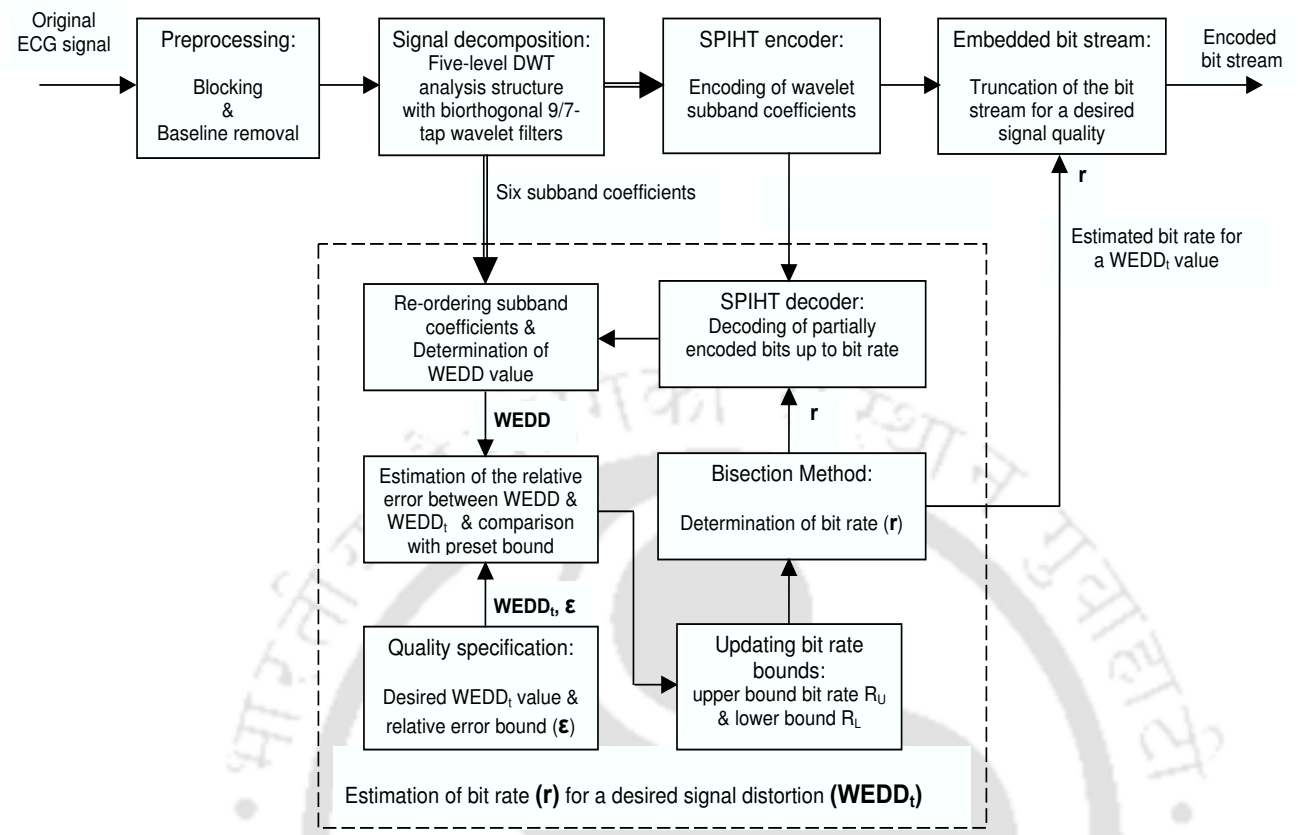

Figure 5.10: Block diagram of the quality controlled ECG compression method based on SPIHT algorithm and WEDD criterion.

reduce significantly, especially when the PRD1 and WWPRD measurement criteria are used for quality control, even if the method can achieve high compression rate with low distortion. This is because these measurement criteria accounts for the insignificant errors due to the filtering of high-frequency noises in the subbands D_2 and D_1. We hereby show the effectiveness of the PRD1, WWPRD and WEDD measures. The entire quality controlled SPIHT coding procedure is shown in Table 5.6. This coding procedure is similar to that in [145, 146] and in Chapter 3. The ECG signals from the `mita` records 100 and 107 are compressed using the SPIHT coder at CR=8:1 and CR=16:1, respectively. These two compressed signal qualities are shown in Figs. 5.11(a) and (c), respectively and the behavior of local and global measures are shown in Table 5.7. In WWPRD criterion, insignificant errors in subbands D_2 and D_1 dominates the global error while significant errors in other subbands are low. Thus, choosing upper bound distortion (D) level is difficult. Moreover, experiments show that the coding performance of the SPIHT coder is poorly reflected in the PRD1 and the WWPRD measurement criteria. Since the WEDD measure is subjectively meaningful in the sense that the small and large values correspond to "good" and "bad" quality, respectively [see Fig. 5.11 and Table 5.7], upper bound distortion D can be easily chosen for clinical application. Therefore, the

Table 5.6: Quality controlled SPIHT coding algorithm.

The quality specification can be specified in PRD1, WWPRD and WEDD in this algorithm.
Step 0: Initialization: given D_m, R_{min}, R_{max} and ε.
Step 1: Get the i^{th} signal block of an input m^{th} ECG record or lead.
Block size, N=1024 samples. Remove mean and store it as $\mu_{m,i}$.
Perform 5-level BW 9/7-tap filters DWT and SPIHT encoding.
Step 2: Desired distortion (d) estimation: Get R_L=R_{min}, R_U=R_{max}, ε.
L and U are lower and upper bounds, respectively. k=0
Loop until $|d_{i,k+1}(r_{i,k+1}) - D_m|/D_m \leq \varepsilon$:
Step 3: Compute rate of the i^{th} block for k+1 iteration, $r_{i,k+1} = \frac{1}{2}(R_L + R_U)$.
Step 4: The truncated bits up to $r_{i,k+1}$ are decoded by the SPIHT decoding process and get the subbands:
original $[\mathbf{A}_J, \mathbf{D}_J, ...\mathbf{D}_1]$ and compressed $[\tilde{\mathbf{A}}_J, \tilde{\mathbf{D}}_J, ...\tilde{\mathbf{D}}_1]$.
Step 5: Compute $d_{i,k+1}(r_{i,k+1})$ using the WEDD measure.
Step 6: If $d_{i,k+1}(r_{i,k+1}) < D$, set lower bound $R_L = r_{i,k+1}$;
Else, set upper bound $R_U = r_{i,k+1}$.
k=k+1, Repeat the process given above until an error percentage falls within the convergence precision ε.
Step 7: **Otherwise, stop**: send or store the encoded bits.
Step 8: $\tilde{D}_{m,i} = d_{i,k+1}$, R=$r_{i,k+1}$, number of iterations N_k=k.
Step 9: Initialization for next $(i+1)^{th}$ block; Go to step 2).

Table 5.7: Local and global assessment of the compressed signals shown in Fig. 5.11.

Rec.	CR	Error Measures	Local/Subband Error, PRD_s (%)						global / total
			$\mathbf{A}_5$	$\mathbf{D}_5$	$\mathbf{D}_4$	$\mathbf{D}_3$	$\mathbf{D}_2$	$\mathbf{D}_1$	
100	8:1	PRD_w	2.83	1.72	2.54	4.49	33.83	84.11	4.93
		WWPRD	0.86	0.31	0.52	0.71	**3.26**	**4.77**	**10.43**
		WEED	0.69	0.57	0.76	0.52	**0.30**	**0.06**	**2.90**
107	16:1	PRD_w	3.01	4.67	18.93	34.72	78.34	99.89	4.851
		WWPRD	**2.09**	0.74	1.35	1.38	**1.90**	**1.19**	**8.65**
		WEDD	**2.69**	0.41	0.24	0.11	**0.03**	**0.01**	**3.49**

WEDD measure is incorporated with the excellent coding procedures given in [146] for providing a better quality controlled compression algorithm.

5.6.2 Results of Quality-Driven SPIHT Coding Scheme

The proposed coding strategy is tested using the `mita` records in [140,146] and the measurement criteria viz. PRD1, WWPRD and WEDD. The dataset-I consists of 1024 samples of data (each) from record numbers

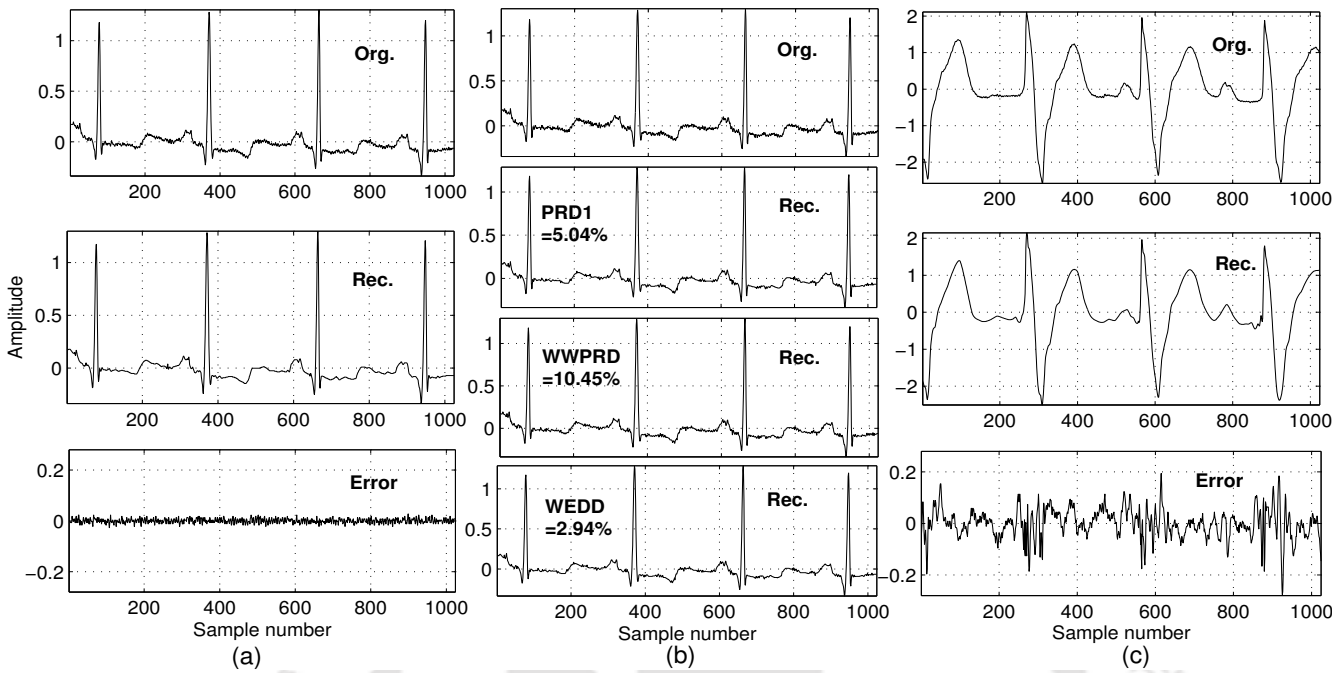

Figure 5.11: Compression results of the SPIHT coder. (a) `mita` rec. 100 (CR=8:1, PRD=4.93%, WWPRD=10.43% and WEWPRD$_s$=2.90%). (b) Compression of noisy signal for a target PRD=5.04%, WWPRD=10.45% and WEWPRD$_s$=2.94%. The CRs obtained are 5.5, 3.92 and CR=7.82, respectively. (c) `mita` rec. 107 (CR=16:1, PRD=4.851%, WWPRD=8.65% and WEWPRD$_s$=3.49%). The error signal shows the features distortion.

100, 101, 102, 103, 107, 109, 111, 115, 117, 118 and 119. Each signal block is transformed and encoded separately. The signal block from the `mita` record 100 with SNR=45 dB is compressed for PRD=4.93%, WWPRD=10.43% and WEDD=2.90% which are obtained at CR=8:1 [see Fig. 5.11(a) and (b)]. The compression ratios obtained are 5.5, 3.92 and 7.82, respectively. Thus, the compression ratio is decreased by 31.2%, 51% and 2.25%, respectively [for example, 100*((8-5.5)/8)=31.2%]. This phenomenon is shown in Fig. 5.11(b) which reveals the clinical quality of the compressed signals for each specified error percentage. We observe that not only the significant feature is retrieved, but also the signal quality is upgraded because the insignificant coefficients dominating in subbands D_2 and D_1 are removed for data compression.

The signal (each) from the dataset-I is compressed for the target error values of 2% ("very good" quality) and 5% ("very bad" quality) with convergence precision $\varepsilon = 2\%$. The coding performances of the quality-controlled SPIHT coding strategy based on the PRD1, WWPRD and WEDD measurement criteria are shown in Fig. 5.12. Since the preservation of clinical information is most important, we have deliberated a desired error value of 2%. We notice severe clinical feature distortions for the error value of 5%. Experiment shows that the proposed coding strategy with WEDD criterion provides a better coding performance for noisy signals from the `mita` database. One can argue that the comparison of the coding performance obtained for different distortion measurement conditions is inappropriate. Note that the compression rates

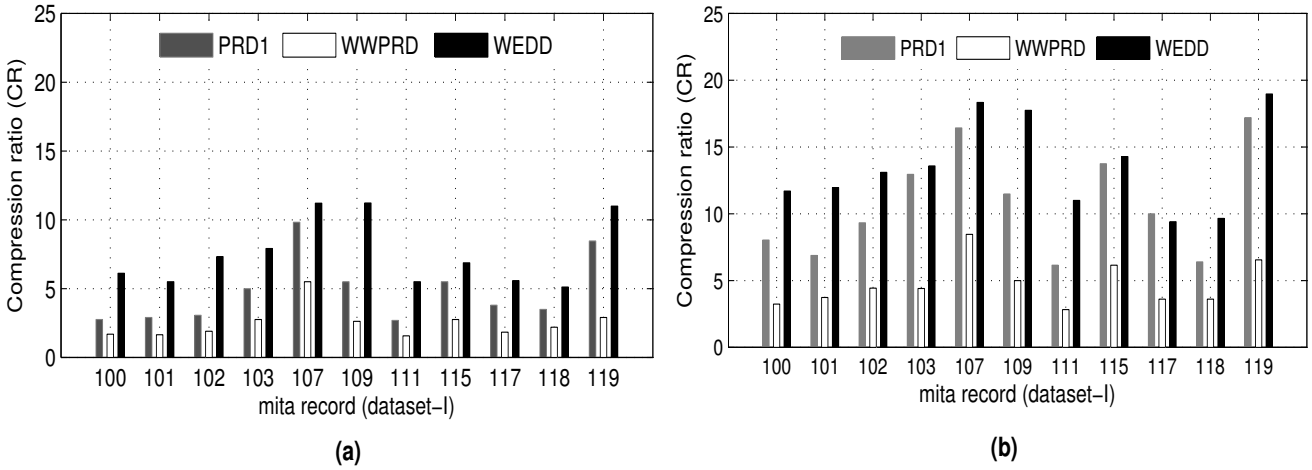

Figure 5.12: Compression performance of the quality-driven SPIHT coding strategy with different objective measures. (a) the performance for a desired error value of 2% ("very good" quality), (b) the performance for a desired error value of 5% ("very bad" quality).

of the PRD, WWPRD and WEDD based strategies are compared with reference to the subjective results obtained for a error value of 2% and the experiment shown in Table 5.7 and Fig. 5.11. Therefore, the lower error percentage is chosen which results in "very good" quality for all tested signals. This investigation shows that the tradeoff between the compression rate and PRD/WWPRD is broken for low error percentage situations.

The main contribution in this section is to study the effectiveness of the distortion measures and illustrate the effect of the noises on the R-D performance of the SPIHT coder. Experiments showed that the overall performance comparison of the compression methods based on the results obtained using the records from the `mita` database and the PRD1 measurement criterion is meaningless. We observed that noise decreases the compression ratio for a specified distortion level. As a remedy, one can then suggest ideal filtering of the background noise [149]. However, the noise filtering may introduce features (amplitude, duration and shape) distortion and sometimes the input noise level is difficult to estimate using the frequency domain filtering as followed in [139]. When the ECG signals are noisy, the distortion measure should be dependent on the signal distortion rather than on the noise level. Regardless of the number of publications that were based on PRD1 measure, such a measure does not significantly reflect the actual behaviors (noise filtering and compression error) of the compression method [190]. Experiments on several noisy records from the widely used `mita` database show that the proposed strategy outperforms conventional PRD1 and a recent WWPRD criteria based coding strategies, especially in low error percentage situations without introducing the signal distortion. Furthermore, Fig. 5.12 shows that the PRD1 and WWPRD criteria based SPIHT coding strategies achieve lower compression rate for the noisy blocks. Experiment shows that this SPIHT coding strategy can provides the best possible compression rate without spending extra bit rate for noise

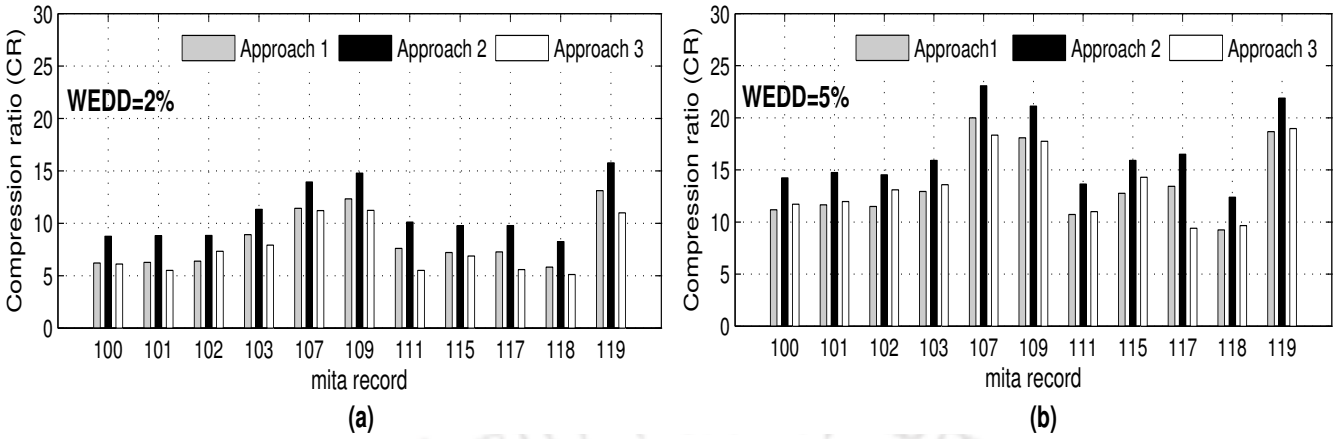

Figure 5.13: Compression performance of the Approach 1, Approach 2 and Approach 3 for the dataset-I records.

coding. Thus, a quality controlled SPIHT coding algorithm combined with a WEDD measurement criterion can provide an effective and efficient compression of biomedical signals.

5.7 Discussion

In this Chapter, quality controlled wavelet ECG compression methods are presented for guaranteeing reconstruction quality measured using the wavelet energy based diagnostic distortion (WEDD) criterion, which appears to be a correct representation of the amount of signal distortion at all subbands. The compression methods are based on: 1) the adaptive wavelet coding with joint thresholding and quantization strategy (Approach 1); 2) the adaptive subband coding with joint thresholding and quantization strategy (Approach 2); and 3) the set partitioning in hierarchical trees (SPIHT) coding strategy (Approach 3). Combining the WEDD measurement criterion and the well-designed coding strategy, the quality control mechanism provides an excellent coding gain. The following modifications distinguish the approaches from the existing works. A new WEDD measure is used for guaranteeing reconstruction quality that outperforms the conventional PRD and the WWPRD consistently measuring the distortion both across different distortion types and within a given distortion type at different distortion levels. A threshold control zero-zone nearly uniform midtread quantization (TCZNUMQ) scheme where the zero-zone width of the quantizer is limited by the threshold parameter is employed for the compression of coefficients. The Approach 1 and Approach 2 are based on the TCZNUMQ and MIC schemes. The following step distinguishes the Approach 2 from the Approach 1. Classification of wavelet coefficients into frames based on the statistics of the subband coefficients. The energy based classification technique used in Approach 2 where a different quantizer resolution is used for quantizing each frame, achieves substantial gains in the compression performance. To validate the performance of the proposed SPIHT coding strategy, PRD and WWPRD based strategies are presented.

Experimental results show that the proposed approaches are superior to the PRD and WWPRD based quality controlled SPIHT coding and the other wavelet thresholding methods in terms of compression performance. The compression performance of the Approaches are shown in Fig. 5.13. The compression performance of the Approach 2 is better than the Approach 1 and the Approach 3. But the maximum computational time required is more as compared to the Approach 1 and Approach 3. However, the computational time is comparable with the duration of the signal block considered. The algorithm performs the quality control quickly, smoothly, and reliably. The experimental results show that a desired WEDD value can be guaranteed with higher compression rate and lesser coding delay than the signal duration in all the approaches. For a given dataset-I, the quality of compressed signals with a WEDD value of 2% are suitable for morphological studies. Experiments show that the subjective tests are the obvious way of measuring clinical quality when working with ECG signals. The final conclusion on the optimal selection of distortion threshold when guaranteeing signal quality is so difficult since it depends on varying characteristics of various ECG signals. However, it can be performed with more subjective test with different records. The experimental results in this Chapter demonstrates the possibility of attaining good compression ratios by using the well-designed quality-driven subband coding scheme and WEDD criterion for guaranteeing reconstruction quality. The WEDD measure can be useful for data compression where the noise level is difficult to avoid or estimate, and for simultaneous noise suppression and signal compression approach.

भारतीय प्रौद्योगिकी संस्थान गुवाहाटी
Indian Institute of Technology Guwahati

6

Wavelet Compression of Phonocardiograms

Contents

6.1 Introduction

With advances in sensors, computer technology and signal processing tools, computer-aided analysis of heart sounds has become part of a routine clinical assessment due to its diagnostic potentials [207]. The phonocardiogram (PCG) is a recording of the acoustic waves produced by the mechanical action of the heart [208, 210, 214]. It is a very useful and effective method for the diagnosis of valvular heart diseases. The PCG may include the heart sounds and the heart murmurs (systolic and diastolic). Heart sound consists of four components namely S1, S2, S3, and S4. The S1 (lup) and S2 (dub) heart sounds are regarded as the normal heart sounds in a cardiac cycle. The S1 and S2 heart sounds are caused by the closure of mitral and tricuspid valves, and the closure of aortic and pulmonary valves, respectively. The S3 and S4 heart sounds are caused by the rapid ventricular filling in early diastole and the ventricular filling due to atrial contraction, respectively. In addition to these four heart sounds, other transient sounds namely opening clicks, snaps and prolapsed sounds are produced by valvular stenosis during systole and diastole. The frequencies of all important sounds are less than 1000 Hz [34]. The PCG signals are digitized at a sampling frequency of 8000-22050 Hz with 8-16 bit resolution. The data rate for PCG (`qdheart` PCG database) data rate is 352.8 kbps [214]. The PCG data rate is much higher than the other cardiac data namely heart rate, cardiac output and ECG, etc., which are discussed in Chapter 1. Consequently, cardiac data management system and real time telecardiology application requires an efficient compression method, without losing the original clinical information, to meet the data rate demands of limited and well established transmission link. In recent years, almost all the attempts have been focused on the compression of ECG signals. But few PCG signal compression methods are reported in literature [34, 211, 212, 214]. Therefore, we attempt to further validate the performance of the proposed schemes for the compression of PCG signal.

The successful results presented in chapters 3-5 have motivated this follow-up study. In this Chapter, we present a better PCG compression method based on the combination of multirate sampling strategy and wavelet transform. The multirate sampling strategy reduces the computational cost and its sampling rate will be chosen according to the interpolation error. Once the signal is decomposed, the wavelet coefficients are classified into three regions based on the relative wavelet subband energy and then the coefficients in each region is compressed using the threshold control zero-zone nearly uniform midtread quantization (TCZNUMQ) and modified index coding (MIC) schemes. The performance of the method is tested using the PCG signal blocks taken from the `qdheart` and `CAHM` databases which include normal sounds, murmurs, stenosis, noise and other pathologies. The quality of the compressed signal is evaluated by different quality tests. The performance of the WEDD measure is evaluated to emphasize the development of quality controlled wavelet based compression method for biomedical signals. The WEDD criterion correlates better with the significant distortions in the compressed signal compared to the conventional PRD1 and PRD_w criteria. This chapter is organized as follows. In Section 6.2, an overview of wavelet based PCG compression methods are presented and then motivations for the present study are presented with different

sets of experiments. In Section 6.3, a new wavelet based PCG compression method is presented based on the energy based classification, TCZNUMQ and MIC schemes. In Section 6.4, performance evaluation of the proposed and other methods is presented. Tests are carried out using the cardiac auscultation of heart murmurs (CAHM) and qdheart databases, and the PRD_w, WWPRD and WEDD measurement criteria. The performance of each compression methodology is discussed in this Section. In Section 6.5, experimental results of the quality controlled PCG compression are presented and then drawbacks of the proposed method is highlighted at the end of this Section.

6.2 Background and Problem Statement

Wavelet threshold based PCG compression methods with good compression performance have been reported during the last few years [34, 211, 212]. The wavelet and wavelet packet based compression for PCG signals are reported [211]. The wavelet coefficient (WC) vector is formed with the coefficients of all subbands, ordered from high to low scales. The threshold value is calculated based on an RE criterion. This method employs the linear quantization scheme and Huffman coding to encode the quantized nonzero wavelet coefficients (QNZWC) vector and the run-length encoding (RLE) and Huffman encoding for BSM. The performance of the wavelet transform based method is better than WP based method. The wavelet based compression methods achieve data reduction using the thresholding or/and quantization scheme(s) based on some target criterion. The zero zone parameter in the quantization step of compression is analogous to the threshold value in the thresholding function. Generally the uniform scalar quantization with step size controlled by desirable CR is used. Because of the large dynamic range of the retained significant coefficients, if the size of the zero zone is chosen to be too large, then some of the retained coefficients around the zero zone may also be rounded to zero. The desired target criterion ensured in the thresholding stage may not be maintained after the quantization process. A way to solve this would be to choose a smaller quantization step such that it matches with the threshold value but this would require more number of bits. Hence, the quantized coefficients may occur with equal probability and, thus it may decrease the overall compression efficiency. The solution that we propose is to use a uniform scalar quantizer with threshold adaptive zero zone.

A wavelet based PCG compression method is focussed for a portable real-time homecare system [34]. First, the input signal with 16384 samples is down-sampled by eight times to reduce the computation time of the WT and to remove the high frequency components fast. The down-sampled input signal with 2048 samples is decomposed by four-level DWT. The high frequency components corresponding to noises in the first level are removed directly by setting the thresholded coefficients to zero. The data size is further reduced by choosing the appropriate threshold values based on the desired compression ratio. However, time varying thresholding process is important rather than zeroing a particular band directly because the PCG signal is a highly non-stationary signal. Zeroing first level may result in large clinical error with

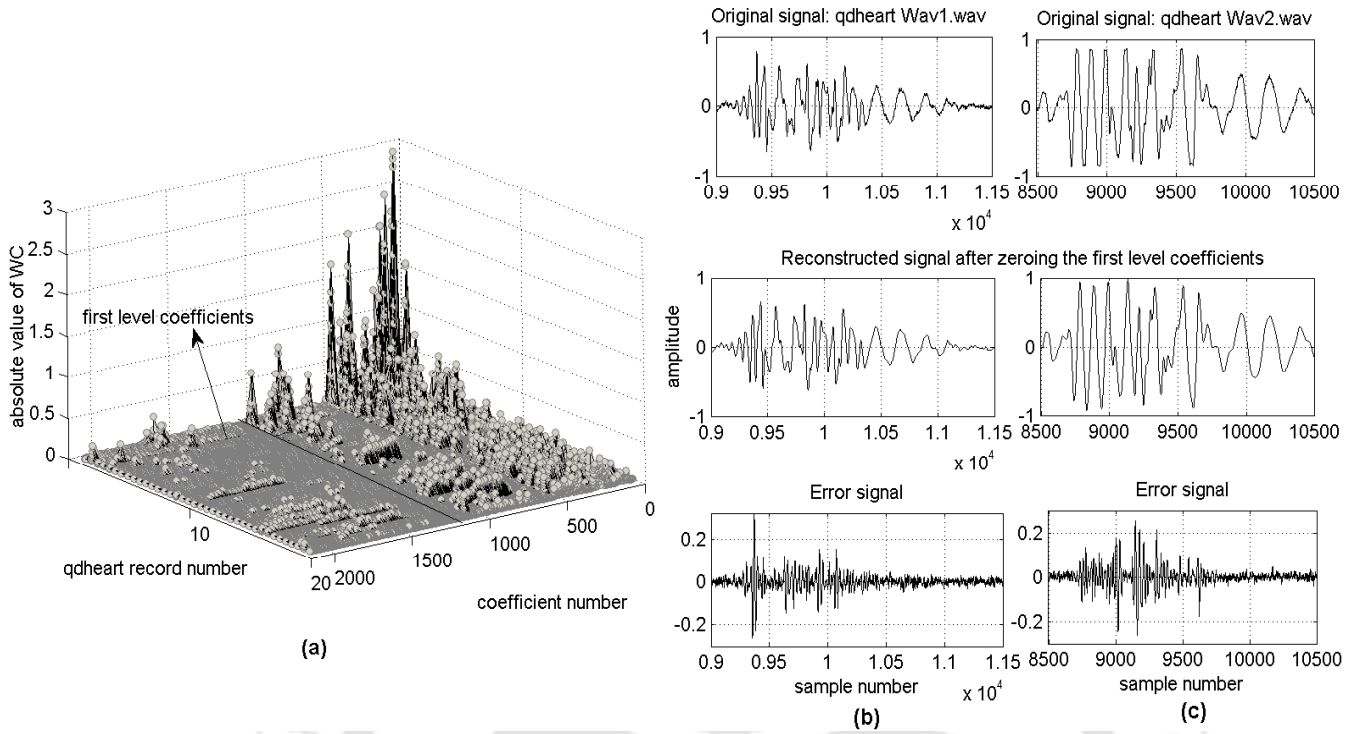

Figure 6.1: Analysis of effect of first level wavelet coefficients. (a) Amplitude distribution: absolute value of wavelet coefficient (WC) vector. Large PRD1 value is reflected due to zeroing of coefficients in the first level: (b) `qdheart` Wav1.wav, PRD1=19.7483%. (c) `qdheart` Wav1.wav, PRD1=12.5939%.

high frequency components such as heart murmurs. The wavelet coefficients of the decimated PCG signal block with 2048 samples are obtained and their amplitude distributions of the wavelet coefficients are also shown in Fig. 6.1(a). We can observe that detail coefficients in the band D_1 (first level) have considerable amplitude level. The distorted PCG signals with PRD values after the zeroing of the first level coefficients are shown in Fig. 6.1(b) and (c). Large PRD1 values are obtained for these two signals due to the presence of significant coefficients in the first level. Since the coefficients in the highest frequency subband have significant contribution, the wavelet coefficients should not be zeroed directly. In this work, this problem is solved by using the thresholding process based on the EPE criterion.

A field programmable gate array (FPGA) based embedded system for compression and transmission of the PCG signal was reported in [211, 212]. Here, the thresholding is done with a threshold value which is determined based on a desired PRD_w criterion. In the iteration, the threshold value is modified until the desired PRD_w is reached. The transform based compression method may produce smooth reconstructed signals with insignificant errors [134, 145]. Similar to time domain, the PRD_w is measured in wavelet domain. The errors are estimated as the difference between the wavelet coefficients of the original signal and the coefficients of the compressed signal. Large PRD_w value may be obtained since the transform based method achieves the compression of the signal block by zeroing large number of insignificant coefficients

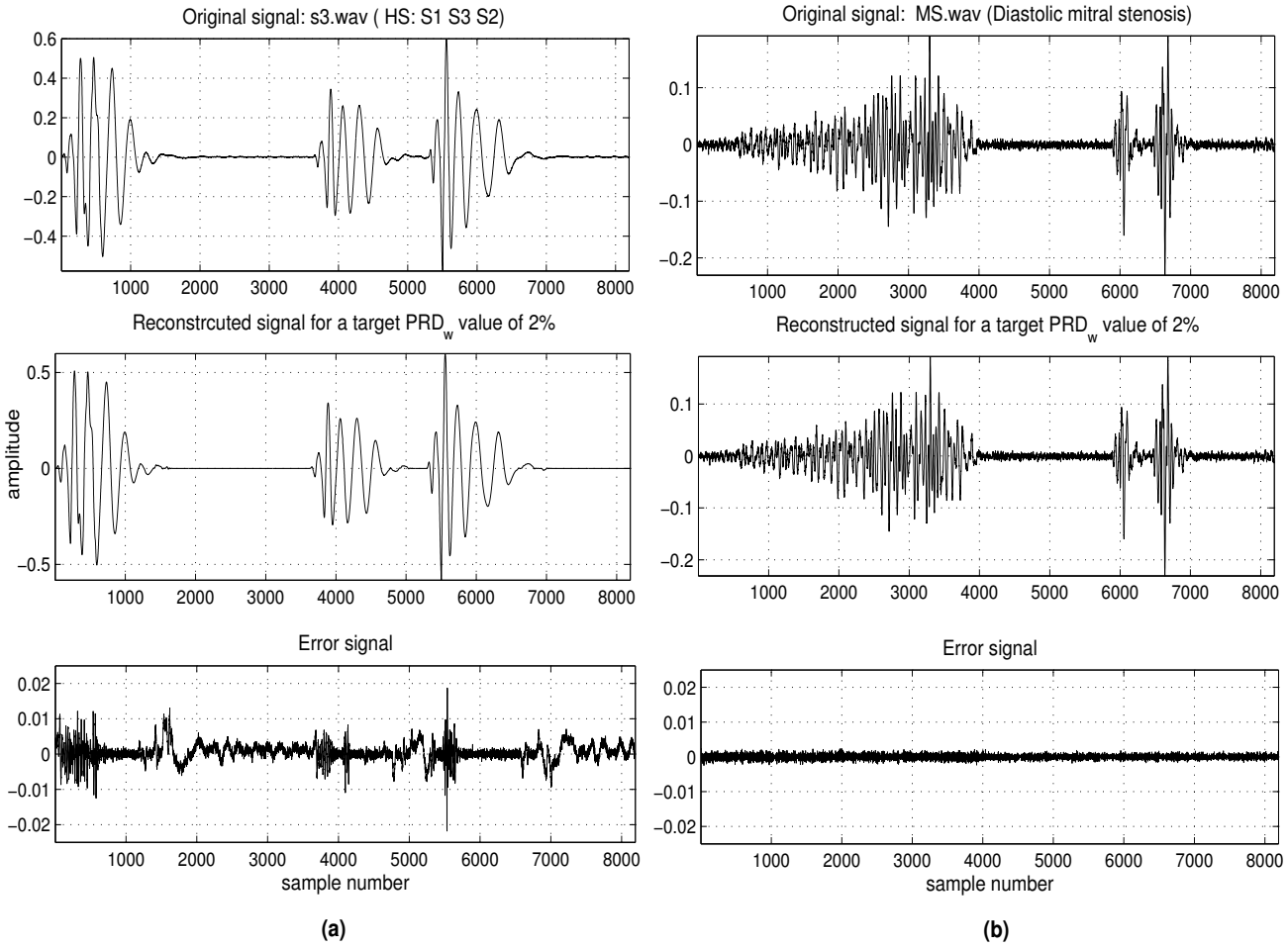

Figure 6.2: Analysis of target PRD_w based compression method. The following specifications are used for the analysis: N=4096 samples, 4-level Daubechies order 10 DWT, two blocks and target PRD_w value of 2%. (a) PCG signal block taken from `CAHM` record S3.wav ($WEDD_{avg} = 1.609$, $CR_{block1} = 33.35 : 1$ and $CR_{block2} = 23.42 : 1$), (b) PCG signal block taken from `CAHM` record MS.wav ($WEDD_{avg} = 0.4716$), $CR_{block1} = 1.90 : 1$ and $CR_{block2} = 1.64 : 1$).

in the wavelet coefficient (WC) vector. The PRD_w criterion aims to gain a compromise between the number of retained wavelet coefficients and the error. The insignificant errors are included in the PRD_w calculation which misleads the judgment of the reconstructed signal quality if the contribution of significant errors is low. Choosing a threshold for error value for clinically acceptable level is difficult in this case. The iteration algorithm ensures the desired error percentage for a noisy PCG signal block. The performance of the PRD_w criterion may affect the number of wavelet coefficients chosen for a given error percentage. The deficiency of the PRD_w is shown in Fig. 6.2 with reference to preliminary results of the WEDD criterion. An algorithm to optimize the efficiency of compression in the wavelet domain based on PRD_w criterion may not reflect the optimum compression rate of the method. The reason lies in the fact that if the same PRD_w is specified for a noiseless PCG signal block and the noisy one, the compression rate obtained for

the noisy block will be lower than that of the noiseless block. This is due to a smaller threshold value used for the noisy signal and this will include extra coefficients in the thresholded coefficient (TC) vector. At this stage, the coefficients reduction ratio is shown in Fig. 6.2 and further investigation is made in Section 6.4. One of the important problems in medical signal compression is the definition of the quality criterion for evaluating different compression methods. The researches in this area are focused on improving rate-distortion optimization algorithm which results in maximum compression rate with minimum distortion. Most of the methods employed the linear quantization scheme and the run-length and Huffman codings. A significant improvement in the compression rate can be achieved by exploiting the redundancy between the time indexes of the retained significant coefficients. This coding methodology will not employ Huffman coding scheme in the iterative algorithm based on data rate or distortion level criterion. This may help to reduce the overall complexity of the compression method. In this chapter, we propose a novel wavelet based lossy PCG compression method. The performance of each stage of the proposed method is first tested using the `qdheart` and `CAHM` databases and the PRD/PRD$_w$ and WEDD measurement criteria. The advantage of the WEDD will be demonstrated over the PRD$_w$ criterion with different sets of experiments.

6.3 Wavelet Compression of PCG Signals

In this work, a compression method based on the combination of the multirate sampling and wavelet transform is presented for PCG signals. Once the signal is down-sampled with an appropriate sampling factor, the signal is decomposed using the 9/7-tap wavelet filters. The resulting wavelet coefficients are compressed using the adaptive threshold control zero-zone nearly uniform midtread quantization and modified index coding schemes. The performance of the each scheme is explained in detail in Sections 3.2.4 and 3.2.5 of the Chapter 3. In this Chapter, we present some of the experimental results of each stage of the compression method.

6.3.1 Preprocessing (Blocking, Mean Removal and Multirate Sampling)

The PCG record is divided into nonoverlapping signal blocks of N samples and the mean value of the PCG signal block is removed in this work. The block size can be chosen by considering the compression system resources. The complexity of the method mainly depends on the iterative algorithm which is employed to achieve a desired rate or distortion and length of the signal block. Each PCG cycle contains a large number of samples since the sampling rate used for recording of the PCG is high. The compression system involves tradeoffs between system resources and the quality of the output [212]. In such a case, large number of wavelet coefficients will be processed at each stage (thresholding, quantization and encoding) of the compression method. Thus, more computation time and memory space is required if the full number of wavelet coefficients of the original signal block is employed in the iterative algorithm. The number of samples within a signal block can be reduced if the multirate sampling strategy restores the original signal

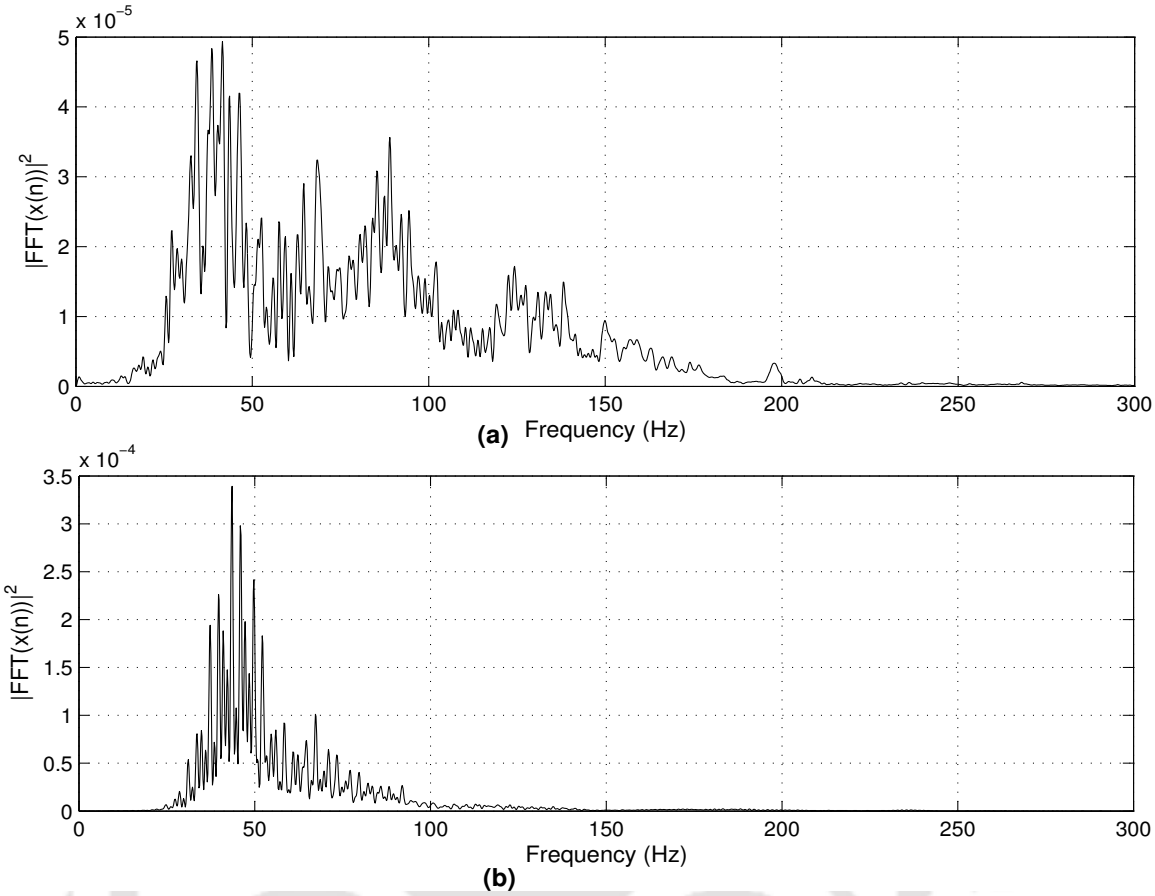

Figure 6.3: Frequency components of the PCG signals taken from the CAHM database. (a) Average spectrum obtained for the 21 PCG signals sampled at 22050 Hz. (b) Average spectrum obtained for the 21 PCG signals sampled at 11025 Hz.

with minimum mean squared error. Therefore we attempt the method for the PCG compression based on the combination of the multirate sampling strategy and the wavelet based compression scheme. In this method, the multirate sampling strategy will be adopted if the resulting interpolation error is negligible and reduces the time and memory requirements of the succeeding stages. The disadvantage of this method is that the minimum target error value depends on the interpolation error percentage. This may be avoided by selecting decimation factor adaptively. One can claim that the computation time can be reduced if the block size is small. But sometimes the small PCG signal block that to be considered does not contain any signal information. This condition is verified in our previous works [213, 214].

In order to design a multirate sampling strategy, we compute the frequency information of the PCG signals taken from the cardiac auscultation of heart murmurs (CAHM) and the qdheart databases. In these databases, PCG records are stored in WAV format with different sampling rates and resolutions. These databases include records of many different valvular pathologies (normal sounds, third heart sound, fourth

heart sound, aortic insufficiency, aortic stenosis, mitral stenosis and murmurs, noises, etc.). To analyze the frequency contents of a PCG signal, the records from the CAHM are used in this section. By studying the specific frequencies of heart sounds and the average spectral density shown in Fig. 6.3, it is found that the frequencies of the sounds are below 500 Hz. Note that the bandwidth of the signal vary according to the contents of the clinical information. The qdheart database PCG records were stored in WAV format with sampling rate of 22050 Hz and resolution of 16-bit. Since heart sounds have frequencies below 500 Hz the PCG signal may be decimated without distorting the perceptual quality of the sounds. They are sampled at very high frequencies as required for normal sound signal. Therefore, at first, the original PCG signal is decimated by a factor of 8/4 from 22050 Hz to 2756/5512 Hz. The decimation factor (DF) can be adapted based on the sampling frequency of the PCG signal. This is seen in the PCG signal taken from CAHM database where the PCG records are stored in WAV format with different sampling frequencies and different resolution. In this work, each signal block size is reduced to block with N samples using the DSI algorithm and its performance for the ECG signal is studied in our previous work [192]. The effect of the DSI algorithm is discussed in terms of the error percentage and computation time in Section 6.4.

6.3.2 Wavelet Decomposition of the PCG Signal

The zero-mean PCG signal $\{x(n), n = 0, 1, 2, ...N-1\}$ is successively decomposed into a set of subsignals $\{A_J, (D_j)_{(1\leq j\leq J)}\}$ using the biorthogonal 9/7-tap filter bank DWT up to J levels. This decomposition process results in $J+1$ subbands. These subbands are the approximation band A_J and the detail bands D_J, D_{J-1}, D_{J-2},..... D_1, where A_J is the smoothed version of $x(n)$ and $(D_j)_{(1\leq j\leq J)}$ are the difference subsignals between $x(n)$ and its smoothed version at j^{th} resolution, respectively. The higher subbands carry finely detailed information and the lower subbands carry shape based information. We notice that the noise is well explained by a few levels that contain fine details and its effect disappears at the coarser scales. After performing the 5-level DWT, histograms of the wavelet coefficients in the subbands are shown Fig. 6.5 that demonstrates the behavior of the wavelet coefficients at each subband. As can be observed, the histograms of a few subbands can be very closely fitted with some distributions. In this case, the estimated values of the shape and scale parameters were used for this modeling. To determine the importance of each subband, statistics of the wavelet coefficients for each subband are further computed like in subsection 3.2.2 of Chapter 3. It is observed that the range of the coefficients ([MIN, MAX]) of the subband D_1 is smaller as compared to other subbands and this remains similar for all the test signals at the same subband. From the behavior of the wavelet coefficients and their statistics, it can be seen that most of the coefficients are small and lie in a very narrow dynamic range around the origin.

The relative wavelet subband energy (RWSE) of the approximation subband (A_J) and the detail subbands $(D_j)_{(1\leq j\leq J)}$ are calculated for the 4-level and the 5-level wavelet transform of the signal are shown in Fig. 6.6. The local energy distribution shown in Fig. 6.6(a) indicates that more energy is concentrated in the lower subbands (A_4, D_4, D_3) with fewer number of coefficients and low energy is concentrated in the

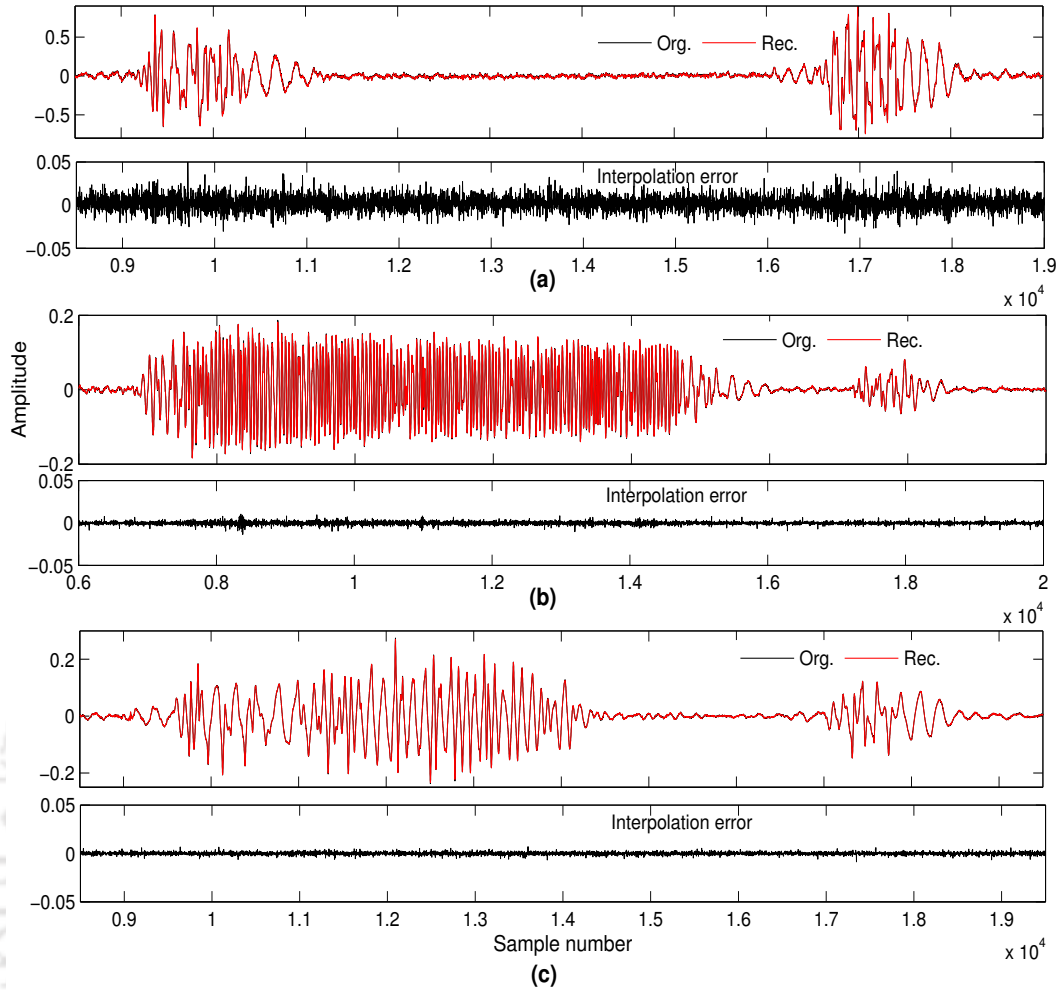

Figure 6.4: Results of the multirate sampling strategy. Three different PCG signals taken from the records in `qdheart` database (Fs=22050 Hz, 16-bit resolution) are down-sampled by factor of 4. The original, reconstructed and error signals for the test records (a) Wav1, (b) Wav20 and (c) Wav30.

higher subbands (D_2, D_1) except for a few PCG signals. It is noticed that the subbands D_1 and D_2 contain most of the energy attributed to the noise and that the noise energy is practically nonexistent at larger scales. For a few signals, the RWSEs of the higher subbands have comparable values. The wavelet coefficients in the higher subbands are important for perfect reconstruction. Hence, zeroing of coefficients in the first level may degrade the quality of the compressed signal. Since the coefficients in the highest frequency subband have significant energy contribution, the wavelet coefficients should not be zeroed directly. As we demonstrated in Section 3.2.2, the performance of a wavelet transform for data compression lies in its ability in concentrating a larger percentage of total signal energy in fewer coefficients. The energy distribution for the 5-level decomposition is shown in Fig. 6.6(b). The experiments shown in Fig. 6.6(b) and Fig. 6.5 demonstrate that the subband A_5 obtained for the 5-level decomposition contain smaller wavelet coefficients and

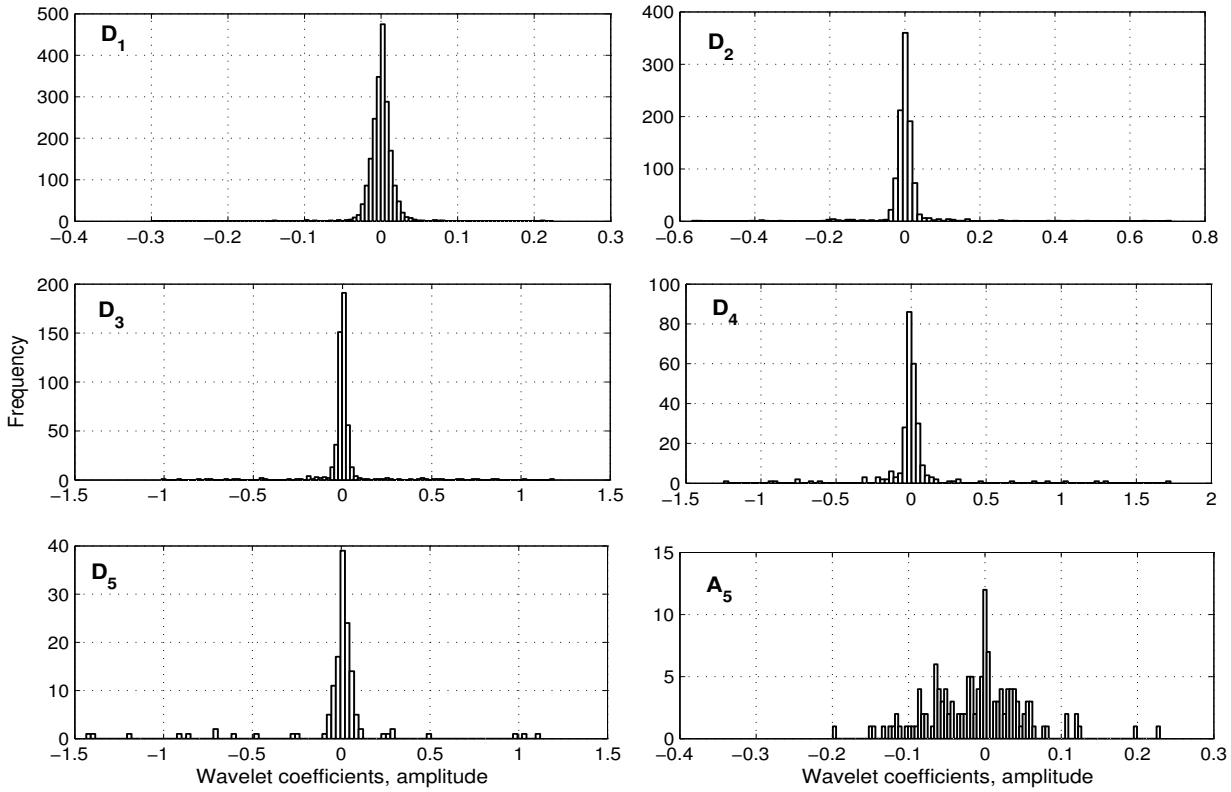

Figure 6.5: Histogram of the coefficients of the PCG signal at each subband. Total number of wavelet coefficients in each subband is: $\{A_5, D_5, D_4, D_3, D_2, D_1\}$=$\{180, 180, 352, 696, 1384, 2760\}$

.

energies compared to the other subbands. It is also noticed that these coefficients are due to signal contents of the PCG signal not from the noises which exists at the higher subbands. The wavelet coefficients in the subband A_5 may be discarded during the thresholding and quantization process since most of the wavelet coefficients in A_5 are small, and this may distort the global shape of the sounds. Reconstruction without wavelet coefficients in approximation subband A_5 and detail subband D_1 is shown in Fig. 6.7. We can see that the wavelet coefficients in lower subband A_5 are important for the reconstruction. In such a case, the further decomposition of the signal may result in a smaller relevant wavelet coefficients and thus signal distortion may be seen during compression. This may affect the diagnostic accuracy. Therefore, they will be quantized with more number of bits which might result in lower compression. However, by considering a higher reconstruction accuracy, the coefficients of the 4-level wavelet decomposition structure is processed in this work. The wavelet coefficients vector (WC) is given by WC = [A_4 D_4 D_3 D_2 D_1]. Experiments show that the modeling of the histograms of the wavelet coefficients is possible for the higher subbands but it may not be feasible for the lower subbands. Each of the subbands has a different energy

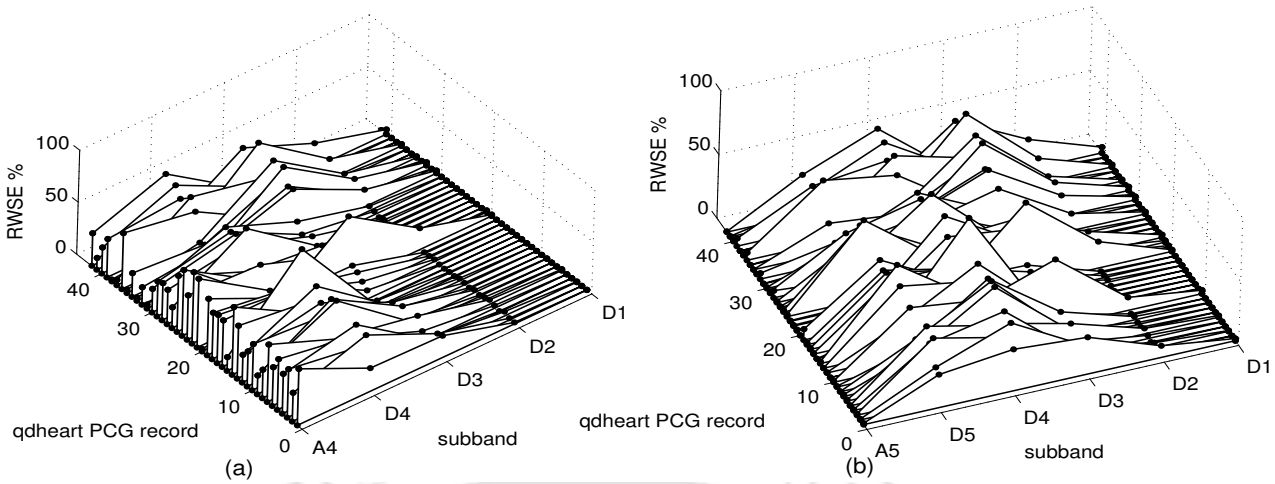

Figure 6.6: Relative wavelet subband energy distributions of the signal blocks taken from `qdheart` PCG records. (a) RWSE distributions obtained for the 4-level decomposition. (b) RWSE distributions obtained for the 5-level decomposition.

level as shown in Fig. 6.6 and variance, with less energy being in the higher detail subbands. Thus, each dataset (each subband or each frame in case of classification) is quantized using a separate quantizer. In this work, these wavelet coefficients are classified into three frames based on the statistical distribution of the coefficients and then compressed based on the presented TCZNUMQ and MIC schemes in Chapter 3.

6.3.3 Coding of the Wavelet Coefficients

Different schemes such as wavelet thresholding, vector quantization and SPIHT methods can be used for coding of wavelet coefficients of the PCG signal. In our previous study [214], the compression of the wavelet coefficients of the PCG signal is attempted using the SPIHT algorithm. In this study, the compression of the wavelet coefficients is performed using the schemes presented in the previous Chapters. For the PCG signal compression, the wavelet coefficients are grouped into three frames, $\{F_1, F_2, F_3\}$ based on the RWSE values of the subbands. The frame classification serves to distinguish between the subband coefficients according to their energy levels for better quantization. These frame coefficients can now be quantized using the presented adaptive quantization scheme, where a different quantizer is used for quantizing each frame. An extensive study in Chapter 3 on the frame classification and the thresholding followed by quantization based compression methods demonstrates substantial gains in wavelet coding applications. Therefore, the data compression is achieved by compression of the wavelet coefficients of the frames using the TCZNUMQ scheme and compression of the significance map using the MIC scheme. After performing the TCZNUMQ process the wavelet indexes stored as shown in Fig. 6.8. It is observed that there is a redundancy between the time indexes of the retained wavelet coefficients. This can be compressed using the MIC scheme.

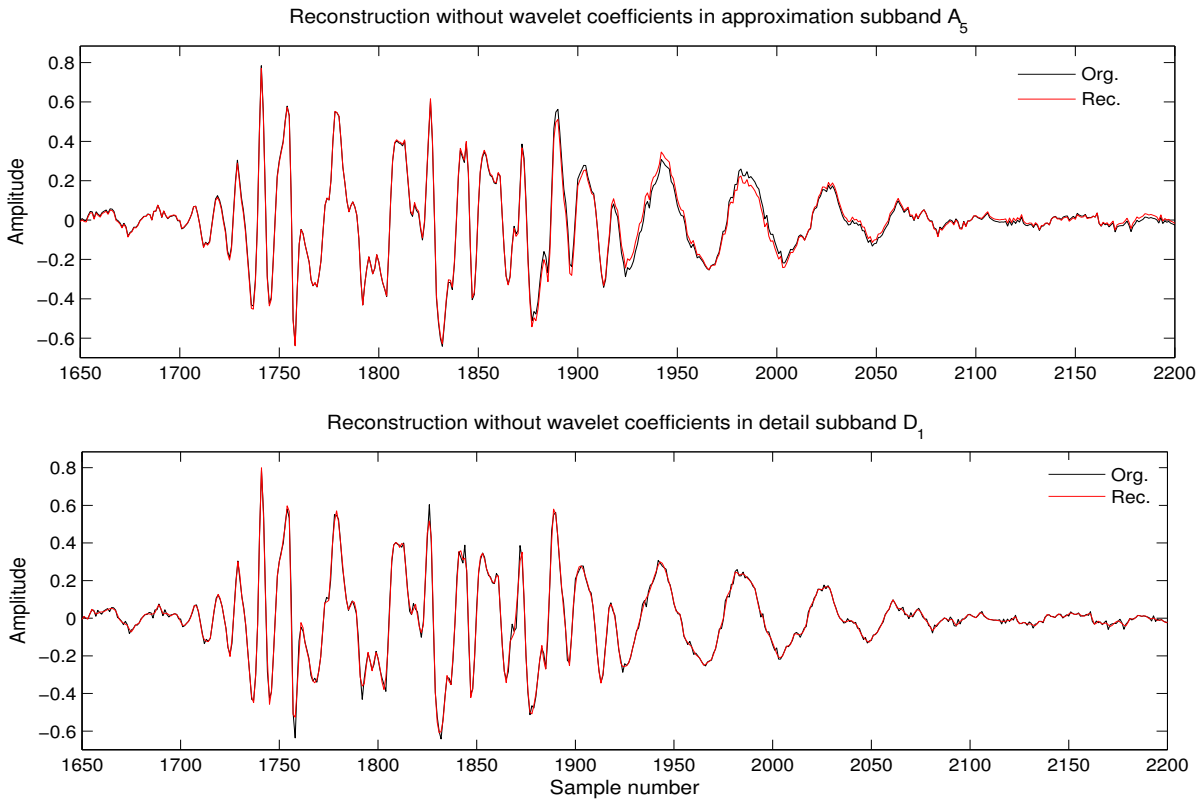

Figure 6.7: Reconstructions without wavelet coefficients in approximation subband A_5 and detail subband D_1. For each reconstruction process, first heart sound of the Wav1 record taken from the `qdheart` database is shown for evaluation purpose.

6.3.4 Distortion Measures

The performance of lossy signal compression methods is measured with compression ratio and distortion. The squared error distortion measures are used for the assessment of the compressed PCG signal. It is well known that the widely used objective measure is the PRD. This PRD measure is performed in time domain whereas PRD_w measure is performed in wavelet domain [212]. The PRD_w measure is defined as

$$\text{PRD}_w = \sqrt{\frac{\sum_{k=1}^{K}[c(k)-\tilde{c}(k)]^2}{\sum_{k=1}^{K}[c(k)]^2}} \times 100 \tag{6.1}$$

where K denotes the number of wavelet coefficients in the vector, $c(k)$ denotes the k^{th} wavelet coefficient of the original signal and $\tilde{c}(k)$ denotes the k^{th} wavelet coefficient of the compressed signal. As we demonstrated in Section 6.2, the correlation between PRD1/PRD_w and clinical quality is not good enough for most test PCG signals. The obvious way of measuring the compressed signal quality is the subjective evaluation by audio/visual perception. But they cannot be incorporated also into automatic quality controlled systems.

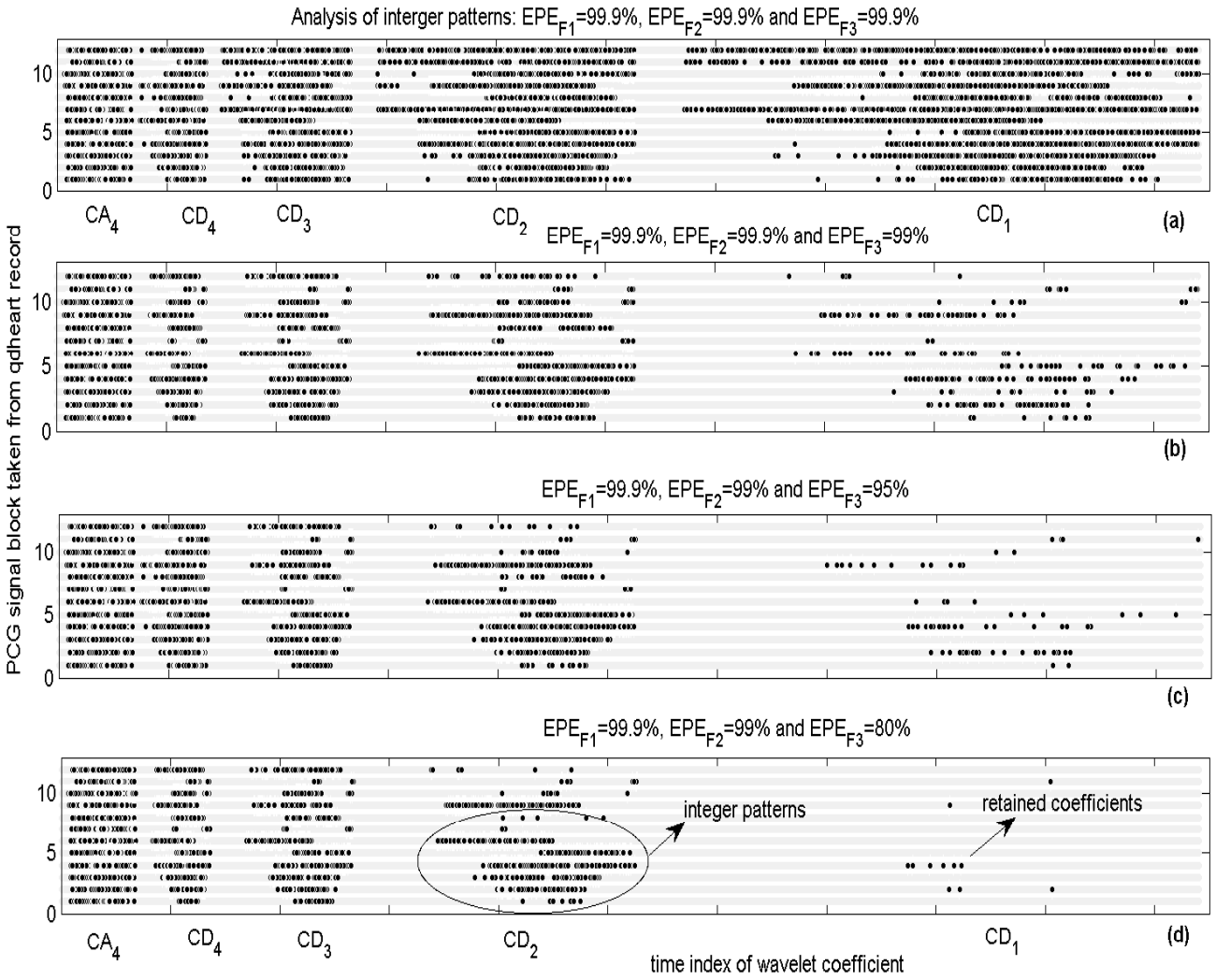

Figure 6.8: Analysis of integer patterns in the ISM vectors: (a-d) Time index redundancy of the retained coefficients for each setting of EPE values.

Table 6.1: Subjective evaluation: The mean opinion score (MOS) rating.

Quality group	Excellent	Good	Fair	Poor	Unsatisfactory
Quality rating	5	4	3	2	1
Level of distortion	No degradation	Little degradation	Somewhat degraded	Fairly degraded	Very degraded

Since the criterion is sensitive to smoothing effect or noise filtering [34], the PRD driven adaptive algorithm cannot provide best rate of the well-designed compression method.

In this work, the performance of the proposed WEDD criterion is tested for the distorted PCG signals. For this test, the clinical quality of the compressed signal is assessed by the subjective evaluation. The main features of the PCG cycle are individually studied and rated in MOS scale as shown in Table 6.1. The

$\text{MOS}_{\text{error}}$ is calculated to correlate with WEDD values. The $\text{MOS}_{\text{error}}$ for z^{th} PCG cycle is given by

$$\text{MOS}_{\text{error}}(z) = \left(\frac{5 - \frac{1}{\text{N}_o \text{N}_f} \sum_{x=1}^{\text{N}_o} \sum_{y=1}^{\text{N}_f} \text{R}(x,y,z)}{5} \right) \times 100 \tag{6.2}$$

where $\text{R}(x,y,z)$ is the rating for y^{th} feature of z^{th} cycle by x^{th} observer, N_f is the number of diagnostic features and N_o is the number of observers. Note that the assessment of heart sounds via audio perceptual quality test is so difficult and thus we have focussed on measuring signal fidelity as a means of assessing visual quality. Typically this comparison involves measuring the distance between the original and reconstructed signals in a perceptually meaningful way. The results of this test is the final one in most of the cases. However, such subjective evaluations are so difficult in many aspects.

6.4 Evaluation of the PCG Compression Method

In this work, the `qdheart` [21] and `CAHM` [22] record databases are used to evaluate the performance of the proposed method and WEDD criterion. The `qdheart` database consists of 42 PCG records which are digitized at a sampling frequency of 22050 Hz with resolution of 16 bits/sample. The `CAHM` database consists of 64 records which are digitized with different sampling frequencies and different resolutions. These databases include different valvular pathologies such as normal sounds, third and fourth heart sounds, heart murmurs (systolic, diastolic), aortic and mitral stenosis, etc. These PCG records are used in the previous work [34, 214]. A direct comparison based only on the numerical results in PRD1 and CR may be misleading because they may be taken in different test conditions such as various records, test PCG signal block, different data length, with or without an entropy coder, filtering effect by the compression method, etc. The coding performances can vary dramatically under different test PCG signal block conditions. Direct comparison of PCG compression methods with PRD1 and CR may not be correct. Therefore, in order to make a standard, the compressed signal quality is measured with WEDD and the MOS tests. The performance of each compression stage is discussed in this section. The computation time for the proposed compression method with and without use of decimation process is shown at the end of this section.

6.4.1 Selection of Signal Block Size

The performance of the DSI algorithm is evaluated using 1-sec (each) PCG signal block taken from the `CAHM` records. The original sample count within the signal block is reduced to N samples using the DSI algorithm. In this experiment, $N = 4096$ and $N = 2048$ samples are chosen for testing purpose and this can be adapted by minimizing the interpolation error. For $N = 4096$ samples from `CAHM` records, the interpolation errors (IE) measured with PRD1 and WEDD are shown in Fig. 6.9(a) and (b). It is observed that the audio and visual perception of the compressed signal quality is good for high PRD1 value obtained for noisy signal

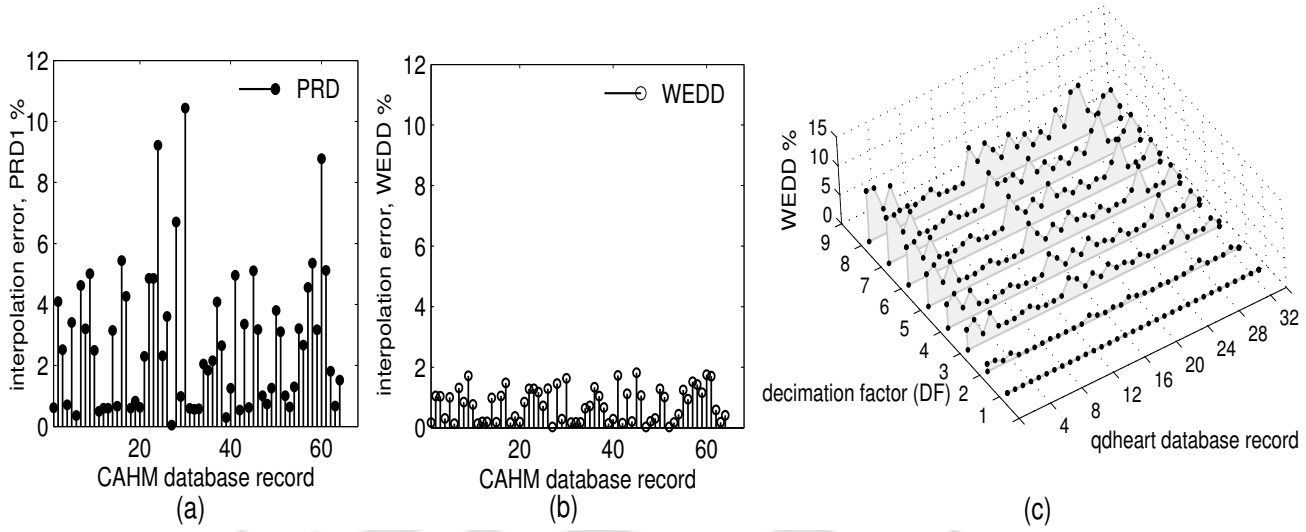

Figure 6.9: Experimental results of the DSI algorithm: Interpolation error (IE) for a processed PCG signal block taken from `CAHM` record. (a) IE measured in terms of PRD1 (%). (b) IE measured in terms of WEDD (%). (c) IE for a processed PCG signal block taken from `qdheart` record.

block. The PRD1 value is dependent on the noise suppression. Therefore, the WEDD is used to measure only the significant information loss. The WEDD value for each interpolated signal is shown in Fig. 6.9(b). The quality of the reconstruction is also assessed by the visual and audio perception. The results show that DSI does not affect the signal quality for these two signal blocks of samples. The WEDD values better correlate with subjective evaluation than the correlation of the PRD1 values. The interpolation errors for different decimation factors are shown in Fig. 6.9(c) for the signal block of 16384 samples taken from the `qdheart` database records. The decimation factor is chosen based on the target error percentage so that the desired percentage of error accuracy is maintained.

6.4.2 Comparison with Other Wavelet Compression Methods

In the first experiment, for different EPE values and quantizer resolutions, each PCG signal block taken from `CAHM` record is compressed independently. The compression results for the threshold values TF_1, TF_2 and TF_3 selected at $EPE_{F1} = EPE_{F2} = 99.9\%$ and $EPE_{F3} = 98\%$, respectively and the 8-bit quantizer resolution are shown in Fig. 6.10. The assessment of results of the compressed signals with distortion measures such as PRD1, WEDD and MOS test are shown in this figure. In Fig. 6.10(d), MOS_{error} for each PCG signal block is shown. This error is the average MOS_{error} value obtained with audio and visual perception tests. The lower the value of the MOS_{error} the better the quality rating of the compressed signal. During the subjective evaluation, the heart sounds in the compressed signal are heard clearly. In this evaluation, signal quality is assessed with respect to the original signal. Typically this comparison involves measuring the distance between the original and the compressed signals in a perceptually meaningful way. For all tested

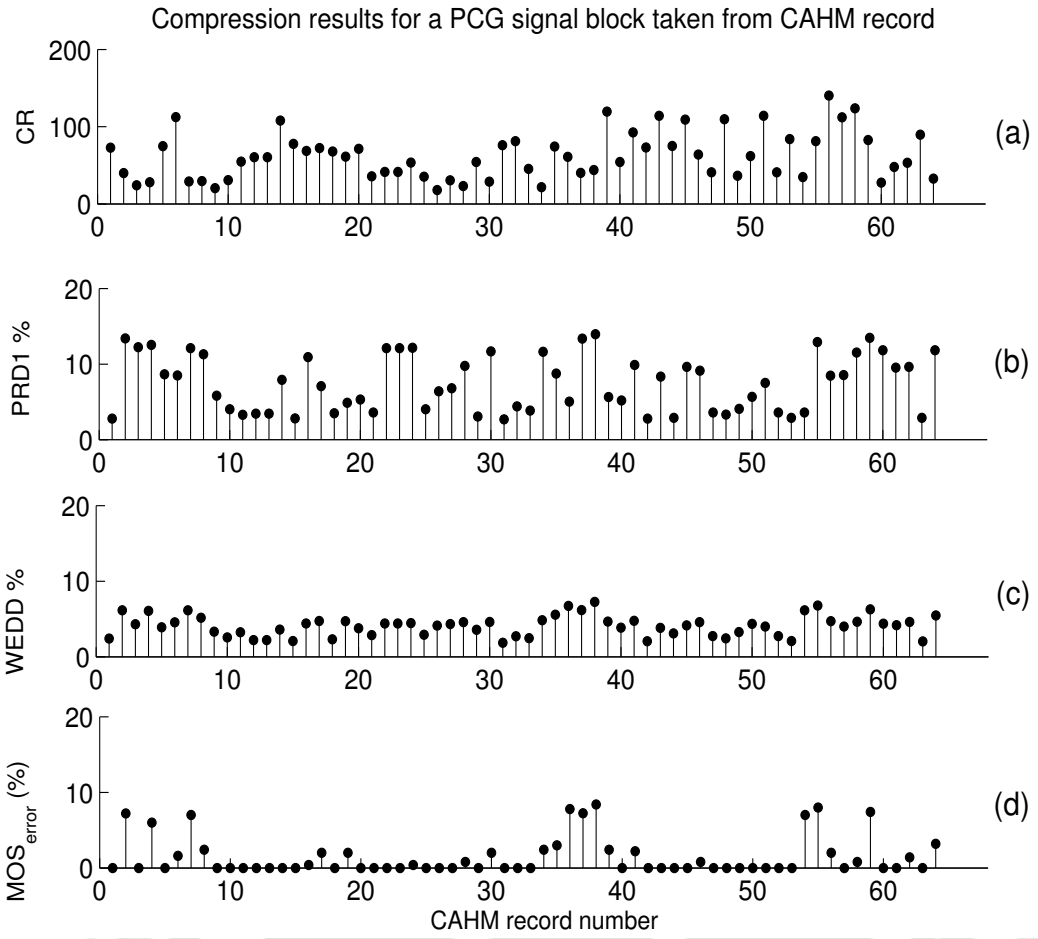

Figure 6.10: Performance of the proposed method for different PCG signals at various sampling rates. (a) CR values for 64 CAHM PCG records compressed with EPE_{F1} = EPE_{F2} = 99.9%, EPE_{F3} = 98% and b = 8. (b) PRD values. (c) WEDD values. (d) MOS_{error} values.

PCG signal blocks taken from each records, the clinical and sound qualities of the compressed signals are assessed. By visual inspection, it is observed that good signal quality is obtained with large PRD1 value for noisy PCG signal blocks. The insignificant errors due to noise suppression is not reflected in measured WEDD values. The WEDD values are correlated well with the MOS_{error} values which are shown in the figure. The experimental results in the figure show that there is a large variation in the CR value for the tested CAHM records. For the above coding parameters, the minimum and the maximum CR value of 18.03 and 140.22 are achieved, respectively. This experiment shows that the CR depends on the specifications of the PCG record such as sampling rate, quantizer resolution, etc. The quality of the compressed signals are degraded when the values of EPE_{F3} and coefficient resolution is below 97% and 8-bit, respectively.

In the second experiment, the signal block taken from 42 qdheart records are considered for testing the procedure of zeroing the first decomposition level using the proposed method. The original block of

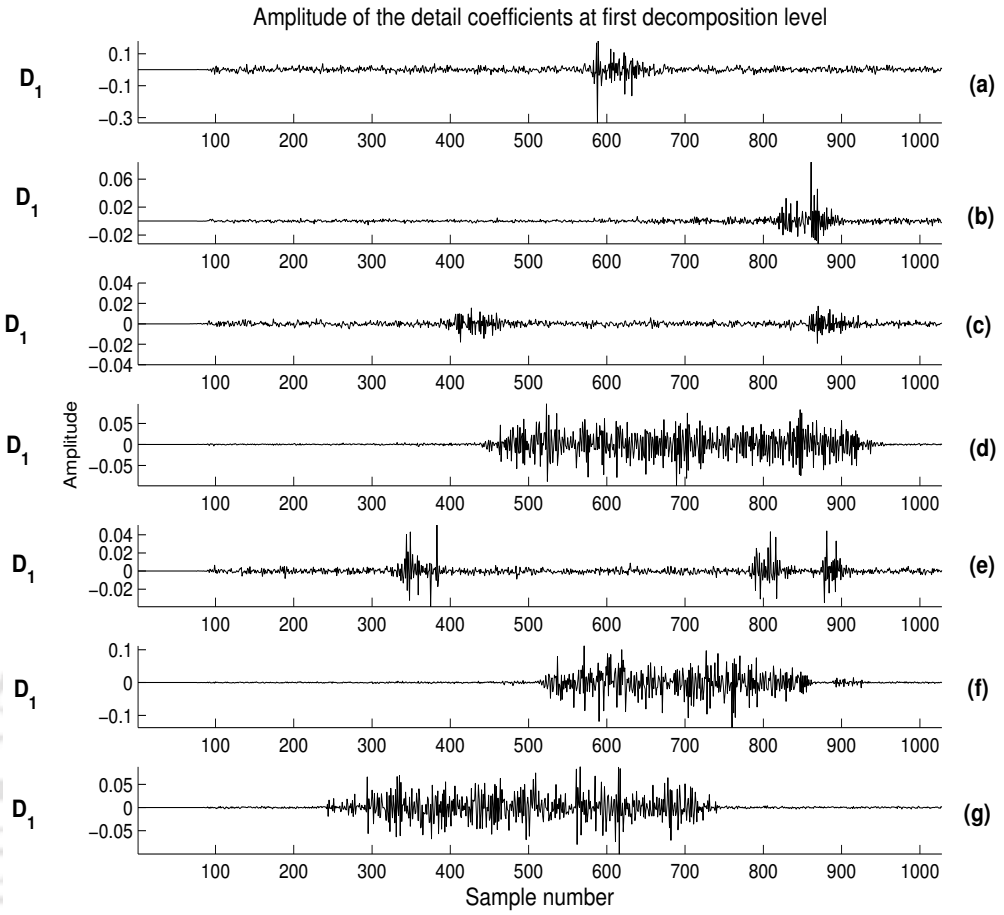

Figure 6.11: Detail coefficients at the first decomposition level for (a) Wav1.wav, (b) Wav11.wav, (c) Wav15.wav, (d) Wav20.wav, (e) Wav27.wav, (f) Wav31.wav, and (g) Wav35.wav.

16384 samples is decimated to 2048 samples. This block size is chosen to demonstrate the role of the significant coefficients in the higher subband. The decimated signal block of 2048 samples is decomposed using the 4-level biorthogonal 9/7 DWT. Fig. 6.11(a-g) shows the wavelet detail coefficients at the first decomposition level for PCG signal blocks taken from `qdheart` record: Wav1, Wav11, Wav15, Wav20, Wav27, Wav31 and Wav35. Examining the detail coefficients shown in Fig. 6.11 shows that the localized coefficients are most important in higher reconstruction accuracy. This is analyzed by reconstructing the signal using the remaining coefficients in the other levels without quantization. The reconstruction errors are estimated using the PRD and WEDD criteria. The RWSE of the D_1 and the error values are shown in the figure. This thresholding procedure, zeroing all the coefficients in subband D_1, results in large PRD1 values which can be seen clearly in Table II of the reported work in [34]. The PRD1 value of 4.4142% is obtained for the signal block taken from the record Wav15 that is lower as compared to values obtained

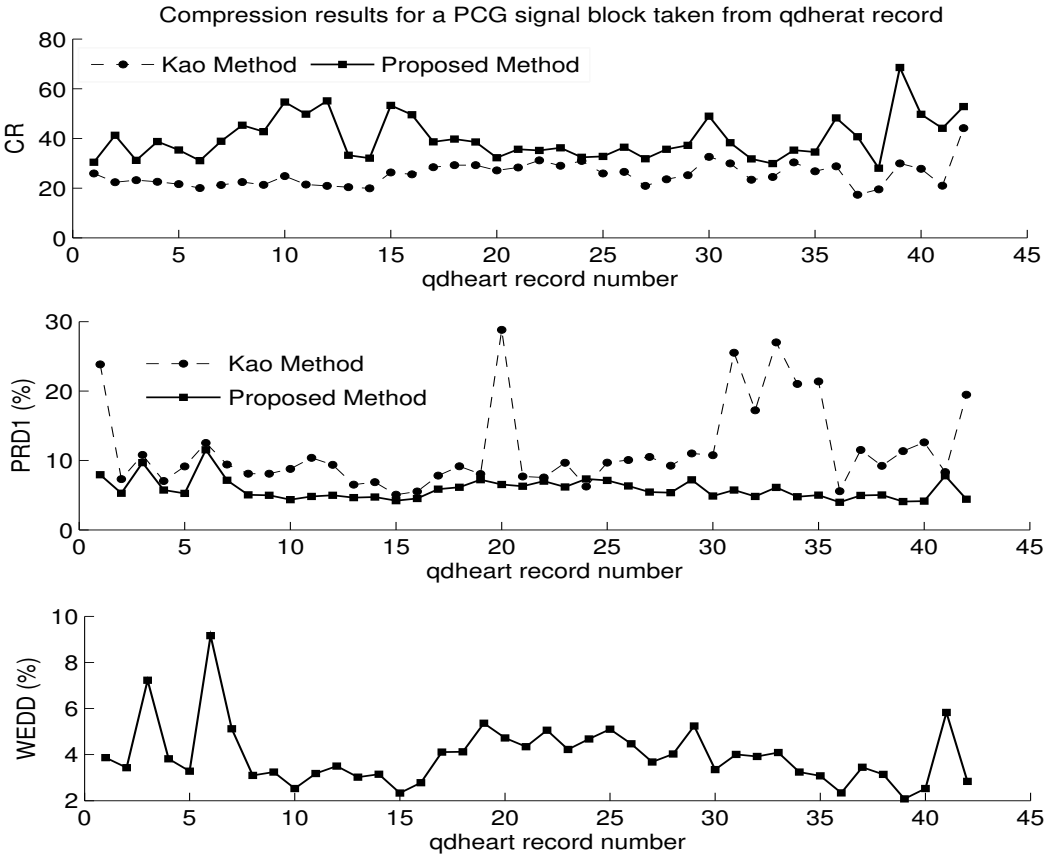

Figure 6.12: Compression performance of the proposed method for the thresholds set $\{0.999, 0.999, 0.999\}$ and the method reported in [34] for the thresholds set $\{0, 0.999, 0.999, 0.999\}$.

for other records. The RWSE of the subband D_1 is 0.1780% which is smaller than others. Since the signal block contains noise, the distortion is evaluated using the WEDD criterion. The WEDD value obtained for the test signal block is 0.2075%. For other test signal blocks, larger WEDD values are obtained when the wavelet coefficients in subband D_1 are removed directly by setting the threshold parameter to zero and the audibility of the compressed signal is degraded significantly.

For comparison purposes, the significant wavelet coefficients are considered based on the desired EPE values. The wavelet coefficients in the frame are compressed using threshold values T_1, T_2 and T_3 selected at $EPE_{F1} = EPE_{F2} = EPE_{F3} = 99.9\%$, 8-bit quantizer and differencing coder. The compression results of the 42 `qdheart` records are shown in Fig. 6.12. The proposed method achieves a minimum and maximum CR value of 28.02 and 68.54 with a PRD value of 5.02% and 4.08%, respectively. The clinical features and the original audio quality are preserved in the compressed signal for the CR achieved as shown in the figure. In many situations, the PCG signal contains noise which may not be important for clinical diagnosis but it provides a nonzero PRD value. Under this situation WEDD provides better evaluation of the compressed signal quality and the measured values are shown in Fig. 6.12. In [34], the high frequency parts in the first

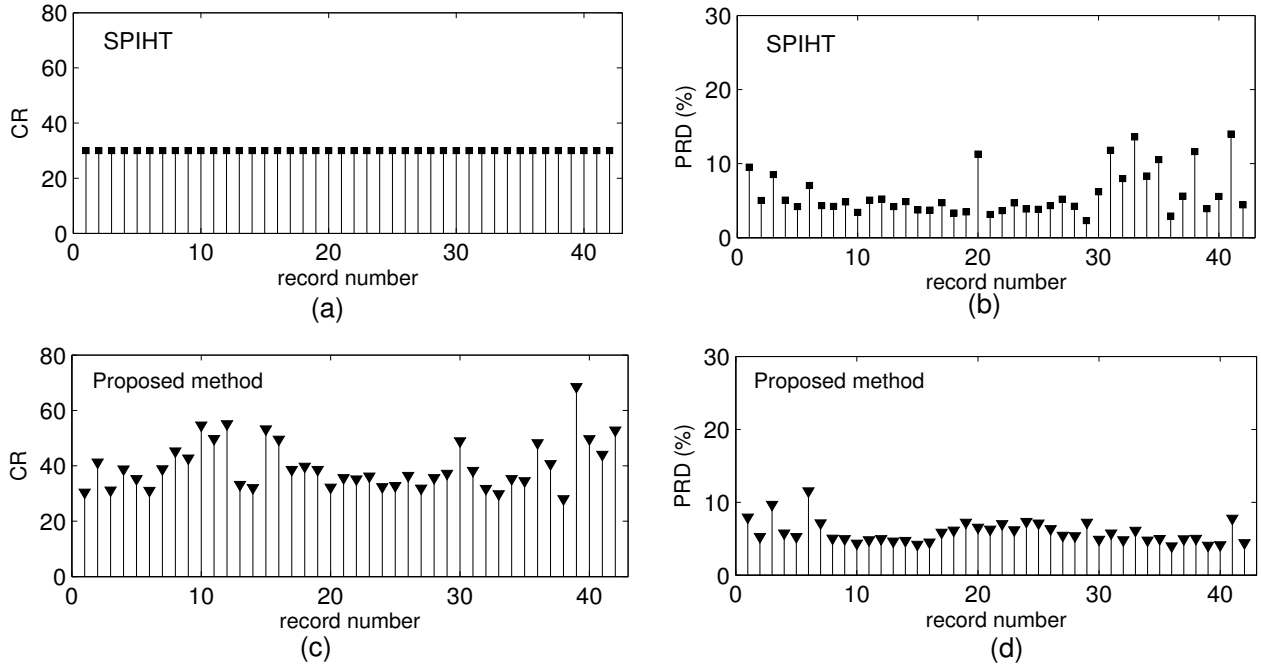

Figure 6.13: Compression results of the proposed method and SPIHT coding based method.

level are removed directly by setting the threshold parameter to zero. This selection may not be pertinent for nonstationary signals. From the Figs. 6.6 and 6.1, it is observed that the RWSE value of the first level (detail band D_1) is considerable for the faithful reproduction. Better compression ratios with lower PRDs are achieved using the proposed method. In Fig. 6.13, the compression performance of the proposed method is compared with SPIHT coding based method [214] for the same PCG signal blocks. The proposed method achieves higher CRs with lower PRD1 values for most of the PCG signal block taken from `qdheart` record. This performance comparison does not consider the amount of noise suppression performed by the coding methodologies. The visual and audio quality of the reconstructed signals for different EPE_{F3} values are analyzed. The reconstructed signals are nearly identical to the original, and the low level background noise is smoothed. The audibility of the heart sounds is good. Higher CR value is achieved with lower PRD value compared to earlier reported results. The audio perception of the error signals are also performed to identify the loss of heart sounds due to the lossy processes such as thresholding and quantization employed in the compression method. The experimental results show that there is no loss of heart sound component and no structured error formation due to the reconstruction of the test signal for the above EPE_{F3} values. The noise filtering capability of the method can be demonstrated in the reconstructed signals of the abnormal PCG signals. All the structural features of the PCG are easily recognized and are faithfully reproduced, and the various heart sounds can be clearly heard and distinguished.

Table 6.2: Performance of the PRD_w and WEDD criteria.

PCG signal block	original S3.wav						original S3.wav+noise						original MS.wav					
	PRD_wtarget of 2%			WEDD target of 2%			PRD_w target of 2%			WEDD target of 2%			PRD_wtarget of 2%			WEDD target of 2%		
	Measured values are given below for each target error criterion																	
	PRD_w	WEDD	CR	PRD_w	WEDD	CR	PRD_w	WEDD	CR	PRD_w	WEDD	CR	PRD_w	WEDD	CR	PRD_w	WEDD	CR
block1	2.02	1.60	33.35	2.55	1.98	37.22	1.98	0.557	11.54	3.28	2.01	36.89	1.95	0.330	1.90	5.81	1.99	6.10
block1	1.95	1.69	23.42	2.35	1.97	24.96	1.99	0.312	8.14	3.27	2.01	24.66	2.02	0.612	1.64	6.07	2.03	3.82

6.4.3 Performance of the WEDD Measure for Distorted PCG Signals

It is observed that in order to ensure that the compressed signals can be properly used for clinical evaluation, the error measure must be taken carefully if noisy signal is compressed. There are several different distortion error measures which are used for quality assessment of the compressed ECG and PCG signals. In this Chapter, performance of the WEDD criterion is therefore used to emphasize the development of quality controlled wavelet compression of biomedical signals. The effectiveness of the widely used distortion criteria such as the PRD/PRD_w and WEDD are analyzed with the noiseless and noisy PCG signal blocks. The iterative algorithm based on target PRD_w/WEDD criterion presented in Chapter 3 is used for this experimental analysis. The algorithm modifies the threshold value to reach the desired error percentage. First two PCG signal blocks with 4096 samples are extracted from the CAHM records: S3.wav and MS.wav which are stored in WAV format with different sampling frequency and different resolution. Each signal block is compressed independently from the other blocks. The CR, PRD_w and WEDD values are calculated for each target error criterion with error percentage of 2% with convergence accuracy of 2.5%. These experimental results are shown in Fig. 6.14 and in Table 6.2. The compression results for the signal block taken from S3.wav shows that WEDD criterion based method achieves higher CR than the PRD_w based method. These CR values are 37.22:1 and 33.35:1, respectively. The CR value of the PRD_w based criterion method is less. Because the desired error percentage accuracy reaches faster with smaller threshold value by including the insignificant errors in the measurement. The threshold value obtained by this criterion may not be an optimum one and it does not reflect the best compression rate of the method. This is demonstrated clearly by compressing the PCG block with signal plus noise. The CR values of 36.89:1 and 11.54:1 are obtained for WEDD and PRD_w based method, respectively. The CR value of the PRD_w criterion based method is drastically reduced. At this stage, the WEDD criterion based method approximately achieves the same CR value of 37.22:1 obtained for the original PCG signal block. The best compression rate of the method is reflected in the WEDD criterion based iterative algorithm. Experiment results shown in the Fig. 6.14 and in the Table 6.2 shows that the WEDD criterion correlates better with the significant distortions in the compressed signal compared to the conventional distortion criteria.

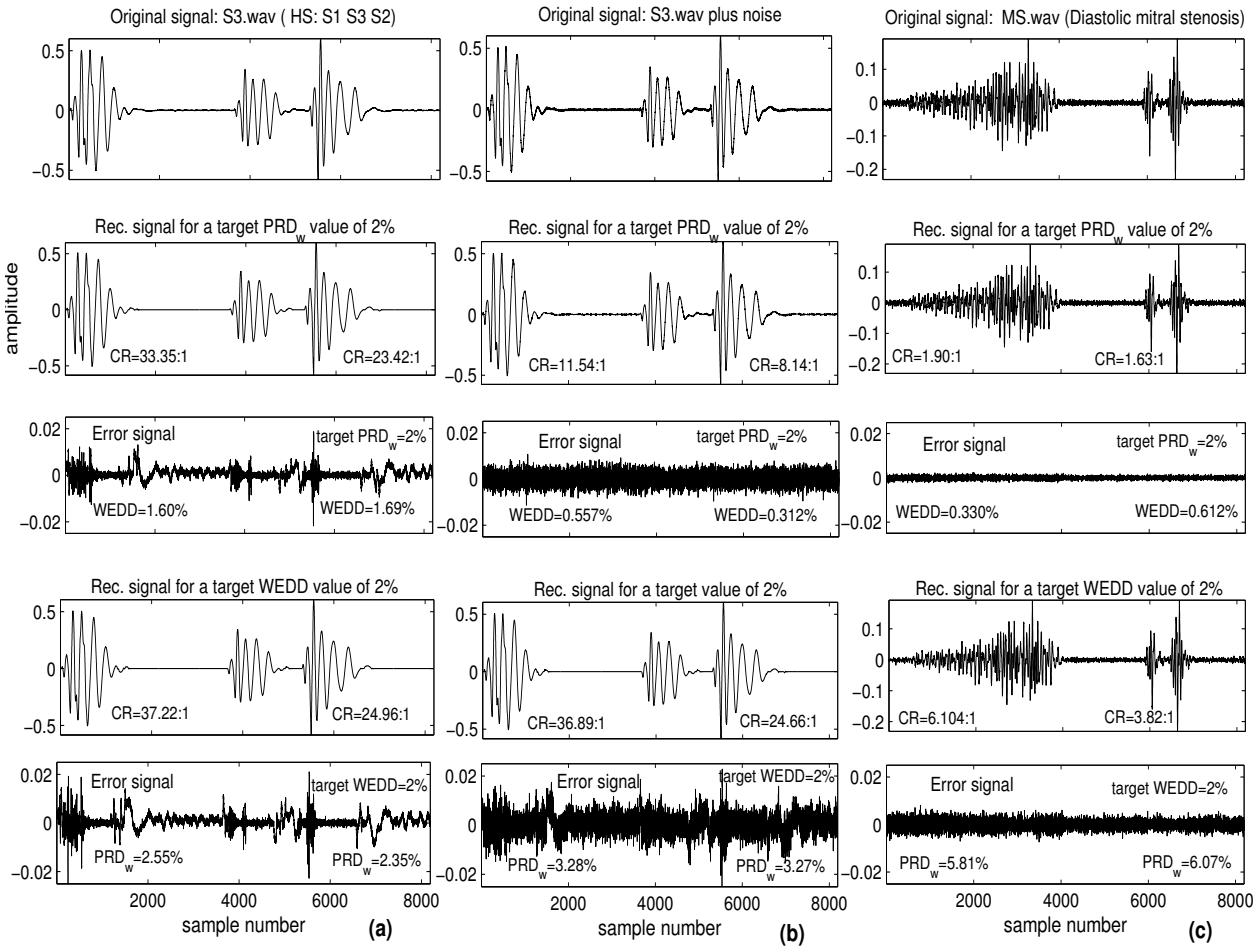

Figure 6.14: Performance of the PRD_w and WEDD criteria. Compression results of the error target criterion based algorithm with the desired error percentage of 2%. Visual inspection of compressed signals: valuation of error signals and their error percentages.

6.4.4 Computational Complexity

In this subsection, computational complexity of the proposed method is discussed. Let us consider M as the number of samples in the PCG signal block and N_i as the number of iterations. The number of operations (additions/multiplications/comparisons/swappings) required in the encoder is calculated for the proposed method with and without DSI algorithm. The computational complexity of the shifted DFT (SDFT) based sinc interpolation algorithms is $O(\mathrm{MlogM})$ operations or $O(\mathrm{logM})$ operations per signal sample [216]. The computational complexity of DSI (forward direction only) is 229376 operations for a PCG signal block of 16384 samples. The computational complexity of the DWT is $2(L_g + L_h)\mathrm{M}$ where L_g and L_h are the number of nonzero coefficients in the high-pass and low-pass filters respectively. For same block size with DF of 8, the complexity of DWT without DSI and with DSI is 524288 operations and 294912 operations, respectively. The order of DWT computation is $O(\mathrm{M})$ [144]. The average case time complexity of the

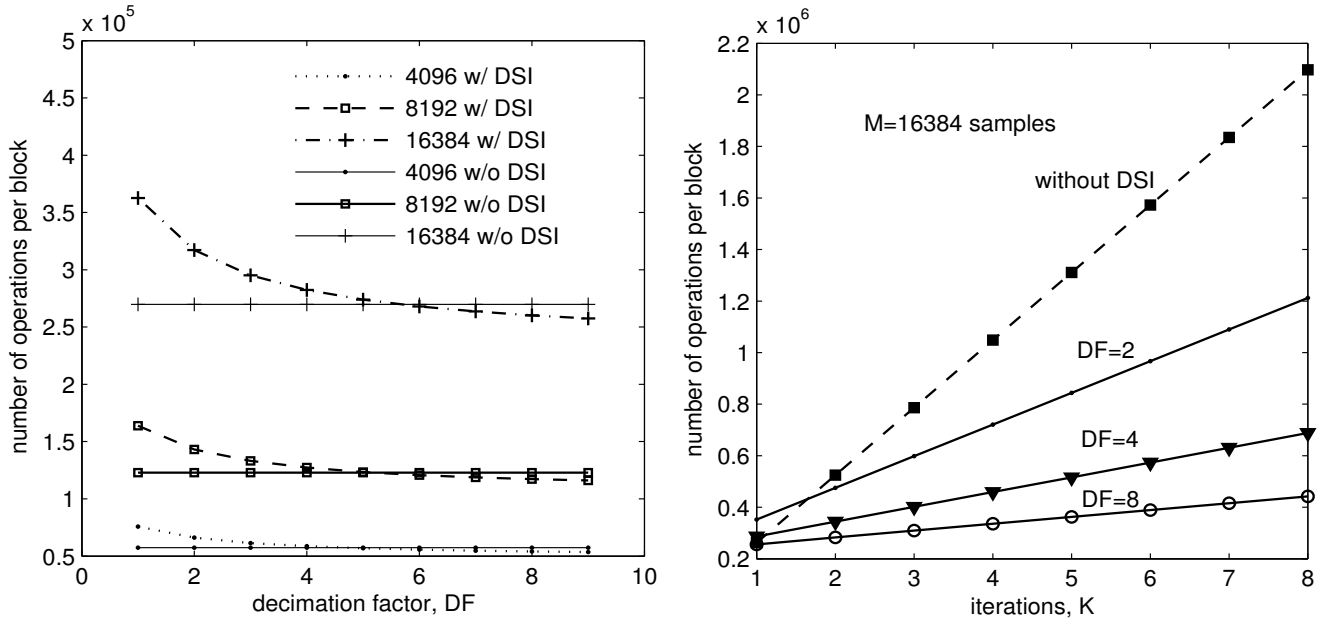

Figure 6.15: Computation time required for the proposed method with and without DSI.

Table 6.3: Average computation time (ms) required for each compression methodology.

stages	DSI	Wavelet	Sorting	Thresholding	ISM vector	Quantization	Differencing	RLE
without DSI	-	15.6	9.6	2.8	2.9	6.4	3.1	1.7
with DSI	2.9	4.4	3.2	1.7	1.8	4.1	1.6	0.82

sorting algorithm is $O(\mathrm{MlogM})$[Quick Sort] [34]. The time complexity of the thresholding function is $O(\mathrm{M})$ operations. The quantization requires one multiplication and addition operation per sample [129]. For quantization section, the complexity depends on the size of the NZTC vector which is controlled by EPE criterion. Therefore, we have calculated the complexity of the method at this stage and shown in Fig. 6.15. The time complexity of the proposed method without DSI is $O(\mathrm{M}) + O(\mathrm{MlogM}) + O(\mathrm{M})$ and with DSI is $O(\mathrm{MlogM}) + O(\mathrm{N}) + O(\mathrm{NlogN}) + O(\mathrm{N})$ where $\mathrm{N} = (\mathrm{M}/\mathrm{DF})$. For M=16384 samples and DF=8, the number of operations without and with DSI is 262144 and 256000 respectively. If we include the number of operations required for quantization and encoding the overall complexity of the proposed method is further reduced.

If the desired target error percentage is greater than the interpolation error value, then the time and memory requirements of the iterative algorithm can be reduced for the proposed method with use of DSI algorithm. At first, the number of samples are reduced by decimation factor and then the decomposition of the decimated PCG signal block is performed using the wavelet transform. Smaller number of wavelet coefficients is processed in the iterative algorithm. The iterative algorithm includes thresholding or/and quantization process. This process iterates until the target error percentage is reached. More time and mem-

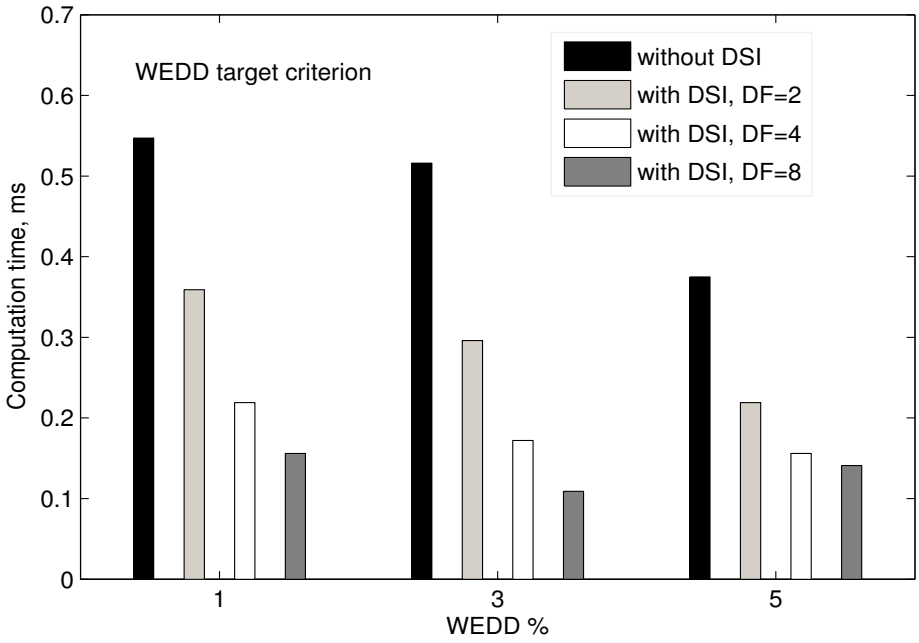

Figure 6.16: Average computation time required for the WEDD criterion based adaptive algorithm with and without DSI process.

ory space is required if the full number of wavelet coefficients of the original signal block is employed in the iterative algorithm. The disadvantage of the proposed method is that the minimum target error value depends on the interpolation error percentage. This may be avoided by selecting decimation factor adaptively. One can claim that the computation time can be reduced if the block size is small. But sometimes the PCG signal block does not contain any clinical information. This is verified in our experiments. Therefore we have considered 1-sec duration signal for testing purpose. The computation time of the proposed method with and without use of the DSI algorithm is evaluated. The DSI step is the lossy portion of the method and hence, the computational complexity is analyzed based on the error criterion rather than the EPE criterion. At this stage, the complete analysis of the interpolation error is important. The computation time required for the proposed method with WEDD criterion, t_e, can be expressed approximately as

$$t_{\mathrm{e}} \;=\; t_{\mathrm{dsi}} + t_{\mathrm{dwt}} + [K \times (t_{\mathrm{ti}} + t_{\mathrm{WEDD}})] + t_{\mathrm{fe}} \tag{6.3}$$

where, t_{dsi}, t_{dwt}, t_{WEDD} and t_{fe} denotes the time required for the DSI implementation, DWT implementation, the WEDD calculation and the final encoding process, respectively. K is the number of quantization b used for rate-distortion optimization and t_{ti} is the total execution time required for iteration per quantization bit which is calculated as, $t_{\mathrm{ti}} \;=\; N_i \times (t_{\mathrm{thresh}} + t_{\mathrm{quantizer}} + t_{\mathrm{entropy}})$. The value of $t_{\mathrm{fe}} = 0$ when $K = 1$. On HCL PC with Microsoft Windows XP, Intel Pentium-4 3.4 GHz CPU, 512 MB RAM and MATLAB 7.0, the time required for the proposed method is calculated. Fig. 6.16 and Table 6.3 gives the times required to compress

a PCG signal block using the proposed compression method and iterative algorithm with WEDD criterion, respectively. The number of iterations depends on the convergence accuracy, the value of the target WEDD or compression rate criterion and the optimization procedure. The complexity of the Huffman coding with RL coding is shown in Fig. 6.16(b) with and without DSI process. The average computation time is less for the Huffman coding with DSI process. Experiments show that the maximum computation time required for the proposed method is less than the duration of the test PCG signal block.

6.5 Results of Quality Controlled PCG Compression

Guaranteeing the quality of a biomedical signal in lossy compression methods is most important since a highly distorted signal can be useless from a clinical point of view. In most of the wavelet based methods, the resulting wavelet coefficients are compressed iteratively until a predefined PRD_w is obtained with a desired tolerance ε. Although PRD_w is easy to calculate and compare, this criterion is not a subjectively meaningful measure since small and large numerical distortions do not correspond to "good" and "bad" subjective quality, respectively. This may lead to confusion in the judgement of the quality of the compressed signal. The PCG database contains many different valvular pathologies and noises. In this case, noise filtering effect can be seen in wavelet transform based compression methods and thus large PRD_w can be obtained for a better compressed signal quality. Moreover, noise decreases compression rate of the coder for a desired PRD value since the coder will spend extra bits on approximating the noise with the specified accuracy.

In this section, we present a simple and efficient method for guaranteeing compressed quality measured using the WEDD metric which reflects in a more accurate way the signal distortion of the compressed signal than the other measures. This property is demonstrated using the two PCG signals with different valvular pathologies. The test signals are taken from the records Wav1 and Wav56 in the CAHM database. These two signals represent the normal heart sound and severe systolic aortic stenosis, respectively. A simulation study is presented where noisy PCG signals are generated from actual PCG records from CAHM database and adding simulated Gaussian white noise. The effectiveness of the three quality measures such as PRD_w, WWPRD and WEDD is shown in Fig. 6.17 for different values of SNR (in dB). The classical wavelet denoising process, based on the Donoho et al. algorithm, is used for this study. The quality of the denoised signals are measured using three criteria which produces three different values. When the noisy signal is compressed, the error signal includes signal error and noise error. If we employ the widely used PRD_w measure between the reconstruction and the noisy signal we can get high values of PRD_w due to the presence of the unwanted noise. The cross validation of the quality reconstruction shows that large values obtained in the PRD_w and WWPRD are due to inclusion of insignificant errors, that are not well correlated with the better quality of the reconstructions. To illustrate this, the original, noisy, reconstructed and error signals are shown in Fig. 6.18. It shows the reconstructed signals when Gaussian white noise is added to the original signals with an SNR=20 dB. The subjective evaluation of the reconstructions establishes that

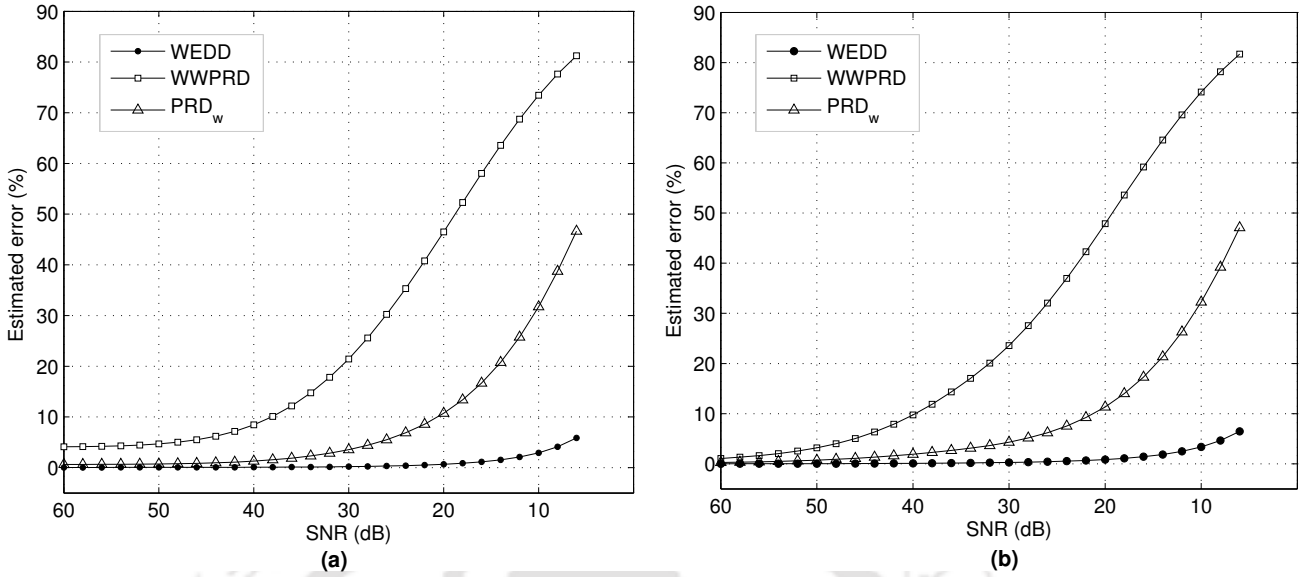

Figure 6.17: Performance evaluation of the distortion criteria such as WEDD, WWPRD and PRD_w in the cases where the data contain signal plus noise: (a) For the PCG signal block taken from the CAHM Normal Heart record. (b) For the PCG signal taken from the CAHM Severe Systolic Aortic Stenosis record. This shows the sensitivity of the objective measures with respect to the noise level present in the original (or reference) signal.

the audibility of the heart sounds are comparable with the original heart sounds. It can be seen that for SNR=20 dB and above, the wavelet based denoising algorithm produces smoothed reconstruction. But the amount of distortion estimated using the PRD_w and WWPRD measures are larger in the case of "excellent" and "very good" reconstructions. The four sets of error values are measured to investigate the performance of the local and global error measures by using the WEDD and WWPRD criteria. The measured values are shown in Table 6.4 and the original, noisy and denoised and error signals, from top to bottom are shown in Fig. 6.18. It is observed that the WEDD measure reflects in estimation of signal errors rather than noise errors across the subbands. Thus, the local and global error values of the WEDD measure correlate well with subjective results. The complete remarks on this experiment are listed in Table 6.4. Experiment shows that the denoising tends to add some amount of denoising artifact to the input signal and if the input noise level is low, the denoising might not serve to improve the quality of the signal. In such a case, WWPRD values measured between the input and denoised signals are large even for a good signal quality. However, the WEDD criterion appears to be a correct representation of the amount of signal distortion at all subbands. The global and local assessments of the signal quality show that the WEDD increases when the signal error increases and the influences of the insignificant errors in some higher subbands are negligible. This property can be seen by correlating the experimental results shown in Figs. 6.17 and 6.18. The compression results with large PRD and WWPRD values are obtained although most of the removed components are irrelevant from the point of signal reconstruction. This experiment shows that such measures do not provide accurate

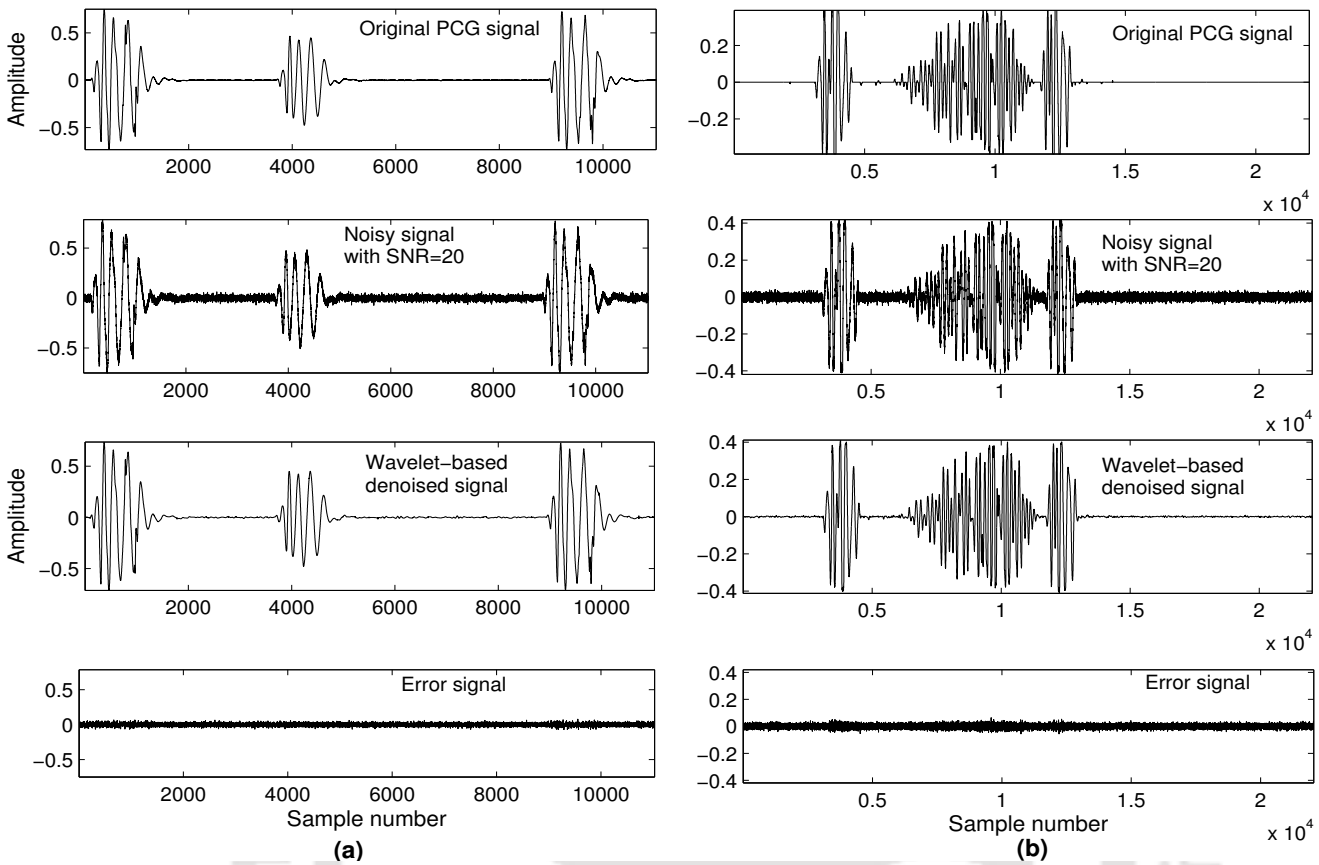

Figure 6.18: Evaluation of WEDD and WWPRD measures under noisy conditions. (a) Original PCG signal, noisy signal with SNR=20 dB and denoised PCG signal of CAHM Normal Heart record. The error values measured between the noisy and denoised signals are WEDD=0.4307%, WWPRD=38.97% and PRD_w=10.02%. The error values measured between the original and denoised signals are WEDD=2.565%, WWPRD=7.2% and PRD_w=3.26%. (b) Original PCG signal, noisy signal with SNR=20 dB and denoised PCG signal of CAHM Severe Systolic Aortic Stenosis record. The error values measured between the noisy and denoised signals are WEDD=0.5349%, WWPRD=39.77% and PRD_w=10.47%. The error values measured between the original and denoised signals are WEDD=2.66%, WWPRD=11.13% and PRD_w=4.359%.

predictions of quality. The experimental results in Fig. 6.17 and in Table 6.4 demonstrates that the WEDD measure reflects in signal distortion in the case of input signal with background noise. In such a case, the noise decreases the compression rate for a specified distortion level measured in PRD_w and WWPRD that is clearly observed in the previous section. Therefore, a distortion-driven wavelet coding scheme with the WEDD measurement criterion for the PCG signals is presented in this section.

The quality controlled compression algorithm with WEDD criterion is tested for the PCG signals. The test PCG signals are taken from the CAHM database which includes records of many different valvular pathologies (normal sounds, third heart sound, fourth heart sound, late systolic, ejection click, tricuspid regurgitation, diastolic aortic insufficiency, murmurs and noises, etc.). Furthermore, the PCG records are

Table 6.4: Performance of local and global error measures for different conditions of distorted and reference signals. Original PCG signal taken from the CAHM Normal Heart record.

Noise SNR	Distortion Measure	A_4 (%)	D_4 (%)	D_3 (%)	D_2 (%)	D_1 (%)	Total (%)	Remarks on the error measures done for different reference and processed signals; x_o,x_n and x_d are the original, noisy and denoised signals, respectively.
20 dB	WEDD(x_o,x_n)	2.4888	0.1042	0.0165	0.0041	0.0034	2.6169	Measures the signal errors introduced by noise; the higher bands include noise;
	WEDD(x_o,x_d)	2.4857	0.0753	0.0042	0.0003	0.0002	**2.565**	Measures the signal errors w.r.t the signal x_o;A_4 dominates but considerable;
	WEDD(x_n,x_d)	0.0774	0.1515	0.0675	0.0702	0.064	**0.4307**	Measures the signal errors w.r.t the x_n; It may provide the denoising artifacts;
	WEDD(x_o,x_d)	0.0274	0.0092	0.0011	0.0002	0.0002	0.0382	Measures the signal errors w.r.t the x_o; No noise is added to the original x_o;
	WWPRD(x_o,x_n)	2.343	1.435	3.931	16.458	33.021	57.18	Insignificant errors in bands D_2 and D_1 dominates global; Very poor correlation;
	WWPRD(x_o,x_d)	2.3405	1.0368	0.9924	1.0382	1.7925	**7.2004**	It measures both the signal errors and noise errors due to the noise filtering;
	WWPRD(x_n,x_d)	0.0464	2.2958	5.2518	10.8241	20.5503	**38.968**	It measures the noise errors knows as insignificant errors;
	WWPRD(x_o,x_d)	0.0258	0.1272	0.2716	0.8945	1.7205	3.0396	High values are obtained due to background noise in the x_o;
35 dB	WEDD(x_o,x_n)	0.4426	0.0185	0.0029	0.0007	0.0006	0.465	Measures the signal errors; Maybe suitable for communications channel testing;
	WEDD(x_o,x_d)	0.4414	0.0222	0.0022	0.0002	0.0002	**0.466**	Measures the signal errors; Useful for denoising method testing case;
	WEDD(x_n,x_d)	0.0203	0.0285	0.0042	0.0024	0.0022	**0.056**	For R-D optimization scheme and simultaneous denoising and compression;
	WEDD(x_o,x_d)	0.0274	0.0092	0.0011	0.0002	0.0002	0.0382	Provides the performance of denoising method when the input noise is low;
	WWPRD(x_o,x_n)	0.4167	0.2552	0.699	2.9267	5.8721	10.17	This may help to know the presence of noise in the input;
	WWPRD(x_o,x_d)	0.4156	0.3053	0.5258	0.9474	1.723	**3.917**	Maybe good if no noise present in the reference signal but less feasible.
	WWPRD(x_n,x_d)	0.0177	0.4236	1.2664	2.9608	5.6352	**10.304**	Predictions of quality of the processed signal is poor for the noisy signals case;
	WWPRD(x_o,x_d)	0.0258	0.1272	0.2716	0.8945	1.7205	3.0396	Not suitable for evaluating the system performance under noisy conditions.

digitized with different sampling rates and resolutions. For different values of WEDD, the PCG signals are compressed and the signal qualities are assessed by subjective evaluation where the similarity between the original signal and the reconstructed one is rated in the Boolean question about the diagnosis (1-YES, 0-NO). The compression results of this experiment are shown in Table 6.5. The algorithm reaches the desired quality specification accurately, quickly and smoothly for all test signals. For each value of WEDD, the compression ratio is computed and the assessment of quality of the compressed signal is performed. Note that the test signals contain different clinical information such as low-frequency and high-frequency sounds. Experiment shows that the compression ratio of the scheme varies according to the clinical information for a given distortion specification. For WEDD=4%, the maximum compression ratio of 186.07 is achieved for the test signal from the Diastolic Fixed S2 Split II record and the minimum compression ratio of 21.16 is obtained for the signal from the Diastolic Atrial Septal Defect record. To reveal the visual quality of the compressed signals, the original signal and the compressed signals obtained for a WEDD value of 4% of the Diastolic Fixed S2 Split II and Diastolic Atrial Septal Defect records are shown in Fig. 6.19. It can be seen that the clinical features are well preserved in the compressed signals and the main effect of the proposed scheme is the smoothing of background noise. However, it is noticed that the clinical features are distorted for a WEDD value of 5% and above. Thus, the WEDD value of 4% may be fixed for the test signals. But there is no optimal selection of distortion when guaranteeing signal quality since it depends on the clinical

Table 6.5: Performance of the proposed quality controlled PCG compression for a user-specified WEDD and the assessment of quality of the compressed signals.

	WEDD=1%		WEDD=2%		WEDD=4%	
PCG record	CR	Quality	CR	Quality	CR	Quality
Normal Heart	61.05	Acceptable	93.28	Acceptable	125.64	Acceptable
Normal Split	70.61	Acceptable	91.30	Acceptable	123.78	Acceptable
S3	56.41	Acceptable	71.85	Acceptable	93.03	Acceptable
S4	56.99	Acceptable	78.60	Acceptable	109.22	Acceptable
Early Systolic	44.90	Acceptable	58.17	Acceptable	99.38	Acceptable
Diastolic Tricuspid Stenosis	18.29	Acceptable	26.25	Acceptable	41.93	Acceptable
Diastolic Pulmonic Regurgitation	6.85	Acceptable	15.05	Acceptable	28.87	Acceptable
Diastolic Fixed S2 Split II	86.72	Acceptable	133.3	Acceptable	186.07	Acceptable
Diastolic Atrial Septal Defect	9.79	Acceptable	15.04	Acceptable	21.16	Acceptable
Diastolic S4 Gallop	53.53	Acceptable	89.18	Acceptable	141.91	Acceptable
Diastolic Summation Gallop II	20.71	Acceptable	39.64	Acceptable	55.62	Acceptable
Systolic Mitral Regurgitation	9.47	Acceptable	13.58	Acceptable	21.28	Acceptable
Systolic Mitral Prolapse 3	6.56	Acceptable	15.12	Acceptable	28.63	Acceptable
Systolic Mitral Value Replacement	7.29	Acceptable	10.84	Acceptable	28.25	Acceptable
Ejection Murmur	22.85	Acceptable	44.48	Acceptable	65.89	Acceptable
Aortic Stenosis 2	62.18	Acceptable	79.29	Acceptable	109.25	Acceptable
Critical Systolic Aortic Stenosis	21.55	Acceptable	29.55	Acceptable	39.58	Acceptable
Systolic Ventricular Septal Defect	13.74	Acceptable	20.44	Acceptable	29.16	Acceptable

accuracy required. However, an optimal selection in WEDD scale leads to provide a better guaranteeing signal quality than in PRD_w and WWPRD scales.

As stated above, one of the major problems with PCG is noise corruption from the contact of the recording device with the skin to the sounds of breath [34]. The proposed wavelet based PCG compression algorithm efficiently removes the high frequency noises while keeping the major features such as S1, S2, S3, S4 and murmurs, etc. The audibility of clinical features are more clear than the original ones for some noisy signal. The compression method with TCZNUMQ and MIC schemes achieves higher compression rate while keeping the important heart sounds more audible. In this experiment, the multirate sampling strategy is employed to reduce the computational complexity of the quality driven wavelet coding algorithm. This strategy may degrade the coding performance when compressing a relatively high frequency heart sounds (e.g., an ejection click, systolic aortic stenosis and murmurs, etc.). In order to preserve clinical information, the multirate sampling process is avoided in the proposed method for those test signals. Thus, the computational complexity of the adaptive wavelet coding method is high in this case. Meanwhile, during the cross validations, a long-interval silent event is seen in each cycle of the test signals. This property shows that the

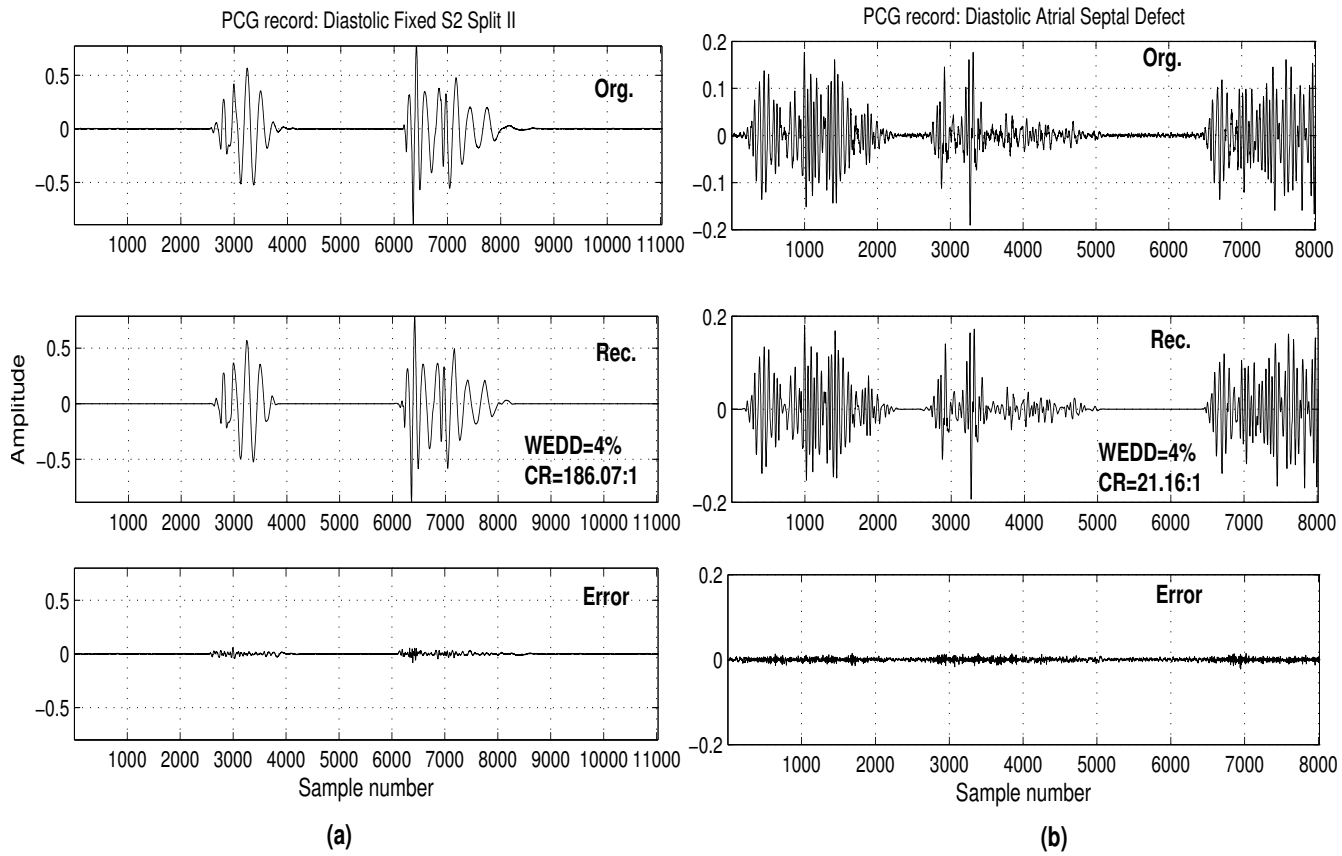

Figure 6.19: Performance of the proposed method for different clinical information. (a) Original and reconstructed PCG signal of CAHM record Diastolic Fixed S2 Split II. Reconstructed signal for WEDD=4% (CR=186.07:1, PRD1 =6.19% and WWPRD=14.6983%). (b) Original and reconstructed PCG signal of CAHM record Diastolic Atrial Septal Defect. Reconstructed signal for WEDD=4%(CR=21.16:1, PRD1 =8.144% and WWPRD=19.72%). Note that the 1-sec PCG signal is presented here.

computational cost can be reduced by extracting the long-interval silent and short-interval sound events of the input signal. Therefore, in this case, effective algorithms for the segmentation are necessary. Continuing our research work, we will attempt to find a robust wavelet based heart sound segmentation scheme which can integrate with the latter preprocessing stage.

भारतीय प्रौद्योगिकी संस्थान गुवाहाटी
Indian Institute of Technology Guwahati

7

Summary and Conclusions

Contents

7.1 Summary of the Work

In this thesis, an adaptive wavelet based compression scheme for cardiovascular signals was presented. In order to design a quality controlled wavelet compression of cardiovascular signals, the three most important components required are: a well-designed adaptive subband coding methodology, a meaningful objective quality measure, and a simple quality controlling algorithm. This research work attempted the compression issues involved in the above three components to develop a better automatic quality controlled compression system.

In Chapter 3, a better adaptive wavelet coding scheme was presented based on the preprocessing, 5-level 9/7-tap filters wavelet decomposition, energy based classification of coefficients, optimal constraint threshold control zero-zone nearly uniform midtread quantizer, modified index coder and Huffman coder. The preprocessing step involved the blocking of incoming ECG signals into non-overlapped blocks of N samples and the mean removal. In this work, the maximum block size was 4096 samples, which is equivalent to 11.38 seconds by considering the computational cost. Once the signal block was decomposed using the multiresolution signal decomposition technique, statistics of the wavelet coefficients at each subband was computed to perform classification of coefficients before compression process for achieving substantial gains in coding performance. The study showed that each of the subbands had a different energy level, dynamic range and variance, with less energy being in the high detail subbands. The relative wavelet subband energy (RWSE) was introduced to provide information about the relative energy associated with different frequency bands present in the ECG/PCG signals. The resulting energy distribution provided a suitable tool for detecting and characterizing signal contents and then the classification into frames was performed that served to distinguish between the subband coefficients according to their relative energy levels. These classified wavelet coefficients were quantized using the presented threshold control zero-zone nearly uniform midtread quantization (TCZNUMQ) scheme in an adaptive manner where a different quantizer was used for quantizing each frame. The TCZNUMQ scheme presented was completely specified by the two design parameters: the zero-zone width and the outer-zone width and the reconstruction value as the center of a zone. In our quantizer design, the zero-zone width was limited by threshold T which allowed to perform signal denoising where the zero-zone width equals noise threshold parameter T_B and the outer-zone width was chosen according to specific applications. For the two-stage scheme, the quantizer design with constraint on the relationship between T and Δ reduces the computation cost when searching for an outer-zone width Δ with a zero-zone width T found in the first stage thresholding algorithm. In quality or rate driven subband coding, the zero-zone width and outer-zone width was adapted to achieve the optimal compression performance. For each signal block, the algorithm starts by searching for the allowable region of the zero-zone width and then searches for optimal outer-zone width and viceversa depending on the criterion specific. This strategy efficiently located the allowable region of the T and Δ as well as reduced the computation cost of the adaptive algorithm. In our two-stage design, the constraint allowed us to reduce the computation time

from $K-1$ to 1 when searching for the optimal outer-zone width for the given zero-zone width. For each signal, the wavelet coefficients vector was thresholded and quantized using the optimal design parameters set. Experiment showed that more energy is concentrated in a few wavelet coefficients that appear very close in the order sequence within a subband. Therefore, the integer significance map (ISM) was created by storing the indexes or locations of the significant coefficients and then the ISM was compressed using the MIC scheme. The performance of the MIC scheme was better than the conventional scheme used for compression of significance map.

Using the above compression methodologies, the target distortion level (TDL) and the target data rate (TDR) driven wavelet compression algorithms were presented. The present work described a method to define the threshold T and quantization bit b such that it minimizes the distortion for a given rate or it minimizes the estimated entropy of the coefficients for a given distortion. The compression performance of these two algorithms was evaluated in terms of number of iterations required to reach a desired specification, quality of compressed signal and coding delay. The data rate variability of TDL algorithm was analyzed under different signal conditions such as mean value variation, noise level and time varying PQRST morphologies. Issues related to real time implementation using fixed block length and fixed data length were also addressed. It was observed that the PRD criterion is not a subjectively meaningful measure since the small and large numerical distortions did not correspond to "good" and "bad" subjective quality, respectively. Experiments showed that the wavelet based method may produce smooth reconstructed signal. Thus, the compression errors include both signal error and noise error. The noise in the input decreases the compression rate of the coder since the coder will spend extra bits on approximating the noise with the specified accuracy. Thus, the distortion measurement criterion played an important role for choosing a set of optimal coding parameters. Therefore, we focussed on the evaluation of the TDR algorithm rather than the TDL algorithm in this Chapter. In this case, the subjective evaluation was used to quantify the dissatisfaction of the compressed ECG signal. The ECG compression based on SPIHT coding scheme was also implemented and considered as a reference for comparison since it had the best compression performance. The compression results of proposed methods and SPIHT based ECG coder were shown in this chapter. The compressed signal quality was evaluated by verifying the diagnostic features of the original and decompressed signal which was referred to as correct diagnosis test in this work. For each set of ECG data the CR bound was determined after correlating the percentage of correct diagnosis and the compression rate. Three sets of ECG data from three different databases, the MIT-BIH Arrhythmia (`mita`) (F_s = 360 Hz, 11 b/sample), the Creighton University Ventricular Tachyarrhythmia (`cuvt`) (F_s = 250 Hz, 12 b/sample) and the MIT-BIH Supraventricular Arrhythmia (`mitsva`) (F_s = 128 Hz, 10 b/sample), were used for this work. These databases are widely used and contains different rhythms, QRS complex morphologies, ectopic beats and noisy signals. For each set of ECG data, the CR range was defined. The CD value of 100% was achieved for CR $\leq$ 12, CR $\leq$ 8 and CR $\leq$ 4 for data from `mita`, `cuvt` and `mitsva` databases, respectively. The performance of the algorithms for the compression of the ECG signals was better than other wavelet based ECG coders.

In chapter 4, we present a wavelet energy based diagnostic distortion (WEDD) measure that can be used as a local or a global measure to predict the distortion introduced by different types of compressors which are very diverse. The proposed WEDD measure is the weighted percentage root mean square difference between the wavelet subband coefficients of the original and compressed signals with weights equal to the relative wavelet subband energies of the corresponding subbands. The multiresolution signal decomposition (MSD) technique characterizes the different frequency contents and noises in the input signal. In this technique, the higher subbands carry finely detailed information and the lower subbands carry shape based information, and it is noticed that the noise is well explained by a few levels that contain fine details and its effect disappears at the coarser scales. The relative wavelet subband energy gives a good measurement of information of the signal contents and can be exploited to characterize the signal and noise contents. Experiments showed that the higher detail subbands contain most of the energy attributed to the noise and that the noise energy is practically nonexistent at larger scales. The dynamic weights based on wavelet energy feature provides the actual contribution of the subbands that are used to discriminate different frequency subbands, particularly subbands corresponding to noise. The WEDD measure appeared to be a correct representation of the amount of signal distortion at all the subbands. This measure gave the idea about the local or subband error estimation since it enabled the calculation of the error between the frequency bands of the original and compressed signals. Based on MSD technique, it reliably measured the distortion not only within a distortion type at different distortion levels but also across different distortion types.

The performance of the subjective measure and several objective quality measures in time and frequency domain was discussed and investigated. This Chapter attempted to evaluate the closeness of the objective quality measures with subjective measure and to develop a simple quality measure to replace PRD, RMSE and WWPRD roles in ECG compression methods. Various distortions introduced by the compression methods was measured using various objective measures and their effectiveness were investigated. The relationship between the subjectively evaluated values and the objectively estimated values was studied quantitatively and qualitatively. The effectiveness of WEDD measure was validated by linear polynomial, cubic polynomial and nonlinear (logistic) regression analysis between the computed WEDD values and subjective scores. The performance of the proposed measure was gauged by its prediction accuracy and prediction monotonicity by using the validation metrics such as correlation coefficient (CC), root mean squared error (RMSE), mean absolute error (MAE), Spearman rank-order correlation coefficient (SROCC). The WEDD provided a better prediction accuracy and exhibited a statistically better monotonic relationship with the subjective scores than the WWPRD, PRD and other objective measures. Both qualitative and quantitative results proved that the proposed WEDD measure was more effective for evaluating the quality of the diagnostic features in the compressed signal. In wavelet based coding schemes, the large number of small coefficients, which are thresholded or quantized to zero value, resulted in insignificant error. The magnitude of this error may not be of much relevance from the point of view of clinical quality of the compressed signal. In WWPRD measure approach, insignificant errors in higher subbands dominated the global error while

significant errors in other bands may not reflect any contribution to the global error. Experiments showed that the WEDD measure is subjectively meaningful since the small and large values correspond to "good" and "bad" quality, respectively. Thus, this criterion can lead to a better evaluation of the rate-distortion performance of any coder. From the results shown in this Chapter, it was concluded that the WEDD measure is much more suitable for evaluating compressed signals than the other measures, and leads naturally to a new method for quality control in ECG signal compression. The WEDD measure is simple and it can be easily incorporated into wavelet based ECG compression scheme for providing automatic quality assessments.

In Chapter 5, quality controlled wavelet ECG compression methods were presented for guaranteeing reconstruction quality measured using the wavelet energy based diagnostic distortion (WEDD) criterion. The compression methods were based on: 1) the adaptive wavelet coding with joint thresholding and quantization strategy (Approach 1); 2) the adaptive subband coding with joint thresholding and quantization strategy (Approach 2); and 3) the set partitioning in hierarchical trees (SPIHT) coding strategy (Approach 3). Combining the WEDD measurement criterion and the well-designed coding strategy, the quality control mechanism provided an excellent coding gain. The following modifications distinguished the approaches from the existing works. The new WEDD measure was used for guaranteeing reconstruction quality. A threshold control zero-zone nearly uniform midtread quantization (TCZNUMQ) scheme where the zero-zone width of the quantizer is defined by the threshold parameter was used for the compression of wavelet coefficients. Approach 1 and Approach 2 are based on the TCZNUMQ and MIC schemes. The following step distinguishes Approach 2 from Approach 1. Classification of wavelet coefficients into frames based on the statistics of the subband coefficients. The energy based classification technique used in Approach 2 where a different quantizer resolution used for quantizing each frame, achieved substantial gains in the compression performance.

The rate-distortion optimization is the key technique in quality controlled compression algorithm to efficiently find a set of coding parameters. In the rate-distortion optimization for ECG coding, the distortion (D) was measured in the PRD and WWPRD. A new wavelet based quality measure was brought forward. It was proved that the WEDD can provide a better approximation to the perceived signal distortion than the currently used PRD and WWPRD. Thus, WEDD criterion provided a better evaluation of the rate-distortion (coding) performance of the proposed methods. In this Chapter, a new rate-distortion optimization for subband coding using WEDD as the distortion metric was presented. The intent of Chapter 5 is also to compare and contrast the three types of distortion measures such as the conventional PRD, the WWPRD and the WEDD in a particular application, lossy compression of noisy ECG signals. The noise degrades the rate-distortion performance of the coder. The study of the effectiveness of the distortion measures and the effect of the noises on the rate-distortion performance of the coder were investigated. Experiments on several noisy records from the widely used MIT-BIH arrhythmia (`mita`) database showed that the proposed strategy with WEDD criterion outperforms the conventional PRD and the wavelet based weighted PRD measurement criteria based strategies. It also demonstrated that the overall performance comparison of the

compression methods based on the results obtained using the signal blocks from the mita database and the PRD measurement criterion is less efficient. The compression results show that the proposed adaptive wavelet coding scheme slightly outperformed the SPIHT coding based scheme. Since a highly distorted compressed signal can be useless from a diagnostic point of view, the quality of compressed signal with a WEDD value of 2% is suitable for morphological studies for test signals. Experiments showed that the proposed quality control strategy reached a desired quality specification smoothly, accurately and quickly. Experiments showed that the subjective tests are the obvious ways of measuring clinical quality when working with ECG signals. The final conclusion on the optimal selection of distortion threshold when guaranteeing signal quality is so difficult since it depends on varying characteristics of various ECG signals. However, it can be performed with more subjective tests with different records. A detailed analytical treatment on the results of the threshold control zero-zone nearly uniform midtread quantization and modified index coding schemes can be carried out.

The successful results presented in Chapters 3-5 motivated to propose an effective quality controlled PCG signal compression using WEDD measurement criterion under noisy environments in Chapter 6. The compression method based on a combination of the multirate sampling and wavelet transform was presented for PCG signals. The multirate rate sampling strategy was employed to reduce the computational complexity of the quality driven wavelet coding algorithm. Once the signal was down-sampled with an appropriate sampling factor, the PCG signal was decomposed using the 9/7-tap wavelet filters. The resulting wavelet coefficients vector was compressed using the adaptive threshold control zero-zone nearly uniform midtread quantization and modified index coding schemes. The proposed scheme used to compress the PCG signal block depends on the following parameters: number of samples of each PCG signal block (M), decimation factor (D), wavelet filter (WF), decomposition level (J), value of the target criterion (EPEs/WEDD/CR) for threshold selection, number of bits used to quantize nonzero thresholded coefficients (b) and the proposed compression methodology. The performance of the lossy PCG compression scheme was evaluated using the compression rate, the objective distortion error criteria such as PRD_w and WEDD. For evaluation of the proposed scheme, the PCG signal blocks were taken from the qdheart and CAHM databases which include PCG records of many different valvular pathologies (normal sounds, third heart sound, fourth heart sound, late systolic, ejection click, tricuspid regurgitation, diastolic aortic insufficiency, murmurs and noises, etc.). Furthermore, the PCG records are digitized with different sampling rates and resolutions, and used for testing purposes in the literature. The effectiveness of the three quality measures such as PRD_w, WWPRD and WEDD are investigated using the simulated Gaussian white noise and different distortion types. Results showed that the performance of the WEDD criterion outperforms the PRD_w and WWPRD criteria. Experiments also proved that the direct comparison may be incorrect because they may be taken in different test conditions such as various records, test PCG signal block, different data length, with or without an entropy coder, filtering effect by the compression method, etc. For different values of WEDD, the PCG signals were compressed and the signal qualities were assessed by subjective evaluation where the similarity between

the original signal and the reconstructed one was rated in the Boolean question about the diagnosis (1-YES, 0-NO). We noticed severe clinical feature distortions for the error value of 5% and above. The algorithm reached the desired quality specification accurately, quickly and smoothly for all test signals. Experiments showed that the compression ratio of the scheme varies according to the clinical information for a given distortion specification. For WEDD=4%, the maximum compression ratio of 186.07 was achieved for the test signal from the Diastolic Fixed S2 Split II record and the minimum compression ratio of 21.16 is obtained for the signal from the Diastolic Atrial Septal Defect record. The overall compression performance was better than the other two-stage schemes. This research work showed that the proposed wavelet coding method based on the classification of wavelet coefficients, threshold control zero-zone nearly uniform midtread quantization and modified index coding schemes for guaranteeing reconstruction quality measured using the WEDD criterion provided a better compression performance for cardiovascular signals.

7.2 Scope for Future Work

(i) We can present the optimal wavelets and number of decomposition levels for compression of biomedical signals based on the WEDD criterion. The selection of a suitable mother wavelet is necessary for the biomedical signal denoising and compression. In this case, one may perform in an optimization criterion based on the minimization of the bit rate for the given signal distortion. Thus, to perform the mother wavelet optimization, we need to define: 1) a family of mother wavelets that can be obtained from the wavelet filter bank library (available in MATLAB library); and 2) a distortion measure for wavelet selection that can be performed using the WEDD criterion. This work can provide a new signal compression based on signal-dependent wavelets.

(ii) We can present the Data rate- or quality-driven subband coding framework based on the threshold control zero-zone nearly uniform midtread quantization with modeling of subband coefficient histograms and modified index coding scheme for compression of other biomedical signals viz. electroencephalogram (EEG), electromyogram (EMG), etc.

(iii) Using the adaptive subband coding scheme and the WEDD measure, a simultaneous denoising and compression based on the threshold control zero-zone nearly uniform midtread quantization and noise estimation technique can be attempted where the zero-zone width equals noise threshold parameter and the optimal outer-zone width according to the distortion specification. This work may lead to present a better adaptive wavelet denoising technique based on the weighted Euclidean wavelet distance criterion.

(iv) Evaluation of automatic quality control for two-dimensional (2-D) wavelet based compression of multilead ECG signals and medical images based on the weighted Euclidean wavelet distance criterion.

(v) Template matching (TM) is a basic task in numerous electrocardiogram (ECG) processing techniques namely ECG beat indexing and retrieval, verification of patient's identity, biometric, and residual based data compression. Typically TM system performs two major tasks: beat extraction and similarity measurement (SM). Among all the metrics, Euclidean distance (ED) is the widely used SM due to its simplicity but the accuracy depends on noise levels of the input beats. In such a case, a low noise level may result in a large ED and may diminish the local effects of small morphology variations. Therefore, we can attempt to present a wavelet based robust template matching using the weighted Euclidean wavelet distance measure.

(vi) Although WEDD measure outperforms the conventional PRD and WWPRD measures, the performance of the WEDD measure has to be studied for the case of low-frequency artifacts. As a continuation of this work, a weighting function can be pursued for the representation of the subband errors and an information fidelity criterion for local and global assessment of distorted signals can be attempted in multiresolution signal decomposition framework.

(vii) We can present a simple technique to select a communication channel for the transmission of biomedical signals. This work can include noise floor estimation and structural similarity measurement to measure varying shape changes due to the background noise introduced.

Bibliography

[1] Arthur C. Guyton, John E. Hall, "Textbook of medical physiology" 10th edition, 2001, Harcourt Asia Pte., Singapore.

[2] R. J. Huszar, "Basic dysrhythmias: interpretation and management," 2nd edition, Mosby-Year Book, Inc. St Louis.

[3] Leo Schamroth, "An introduction to electrocardiology," 1990, Blackwell Science, UK.

[4] F. Morris, J. Edhouse, J. W. Brady, J. Camm, "ABC of Clinical Electrocardiography," 2003, BMJ Publishing Group, London.

[5] W. J. Tompkins, "Biomedical digital signal processing," 1993, Prentice-Hall, New Jersey.

[6] R. McFee, M. G. Baule, "Research in electrocardiography and magnetocardiography," *Proceedings of the IEEE*, vol. 60, no. 3, pp. 290-321, March 1972.

[7] D. B. Geselowitz, "Origin of the electrocardiogram," *IEEE Engineering in Medicine and Biology Magazine*, vol. 13, no. 4, pp. 479-486, August/September 1994.

[8] A. Mattu, W. Brady, "ECGs for the emergency physician," 2003, BMJ Publishing Group, London.

[9] H. E. Awtry, V. A. Gururaj, M. Maytic, W. M. Tsang, J. B. Zachariah, J. Loscalzo, "Blueprints in cardiology," 2003, Blackwell Science, UK.

[10] S. Chauhan, P. Wang, C. S. Lim, V. Anantharaman, "A computer-aided MFCC-based HMM system for automatic auscultation," *Computers in Biology and Medicine*, vol. 38, no. 2, pp. 221-233, February 2008.

[11] X. Zhang, L. G. Durand, L. Senhadji, H. C. Lee, J. L. Coatrieux, "Analysis-synthesis of the phonocardiogram based on the matching pursuit method," *IEEE Transactions on Biomedical Engineering*, vol. 45, no. 8, pp. 962-971, August 1998.

[12] S. M. Debbal, F. B. Reguig, "Automatic measure of the split in the second cardiac sound by using the wavelet transform technique," *Computers in Biology and Medicine,* vol.37, no. 3, pp. 269-276, March 2007.

[13] R. J. Lehner, R. M. Rangayyan, "A three-channel microcomputer system for segmentation and characterization of the phonocardiogram," *IEEE Transactions on Biomedical Engineering*, vol. BME-34, no. 6 pp. 485-489, June 1987.

[14] Report of committee on electrocardiography, American heart association, "Recommendations for standardization of leads and of specifications for instruments in electrocardiography and vectorcardiography," *Circulation*, vol. XXXV, pp. 583-602, March 1967.

[15] N. V. Thakor, J. G. Webstor, W. J. Tompkins, "Estimation of QRS complex power spectra for design of a QRS filter," *IEEE Transactions on Biomedical Engineering*, vol. BME-31, no. 11, pp. 702-705, November 1984.

[16] G. J. Guang, W. J. Tompkins, "High-frequency electrocardiogram analyzer," *IEEE Transactions on Biomedical Engineering*, vol. BME-33, no. 12, pp. 1137-1140, December 1986.

[17] László Gerencsr, Gyrgy Kozmann, Zsuzsanna Vágó, Kristóf Haraszti, "The Use of the SPSA Method in ECG Analysis," *IEEE Transactions on Biomedical Engineering*, vol. 49, no. 10, pp. 1094-1101, October 2002.

[18] G. B. Moody, R. G. Mark, "The MIT-BIH arrhythmia database in CD-ROM and software for use with it," in *Computers in Cardiology*, pp. 185-188, 1990.

[19] G. B. Moody, R. G. Mark, "The impact of the MIT-BIH arrhythmia database," *IEEE Engineering in Medicine and Biology Magazine*, vol. 17, no. 1, pp. 45-50, May/June 2001.

[20] G. B. Moody, R. G. Mark, A. L. Goldberger, "PhysioNet: A web-based resource for study of physiologic signals," *IEEE Engineering in Medicine and Biology Magazine*, vol. 20, no. 1, pp. 70-75, May/June 2001.

[21] qdheart PCG database available at http://www.qdheart.com/cgz/jcxt/tyvf/tyvf1.htm.

[22] eGeneralMedical PCG database at http://egeneralmedical.com/listohearmur.html

[23] S. Pavlopoulos, E. Kyriacou, A. Berler, S. Dembeyiotis, D. Koutsouris, "A novel emergency telemedicine system based on wireless communication technology-AMBULANCE," *IEEE Transactions on Information Technology in Biomedicine*, vol. 2, no. 4, pp. 261-267, December 1998.

[24] Ren-Guey Lee, Heng-Shuen Chen, Chung-Chih Lin, Kuang-Chiung Chang, Jyh-Horng Chen, "Home telecare system using cable television plants-an experimental field trial," *IEEE Transactions on Information Technology in Biomedicine*, vol. 4, no. 1, pp. 37-44, March 2000.

[25] B. Woodward, R. S. H. Istepanian, C. I. Richards, "Design of a telemedicine system using a mobile telephone," *IEEE Transactions on Information Technology in Biomedicine*, vol. 5, no. 1, pp. 13-15, March 2001.

[26] A. I. Hernandez, F. Mora, M. Villegas, G. Passariello, G. Carrault, "Real-time ECG transmission via Internet for nonclinical applications," *IEEE Transactions on Information Technology in Biomedicine*, vol. 5, no. 3, pp. 253-257, September 2001.

[27] C. S. Pattichis, E. Kyriacou, S. Voskarides, M. S. Pattichis, R. Istepanian, C. N. Schizas, "Wireless telemedicine systems: an overview," *IEEE Antennas and Propagation Magazine*, vol. 44, no. 2, pp. 143-153, April 2002.

[28] J. Garcia, I. Martinez, L. Sornmo, S. Olmos, A. Mur, P. Laguna, "Remote processing server for ECG-based clinical diagnosis support," *IEEE Transactions on Information Technology in Biomedicine,* vol. 6, no. 4, pp. 277-284, December 2002.

[29] K. Hung, Yuan-Ting Zhang, "Implementation of a WAP-based telemedicine system for patient monitoring," *IEEE Transactions on Information Technology in Biomedicine,* vol. 7, no. 2, pp. 101-107, June 2003.

[30] L. Sharpe, "Doctors at a distance [telemedicine]," *IEE Review*, vol. 49, no. 9, pp. 44-47, September 2003.

[31] L. Hadzievski, B. Bojovic, V. Vukcevic, P. Belicev, S. Pavlovic, Z. V. Pokrajcic, M. Ostojic, "A novel mobile transtelephonic system with synthesized 12-lead ECG," *IEEE Transactions on Information Technology in Biomedicine,* vol. 8, no. 4, pp. 428-438, December 2004

[32] M. F. A. Rasid, B. Woodward, "Bluetooth telemedicine processor for multichannel biomedical signal transmission via mobile cellular networks," *IEEE Transactions on Information Technology in Biomedicine,* vol. 9, no. 1, pp. 35-43, March 2005.

[33] J. Rodriguez, A. Goni, A. Illarramendi, "Real-time classification of ECGs on a PDA," *IEEE Transactions on Information Technology in Biomedicine,* vol. 9, no. 1, pp. 23-34, March 2005.

[34] W. C. Kao, W. H. Chen, C. K. Yu, C. M. Hong, S. Y. Lin, "Portable real-time homecare system design with digital camera platform," *IEEE Transactions on Consumer Electronics*, vol. 51, no. 4, pp. 1035-1041, November 2005.

[35] D. A. Lelewer, D. S. Hirschberg, "Data compression," *ACM Computing Surveys,* vol. 19, no. 3, pp. 261-296, September 1987.

[36] N. S. Jayant, P. Noll, "Digital coding of waveforms," *New Jersey: Prentice-Hall*, 1984.

[37] K. Sayood, "Introduction to data compression," *Elsevier Inc.*, 2006.

[38] A. Gersho,"Principles of quantization," *IEEE Transaction on Circuits and Systems*, vol. CAS-25 no. 7, PP. 427-436, July 1978.

[39] A. Buzo, A. J. Gray, R. Gray, J. D. Markel, "Speech coding based upon vector quantization," *IEEE Transactions on Acoustics Speech and Signal Processing ASSP-28*, vol. 28, no. 5, pp. 562-574, October 1980.

[40] R. M. Gray, "Vector quantization," *IEEE Acoustics Speech and Signal Processing Magazine*, pp. 4-29, April 1984.

[41] M. N. Nasrabadi, A. R. King, "Image coding using vector quantization: a review," *IEEE Transactions on communications,* vol. 36, no. 8, pp. 957-971, August 1988.

[42] A. Cohen, P. M. Poluta, R. S. Millar, "Compression of ECG signals using vector quantization," in *Proceedings of IEEE-90 S. A. Symposium on Communications and Signal Processing,* COMSIG-90, pp. 45-54, 1990.

[43] J. P. Abenstein, W. J. Tompkins, "A new data reduction algorithm for real time ECG analysis," *IEEE Transactions on Biomedical Engineering,* vol. BME-29, no. 1, pp. 43-48. Junauary 1982.

[44] C. M. Kortman, "Redundancy reduction-a practical method of data compression," *Proceedings of IEEE,* vol. 55, no. 3, pp. 253-263, March 1967.

[45] C. A. Andrews, J. M. Davies, G. R. Schwarz, "Adaptive data compression," *Proceedings of IEEE,* vol. 55, no. 3, pp. 267-277, March 1967.

[46] P. Elias, "Predictive coding," *IEEE Transactions on Information Theory,* vol. 1, no. 1, pp. 16-33, March 1955.

[47] J. R. Cox, K. L. Ripley, "Compact digital coding of electrocardiographic data," in *Proceeding of 6th Hawaii International Conference on System Sciences*, pp. 333-336. 1973.

[48] O. Pahlm, O. P. Borjesson, O. Werner, "Compact digital storage of ECGs," *Computer Programs in Biomedicine*, Vol. 9, pp. 293-300, May 1979.

[49] U. E. Ruttimann, H. V. Pipberger, "Compression of the ECG by prediction or interpolation and entropy encoding," *IEEE Transactions on Biomedical Engineering,* vol. BME-26, no. 11, pp. 613-623, Nov. 1979.

[50] A. Sandman, B. Sapir, "Third order polynomialIts use in data compression," *Signal Processing*, vol. 15, no. 4, pp. 405-418, December 1988.

[51] L. W. Gardenhire, "Redundancy reduction, the key to adaptive telemetry," in *Proceedings of National Telemetering Conference,* pp. 1-16, 1964.

[52] L. W. Gardenhire, "Data redundancy reduction for biomedical telemetry," *Biomedical telemetry,* C. A. Caceres, Ed. New York: Academic, pp. 255-298, 1965.

[53] S. M. Blanchard, R. C. Barr, M. S. Spach, "A voltage-triggered system for adaptive sampling in body surface mapping," *IEEE Transactions on Biomedical Engineering,* vol. BME-29, no. 11, pp. 726-730, November 1982.

[54] S. M. Blanchard, R. C. Barr, "Comparison of methods for adaptive sampling of cardiac electrograms and electrocardiograms," *Medical and Biological Engineering and Computing,* vol. 23, no. 4, pp. 377-386, July 1985.

[55] J. R. Cox, F. M. Nolle, H. A. Fozzard, G. C. Oliver, "AZTEC, a preprocessing program for real-time ECG rhythm analysis," *IEEE Transactions on Biomedical Engineering,* vol. BME-15, pp. 128-129, April 1968.

[56] W. C. Mueller, "Arrhythmia detection program for an ambulatory ECG monitor," *Biomedical Science Instrumentation,* vol. 14, pp. 81-85, 1978.

[57] M. Ishjima, S. B. Shin, G. H. Hostetter, J. Sklansky, "Scan-along polygon approximation for data compression of electrocardiograms," *IEEE Transactions on Biomedical Engineering,* vol. 30, pp. 723-729, 1983.

[58] R. C. Barr, S. M. Blanchard, D. A. DiPersio, "SAPA-2 is the fan," *IEEE Transactions on Biomedical Engineering,* vol. BME-32, no. 5, 337, May 1985.

[59] D. A. Dipersio, R. C. Barr, "Evaluation of the fan method of adaptive sampling on human electrocardiograms," *Medical and Biological Engineering and Computing,* vol. 23, no. 5, pp. 401-410, September 1985.

[60] A. E. Pollard, R. C. Barr, "Adaptive sampling of intracellular and extracellular cardiac potentials with the fan method," *Medical and Biological Engineering and Computing,* vol. 25, no. 3, pp. 261-268, May 1987.

[61] M. Giallorenzo, J. Cohen, F. Mora, G. Passariello, L. O. Lara, "Ambulatory monitoring device using the fan method as data-compression algorithm," *Medical and Biological Engineering and Computing,* vol. 26, no. 4 pp. 439-443, July 1988.

[62] B. Furht, A. Perez, "An adaptive real-time ECG compression algorithm with variable threshold," *IEEE Transactions on Biomedical Engineering,* vol. 35, no. 6, pp. 489-494, June 1988.

[63] S. C. Tai, "Slope-a real-time ECG data compressor," *Medical and Biological Engineering and Computing,* vol. 29, no. 2, pp. 175-179, March 1991.

[64] S. C. Tai, "ECG data compression by corner detection," *Medical and Biological Engineering and Computing,* vol. 30, no. 6, pp. 584-590, March 1992.

[65] X. B. Huang, M. J. English, R. Vincent, "Fast ECG data compression algorithms suitable for microprocessor systems," *Journal of Biomedical Engineering,* vol. 14, no. 1, pp. 64-68, January 1992.

[66] S. C. Tai, "AZTDIS-a two-phase real-time ECG data compressor," *Journal of Biomedical Engineering,* vol. 15, no. 6, pp. 510-515, November 1993.

[67] H. I. Shahein, H. M. Abbas, "ECG data compression via cubic-splines and scan-along polygonal approximation," *Signal Processing,* vol. 35, no. 3, pp. 269-283, February 1994.

[68] G. Lachiver, J. M. Eichner, F. Besette, W. Seufert, "An algorithm for ECG data compression using spline functions," in *Computer in Cardiology*, pp. 575-578, 1986.

[69] M. Karczewicz, M. Gabbouj, "ECG data compression by spline approximation," *Signal Processing*, vol. 59, no. 1, pp. 43-59, May 1997.

[70] Vinod Kumar, S. C. Saxena, V. K. Giri, Dilbag Singh, "Improved modified AZTEC technique for ECG data compression: Effect of length of parabolic filter on reconstructed signal," *Computers and Electrical Engineering,* vol. 31, no. 4-5, pp. 334-344, June-July 2005.

[71] S. C. Tai, C. W. Chang, C. F. Chen, "Designing better adaptive sampling algorithms for ECG holter systems," *IEEE Transactions on Biomedical Engineering,* vol. 44, no. 9, pp. 901-903, September 1997.

[72] L. N. Bohs, R. C. Barr, "Real-time adaptive sampling with the fan algorithm," *Medical and Biological Engineering and Computing,* vol. 26, no. 6, pp. 565-573, November 1988.

[73] M. Bertinelli, A. Castelli, C. Combi, F. Pinciroli, "Data compression applied to dynamic electrocardiography," *Medical and Biological Engineering and Computing,* vol. 27 no. 1, pp. 33-40, January 1989.

[74] S. M. S. Jalaleddine, C. G. Hutchens, R. D. Strattan, W. A. Coberly, "ECG data compression techniques-a unified approach," *IEEE Transactions on Biomedical Engineering,* vol. 37, no. 4, pp.329-343, April 1990.

[75] H. El-Sherief, S. Pham, N. El-Sherif, E. Caref, "Clinical evaluation of ECG data compression techniques for ambulatory recording," in *Proceedings of 19th Annual International Conference of the IEEE EMBS*, vol. 2, pp. 1306-1307, 1994.

[76] P. S. Hamilton, W. J. Tompkins, "Compression of the ambulatory ECG by average beat subtraction and residual differencing," *IEEE Transactions on Biomedical Engineering,* vol. 38, no. 3, pp. 253-259, March 1991.

[77] G. Einarsson, "An improved implementation of predictive coding compression," *IEEE Transactions on Communications*, vol. 39, no. 2, pp. 169-171, February 1991.

[78] P. S. Hamilton, W. J. Tompkins, "Theoritical and experimental rate distortion performace in compression of ambulatory ECG's," *IEEE Transactions on Biomedical Engineering,* vol. 38, no. 3, pp. 260-266, March 1991.

[79] G. Nave, A. Cohen, "ECG compression using long-term prediction," *IEEE Transactions on Biomedical Engineering,* vol. 40, no. 9, pp. 877-885, September 1993.

[80] C. Paggetti, M. Lusini, M. Varanini, A. Taddei, C. Marchesi, "A multichannel template based data compression algorithm," in *Computer in Cardiology,* pp. 629-632, 1994.

[81] Y. Zigel, A. Cohen A. Katz, "A diagnostic meaningful distortion measure for ECG compression," in *Proceedings of 19th Convention of Electrical and Electronic Engineering* pp. 117-120, 1996.

[82] A. Cohen, Y. Zigel, "Compression of multichannel ECG through multichannel long-term prediction," *IEEE Engineering in Medicine and Biology Magazine,* vol. 17, no. 1, pp. 109-115, January/February 1998.

[83] Y. Zigel, A. Cohen, A. Katz, "ECG signal compression using analysis by synthesis coding," *IEEE Transactions on Biomedical Engineering,* vol. 47, no. 10, pp. 1308-1316, October 2000.

[84] Wen-Shiung Chena, Lili Hsiehb, Shang-Yuan Yuana, "High performance data compression method with pattern matching for biomedical ECG and arterial pulse waveforms," *Computer Methods and Programs in Biomedicine,* vol. 74, no. 01, pp. 11-27, April 2004.

[85] C. P. Mammen, B. Ramamurthi, "Vector quantization for compression of multichannel ECG," *IEEE Transactions on Biomedical Engineering,* vol. 37, no. 9, pp. 821-825, September 1990.

[86] A. Cohen, P. M. Poluta, R. Scott-Millar, "Compression of ECG signals using vector quantization," in *Proceedings of IEEE-90 S. A. Symposium Communications and Signal Processing,* COMSIG-90, pp. 45-54, 1990.

[87] J. L. C. Barrera, J. V. Lorenzo-Ginori, "Mean-shape vector quantizer for ECG signal compression," *IEEE Transactions on Biomedical Engineering,* vol. 46, no. 1, pp. 62-70, January 1999.

[88] Shaou-Gang Miaou, Heng-Lin Yen, "Multichannel ECG compression using multichannel adaptive vector quantization," *IEEE Transactions on Biomedical Engineering,* vol. 48, no. 10, pp. 1203-1207, October 2001.

[89] Chia-Chun Sun, Shen-Chuan Tai, "Beat-based ECG compression using gain-shape vector quantization," *IEEE Transactions on Biomedical Engineering,* vol. 52, no. 11, pp. 1882-1888, November 2005.

[90] A. Iwata, Y. Nagasaka, N. Suzumura, "Data compression of the ECG using neural network for digital Holter monitor," *IEEE Engineering in Medicine and Biology Magazine,* vol. 9, no. 3, pp. 53-57, September 1990.

[91] Yong Zhao, Boxiang Wang, Wei Zhao, Lida Dong, "Applying incompletely connected feedforward neural network to ambulatory ECG data compression," *IET Electronics Letters*, vol. 33, no. 3, pp. 220-221, 30 January 1997.

[92] A. Chatterjee, A. Nait-Ali, P. Siarry, "An input-delay neural-network-based approach for piecewise ECG signal compression," *IEEE Transactions on Biomedical Engineering,* vol.52, no.5, pp. 945-947, May 2005.

[93] N. Ahmed, P. J. Milne, S. G. Hams, "Electrocardiographic data compression via orthogonal transforms," *IEEE Transactions on Biomedical Engineering,* vol. BME-22, no. 6, pp. 484-487, November 1975.

[94] M. E. Womble, J. S. Halliday, S. K. Mitter, M. C. Lancaster, J. H. Triebwasser, "Data compression for storing and transmitting ECG's/VCG's," *Proceedings of IEEE,* vol. 65, no. 5, pp. 702-706, May 1977.

[95] R. L. Lux, "Karhunen-loeve representation of ECG data," *Journal of Electrocardiology,* vol. 25, Supplement 1, pp. 195-198, 1992.

[96] S. Olmos, J. Garca, R. Jan, P. Laguna, "ECG signal compression plus noise filtering with truncated orthogonal expansions," *Signal Processing*, vol. 79, no. 1, pp. 97-115, November 1999.

[97] T. Blanchett, G. C. Kember, G. A. Fenton, "KLT-based quality controlled compression of single-lead ECG," *IEEE Transactions on Biomedical Engineering,* vol. 45, no. 7, pp. 942-945, July 1998.

[98] W. S. Kuklinski, "Fast Walsh transform data-compression algorithm; ECG applications," *Medical and Biological Engineering and Computing,* vol. 21 pp. 465-472, 1983.

[99] G. P. Frangakis, G. Papakonstantinou, S. G. Tzafestas, "A fast Walsh transfrom-based data compression multi-microprocessor system: application to ECG signals," *Mathematics and Computers in Simulation,* vol. 27, no. 5-6, pp. 491-502, October 1985.

[100] E. Berti,F. Chiaraluce, N. E. Evans, J. J. McKee, "ECG data compression using double logarithmic quantisation of Walsh spectrum," *IET Electronics Letters,* vol . 31, no. 13, pp. 1025-1026, June 1995.

[101] E. Berti,F. Chiaraluce, N. E. Evans, J. J. McKee, "Double logarithmic quantisation of the Walsh spectrum: application to real ECGs," *IET Electronics Letters,* vol . 33, no. 18, pp. 1513-1515, August 1997.

[102] E. Berti,F. Chiaraluce, N. E. Evans, J. J. McKee, "Reduction of Walsh-transformed electrocardiograms by double logarithmic coding," *IEEE Transactions on Biomedical Engineering,* vol. 47, no. 11, pp. 1543-1547, November 2000.

[103] B. R. S. Reddy, I. S. N. Murthy, "ECG Data Compression Using Fourier Descriptors," *IEEE Transactions on Biomedical Engineering,* vol. BME-33, no. 4, pp. 428-434, April 1986.

[104] H. A. M. Al-Nashash, "ECG data compression using adaptive Fourier coefficients estimation," *Medical Engineering and Physics*, vol. 16, no. 1, pp. 62-66, January 1994.

[105] H. A. M. Al-Nashash, "A dynamic fourier series for the compression of ECG using FFT and adaptive coefficient estimation," *Medical Engineering and Physics*, vol. 17, no. 3, pp. 197-203, April 1995.

[106] V. A. Allen, J. Belina, "ECG data compression using the discrete cosine transform, *Computers in Cardiology,* pp. 687-690, October 1992.

[107] U. C. Niranjan, I. S. N. Murthy, "ECG component delineation by Prony's method," *Signal Processing,* vol. 31, no. 2, pp. 191-202, March 1993.

[108] B. Madhukar, I. S. N. Murthy, "ECG Data Compression by Modeling," *Computers and Biomedical Research,* vol. 26, no. 3, pp. 310-317, June 1993.

[109] L. V. Batista, E. U. Kurt Melcher, L. C. Carvalho, "Compression of ECG signals by optimized quantization of discrete cosine transform coefficients," *Medical Engineering and Physics,* vol. 23, no. 2, pp. 127-134, March 2001.

[110] R. Borsali, A. Nait-Ali, J. Lemoine, "ECG Compression Using an Ensemble Polynomial Modeling: Comparison With the DCT Based Technique," *Cardiovascular Engineering: An International Journal,* vol. 4, No. 3, pp. 237-244, September 2004.

[111] R. Benzid, A. Messaoudi, A. Boussaad, "Constrained ECG compression algorithm using the block-based discrete cosine transform," *Digital Signal Processing,* vol. 18, no. 1, pp. 56-64, January 2008.

[112] W. Philips, G. De Jonghe, "Data compression of ECG's by high-degree polynomial approximation," *IEEE Transactions on Biomedical Engineering,* vol. 39, no. 4, pp. 330-337, April 1992.

[113] W. Philips, "ECG data compression with time-warped polynomials," *IEEE Transactions on Biomedical Engineering,* vol. 40, no. 11, pp. 1095-1101, November 1993.

[114] Alberto Albiol Colomer, Antonio Albiol Colomer, "Adaptive ECG data compression using discrete legendre transform," *Digital Signal Processing*, vol. 7, no. 4, pp. 222-228, October 1997.

[115] S. C. Tai, "Six-band sub-band coder on ECG waveforms," *Medical and Biological Engineering and Computing,* vol. 30, pp. 187-192, 1992.

[116] M. C. Aydin, A. E. Cetin, H. Koymen, "ECG data compression by sub-band coding," *IET Electronics Letters*, vol. 27, no. 4, pp. 359-360, February 1991.

[117] S. C. Tai, "Improving the performance of electrocardiogram sub-band coder by extensive Markov system," *Medical and Biological Engineering and Computing,* vol. 33, pp. 471-475, May 1995.

[118] J. H. Husy, T. Gjerde, "Computationally efficient subband coding of ECG signals," *Medical Engineering and Physics,* vol. 18, no. 2 pp. 132-142, March 1996.

[119] A. G. Ramakrishnan, S. Saha, "ECG compression by multirate processing of beats," *Computers and Biomedical Research*, vol. 29, no. 5, pp. 407-409, October 1996.

[120] M. B. Velasco, F. C. Roldn, F. L. Ferreras, A. B. Santos, D. M. Muoz, "A low computational complexity algorithm for ECG signal compression," *Medical Engineering and Physics,* vol. 26, no. 7 pp. 553-568, September 2004.

[121] M. B. Velasco, F. C. Roldn, J. I. G. Llorente, K. E. Barner, "ECG compression with retrieved quality guaranteed," *IET Electronics Letters,* vol. 40, no. 23, pp. 1466-1467, November 2004.

[122] J. A. Crowe, N. M. Gibson, M. S. Woolfson, M. G. Somekh, "Wavelet transform as a potential tool for ECG analysis and compression," *Journal of Biomedical Engineering*, vol. 14, no. 3, pp. 268-272, May 1992.

[123] J. Chen, S. Itoh, T. Hashimoto, "ECG data compression by using wavelet transform," *IEICE Transaction on Information and Systems,* vol. E76-D, no. 12, pp. 1454-1461, December 1993.

[124] N. Thakor, Y. Sun, H. Rix, P. Caminal, "Multiwave: A wavelet based ECG data compression algorithm," *IEICE Transaction on Information and Systems,* vol. E76-D, no. 12, pp. 14621469, 1993.

[125] I. Provaznk, J. Kozumplk, "Wavelet transform in electrocardiography-data compression," *International Journal of Medical Informatics*, vol. 45, no. 1-2, pp. 111-128, June 1997.

[126] B. Bradie, "Wavelet packet-based compression of single lead ECG," *IEEE Transactions on Biomedical Engineering,* vol. 43, no. 5, pp. 493-501, May 1996.

[127] K. Nagarajan, E. Kresch, S. S. Rao, Y. Kresh, "Constrained ECG compression using best adapted wavelet packet bases," *IEEE Signal Processing Letters,* vol. 3, no. 10, pp. 273-275, October 1996.

[128] A. G. Ramakrishnan, S. Saha, "ECG coding by wavelet-based linear prediction," *IEEE Transactions on Biomedical Engineering,* vol. 44, no. 12, pp. 1253-1261, December 1997.

[129] J. Chen, S. Itoh, "A wavelet transform-based ECG compression method guaranteeing desired signal quality," *IEEE Transactions on Biomedical Engineering,* vol. 45, no. 12, pp. 1414-1419, December 1998.

[130] M. A. Sabah, A. Al-Shrouf, M. Abo-Zahhad, "ECG data compression using optimum non-orthogonal wavelet transform," *Medical Engineering and Physics*, vol. 22, no. 1 pp. 39-46, January 2000.

[131] R. S. H. Istepanian, A. A. Petrosian, "Optimal zonal wavelet-based ECG data compression for a mobile telecardiology system," *IEEE Transactions on Information Technology in Biomedicine,* vol. 4, no. 3, pp. 200-211, September 2000.

[132] R. S. H. Istepanian, L. J. Hadjileontiadis, S. M. Panas, "ECG data compression using wavelets and higher order statistics methods," *IEEE Transactions on Information Technology in Biomedicine,* vol. 5, no. 2, pp. 108-115, June 2001.

[133] S. M. Ahmeda, M. Abo-Zahhad, "A new hybrid algorithm for ECG signal compression based on the wavelet transformation of the linearly predicted error," *Medical Engineering and Physics,* vol. 23, no. 2, pp. 117-126, March 2001.

[134] B. A. Rajoub, "An efficient coding algorithm for the compression of ECG signals using the wavelet transform," *IEEE Transactions on Biomedical Engineering,* vol. 49, no. 4, pp. 355-362, April 2002.

[135] M. Abo-Zahhad; B. A. Rajoub, "An effective coding technique for the compression of one-dimensional signals using wavelet transforms," *Medical Engineering and Physics,* vol. 24, no. 3, pp. 185-199, April 2002.

[136] A. Al-Shrouf, M. Abo-Zahhad, Sabah M. Ahmed, "A novel compression algorithm for electrocardiogram signals based on the linear prediction of the wavelet coefficients," *Digital Signal Processing*, vol. 13, no. 4, pp. 604-622, October 2003.

[137] R. Benzid, F. Marir, A. Boussaad, M. Benyoucef, D. Arar, "Fixed percentage of wavelet coefficients to be zeroed for ECG compression," *IET Electronics Letters,* vol. 39, no. 11, pp. 830-831, May 2003.

[138] B . S. Kim, S. K. Yoo, M. H. Lee, "Wavelet-based low-delay ECG compression algorithm for continuous ECG transmission," *IEEE Transactions on Information Technology in Biomedicine,* vol. 10, no. 1, pp. 77-83, January 2006.

[139] A. Alesanco, S. Olmos, R. S. H. Istepanian, J. Garcia, "Enhanced real-time ECG coder for packetized telecardiology applications," *IEEE Transactions on Information Technology in Biomedicine,* vol. 10, no. 2, pp. 229-236, April 2006.

[140] C. T. Ku, H. S. Wang, K. C. Hung, Y. S. Hung, "A novel ECG data compression method based on nonrecursive discrete periodized wavelet transform," *IEEE Transactions on Biomedical Engineering,* vol. 53, no. 12, pp. 2577-2583, December 2006.

[141] C. T. Ku, K. C. Hung, H. S. Wang, Y. S. Hung, "High efficient ECG compression based on reversible round-off non-recursive 1-D discrete periodized wavelet transform," *Medical Engineering and Physics,* vol. 29, no. 10, pp. 1149-1166, December 2007.

[142] M. B. Velasco, F. C. Roldan, J. I. G. Llorente, K. E. Barner, "Wavelet Packets Feasibility Study for the Design of an ECG Compressor," *IEEE Transactions on Biomedical Engineering,* vol. 54, no. 4, pp. 766-769, April 2007.

[143] R. Benzid, F. Marir, N. E. Bouguechal, "Electrocardiogram compression method based on the adaptive wavelet coefficients quantization combined to a modified two-role encoder," *IEEE Signal Processing Letters,* vol. 14, no. 6, pp. 373-376, June 2007.

[144] M. L. Hilton, "Wavelet and wavelet packet compression of electrocardiograms," *IEEE Transactions on Biomedical Engineering,* vol. 44, no. 5, pp. 394-402, May 1997.

[145] Z. Lu, D. Y. Kim, W. A. Pearlman, "Wavelet compression of ECG signals by the set partitioning in hierarchical trees algorithm," *IEEE Transactions on Biomedical Engineering,* vol. 47, no. 7, pp. 849-856, July 2000.

[146] Shaou-Gang Miaou, Chih-Lung Lin, "A quality-on-demand algorithm for wavelet-based compression of electrocardiogram signals," *IEEE Transactions on Biomedical Engineering,* vol. 49, no. 3, pp. 233-239, March 2002.

[147] W. J. Hwang, C. F. Chine, K. J. Li, "Scalable medical data compression and transmission using wavelet transform for telemedicine applications," *IEEE Transactions on Information Technology in Biomedicine,* vol. 7, no. 1 pp. 54-63, March 2003.

[148] G. Tohumoglu, K. E. Sezgin, "ECG signal compression by multi-iteration EZW coding for different wavelets and thresholds," *Computers in Biology and Medicine,* vol. 37, no. 2, pp. 173-182, February 2007.

[149] A. Alesanco, J. Garcya "A simple method for guaranteeing ECG quality in real-time wavelet lossy coding," *EURASIP Journal on Advances in Signal Processing,* vol. 2007, Article ID 93195, 9 pages, 2007.

[150] K. Anant, F. Dowla, G. Rodrigue, "Vector quantization of ECG wavelet coefficients," *IEEE Signal Processing Letters,* vol. 2, no. 7, pp. 129-131, July 1995.

[151] Shaou-Gang Miaou, Heng-Lin Yen, "Quality driven gold washing adaptive vector quantization and its application to ECG data compression," *IEEE Transactions on Biomedical Engineering,* vol. 47, no. 2, pp. 209-218, February 2000.

[152] Shaou-Gang Miaou, Heng-Lin Yen, Chih-Lung Lin, "Wavelet-based ECG compression using dynamic vector quantization with tree codevectors in single codebook," *IEEE Transactions on Biomedical Engineering,* vol. 49, no. 7, pp. 671-680, July 2002.

[153] Shaou-Gang Miaou, Shu-Nien Chao, "Wavelet-based lossy-to-lossless ECG compression in a unified vector quantization framework," *IEEE Transactions on Biomedical Engineering,* vol. 52, no. 3, pp. 539-543, March 2005.

[154] X. Wang, J. Meng, "A 2-D ECG compression algorithm based on wavelet transform and vector quantization," *Digital signal Processing*, vol. 18, no. 2, pp. 179-188, March 2008.

[155] H. Lee, K. M. Buckley, "ECG data compression using cut and align beats approach and 2-D transforms," *IEEE Transactions on Biomedical Engineering,* vol. 46, no. 5, pp. 556-564, May 1999.

[156] A. R. A. Moghaddam, K. Nayebi, "A two dimensional wavelet packet approach for ECG compression," in *Proceedings of International Symposium Signal Processing Applications,* pp. 226-229, August 2001.

[157] K. Uyar, Y. Z. Ider, "Development of a compression algorithm suitable for exercise ECG data," in *Proceedings of 23rd Annual International Conference of the IEEE EMBS*, pp. 3521-3524, October 2001.

[158] J. J. Wei, C. J. Chang, N. K. Chou, G. J. Jan, "ECG data compression using truncated singular value decomposition ," *IEEE Transactions on Information Technology in Biomedicine,* vol. 5, no. 4, pp. 290-299, December 2001.

[159] A. Bilgin, M. W. Marcellin, M. I. Altbach, "Compression of electrocardiogram signals using JPEG2000," *IEEE Transactions on Consumer Electronics,* vol. 49, no. 4, pp. 833-840, November 2003.

[160] S. C. Tai, C. C. Sun, W. C. Yan, "A 2-D ECG compression method based on wavelet transform and modified SPIHT," *IEEE Transactions on Biomedical Engineering,* vol. 52, no. 6, pp. 999-1008, June 2005.

[161] H. H. Chou, Y. J. Chen, Y. C. Shiau, T. S. Kuo, "An effective and efficient compression algorithm for ECG signals with irregular periods," *IEEE Transactions on Biomedical Engineering,* vol. 53, no. 6, pp. 1198-1205, June 2006.

[162] E. Alexandre, A. Pena, M. Sobreira, "On the use of 2-D coding techniques for ECG signals," *IEEE Transactions on Information Technology in Biomedicine,* vol. 10, no. 4, pp. 809-811, October 2006.

[163] P. O. Borjesson, G. Einarsson, O. Pahlm, "Comments on "Compression of the ECG by prediction or interpolation and entropy encoding," *IEEE Transactions on Biomedical Engineering,* vol. BME-27, no. 11, pp. 674-674, November 1980.

[164] P. S. Hamilton, W. J. Tompkins, "Theoretical and experimental rate distortion performance in compression of ambulatory ECGs," *IEEE Transactions on Biomedical Engineering,* vol. 38, no. 3, pp. 260-266, March 1991.

[165] A. Alshamali, A. S. Al-Fahoum, "Comments on "An efficient coding algorithm for the compression of ECG signals using the wavelet transform," *IEEE Transactions on Biomedical Engineering,* vol. 50, no. 8, pp. 1034-1037, August 2003.

[166] M. B. Velasco, F. C. Roldn, J. I. G. Llorente, J. B. Velasco, C. A. Aparicio. F. L. Ferreras, "On the use of PRD and CR parameters for ECG compression," *Medical Engineering and Physics*, vol. 27, no. 9, pp. 798-802, November 2005.

[167] J. Pan, W. J. Tompkins, "A Real-Time QRS Detection Algorithm," *IEEE Transactions on Biomedical Engineering,* vol. BME-32, no. 3, pp. 230-236, March 1985.

[168] V. X. Afonso, W. J. Tompkins, T. Q. Nguyen, Shen Luo, "ECG beat detection using filter banks," *IEEE Transactions on Biomedical Engineering,* vol. 46, no. 2, pp. 192-202, February 1999.

[169] L. Senhadji, J. J. Bellanger, G. Carrault, J. L. Coatrieux, "Wavelet analysis of E.C.G. signals," in *Proceedings of 12th Annual International Conference of the IEEE EMBS*, pp. 811-812, November 1990.

[170] L. Cuiwei, C. Zheng, C. Tai, "Detection of ECG characteristic points using wavelet transforms," *IEEE Transactions on Biomedical Engineering,* vol. 42, no. 1, pp. 21-28, January 1995.

[171] M. Unser, A. Aldroubi, "A review of wavelets in biomedical applications," *Proceedings of IEEE,* vol. 84, no. 4, pp. 626-638, April 1996.

[172] J. S. Sahambi, S. N. Tandon, R. K. P. Bhatt, "Using wavelet transforms for ECG characterization. An on-line digital signal processing system," *IEEE Engineering in Medicine and Biology Magazine,* vol. 16, no. 1, pp. 77-83, January/February 1997.

[173] A. Figliola, E. Serrano, "Analysis of physiological time series using wavelet transforms," *IEEE Engineering in Medicine and Biology Magazine,* vol. 16, no. 3, pp. 74-79, May/June 1997.

[174] S. Kadambe, R. Murray, G. F. B. Bartels, "Wavelet transform-based QRS complex detector," *IEEE Transactions on Biomedical Engineering,* vol. 46, no. 7, pp. 838-848, July 1999.

[175] J. S. Sahambi, S. N. Tandon, R. K. P. Bhatt, "An automated approach to beat-by-beat QT-interval analysis," *IEEE Engineering in Medicine and Biology Magazine,* vol. 19, no. 3, pp. 97-101, May/June 2000.

[176] D. Lemire, C. Pharand, J. Rajaonah, B. Dube, A. R. LeBlanc, "Wavelet time entropy, T wave morphology and myocardial ischemia," *IEEE Transactions on Biomedical Engineering,* vol. 47, no. 7, pp. 967-970, July 2000.

[177] B. U. Kohler, C. Hennig, R. Orglmeister, "The principles of software QRS detection," *IEEE Engineering in Medicine and Biology Magazine,* vol. 21, no. 1, pp. 42-57, January/February 2002.

[178] J. P. Martinez, R. Almeida, S. Olmos, A. P. Rocha, P. Laguna, "A wavelet-based ECG delineator: evaluation on standard databases," *IEEE Transactions on Biomedical Engineering,* vol. 51, no. 4, pp. 570-581, April 2004.

[179] C. Meyer, J. F. Gavela, M. Harris, "Combining Algorithms in Automatic Detection of QRS Complexes in ECG Signals," *IEEE Transactions on Information Technology in Biomedicine,* vol. 10, no. 3, pp. 468-475, July 2006.

[180] I. Daubechies, "Orthonormal bases of compactly supported wavelets," *Communications on Pure and Applied Mathematics,* vol. 41, no. 7, pp. 909-996, October 1998.

[181] S. Mallat, "A theory for multiresolution signal decomposition: The wavelet representation', *IEEE Transactions on Pattern Analysis and Machine Intelligence,* vol. 11, no. 7, pp. 674-693, July 1989.

[182] O. Rioul, M. Vetterli, "Wavelets and signal processing," *IEEE Signal Processing Magazine,* vol. 8, no. 4, pp. 14-38, October 1991.

[183] S. Mallat, S. Zhong, "Characterization of signals from multi-scale edges," *IEEE Transactions on Pattern Analysis and Machine Intelligence,* vol. 14, no. 7, pp. 710-732, July 1992.

[184] I. Daubechies, "Ten Lectures on Wavelets," Philadelphia: SIAM, 1992.

[185] S. Mallat, "A Wavelet Tour of Signal Processing," second ed. San Diego:Academic Press, 1999.

[186] M. Antonini, "Image coding using wavelet transform," *IEEE Transactions on Image Processing,* vol. l, no. 2 pp. 205-220, April 1992.

[187] B. E. Usevitch, "A tutorial on modern lossy wavelet image compression: Foundation of JPEG 2000," *IEEE Signal Process. Magazine,* vol. 18, no. 5, pp. 22-35, September 2001.

[188] David Salomon "Data Compression," 3rd Edition, Springer-Verlag, New York, Inc.

[189] Pankaj N. Topiwala (Editor), "Wavelet image and video compression (The springer international series in engineering and computer science)," Kluwer Academic Publishers.

[190] A. S. Al-Fahoum, "Quality assessment of ECG compression techniques using a wavelet-based diagnostic measure," *IEEE Transactions on Information Technology in Biomedicine,* vol. 10, no. 1, pp. 182-191, January 2006.

[191] Y. Zigel, A. Cohen, A. Katz, "The weighted diagnostic distortion (WDD) measure for ECG signal compression," *IEEE Transactions on Biomedical Engineering,* vol. 47, no. 11, pp. 1422-1430, Novemeber 2000.

[192] M. S. Manikandan, S. Dandapat, "ECG Signal Compression using Discrete Sinc Interpolation," in *Proceedings of 3rd IEEE International Conference on Intelligent Sensing and Information Processing,* pp. 14-19, December 2005.

[193] A. Caral, H. D. Ambrosio, A. Oritz-Conde, F. J. Garcia Sanchez, "Percent area difference as a measure of distortion and its use in maximum enclosed area (MEA), a new ECG signal compression algorithm," in *Proceedings of 4th IEEE international Caracas Conference on Devices, Circuits and Systems,* pp. 1035-1-1035-5, 2002.

[194] VQEQ, Final report from the video quality experts group on the validation of objective models of video quality assessment, March 2000. http://www.vqeg.org/.

[195] M. W. Marcellin, M. A. Lepley, A. Bilgin, T. J. Flohr, T. T. Chinen, J. H. Kasner "An overview of quantization in JPEG 2000," *Signal Processing: Image Communication,* vol. 17, no. 1, pp. 73-84, January 2002.

[196] M. Long, H. M. Tai, S. Yang, "Quantisation step selection schemes in JPEG2000," *IET Electronics Letters,* vol. 38, no. 12, pp. 547-549, June 2002.

[197] O. K. Al-Shaykh, R. M. Mersereau, "Lossy compression of noisy images," *IEEE Transactions on Image Processing,* vol. 7, no. 12, pp. 1641-1652, December 1998.

[198] Bo Tao, "On optimal entropy-constrained deadzone quantization," *IEEE Transactions on Circuits and Systems for Video Technology,*, vol. 11, no. 4, pp. 560-563, April 2001.

[199] A. Alecu, A. Munteanu, J. Cornelis, S. Dewitte, P. Schelkens, "On the optimality of embedded dead-zone scalar-quantizers for wavelet-based L-infinite-constrained image coding," *IEEE Signal Processing Letters,* vol. 11, no. 3, pp. 367-370, March 2004.

[200] Jinhua Yu, "Advantages of Uniform Scalar Dead-zone Quantization in Image Coding System," in *Proceedings of International Conference on Communications, Circuits and Systems,* vol 2, pp. 805-808, June 2004.

[201] Jianhua Chen, Yufeng Zhang, Xinling Shi "Image coding based on wavelet transform and uniform scalar dead zone quantizer," *Signal Processing: Image Communication,* vol. 21, no. 7, pp. 562-572, August 2006.

[202] M. S. Manikandan, S. Dandapat, "Wavelet based ECG compression with large zero zone quantizer," in *Proceedings of IEEE Annual India Conference,* pp. 1-5, September 2006.

[203] Jianhua Chen, Fuyan Wang, Yufeng Zhang, Xinling Shig, "ECG compression using uniform scalar dead-zone quantization and conditional entropy coding," *Medical Engineering and Physics,* vol. 30, no. 4, pp. 523-530, May 2008.

[204] Z. Xiong, K. Ramchandran, M. T. Orchard, "Space-frequency quantization for wavelet image coding," *IEEE Transactions on Image Processing,* vol. 6, no. 5, pp. 677-693, May 1997.

[205] S. Grace Chang, Bin Yu, Martin Vetterli, "Adaptive wavelet thresholding for image denoising and compression," *IEEE Transactions on Image Processing,* vol. 9, no. 9, pp. 1532-1546, September 2000.

[206] N. Gupta, M. N. S. Swamy, E. Plotkin, "Despeckling of medical ultrasound images using data and rate adaptive lossy compression," *IEEE Transactions on Medical Imaging,* vol. 24, no. 6, pp. 743-754, June 2005.

[207] Ping Zhou, Zhigang Wang, "A computer location algorithm for ECG, PCG and CAP," in *Proceedings of the 20th Annual International Conference of the IEEE EMBS*, vol. 1, pp. 220-222, 1998.

[208] Z. Syed, D. Leeds, D. Curtis, F. Nesta, R. A. Levine, J. Guttag, "A framework for the analysis of acoustical cardiac signals," *IEEE Transactions on Biomedical Engineering,* vol. 54, no. 4, pp. 651-662, April 2007.

[209] K. Phua, J. Chen, T. H. Dat, L. Shue, "Heart sound as a biometric," *Pattern Recognition,* vol. 41 no. 3, pp. 906-919, March 2008.

[210] S. Choi, Z. Jiang, "Comparison of envelope extraction algorithms for cardiac sound signal segmentation," *Expert Systems with Applications,* vol. 34, no. 2, pp. 1056-1069, February 2008.

[211] J. M. Alajarín, R. R. Merino, "Wavelet and wavelet packet compression of phonocardiograms," *IET Electronics Letters,* vol. 40, no. 17, pp. 1040-1041, August 2004.

[212] F. J. Toledo-Moreo, A. Legaz-Cano, J. J. Martlinez-Alvarez J. M. Alajarin, R. R. Merino, "Compression system for the phonocardiographic signal," in *Proceedings of International Conference on Field Programmable Logic and Applications,* pp. 770-773, 2007.

[213] M. S. Manikandan and S. Dandapat, "An efficient wavelet energy based phonocardiogram (PCG) data compression," in *Proceedings of IEEE International Conference on Signal and Image Processing*, pp. 424-429, December 2006.

[214] M. S. Manikandan, S. Dandapat, "PCG Signals Compression Method Based on Wavelet Transform and SPIHT Algorithm," *Proceedings of IEEE Annual India Conference,* pp. 150-156, September 2007.

[215] R. Benzid, M. Benyoucef, L. Saidi, "Quality-on-request phonocardiogram compression algorithm using the discrete cosine transform: Comparison between the linear and the Lloyd quantizers," *International Review on Computers and Software,* November 2007.

[216] L. P. Yaroslavsky, "Efficient algorithm for discrete sinc interpolation," *Applied optics,* vol. 36, no. 2, pp. 460-463, January 1997.

[217] Jun Tian, Wells, R.O., Jr., "A lossy image codec based on index coding," in *Proceedings of Data Compression Conference, 1996. DCC '96*, page 456, March/April 1996.

List of Publications

Refereed Journal Publications

Published papers and Accepted publications

(i) M. S. Manikandan and S. Dandapat, "Wavelet threshold based ECG compression using USZZQ and Huffman coding of DSM," *Biomed. Signal Process. Control,* Elsevier, vol. 1, no. 4, pp. 261-270, October 2006.

(ii) M. S. Manikandan and S. Dandapat, "Wavelet energy based diagnostic distortion measure for ECG," *Biomed. Signal Process. Control,* Elsevier, vol. 2, no. 2, pp. 80-96, April 2007.

(iii) M. S. Manikandan and S. Dandapat, "Wavelet threshold based TDL and TDR algorithms for real-time ECG signal compression," *Biomed. Signal Process. Control,* Elsevier, vol. 3, no. 1, pp. 44-66, January 2008.

(iv) M. S. Manikandan and S. Dandapat, "Multiscale entropy based weighted distortion measure for ECG coding," accepted for publication in *IEEE Signal Processing Letters,* June 2008.

Manuscripts Revised and Submitted

(i) M. S. Manikandan and S. Dandapat, "Wavelet Energy based Lossy PCG Compression and Quality Assessment of the Compressed Signal using WEDD Criterion," *Digital Signal Processing,* Elsevier, March 2008.

Manuscripts under Review

(i) M. S. Manikandan and S. Dandapat, "Effective quality-controlled SPIHT based ECG coding under noise environments", *IEE Electronics Letters,* May 2008.

Manuscripts to be Submitted

(i) M. S. Manikandan, and S. Dandapat, "Quality-driven subband coding of cardiac signals," *IEEE Transactions on Biomedical Engineering,* 2008.

(ii) M. S. Manikandan, and S. Dandapat, "Wavelet based cardiac sound classification and compression," *IEEE Transactions on Biomedical Engineering,* 2008.

(iii) M. S. Manikandan, and S. Dandapat, "Multiscale entropy based weighted distortion measure for cardiac beat recognition," *Biomed. Signal Process. Control,* 2008.

Refereed Conference Publications

Published papers and Accepted publications

(i) M. S. Manikandan and S. Dandapat, "ECG signal compression using discrete sinc interpolation," in *Proc. 3rd IEEE Int. Conf. Intelligent Sensing and Information Processing,* pp. 14-19, Dec. 2005.

(ii) M. S. Manikandan and S. Dandapat, "Wavelet-threshold based ECG compression with smooth retrieved quality for telecardiology," in *Proc. 4th IEEE Int. Conf. Intelligent Sensing and Information Processing,* pp. 138-143, Dec. 2006.

(iii) M. S. Manikandan and S. Dandapat, "An efficient wavelet energy based phonocardiogram (PCG) data compression," *in Proc. IEEE Int. Conf. Signal and Image Proc. (ICSIP 2006),* pp. 424-429, Dec. 2006.

(iv) M. S. Manikandan and S. Dandapat, "Quality controlled wavelet compression of ECG signals by WEDD," in *Proc. 9th Int. conf. Computational Intelligence and Multimedia Applications (ICCIMA 2007),* IEEE CS Press, vol.1, pp. 581-586, Dec. 2007.

(v) M. S. Manikandan and S. Dandapat, "Wavelet-based ECG and PCG signals compression technique for mobile telemedicine," in *Proc. 15th Int. Conf. Advanced Computing and Communication 2007,* IEEE CS Press, pp. 164-169, Dec. 2007.

(vi) M. S. Manikandan and S. Dandapat, "Wavelet energy based compression of phonocardiogram (PCG) signal for telecardiology," in *Proc. IET Int. Conf. Information and Communication Technology in Electrical Sciences (ICTES 2007),* Dec. 2007.

(vii) M. S. Manikandan and S. Dandapat, "ECG Distortion Measures and their Effectiveness," icetet, IEEE CS Press, pp. 705-710, *International Conference on Emerging Trends in Engineering and Technology,* July 2008.

(viii) M. S. Manikandan and S. Dandapat, "An effective wavelet-based lossy compression of noisy ECG signals", accepted for *IEEE TENCON 2008,* Hyderabad, India.

(ix) M. S. Manikandan and S. Dandapat, "Wavelet based ECG Compression with large zero zone quantizer," in *Proc. IEEE India Annual Conference (INDICON 2006),* Sep. 2006.

(x) M. S. Manikandan and S. Dandapat, "An efficient wavelet-based cardiac signal compression for telemedicine," in *Proc. Indian Conf. Medical Informatics and Telemedicine,* IIT Kharagpur, pp. 132-136, Dec. 2006, India.

(xi) M. S. Manikandan and S. Dandapat, "PCG signals compression method based on wavelet transform and SPIHT algorithm," in *Proc. IEEE India Annual Conference (INDICON 2007),* pp. 222-227, Sep. 2007.

(xii) L. N. Sarma, S. R. Nirmala, M. S. Manikandan and S. Dandapat, "Compression of multi-lead ECG signals and retinal images using 2-D wavelet transform and SPIHT coding scheme for mobile telemedicine," in *Proc. Workshop on Image and Signal Processing (WISP 2007),* pp. 18-27, Dec. 2007.

Manuscripts and Abstracts under Review

(i) M. S. Manikandan and S. Dandapat, "Wavelet-Based Robust Template Matching Using Multiscale Energy Weighted Euclidean Wavelet Distance," abstract submitted to *13th International conference on biomedical engineering (ICBME2008),* Singapore, August 2008.

(ii) M. S. Manikandan and S. Dandapat, "Optimal Constraint Threshold Control Zero-zone Nearly Uniform Midtread Quantizer for Simultaneous Denoising and Compression of Biomedical Signals," abstract submitted to *13th International conference on biomedical engineering (ICBME2008)*, Singapore, August 2008.